# REGULATION OF HUMAN MONOCYTE DIFFERENTIATION INTO M1- AND M2-LIKE MACROPHAGES

A DISSERTATION SUBMITTED TO

THE GRADUATE SCHOOL OF ENGINEERING AND SCIENCE

OF BILKENT UNIVERSITY

IN PARTIAL FULFILLMENT OF THE REQUIREMENTS

FOR THE DEGREE OF

DOCTOR OF PHILOSOPHY

IN

MOLECULAR BIOLOGY AND GENETICS

By

Defne Bayık

May 2016

**REGULATION OF HUMAN MONOCYTE DIFFERENTIATION INTO M1- AND M2-LIKE MACROPHAGES**

By Defne Bayık

May, 2016

We certify that we have read this dissertation and that in our opinion it is fully adequate, in scope and in quality, as a thesis for the degree of Doctor of Philosophy.

İhsan Gürsel
(Advisor)

Dennis M. Klinman
(Co-Advisor)

Mayda Gürsel

Özlen Konu

Ali Güre

Mesut Muyan

Approved for the Graduate School of Engineering and Science

Levent Onural

Director of the Graduate School of Engineering and Science

# Abstract


REGULATION OF HUMAN MONOCYTE
DIFFERENTIATION INTO M1- AND M2-LIKE MACROPHAGES

Defne Bayık

Ph.D. in Molecular Biology and Genetics

Supervisor: İhsan Gürsel

Co-supervisor: Dennis M. Klinman

May, 2016

Myeloid-derived suppressor cells (MDSC) play a key role in down-regulating activated T and NK cells. MDSC are emerging as targets for cancer immunotherapy since they protect tumor cells from immune elimination. We previously showed that the TLR7/8 agonist R848 and the TLR2/1 dual agonist PAM3 had opposite effect on the maturation of human monocytic MDSC (mMDSC). While the former triggered them to differentiation in M1-like macrophages with pro-inflammatory/anti-tumoricidal capacity, the latter generated immunosuppressive M2-like macrophages. This work seeks to identify the soluble factors that regulate the differentiation of mMDSC into macrophages. Our studies reveal that TNFα and M-CSF are essential for mMDSC to mature into functional M1- and M2-like macrophages, respectively. IL-6 and IL-10 play secondary roles but when used in combination with TNFα or M-CSF exceed the effects of TLR agonists. Understanding the response of mMDSC to cytokines should help efforts to direct the mMDSC maturation to therapeutic benefit.

The finding that PAM3 could induce human mMDSC to mature into M2-like macrophage triggered us to study the effect of this TLR agonist on other monocyte populations. Our findings reveal that PAM3 was unique among TLR agonists in generating M2-like macrophages. We compared the polarizing activity of PAM3 to that of M-CSF. PAM3 was slightly less efficient than M-CSF in driving maturation of HLA-$DR^+$ monocytes based on phenotypic characterization and phagocytic ability. Yet macrophages generated by PAM3 or M-CSF were equally capable of suppressing T cell proliferation. Analysis of gene regulatory networks by microarray and subsequent validation of the pathways identified by using specific inhibitors defined the NF-κB – COX-2 axis as playing a primary role. However, PAM3 also induced monocyte differentiation via an IL-6-dependent pathway that was largely absent from M-CSF-

driven cultures. Our findings clarified the pathways by which immunosuppressive M2-like macrophage arise from human monocytes and identify PAM3 as a potential therapeutic modulator of monocyte differentiation in patients with autoimmune disease.

Extracellular vesicles (EV) are a heterogeneous population of biological nanoscaled particles that serve as vectors to enhance intercellular communication. In addition to this physiological role evidence indicates that EV can be harnessed as therapeutic agents for cancer. The major limitation to EV-based therapeutics is their rapid clearance by the reticuloendothelial system (RES). To overcome this problem, we sought to reduce macrophage uptake of EV by blocking scavenger receptors. *In vitro* results using human and murine cells suggests that inhibiting class A scavenger receptors selectively impairs EV uptake by monocytes and macrophages. *In vivo* studies document reduced liver accumulation and enhanced plasma circulation of i.v. injected EV after such blockade. These findings provide a strategy for reducing EV uptake by the RES thereby increasing their targeting and activity.

***Keywords:*** Myeloid-derived suppressor cells, HLA-$DR^+$ human monocytes, M1-like macrophages, M2-like macrophages, TLR agonists, cytokines, extracellular vesicles, scavenger receptors

# Özet

## İNSAN MONOSİTLERİNİN M1- VE M2-BENZERİ MAKROFAJLARA DÖNÜŞÜMÜNÜN DÜZENLENMESİ

Defne Bayık

Moleküler Biyoloji ve Genetik Bölümü, Doktora

Tez Danışmanı: İhsan Gürsel

Eş Tez Danışmanı: Dennis M. Klinman

Mayıs, 2016

Miyeloid türevi baskılayıcı hücreler (MDSC) aktive olmuş T ve NK hücrelerini susturulmasında önemli rol oynarlar. Tümör hücrelerinin bağışıklık sistemi tarafından elemesini engelledikleri nden dolayı, MDSC kanser immünoterapi için yeni bir hedef olarak ortaya çıkmaktadır. Önceki sonuçlarımız TLR7/8 agonisti R848 ve TLR2/1 ikili agonisti PAM3'ün insan monositik MDSC (mMDSC) olgunlaşması üzerinde ters bir etkiye sahip olduğunu göstermişti. İlk agonist mMDSClerin pro-inflamatuar/anti-tümorisidal kapasiteli M1 benzeri makrofajlara farklılaşmasını tetiklerken, ikinci agonist immunsupresif M2 benzeri makrofajlar oluşturmuştur. Bu çalışma mMDSClerin makrofajlara farklılaşmasını düzenleyen çözünür faktörler tespit etmeyi amaçlamaktadır. Araştırmalarımız mMDSClerin fonksiyonel M1 ve M2 benzeri makrofajlara olgunlaşması için sırasıyla TNFα ve M-CSF'in önemli olduğunu ortaya koymaktadır. IL-6 ve IL-10 ikincil bir rol oynamakla birlikte TNFα veya M-CSF ile kombinasyon halinde kullanıldığında TLR agonistlerinden daha etkilidir. mMDSC sitokinlere nasıl tepki verdiğini anlamak bu hücrelerin terapötik amaçla olgunlaşmasını yönlendirmek açısından yardımcı olacaktır.

PAM3'ün insan mMDSClerini M2-benzeri makrofajlara dönüştürdüğüne dair bulgular, bu TLR agonistinin diğer monosit popülasyonları üzerinde etkisini araştırmaya yönlendirmiştir. Bulgularımız PAM3'ün M2-benzeri makrofajlar oluşturabilme kapasitesinin TLR agonistleri arasında benzersiz olduğunu ortaya koymaktadır. PAM3 ve M-CSF'in kutuplaştırıcı aktivitesinin fenotipik nitelendirilme ve fagositik yetenek açısından karşılaştırılması PAM3' ün M-CSF'e oranla HLA-DR$^{+}$ monositleri dönüştürmede daha az etkili olduğunu göstermiştir. Yine de PAM3 veya M-CSF tarafından oluşturulan makrofajlar T hücresi çoğalmasını eşit derecede bastırabilmektedirler. Mikrodizi analizi yöntemi ile düzenleyici gen şebekelerinin tespit edilmesi ve devamında spesifik inhibitörler kullanılarak bu şebekelerin doğrulanması

sonucunda NF-κB–COX-2 ekseninin makrofaj dönüşümünde birincil rol oynadığı tespit edilmiştir. PAM3 aynı zamanda IL-6 bağımlı bir yol üzerinden monosit farklılaşmasını neden olurken, bu şebeke M-CSF tarafından kullanılmamaktadır. Bulgularımız, insan monositlerinin bağışıklık baskılayıcı M2 makrofajlara kutuplaşmasını yönlendiren yollara açıklık getirmiş ve PAM3'ü otoimmün hastalarda monosit farklılaşmasını kontrol edebilecek potansiyel bir terapötik modülatör olarak tanımlamıştır.

Hücre dışı kesecikler (EV), hücreler arası iletişimi arttırmak için hizmet eden biyolojik kökenli, nano büyüklükte heterojen parçacıklar topluluğudur. Fizyolojik rolüne ek olarak EVlerin kanser tedavisinde kullanılabileceğine dair kanıtlar bulunmaktadır. EV-bazlı tedavilerdeki başlıca sınırlama EVlerin retikülo-endotelyal sistem (RES) tarafından hızlı bir şekilde temizlenmeleridir. Bu sorunu aşmak için, çöpçü reseptörlerini bloke ederek EVlerin makrofajlar tarafından alımını azaltmak hedeflenmiştir. İnsan ve fare hücrelerini kullanarak elde edilen *in vitro* sonuçlar A sınıfı çöpçü reseptörlerinin bloke edilmesinin seçici olarak monosit ve makrofajlar tarafından EV alımını engellediğini göstermektedir. *İn vivo* çalışmalar A sınıfı çöpçü reseptörleri bloklanmasının damar içi enjekte edilerin EVlerin karaciğer birikimi azaltırken plazma dolaşımını arttırdığını belgelemiştir. Bu çalışma RES alımını engelleyerek EVlerin hedef ve aktivitelerini geliştirmeye yönelik bir strateji tanımlamıştır.

***Anahtar Kelimeler:*** Myeloid türevi baskılayıcı hücreler , HLA-DR$^{+}$ insan monositler, M1-benzeri makrofajlar , M2-benzeri makrofajlar, TLR agonistleri , sitokinler , hücre dışı kesecikler, çöpçü reseptörleri

*To my precious family…*

# Acknowledgements

First and foremost I would like to express my deepest gratitude to my supervisors Prof. Dr İhsan Gürsel and Dr. Dennis M. Klinman for their care, trust, patience and guidance. It has been a privilege to work with them. I am grateful for all the knowledge they shared and the values they taught. I cannot thank them enough for helping me to become a researcher and to develop as a person. I hope that I can make them proud.

I would also like to express my heartfelt thanks to Assoc. Prof. Dr. Mayda Gürsel for broadening my perspective on life and science. She has been a true inspiration for me. I am extremely thankful to Assoc. Prof. Dr. Işık G. Yuluğ for her support throughout my graduate life. I would like to express my gratitude to Assoc. Prof. Dr. Özlen Konu for being part of my Ph.D. progress committee and for her feedbacks. I also would like to thank Assoc. Prof. Dr. Ali Güre and Assoc. Prof. Dr. Mesut Muyan for accepting to become members of my thesis jury, and sparing time to evaluate and improve my thesis.

I would like to express my gratitude to Debra Tross for her help, especially with the microarray experiments. I am grateful to Roberta Matthai and Kathleen Noer for all the sorting that they have done and to the NIH Blood Bank staff for the samples they provided. Special thanks to Dr. Dionysios C. Watson and Dr. Avinash Srivatsan for collaborating on studies with extracellular vesicles.

I am really grateful to past and present members of the Gürsel group: Fuat Cem Yağcı, Tamer Kahraman, Arda Gürsel, Mehmet Şahin, İhsan Dereli, Yusuf İsmail Ertuna, Merve Deniz Abdüsselamoğlu, Kübra Almacıoğlu, Begüm Han Horuluoğlu, Gözde Güçlüler, particularly to Banu Bayyurt and Gizem Tinçer-König for their support and friendship. I had to privilege to work alongside great people. I am thankful to the Klinman Group members Emilie Goguet, Julia Scheiermann, Kathy Parker and Neslihan Turan and Debra Tross for their collegiality, discussions and support.

I feel lucky to be a part of the MBG family, where I met amazing people with whom I will remain lifetime friends, especially Gülşah Dal-Kılınç, Özlem Tufanlı, Büşra Yağbasan, Şeyma Demirsoy, Füsun Doldur-Ballı, Merve Mutlu and Dilan Çelebi-Birand. I would like to dedicate special thanks to Gözde Güçlüler and Begüm Han Horuluoğlu for their invaluable friendship and support.

I am especially grateful to Verda Bitirim for her incredible friendship. Through good times and bad, she will remain as my best friend.

Last but not least, I want to thank all my family for their life-long support and encouragement. I would like to express my deepest love to my parent Sedef and Nezihi; and my grandmothers Gül and Göksel. Thank you for being awesome parents and grandparents. I would like to express my heartfelt gratitude Dennis Watson. Without his constant love and patience, I couldn't have completed this thesis. We will remain united in work as in life. Finally I would like to dedicate this thesis to my grandfather, whom will be deeply missed.

I was financially supported by The Scientific and Technological Research Council of Turkey (TÜBİTAK) BİDEB 2211 scholarship during my Ph.D. studies. My work at the NIH as part of the NIH-Bilkent University individual Graduate Partnership Program (GPP) was supported by the NIH intramural funds.

# Table of contents

Abstract..... iii

Özet..... v

Acknowledgements..... viii

Table of contents..... x

List of figures..... xv

List of tables..... xix

Abbreviations..... xx

Chapter 1....Introduction..... 1

1.1 The Immune System..... 1

1.2 Myeloid Cells..... 2

1.2.1 Monocytes..... 2

1.2.2 Macrophages..... 3

1.2.2.1 M1 Macrophages..... 3

1.2.2.2 M2 Macrophages..... 6

1.2.2.3 Macrophages Generated by M-CSF and GM-CSF..... 9

1.2.2.4 Tumor-associated Macrophages..... 10

1.2.3 Myeloid Derived Suppressor Cells..... 12

1.2.3.1 MDSC under disease conditions..... 13

1.2.3.2 MDSC-Mediated Immune Suppression..... 14

1.2.3.3 Response of MDSC to Soluble Factors..... 16

1.2.3.4 Therapeutic strategies for MDSC targeting..... 19

1.2.3.4.1 Response of MDSC to TLR Agonists..... 22

1.3 Extracellular Vesicles..... 25

1.3.1 Therapeutic Potential of EV..... 26

1.3.2 Problems associated with EV-based therapeutics ..... 27
1.3.3 EV Uptake Receptors ..... 29
1.3.4 Scavenger Receptors Class A and B Families ..... 31
1.4 Aim and outline of the thesis ..... 33
Chapter 2....Materials and Methods ..... 34
2.1 Materials ..... 34
2.1.1 TLR Ligands ..... 34
2.1.2 Recombinant Cytokines ..... 35
2.1.3 Cytokine Neutralizing Antibody ..... 36
2.1.4 Flow Cytometry Antibody ..... 37
2.1.5 ELISA Antibodies ..... 39
2.1.6 Cell Culture Media and Standard Solutions Components ..... 39
2.2 Methods ..... 40
2.2.1 Collection and isolation of human blood samples ..... 40
2.2.1.1 Sorting of mMDSC and HLA-DR$^+$ monocytes ..... 40
2.2.1.2 Sorting of naïve CD4$^+$ T Cells ..... 41
2.2.2 Stimulation of mMDSC and HLA-DR$^+$ monocytes ..... 42
2.2.3 Effect of cytokines on re-polarization of HLA-DR$^+$ monocytes ..... 42
2.2.4 Microscopy image of HLA-DR$^+$ monocytes ..... 42
2.2.5 Analysis of surface and intracellular markers with flow cytometry ..... 43
2.2.6 Functional analysis of differentiated cells ..... 43
2.2.6.1 Cytotoxicity functional assay ..... 43
2.2.6.2 T Cell proliferation assay ..... 44
2.2.6.2.1 Staining of naïve CD4$^+$ T cells with CFSE ..... 44
2.2.6.2.2 Preparation of Dynabeads® Human T Actiator CD3/CD28 ..... 44
2.2.6.2.3 Assay procedure ..... 45

2.2.6.3 Phagocytosis Assay ..... 45
2.2.7 ELISA for cytokines ..... 45
2.2.8 Analysis of gene expression with microarray ..... 46
2.2.8.1 RNA isolation ..... 46
2.2.8.2 Expression analyses ..... 46
2.2.9 Generation of bone marrow-derived macrophages ..... 47
2.2.9.1 Isolation of bone marrow cells ..... 47
2.2.9.2 Sorting for mouse mMDSC ..... 47
2.2.9.3 Sorting of mouse monocytes ..... 47
2.2.9.4 Stimulation of bone marrow-derived cells ..... 48
2.2.10 Cell lines ..... 48
2.2.11 Isolation of extracellular vesicles ..... 49
2.2.12 Staining of extracellular vesicles ..... 49
2.2.12.1 Staining with SYTO® RNASelect™ Green Fluorescent Stain ..... 49
2.2.12.2 Staining with DiR ..... 50
2.2.13 Uptake of EV by mouse cell lines ..... 50
2.2.14 Uptake of EV by primary murine macrophages ..... 51
2.2.15 Uptake of EV by human peripheral blood mononuclear cells ..... 51
2.2.16 *In vivo* biodistribution of EV ..... 52
2.2.17 Statistical analyses ..... 52
Chapter 3....Results ..... 53
3.1 Efforts to Regulate Macrophage Differentiation ..... 53
3.1.1 PAM3 and R848 induce mMDSC to differentiate into M1- and M2-like macrophages ..... 53
3.1.2 Co-stimulation of TLR7 and TLR8 is required for effective M1-like macrophage polarization of mMDSC ..... 54

3.1.3 IL-6 and IL-10 are important but not sufficient to induce the complete differentiation of mMDSC ..... 55

3.1.4 TNFα but not IL-12 supports the differentiation of mMDSCs into M1-like macrophages ..... 59

3.1.5 Combining TNFα with IL-6 recapitulates the effect of R848 on mMDSC ..... 62

3.1.6 M1-like macrophages generated by R848 vs IL-6 and TNFα combination differ in morphology ..... 65

3.1.7 Macrophages generated by stimulation of mMDSC with IL-6 and TNFα lyse tumor cells effectively ..... 65

3.1.8 IFNγ is efficient driver of M1-like macrophage differentiation from mMDSC . 66

3.1.9 Regulatory networks of R848, IFNγ and IL-6 plus TNFα-dependent differentiation of mMDSC ..... 67

3.1.10 GM-CSF does not induce differentiation of the mMDSC into macrophages ..... 70

3.1.11 $PGE_2$ alters the pattern of macrophage differentiation from mMDSC ..... 72

3.1.12 IL-4, IL-8, IL-13 and TGF-β are not essential for M2-like macrophage differentiation from mMDSC ..... 73

3.1.13 IL-1β partially supports M2-like macrophage differentiation from mMDSC .... 74

3.1.14 High dose M-CSF supports M2-like macrophage differentiation from mMDSC as an independent signal ..... 77

3.1.15 Low dose M-CSF in combination with IL-6 and IL-10 recapitulates the effect of PAM3 ..... 80

3.1.16 mMDSC stimulated with PAM3 or combination of IL-6, IL-10 and low dose M-CSF remain functionally suppressive ..... 83

3.1.17 mMDSC preferentially differentiate into M2- rather than M1-like macrophages .. ..... 84

3.1.18 Macrophages differentiated from HLA-$DR^+$ monocytes are plastic ..... 85

3.1.19 TLR2/1 signaling polarizes HLA-$DR^+$ monocytes into M2-like macrophages .. 86

3.1.20 PAM3 response of mMDSC and HLA-$DR^+$ monocytes are indistinguishable ... 90

3.1.21 Variation in PAM3 response of human and mouse monocytes ..... 90

3.1.22 PAM3 and M-CSF generate M2-like macrophages from HLA-DR$^+$ monocytes 92

3.1.23 PAM3 and M-CSF differ in their ability to induce HLA-DR$^+$ monocytes to differentiate into M2-like macrophage ..... 94

3.1.24 Functional activity of PAM3 and M-CSF induced M2-like macrophages ..... 94

3.1.25 Morphology of PAM3 and M-CSF induced M2-like macrophages ..... 95

3.1.26 PAM3 and M-CSF-induced M2-like macrophages originated from HLA-DR$^+$ monocytes differ in lineage and functional marker expression ..... 96

3.1.27 PAM3 and M-CSF generate M2-like macrophages from HLA-DR$^+$ monocytes that differ in phagocytic activity ..... 98

3.1.28 Regulatory network underlying PAM3 and M-CSF-induced M2-like macrophage differentiation of HLA-DR$^+$ monocytes ..... 100

3.1.29 Validation of selected targets identified with microarray ..... 103

3.1.30 Mouse macrophage cell line uptakes EV in Scavenger Receptor Class A-dependent manner ..... 104

3.1.31 Primary mouse macrophages differentially uptake EV depending on the level of scavenger receptor expression ..... 106

3.1.32 Human monocytes uptake EV in scavenger receptor-dependent manner..... 107

3.1.33 Administration of scavenger-receptor inhibitor alters the biodistribution of EV ... ..... 108

Chapter 4....Discussion ..... 110

Chapter 5....Future Perspectives ..... 130

Bibliography ..... 133

Appendices ..... 172

Appendix A - Gene Lists ..... 172

Appendix B - Figures ..... 181

Curriculum Vitae and Publications ..... 184

# List of figures

Figure 1.1: Subsets of myeloid-derived suppressor cells..... 12

Figure 1.2: Biogenesis and properties of three main classes of extracellular vesicles. ..... 25

Figure 3.1: TLR agonists selectively drive mMDSC differentiation into M1- and M2-like macrophages. ..... 54

Figure 3.2: Stimulation through both TLR7 and TLR8 is required for differentiation of mMDSC into M1-like macrophages. ..... 55

Figure 3.3: PAM3 and R848 induce mMDSC to secrete IL-6 and IL-10. ..... 56

Figure 3.4: IL-6 and IL-10 have regulatory roles in R848- and PAM3-induced differentiation of mMDSC. ..... 57

Figure 3.5: IL-6 and IL-10 partially support macrophage differentiation from mMDSC. ..... 58

Figure 3.6: Addition of IL-6 plus IL-10 has the same effect as each cytokine separately on mMDSC differentiation. ..... 59

Figure 3.7: TNFα is secreted in the course of R848-induced mMDSC differentiation. ..... 60

Figure 3.8: IL-12 and TNFα regulate R848- but not PAM3-induced macrophage differentiation from mMDSC. ..... 61

Figure 3.9: TNFα but not IL-12 supports the differentiation of mMDSC into M1-like macrophage. ..... 62

Figure 3.10: TNFα and IL-6 cocktail is the most effective cytokine combination inducing M1-like macrophage differentiation. ..... 63

Figure 3.11: Combination of IL-6 with TNFα is superior to R848 in generating M1-like macrophages. ..... 64

Figure 3.12: Distinct morphology of unstimulated, R848 or IL-6 + TNFα stimulated mMDSC at Day 5. ..... 65

Figure 3.13: mMDSC stimulated with R848 or the combination of IL-6 plus TNFα effectively lyse tumor cells. ..... 66

Figure 3.14: IFNγ polarizes mMDSC towards M1-like macrophages. ..... 67

Figure 3.15: R848, IL-6 plus TNFα and IFNγ-induced M1-like macrophage differentiation is regulated by a NF-κB-dependent network. ..... 69

Figure 3.16: GM-CSF does not induce mMDSC to become macrophage. ..... 71

Figure 3.17: $PGE_2$ regulates differentiation status of mMDSC. ..... 73

Figure 3.18: IL-4, IL-8, IL-13 and TGF-β do not support the differentiation of mMDSC into M2-like macrophages. ..... 74

Figure 3.19: IL-1β partially supports M2-like macrophage differentiation by mMDSC. ..... 76

Figure 3.20: High dose M-CSF is effective inducer of M2-like macrophages from mMDSC... 79

Figure 3.21: Combination of 1 ng/ml M-CSF with IL-6 and IL-10 is not sufficient to recapitulate the effect of PAM3. ..... 81

Figure 3.22: Combination of 5ng/ml M-CSF with IL-6 and IL-10 drives M2-like macrophage polarization as effectively as PAM3. ..... 82

Figure 3.23: mMDSC stimulated with PAM3 or IL-6, IL-10 and low dose M-CSF combination retain the suppressive activity. ..... 84

Figure 3.24: mMDSC preferentially differentiate into M2-like macrophages when exposed to TNFα and M-CSF simultaneously. ..... 85

Figure 3.25: M1-like and M2-like macrophages generated from HLA-$DR^+$ monocytes can change their phenotype when exposed to opposing stimuli. ..... 86

Figure 3.26: PAM3 preferentially generates M2-like macrophages from HLA-$DR^+$ monocytes. ..... 88

Figure 3.27: Differences in HLA-$DR^+$ monocyte differentiation after stimulation with PAM3 vs FSL-1. ..... 89

Figure 3.28: mMDSC and HLA-$DR^+$ monocytes respond similarly to PAM3. ..... 90

Figure 3.29: Mouse mMDSC and monocytes do not primarily differentiate into M2 macrophages in response to PAM3. ..... 92

Figure 3.30: M-CSF and PAM3 polarized HLA-$DR^+$ monocytes towards M2-like macrophage phenotype. ..... 93

Figure 3.31: PAM3-induced M2-like macrophage differentiation of HLA-$DR^+$ monocytes is independent of M-CSF. ..... 94

Figure 3.32: Macrophages generated from HLA-DR$^+$ monocytes in the presence of PAM3 and M-CSF suppress proliferation of T cells. ..... 95

Figure 3.33: Distinct morphology of unstimulated, PAM3 or M-CSF stimulated HLA-DR$^+$ monocytes at Day 5. ..... 96

Figure 3.34: CD16 is differentially up-regulated in PAM3 and M-CSF macrophages. ..... 97

Figure 3.35: PAM3 and M-CSF induced macrophages slightly differ in marker expression. ..... 98

Figure 3.36: PAM3 vs M-CSF-induced macrophages differ in their ability to phagocytose. ..... 99

Figure 3.37: Shared network of genes up-regulated during the course of PAM3- and M-CSF-induced macrophage differentiation. ..... 100

Figure 3.38: Interaction of distinct set of genes up-regulated by PAM3 vs M-CSF with shared regulatory network. ..... 102

Figure 3.39: NF-κB is the main regulator of PAM3- and M-CSF-induced M2-like macrophage differentiation ..... 104

Figure 3.40: Scavenger receptor class A blockade with DS interferes with EV uptake of murine macrophage cell line. ..... 105

Figure 3.41: Scavenger receptor class A blockade with DS interferes reduces EV uptake of primary murine macrophages. ..... 106

Figure 3.42: Human monocytes take up EV in a scavenger receptor class A dependent manner. ..... 108

Figure 3.43: Scavenger receptor blockade decreases the uptake of EV by the liver. ..... 109

Figure 4.1: Schematic representation of differentiation of mMDSC into M1-like macrophages. ..... 115

Figure 4.2: Schematic representation of differentiation of mMDSC HLA-DR$^+$ monocytes into M2-like macrophages. ..... 126

Figure B1: Confirmation of IL-10 and TNFα neutralization with ELISA ..... 181

Figure B2: Expression pattern of additional surface markers in PAM3 vs M-CSF stimulated HLA-DR$^+$ monocytes ..... 181

Figure B3: Secreted IL-6 levels are higher in PAM3 treated cultures as compared to M-CSF treated cultures. ..... 182

Figure B4: DS and CS-treatment has no influence on the viability of cells. ..... 182

Figure B5: FCS concentration determines the level of spontaneous macrophage differentiation from human monocytes. ..... 183

# List of tables

Table 1.1: Ligands of TLR ..... 3

Table 1.2: Therapeutic agents for MDSC targeting ..... 19

Table 1.3: EV uptake receptors ..... 29

Table 2.1: Ligands for TLR ..... 34

Table 2.2: Recombinant Cytokines ..... 35

Table 2.3: Neutralizing antibodies against secreted cytokines. ..... 36

Table 2.4: Fluorescence-conjugated antibodies ..... 37

Table 2.5: Staining volume and antibody amounts ..... 40

Table 2.6: Cell lines and culture conditions ..... 48

Table 2.7: EV concentrations ..... 50

Table 3.1: Comparison of M2:M1 Ratio and actual M2-like macrophage numbers of PAM3 or IL-6 + IL-10 + IL-1β stimulated mMDSC cultures. ..... 77

Appendix Table 1: Symbol of genes upregulated more 2-fold in R848, IL-6 plus TNFα or IFNγ stimulated HLA-DR$^+$ monocytes (alphabetically ordered)……172

Appendix Table 2: Symbol of genes upregulated more than 2-fold in PAM3 and M-CSF stimulated HLA-DR$^+$ monocytes (alphabetically ordered). ..... 174

# Abbreviations

| | |
|---|---|
| Ab | Antibody |
| APC | Antigen presenting cell |
| asRNA | Antisense RNA |
| ARG1 | Arginase 1 |
| ATCC | American Type Culture Collection |
| BSA | Bovine serum albumin |
| BMDC | Bone marrow-derived dendritic cell |
| BMDM | Bone marrow-derived macrophage |
| CCL/CXCL | Chemokine ligand |
| cDNA | Complementary deoxyribonucelaic acid |
| COX-1 (PTGS1) | Cyclooxygenase 2/Prostaglandin-endoperoxide synthase 1 |
| COX-2 (PTGS2) | Cyclooxygenase 2/Prostaglandin-endoperoxide synthase 2 |
| CS | Chondroitin sulfate |
| dd$H_2O$ | Double-distilled water |
| DC | Dendritic cell |
| DMEM | Dulbecco's modified eagle medium |
| DMSO | Dimethyl sulfoxide |
| DS | Dextran sulfate |
| ELISA | Enzyme linked-immunosorbent assay |
| EV | Extracellular vesicles |
| GvHD | Graft-versus-host disease |
| gMDSC | Granulocytic myeloid-derived suppressor cells |
| Hsp | Heat shock protein |
| FCS | Fetal bovine/calf serum |

| | |
|---|---|
| FLA | Flagellin |
| GM-CSF (CSF-2) | Granulocyte macrophage colony-stimulating factor |
| Gr-1 | Granulocyte receptor 1 |
| HLA-DR | Human leukocyte antigen – antigen D related |
| IFNα | Interferon alpha |
| IFNγ | Interferon gamma |
| IL | Interleukin |
| iNOS | Inducible nitric oxide synthase |
| IPA | Ingenuity Pathway Analysis |
| I.P. | Intraperitoneal |
| IRF | Interferon regulatory factor |
| I.V. | Intravenous |
| KO | Knockout |
| L-Arg | L-Arginine |
| LPS | Lipopolysaccharide |
| MAPK | Mitogen-activated protein kinase |
| M-CSF (CSF-1) | Macrophage colony stimulating factor |
| MDSC | Myeloid-derived suppressor cells |
| MFI | Mean fluorescence intensity |
| MHC | Major histocompatibility complex |
| mMDSC | Monocytic myeloid-derived suppressor cell |
| MPLA | Monophosphoryl Lipid A |
| MSC | Mesenchymal stem cell |
| MSR1 (SR-A) | Macrophage Scavenger Receptor 1 |
| MyD88 | Myeloid differentiation factor 88 |
| NAMPT | Nicotinamide phosphoribosyltransferase |

| | |
|---|---|
| NCI | National Cancer Institute |
| NF-κB | Nuclear factor-kappa B |
| NIBIB | National Institute of Biomedical Imaging and Bioengineering |
| NIH | National Institutes of Health |
| NK | Natural Killer |
| NO | Nitric oxide |
| OMV | Outer membrane vesicle |
| O/N | Overnight |
| PAM3 | Pam3CysSerLys4 |
| PAMP | Pathogen-associated molecular patterns |
| PBMC | Peripheral blood mononuclear cells |
| PBS | Phosphate buffered saline |
| PGN | Peptidoglycan |
| PRR | Pathogen recognition receptor |
| PS | Phosphatidylserine |
| R848 | Resiquimod |
| RES | Reticuloendothelial system |
| RNA | Ribonucleic acid |
| RPMI | Roswell Park Memorial Institute |
| RT | Room temperature |
| SR-BI | Scavenger receptor class B I |
| STAT | Signal transducers and activators of transcription |
| TGF-β | Transforming growth factor beta |
| TLR | Toll-like Receptor |
| TNFα | Tumor necrosis factor alpha |
| VEGF | Vascular endothelial growth factor |

# Chapter 1
# Introduction

## 1.1 The Immune System

The mammalian immune system is a network of physical barriers, leukocytes and soluble factors that provide host resistance to non-self or altered/missing-self [1]. The immune system has been broadly divided into two arms - innate and adaptive - based on the specificity, type and rapidity of the response, [2].

Monocytes/macrophages, dendritic cells (DC), neutrophils, natural killer cells (NK cells), mast cells, eosinophils and basophils comprise the cellular elements of the innate immune system that provides the first line of host defense against pathogenic microorganisms. These cells express germline-encoded receptors, so called pattern recognition receptors (PRR), specialized to recognize pathogen and danger-associated molecules and to discriminate between self, altered-self and non-self [3]. PRR include several receptor families: AIM2-like receptors (ALR), C-type lectin receptors (CLR), nucleotide-binding oligomerization domain (Nod)-, leucine-rich repeat-containing receptors (NLR), RIG-I-like receptors Toll-like receptors (TLR) and cytosolic DNA sensors, all of which are primarily classified based on structural similarities and target molecule specificity [4-6]. PRR recognize common microbial pathogen/danger-associated molecular patterns (PAMPs or DAMPs) including nucleic acids (double- or single-stranded DNA and RNA) protein components, lipids, lipoproteins, glycolipids and polysaccharides expressed by bacteria, viruses, fungi and parasites and to a lesser extent the cellular contents of dying host cells [3, 4, 7, 8]. Detection of PAMPs or DAMPs initiates an inflammatory response that involves pathogen killing, elimination of debris via phagocytosis, release of pro-inflammatory mediators, and the recruitment/activation of innate and/or adaptive immune cells [9]. This process is followed by a resolution phase which involves different set of mediators and cells specialized to restore the homeostasis [10].

The adaptive immune system, also known as the acquired immune system, is the second arm of immune defense. T cells and B cells belong to this arm, mount pathogen-specific immune responses, and confer long-lasting protection against the same pathogen [2]. The type of response generated by these cell types is different. T cells are important for cell-mediated immunity, whereas B cells secrete antibodies as part of the humoral immune response [11].

Activation of both T and B cells is regulated by cellular interactions and factors released by the innate immune cells [12].

## 1.2 Myeloid Cells

### 1.2.1 Monocytes

Monocytes are elements of the mononuclear phagocytose system (MPS) which also includes macrophages and dendritic cells. These cells help maintain immune homeostasis and support the induction of immunity through their ability to phagocytose a large spectrum of particles [13]. Monocytes originate from myeloid precursors in the bone marrow or fetal liver from which they are released into the systemic circulation [14, 15]. Colony stimulating factors (CSFs) regulate the generation of monocytes and their maturation into tissue-resident macrophages. Severe monocytopenia develops in mice deficient in M-CSF or the M-CSF receptor CSF-1R [16, 17]. Conversely, i.v. injection of M-CSF for several days enhances the frequency of peripheral monocytes by 10-fold [18].

Monocytes constitute 5-10% of human and 2-5% of mice circulating leukocytes. Most of these monocytes survive for only 2-3 days. Yet microbial products, pro-inflammatory mediators and growth factors can trigger monocytes to migrate into tissues where they replenish tissue-resident macrophages and/or give rise to DC and inflammatory macrophages [19, 20].

Human monocytes are broadly categorized in three subclasses depending on their expression of CD14 (co-receptor for TLR4) and CD16 (FcγRIII). Classical monocytes represent the largest subset (85%) and have a $CD14^{high}CD16^{low}$ expression profile. Non-classical monocytes represent 10% of the population and are $CD14^{dim}CD16^{high}$. The remaining 5% are composed of intermediate monocytes that are $CD14^{high}CD16^{med}$ [21, 22]. These subsets express different levels of HLA-DR, which can be used to discriminate the CD16 expressing subset from NK cells [23]. These chemokine receptors similarly define monocyte subsets in mice. The classical monocyte population is $CD11b^{high}Ly6C^{high}CCR2^{high}$ while the non-classical and intermediate monocytes are represented by $Ly6C^{low}$ and $CX3CR1^{high}$ cells, respectively [24, 25].

Transcriptome profiling of monocytes shows that intermediate and non-classical monocytes are closely related and might have a developmental relationship [26]. Although the *in vivo* roles of the monocyte subsets are not well defined, several behavioral and functional differences have been noted. CCR2 is expressed by classical monocytes, aiding their recruitment to sites of infection/inflammation by CCL2 (MCP-1) and CCL7 (MCP-3), where they differentiate into phagocytes [27-29]. In contrast, trafficking of non-classical monocytes is regulated through

CX3CR1 [30]. Unlike classical monocytes, intermediate and non-classical monocytes engage in patrolling behavior by circulating through vessels and entering uninflamed tissues [31, 32].

### 1.2.2 Macrophages

Inflammation occurs when the host responds to infection or tissue damage [33]. This response includes the maturation of monocytes into macrophages that play a critical role in limiting the infection and subsequently resolving the inflammation [34]. Macrophages also contribute to the regulation of metabolism, wound healing, organogenesis and tissue remodeling [35, 36]. Based on differences in function, macrophages are broadly categorized into two sub-groups: M1 and M2 (in humans M1-like and M2-like macrophages). This nomenclature is linked to the Th1-Th2 paradigm, which reflects the activation status of functionally distinct types of T cells [37]. When stimulated by bacteria or viruses, macrophages undergo "classical" activation towards and M1 phenotype [37, 38]. In contrast, parasitic infections and allergens trigger "alternative" activation into M2 macrophages. These help downregulate the immune response during the resolution phase of inflammation and promote tissue remodeling and repair [34, 39].

#### 1.2.2.1 M1 Macrophages

M1 macrophages are primarily activated by bacterial or viral products that are recognized by PRRs in particular TLRs [7]. Following recognition of PAMPs or endogenous danger molecules these receptors initiate a highly conserved signaling cascade to generate an immune response that involves the release of pro-inflammatory mediators, pathogen killing and attraction of cytotoxic T lymphocytes [40, 41]. Each TLR has evolved to recognize a different set of ligands and their specificity is influenced by the subcellular localization of the receptors [42]. A list of well characterized TLRs expressed by monocytes is provided in **Error! Not a valid bookmark self-reference.**. More recently TLR10, TLR11, TLR12 and TLR13 were identified [43].

**Table 1.1: Ligands of TLR**

| Receptor | Ligand | Origin | Subcellular Localization |
|---|---|---|---|
| TLR2/1 | Triacetylated lipoprotein | Mycobacteria | Plasma membrane |

| Receptor | Ligand | Origin | Subcellular Localization |
|---|---|---|---|
| TLR2 | Lipoprotein, peptidoglycan, glycolipid, lipoteichoic acid, zymosan, heat-shock protein | Bacteria, Mycobacteria, Fungi, Host | Plasma membrane |
| TLR2/6 | Diacetylated lipoprotein, zymosan | *Mycoplasma*, gram-positive bacteria, fungi | Plasma membrane |
| TLR3 | Double-stranded RNA | Viruses | Endolysosome |
| TLR4 | Lipopolysaccharide, heat-shock protein | Gram-negative bacteria, Host | Plasma membrane |
| TLR5 | Flagellin | Bacteria | Plasma membrane |
| TLR7/8 | Single-stranded RNA | Viruses | Endolysosome |
| TLR9 | Unmethylated CpG ODN | Bacterial DNA | Endolysosome |

*Modified from Akira and Takeda [44]* .

Several studies indicate that the M1 macrophages generated by TLR signaling (tested with LPS) do not exhibit a full pro-inflammatory response and that co-stimulation with IFNγ might be required for complete activity. This conclusion is based on experiments examining the expression pattern of IL-12 which is an important cytokine that regulates early events in the anti-microbial response and activates NK cells and CTL [45]. IL-12 is a heterodimer formed by p35 and p40 subunits expressed from different promoters [46]. Although constitutively expressed at low levels, expression of the p35 subunit is augmented with stimulation with IFNγ [47, 48]. In contrast, p40 subunit expression is induced by LPS and levels are increased further with IFNγ [47, 49]. Thus, IFNγ primes monocytes to more efficiently produce IL-12 in response

to TLR agonists. Macrophage polarization and function is regulated by a combination of transcription factors. NF-κB and AP-1 are up-regulated through the TLR signaling pathway [50]. For M1 macrophages, STAT1 and interferon regulator factors (IRF) are crucial for the expression of pro-inflammatory mediators [51, 52].

The anti-microbial function of M1 macrophages has two arms. These cells can directly kill pathogens by producing nitric oxide (NO) and reactive oxygen intermediates (ROI) [53]. In addition, they generate a Th1 biased immune response characterized by the release of factors that activate and recruit other cells. Polarization of the type I T cell response is mediated by production of pro-inflammatory molecules and expression of the co-stimulatory molecules CD80 and CD86 along with MHC Class II to present antigens to T cells [54]. These mediators include are IL-1β, IL-6, IL-12, IFNγ and TNFα, which are required for activation of Th1 immune responses [55-58]. Moreover, secretion of chemoattractants (such as CCL15, CCL20, CXCL9, CXCL10, CXCL11 and CXCL13) drives recruitment of NK and Th1 T cells at the site of infection [39, 59].

Unrestrained activation of M1 macrophages has been linked to the pathogenesis of chronic inflammatory conditions and autoimmune diseases [60]. Chronic inflammation and infection can increase cancer incidence [61, 62]. For example, patinets with Crohn's disease and other inflammatory bowel abnormalities have an increased prevalence of colorectal cancer [63]. Approximately 25% of cirrhotic patients develop hepatocellular carcinoma within 12 years [64]. Hepatitis B and *Helicobacter pylori* are linked to liver and stomach cancers, respectively [65]. Mechanistically, there is a relationship in which pro-inflammatory macrophages produce reactive oxygen species that can induce spontaneous cancer driving mutations in surrounding cells [66]. Furthermore, unresolved inflammation drives stromal cell accumulation and activation which creates a pro-tumorigenic niche [67]. Elevated TNFα or IL-12 levels have been linked to development and progression of inflammatory and autoimmune diseases including ankylosing spondylitis, Crohn's disease, multiple sclerosis, psoriasis, rheumatoid arthiritis, Sjögren's syndrome and ulcerative colitis [68-74].

Considering the role of macrophages in different disease and conditions, therapeutic strategies were developed in preclinical and clinical setting to target maturation, migration and effector functions of the macrophages [75]. Monoclonal antibodies against TNFα, IL-1 or IL-12 family are the mostly studied treatment applications for autoimmune diseases [76, 77]. Due to side effects of these systemic therapies, new approaches were investigated to increase the specificity of the antibodies. In murine model of LPS/D-Galactosamine-induced hepatotoxicity, anti-TNFα antibody conjugated to anti-F4/80 antibody was tested to increase targeting of active macrophages. Targeted TNFα antibody significantly more effective than untargeted antibody

and completely abolished the serum TNFα levels [78]. Still, human trials with monoclonal antibody against TNFα infliximab were unsuccessful, exacerbating the symptoms [79]. These results suggest that alternative treatment options are required.

#### 1.2.2.2 M2 Macrophages

The designation M2 encompasses a heterogeneous population of immunomodulatory macrophages. Three main sub-groups have been defined based on the polarizing stimuli (IL-4, IL-13, immunoglobulin complexes, IL-10 and glucocorticoids). These have somewhat different phenotypes and primary functions. However it is unclear whether these subgroups are distinct or whether they represent different parts of a shared spectrum of activation [80].

IL-4 and IL-13 produced by mast cells, Th2 cells, eosinophils, basophils or macrophages during parasite infection or allergen exposure are the main drivers of "M2a" type macrophages [81]. In conditions of tissue damage and helminthic infection, IL-4 induces the expansion of tissue-resident macrophages and the recruit of additional macrophages from distinct sites [82-84]. IL-4 and IFNγ work in an antagonistic manner to regulate expression of markers and macrophage function. FIZZ1, Ym1, macrophage mannose receptor (MMR, CD206), C-type lectin receptor DC-SIGN (CD209), scavenger receptors SR-A (CD204) and CD163, are markers of M2 macrophages and are significantly enhanced in macrophages following IL-4 and/or IL-13 but not IFNγ stimulation [85-90]. Their expression is regulated by the cooperation of transcription factors STAT6 and KLF4, which are activated by IL-4R and IL-13R-mediated signaling cascades [91-93]. Stimulation of peritoneal macrophages with IL-4 or IL-13 also up-regulates MHC Class II, although the level of expression was modest when compared to IFNγ-treated macrophages [87, 94]. In addition to surface marker expression, IL-4 and IL-13 regulate the cytokine profile of macrophages, most notably by blocking LPS-induced IL-1β, IL-10, IL-12 and TNFα production from monocytes [95-98]. Instead, IL-4 stimulation induces the production of anti-inflammatory cytokines such as TGF-β, IL-10, CCL18 (AMAC-1) and IL-1Ra [96, 99, 100]. Unlike IFNγ and LPS stimulated murine BMDM, which produce iNOS, IL-4 and IL-13, IL-4 treatment favors expression of arginase [101]. The most important difference between M1 and M2 macrophages is their functional activity. M2a macrophages have impaired killing function, associated with a lack of superoxide production [102]. Rather, macrophages activated by a combination of IL-4 plus glucocorticoids secrete growth factors which promote the proliferation of epithelial cells *in vitro* [100]. These macrophages also have pro-fibrotic function and produce TGFβ and PDGF to modulate collagen formation [103]. Thus, M2a macrophages have pro-angiogenic and remodeling capacity like tissue-resident macrophages [34]. Of note, the primary role of macrophages generated by IL-4 or IL-13 is to mediate Th2 type immune responses [83]. Alternatively activated macrophages are generated in response to parasites

including protozoa, fungi and helmiths, such as *Trypanosoma cruzi*, *Heligmosomoides polygyru* and *Nippostrongylus brasiliensis* to eliminate parasites and generate Th2 memory $CD4^+$ T cells [83, 104, 105]. Although their roles are slightly different both IL-4 and IL-13 are required for a anti-parasite response [106].

Uncontrolled alternatively activated macrophage have been linked to recurrent infections and asthma. *Francisella tularensis* is an intracellular bacterium that causes tulameria. Although initial recognition of the bacteria triggers pro-inflammatory macrophages, at later stages this pathogen restrains classical activation and triggers an alternative macrophage response characterized by IL-4 and IL-13 production. This mechanism enables immune escape of the bacteria [107]. A similar response is induced by *Mycobacterium tuberculosis* and *Leishmania major* [108, 109]. IL-4 and IL-13 levels as well as M2 macrophage frequency are elevated in patients with asthma and allergen-induced asthma in animal models [110-113]. In this setting targeting M2 macrophages or reducing IL-13 provides protection [114, 115]. A phase II clinical trial demonstrated that administration of recombinant IL-4 variant that recognizes IL-4Rα subunit ameliorates asthma symptoms [116].

TLR desensitization is a negative feedback loop that protects the host from a dysregulated TLR response. This mechanism includes the release of receptor antagonists and expression of genes that downregulate various components of the TLR signaling pathway [117]. One such desensitization mechanism includes the promotion of "M2b" macrophages. Analysis of gene regulatory networks of LPS tolerant murine BMDM indicate that there are two distinct sets of genes that are differentially regulated by TLR4. The first genes activated after LPS exposure mainly contains pro-inflammatory mediators. Repeated LPS exposure generates tolerant macrophages that upregulate a second set of genes specifically involved in pathogen recognition and clearance but not in pro-inflammatory responses. p38 MAPK signaling was important for the regulation of both sets of genes [118]. In this context, desensitized macrophages expressed higher levels of the p50 subunit of the NF-κB complex. Homodimerization of p50 impairs p65/p50-dependent signaling events such as the production of IFNβ and phosphorylation of STAT1 [119]. These studies suggest that prolonged exposure to LPS can generate tolerant macrophages by altering the gene signature. However several other groups concluded that treatment with LPS alone was not sufficient to drive polarization of immunoregulatory macrophages and additional signaling through the FcγRI or complement receptor was required [120-123]. For example, ligation of the immunoglobulin complex (IgG) with FcγRI on BMDM reversed the pro-inflammatory response by blocking LPS-dependent transcription of IL-12 while enhancing IL-10 production [121, 124]. This change in macrophage phenotype affected the T cell response: stimulation of T cells with antigens in the presence of FcγRI-ligated macrophages resulted in high IL-4 and low IFNγ whereas in the absence of macrophages high

IFNγ secreting Th1 cells arose [125, 126]. The *in vivo* implication of this interaction was tested in an LPS-induced endotoxin shock model, in which FcγR-ligated macrophages were adoptively transferred into mice injected with a lethal dose of LPS. Mice receiving ligated macrophages were protected against this lethal challenge in a response that involved the up-regulation of IL-10 [127]. The effect of complement engagement was slightly dissimilar as C5a or anti-C3R antibodies interfered with IL-12 production by IFNγ-primed, LPS-treated human and mouse macrophages but did not influence IL-10 secretion [122, 123]. Neither FcγR nor complement activation reduced TNFα production suggesting that these macrophages are different from M2a macrophages in their immunosuppressive capacity [120, 122]. Transcriptome analysis demonstrated that M2b macrophages uniquely secreted CCL1 to attract Treg and eosinophils, which express CCR8 [128-130]. Functional and phenotypical comparisons revealed that this subset of macrophage more closely resemble M1 than M2a macrophages, the only difference being reduced IL-12 and elevated IL-10 levels [54]. Similar to M2a macrophages, M2b macrophages increase susceptibility in leishmaniasis [131].

"M2c" macrophages are a heterogeneous population defined by the stimulus used to induce them: IL-10, glucocorticoids (GC) or TGFβ [132]. IL-10 induced macrophage are considered to be deactivated [133]. IL-10 treatment prevents the production of pro-inflammatory mediators such as NO, TNFα, IL-12, IL-1β and IFNγ, and interferes with macrophage function such as oxidative burst and cytotoxicity [133-135]. Similarly, TGFβ antagonizes the production of TNFα, IL-1β and IL-18 [136]. GC induces anti-inflammatory macrophages by elevating IL-10, IL-1RII decoy receptor and CD163 expression [137]. Unlike IL-4/IL-13, IL-10 interferes with the antigen presenting capacity of macrophages by reducing the expression of MHC Class II [138]. IL-10 macrophages primarily rely on phophorylation of STAT3 [139]. Studies using IL-10 KO mice established that macrophages generated by IL-10 enhance susceptibility to intracellular infections *(L. major*, *L. monocytogenes, C. trachomatis*, *M. bovis* bacille Calmette-Guérin (BCG)) due to reduced pro-inflammatory mediator production, such as IL-6, IL-12, TNFα, NO, prostaglandins [140-144]. Still these macrophages play a protective role in reducing pathogenic immune responses with colonic macrophages generated by exposure to IL-10 helping to suppress the response against gut flora [145].

The categories M2a, M2b and M2c do not include the full spectrum of M2 macrophages such as tumor-associated macrophages (TAMs) that are generated by combinations of various polarizing agents. It is also debatable whether tissue-resident macrophages generated by M-CSF, which share a resemblance to M2 macrophages should be categorized separately [146]. These subsets of M2 macrophages are discussed under different topics. Due to the enormous heterogeneity and ongoing debates about M2 subsets, a consortium of scientists has

recommended that the stimulant(s) used to generate monocytes and macrophages should be clearly described when reporting results [147].

#### 1.2.2.3 Macrophages Generated by M-CSF and GM-CSF

Tissue-resident macrophages include Kupffer cells, splenic and alveolar macrophages, histiocytes and microglia [148]. While these cells are heterogeneous and have specialized functions associated with their anatomic location, they share the same primary role of clearing cellular debris and apoptotic/necrotic cells [149].

Experiments in mouse models indicate that tissue-resident macrophages originate from hematopoietic organs prior to birth as well as blood monocytes and can proliferate to replenish their numbers under homeostatic conditions or following an inflammatory response [150-155]. M-CSF is responsible for maintaining microglia and osteoclasts whereas GM-CSF is critical for the generation of alveolar and peritoneal macrophages [156]. M-CSF binds to the c-fms receptor (also known as CSF-1R or CD115) expressed on myeloid cells [157].

Treating mice repeatedly with anti-M-CSF Ab resulted in a depletion of tissue-resident macrophages particularly in the liver, gut, kidney and testis whereas thioglycollate-elicited peritoneal and LPS-driven lung inflammatory macrophages were unaffected [158]. One of the properties of tissue-resident macrophages is believed to involve maintaining organogenesis by regulating the tissue microenvironment. In line with this hypothesis, M-CSF or CSF-1R KO mice exhibit defects in osteopetrosis and were infertile [16, 159]. Conversely, daily injection of recombinant M-CSF conjugated to Fc increased the absolute number of osteoclasts in the epiphyseal plate by 2.5-fold and significantly increased the frequency of testicular macrophages [160]. Another property of these cells is to trigger tissue regeneration following injury. This function was tested in a dextran sodium sulfate-induced colitis model. The proliferation of epithelial cells was impaired in M-CSF deficient mice, suggesting that regenerating colonic epithelium from progenitors required the presence of macrophage [161].

For these reasons, culturing with M-CSF and GM-CSF was established as the standard protocol for inducing the maturation of murine bone marrow and human peripheral blood monocytes into macrophages *in vitro*. Such cells can then be further stimulated with TLR agonists, cytokines and soluble factors to induce differentiation into M1 and M2 subsets [147]. In this context, macrophages generated in the presence of CSFs exhibit characteristics of both M1 and M2 macrophages that differ in transcriptome profile. Analysis of murine BMDM revealed that macrophages generated with GM-CSF can stimulate T cells 30-fold more effective than those produced by M-CSF. Consistent with pro-inflammatory properties, GM-CSF macrophages expressed 60-fold higher levels of TNFα when compared to M-CSF macrophages, which

primarily produced IL-10 and CCL2. Additional differences were observed after LPS stimulation. GM-CSF but not M-CSF generated macrophages up-regulated IL-12 in response to LPS [162]. Culturing human $CD14^+$ monocytes with GM-CSF for 6 days resulted in a IL-12 producing macrophages with the ability to present antigens to T cells. In contrast, macrophages generated in the presence of M-CSF secreted high levels of IL-10 and failed to activate Th1 cells [55]. Gene expression analysis of human monocytes stimulated with M-CSF showed that further activation with IL-4 did not significantly alter the gene expression pattern [163]. These results suggest that the default polarization pathway of monocytes under physiological conditions could be M2-like and that M-CSF-driven macrophages should be categorized as M2 macrophages.

#### 1.2.2.4 Tumor-associated Macrophages

M2 macrophages can contribute during the latter stages of cancer progression [132]. Tumor-associated macrophages (TAM) originate from bone marrow-derived monocytes that are recruited to tumor sites by the chemoattractants CCL2, VEGF and M-CSF produced by tumor cells [164-167]. The activation state of these macrophages is heterogeneous as determined by local stimuli [168, 169]. During the late stages of the tumorigenesis, TAM are characterized by an inability to produce IL-12 or NO due to altered classical NF-κB signaling [170-172]. Instead, they secrete very low levels of TNFα, high levels of IL-6, and the anti-inflammatory cytokines IL-10 and TGF-β which inhibit cytotoxic T cell activation, induce generation/recruitment of Tregs, and support tumor cell survival [37, 39, 170, 173, 174]. Furthermore, TAM release pro-angiogenic factors and growth hormones (particularly VEGF and MMP-9) to promote vascular development and regulate the proliferation of tumor cells [175-177]. Enzymes (including metalloproteases, plasmin and cathepsins) produced by TAM are essential for remodeling of extracellular matrix, and activity that triggers migration of tumor cells to distant sites [178-180]. Thus, TAM collectively protect established tumors by enabling their escape from immune recognition, supporting angiogenesis, tumor growth and metastasis [181]. These macrophages are phenotypically characterized by high levels of CD68 and CD163 expression [182, 183]. TAM have been detected in the solid tumors of patients with breast, pancreatic, and non-small cell lung cancer, endometrial and ovarian carcinoma, colon adenocarcinoma, and the lymph nodes of patients with Hodgkin's or angioimmunoblastic T cell lymphoma [182-189]. Several studies demonstrated a correlation between high numbers of TAM and poor disease outcome in breast cancer, melanoma, lymphoma and pancreatic cancer [185, 189-192]. For these reasons, efforts have concentrated on understanding the mechanisms by which TAM are generated and in developing approaches to target them therapeutically.

Following identification of TAM, therapeutic approaches to prevent the recruitment and action of these cells were recently tested [178]. Most of these strategies focuses on preventing TAM infiltration [193]. Among multiple soluble targets, M-CSF is the one studied extensively. High M-CSF is detected in the microenvironment many types of cancer and linked to poor prognosis [181, 194]. Indeed, M-CSF was shown to support both accumulation and maintenance of TAM in the tumor microenvironment [167, 195, 196]. The importance of M-CSF was tested in several pre-clinical setting using monoclonal antibodies, kinase inhibitors and antisense oligonucleotides [197, 198]. Systemic treatment of breast cancers with tyrosine kinase inhibitor PLX3397, which block CSF-1R signaling, depleted >70% of the TAM and decreased the metastatic rate >85%. This reduction in TAM frequency associated with improved response to chemotherapeutic agent PTX as measured by the degree of tumor shrinkage and enhanced cytotoxic T cell influx [196]. Daily oral delivery of another CSF-1R inhibitor JNJ-28312141 also significantly reduced the tumor growth. Injection of siRNA against M-CSF significantly reduced the growth rate of neuroblastoma cells prolonging the survival period [199]. Limited evidence indicates that these preclinical findings can be translated into human. One such example is diffuse-type giant cell tumor (Dt-GCT), in which chromosal translocation is leads to overproduction of M-CSF [200]. In patients with Dt-GCT (n=7), a phase I trial with anti-CSF-1R antibody named RG7155 reduced the percentage of TAMs in tumor biopsies and resulted in significant symptomatic improvement [201]. Similarly anti-CCL2 antibodies were tested in patient with various cancers either alone or in combination with conventional chemotherapy in phase I and phase II studies [202-204]. Based on clinical criteria, all these studies observed better outcome. Yet, they have not checked for the changes in the TAM percentages in the tumor microenvironment. However, more recent studies indicated that interrupted anti-CCL2 may associate with increased metastasis due to enhanced angiogenesis [205]. Another approach is to reeducate TAM towards anti-tumoricidal phenotype. IFNγ and anti-CD40 agonist antibody was tested for this purpose [206, 207]. In mouse models of pancreas cancer, administration of CD40 agonist resulted in up-regulation of CD86 and MHC Class II indicating that TAM acquire M1 macrophage properties [208]. A phase I clinical trial combining CD40 agonist with gemcatibine in patients with pancreatic adenocarcinoma (n=21) detected an increase in serum cytokine levels of IL-6, IL-8 and IL-10; and reduced tumor mass [209]. TLR receptors a

### 1.2.3 Myeloid Derived Suppressor Cells

Myeloid-derived suppressor cells (MDSCs) are a heterogenous population of immature myeloid cells that arise in the bone marrow. Under normal physiological conditions, these cells rapidly differentiate into macrophages, DCs or neutrophils [210, 211]. C/EBPβ, HIF-1α and STAT3 maintain the MDSC survival and activity [212-218]. In certain disease and inflammatory states MDSCs can proliferate and migrate into affected tissues where they suppress ongoing immunity [219-221]. Several studies found that the differentiation of MDSC into antigen-presenting cells is abrogated under these conditions [210, 217, 222]. There are two major types of MDSC: monocytic (mMDSC) and granulocytic (gMDSC, also known by polymorphonuclear MDSC) (Figure 1.1).

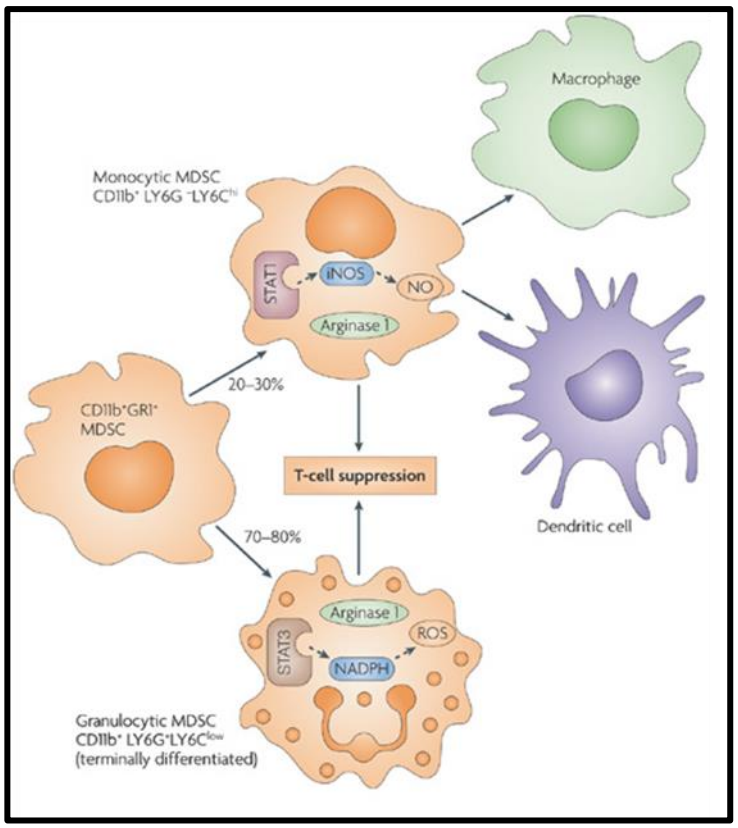


**Figure 1.1: Subsets of myeloid-derived suppressor cells**

*Monocytic and granulocytic are the two main sub-types of MDSC. These cells differ in their frequency, marker expression, suppressive mechanism and capacity to mature into macrophages. Adapted from Gabrilovich and Nagaraj [210].*

These subsets differ in their expression of markers, mechanism by which they exert suppressive activity, and biological function [210]. Murine MDSCs are CD11b positive cells defined by the differential expression of granulocyte receptor-1 (Gr-1), which consists of two epitopes Ly6C and Ly6G. mMDSC have high levels of Ly6C and low levels of Ly6G while the gMDSC are

Ly6G high and Ly6C low [223]. gMDSC constitute 70-80% of the total MDSC population with the remaining being mMDSC [223, 224]. In humans, MDSCs are characterized by the expression of the myeloid cell markers CD11b and CD33 and by lack of lineage specific markers (CD3/CD19/CD56) and MHC Class II (HL-DR) [210, 220]. Discrimination between subgroups is mainly accomplished based on their expression of CD14 and CD15. Cells expressing high levels of CD15 but negative for CD14 are gMDSC [225-228] while $CD14^{high}HLA\text{-}DR^{low/-}$ cells are mMDSC [229-235].

#### 1.2.3.1 MDSC under disease conditions

MDSC frequency is enhanced in many diseases including cancer, sepsis, allergy, traumatic stress, infection and autoimmunity. In healthy individuals MDSC constitute <0.5% of the total PBMC, while the percentage of MDSC in the peripheral blood can increase up to 10-fold in patients with HNSCC, multiple myeloma, non-Hodgkin's lymphoma, prostate, renal, thyroid, bladder, pancreatic, breast, colorectal, esophageal, gastrointestinal, hepatocellular and non-small cell lung carcinoma, [225, 226, 229, 231-253]. In patients with renal cell carcinoma, the increase in the gMDSC population (almost 25-fold) was more profound than in the mMDSC population (7-8-fold) and a direct correlation between the absolute number and percentage of circulatory mMDSC with clinical stage was detected [241, 254]. MDSC constitute 1-15% of the total tumor mass in a number of different cancers [236, 237]. Several murine models yielded the same observations. The accumulation of MDSC in the tumor microenvironment correlated with enhanced growth, angiogenesis, and metastasis [236, 241, 255-257].

It is also noteworthy that MDSCs can dampen immunological responses against parasitic, bacterial and viral infections and interfere with the efficacy of vaccines. A number of studies reported that MDSC expand in patients with toxoplasmosis or trypanosomiasis [258, 259]. By suppressing T cell activation, MDSC reduce responsiveness against these parasites [260]. Exposure to vaccinia or influenza A virus can also trigger the accumulation of MDSC at the site of infection [261, 262]. Although the frequency of hepatic MDSCs in HBV-infected mice was twice as the frequency in uninfected mice [263], no correlation between the frequency of mMDSC and the stage of hepatitis B/C virus infection was found in humans [234]. In this context, human myeloid cells co-cultured with HCV-infected hepatocytes acquired the ability to suppress T and NK cells by up-regulating ARG1 and ROS, suggesting a potential link between the HCV infection and MDSC generation [264, 265]. Both mMDSC and gMDSC frequencies are significantly increased in patients with human immunodeficiency virus type 1 (HIV-1) [266, 267]. *In vitro* findings demonstrate that the HIV-1 transactivator protein and gp120 are directly responsible for the expansion of mMDSC by 2-3-fold [266, 268]. This increase in MDSC inhibits HIV-specific $CD8^+$ T cell responses such that MDSC accumulation positively correlates

with viral load and disease progression [266, 267]. In line with these finding, vaccination of macaques against Simian immunodeficiency virus (SIV) resulted in a 2-fold increase in the MDSC frequency [269]. Priming mice with Complete Freud's Adjuvant (CFA) containing heat-killed *Mycobacteria* triggered expansion of splenic gMDSC by 10-fold over the course of 10 days [270, 271]. Similarly, vaccination with *Mycobacterium bovis* bacillus Calmette-Guérin (BCG) led to accumulation of mMDSC at the site of injection [272]. For these reasons, MDSC are considered a targetable population that can be manipulated to boost immunity.

Studies using murine models support the observation that MDSC frequencies change as a function of disease state and inflammation. In a murine model of polymicrobial sepsis, splenic MDSC numbers increased by 50-fold [273]. Traumatic stress was examined in mice by performing midline incision under anesthesia. 12 hours after surgery, the number of splenic MDSCs was increased by 6-fold and remained at high levels for >3 days [274]. It should be recognized that increasing MDSC frequency can be beneficial in certain disease states. For example in murine models of experimental autoimmune encephalomyelitis (EAE) and inflammatory bowel disease (IBD), MDSC were expanded in the spleen and blood and served to inhibit autoreactive T cells and reduce disease burden [221, 275]. Adoptive transfer of MDSC attenuated the symptoms of EAE, IBD, uveitis and rheumatoid arthritis [276-280]. Similarly, following transplantation, MDSC percentages were enhanced to suppress alloreactive T cells and induce generation of Tregs [281, 282]. In a murine model of graft-versus-host disease, adoptive transfer MDSCs significantly increased the number of surviving mice [283].

#### 1.2.3.2 MDSC-Mediated Immune Suppression

The primary function of an MDSC is to suppress cytotoxic $CD8^+$ T and NK cell responses [222, 284]. This role is of particular relevance in the tumor microenvironment where MDSC down-regulate anti-tumor immunity via several mechanisms [285]. MDSC interfere with activation of T cells by altering availability of amino acids. L-Arg is a nonessential amino acid important to immune metabolism [286]. L-Arg starvation of T cells triggers cell-cycle arrest at the $G_o$-$G_1$ phase by preventing up-regulation of cyclinD3 and Cdk4 [287]. Additionally, depletion of L-Arg downregulates (by approximately 3-fold) the expression of the T cell receptor ζ chain, which is crucial for the formation of the T cell antigen receptor [288, 289]. L-Arg is metabolized into L-ornithine and urea by arginase (ARG1) or into citrulline by inducible nitric oxide synthase (iNOS) [286]. In line with these observations both enzymes are highly but differentially expressed by tumor-infiltrating MDSC [288, 290, 291]. The inhibitory activity of mMDSC is mediated by iNOS expression, whereas gMDSC has higher levels of ARG1 [223, 251, 292]. MDSC also deplete L-Arg by internalization through the cationic amino-acid transporter 2B [293, 294]. Expression of iNOS supports the production of nitric oxide (NO) by

MDSC. NO suppresses effector T cell proliferation by interfering with the downstream of IL-2R signaling pathway [291].

T cells also depend on exogenous cystine for proliferation and protein synthesis. Cystine is generated by joining two molecules of cysteine, a function performed by macrophages and DC [295, 296]. MDSCs complete with macrophages and DC for the uptake of cysteine, thereby reducing the availability of cystine to T cells [297]. Another mechanism of MDSC-dependent suppression involves the generation of reactive oxygen species (ROS). gMDSC are the main source of ROS and produce 3-fold more ROS per cell than mMDSC [224, 270]. Constitutive STAT3 signaling results in up-regulation of NADPH oxidase subunits, which generates superoxide [298]. Superoxide spontaneously reacts with a variety of molecules to induce ROS including $H_2O_2$ and hydroxyl radicals. $H_2O_2$ contributes to the maintenance of MDSC and at the same time suppresses the activity of cytotoxic T cells [299, 300]. Superoxide produced by gMDSC also reacts with NO secreted by mMDSC and forms peroxynitrite (PNT) [292]. By preventing formation MHC Class I-tumor peptide complex, PNT protects tumor cells from recognition by cytotoxic T cells [301]. Finally, MDSCs can inhibit the migration of $CD4^+$ and $CD8^+$ T cells by expressing ADAM17; an enzyme that cleaves L-selectin on the T cells [302-304].

Suppression of NK cells is mediated by production of TGF-β and/or contact inhibition. IL-2 activated NK cells co-cultured with murine MDSC fail to phosphorylate STAT5, activate the JAK3 pathway, or produce perforin (which is crucial to their cytotoxic activity) [305]. Murine MDSC induce NK cells to down-regulate expression of the activation markers NKG2D, NKp46 and NKp44 and the production of IFNγ *in vitro* and *in vivo* by producing TGF-β1 [306, 307]. TGF-β produced by MDSC also suppresses the activation of human NK cells [235].

Additionally, MDSC support immunosuppressive responses by directing the differentiation of myeloid and T cells into suppressive subpopulations. The only study investigating the interaction between MDSC and myeloid cells revealed that contact-dependent cross-talk between MDSCs and tumor infiltrating macrophages drove the latter population towards M2 macrophages by preventing IL-12 secretion [308]. In humans and in murine models, the frequency of Tregs correlated with MDSC levels [254, 309]. MDSC can induce Tregs by three mechanisms. *In vitro* and *in* vivo studies confirm that IL-10 and IL-10-dependent TGF-β production by MDSC can increase the frequency of Tregs by 2-fold by converting non-dividing $CD4^+$ T cells or Th17 cells into Foxp3 expressing Tregs [234, 310, 311]. MDSC also induce expansion of Tregs in a CD40-dependent manner such that CD40-deficient MDSC fail to support Treg expansion [312]. Lastly, ARG1 can double the size of pre-existing Treg

populations [313]. Consistent with these observations, blockade of MDSC accumulation at the tumor site (with c-Kit antibody) reduces the number of Foxp3 cells by 3-fold [309].

#### 1.2.3.3 Response of MDSC to Soluble Factors

The effects of soluble factors on the generation, migration and expansion of murine and human MDSC were evaluated. These factors included cytokines, chemokines, growth factors and other inflammatory mediators secreted by cells under inflammatory conditions and in the tumor microenvironment [314, 315].

GM-CSF secreted from tumors is essential to the expansion of MDSC. Mice inoculated with GM-CSF-producing melanoma clones had 4-fold more MDSCs in the spleen compared to the mice with parental melanoma. Injection of GM-CSF recapitulated this effect [222]. Consistent with this observation, anti-tumor vaccines containing high dose of GM-CSF (more than 300 ng) generated impaired T cell-mediated immune responses due to the enhancement of MDSC in the lymph node (0.8%) and spleen (15%) [316]. *In vitro* experiments provided insight in to the activity of GM-CSF. Twenty-five to fifty percent of unfractionated bone marrow cells from normal or tumor-bearing mice cultured with GM-CSF differentiated into CD11b+GR-1+ MDSC by day 6 [317]. Bone marrow cells incubated with supernatants from Lewis lung carcinoma also supported and 8-fold increase in the proportion of MDSC. Nonetheless, GM-CSF was only partially responsible for this activity since neutralization did not completely abolished this enhancement and GM-CSF alone failed to fully recapitulate the effect of the tumor supernatants. [318]. Stimulation of bone marrow with murine colon carcinoma supernatants triggered a 2.5-fold expansion of MDSC by inducing the phosphorylation of Erk. This effect could be blocked with neutralization antibodies against GM-CSF and replicated by the addition of recombinant GM-CSF to the cultures [212]. GM-CSF improved the viability of splenic MDSC from mice with cervical cancer by> 90% [319]. One report suggests that i.p. administration of GM-CSF confers protection to MDSC against tyrosine-kinase inhibitors by inducing phosphorylated of the STAT5 signaling pathway [320].

Although GM-CSF treatment did not convert MDSCs from naïve mice into DCs or reverse their suppressive potential, it did reduce expression of Gr-1, MHC Class II and C86 suggesting that GM-CSF might be affecting the differentiation state of the cells [284, 319]. In contrast, GM-CSF treatment of MDSC from the spleen of mice with infection or breast cancer induced differentiation of approximately 20% of the cells into DCs and 25% into macrophages [273, 321]. Consistent with the reports from murine models, culturing of human PBMC with GM-CSF supported the survival of MDSC [225, 237]. When CD33 expressing cells were isolated from PBMC cultured with GM-CSF for one week they inhibited the proliferation of T cells by 60% [322]. However, increased expression of CD11c and CD68 coupled with an absence of

ARG1, iNOS or NAPH oxidase levels in these cells suggest that they may not be typical MDSCs [322].

Prostaglandin E2 ($PGE_2$) was identified as an important factor released by MDSC in the tumor microenvironment [323, 324]. Studies in a lung carcinoma model showed that $PGE_2$ was released by tumor cells in a COX-2-dependent manner induced phosphorylation of STAT3 and expression of ARG1 in bone marrow-derived or tumor infiltrating MDSCs [215, 324]. A second study confirmed that $PGE_2$ triggered the *in vitro* differentiation of bone marrow cells into MDSC by binding to E-prostanoid receptors expressed on the myeloid cells. In a model of mammary carcinoma this resulted in a 2-fold increase in the frequency of MDSC in the tumor and circulation [323]. Using human mMDSC isolated from melanoma samples, inhibition of COX-2 reversed T cell suppression [303]. Culturing human monocytes or dendritic cells with $PGE_2$ initiated a $PGE_2$-COX-2 positive feedback loop which drove the cells to differentiate into mMDSC [303, 325]. The frequency of mMDSC in human ovarian cancers correlated positively with $PGE_2$ and CXCL12 (SDF-1) levels in patient ascites [326]. CXCL12 is a chemoattractant that triggers recruitment of different cell types to the tumor microenvironment by interacting with CXCR4 [327]. Tumor infiltrating mMDSC expressed high levels of CXCR4, and inhibition of COX-2 in this environment halved the level of expression of both CXCL12 and CXCR4 [326].

Studies with murine and human cells suggest that vascular endothelial growth factor (VEGF) released by tumor cells might be important for MDSC maintenance. In a murine model of spontaneous breast cancer, serum VEGF levels correlated positively with MDSC frequency in the peripheral blood. The ability of tumor supernatants to induce colony formation by bone marrow cells was reduced 5-fold following neutralization of VEGF [321]. Likewise, the ability of conditioned media from primary head and neck squamous cell carcinoma (HNSCC) to trigger the migration of human MDSC was abolished by anti-VEGF Ab [253]. The number of Gr-1 expressing myeloid cells increased 4-fold in the lymph nodes and 30-fold in the spleen of mice treated for one month with VEGF, consistent with VEGF driving MDSC generation *in vivo* [328]. However, in murine models of thymoma, melanoma and colon carcinoma, neutralization of VEGF did not alter the frequency of tumor associated MDSCs [329]. Similarly, VEGF-Trap did not reduce the number of circulatory MDSC in patients with different kinds of solid refractory cancers (n=15) [240].

IL-1β was also shown to regulate the accumulation and suppressive activity of MDSC in various tumor models. MDSCs were enriched by 4-5-fold in the blood and splenocytes of mice bearing an IL-1β secreting fibrosarcoma [330]. Comparison of an IL-1β producing mammary carcinoma cell line to non-transduced cancer cells indicated that IL-1β accelerated the

accumulation of MDSC in the spleen and tumor by 3-fold [331]. MDSCs generated in the presence of IL-1β produced more ROS and were more effective suppressors of $CD8^+$ T cell proliferation. Similarly, splenic MDSCs generated in the presence of 4T1/IL-1β tumors suppressed NK activation more effectively than MDSC isolated from mice bearing WT 4T1 tumors ($p<0.05$)[306]. This enhanced suppressive environment was associated with faster tumor growth rate, although there was no increase in the tumor burden [306, 330, 331]. Of note, murine MDSC lack IL-1R making it unlikely that these changes were a direct consequence of exposure of MDSCs to IL-1β [331].

IL-6 acts as a downstream mediator of IL-1β. Whereas tumor growth was delayed and MDSC accumulation impaired in IL-1R KO mice, tumor cells that overexpressed IL-6 restored MDSC accumulation (increasing MDSC in the blood by 3-fold). This effect was accompanied by rapid tumor growth [332]. Several findings indicate that IL-6 released by tumor cells or MDSC can have this effect. IL-6 produced by tumorigenic MDSCs induces phosphorylation of STAT3, which supports suppressive activity [212]. Exposure of bone marrow cells to IL-6 plus GM-CSF significantly enhanced MDSC suppressive function [333]. Similarly, human MDSC generated by treating PBMC with a combination of GM-CSF and IL-6 suppressed T cell proliferation significantly more effectively than those generated using GM-CSF alone [322].

Stem cell factor (SCF) can also enhance the accumulation of MDSCs at the tumor site by inducing their generation in the bone marrow. SCF is secreted by colon cancer, breast cancer and melanoma cell lines of human or murine origin. Comparison of the number of tumor-infiltrating MDSC in SCF-expressing colon tumor with SCF-knockdown colon tumor revealed a 2-fold difference [309]. Consistent with these observations mice with mutated c-Kit (receptor for SCF) had 4-fold less MDSC at the site of the colon tumors compared to the wild-type mice [334].

Another regulator of MDSC are the S100A8/A9 proteins which bind to N-glycans receptors. These proteins are secreted by tumor cells and MDSCs and promote the accumulation of the MDSC at the tumor site [335-337]. Treating tumor-bearing mice with glycan specific Ab can reduce MDSC in the circulation by 2-3-fold [251, 335]. STAT3-dependent S100A9 production interferes with the differentiation of bone marrow cells into DCs and facilities ROS production. Consistent with these findings, S100A9 KO mice had significantly smaller tumors and lower percentage of splenic MDSC (3-fold). [336].

Extracellular adenosine, which is generated in the tumor microenvironment under hypoxic conditions, has been linked to tumor immunosurvelliance and MDSC biology [338, 339]. Initial studies indicated that stimulation through the adenosine A2B receptor induced a 2-fold expansion of gMDSC in bone marrow cultures [338]. Consistent with this observation,

pharmacological inhibition of the A2B receptor in the tumor microenvironment or genetic deletion of the A2B receptor reduced the number of tumor-infiltrating gMDSC by >2-fold [338, 340, 341]. While it has not determined that the adenosine A2A receptor is required for MDSC accumulation, it might be required for the suppressive function of MDSC as myeloid specific deletion of A2A receptor significantly reduced the frequency of IL-10 producing mMDSC [342]. Collectively, these results demonstrate that adenosine is an important component of MDSC metabolism in tumor microenvironment.

More recently, High Mobility Group Box Protein 1 (HMGB1) protein was shown to facilitate the survival of MDSC. *In vitro* HMGB1 induces differentiation of bone marrow cells into MDSC. Inhibition of HMGB1 decreases MDSC numbers by 80% [304]. When MDSC are cultured with tumor conditioned media they increase autophagic activity by 3-fold in an HMGB1-dependent manner. Blocking HMGB1 under starvation conditions reduces the viability of MDSC by 85% [343]. Consistent with these observations, neutralization of endogenous HMGB1 reduces the growth rate of tumors and percent of MDSC by up to 4-fold [304].

Whereas conventional monocytes differentiate into pro-inflammatory or immunosuppressive macrophages when exposed to different combinations of cytokines [146], the effect of such cytokines on MDSC and their precursors has not been investigated.

#### 1.2.3.4 Therapeutic strategies for MDSC targeting

Several therapeutic strategies have been considered in an attempt to block MDSC activity in the tumor microenvironment [219, 344]. A list of tested therapeutic agents is provided in Table 1.2.

**Table 1.2: Therapeutic agents for MDSC targeting**

| Therapeutic Agent | Type of Cancer | Effects on MDSC | Reference |
|---|---|---|---|
| 1,25-dihydroxyvitamin D3 | Human HNSCC (n=6) | Decreases the percent of circulatory MDSC in human peripheral blood | [238] |
| 5-Fluorouracil | Murine thymoma, lung carcinoma | Reduces the number of splenic and tumor-localized MDSC (by triggering apoptosis) | [329, 345] |

| Therapeutic Agent | Type of Cancer | Effects on MDSC | Reference |
|---|---|---|---|
| All-*trans*-retinoic acid | Murine mammary adenocarcinoma, sarcoma and colon carcinoma<br>Human renal cell carcinoma (n=18) | Reduces the number of MDSC in spleen, lymph node and bone marrow by inducing differentiation into DC and macrophages (by increasing glutathione synthase)<br>Decreases the percent of circulatory MDSC in human peripheral blood | [239, 319, 346, 347] |
| Amino-biphosphonates | Murine mammary carcinoma | Reduces the number of peripheral blood, tumor infiltrating MDSC (by inhibiting MMP-9, VEGF) | [348] |
| c-Kit antibody | Murine colon carcinoma | Reduces the number of tumor-infiltrating MDSC and their suppressive activity | [309] |
| COX-2 inhibitor | Murine lung carcinoma, mammary carcinoma, glioma | Blocks suppressive activity of MDSC (by reducing ARG1 expression), reduces generation of gMDSC in bone marrows and accumulation at the tumor sites | [323, 324, 349] |
| CXCR2 and CXCR4 antagonists | Murine mammary carcinoma | Reduces the migration of MDSC | [236] |

| Therapeutic Agent | Type of Cancer | Effects on MDSC | Reference |
|---|---|---|---|
| Docetaxel | Murine mammary carcinoma | Reduces the percentage of splenic gMDSC, triggers apoptosis and differentiation of gMDSC (by inhibiting phosphor-STAT3 signaling) | [213] |
| Gemcitabine | Murine thymoma, lung carcinoma, mesothelioma tumors, mammary carcinoma, colon carcinoma | Reduces the quantity of splenic, circulatory and tumor-localized MDSC | [308, 329, 345, 350-352] |
| Nitroaspirin | Murine colon carcinoma | Reduces the number of tumor-infiltrating MDSC<br>Blocks suppressive activity of MDSC (by inhibiting ARG1 and NOS2) | [353] |
| Phosphodiesterase-5 inhibitor | Murine colon carcinoma, mammary adenocarcinoma, fibrosarcoma, melanoma | Abrogates suppressive activity of MDSC (by downregulating ARG1 and NOS2) | [354, 355] |
| PROK2 antibody | Murine models bearing human lung carcinoma, T cell leukemia, colorectal carcinoma, pancreatic adenocarcinoma | Reduces circulatory and tumor infiltrating MDSC | [356] |

| Therapeutic Agent | Type of Cancer | Effects on MDSC | Reference |
|---|---|---|---|
| Sunitinib | Murine melanoma, colon carcinoma, kidney tumors, mammary carcinoma<br>Human renal cell carcinoma patient blood samples (n=26+23), tumor samples (n=37) | Reduces the number of bone marrow-derived, splenic, tumor-infiltrating MDSC<br>(by inhibiting proliferation of mMDSC and triggering apoptosis of gMDSC)<br>Decreases the number of circulatory but not tumor-infiltrating mMDSC and gMDSC | [254, 320, 334, 357, 358] |
| Triterpenoid (CDDO-Me) | Murine thymoma, lung carcinoma, colon carcinoma<br>Human renal cell carcinoma (n=9) | Reduces ROS production from MDSC<br>Abrogates suppressive activity of MDSC | [359] |

*Modified from Najjar and Finke [344].*

Preventing the accumulation and/or function of MDSC within the tumor improved the activity of NK, $CD4^+$ and $CD8^+$ T cells [213, 254, 309, 319, 320, 323, 324, 334, 345, 346, 349-355, 357, 359]. To date, however, none of these interventions resulted in complete remission but rather they delayed tumor growth, extended survival and/or reduced metastases [213, 308, 309, 320, 329, 345, 346, 348-351, 354-357, 359].

#### 1.2.3.4.1 Response of MDSC to TLR Agonists

Our group is interested in whether TLR agonists can be used to regulate MDSC maturation. We found that intratumoral or systemic delivery of the TLR9 agonist CpG ODN significantly slowed the rate of tumor growth in murine models. This effect associated with a CpG mediated decrease in the frequency of tumor infiltrating mMDSC (> 3-fold) [360]. *In vitro* treatment of splenic mMDSC from tumor-bearing mice with CpG ODN reversed their suppressive activity by decreasing iNOS and arginase-1 production and interfering with their ability to inhibit T cell proliferation by inducing the differentiation of the cells into M1 macrophages [360]. Other

showed that treating tumor bearing mice with CpG ODN induced splenic gMDSC to differentiate into macrophages. This was an indirect effect mediated by IFNα secreted by plasmacytoid DCs [361]. Both studies confirmed the role of TLR9 agonists in generating macrophages from MDSC.

Investigation of the other ligands identified the TLR7 agonist imiquimod as a regulator of mMDSC maturation [360]. In an effort to increase the differentiation efficiency of MDSC, ligands targeting TLR9 and TLR7 were combined. Intratumoral delivery of CpG ODN plus the the TLR7/8 agonist 3M-052 reduced the frequency of mMDSC by 90% as opposed to 50% by the each agonist alone [362]. This reduction in mMDSC frequency in the tumor microenvironment was accompanied by an increase in NK cells (25%), $CD8^+$ T cells (5-fold) and change in the inflammatory mediators. IL-12, IFNγ and Granzyme B levels were enhanced, whereas Arg1, Nos2, CTLA-4 and TGFβ levels were reduced. The combination of the TLR agonists effectively eradicated even large established tumors and provided long lasting tumor-specific immunity to 85-90% of mice [362].

The role of the TLR3 signaling pathway in MDSC differentiation is more controversial. Previous results demonstrated that the TLR3 agonist poly(I:C) had no influence on mMDSC but increased the differentiation of splenic gMDSC [360, 361]. More recently, two groups demonstrated that poly(I:C) treatment reduced the tumor growth by half by altering MDSC response and frequency. *In vitro* stimulation of splenic MDSCs ($CD11b^+Gr\text{-}1^+$) of tumor-bearing mice with poly(I:C) confirmed that treatment increased expression of pro-inflammatory surface markers and cytokines such as TNFα and IFNγ [363, 364]. Differentiation of MDSC into macrophages also reversed the suppression of NK cells as observed by an IFNα-dependent change in CD69 levels [364]. These studies demonstrate that targeting TLR3, TLR7 or TLR9 can dampen the immunosuppressive activity of MDSC in murine models. This approach is distinct in its ability to convert MDSCs into tumoricidial macrophages, whereas the majority of the methods listed in Table 1.2 focus on methods of blocking MDSC activity.

However not all TLR agonists have the same effect. TLR4 agonists reportedly support MDSC generation in a MyD88-dependent manner. The role of MyD88 was defined in cecal ligation and puncture model [273]. MDSC expanded in WT by not MyD88KO mice after infection. Delivering a sublethal dose of LPS i.p. similarly stimulated an increase in the percentage of MDSC in spleens [273]. Instilling LPS into the lungs of mice triggered a 50-fold accumulation of gMDSC in a TLR4-MyD88-dependent manner as the effect was not observed in relevant KO strains [365]. These cells produced ARG1 and IL010 that suppressed the activity of Th2 cells in the lungs [365]. Moreover, treatment of MDSC in the peripheral circulation of tumor bearing

mice with LPS and IFNγ induced changes in the TLR4/CD14 pathway that increased IL-10 and decreased IL-12 production by MDSC [366].

Findings involving TLR2 are inconsistent. Incubation of splenic MDSC with tumor supernatants induced a 3-fold increase in IL-6-dependent p-STAT3 levels. This was attributed to activation of TLR2-MyD88 pathway by heat shock protein 72 (Hsp 72) present on tumor-derived exosomes [212]. That conclusion was challenged by another group which demonstrated that tumor derived exosomes vary in their ability to activate the TLR2 pathway, although they confirmed that exosomes could support the generation of MDSC in a MyD88-dependent manner [367, 368]. In a model of DEN-induced hepatic cell carcinoma, hepatocyte derived IL-18 preferentially supported the generation of mMDSC in IL-2 KO mice [369]. Administering the TLR2/1 agonist PAM3 for 7 months reduced tumor growth and prevalence by 3-fold, effects associated with decreased serum IL-18 levels and a 2-fold reduction in mMDSC frequency [369]. Yet in a murine model of atopic dermatitis, *Staphylococcus aureus* infection increased MDSC numbers ($CD11b^{+}Gr\text{-}1^{+}$), and effect mimicked by the TLR2/6 agonists FSL-1 and Pam2Cys but not PAM3 [333]. Cutaneous exposure to Pam2Cys triggered IL-6 production by keratinocytes, which in return promoted expansion of MDSC in the bone marrow and spleen. Although both subtypes of MDSCs migrated to the skin by Day 10, only NO producing mMDSC were responsible for the suppression of T cells [333].

There is limited evidence that mouse MDSCs are predictive of the response of human MDSCs. Phosphorylated STAT3 levels were increase in both mouse and blood-derived human MDSCs in response to Hsp 72 [212]. As mMDSC are more suppressive than gMDSC on per cell basis, our group investigated the TLR response human mMDSC [223, 224, 370]. Consistent with murine findings, human mMDSC (purified from healthy individuals or patients with cancer) responded to culture with the TLR7/8 dual agonist R848 by differentiating primarily into pro-inflammatory macrophages with the ability to lyse tumor cells. The TLR2/1 dual agonist PAM3 had the opposite effect and induced maturation of the human mMDSC into immunosuppressive macrophages that interfered with T cell proliferation [230]. Of importance, some degree of heterogeneity was always observed when human mMDSC were cultured with either one of these agonists.

## 1.3 Extracellular Vesicles

Extracellular vesicles (EV) are biological nanoparticles secreted by prokaryotic and eukaryotic cells. EV are heterogeneous and have been classified based on the size, composition and cellular origin [371]. Three major subpopulations of EV are depicted in **Figure 1.2.**

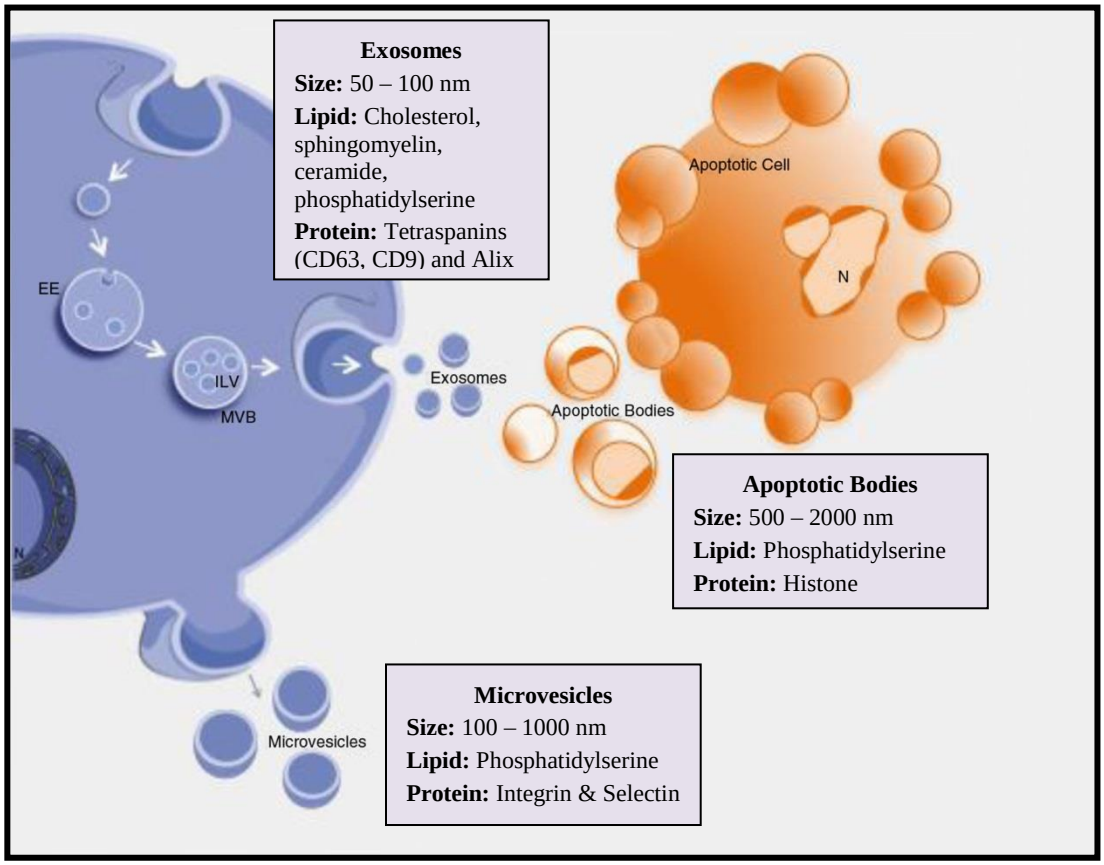


**Figure 1.2: Biogenesis and properties of three main classes of extracellular vesicles.**

*Exosomes are 50-100 nm sized vesicles derive from multi-vesicular bodies. Microvesicles bud from the plasma membrane. Apoptotic bodies are produced as a result of blebbing. EE = early endosome; ILV = intraluminal vesicles; MVB = multi-vesicular body; N =nucleus. Adapted from Yáñez-Mó et al. [371].*

EV serve as intercellular communication vectors that carry information, including nucleic acids, proteins and lipids from the donor cell to the recipient [372, 373]. EV have a number of physiological roles and act in both an autocrine and paracrine fashion to maintain homeostasis. Their roles are directly linked to the cellular origin and the content of the cargo. EV can participate in regulation of angiogenesis, blood coagulation, embryonic development, tissue repair, neuronal communication and reproduction [371, 374]. The roles of EV in the immune system, especially in antigen presentation, are well defined [375, 376]. EV derived from APCs express MHC class I and class II complexes and co-stimulatory molecules. These EV can cross-

present antigens and activate $CD4^+$ and $CD8^+$ T cells [377-381]. This property of DC-derived EV has supported studies investigating the therapeutic potential [382, 383]. On the other hand, the effect of EV changes under pathophysiological conditions. EV released from altered cells can contribute to progression of the diseases, by when EV released by cancer cells suppressing the immune response or cells affected by Alzheimer's or Parkinson's disease spreading the mutated proteins [384, 385]. Of importance, EV can therefore be used as diagnostic biomarkers for cancer, neurodegenerative, cardiovascular, infectious and autoimmune diseases [386-389].

### 1.3.1 Therapeutic Potential of EV

The potential of EV to serve as drug/vaccine delivery vehicles is a topic of considerable interest. EV are similar to synthetic nanoparticles in that both can be loaded externally to carry therapeutic cargos. EV offer the added benefit of being immunologically inert and biocompatible [390, 391]. Techniques including chemical conjugation and physical entrapment can be sued to encapsulate chemicals, proteins, siRNAs or viral vectors within EV [392-397]. The therapeutic potential of these loaded EV was tested in different disease settings. For example, a study was conducted in which orthotopic Schwannoma tumors were targeted with EV containing a cytosine deaminase fused to a uracil phosphoribosyltransferase (CD-UPRT) construct [398]. CD converts the pro-drug 5-flurocytosine into its active form of 5-fluorouracil, which is then converted by UPRT into 5-fluoro-deoxyuridine monophosphate, an inhibitor of thymidine synthetase [399]. Weekly intratumoral injection of EV isolated from cells that overexpress this construct combined with daily injection of the prodrug caused significant tumor regression in 60% of mice over 2 months of treatment [398].

EV derived from tissues are also preferentially taken up by local resident or circulatory macrophages [400, 401]. This knowledge was applied to prevent septic shock in murine models. EV modified to contain the anti-inflammatory agent curcumin protected mice against LPS-induced mortality by reducing the serum levels of the pro-inflammatory cytokines TNFα and IL-6 by at least 3-fold. [395]. Intranasal delivery can be used to noninvasively bypass the blood-brain barrier and target the brain and central nervous system [402]. EV delivered by the intranasal route localized to microglia with an hour of administration. Use of curcumin-loaded EV resulted in a decrease in microglia-driven IL-1β production by 4-5-fold in experimental autoimmune encephalomyelitis (EAE) or mice challenged with LPS [403]. This improvement in the activity was a consequence of encapsulation-dependent increase in the stability, solubility and bioavailability of the drug combined with the elimination of off-target effects [395]. As a result of these promising findings, a Phase I clinical trial was initiated to study the ability of curcumin conjugated EV to target colon cancer [NCT01294072]. Another approach involves packaging chemotherapeutic drugs within tumor-derived EV. In mouse models, EV

encapsulating doxorubicin or cisplatin effectively inhibited the growth of peritoneal neoplasia with reduced drug-related side effects [396]. Although Phase II studies were completed in 2014, no final report has been published [NCT01854866].

One advantage of EV is that they can be used as vehicles for personalized medicine. In murine models, EV isolated from bone marrow-derived DCs and pulsed with tumor antigens eradicated established tumors in a T cell-dependent manner [404]. This approach is being evaluated in humans, which requires the development of clinical grade EV production protocols [405, 406]. In phase I clinical trials, EV were derived from autologous immature DCs and loaded with tumor antigens before being administered back to patients with melanoma or non-small cell lung carcinoma [407, 408]. Both studies concluded that EV administration was safe and feasible but that the resulting T cell stimulation was limited. To increase the immunogenicity of DC-derived EV, alternative EV production methods using mature DCs in compliance with Good Manufacturing Practice (GMP) guidelines were established [409]. Phase II clinical trials with patients with inoperable non-small cell lung carcinoma (N=22) found that these improved EV loaded with cancer antigens modestly increased NK cell responses but still failed to activate tumorigenic T cells [410]. Those results suggest that DC-derived EV alone are insufficient to induce anti-tumor immunity. This led to animal testing of DC-derived EV bearing MHC/peptide complexes combined with TLR agonists, chemotherapeutic reagents or NK ligands and showed that synergistic anti-tumor activity could be obtained [411-413]. Similar non-cell-based therapy was attempted using EV derived from mesenchymal stem cells (MSCs). MSCs were introduced as a treatment option for graft-versus-host disease (GvHD) in recent years [414]. Earlier studies found that factors released by MSC rather than the cells themselves had immunomodulatory activity [415]. The potential of MSC-derived EV was investigated in a therapy-refractory GvDH patient. Administration of EV every 2-3 days for a 2 week period significantly reduced the number if IL-1β and TNFα producing cells. The volume of diarrhea was reduced by approximately half and remained low for 4 months after the cessation of therapy [416].

### 1.3.2 Problems associated with EV-based therapeutics

EV based therapeutics have several potential limitations. These include a lack of standardized isolation, characterization and storage procedures [410, 417, 418]. EV have been derived from a variety of different sources including primary donor cells, cultures of eukaryotic and prokaryotic organisms and host body fluids (plasma, saliva, breast milk etc.) [410]. The functional properties of EV vary by cell type as well as donor. For example, a study using MSC-derived EV found that TGF-β levels and suppressive capacity of EV differed among donors [416]. It has also been shown that culture conditions can alter the quantity and composition of EV. Using fetal bovine serum increases the risk of contamination, whereas the

absence of serum increases the percentage of apoptotic bodies in EV preparations [419-421]. The canonical technique for isolating EV involves ultracentrifugation at 100,000 *g* [422, 423]. However platelet-derived EV have tendency to form aggregates following centrifugation unlike EV secreted form erythrocytes [423]. Moreover, ultracentrifugation can lead to the contamination of EV preparations with plasma proteins [424]. For these reasons, alternative methods for isolating EV (particularly body fluids) based on size-exclusion chromatography or precipitation of organic material were developed [425, 426].

Storage conditions including temperature and buffer affect the stability and aggregation rate of EV. Limited evidence suggests that storing EV in isotonic buffers at -20$^{o}$C or -80$^{o}$C is optimal for stability, although freezing-thawing of EV remains a problem [419, 424, 427, 428]. Standard methods of EV characterization are based on bulk analysis of size, concentration and expression of surface markers [429]. These methods do not evaluate differences in the RNA, lipid and protein composition of EV despite evidence that they vary as a function of cell type and activation status [430, 431]. These concerns limit the batch-to-batch reproducibility of current generation EV [418].

EV are similar to liposomes and adenoviruses in being rapidly cleared by the reticuloendothelial system (RES, also known as mononuclear phagocyte system). This includes Kupffer cells in the liver. The non-specific removal of these agents remains a major obstacle to EV-based therapeutics [395, 432-438]. RES uptake of EV is influenced by their route of administration. More than 75% of i.v. injected EV ended up in the liver or spleen whereas only 40% of EV are removed by those organs after i.p. or s.c. delivery. Instead, EV administered via these routes preferentially accumulate in the pancreas and gastrointestinal tract. It is also noteworthy that s.c. injection resulted in 4-6-fold lower total fluorescence signal from the organs suggesting that EV remain at the site of injection [439]. Depleting circulatory and tissue-resident macrophages with clodronate liposomes prior to EV administration almost significantly inhibited the clearance of EV and thereby increased distribution throughout the body [440].

Efforts to overcome this problem included engineering EV to express moieties that target specific receptors expressed by selected cell types. One such attempt involved coating EV with rabies virus glycoprotein peptide (RVG) which recognizes acetylcholine receptors expressed by neurons [441]. The intensity of the fluorescent signal from brains of mice injected with RVG bearing labeled EV was 3.5-fold higher after 24 hours than the background signal of untreated mice [442]. The accumulation of the RVG-EV in the brain was 2-fold greater than that of untargeted EV [439]. Nevertheless, considering that the receptor for RVG is only expressed in neurons and that EV expressing that protein also selectively accumulated in the heart, it is clear that tissue specific targeting was not fully achieved. These modified EV were loaded with

siRNAs against either BACE1 (which regulates the formation of β-amyloid plaques in patients with Alzheimer's disease) or alpha-synuclein (a protein aggregated especially in the neurons of patients with Parkinson's disease) to test their therapeutic potential. RVG-EV encapsulating siRNA reduced target mRNA levels by half in brain tissue but depending on their exact location (midbrain, striatum or cortex) decreased the protein levels by only to 20-45% [441, 442].

Another effort to improve EV targeting involved the use of EV expressing the Tspan8 complex. This complex recognizes integrin subunit α which is expressed preferentially on endothelial cells [443, 444]. However when EV isolated from cell lines that overexpress Tspan8 were injected to rats, no selective enhancement cell or tissue localization was found [445]. These studies suggest that targeting a surface molecule fails to significantly improve EV specificity and that RES clearance needs to be reduced to improve the therapeutic utility of these agents.

### 1.3.3 EV Uptake Receptors

Considering the physiologic role and therapeutic potential of EV, it is important to understand the interaction of EV with recipient cells. EV are internalized by target cells via endocytic pathways (lipid raft-mediated, clathrin-dependent, caveolin-dependent), phagocytosis, micropinocytosis or membrane fusion [446]. Depending on the cell type, different uptake mechanisms can co-exist. For the most part, EV uptake is an energy-dependent process [400, 434, 447-449]. Protein-protein and protein-lipid interactions are required for EV internalization and several receptors (mostly integrins) have been identified by *in vitro* studies. These receptors and relevant reference are listed in Table 1.3.

**Table 1.3: EV uptake receptors**

| Receptors | Target Cells | Possible/Identified Exosomal Ligands | Reference |
|---|---|---|---|
| CD11b, CD11c, CD44, CD62L | Murine lymph node cells, splenocytes | CD9, CD81 | [401] |
| CD51, CD61, CD11a | Murine bone marrow-derived dendritic cells (BMDC) | CD11a, CD9, CD81, ICAM-1, MFG-E8 (lactadherin) - Phosphatidylserine (PS) | [434] |
| VCAM-1 | Rat aortic endothelial cells | Tspan8 | [443] |

| Receptors | Target Cells | Possible/Identified Exosomal Ligands | Reference |
|---|---|---|---|
| CD49c, CD151 | Rat lung fibroblasts | Tetraspanins (?) | [443] |
| ICAM-1 | Murine lymph node cells, splenocytes, BMDC | CD9, CD81 | [401, 434] |
| CD49d | Rat aortic endothelial cells, murine lymph node cells, splenocytes, BMDC | Tspan8 | [401, 434, 443] |
| N/A | J774 murine macrophage cell line, rat peritoneal macrophages | Galectin-5 | [449] |
| N/A | THP-1 human macrophage cell line, murine splenic macrophage | MFG-E8-PS | [450] |
| CD91 | BMDC | Heat shock proteins | [451] |
| Fibronectin | N/A | VLA-4 | [452] |
| CD205 | BMDC | Unknown mannose/glucosamine-rich C-type lectin receptor | [453] |
| MHC Class I H-2K$^{b}$ | BMDC | T cell receptor | [454] |
| LFA-1 | BMDC, murine T cells, CD8$^{+}$ DCs | ICAM-1 | [453-458] |
| CD209 | Human monocyte-derived dendritic cells | MUC1 | [459] |

| Receptors | Target Cells | Possible/Identified Exosomal Ligands | Reference |
|---|---|---|---|
| TIM4 | Ba/F3 murine pro B cell line, RAW264.7 murine macrophage cell line | PS | [400, 460] |
| TIM3 | Murine $CD4^+$ T cell clones | Galectin-9 | [461] |
| CD169 | Murine macrophages of spleen and lymph nodes | α2,3-linked sialic acid | [462] |
| SR-BI | RAW264.7, human dermal microvascular epithelial cells, A-375 human melanoma cell line | N/A | [463] |

*Modified from Mulcahy et al.* [446]

Identification of the receptors recognized by EV is useful but of limited therapeutic value since few of these receptors is expressed at high levels in the RES and their ligands are not expressed by all types of EV. On the other hand, studies of liposomes and adenoviral vectors demonstrated that scavenger receptors play an important role in clearance by Kupffer cells [464-467]. Considering that synthetic particles and biological EV have the same biodistribution, it is probable that their uptake by RES is regulated by the same receptors.

### 1.3.4 Scavenger Receptors Class A and B Families

The mammalian scavenger receptor superfamily consists of 8 classes with little structural homology, although members of each class share common structural motifs [468]. These receptors are identified by their ability to recognize wide variety of endogenous and exogenous ligands, including pathogen or danger-associated molecular patterns such as heat shock proteins, modified lipoproteins and apoptotic cells [469, 470]. The physiological role of the scavenger receptors is to clear target ligands from the circulation by endocytosis or phagocytosis [471]. These properties make scavenger receptors important regulators of homeostasis. Abnormalities in scavenger receptor function have been linked to pathogenesis of atherosclerosis, Alzheimer's disease, cancer, chronic liver diseases and type 2 diabetes mellitus [472-477]. The expression pattern of scavenger receptor families suggests that Class A and

Class B members are present in hepatic Kupffer cells, suggesting that these cells might regulate the clearance of foreign particles [478]

The A class of scavenger receptors has five members. Macrophage scavenger receptor (MSR1) also named scavenger receptor A (SR-A), SCARA1 or CD204 was the first member to be cloned [479]. SR-A has three alternatively spliced forms: SR-AI, -AII and -AIII. Because SR-AIII is trapped in the endosomes, it is not considered to be a major isoform and SR-AI/II are referred to together as SR-A [480, 481]. The second member is macrophage receptor with collagenous structure (MARCO or SCARA2) [482]. SR-A and MARCO are predominantly expressed by macrophages, although inducible SR-A expression was detected in endothelial and smooth muscle cells [470, 483-488]. SCARA3 is an intracellular stress protein that protects cells from oxidative damage [489]. Expression of the remaining class A members (SCARA4 and SCARA5) is limited to endothelial and epithelial cells [490, 491]. Class A receptors share a positively charged collagen-like domain, which serves as a binding site for negatively charged macromolecules [492, 493]. For this reason, these receptors recognize oxidized, (and with higher affinity) acetylated low density lipoproteins (LDL), polyribonucleotides, polysachharides, polyanionic molecules and apoptotic cells [470, 488, 494-500].

A number of other scavenger receptors also recognize those ligands, with class B members binding to the same set of molecules as class A [501]. Class B consists of CD36 and two alternatively spliced proteins SR-BI and SR-BII [502-505]. These receptors form dimers and multimers and bind their ligands via the central part of their extracellular domain [504, 506, 507]. The ligands for scavenger receptor Class B members SR-BI and CD36 include oxidized LDL, native or modified high-density lipoprotein (HDL) and phosphatidylserine [508-513]. As opposed to SR-A and MARCO, SR-BI and CD36 are expressed in multiple cell types in addition to myeloid cells including platelets, epithelial cells, endothelial cell and adipocytes [478, 507].

Macrophage-restricted expression of Class A members SR-A and MARCO combined with their ability to recognize negatively charged particles make them good candidates as EV uptake receptors. A role for scavenger receptor BI (SR-BI) in EV uptake was recently demonstrated in macrophage and melanoma cells. *In vitro* blockade of this receptor reduced EV uptake by 25% [463]. The role of the remaining scavenger receptor families, especially class A members, in the EV recognition by the cells remains to be investigated.

## 1.4 Aim and outline of the thesis

Macrophages differentiate from monocytes and play a critical role in the maintenance of immune homeostasis and recognition of pathogens. Reflecting their essential role in normal physiology, alterations in macrophage activation are associated with various pathophysiological conditions. Thus, understanding the differentiation pathways of mMDSC and HLA-DR$^+$ monocytes into macrophages can aid the development of strategies to regulate their behavior and potentially alter disease progression.

The first aim of this thesis was to identify the soluble factors involved in the maturation of human mMDSC into M1- and M2-like macrophages. The role of various cytokines druing R848-induced M1- or PAM3-dependent M2-like macrophage polarization was initially evaluated by neutralizing their activity in cultures stimulated by TLR agonists. To identify optimal cytokine mixtures, human mMDSC were cultured with select cytokines alone or in combination. The functionality of mMDSC-derived M1- and M2-like macrophages was assessed by tumor lysis and T cell proliferation assays. Gene expression arrays together with Ingenuity Pathway Analysis (IPA) was performed to identify regulatory networks associated with the differentiation of mMDSC into M1-like macrophages.

The second aim of this thesis sought to characterize the effect of PAM3 on human HLA-DR$^+$ monocytes, following its identification as a novel inducer of M2-like macrophages from human mMDSC. The phenotype of M2-like macrophages generated in the presence of PAM3 was compared to those generated by M-CSF while their functional activity was investigated using T cell proliferation and dextran uptake assays. The regulatory networks utilized in the progess of M2-like macrophage polarization were identified by gene expression assays. The importance of these pathways during PAM3 and M-CSF-dependent M2-like macrophage differentiation was confirmed by inhibition assay.

The third part of this thesis investigated the role of class A scavenger receptors in the interaction of EV with macrophages with the intent of using EV as vehicles for TLR agonist based therapy. The influence of SR-A blockade on EV binding by various cell lines and primary cells was analyzed *in vitro*. Subsequently, the biodistribution of EV was monitored *in vivo* following administration of SR-A inhibitors.

# Chapter 2

# Materials and Methods

## 2.1 Materials

### 2.1.1 TLR Ligands

Receptor specificities, catalog numbers, vendors and working concentrations of TLR ligands used in stimulation experiments are listed in Table 2.1

**Table 2.1: Ligands for TLR**

| Name | Specificity | Catalog # | Company | Working Concentration |
|---|---|---|---|---|
| FSL-1 | TLR2/6 | tlr-fsl | Invivogen (USA) | 10 ng/ml |
| Poly(I:C) HMW (polyinosinic-polycytidylic acidhigh molecular weight) | TLR3 | tlrl-pic | Invivogen (USA) | 30 μg/ml |
| LPS-B5 (*E. coli* 055:B5) | TLR4 | tlrl-b5lps | Invivogen (USA) | 1 μg/ml |
| MPLA-SM (*S. Minnesota* R595) | TLR4 | tlrl-mpla | Invivogen (USA) | 1 μg/ml |
| FLA-BS (*B.subtilis*) | TLR5 | tlrl-bsfla | Invivogen (USA) | 1 μg/ml |

| Name | Specificity | Catalog # | Company | Working Concentration |
|---|---|---|---|---|
| R848 | TLR7/8 | tlrl-r848-5 | Invivogen (USA) | 3 μg/ml |
| 3M-055* | TLR7 | N/A | 3M Drug Delivery Systems, USA | 100 ng/ml |
| CL-075* | TLR8 | N/A | 3M Drug Delivery Systems, USA | 200 ng/ml |

*3M-055 and CL-075 were gifts of Dr. John Vasilakos.

### 2.1.2 Recombinant Cytokines

All human recombinant cytokines were purchased from Miltenyi Biotec, Germany, with the exception of human TGF-β1, which was acquired from Sigma Aldrich, and used at a concentration of 50-500 ng/ml. Catalog numbers of the recombinant cytokines are listed in Table 2.2.

**Table 2.2: Recombinant Cytokines**

| Name | Catalog # |
|---|---|
| Human GM-CSF, premium grade | 130-093-866 |
| Human IFNγ, research grade | 130-096-873 |
| Human IL-1β, premium grade | 130-093-898 |
| Human IL-4, premium grade | 130-093-922 |
| Human IL-6, premium grade | 130-093-932 |

| Name | Catalog # |
|---|---|
| Human IL-8, research grade | 130-093-943 |
| Human IL-10, research grade | 130-098-448 |
| Human IL-12, premium grade | 130-096-798 |
| Human IL-13, research grade | 130-103-440 |
| Human M-CSF, premium grade | 130-096-492 |
| Human TGF-β1 | T7039 |
| Human TGF-β2, research grade | 130-094-005 |
| Human TNFα, premium grade | 130-094-562 |

### 2.1.3 Cytokine Neutralizing Antibody

All anti-cytokine neutralizing antibodies were used at a concentration of 25 μg/ml. Clones, catalog numbers and vendors are listed in Table 2.3

**Table 2.3: Neutralizing antibodies against secreted cytokines.**

| Name | Clone | Catalog # | Company |
|---|---|---|---|
| LEAF™ Purified anti-human GM-CSF | BVD2-23B6 | 502204 | Biolegend, USA |
| LEAF™ Purified anti-human IFNβ | IFNb/A1 | 514004 | Biolegend, USA |
| LEAF™ Purified anti-human IFNγ | MD-1 | 507513 | Biolegend, USA |
| LEAF™ Purified anti-human IL-1β | H1b-27 | 511604 | Biolegend, USA |
| LEAF™ Purified anti-human IL-4 | 8D4-8 | 500707 | Biolegend, USA |

| Name | Clone | Catalog # | Company |
|---|---|---|---|
| LEAF™ Purified anti-human IL-6 | MQ2-13A5 | 501110 | Biolegend, USA |
| LEAF™ Purified anti-human IL-10 | JES3-9D7 | 501407 | Biolegend, USA |
| LEAF™ Purified anti-human IL-12/IL-23 p40 | C8.6 | 508804 | Biolegend, USA |
| anti-hM-CSF | N/A | MAB216 | R&D Systems, USA |
| LEAF™ Purified anti-human/mouse TGF-β1 | 19D8 | 521704 | Biolegend, USA |
| LEAF™ Purified anti-human TNFα | Mab11 | 502922 | Biolegend, USA |
| LEAF™ Purified Mouse IgG1, κ isotype Ctrl | MOPC-21 | 400124 | Biolegend, USA |
| IgG2A Isotype Control | N/A | MAB003 | R&D Systems, USA |

### 2.1.4 Flow Cytometry Antibody

Fluorescence-conjugated antibodies used for the flow cytometric analysis of the cells are listed in Table 2.4.

**Table 2.4: Fluorescence-conjugated antibodies**

| Name | Clone | Catalog # | Company |
|---|---|---|---|
| Anti-human Mature Macrophage | eBio25F9 | 50-0115-42 | eBioscience, USA |
| Anti-human CCR7 | 150503 | FAB197P | R & D Systems, USA |
| Anti-human CD1d | 51.1 | 350310 | Biolegend, USA |
| Anti-human CD3 | SK7 | 557832 | BD Pharmingen, USA |

| Name | Clone | Catalog # | Company |
|---|---|---|---|
| Anti-human CD4 | SK3 | 341654 | BD Pharmingen, USA |
| Anti-human CD11b | ICRF44 | 301330 | Biolegend, USA |
| Anti-human CD11c | 3.9 | 301624 | Biolegend, USA |
| Anti-human CD14 | MΦP9 | 560349 | BD Pharmingen, USA |
| Anti-human CD16 | B73.1 | 360716 | Biolegend, USA |
| Anti-human CD19 | HIB19 | 555415 | BD Pharmingen, USA |
| Anti-human CD36 | AC106 | 130-095-470 | Miltenyi Biotec, USA |
| Anti-human CD40 | HB14 | 313014 | Biolegend, USA |
| Anti-human CD45RA | HI100 | 550855 | BD Pharmingen, USA |
| Anti-human CD56 (NCAM) | 5.1H11 | 362508 | Biolegend, USA |
| Anti-human CD80 | 2D10 | 305218 | Biolegend, USA |
| Anti-human CD86 | IT2.2 | 305422 | Biolegend, USA |
| Anti-human CD163 | GHI/61 | 333618<br>333608<br>333614 | Biolegend, USA |
| Anti-human CD204 | REA460 | 130-107-036 | Miltenyi Biotec, USA |
| Anti-human CD206 | 15-2 | 321122<br>321104<br>321120 | Biolegend, USA |
| Anti-human CD209 (DC-SIGN) | 9E9A8 | 330104 | Biolegend, USA |

| Name | Clone | Catalog # | Company |
|---|---|---|---|
| Anti-human CD273 (PD-L2) | 24F.10C12 | 329606 | Biolegend, USA |
| Anti-human CD274 (B7-H1, PD-L1) | 29E.2A3 | 329718 | Biolegend, USA |
| Anti-human EGF Receptor | EGFR.1 | 555997 | BD Pharmingen, USA |
| Anti-human HLA-DR | TU36 | 555561<br>559868 | BD Pharmingen, USA |
| Anti-mouse/human CD11b | M1/70 | 101206 | Biolegend, USA |
| Anti-mouse CD204 | REA148 | 130-102-328 | Miltenyi Biotec, USA |
| Anti-mouse CD206 | C068C2 | 141716 | Biolegend, USA |
| Anti-mouse F4/80 | BM8 | 123116 | Biolegend, USA |
| Anti-mouse Ly6C | HK1.4 | 128008<br>128032 | Biolegend, USA |
| Anti-mouse Ly6G | 1A8 | 127624 | Biolegend, USA |

### 2.1.5 ELISA Antibodies

Coating antibodies, recombinant proteins and detection antibodies for IL-6, IL-10, IL-12 and TNFα ELISA were purchased from R & D Systems, USA.

### 2.1.6 Cell Culture Media and Standard Solutions Components

DMEM high glucose without L-glutamine (Catalog # 12-614F), FCS (Catalog # 14-502F), 1X PBS (Catalog # 17-516F), 10X PBS (Catalog # 17-516Q), RPMI-1640 without L-glutamine (Catalog # 12-167F), RPMI-1640 without pheonel red & L-glutamine (Catalog # 12-918F) were purchased from Lonza, USA. Sodium Pyruvate (100 mM; Catalog # 11360-070), L-glutamine (200mM; Catalog # 25030-081) and Pen Strep (5,000 unitsl/ml Penicillin and 5,000 µg/ml Streptomycin; Catalog # 25070-063) were supplied from ThermoFisher Scientific, USA; BSA

(Catalog # BSA-50) from Rockland Immunochemicals, USA, and Tween-20 (Catalog # P1379) from Sigma-Aldrich, USA. Complete RPMI-1640 and DMEM were prepared by adding 1 x Sodium Pyruvate and 1 x L-glutamine and different amounts of FCS (heat-inactivated at 56$^{o}$C for 1 hour). Oligo RPMI-1640 was prepared using FCS heat-inactivated at 65$^{o}$C and also contained 1 x Pen Strep. For each experiment FCS percentage of the media is specified in Methods Section.

## 2.2 Methods

### 2.2.1 Collection and isolation of human blood samples

Apharesis collections, elutriated monocytes and elutriated lymphocytes were obtained from healthy volunteers who gave written consent to participate in an Institutional Review Board (IRB) approved study (National Institutes of Health, Bethesda, MD). Human samples were shipped to the laboratory within 2 hours of collection. The apharesis samples and elutriated lymphocytes were diluted in RMPI and slowly layered over Ficoll (Histopaque® 1077, Sigma Aldrich, USA) at a volume:volume ratio of 5:3. They were then centrifuged at 400 *g* for 30 minutes and allowed to slow without added deceleration. Material at the interphase (just above the Ficoll) was collected and transferred to a 50 ml falcon tube using a sterile Pasteur pipette. Samples were washed twice with 50 ml RPMI-1640 supplemented with 2% FCS and centrifuged at 400 *g* for 10 minutes. Elutriated monocytes were washed twice using the same approach. Cell numbers were determined using a KX-21N Automated Hematology Analyzer (Sysmex, USA). Apharesis collections and elutriated lymphocytes were cultured in 5% FCS containing RPMI-1640 and elutriated monocytes in 2% FCS supplemented RPMI-1640 at a density of 2x10$^{6}$ cells/ml media in T-175 tissue culture flasks.

#### 2.2.1.1 Sorting of mMDSC and HLA-DR$^{+}$ monocytes

Apheresis samples and elutriated monocytes were cultured overnight. Cells were centrifuged at 400 *g* for 5 minutes and re-suspended in 30 ml of RPMI-1640 supplemented with 2% FCS. Cell numbers were determined after passage through a 70 μm cell strainer (Falcon, USA). Cells were centrifuged at 400 *g* for 5 minutes before staining in sorting buffer (2.5% FCS containing PBS) containing Brilliant Violet V421- and V450-conjugated anti-human CD14, and PE-conjugated anti-human HLA-DR antibodies for 30 minutes on ice. The volume of staining solution and the amount of antibodies were determined according to the criteria listed in Table 2.5

**Table 2.5: Staining volume and antibody amounts**

| Cell # | Sorting Buffer Volume | anti-CD14 antibody amount (each) | anti-HLA-DR antibody amount |
|---|---|---|---|
| < 75 million | 180 µl | 15 µl | 60 µl |
| 75 – 150 million | 240 µl | 20 µl | 80 µl |
| > 150 million | 300 µl | 25 µl | 100 µl |

After the incubation period, cells were washed with 10 ml Sorting Buffer, centrifuged at 400 g for 5 minutes, and resuspended in 500 µl sorting buffer. Single stained and unstained controls were prepared from the same donors using $5x10^5$ cells. For single stained controls, cells were stained in 10 µl sorting buffer with either 0.5 µl anti-CD14 antibodies or 1 µl anti-HLA-DR antibody. Cells were washed with 100 µl sorting buffer, centrifuged at 5200 rpm for 2 minutes on tabletop centrifuge and resuspended in 200 µl sorting buffer. $CD14^{bright}HLA\text{-}DR^-$ (mMDSC) and $CD14^{bright}HLA\text{-}DR^+$ cells were purified by sorting using FACSAria II (BD Bioscience, USA). Sorted cells were retrieved in collection buffer (20% FCS containing RPMI-1640).

#### 2.2.1.2 Sorting of naïve $CD4^+$ T Cells

Apharesis collections and elutriated lymphocytes were cultured for 2 days. Cell numbers were determined with hematology analyzer after passing through 70 µm cell strainer. 40 million cells were MACS sorted for naïve CD4+ T cells using Naïve CD4+ T Cell Isolation Kit II, human (miltenyi Biotec, USA) according to the manufacturer's instructions. Briefly, cells were centrifuged at 400 *g* for 5 minutes and then resuspended in 160 µl MACS Separation Buffer (PBS pH 7.2, BSA, EDTA, 0.09% azide). 40 µl Naïve CD4+ T Cell Biotin-Antibody Cocktail II was added and cells were incubated in the $4^oC$ refrigerator for 5 minutes. 120 µl MACS Separation Buffer and 80 µl Naïve CD4+ T Cell Microbead Cocktail II were included and cells were incubated in the refrigerator for an additional 10 minutes. Meanwhile, LS columns were equilibrated with 3 ml MACS Separation Buffer. Final volumes of the cell suspensions were increased to 500 µl with MACS Separation Buffer and cells were applied onto the LS Columns. Flow-through was collected and columns were washed two times with 3 ml MACS Separation Buffer. These fractions containing the unlabeled naïve $CD4^+$ T cells were combined and cell numbers were determined with hematology analyzer. The sorting efficiencies were confirmed with staining the initial cell suspension and the flow through with fluorescence-conjugated anti-CD4, anti-CCR7 and anti-CD45RA antibodies.

### 2.2.2 Stimulation of mMDSC and HLA-DR$^+$ monocytes

$5x10^4$-$1x10^5$ purified mMDSC were cultured in 96-well flat bottom plates in 200 µl RPMI-1640 supplemented with 2% FCS. Cells were stimulated with PAM3, R848, 3M-055, CL-075 and combination of 3M-055 with CL-075 for 3 or 5 days. mMDSC were also cultured for 5 days with 500 ng/ml recombinant human cytokines (listed in Table 2.2) and 100ng/ml $PGE_2$ (Cayman Chemical, USA) either alone or in various combinations. In some experiments 25 µg/ml neutralizing antibodies against cytokines (listed in Table 2.3) were added into PAM3 and R848 cultures for 3 days (Figure B1). $1x10^5$-$2x10^5$ HLA-DR+ monocytes were stimulated with the TLR ligands listed in Table 2.1 (with the exception of 3M-055 and CL-075) or 500 ng/ml M-CSF for 3 or 5 days. In some experiments 25 µg/ml αM-CSF, αIL-6, αIL-10 or αIFNβ, 2.5 µM Celastrol (Invivogen, USA, an inhibitor of NF-κB complex), 5nM FK866 (Sigma Aldrich, USA, an inhibitor of NAMPT), 10 µM Celecoxib (Sigma Aldrich, USA, an inhibitor of COX-2) or 50 nM FR122047 (Cayman Chemical, USA, an inhibitor of COX-1) were included in PAM3 and M-CSF cultures for 5 days. For blockade of p38 MAPK, cells were incubated with the inhibitor 10µM SB203580 (Invivogen, USA) for 45 minutes prior to stimulation. At the end of the incubation period, differentiation of monocytes into M1- or M2-like macrophages was determined by staining with fluorescence-conjugated anti-CD163, anti-CD206 and anti-25F9 antibodies.

### 2.2.3 Effect of cytokines on re-polarization of HLA-DR$^+$ monocytes

8 x $10^6$ HLA-DR$^+$ monocytes were stimulated with 250 ng/ml TNFα or M-CSF for 2 days in 6-well plates containing 2 ml 2% FCS supplemented RPMI-1640. Cells were centrifuged at 5,2000 rpm for 2 minutes and re-suspended in 45 µl sorting buffer containing 2.5 µl FITC-conjugated anti-human CD163 and eFluor660-conjugated anti-human 25F9 mature macrophage antibodies. After incubation on ice in the dark for 30 minutes, macrophages were washed with 200 µl sorting buffer and re-suspended in 500 µl sorting buffer. Single stained controls were prepared from fixed elutriated monocytes. FACS purified HLA-DR$^+$ monocytes isolated and fixed on day 0 were used to establish the gates. 25F9$^+$CD163$^-$ M1-like and 25F9$^+$CD163$^+$ M2-like macrophages were FACS sorted from TNFα and M-CSF stimulated monocyte cultures, respectively. 5 x $10^4$- 1 x $10^5$ purified macrophages were stimulated with 250 ng/ml TNFα or M-CSF for an additional 5 days in 96-well flat-bottom plates containing RPMI-1640 supplemented with 2% FCS. Macrophage percentages were determined by staining with fluorescence-conjugated anti-CD163, anti-CD206 and anti-25F9 antibodies.

### 2.2.4 Microscopy image of HLA-DR$^+$ monocytes

mMDSC stimulated with R848 and/or IL-6 plus TNFα for 5 days were imaged using the 40x objective of a Nikon Eclipse Ti equipped with a DS-Ri2 camera. HLA-DR$^+$ monocytes stimulated with PAM3 or M-CSF for 5 days were imaged using 20x objective of a Nikon Eclipse Ti equipped with a DS-Ri2 camera. Images were processed with NIS Element software (Nikon Instruments, USA).

### 2.2.5 Analysis of surface and intracellular markers with flow cytometry

For staining of human samples, plates were centrifuged at 400 *g* for 10 minutes, or 1.5 ml microtubes at 5200 rpm for 2 minutes. Supernatants were removed and cell pellets were resuspended in 50 µl staining buffer (PBS containing 2% BSA) and 2.5 µl fluorescence-conjugated antibodies, unless otherwise stated. Plates or microtubes were incubated on ice, at dark for 30 minutes. Samples were washed with 250 – 1000 µl of staining buffer and centrifuged as before. Pellets were resuspended in 30 – 50 µl of Fixation Medium A (Fix & Perm® Cell Fixation & Cell Permeabilization Kit, ThermoFisher Scientific, USA). Cells were incubated at room temperature, dark for 15 minutes and washed as previously mentioned. In case of intracellular staining, fixed cells were resuspended in 50 µl Permeabilization Buffer B, containing 2.5 µl fluorescence-conjugated antibodies. The mixture was incubated at room temperature, dark for 20 minutes and washed again as described. Final resuspension was done in 250 – 500 µl of PBS. For stimulation experiments, $5x10^4$-$1x10^5$ mMDSC and HLA-DR$^+$ monocytes were fixed at Day 0 to use as control and stained simultaneously with the stimulated samples.

For staining of mouse samples, first cells were incubated with 5 µl FcR Blocking Reagent (Miltenyi Biotec, USA) in 50 µl staining buffer on ice for 10 minutes. After washing step, cells were incubated for an addition 20 minutes on ice with 50 µl staining buffer containing 1 µl of fluorescence-conjugated antibodies. Samples were washed as previously described and resuspended in 300 µl PBS. For stimulation experiments, $5x10^4$-$1x10^5$ bone marrow-derived mMDSC or monocytes were fixed at Day 0 to use as control and stained simultaneously with the stimulated samples.

For each fluorophore used in the staining of the samples, unstained and single stained controls were prepared from fixed elutriated monocytes, lymphocytes or mouse splenocytes. These controls were used to set voltages and adjust compensation values of the machine. In different experiments, 2,000-20,000 viable cells were acquired with LSRFortessa (BD Biosciences, USA).

### 2.2.6 Functional analysis of differentiated cells

#### 2.2.6.1 Cytotoxicity functional assay

Minimum $2x10^5$ mMDSC were stimulated with 3 μg/ml R848 and combination of 500 ng/ml IL-6 with TNFα for 5 days in 2% FCS containing RPMI-1640 (without phenol red). Minimum $4x10^5$ unstimulated mMDSC were cultured under similar conditions in 96-well flat bottom plates. At the end of the incubation period, cells were transferred into sterile 1.5 ml microtubes and cell numbers were determined by counting 10 μl of cell supernatant with C-Chip disposable hemocytometer (iN CYTO, USA). Meanwhile, A549 *Homo sapiens* lung carcinoma cell lines (ATCC) cultured in T-75 tissue culture flasks were trypsinized for 5 minutes (please see Section 2.2.9 for culture details). Cells were washed with 10 ml media by centrifuging at 400 *g* for 5 minutes and resuspended in 10 ml of DMEM supplemented with 10% FCS. 10 μl of A549 cell supernatant was mixed with 40 μl media and 50 μl Trypan Blue (Amresco, USA). 10 μl of the mixture was used to determine cell numbers by counting with C-Chip hemocytometer. Total cell numbers of mMDSC and A549 cells were calculated according to the following formula:

(Counted cell # / 4) x (dilution factor) x $10^4$ = Total cell # / ml

Microtubes were centrifuged at 5200 rpm for 2 minutes and mMDSC were resuspended in 200 μl fresh 2% FCS containing RPMI-1640 (without phenol red). mMDSC were incubated with A549 cells at a 1:40 ratio for 6 hours in 96-well flat bottom plates. A549 cells were also cultured alone to use as a control group. At the end of the incubation period, cells were stained with Live/Dead® Fixable Near-IR Dead Stain Kit (ThermoFisher Scientific, USA) according to the manufacturer's instructions. Briefly, for $1x10^6$ 1 μl dye was mixed with 1 ml PBS. Depending on the number of cells final staining volume was adjusted and cells were stained on ice for 30 minutes. Cells were then washed with 1ml 2% BSA containing PBS and centrifuged at 5200 rpm for 2 minutes. Cells were then stained with fluorescence-conjugated anti-EGFR (10 μl antibody in 50 μl PBS containing 2% BSA) and anti-CD14 antibodies as previously described in Section 2.2.5.

#### 2.2.6.2 T Cell proliferation assay

##### 2.2.6.2.1 Staining of naïve $CD4^+$ T cells with CFSE

Up to $6x10^6$ purified naïve CD4+ T cells were incubated with 1 μM CFSE (Biolegend, USA) in 1 ml PBS at 37°C for 3 minutes. Cells were washed with ice cold 10% FCS supplemented RPMI-1640 twice and centrifuged at 400 *g* for 5 minutes. Cell pellets were resuspended in 5% FCS containing RPMI-1640 at a density of $1x10^5$ cells/100 μl.

##### 2.2.6.2.2 Preparation of Dynabeads® Human T Actiator CD3/CD28

2.5 μl of Dynabeads® Human T-Activator CD3/CD28 (ThermoFisher Scientific, USA) per well (to obtain 1:1 bead-to-T cell ratio) were transferred into a sterile 1.5 ml microtube. Beads were

washed with 1 ml PBS containing 0.1% BSA and vortexed vigorously for 5 seconds. The microtube was placed over magnetic separation stand (Promega, USA) for 1 minute and the supernatant was discarded. Beads were then washed with 1 ml 2% FCS containing media with similar approach. At last beads were re-suspended in 10-fold volume of the original bead amount with 2% FCS supplemented RPMI-1640.

#### 2.2.6.2.3 Assay procedure

2 x $10^5$ mMDSC were cultured in 96-well U-bottom plates in 75 µl of RPMI-1640 supplemented with 2% FCS. Cells were stimulated with 1µg/ml or a combination of 500 ng/ml of IL-6 and IL-10 with 5 ng/ml M-CSF for 4 hours. $10^5$ CFSE-stained naïve CD4+ T cells in 100 µl of medium and 25 µl of beads (described above) were added to the cultures and samples were co-cultured for 3 days. $2x10^5$ HLA-$DR^+$ monocytes were cultured into 96-well U-bottom plates in 75 µl RPMI-1640 supplemented with 2% FCS. Cells were stimulated with 1 µg/ml PAM3 and 500 ng/ml M-CSF overnight. The following day $1x10^5$ CFSE-stained naïve CD4+ T cells in 100 µl media and 25 µl beads were added to the cultures and samples were co-cultured for an additional 4 days. At the end of the incubation period samples were stained with fluorescence-conjugated anti-CD14 antibody and fixed as described Section 2.2.5. The rate of proliferation was assessed by dilution in the CFSE content with flow cytometry, based on naïve $CD4^+$ T cells cultured alone.

#### 2.2.6.3 Phagocytosis Assay

5 x $10^4$ HLA-$DR^+$ monocytes stimulated with PAM3 or M-CSF were incubated with 50 µg/ml of Dextran, Alexa Fluor 488®, 3,000 MW, Anionic (ThermoFisher Scientific, USA) for 45 minutes in 200 µl of 2% FCS containing RPMI Reg. The rate of uptake was assessed with flow cytometry.

### 2.2.7 ELISA for cytokines

At the end of the incubation period at Day 3 or Day 5, 96-well flat bottom plates used culturing mMDSC or HLA-DR+ monocytes were centrifuged at 400 *g* for 10 minutes. Supernatants were transferred into 96-well plates, frozen immediately and stored at -20$^o$C until further use. Immulon 2HB microtiter plates (ThermoFisher Scientific, USA) were coated with 50 µl/well 1/200 diluted anti-cytokine antibodies in PBS, overnight at 4$^o$C refrigerator. Wells were blocked with 200 µl blocking buffer (PBS containing 2% BSA) for 2 hours at room temperature. Plates were washed three times with washing buffer (1x PBS containing %0.05 Tween) for five minutes followed by rinsing three times with $ddH_2O$. 50 µl cell supernatants or 50 µl 3-fold serially diluted recombinant proteins (in blocking buffer starting from 200ng/ml) were added to

the wells. Following overnight incubation at 4°C, plates were washed as previously described. Plates were incubated with 1/1000 diluted biotin-conjugated detection antibodies (prepared in blocking buffer) at room temperature for 2 hours. Plates were again washed and incubated for addition 45 minutes – 1 hour with 1/5000 diluted phosphatase-streptavidin (in blocking buffer; BD Biosciences, USA). After the last washing step, 70 µl of K-Gold PNPP substrate (Neogen Corporation, USA) was added to the wells. Multiple optical density readings at 405 nm wavelength were acquired using Spectra Max M5 Microplate Reader, and SoftMax Pro Acquisition and Analysis Software (both Molecular Devices, USA).

### 2.2.8 Analysis of gene expression with microarray

#### 2.2.8.1 RNA isolation

A minimum of $5x10^5$ mMDSC were cultured in 48-well Linbor plates in 400 µl of 2% FCS containing RPMI-1640. Cells were either left unstimulated or stimulated with i) 3 µg/ml R848, ii) 500 ng/ml IFNγ, iii) combination of 500 ng/ml IL-6 with TNFα for 4 hours. Similarly, $1x10^6$ HLA-DR$^+$ monocytes were either stimulated with i) 1 µg/ml PAM3, ii) 500ng/ml M-CSF or left unstimulated for 4 hours in 400 µl 2% FCS supplemented RPMI-1640. Cells were transferred into 1.5 ml microtubes and centrifuged at 5200 rpm for 2 minutes. Pellets were resuspended in 350 µl RLT Buffer (Qiagen, USA) and immediately stored at -80°C until further use. Total RNAs were extracted using RNeasy Mini Kit (Qiagen, USA) according the manufacturer's instructions. Total RNA was amplified with Amino Allyl Messeage Amp II aRNA kit (Ambion, USA.

#### 2.2.8.2 Expression analyses

Expression analyses were conducted by Ms. Debra Tross-Curie. Briefly, total RNA was first reverse transcribed into cDNA, which was then transcribed into antisense amplified RNA (asRNA) using T7 RNA polymerase. During *in vitro* transcription aminoallyl modified UTPs were incorporated for Cy-dye coupling. asRNA from mMDSC or HLA-DR$^+$ monocyte samples were labeled with Cy5 monoreactive dye (GE Healthcare and Life Sciences, USA). A reference human sample (Stratagene, USA) was labeled in parallel with Cy3. Up to 10 µl of asRNA (2-4 mg) was mixed with 0.1M sodium bicarbonate buffer (pH 8.7) and 20 µl of Cy3 or Cy5 dissolved in DMSO in total volume of 40 µl. The mixture was incubated in the dark for 120 minutes. 18 µl of 4M hydroxylamine was added for 15 minutes to quench unreacted Cy-dye. Cleaning up of samples was performed with the Rneasy MinElute kit (Qiagen, USA).

Cy3-labeled reference and Cy5-labeled sample asRNAs (20 µl each) were combined, denaturated by heating for 2 minutes at 98°C, and mixed with 50 µl water and 60 µl

hybridization solution at 42°C (Ambion, USA). Human microarrays (Microarrays Inc., USA) were overlaid with this mixture and hybridized for 18 hours at 42°C using a static gasket to contain the sample. The arrays were washed post-hybridization and scanned using an Axon scanner equipped with GenePix software 5.1 (Molecular Devices, USA). Data were uploaded and analyzed on the microarray database [of Center for Information Technology/BioInformatics and Molecular Analysis Section; and NCI/Center for Cancer Research; http://nciarray.nci.nih.gov/]. Upregulated genes were mapped into regulatory networks using Ingenuity Pathway Analysis (IPA) software (Qiagen, USA).

### 2.2.9 Generation of bone marrow-derived macrophages

#### 2.2.9.1 Isolation of bone marrow cells

C57BL/6 mice were housed in NCI-Frederick Animal Facility. All procedures conducted were in compliance with the ethical guidelines for the care and use of laboratory animals and approved by Animal Care and Use Committee (ACUC) of the National Institutes of Health. Femur and tibia bones were removed from 6-8 week old female mice. Bone marrow cells were washed through the bones using 27G needle with 10ml RPMI Oligo supplemented with 2% FCS. Cells were washed with 50 ml media by centrifuging at 400 *g* for 5 minutes. Cell numbers were counted using KX-21N Automated Hematology Analyzer after passing through 70 μm cell strainer. Cells were again pelleted with centrifugation.

#### 2.2.9.2 Sorting for mouse mMDSC

Up to $5x10^6$ bone marrow cells were stained in 150 μl sorting buffer with 5 μl of CD11b-FITC, Ly6C-PE and Ly6G-APC-Cy7 antibodies for 30 minutes on ice. Single stained controls were prepared with $3x10^5$ in 10 μl of sorting buffer and 0.5 μl fluorescence-conjugated antibodies. At the of the incubation period, cells were washed with 10 ml sorting buffer by centrifuging at 400 *g* for 5 minutes. Single stain controls were washed with 100 μl sorting buffer and centrifuged at 5200 rpm for 2 minutes. $CD11^{bright}Ly6C^{high}Ly6G^{low}$ cells representing the mouse monocytic MDSCs were collected in RPMI Oligo containing 20% FCS.

#### 2.2.9.3 Sorting of mouse monocytes

Up to $5x10^6$ bone marrow cells were sorted for monocytes using Monocyte Isolation Kit (BM) (Miltenyi Biotec, USA). Briefly, cells were resuspended in 175 μl MACS Separation Buffer and incubated with combination of 25 μl FcR blocking reagent and 50 μl monocyte biotin-antibody cocktail for 5 minutes at 4°C fridge. Cells were washed with 3 ml MACS Separation Buffer be centrifuging at 400 *g* for 5 minutes. Pellets were resuspended in 400 μl MACS Separation Buffer and 100 μl anti-biotin microbeads. Meanwhile, LS columns were equilibrated with 3 ml

MACS Separation Buffer. Mixture was loaded into the columns and bone marrow monocytes were negatively selected by collecting the effluent and combining with 6 ml of MACS Separation Buffer used to wash the columns afterwards. Efficiency of sorting was confirmed by staining with Ly6C and CD11b antibodies as mentioned in Section 2.2.5.

#### 2.2.9.4 Stimulation of bone marrow-derived cells

5 x $10^4$ – 1 x $10^5$ mouse mMDSC were incubated with PAM3, PGN or LPS (concentrations provided in Table 2.1) in 96-well flat-bottom plates containing 200 µl of RPMI Oligo supplemented with 5% FCS. Mouse monocytes were stimulated under similar condition with PAM3, PGN, FSL-1, LPS or MPL for 4 days. Differentiation efficiency of cells was confirmed with staining for F4/80 and CD206 as described in Section 2.2.5.

### 2.2.10 Cell lines

All cell lines were cultured under sterile conditions. Frozen cell vials were removed from liquid nitrogen or -80$^o$C freezers and immediately immersed in 37$^o$C water bath. 9 ml of cold media was added into the vials and cells were centrifuged at 350 *g* for 5 minutes. Cells were resuspended in 10 ml complete media and cultured in T-25 flasks. The following day, media was replaced and once cells reached confluency they were transferred in in T-75 flasks. From then on cells were split every 2-3 days, once they reach to 80-90% confluency. Cells were collected with different dissociation methods in 10 ml media, centrifuged at 400 *g* for 5 minutes and plated in new culture plates at a ratio of 1:5. Cell lines, different media conditions and dissociation methods used for culturing are listed in Table 2.6.

**Table 2.6: Cell lines and culture conditions**

| Cell Line | Media | Dissociation Method |
|---|---|---|
| A549 | Complete High-glucose DMEM supplemented with 10% FCS | Trypsination |
| B16-F10 *Mus musculus* melanoma (ATCC) | Complete RPMI-1640 supplemented with 5% FCS | Trypsination |
| E.G7 *Mus musculus* lymphoma (ATCC) | Complete RPMI-1640 supplemented with 5% FCS | N/A (Suspension Culture) |

| Cell Line | Media | Dissociation Method |
|---|---|---|
| LLC1 *Mus musculus* Lewis cell carcinoma (ATCC) | Complete High-glucose DMEM supplemented with 10% FCS | Trypsination |
| MC-38 *Mus musculus* colon adenocarcinoma | Complete High-glucose DMEM supplemented with 10% FCS | Trypsination |
| RAW264.7 *Mus musculus* macrophage (ATCC) | Complete RPMI-1640 supplemented with 5% FCS | Scraping |
| 4T1 *Mus musculus* mammary gland (ATCC) | Complete High-glucose DMEM supplemented with 10% FCS | Trypsination |

### 2.2.11 Isolation of extracellular vesicles

Extracellular vesicles (EV) isolated from HEK293 *Homo sapiens* embryonic kidney cell lines (ATCC) were kindly provided by Dr. Dionysios C. Watson from NCI. Briefly, HEK293 cells were cultured in a hollow-fiber bioreactor using DMEM supplemented with protein-free 5% CDM-HD (FiberCell Systems, USA) and 100 U/ml penicillin/streptomycin (Lonza, USA). 20 ml conditioned media from the bioreactor was centrifuged sequentially at 300 *g* for 10 minutes, 3000 *g* for 15 minutes and 20,000 *g* for 1 hour. Supernatants were filtered through 0.2 μm Stericup device (EMD Millipore, USA) and dialyzed overnight with Snakeskin 10 kDa MWCO dialysis tubing (ThermoFisher Scientific, USA) in TBS 30-fold volume of the supernatant. Dialyzed supernatants were centrifuged at 110,000 *g* for 2 hours. The pellet was resuspended to the original volume with TBS and centrifuged for additional 2 hours at 110,000 *g*. Pellets were resuspended in 1/50 original volume of TBS and protein amount was quantified using Quick Start™ Bradford Protein Assay (Bio-Rad, USA) according to the manufacturer's instructions. Extracellular vesicle preparations at concentrations of 1 – 2 mg/ml were stored at -80$^{o}$C until further use.

### 2.2.12 Staining of extracellular vesicles

#### 2.2.12.1 Staining with SYTO® RNASelect™ Green Fluorescent Stain

SYTO® RNASelect™ Green Fluorescent dye (ThermoFisher Scientific, USA) was diluted at a 1/5 ratio in DMSO. 100 µg of EV were stained with 1 µl diluted dye in 100 µl TBS (to achieve 10 µM dye concentration) for 30 minutes at 37°C. Meanwhile, Exosome Spin Columns (mW 3000) (ThermoFisher Scientific, USA) were hydrated with 650 µl PBS for 15 minutes at room temperature. Extraneous PBS was removed from the column by centrifugation at 350 *g* for 2 minutes. EV – dye mixture was loaded onto the columns and spun at 350 *g* for 2 minutes into microtubes to get rid of unbound dye molecules. Stained EV were stored at 4°C and used within a week of preparation.

#### 2.2.12.2 Staining with DiR

62.5 µg of EV were stained with 100 ng DiR dye (ThermoFisher Scientific, USA) per µg EV in 100 µl TBS. EV were incubated with the dye at 37°C for 1 hour. Unbound dye was washed as previously described in Section 2.2.12.1.

### 2.2.13 Uptake of EV by mouse cell lines

B16-FO, LLC1, MC-38, RAW264.7 and 4T1 cells were counted (as described for A549 cells in Section 2.2.6.1) and cultured in 12-well plates at a density of $2.5x10^5$ / ml a day prior to the experiment. E.G7 cells were counted at the day of the experiment and $2.5x10^5$ cells were transferred into 15 ml falcons. All cell lines were pre-treated with 100 µg/ml dextran sulfate (DS; Sigma Aldrich, USA) and 100 µg/ml chondroitin sulfate (CS; Sigma Aldrich, USA), or left untreated in 500 µl 5% FCS containing RPMI-1640 for 30 minutes at 37°C. For adherent cell lines, conditioned media was sucked and cells were washed with 1 ml fresh media. For E.G7 cells, volume was increased to 10 ml with media and cells were centrifuged at 400 *g* for 5 minutes. Cell lines were incubated with different concentrations of SYTO RNASelect stained EV for 2 hours at 37°C. EV concentrations were adjusted for each cell line to have 2-4 fold increase in fluorescent signal above the autofluorescence. Concentration of EV for each cell type is listed in Table 2.7.

**Table 2.7: EV concentrations**

| Cell Line | EV Concentration |
|---|---|
| B16-FO | 0.8 µg/ml |
| E.G7 | 1.6 µg/ml |
| LLC1 | 0.8 µg/ml |

| Cell Line | EV Concentration |
|---|---|
| MC-38 | 1.6 μg/ml |
| RAW264.7 | 3.2 μg/ml |
| 4T1 | 1.6 μg/ml |

At the end of the incubation period, E.G7 cells were washed with 9 ml of PBS and resuspended in 300 μl PBS. The remaining cells types were washed with 1 ml of PBS after sucking media, scraped and collected in 300 μl PBS. EV uptake ratios of different cell lines were assessed with flow cytometry. In some experiments, untreated cells were stained with anti-CD204 and REA control antibody (0.2 μl antibody in 50 μl PBS containing 2% BSA per sample) for 15 minutes on ice. Cells were washed with 1 ml PBS containing 2% BSA, centrifuged at 5200 rpm for 2 minutes and resuspended in 300 μl PBS containing 2% BSA. Cells pre-treated with DS and CS for 30 minutes and incubated with plain medium for 2 hours were also stained with Live/Dead dye as described in **Section 2.2.6.1**.

### 2.2.14 Uptake of EV by primary murine macrophages

Murine macrophages were induced to differentiate from bone marrow monocytes by treatment with 1 μg/ml of LPS or 10 ng/ml of FSL-1 for 4 days as described in Section 2.2.9. 1 x $10^5$ macrophages were pre-treated with 100 μg/ml DS or CS for 30 minutes in 200 μl of 5% RPMI Oligo or left untreated at 37$^o$C. After washing with 1 ml of media, cells were incubated with 1 μg/ml of SYTO RNASelect stained EV for 2 hours at 37$^o$C. Cells were washed with 1 ml PBS and resuspended in 250 μl of PBS. EV uptake potentials of different macrophage populations were assessed with flow cytometry.

### 2.2.15 Uptake of EV by human peripheral blood mononuclear cells

Human peripheral blood mononuclear cells (PBMCs) were isolated from apharesis collections as described in Section 2.2.1. The next day, 2x$10^6$ cells were pre-treated with 500 μg/ml DS, 500 μg/ml CS, or left untreated in 1 ml 5% FCS containing RPMI-1640 for 30 minutes at 37$^o$C. Cells were washed with 10 ml media and centrifuged at 400 *g* for 5 minutes. Cell pellets were resuspended in 500 μl of 5% FCS supplemented RPMI-1640 containing 800 ng/ml SYTO RNASelect stained EV. Cells were incubated for two additional hours and then stained with

fluorescence-conjugated anti-CD14, anti-CD19, anti-CD3 and anti-CD56 as described in Section 2.2.5. EV uptake ratios of different cell populations were assessed with flow cytometry.

### 2.2.16 *In vivo* biodistribution of EV

FVB mice were housed in the NIH Animal Facility, Bethesda, MD. All procedures conducted were in compliance with the ethical guidelines for the care and use of laboratory animals and approved by Animal Care and Use Committee (ACUC) of the National Institutes of Health. 6-8 week old female FVB mice were injected with 0.6mg of DS or CS in 100 µl of PBS from tail vein. Control mice were injected with the same amount of PBS. Two hours later in 15 µg of DiR stained EV were injected intravenously from tail vein in 100 µl PBS. Two hours later mice were first imaged alive with Maestro™ 2 imaging system (Perkin Elmer, USA) with the help of Dr. Avinash Srivatsan from NIBIB. Mice were then utinized; and excised organs and plasma were imaged again.

### 2.2.17 Statistical analyses

All statistical analyses were performed in GraphPad Prism 6.0 software, if not otherwise stated. Comparison of data for *in vitro* stimulation assays were performed with two tailed t-test. For comparison of expression levels of multiple markers in macrophages, EV uptake in cell lines multiple t-test with Bonferroni correction (alpha-error < 0.05) was performed.

# Chapter 3

# Results

## 3.1 Efforts to Regulate Macrophage Differentiation

### 3.1.1 PAM3 and R848 induce mMDSC to differentiate into M1- and M2-like macrophages

Intratumoral injection of TLR7 and TLR9 agonists eradicates established tumors. One of the critical mechanisms involves inducing the differentiation of tumor localized mMDSC into anti-tumoricidal macrophages [360, 362]. The relevance of these findings was confirmed by stimulating human mMDSC with TLR agonists for 3 days. Based on changes in the expression level of the M2-like macrophage associated marker CD200R and marker of macrophage activation 25F9, we showed that the TLR7/8 agonist R848 drives MDSC to differentiate into M1-like macrophage whereas the TLR2/1 agonist PAM3 induces them to mature into M2-like macrophage [230]. The reproducibility of these patterns was verified by increasing the number of donors, using additional markers to discriminate between M2-like vs M1-like macrophages and changing *in vitro* culture conditions. In the absence of any further stimulus, <20% of mMDSC survive in vitro and differentiated into macrophages by acquiring the 25F9 marker . We postulate these represent MDSC that had been activated in vivo prior to isolation. In contrast, >70% mMDSC stimulated with 3 μg/ml of R848 or 1 μg/ml of PAM3 for 3 days matured into macrophages (Figure 3.1A). Further phenotypic characterization of M2-like macrophages included expression of the scavenger receptor CD163 and mannose receptor CD206, both of which are expressed at high levels by M2-like macrophages [85, 88]. Stimulation of mMDSC with TLR agonists tended to generate a heterogeneous population of macrophage. >50% of the macrophages generated by R848 lacked CD163 and CD206 and thus were phenotypically characterized as M1-like. On the other hand, ≈20% of the macrophages in R848 cultures and >60% of the macrophages in the PAM3 cultures co-expressed CD163 and CD206, suggesting that these cells represented M2-like macrophages (Figure 3.1B). This difference in frequency of M1- vs M2-like macrophages was analyzed by calculating their ratio. ~2.5-fold more M1-like macrophages were present in R848 cultures, whereas ~3-fold more M2-like macrophages were present in PAM3 cultures (Figure 3.1C). Culturing mMDSC with TLR agonists for additional 2 days slightly increased the percentage of active macrophages but did

not significantly alter the pattern of macrophage differentiation (Figure 3.1D-E-F-G).

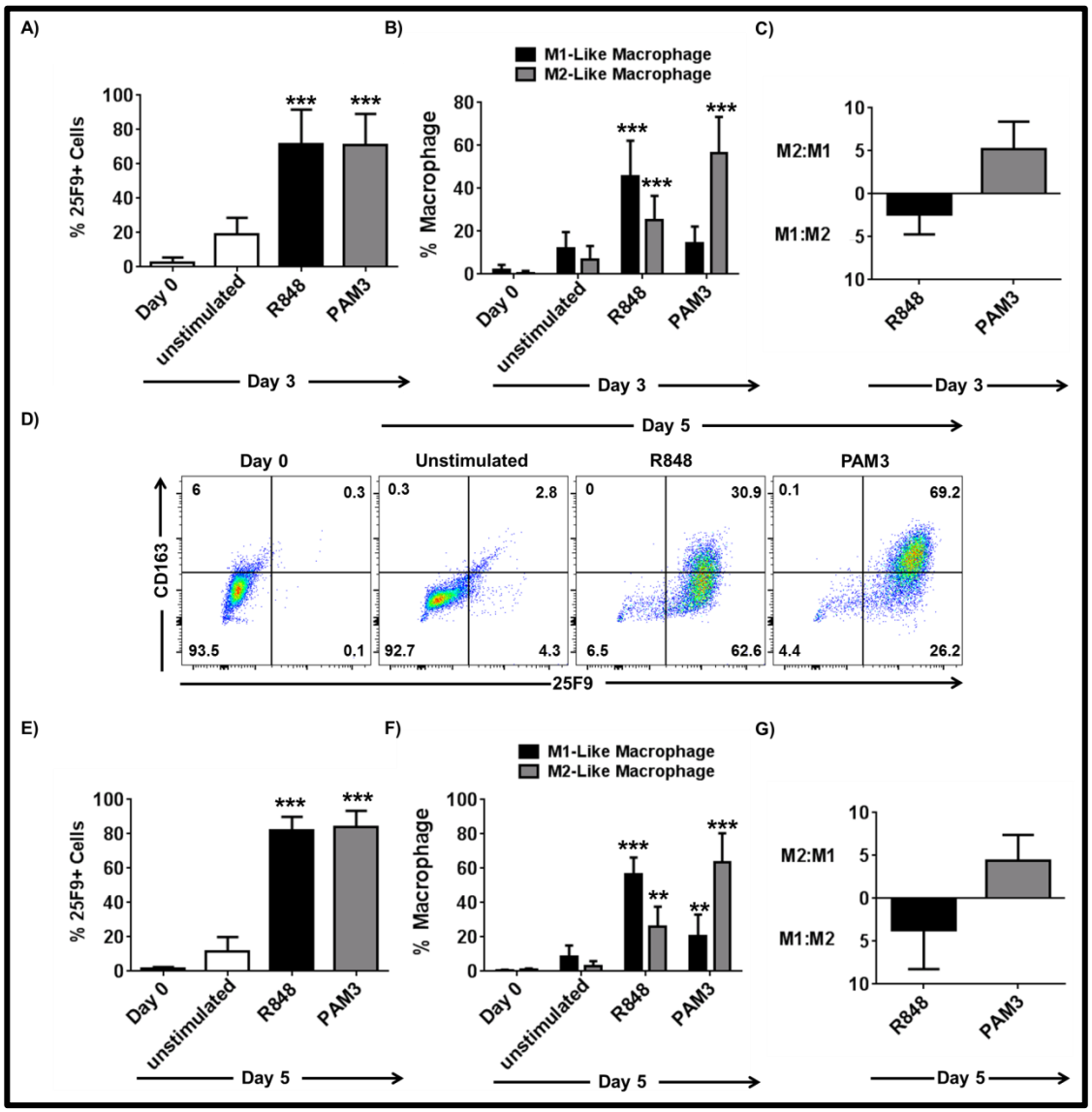


**Figure 3.1: TLR agonists selectively drive mMDSC differentiation into M1- and M2-like macrophages.**

*A) Percentage of 25F9+ monocytes following 3 of treatment with R848 or PAM3 (mean ± SD of 24-26 independently analyzed donors). B) Percentage of M1- and M2-like macrophages following stimulation with R848 or PAM3 for 3 days (mean ± SD of 24-26 independently analyzed donors) C) Ratio of macrophages from each sample evaluated on Day 3. D) Representative dot plots depicting change in 25F9 and CD163 levels following stimulation of mMDSC with R848 or PAM3 for 5 days. E) Frequency of cells expressing 25F9 after 5 days of stimulation with R848 or PAM3 (mean ± SD of 7-15 independently analyzed donors). F) Percentage of M1- and M2-like macrophages following stimulation with R848 or PAM3 for 5 days (mean ± SD of 7-15 independently analyzed donors). G) Ratio of macrophages from each sample evaluated for 5 days. ** p<0.01; *** p<0.001 R848/PAM3 treated samples vs. unstimulated samples.*

### 3.1.2 Co-stimulation of TLR7 and TLR8 is required for effective M1-like macrophage polarization of mMDSC

In order to identify whether stimulation through both TLR7 and TLR8 is required for R848-induced M1-like macrophage differentiation, human mMDSC were incubated with TLR7 and/or TLR8 specific agonists. The TLR7 specific agonist 3M-05 had limited effect and failed to induce macrophage to significantly differentiate from mMDSC (Figure 3.2A-B). In contrast, the TLR8 specific ligand CL-075 alone or in combination with 3M-055 promoted maturation of more than 80% of the mMDSC (Figure 3.2A-B). Phenotypic characterization of these macrophages showed that a majority of these macrophages were M2-like. In contrast, more than 60% of the macrophages generated by the combination of 3M-055 plus CL-075 were M1-like (Figure 3.2C). These results demonstrate that activation of both TLR7 and TLR8 is required to recapitulate R848-driven macrophage differentiation.

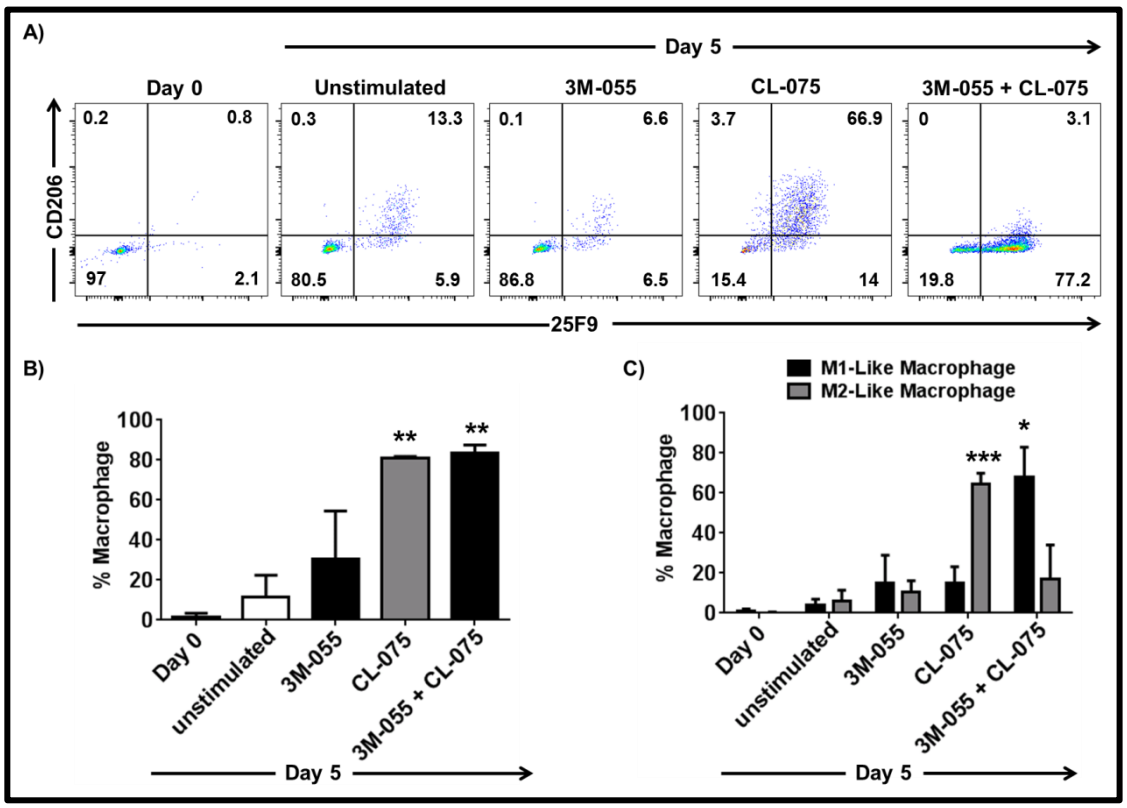


**Figure 3.2: Stimulation through both TLR7 and TLR8 is required for differentiation of mMDSC into M1-like macrophages.**

*A) Representative dot plots depicting changes in the expression of macrophage markers. B) Percentage of 25F9+ cells following treatment with 3M-055, CL-075 or their combination for 5 days (mean ± SD of 3 independently analyzed donors). C) Frequency of M1- and M2-like macrophages following stimulation with 3M-055, CL-075 or their combination for 5 days (mean ± SD of 3 independently analyzed donors). * p<0.05; ** p<0.01; *** p<0.001 unstimulated vs. stimulated samples.*

### 3.1.3 IL-6 and IL-10 are important but not sufficient to induce the complete differentiation of mMDSC

Previous results from our group showed that both R848 and PAM3 could stimulate mMDSC to produce IL-6. PAM3 treated samples uniquely produced IL-10 while R848 treated samples preferentially secreted IL-12 [230]. My initial studies sought to confirm these findings by measuring the cytokines present after mMDSC were treated for 3 days in vitro. Both IL-6 and IL-10 were undetectable in cultures of unstimulated cells. In contrast, stimulation of mMDSC with either R848 or PAM3 induced the secretion of IL-6 with R848 triggering the production of the larger amount of this cytokine (Figure 3.3, Graph 1). Unexpectedly, a similar pattern was observed for IL-10 with R848 stimulated cultures containing 3-fold more IL-10 than those incubated with PAM3 (Figure 3.3, Graph 2).

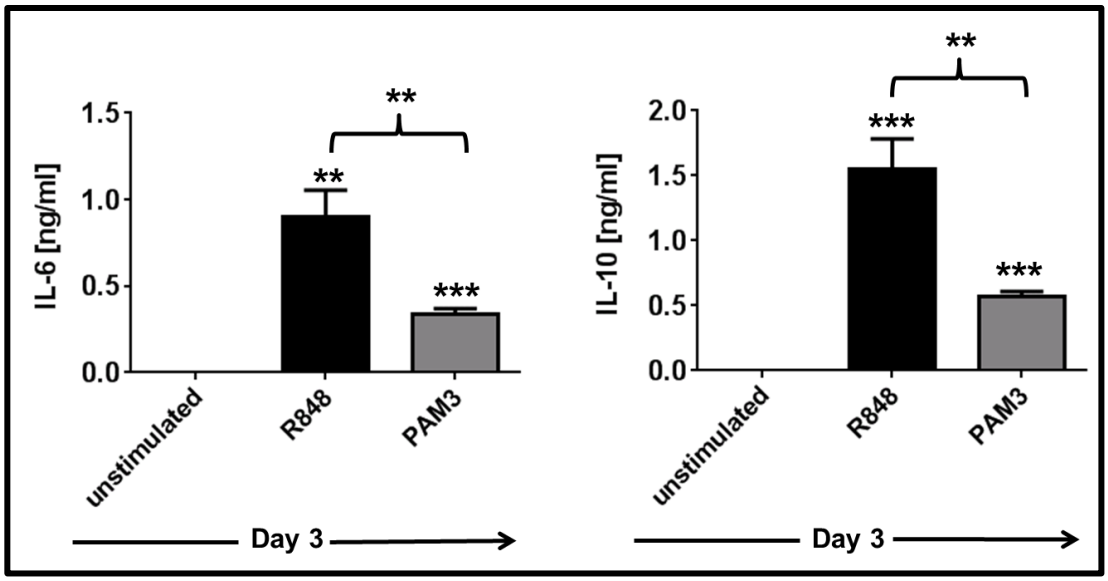


**Figure 3.3: PAM3 and R848 induce mMDSC to secrete IL-6 and IL-10.**

*Data shown are the mean cytokine concentration (± SD) of four donors. ** p<0.01; *** p<0.001 R848 or PAM3 cultures vs. untreated cultures.*

The production of IL-6 and IL-10 might play a central role in the generation of macrophage during PAM3- and R848-induced differentiation. To assess possible contribution of these cytokines, IL-6 and IL-10 neutralizing antibodies were added to the cultures on Day 0 at a concentration of 25 μg/ml. Neutralization of IL-6 or IL-10 interfered with the R848-dependent generation of M1-like macrophage as seen by the 3 and 4 fold reduction in M1-like macrophage frequency after the addition of anti-IL-6 or anti-IL-10 Abs ($p<0.001$ and $p<0.05$; Figure 3.4A). Similarly, PAM3-induced differentiation was partially dependent on both IL-6 and IL-10. Neutralization of either one of these cytokines decreased the percentage of M2-like macrophages by ≈2.5 fold ($p<0.01$ and $p<0.001$) (Figure 3.4B). Antibody isotype controls did not alter the generation of macrophages in R848 or PAM3 stimulated samples (Figure 3.4).

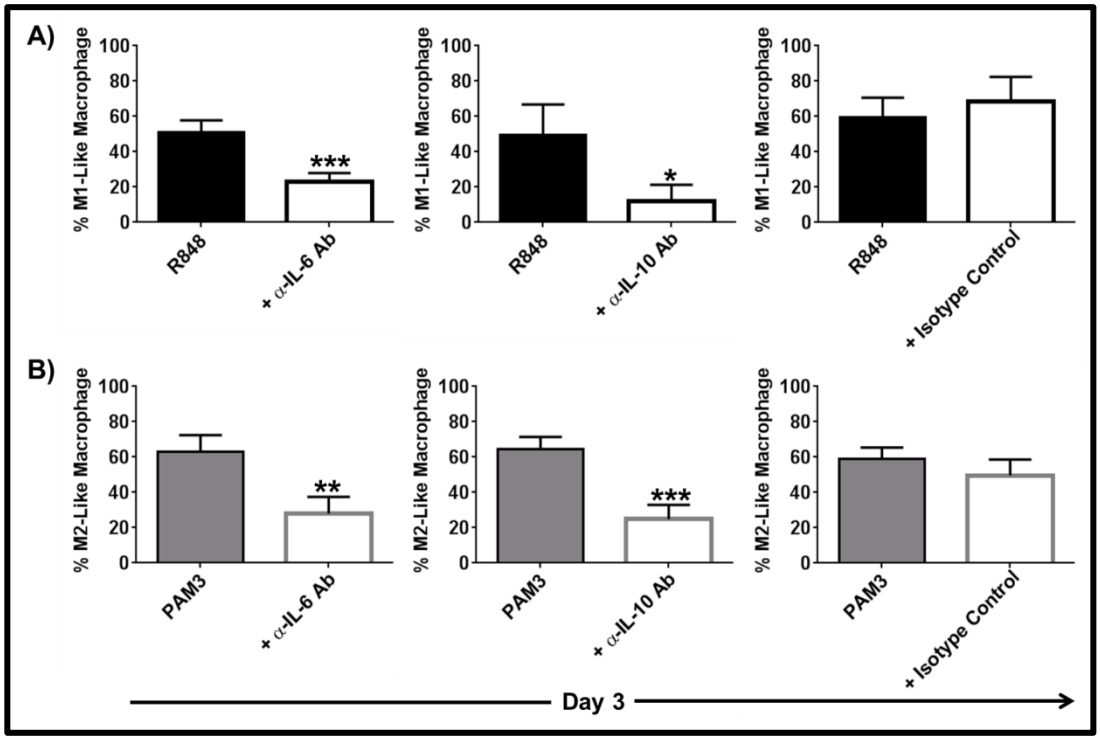


**Figure 3.4: IL-6 and IL-10 have regulatory roles in R848- and PAM3-induced differentiation of mMDSC.**

*A) Percentage of M1-like macrophage after R848 treatment and B) Percentage of M2-like macrophage after PAM3 treatment of samples in the presence of neutralizing antibodies against IL-6 or IL-10 (isotype control also included). Data represent the (mean ± SD of four independently analyzed donors). * p<0.05; ** p<0.01; *** p<0.001 neutralizing antibody containing cultures vs. stimulant cultures.*

Recombinant IL-6 and IL-10 were added to mMDSC cultures for 3 or 5 days and their contribution to the differentiation process assessed. Preliminary experiments established that a minimum of 50 ng/ml of cytokine reproducibly induced MDSC differentiation and that the same effect was observed using 500 ng/ml. All experiments using recombinant cytokines were therefore conducted at an initial concentration of 500 ng/ml to avoid the need to replenish the cytokines over time. The activity of IL-6 and IL-10 on mMDSC was initially evaluated by incubating cells for 3 days. Both cytokines triggered a significant increase the percent of active macrophages (Figure 3.5A). However, these changes failed to achieve statistical significance due to heterogeneity in the response of cells from different donors (N=4) (Figure 3.5B). To overcome this limitation, the duration of the experiment was extended to 5 days. After 5 days in vitro, approximately half of the cells survived and differentiated into macrophages when cultured with IL-6 or IL-10. This was 3-6 fold higher than observed in the absence of stimulation with $p<0.001$ (Figure 3.5C). As with shorter cultures, considerable inter-donor variation was observed in the response to IL-6 and IL-10. A majority of samples responded to

IL-10 stimulation by preferentially generating M1-like macrophages whereas the response to IL-6 was highly heterogeneous (Figure 3.5D-E).

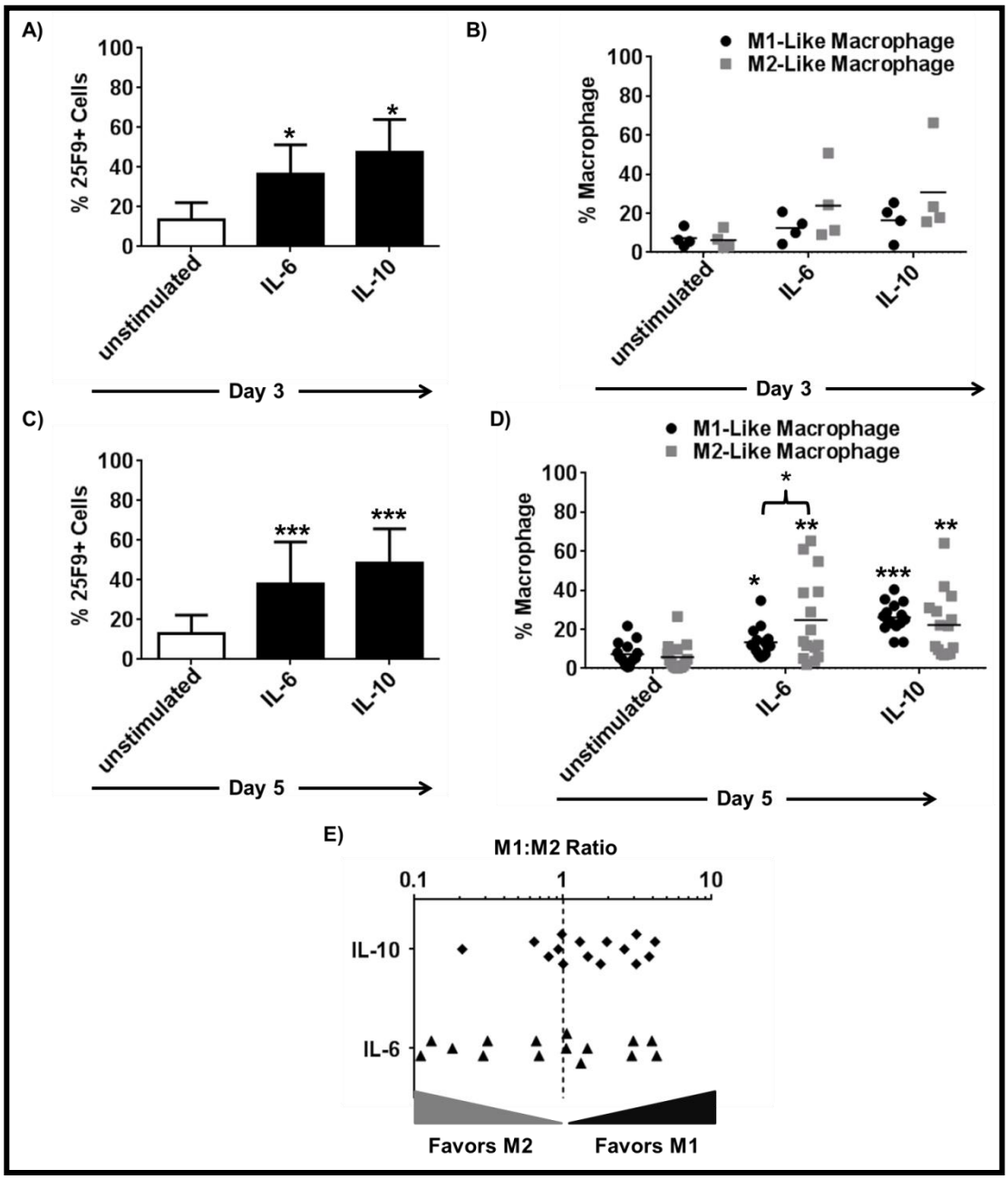


**Figure 3.5: IL-6 and IL-10 partially support macrophage differentiation from mMDSC.**

*A) Percentage of 25F9+ cells and B) Frequency of M1- and M2-like macrophages following stimulation with IL-6 or IL-10 for 3 days (mean ± SD of 4 independently analyzed donors). C,D) Results of the same experiment conducted for 5 days (mean ± SD of 15 independently analyzed donors). E) Ratio of M1-to-M2-like macrophages from each sample evaluated for 5 days.* $p<0.05$; ** $p<0.01$; *** $p<0.001$ IL-6 or IL-10 stimulated vs. unstimulated samples.*

Given the observed variability, we evaluated the effect of IL-6 plus IL-10 in combination. The generation of macrophages from mMDSC was slightly but not significantly improved by the addition of IL-6 plus IL-10 (Figure 3.6A). Moreover, the frequency of M1- versus M2-like macrophages generated from mMDSC showed the same range of variability observed using single cytokines (Figure 3.6B). From this we concluded that IL-6 and IL-10 contributed to but were insufficient to drive the differentiation of mMDSC into macrophages, and that these cytokines only partially recapitulated the effects of R848 and PAM3.

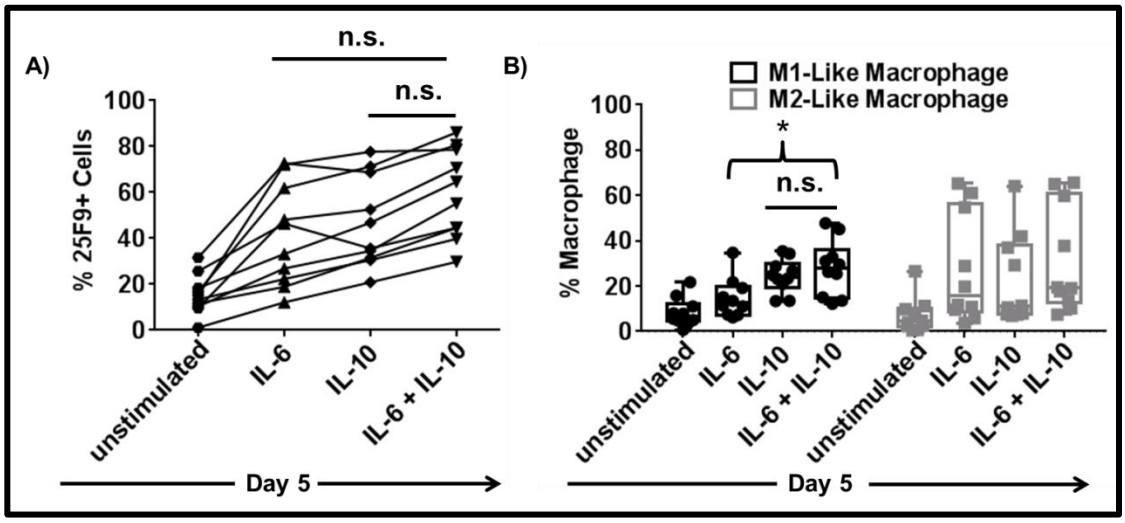


**Figure 3.6: Addition of IL-6 plus IL-10 has the same effect as each cytokine separately on mMDSC differentiation.**

*A) Percentage of 25F9+ cells following treatment IL-6 or IL-10 alone vs the combination for 5 days (mean ± SD of 10 independently analyzed donors). B) Percentages of M1- and M2-like macrophage after stimulation with IL-6 or IL-10 alone vs their combination for 5 days (mean ± SD of 10 independently analyzed donors). * $p<0.05$.*

### 3.1.4 TNFα but not IL-12 supports the differentiation of mMDSCs into M1-like macrophages

Intracellular cytokine staining showed that mMDSC produced IL-12 when stimulated with R848 but not with PAM3 [230]. However when supernatants from these cultures were analyzed by ELISA, IL-12 could not be detected after stimulation with either PAM3 or R848 (assay sensitivity was 45 pg/ml). In contrast, TNFα could be detected in the supernatants of mMDSC cultures stimulated with R848 but not PAM3 (Figure 3.7).

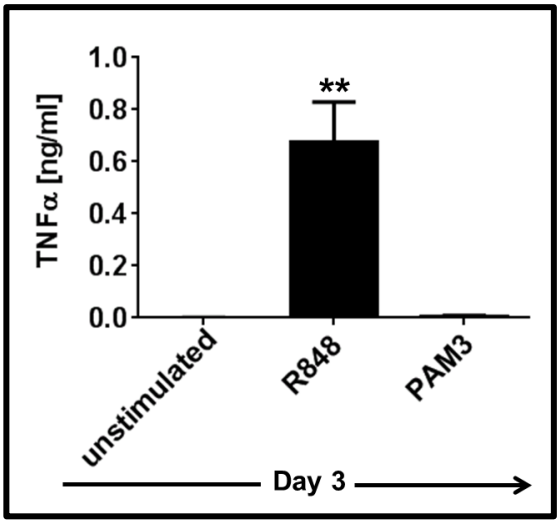


**Figure 3.7: TNFα is secreted in the course of R848-induced mMDSC differentiation.**

*Data show the TNFα concentration in culture supernatants on day 3 (mean ± SD of four donors). ** p<0.01 R848 treated samples vs. unstimulated or PAM3 stimulated samples.*

To determine whether any/all of these cytokines were required to enable M1-like macrophage differentiation of mMDSC, neutralizing antibodies were added to R848 stimulated cultures for 3 days. Despite the inability to detect IL-12 in culture supernatants by ELISA, neutralization of IL-12 reduced the generation of M1-like macrophages by ≈50% (Figure 3.8A, Graph 1). Inhibiting TNFα had an even greater effect in that it almost completely abolished R848-dependent M1-like macrophage differentiation (Figure 3.8A, Graph 2). The selectivity of these responses was confirmed by examining the effects of neutralizing Abs on PAM3 stimulated mMDSC. Neither anti-IL-12 nor anti-TNFα Ab reduced the frequency with which M2-like macrophage were generated (Figure 3.8B).

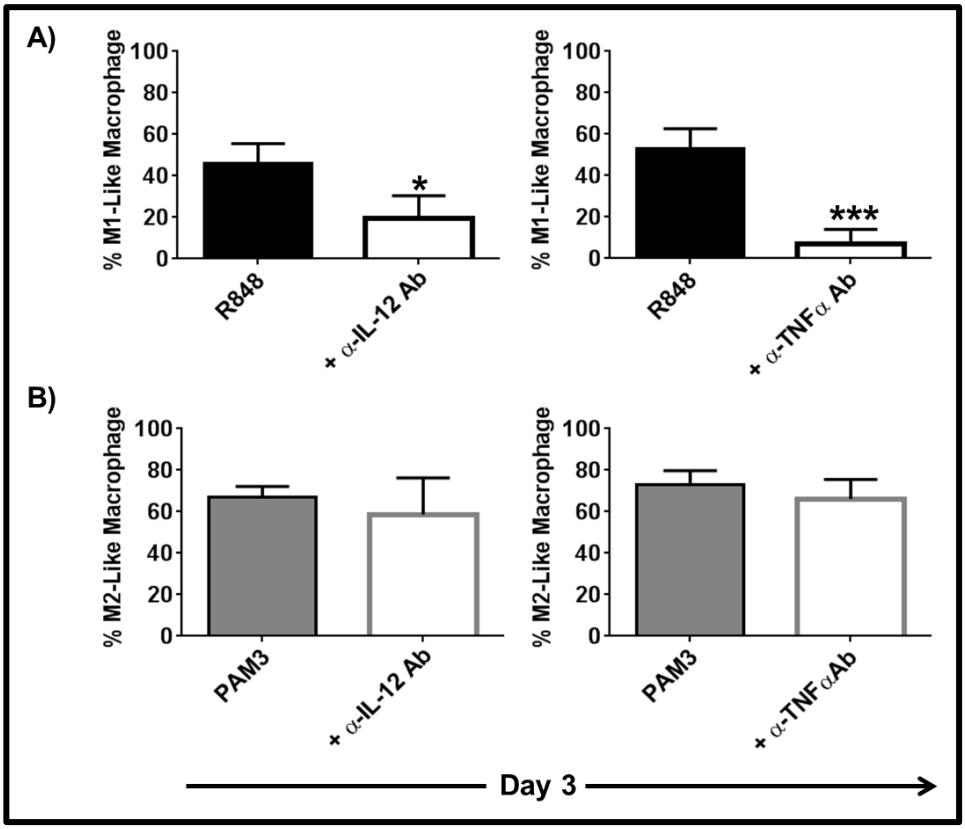


**Figure 3.8: IL-12 and TNFα regulate R848- but not PAM3-induced macrophage differentiation from mMDSC.**

*A) Percentage of M1-like macrophage in R848 treated samples in the presence of neutralizing antibodies against IL-12 or TNFα (mean ± SD of four independently analyzed donors). B) Percentage of M2-like macrophage in PAM3 treated samples in the presence of neutralizing antibodies IL-12 or TNFα (mean ± SD of three and four independently analyzed donors, respectively). * $p<0.05$; *** $p<0.001$ neutralizing antibody containing cultures vs. stimulant cultures.*

Contribution of IL-12 and TNFα to M1-like macrophage polarization was evaluated by culturing mMDSC with recombinant cytokines for 3 or 5 days. IL-12 alone failed to support differentiation (Figure 3.9A). In contrast, TNFα induced 25% of MDSC to express an M1 phenotype after 3 days in culture ($p<0.05$) (Figure 3.9B; Graph 1). This rose to 50% after 5 days of culture. There was no effect on M2-like macrophage frequency (Figure 3.9B; Graph 1). These results suggest that TNFα plays a major role in the generation of M1-like macrophages whereas IL-12 contributes to such differentiation but plays a lesser role. However, it was noteworthy that TNFα alone did not recapitulate the full effect of R848, suggesting that this single cytokine was insufficient to mimic the activity of the TLR agonist.

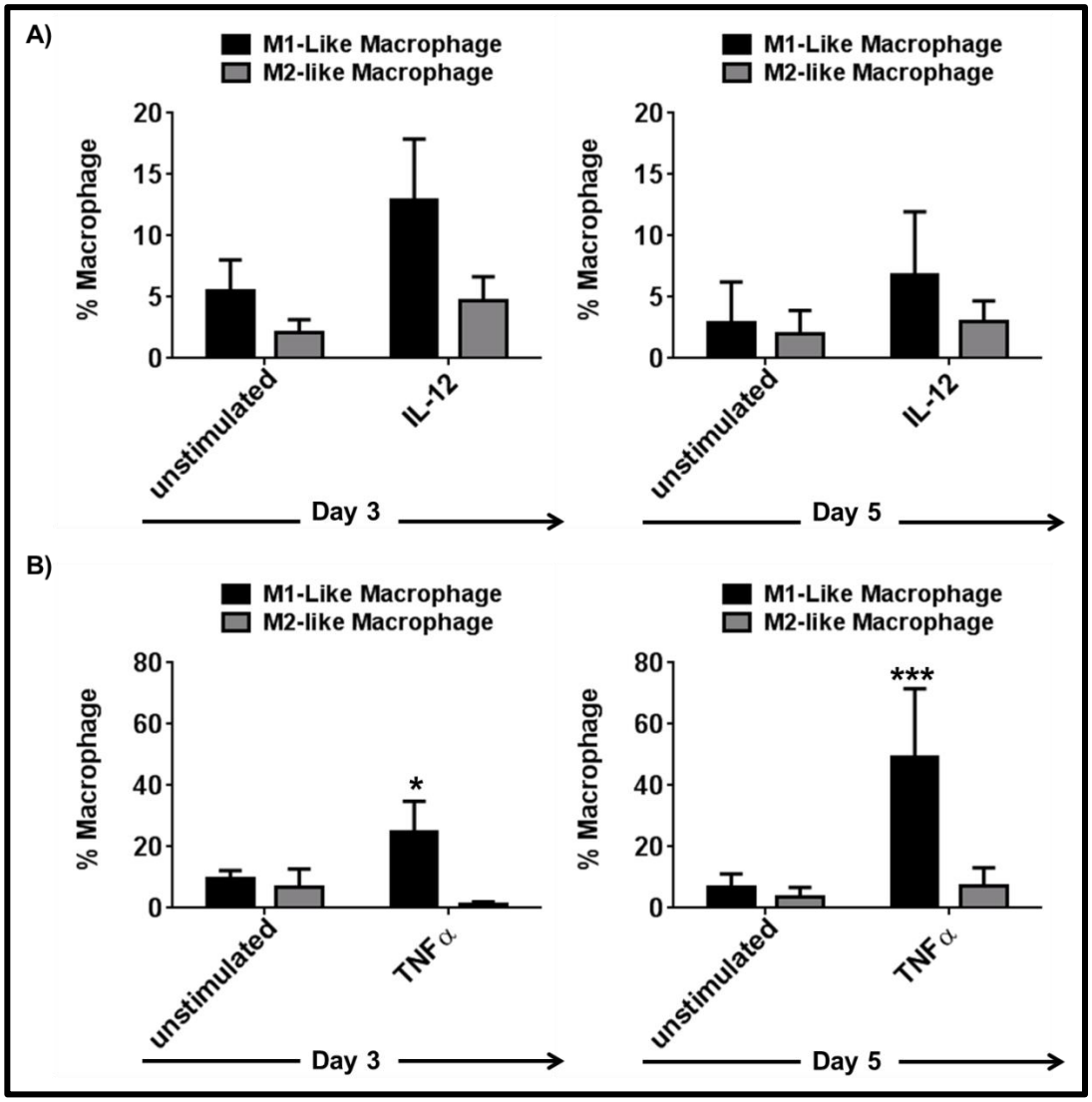


**Figure 3.9: TNFα but not IL-12 supports the differentiation of mMDSC into M1-like macrophage.**

*A,B) Mean percentage (± SD) of M1- and M2-like macrophages in culture when mMDSC were treated with IL-12 (A) or TNFα (B) for 3 or 5 days (N = 4-10 independently analyzed donors/time point). * p<0.05; *** p<0.001 TNFα treated samples vs. untreated samples.*

### 3.1.5 Combining TNFα with IL-6 recapitulates the effect of R848 on mMDSC

Since single cytokines failed to replicate the effect of R848, cytokine combinations were tested for their ability to mimic the M1-like macrophage polarizing activity of R848. Our previous experiments established that TNFα played a significant role in the differentiation of mMDSC into M1-like macrophages. Thus, we focused on combination of TNFα with IL-6, IL-10 and IL-12, all of which had some effect on mMDSC differentiation. Whereas individual cytokines (with the exception of IL-12) and cocktails generated significant numbers of macrophages after 5 days of culture only the combination of TNFα with IL-6 was more effective than TNFα in driving macrophage differentiation (p<.05; Figure 3.10A). Phenotypic characterization of these

cells revealed that more 60% of the macrophages generated in the presence of IL-6 plus TNFα were M1-like macrophages which was significantly higher than the percentages observed in samples stimulated with TNFα only (Figure 3.10B). Even though the combinations of TNFα with IL-10 and IL-12 were slightly better than TNFα in generating M1-like macrophages, these differences were not statistically significant. For these reasons, further experiments focused on the combination of IL-6 with TNFα.

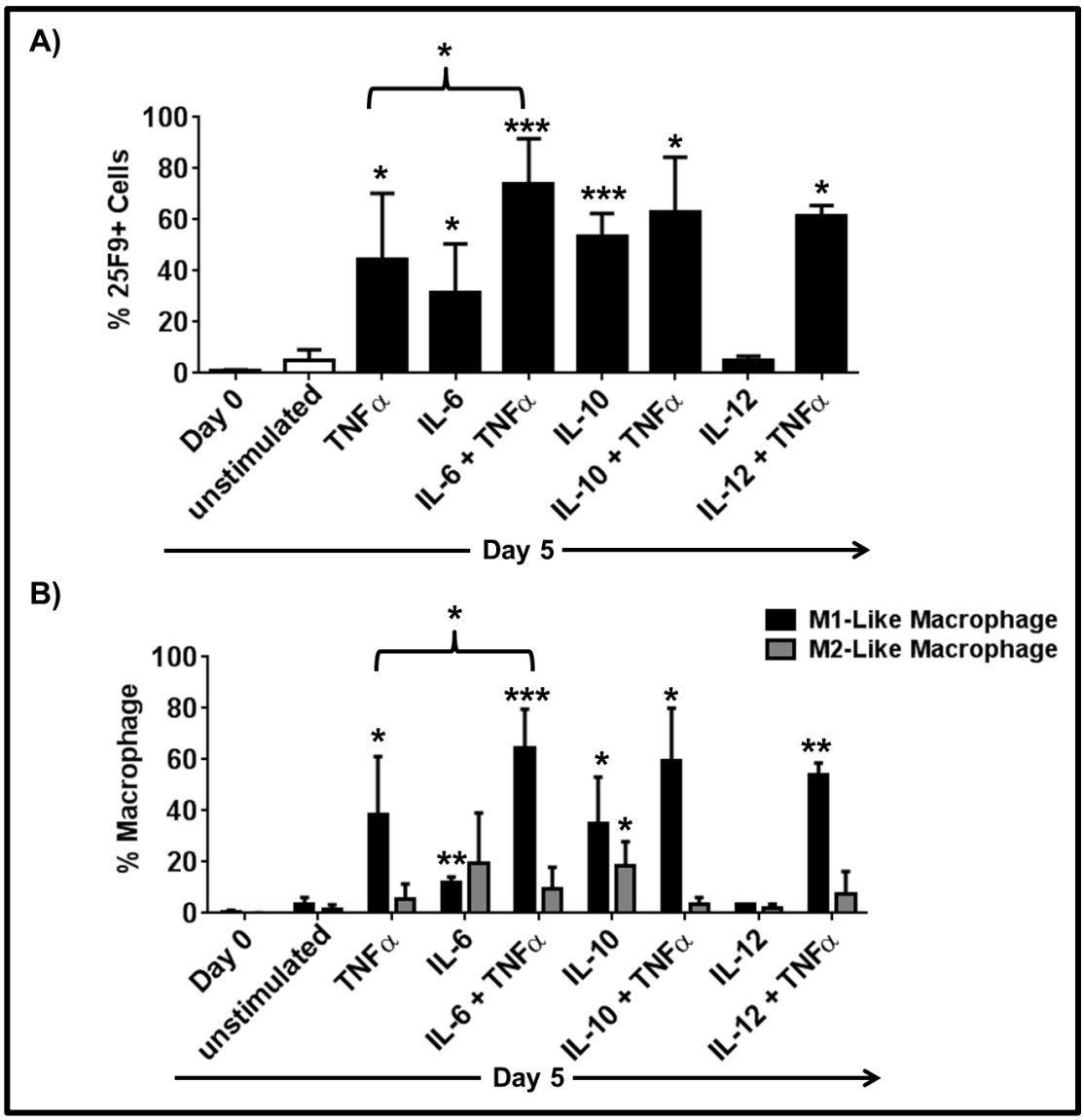


**Figure 3.10: TNFα and IL-6 cocktail is the most effective cytokine combination inducing M1-like macrophage differentiation.**

*A) Percentage of 25F9+ cells following treatment TNFα alone or in combination with IL-6, IL-10 and IL-12 for 5 days (mean ± SD of 2-6 independently analyzed donors). B) Frequency of M1- and M2-like macrophages following stimulation with TNFα combination for 5 days (mean ± SD of 2- independently analyzed donors). * p<0.05; ** p<0.01, *** p<0.001 unstimulated vs. stimulated samples.*

To compare the polarizing activity of IL-6 plus TNFα relative to R848, mMDSC from three healthy donors were incubated with these agents for 5 days. Both R848 and the cytokine combination caused >80% of the mMDSC to mature into macrophages (Figure 3.11A-B). Yet, stimulation with combination of IL-6 with TNFα significantly generated more M1- and fewer M2-like macrophages than did R848 (Figure 3.11A-C). This resulted in an M1:M2-like macrophage ratio following cytokine combination treatment that was almost 20-fold higher than that induced by R848 ($p<.001$; Figure 3.11C).

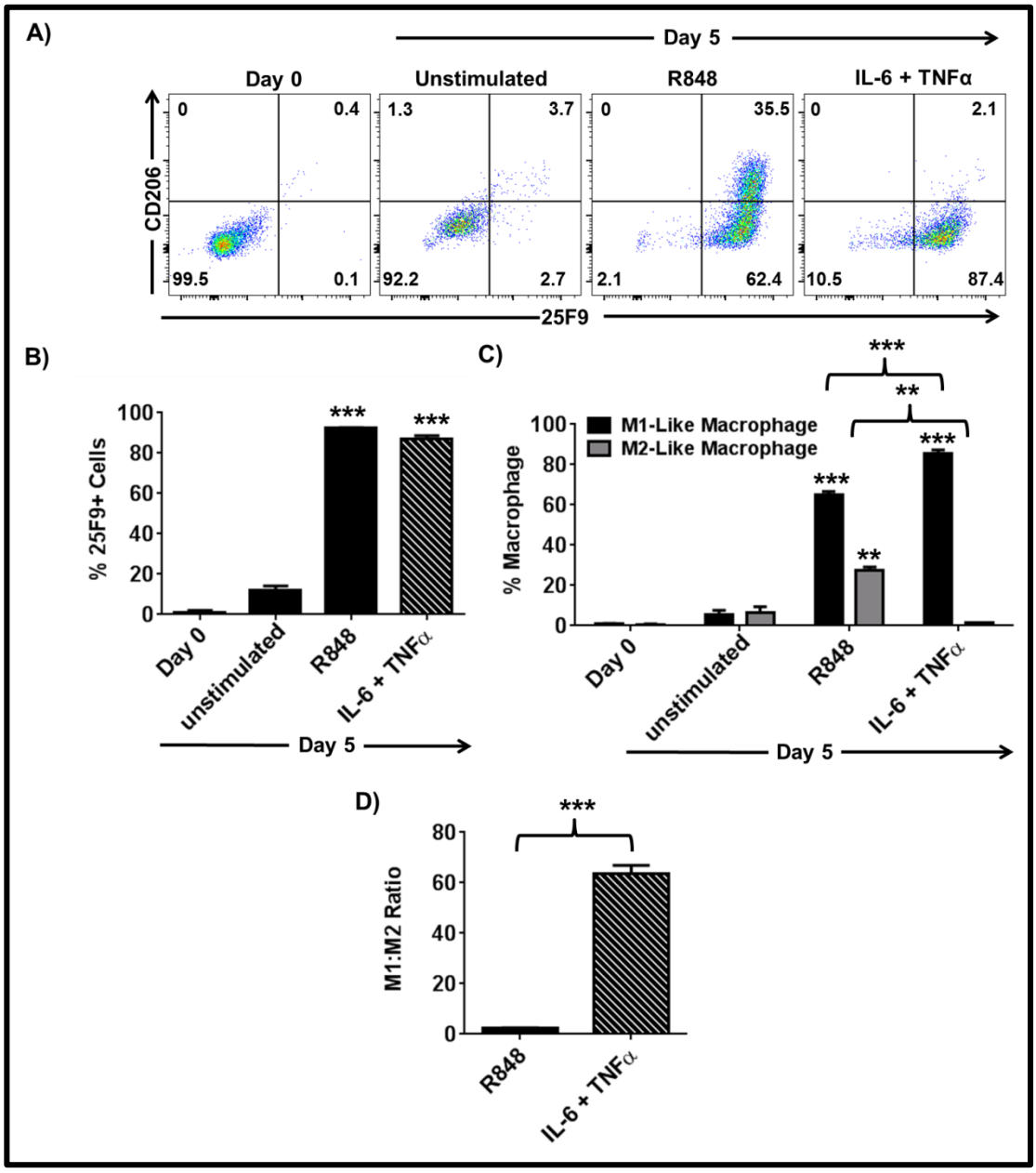


**Figure 3.11: Combination of IL-6 with TNFα is superior to R848 in generating M1-like macrophages.**

*A) Representative dot plots depicting changes in CD206 and 25F9 expression upon differentiation. B) Percent of cells expressing the active macrophage marker 25F9 (mean ± SD*

*of 3 independently analyzed donors). C) Percentages of M1- and M2-like macrophages (mean ± SD of 3 independently analyzed donors). D) Ratio of M1-to-M2-like macrophages (mean ± SD of 3 independently analyzed donors). ** p<0.01; *** p<0.001 unstimulated vs. R848/IL-6 + TNFα stimulated samples.*

### 3.1.6 M1-like macrophages generated by R848 vs IL-6 and TNFα combination differ in morphology

The shape of a macrophage is influenced by its polarization state in response to stimuli. The differentiation of monocytes into macrophages is accompanied by a change in morphology: the cells become elongated [514]. Unstimulated mMDSC were small, fragmented and unattached, which are hallmarks of dying monocytes. In contrast, cells stimulated with R848 or the combination of IL-6 plus TNFα were enlarged nearly 3-fold reaching ≈30 μm in diameter. These cells were attached to the surface of the plates and had short dendrites, consistent with the description of pro-inflammatory macrophages. While the cellular morphology of macrophages generated in the presence of R848 or IL-6 plus TNFα were similar, R848-induced macrophages were distributed throughout the plate whereas macrophages generated in the presence of the cytokine combination were clustered (Figure 3.12).

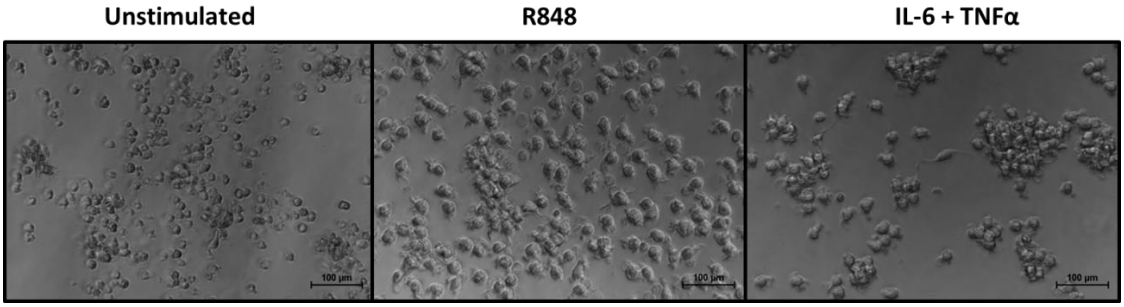


**Figure 3.12: Distinct morphology of unstimulated, R848 or IL-6 + TNFα stimulated mMDSC at Day 5.**

### 3.1.7 Macrophages generated by stimulation of mMDSC with IL-6 and TNFα lyse tumor cells effectively

Our phenotypic analysis demonstrated that the combination of IL-6 plus TNFα was superior to R848 at inducing mMDSC to differentiate into M1-like macrophage. To examine the function of these cells, M1-like macrophages generated after 5 days of treatment with R848 or IL-6 plus TNFα treatment were incubated with A549 tumor cells as described in Section 2.2.6.1. Although macrophage from different donors varied in their ability to lyse the tumor cells, those generated by treatment with R848 lysed approximately 7% of the A549 cells after 6 hours of incubation. By comparison, macrophages generated by treatment with IL-6 plus TNFα lysed nearly twice as many tumor cells (Figure 3.13). Control unstimulated mMDSC did not increase tumor cell lysis over background. These results established that the M1-like macrophages

generated from mMDSC in the presence of R848 or IL-6 plus TNFα were functionally active and that IL-6 plus TNFα produced macrophages that were more efficient at tumor cell lysis.

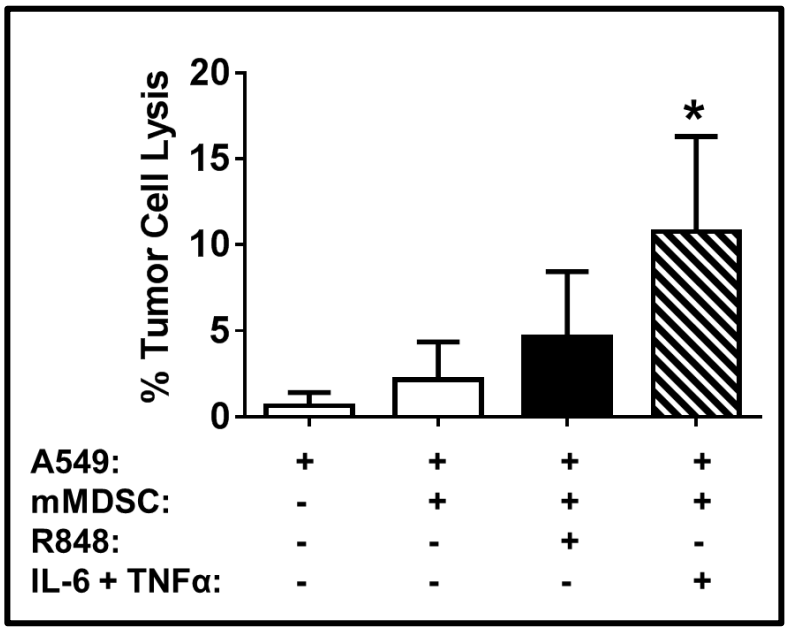


**Figure 3.13: mMDSC stimulated with R848 or the combination of IL-6 plus TNFα effectively lyse tumor cells.**

*Percent of dead A549 cells following 6 hours of incubation with unstimulated or R848 and IL-6 plus TNFα stimulated mMDSC (mean ± SD of four independently analyzed donors). * $p<0.05$ IL-6 plus TNFα treated samples vs. unstimulated samples.*

### 3.1.8 IFNγ is efficient driver of M1-like macrophage differentiation from mMDSC

IFNγ is an important regulator of classically activated macrophages [515, 516]. We considered the possibility that it could be play a role in the differentiation of mMDSC into M1-like macrophages. To test this hypothesis, IFNγ was neutralized in R848 cultures. Although the percentage of M1-like macrophages in such cultures fell, the effect was not significant (Figure 3.14A). The activity of IFNγ was further examined by adding recombinant cytokines to mMDSC cultures for 5 days. Comparison of R848 vs IFNγ showed that both stimuli triggered mMDSC maturation (Figure 3.14B). While the absolute frequency of M1-like macrophages was similar, R848 also induced a significant portion (≈20%) of the cells to become M2-like macrophages (Figure 3.14C). In contrast, IFNγ treated samples generated very few M2-like macrophages and thus had significantly higher M1-to-M2-like macrophage ratio (Figure 3.14D).

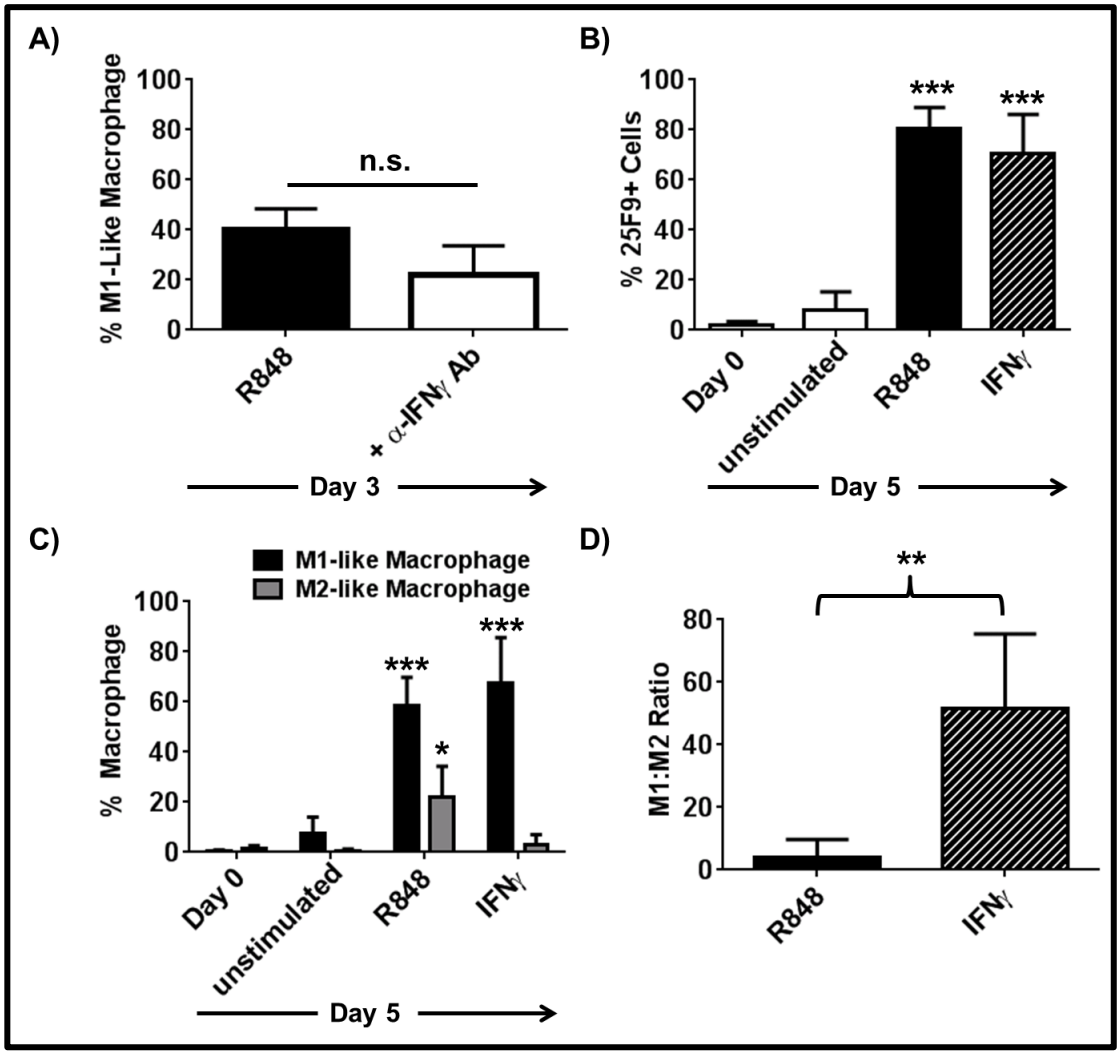


**Figure 3.14: IFNγ polarizes mMDSC towards M1-like macrophages.**

*A) Percentage of M1-like macrophage in R848 treated samples in the presence of neutralizing antibodies against IFNγ. Data represent the mean ± SD of three independently analyzed donors. B) Percentage of 25F9+ monocytes following 5 days of stimulation with R848 or IFNγ. Mean ± SD of 5 independently analyzed donors. C) Percentage of M1- and M2-like macrophages following stimulation with R848 or IFNγ for 5 days. Mean ± SD of 5 independently analyzed donors. D) Ratio of macrophages from each sample evaluated at Day 5. * p<0.05; *** p<0.001 R848/IFNγ treated samples vs. unstimulated samples.*

### 3.1.9 Regulatory networks of R848, IFNγ and IL-6 plus TNFα-dependent differentiation of mMDSC

The results shown above indicated that IFNγ was not a primary regulator of R848-induced M1-like macrophage differentiation. Yet it was as effective as the combination of IL-6 plus TNFα in driving mMDSC to polarize into M1-like macrophages. To identify the core network responsible for the maturation of mMDSC into M1-like macrophage, we analyzed and compared the gene expression pattern triggered by R848, IL-6 plus TNFα, and IFNγ stimulated samples. Previous *in vivo* and *in vitro* studies demonstrated that relevant signaling networks

tend to become activated within a few hours of macrophage differentiation [230, 517, 518]. For this reason, changes in gene expression were assessed at the 4 hour time point by identifying up-regulated genes in stimulated samples vs baseline expression of untreated cells from the same donor (N=5). A full list of genes upregulated >2-fold following R848, IFNγ or IL-6 plus TNFα stimulation is provided in Appendix Table 1. Notably, each of these stimulants up-regulated discrete genes sets consistent with their differential effects on mMDSC polarization. However mapping these genes into the regulatory networks using Ingenuity Pathway Analysis (IPA) software identified three convergent signaling pathways used in common by all three stimulants. The strongest association was with the NF-κB complex, suggesting that this is the main axis driving M1-like macrophage polarization (Figure 3.15). Although TNFα was predicted to have a central role in polarization triggered by all three stimulants, genes selectively up-regulated following R848 treatment had the strongest association with TNFα consistent with the empirical findings. IFNγ-linked pathways, particularly IRF7 and STAT1/2 signaling (which was also linked to NF-κB), were also identified as common nodes, indicating their importance in M1-like macrophage differentiation (Figure 3.15). These observations suggest that despite their differences, R848, IFNγ, and IL-6 plus TNFα treatment activated shared pathways to drive the differentiation of mMDSC into M1-like macrophages. These pathways involved the transcription factors NF-κB, STAT1/2 and IRF7, and the pro-inflammatory cytokines IFNγ and TNFα.

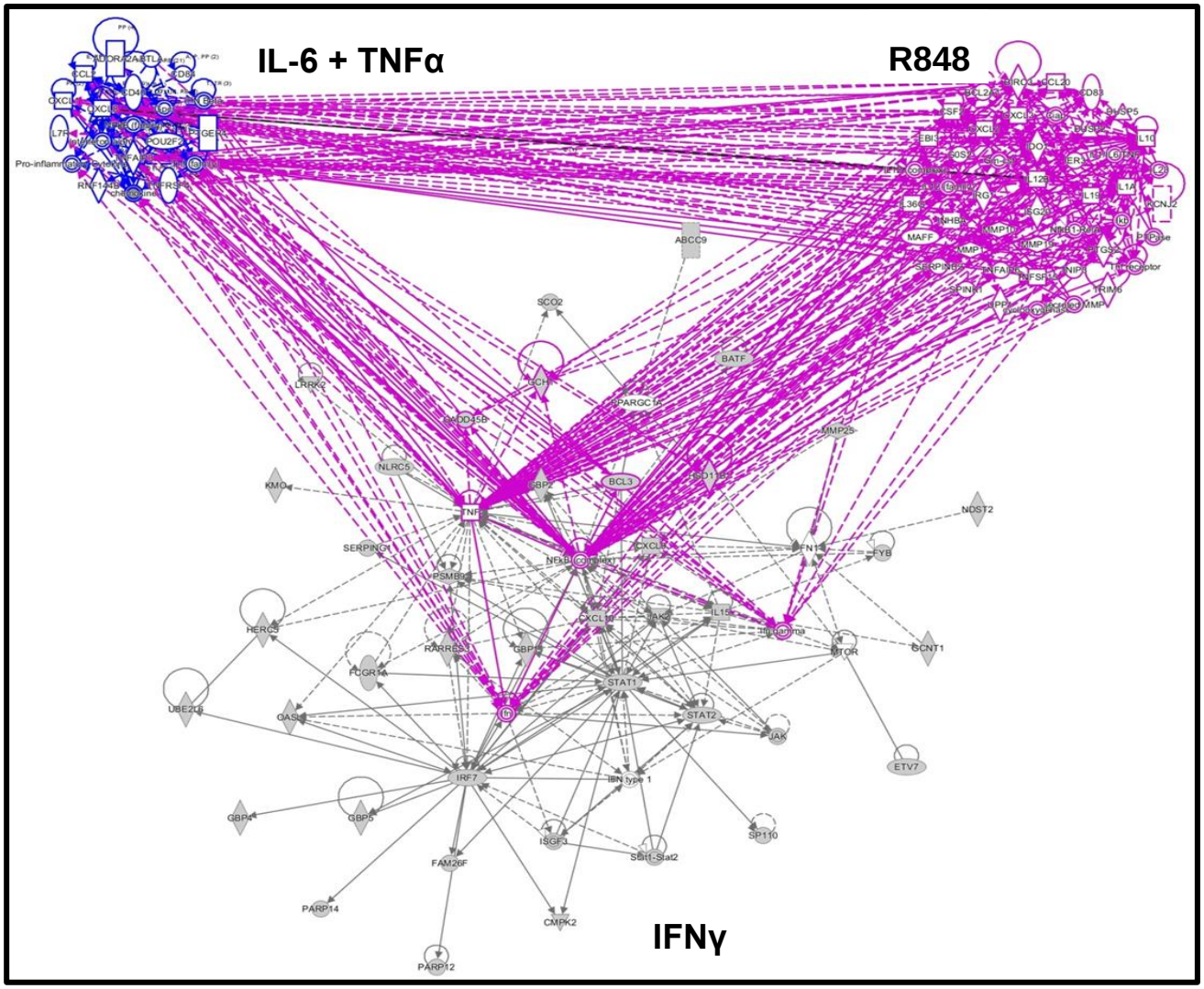


**Figure 3.15: R848, IL-6 plus TNFα and IFNγ-induced M1-like macrophage differentiation is regulated by a NF-κB-dependent network.**

*Scheme demonstrating interaction of regulatory networks (connected with pink lines) activated by R848, IL-6 plus TNFα or IFNγ (based on N=5).*

### 3.1.10 GM-CSF does not induce differentiation of the mMDSC into macrophages

Studies from other groups using murine and human cells indicated that GM-CSF was important for the generation of MDSC from bone marrow [222, 322]. GM-CSF was also shown to induce human peripheral blood and murine bone marrow monocytes to differentiate into pro-inflammatory macrophages [162, 519]. However, the activation status of MDSCs following exposure to GM-CSF was not investigated. For these reasons we hypothesized that GM-CSF might support M1-like macrophage differentiation of mMDSC as well. Culturing mMDSC with GM-CSF for 3 or 5 days resulted in significant increase in the percent of cells expressing the mannose-receptor CD206 (Figure 3.16A-C). However these cells failed to up-regulate the M2-like macrophage marker CD163 or the marker of activated macrophages 25F9 (Figure 3.16A-B-C). In line with these findings, neutralization of GM-CSF did not alter the percent of M1-like macrophages generated by R848 (Figure 3.16D). These findings indicated that GM-CSF does not promote macrophage differentiation from mMDSC. Drawing on reports that GM-CSF triggers the generation of DCs from monocytes, additional lineage markers were investigated [520, 521]. As defined in the literature, unstimulated human mMDSC were positive for CD11b and CD11c while being negative for CD1d [257] (Figure 3.16E). Culturing cells with GM-CSF had no effect on CD11c levels and caused only a slight increase CD1d. In contrast, CD11b levels were increased over background by 4-fold (n=3, Figure 3.16E). These results confirm that mMDSC exposed to GM-CSF persist as monocytes. Other groups believe that GM-CSF regulates maintenance of MDSC in the tumor microenvironment [237, 317]. To investigate whether exposure to GM-CSF provides resistance to differentiation, mMDSC from a single donor were stimulated with a combination of TLR agonists including GM-CSF. M1- and M2-like macrophage frequencies were not altered by the presence of GM-CSF (Figure 3.16F).

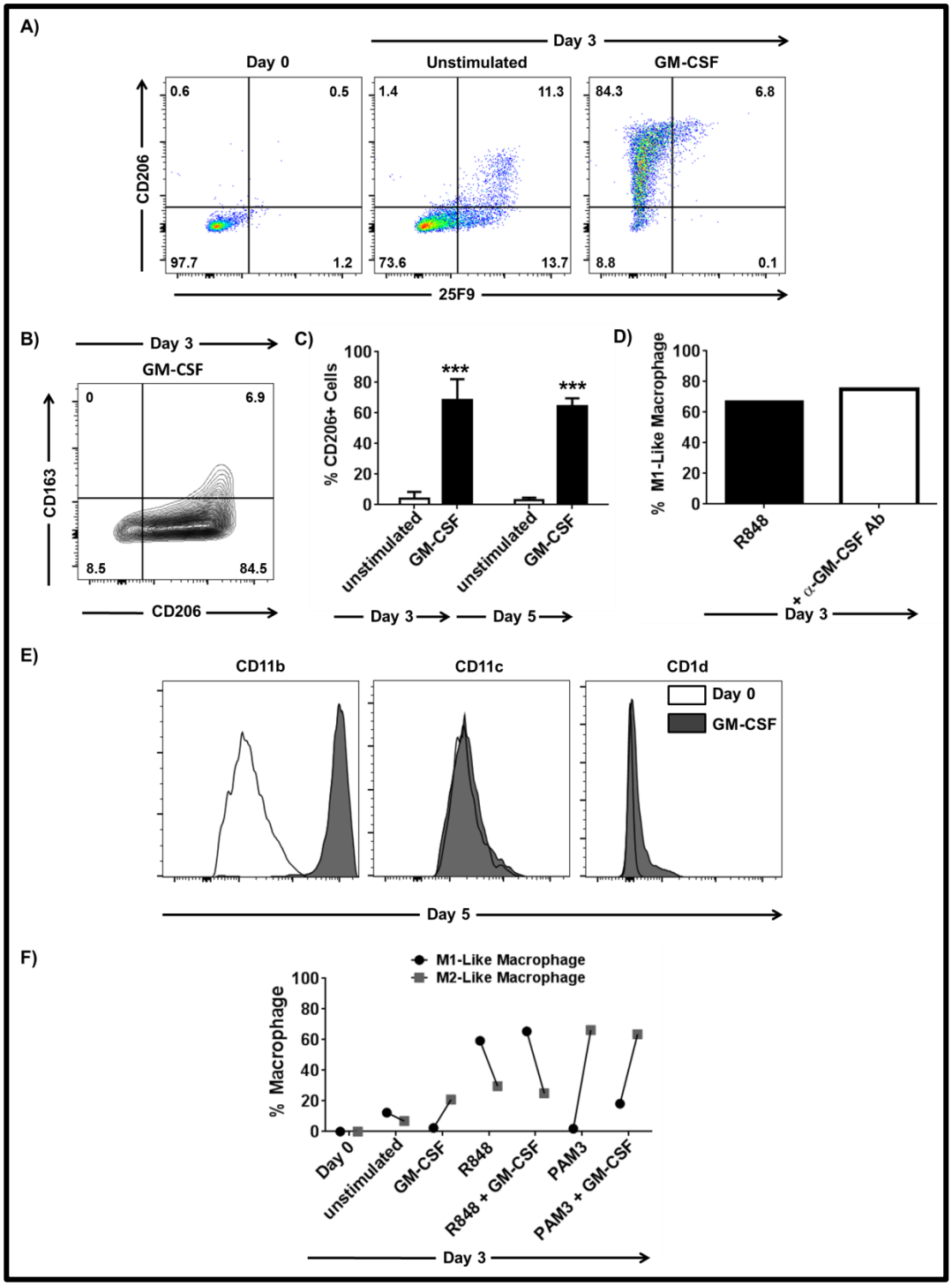


**Figure 3.16: GM-CSF does not induce mMDSC to become macrophage.**

*A) Representative dot plots depicting changes in CD206 and 25F9 expression upon differentiation. B) Representative dot plots showing co-expression pattern of M2-like macrophage markers CD163 and CD206. C) Percent of cells expressing CD206 but not 25F9 following 3 or 5 days of stimulation (mean ± SD of three independently analyzed donors). D) Percent of R848-induced M1-like macrophages in the presence of anti-GM-CSF neutralizing antibody. E) Histograms depicting CD11b, CD11c and CD1d expression following differentiation. F) Percentages of M1- and M2-like macrophage after stimulation with PAM3*

*and R848 alone vs in combination with GM-CSF for 3 days. *** p<0.001 unstimulated vs. GM-CSF stimulated samples.*

### 3.1.11 $PGE_2$ alters the pattern of macrophage differentiation from mMDSC

$PGE_2$ can support the generation of mMDSC and their recruitment to tumor sites [303, 323, 325, 326]. However, the COX-2 - $PGE_2$ axis has a complex role in the regulation of the immune response and can have either stimulatory or inhibitory effects on different stages of APC maturation and the inflammatory response [522]. Such studies suggest that $PGE_2$ might potentially regulate the maturation of mMDSC in the tumor microenvironment and could influence their response to TLR agonists. To test these possibilities, human mMDSC were cultured with 100 ng/ml $PGE_2$ for 3 days. Approximately 20% of the cells differentiated into M1-like macrophages with little donor variability suggesting that at least a portion of mMDSC respond to $PGE_2$ by altering their activation status **(**p<.01; Figure 3.17A). Next the effect of combining $PGE_2$ with TLR agonists was investigated. The percentage of PAM3- or R848-generated macrophages remained unaltered in the presence of $PGE_2$ (Figure 3.17B). However, the phenotype of these macrophages was significantly affected. To account for differences in sample size and donor variance, M1:M2-like macrophage ratios were normalized based on the mean found in Figure 3.1. Comparison of the R848 alone group to R848 plus $PGE_2$ group revealed on average a 6-fold increase in the M1:M2-like macrophage ratio (p<.01; Figure 3.17C). In contrast, $PGE_2$ reversed the pattern of PAM3-mediated macrophage differentiation by abolishing the M2-like macrophage generation and promoting M1-like macrophages instead (Figure 3.17B-C). These findings support the conclusion that $PGE_2$ can influence the maturation of mMDSC into pro-inflammatory macrophages.

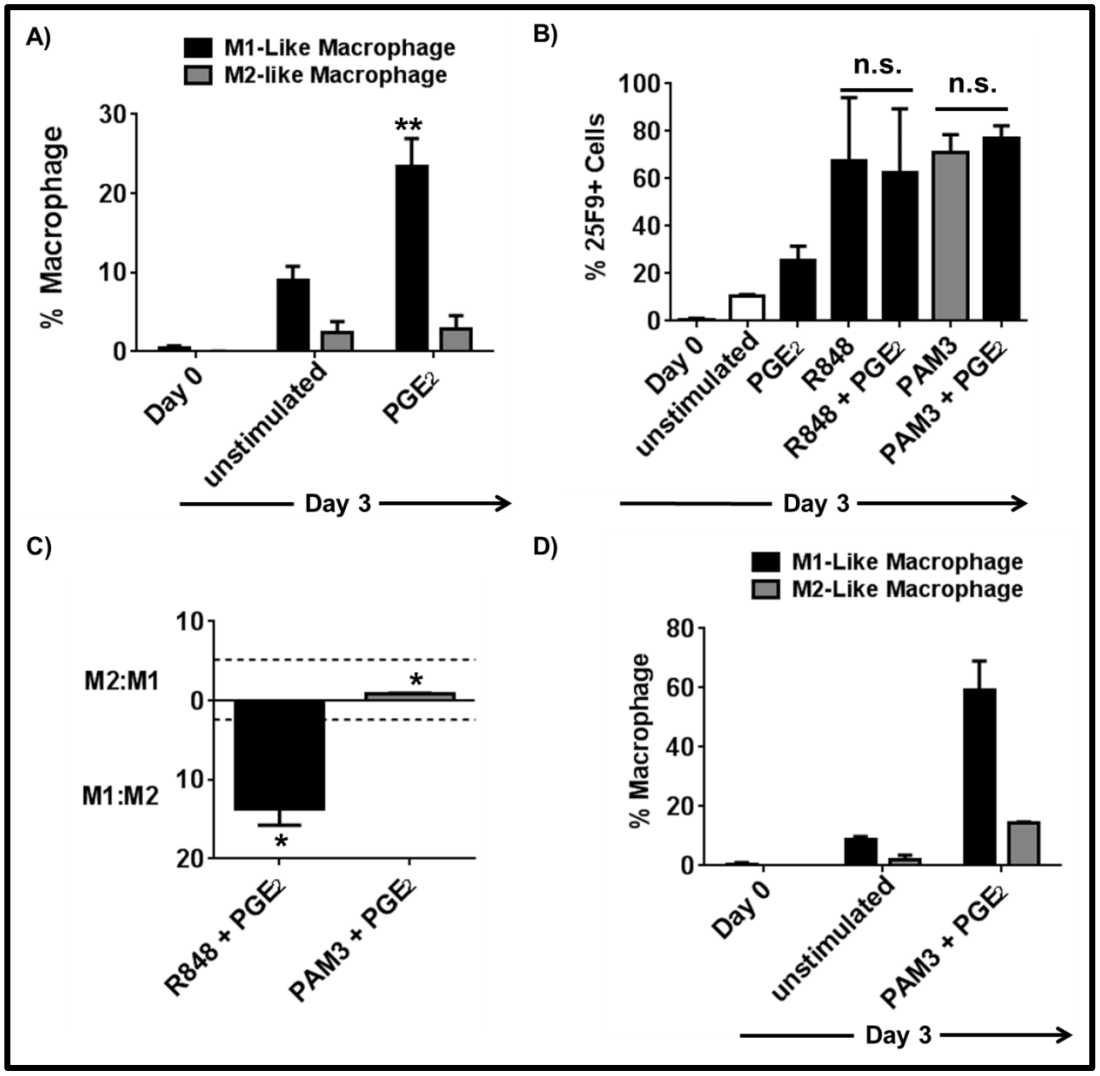


**Figure 3.17: $PGE_2$ regulates differentiation status of mMDSC.**

*A) Frequency of M1- and M2-like macrophages following stimulation with $PGE_2$ for 3 days (mean ± SD of 4 independently analyzed donors). ** $p<0.01$ unstimulated vs. $PGE_2$ stimulated samples. B) Percentage of 25F9+ cells following treatment with $PGE_2$ alone vs. in combination with PAM3 or R848 for 3 days (mean ± SD of 2 independently analyzed donors). C) Ratio of macrophages (mean ± SD of 2 independently analyzed donors stimulated with TLR agonists plus $PGE_2$). Dashed lines represent the mean ratio for PAM3 (top) and R848 (bottom). D) Frequency of M1- and M2-like macrophages following stimulation with the combination of PAM3 and $PGE_2$ for 3 days (mean ± SD of 2 independently analyzed donors). * $p<0.05$ TLR alone vs. $PGE_2$ combination stimulated samples.*

### 3.1.12 IL-4, IL-8, IL-13 and TGF-β are not essential for M2-like macrophage differentiation from mMDSC

We then hypothesized that specific cytokines or cytokine combinations might play a role in PAM3-dependent M2-like macrophage generation. In an effort to clarify the factors that regulate PAM3-induced mMDSC differentiation, a series of cytokines and chemokines known to be contribute to M2 macrophage differentiation were tested [210, 523]. mMDSC were cultured in the presence of 500ng/ml IL-4, IL-8 (CXCL8), IL-13, TGF-β1 or TGF-β2 for 5 days

as described previously. None of the cytokines significantly improved the generation of macrophage (Figure 3.18A). Consistent with that lack of effect, the addition of neutralizing Abs against IL-4 or TGF-β1 to PAM3 stimulated cultures did not interfere with the generation of M2-like macrophages (Figure 3.18B). Thus, PAM3-mediated M2-like macrophage polarization of mMDSC was independent of IL-4, IL-8, IL-13, TGF-β1 and TGF-β2.

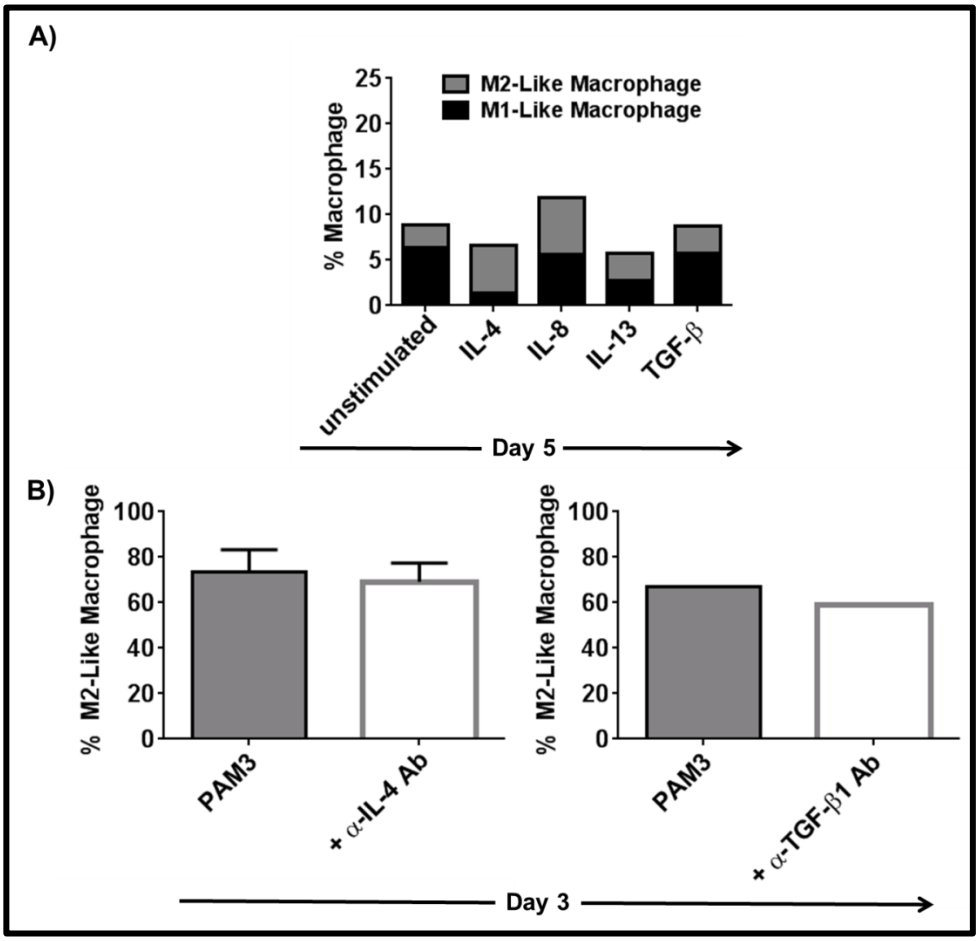


**Figure 3.18: IL-4, IL-8, IL-13 and TGF-β do not support the differentiation of mMDSC into M2-like macrophages.**

*A) Frequency of M1- and M2-like macrophages when mMDSC are cultured for 5 days with IL-4, IL-8, IL-13 and TGF-β1/2. For unstimulated group (mean ± SD) of seven; for stimulants (mean ± SD of three independently analyzed donors). B) Percentage of PAM3-induced M2-like macrophages in the presence of neutralizing antibodies against IL-4 (mean ± SD of two independently analyzed donors or TGF-β1 (N=1)).*

### 3.1.13 IL-1β partially supports M2-like macrophage differentiation from mMDSC

Although being considered a pro-inflammatory cytokine, IL-1β has been shown to mediate tumor immunosuppression (at least in part by recruiting and enhancing suppressive function of granulocytic MDSCs [306, 330, 331]. This led us to investigate whether IL-1β had a role in human mMDSC differentiation, especially considering that other cytokines linked to the activation and differentiation of mouse mMDSC (such as IL-4, IL-8, IL-13, TGF-β [210]),

failed to have such activity on human mMDSC in vitro. Initial experiments demonstrated that culturing mMDSC for 5 days with IL-1β induced the expression of the macrophage marker 25F9 in ≈50% of the cells (Figure 3.19A). Although both macrophage subtypes were detected in IL-1β supplemented mMDSC cultures, M2-like macrophages typically dominated although considerable variability in the M1:M2 ration was observed (Figure 3.5D; Figure 3.19B). To address the possible role of IL-1β in PAM3-induced M2-like macrophage polarization, neutralizing anti-cytokine Ab was added during culture. This significantly impaired the differentiation of mMDSC into M2-like macrophages (Figure 3.19D). Having identified IL-6 and IL-10 as regulators of mMDSC activation, IL-1β was added to these cytokines to determine if such a combination better replicated the activity of PAM3. The triple combination was similar to PAM3 in supporting low amounts of M1-like macrophage polarization and higher levels of M2-like macrophage generation (Figure 3.19E).

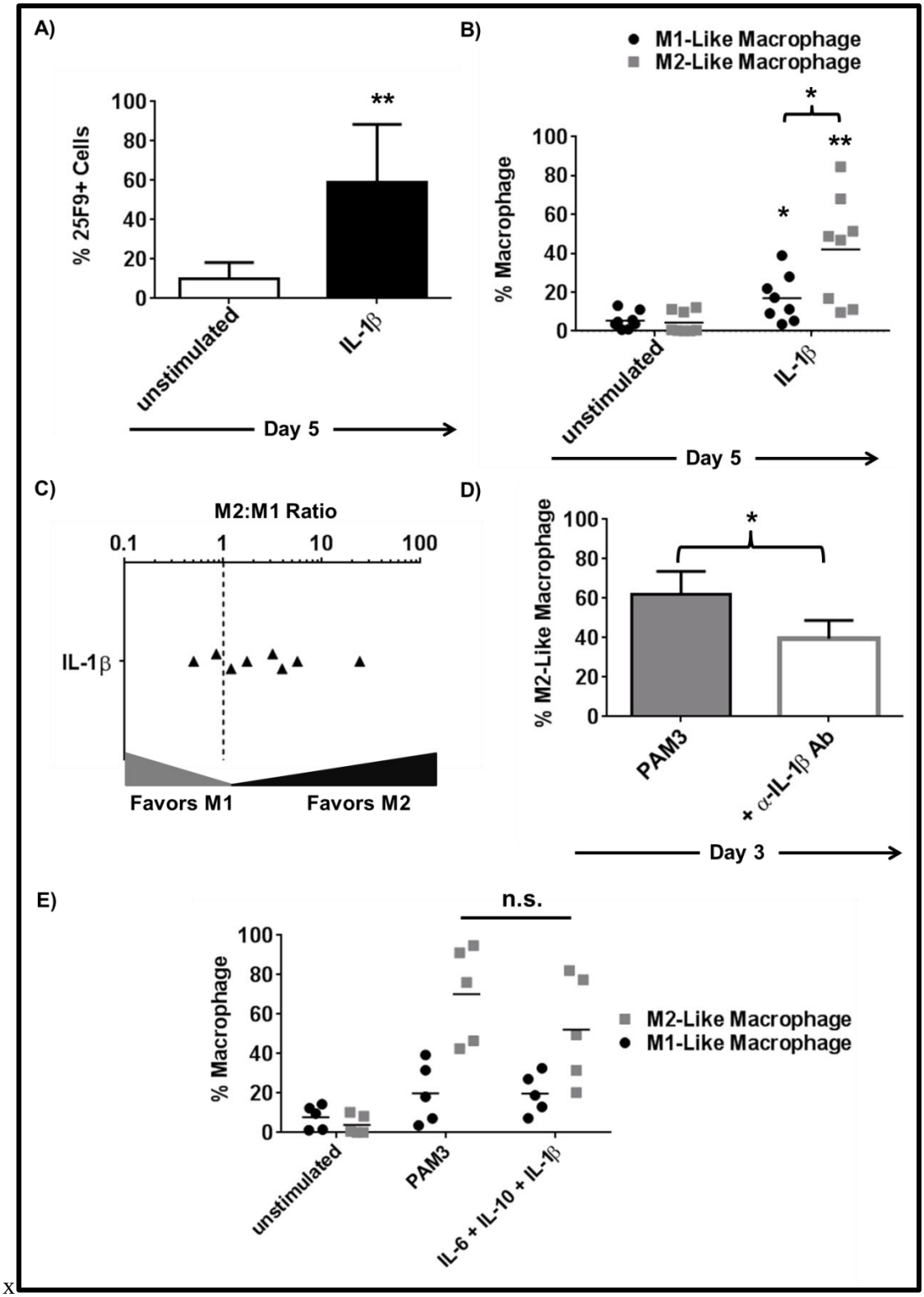


x

**Figure 3.19: IL-1β partially supports M2-like macrophage differentiation by mMDSC.**

*A) Percentage of 25F9+ cells following stimulation with IL-1β for 5 days (mean ± SD of 8 independently analyzed donors). B) Frequency of M1- and M2-like macrophage following stimulation IL-1β for 5 days (mean ± SD of 8 independently analyzed donors). C) Ratio of M1-to-M2-like macrophages from each sample evaluated for 5 days. D) Percentage of PAM3-induced M2-like macrophages in the presence of neutralizing antibody against IL-1β for 3 days*

*(mean ± SD of 4 independently analyzed donors). E) Frequency of M1- and M2-like macrophage following stimulation with combination of IL-6, IL-10 with IL-1β or PAM3 for 5 days (mean ± SD of 5 independently analyzed donors). * p<0.05; ** p<0.01 IL-1β stimulated vs. unstimulated samples or neutralizing antibody containing cultures vs. stimulant cultures.*

However a detailed analysis of the data showed that samples treated with PAM3 on average generated 1.8 fold more M2-like macrophages that those stimulated with the combination of IL-6, IL-10 with IL-1β (Table 3.1). Thus, we conclude that this cytokine combination could not fully mimic the activity of PAM3.

**Table 3.1: Comparison of M2:M1 Ratio and actual M2-like macrophage numbers of PAM3 or IL-6 + IL-10 + IL-1β stimulated mMDSC cultures.**

| | **PAM3 vs. IL-6 + IL-10 + IL-1β** **Relative M2:M1 Ratio** | **PAM3 vs. IL-6 + IL-10 + IL-1β** **Relative Actual # of M2-like Macrophage** |
|---|---|---|
| **Donor #1** | 4.4 | 1.4 |
| **Donor #2** | 1.4 | 3.3 |
| **Donor #3** | 1.6 | 2.3 |
| **Donor #4** | 1.1 | 1.2 |
| **Donor #5** | 1.5 | 0.6 |
| **Mean:** | **2** | **1.8** |

### 3.1.14 High dose M-CSF supports M2-like macrophage differentiation from mMDSC as an independent signal

M-CSF generates macrophage with suppressive properties. Thus, we hypothesized that M-CSF might be required to recapitulate the activity of PAM3 [18]. Incubation of mMDSC with 500 ng/ml M-CSF for 5 days triggered >80% of mMDSC to mature into macrophages (Figure 3.20A-B). 80% of these 25F9+ cells co-expressed CD163 and thus were phenotypically M2-like macrophage (Figure 3.20A-C). The average M2:M1-like macrophage ratio in M-CSF stimulated cultures was 50:1, exceeding the ratio generated by PAM3 by 5-fold (Figure 3.20D-E). Having

identified M-CSF as a strong inducer of M2-like macrophages, we investigated the effect of combining it with IL-6 and IL-10. None of these combinations significantly improved the activity of M-CSF (Figure 3.20A-B-C-D-E). Since these findings suggested that at high doses M-CSF alone was sufficient to recapitulate (or exceed) the effect of PAM3, we neutralized the cytokine to evaluate its role in PAM3-induced macrophage differentiation. Addition of anti-M-CSF antibody to PAM3 stimulated cultures did not significantly reduce the percentage of M2-like macrophages generated (Figure 3.20F). These results suggest that either PAM3-dependent differentiation is independent of M-CSF.

.

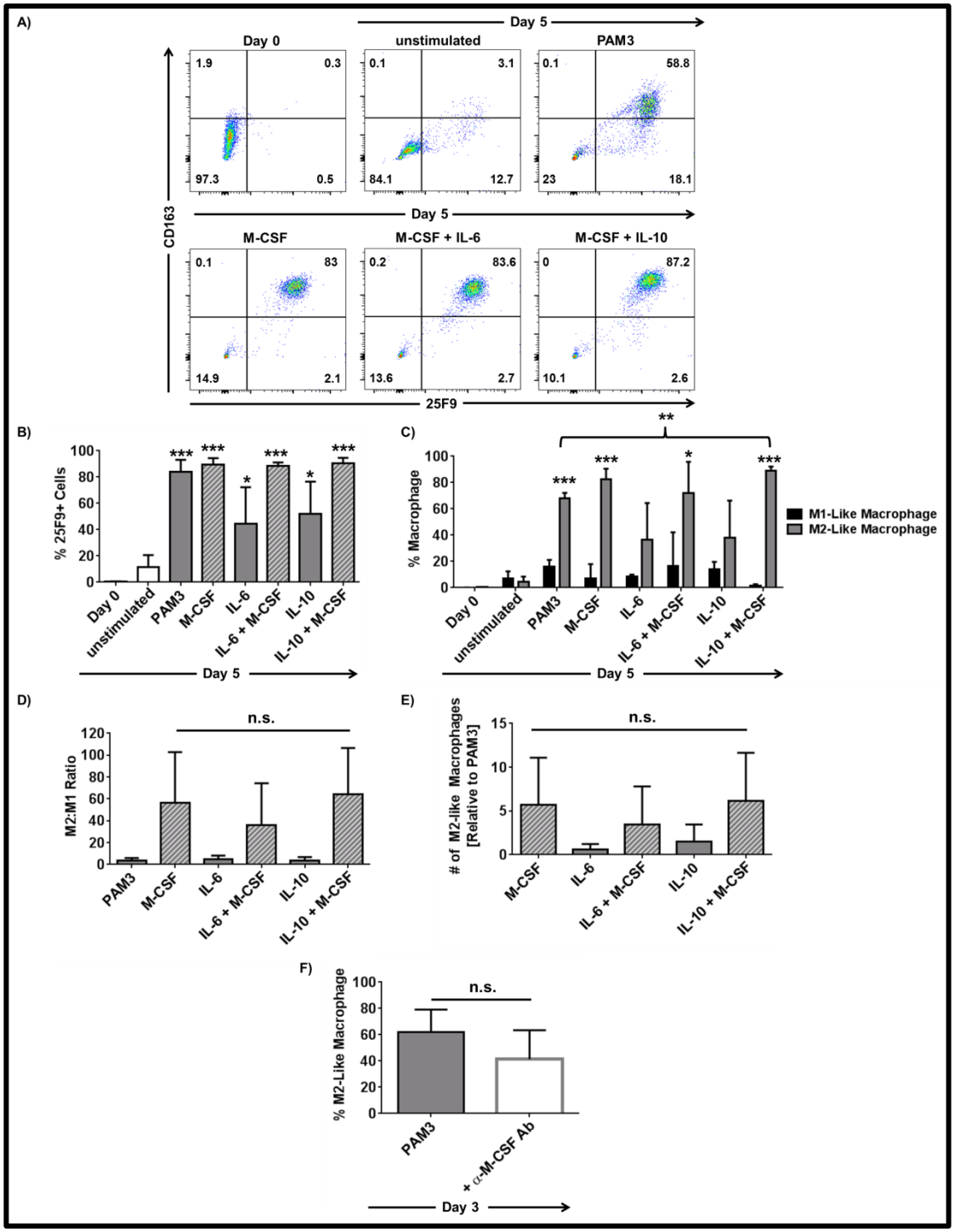


**Figure 3.20: High dose M-CSF is effective inducer of M2-like macrophages from mMDSC.**

*A) Representative dot plots showing change in the expression level of CD163 and 25F9 following stimulation with PAM3, M-CSF and combination of M-CSF with IL-6 or IL-10 for 5 days. B) Percentage of cells expressing the active macrophage marker 25F9 (mean ± SD of 3-4 independently analyzed donors). C) Percentages of M1- and M2-like macrophages (mean ± SD of 3-4 independently analyzed donors). ** p<0.01. D) Ratio of M2-to-M1-like macrophages (mean ± SD of 3-4 independently analyzed donors). E) Ratio of actual number of M2-like macrophages produced in cytokine vs. PAM3 cultures (mean ± SD of 3-4 independently analyzed donors). F) Percentage of PAM3-induced M2-like macrophages in the presence and*

*absence of anti-M-CSF neutralizing antibody. * $p<0.05$; *** $p<0.001$ unstimulated vs. stimulated samples.*

### 3.1.15 Low dose M-CSF in combination with IL-6 and IL-10 recapitulates the effect of PAM3

The results shown above established that M-CSF could induce mMDSC to differentiate into M2-like macrophage more effectively than IL-6 or IL-10. Yet neutralizing IL-6 or IL-10 but not M-CSF impaired PAM3-induced M2-like macrophage generation (Figure 3.4B). This led us to consider whether low doses of M-CSF combined with IL-6 and IL-10 might better replicate the activity of PAM3. Initial studies found that adding 1 ng/ml of M-CSF (a dose that had no effect on mMDSC maturation) to IL-6 plus IL-10 did not improve macrophage differentiation rates (Figure 3.21). When the concentration of M-CSF was increased to 5 ng/ml, 80% of the mMDSC matured into macrophages of which 60% were phenotypically M2-like, similar to the effect of PAM3 (Figure 3.22A-B-C). Adding IL-6 plus IL-10 to the 5 ng/ml M-CSF resulted in higher M2:M1-like macrophages ratios compared to PAM3 alone. Due to variation between donors, however, this effect did not reach statistical significance. (Figure 3.22D,E).

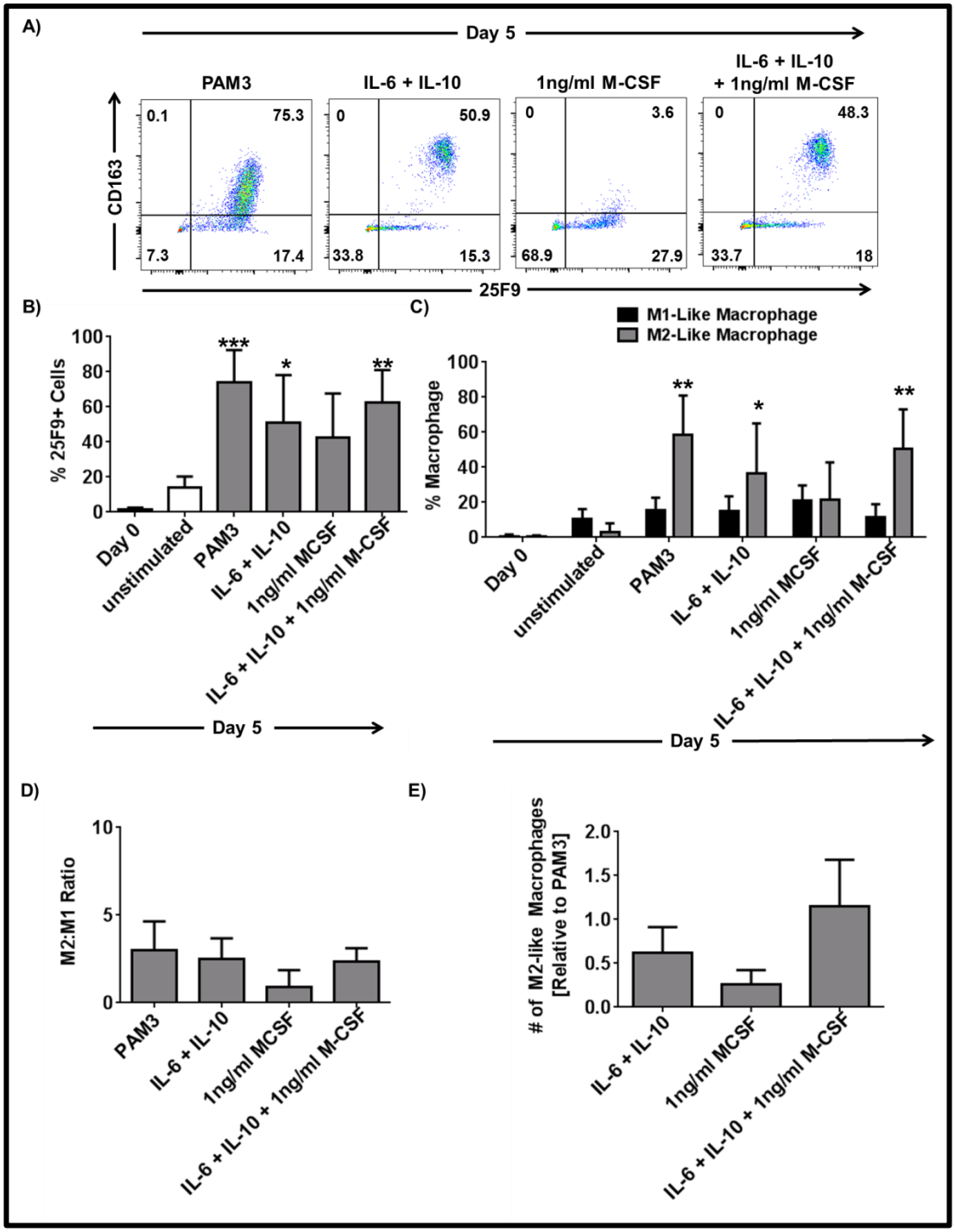


**Figure 3.21: Combination of 1 ng/ml M-CSF with IL-6 and IL-10 is not sufficient to recapitulate the effect of PAM3.**

*A) Representative dot plots showing CD163 and 25F9 expression upon differentiation. B) Percent of cells expressing the active macrophage marker 25F9 (mean ± SD of 5 independently analyzed donors).C) Percentages of M1- and M2-like macrophages (mean ± SD of 5 independently analyzed donors). D) Ratio of M2-to-M1-like macrophages (mean ± SD of 3 independently analyzed donors). E) Ratio of actual number of M2-like macrophages produced in cytokine vs. PAM3 cultures (mean ± SD of 5 independently analyzed donors). * $p<0.05$; ** $p<0.01$; *** $p<0.001$ unstimulated vs. stimulated samples.*

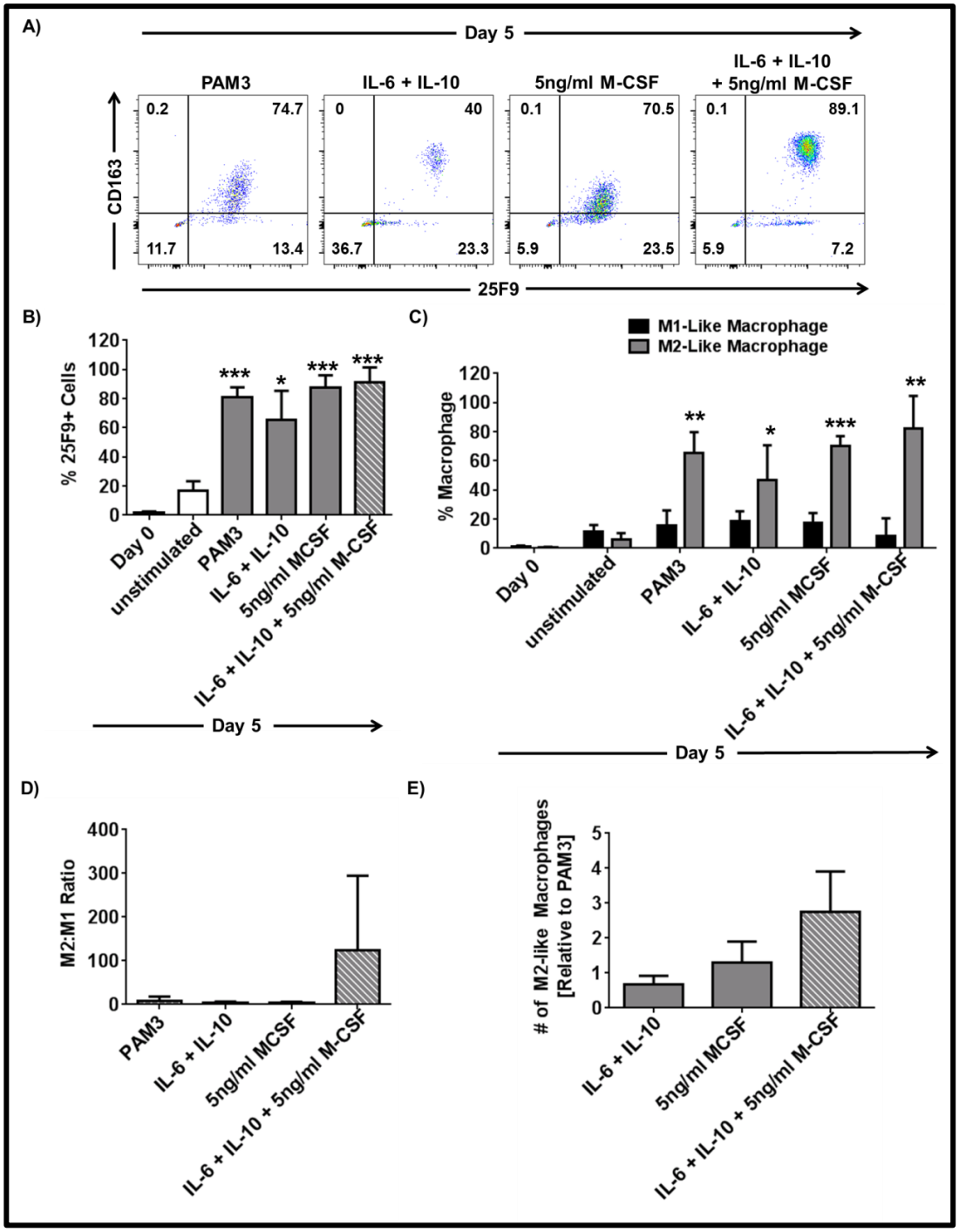


**Figure 3.22: Combination of 5ng/ml M-CSF with IL-6 and IL-10 drives M2-like macrophage polarization as effectively as PAM3.**

*A) Representative dot plots showing CD163 and 25F9 expression upon differentiation. B) Percentage of cells expressing the active macrophage marker 25F9 (mean ± SD of 4 independently analyzed donors). C) Percentages of M1- and M2-like macrophages (mean ± SD of 4 independently analyzed donors). D) Ratio of M2-to-M1-like macrophages (mean ± SD of 4 independently analyzed donors). E) Ratio of actual number of M2-like macrophages produced in cytokine vs. PAM3 cultures (mean ± SD of 4 independently analyzed donors). * $p<0.05$; ** $p<0.01$; *** $p<0.001$ unstimulated vs. stimulated samples.*

### 3.1.16 mMDSC stimulated with PAM3 or combination of IL-6, IL-10 and low dose M-CSF remain functionally suppressive

Previous results from our group demonstrated that mMDSC and PAM3-stimulated macrophages could suppress the proliferation of autologous naïve $CD4^+$ T cells [230]. To confirm the functionality of the macrophages generated by the combination of IL-6, IL-10 and low dose M-CSF (5 ng/ml), a T cell proliferation assay was performed as described in Section 2.2.6.2 by co-incubating suppressor cells with activated $CD4^+$ T cells. Macrophage generated by both PAM3 and IL-6, IL-10 and low dose M-CSF treatment of mMDSC were equivalent in their ability to suppress T cell proliferation (Figure 3.23). Since the addition of PAM3 or IL-6, IL-10 and low dose M-CSF had no direct effect on T cell proliferation we concluded that suppression was mediated by the M2-like macrophages generated during culture (Figure 3.23).

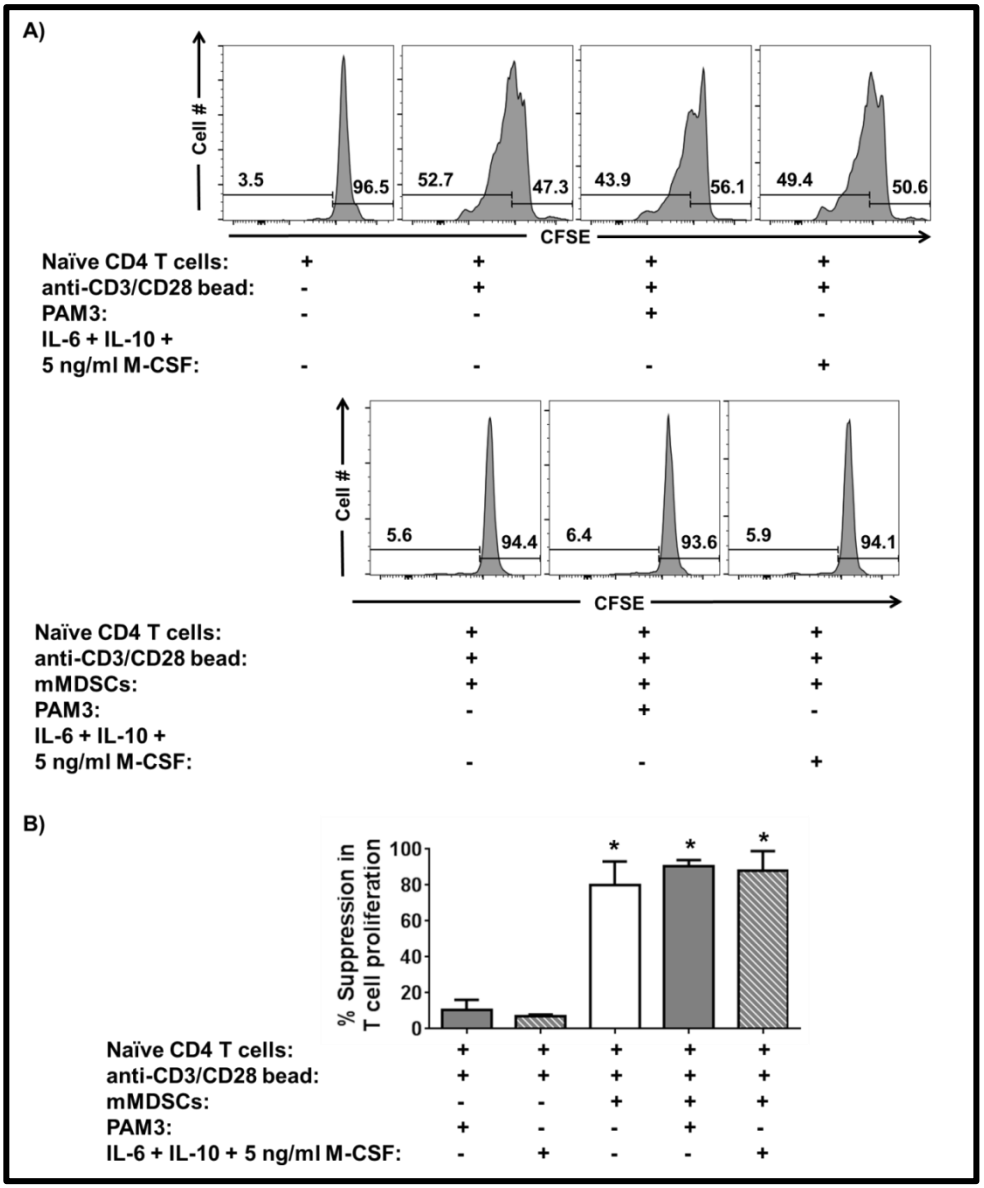


**Figure 3.23: mMDSC stimulated with PAM3 or IL-6, IL-10 and low dose M-CSF combination retain the suppressive activity.**

*A) Representative histograms depicting the proliferation rates of naïve CD4+ T cell in the presence and absence of mMDSC and stimulants. B) Percent suppression in T cell proliferation following 3 days of co-incubation of activated T cells with mMDSC in the presence and absence of PAM3 or IL-6, IL-10 and 5 ng/ml M-CSF (mean ± SD of 3 independently analyzed donors). * $p<0.05$ activated T cells vs. MDSC co-cultures.*

### 3.1.17 mMDSC preferentially differentiate into M2- rather than M1-like macrophages

The cytokines that influence human mMDSC to differentiate into macrophages were defined in the studies described above. However, it is likely that under physiological conditions an mMDSC may encounter two opposing signals simultaneously. Because mMDSC are suppressive cells, we predicted that they might preferentially differentiate into alternatively activated macrophages if exposed to both types of stimulation. To investigate this hypothesis,

mMDSC were treated with IL-6 plus TNFα and/or M-CSF for 5 days. As expected, IL-6 plus TNFα generated primarily M1-like macrophages ($p<0.01$) while M-CSF induced M2-like macrophages. When exposed simultaneously to IL-6, TNFα and M-CSF the overwhelming majority of mMDSC differentiated into M2-like macrophages although such cultures contained fewer M2-like and more M1-like macrophages that M-CSF alone cultures ($p<0.05$, Figure 3.24A-B). These findings indicated that mMDSC preferentially differentiate into M2-like macrophages when exposed to opposing stimuli.

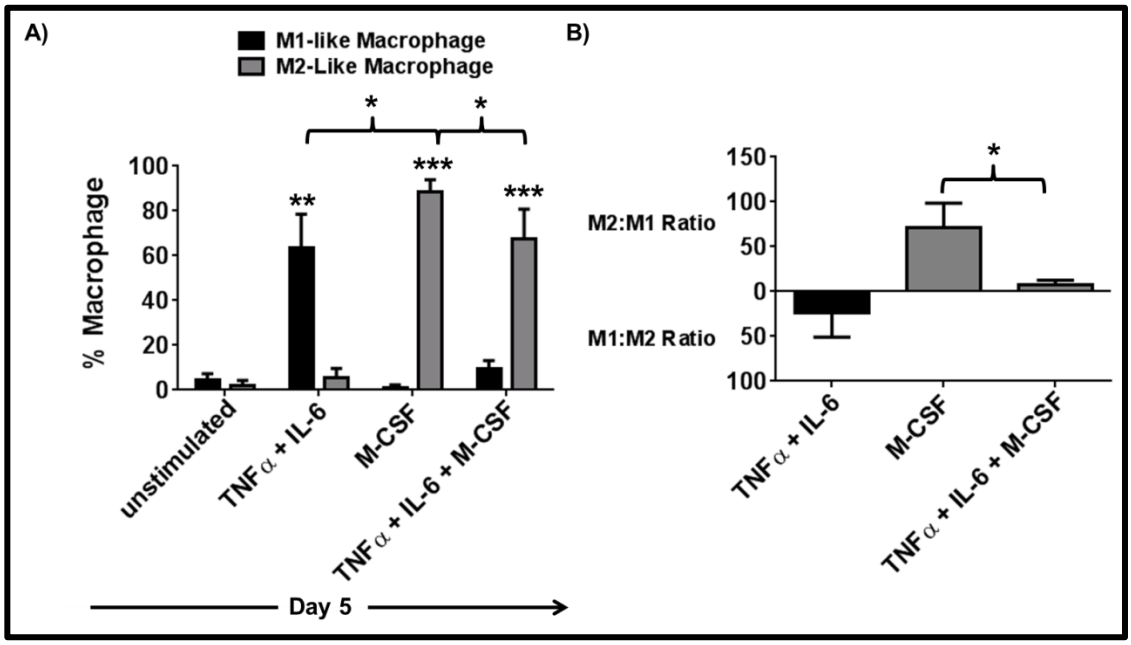


**Figure 3.24: mMDSC preferentially differentiate into M2-like macrophages when exposed to TNFα and M-CSF simultaneously.**

*A) Percentage of M1- and M2-like macrophages following treatment with IL-6 plus TNFα, M-CSF or combination of IL-6 plus TNFα with M-CSF (mean ± SD of four independently analyzed donors). B) Ratio of macrophages from each sample evaluated for 5 days. * $p<0.05$; ** $p<0.01$; *** $p<0.001$ stimulated vs. unstimulated samples.*

### 3.1.18 Macrophages differentiated from HLA-DR$^+$ monocytes are plastic

The experiments described above identified TNFα and M-CSF as strong inducers of monocyte polarization. To evaluate whether these stimuli caused the terminal differentiation of target macrophages, we analyzed the susceptibility of such cells to re-polarization. These assays thus were performed on HLA-DR$^+$ monocytes as very large numbers of starting cells were needed. As shown above, monocytes and mMDSC respond identically to TNFα and M-CSF [21, 146]. Monocytes were initially stimulated with TNFα (or M-CSF) for 2 days. Approximately 40% of the monocytes differentiated into M1-like (or M2-like when cultured with M-CSF) macrophages during this brief culture. These macrophages were FACS purified and cultured for 5 additional days with either with TNFα or M-CSF. The overwhelming majority of M1-like

macrophages retained that phenotype when treated with TNFα (Figure 3.25A). In contrast, nearly half of those cells 'switched' to express an M2-like phenotype when incubated with M-CSF (Figure 3.25B). The same effect was observed in studies of M-CSF generated M2-like macrophages: they remained M2-like when cultured with M-CSF but half re-polarized into M1-like macrophages in the present of TNFα. These observations indicate that a majority of monocytes can differentiate into either M1- or M2-like macrophages and are susceptible to re-polarization when exposed to the proper cytokine/chemokine milieu.

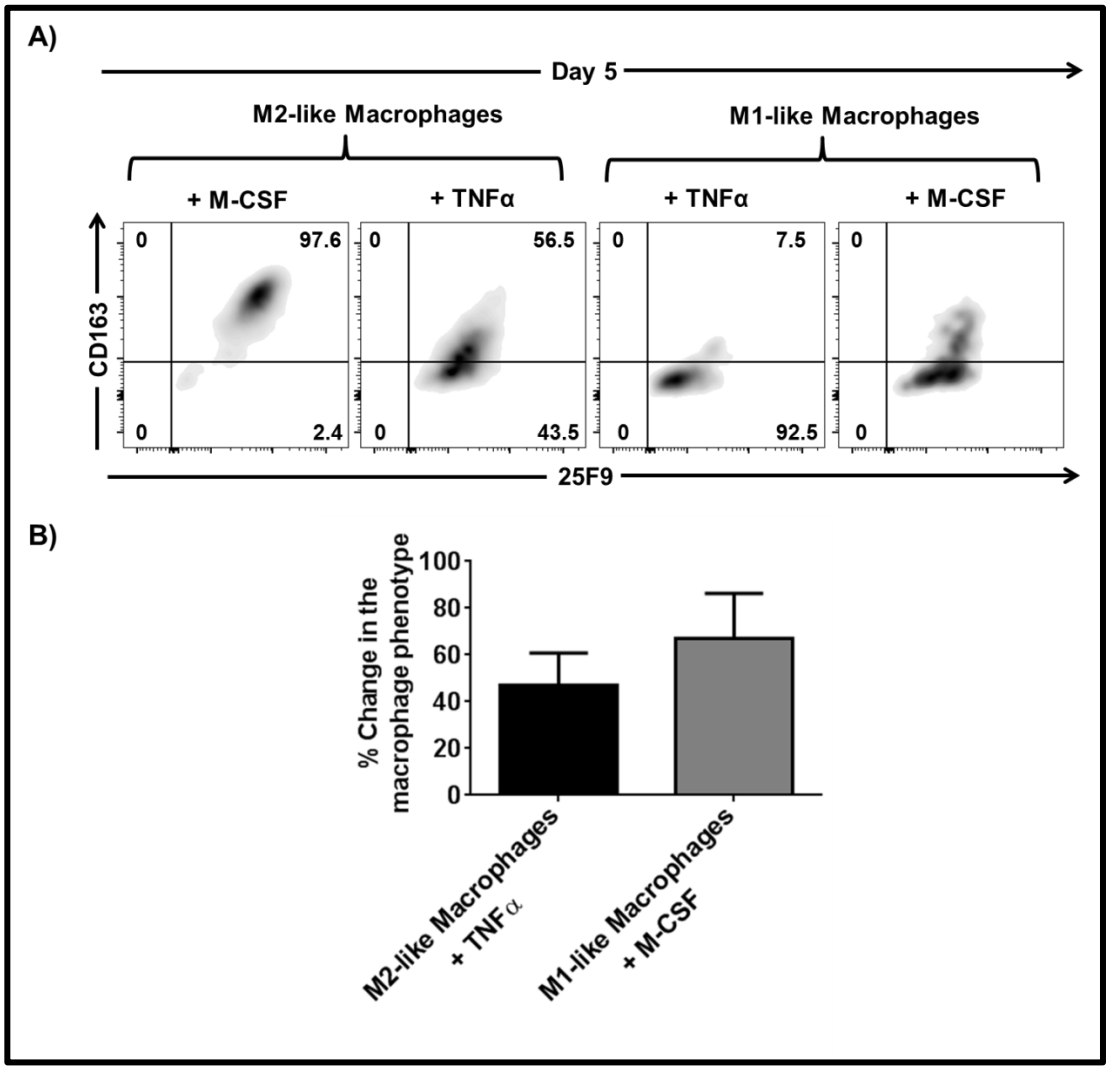


**Figure 3.25: M1-like and M2-like macrophages generated from HLA-DR$^+$ monocytes can change their phenotype when exposed to opposing stimuli.**

*A) Representative dot plots depicting changes in CD163 and 25F9 expression upon incubation of purified M2-like and M1-like macrophages with TNFα and M-CSF for 5 days. B) Percent change in the phenotype of macrophages when exposed to opposing stimuli (mean ± SD of 3 independently analyzed donors).*

### 3.1.19 TLR2/1 signaling polarizes HLA-DR$^+$ monocytes into M2-like macrophages

We identified the TLR2/1 agonist PAM3 as an inducer of M2-like macrophages from mMDSC. Since mMDSC are intrinsically immunosuppressive, we hypothesized that the effect of PAM3 might be restricted to mMDSC. To determine whether conventional monocytes respond to TLR agonists by differentiation into M2-like macrophages, mMDSC were removed from elutriated monocytes by FACS and the remaining monocytes isolated on the basis of high HLA-DR expression. These cells were then stimulated with a panel of TLR2, 3, 4, 5, or 7/8 agonists for 3 days and examined for markers of classically and alternatively activated macrophages. All TLR agonists with the exception of the TLR3 agonist poyI:C induced a significant increase in the activated monocyte population. PAM3 was the most potent, stimulating ≈70% of the monocytes whereas for the remaining TLR ligands triggered from 40-60% of these cells (Figure 3.26A). PAM3 was also unique in its ability to drive monocytes to primarily differentiate into M2-like macrophages. 50-60% of the macrophages in PAM3 cultures co-expressed CD206 and CD163 along with 25F9 and thus were phenotypically M2-like macrophages (Figure 3.26B). The M2:M1-like macrophage ratio of six donors stimulated with PAM3 contained 2-5 fold more M2- than M1-like macrophage (Figure 3.26C).

Cultures of the TLR2 agonist PGN, the TLR2/6 dual agonist FSL-1 and the TLR7/8 dual agonist R848 preferentially generated M1-like macrophages while producing lower but significant numbers of M2-like macrophages. The TLR5 ligand FLA showed a similar trend although the increase in M2-like macrophage did not reach statistical significance (Figure 3.26B). Plotting the ratio of M1:M2-like macrophages showed that these cultures contain 2-10 fold more M1-like macrophages (Figure 3.26C). In contrast, stimulation with the TLR4 agonists LPS and MPL polarized HLA-$DR^+$ monocytes towards those expressing an M1-like phenotype (Figure 3.26B-C).

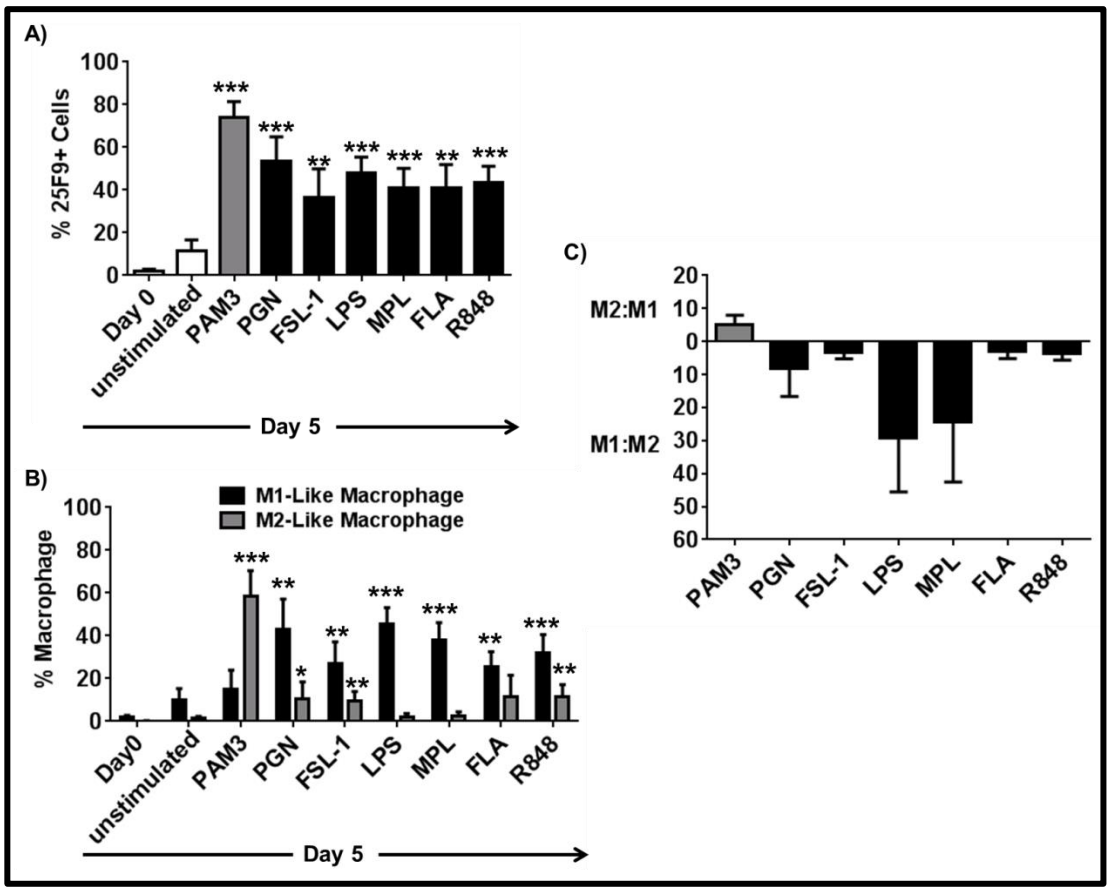


**Figure 3.26: PAM3 preferentially generates M2-like macrophages from HLA-DR$^+$ monocytes.**

*A) Percentage of cells expressing the macrophage marker 25F9 after 3 days of stimulation with various TLR agonists (mean ± SD of 5-7 independently analyzed donors/agonist). B) Frequency of M1- and M2-like macrophages in the same experiment. C) Ratio of macrophages from each sample. * $p<0.05$; ** $p<0.01$; *** $p<0.001$ stimulated samples vs. unstimulated samples.*

To further evaluate the dynamics of the PAM3 response, HLA-DR$^+$ monocytes from six donors were stimulated for 3 or 5 days. The two additional days of culture increased the percent of activated monocytes without altering the M2:M1 ratio suggesting that the longer period allowed more monocytes to differentiate (Figure 3.27A-B). Signaling requirements over this prolonged culture was investigated. The percent of activated HLA-DR$^+$ monocytes was lower in cells stimulated with FSL-1 vs PAM3 (60% vs 80%, Figure 3.27C). Phenotypic analysis of macrophage subtypes showed that both cultures were heterogeneous but exhibited opposite trends: the majority of PAM3 treated HLA-DR$^+$ monocytes differentiated into M2-like macrophages while those treated with FSL-1 were predominantly M1-like (Figure 3.27D). Thus, PAM3 treated samples had 3.5-fold more M2-, whereas FSL-1 treated cultures contained 3-fold more M1-like macrophages (Figure 3.27E). These results support the conclusion that

signaling through the TLR2/1 heterodimer but not through TLR2/6 heterodimer preferentially supported the generation of M2-like macrophages.

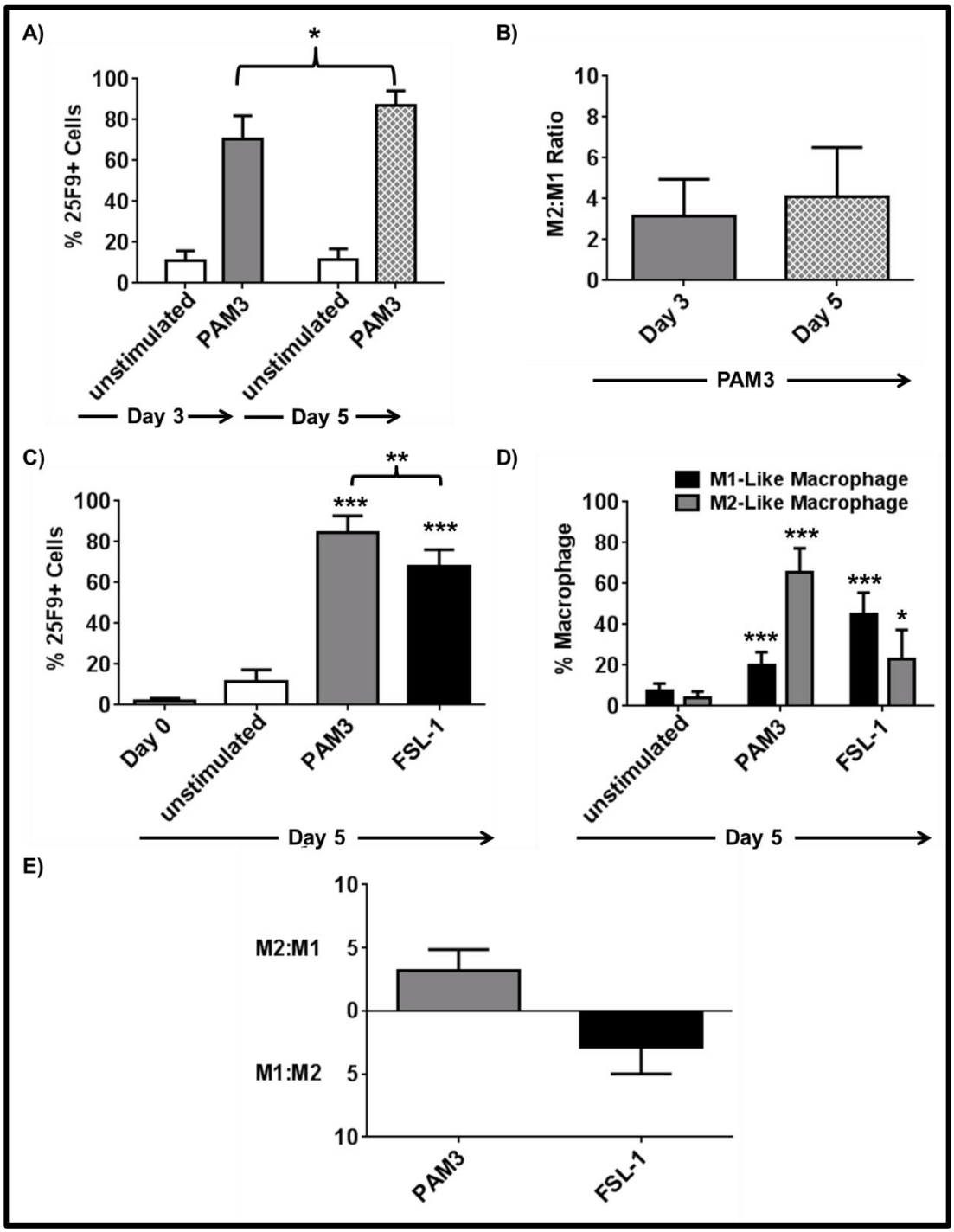


**Figure 3.27: Differences in HLA-DR$^+$ monocyte differentiation after stimulation with PAM3 vs FSL-1.**

*A) Percentage of 25F9+ monocytes following 3 or 5 days of treatment with PAM3 (mean ± SD of 6 independently analyzed donors). B) Ratio of macrophages from each sample evaluated on Day 5. C) Frequency of cells expressing 25F9 after 5 days of stimulation with PAM3 or FSL-1 (mean ± SD of 7 independently analyzed donors). D) Percentage of M1- and M2-like macrophages following stimulation with PAM3 or FSL-1 for 5 days (mean ± SD of 7*

*independently analyzed donors). E) Ratio of macrophages from each sample evaluated for 5 days. * p<0.05; ** p<0.01; *** p<0.001 PAM3/FSL-1 treated samples vs. unstimulated samples.*

### 3.1.20 PAM3 response of mMDSC and HLA-DR$^+$ monocytes are indistinguishable

We next compared the efficiency with which PAM3 generated M2-like macrophage from mMDSC vs HLA-DR$^+$ cells. Both cell types were purified from the same donors and stimulated for 5 days. The percent of cells maturing into M1- and M2-like macrophages from mMDSC or HLA-DR$^+$ monocytes was similar (Figure 3.28A-B) and the resultant M2-:M1-like macrophage ratios indistinguishable (Figure 3.28C). These results establish that PAM3 uniformly actives monocytic populations and polarizes them towards M2-like macrophage.

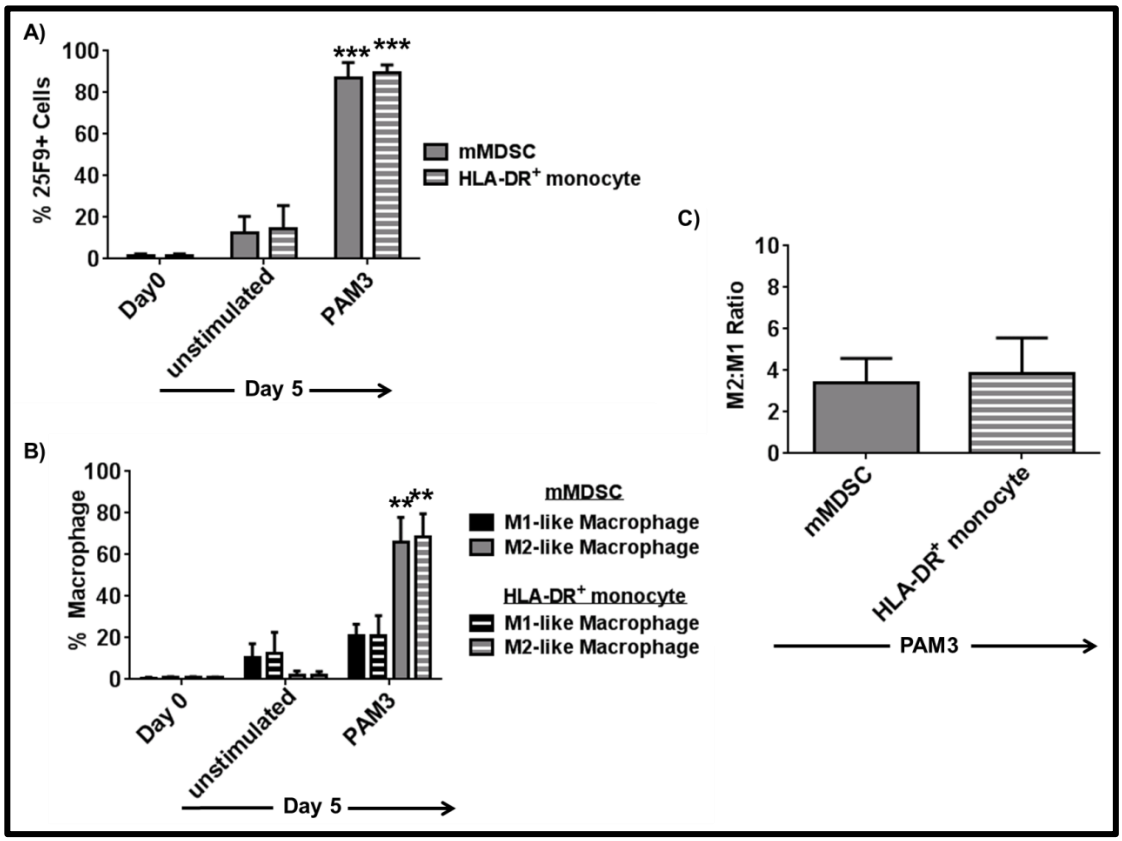


**Figure 3.28: mMDSC and HLA-DR$^+$ monocytes respond similarly to PAM3.**

*A) Percentage of 25F9+ monocytes following 5 days of stimulation with PAM3 (mean ± SD of 4 independently analyzed donors). B) Percentage of M1- and M2-like macrophages following stimulation with for 5 days (mean ± SD of 4 independently analyzed donors). C) Ratio of macrophages from each sample evaluated at Day 5. ** p<0.01; *** p<0.001 PAM3 treated samples vs. unstimulated samples.*

### 3.1.21 Variation in PAM3 response of human and mouse monocytes

We sought to examine whether the activity of PAM3 observed *in vitro* could be reproduced *in vivo* (as was the case for the TLR7/8 agonists, [362]). Towards that end, mMDSC and

monocytes were isolated from bone marrow of C57BL/6 mice as described Section 2.2.9 and stimulated for 3-4 days with various TLR agonists. The effect on macrophage number was determined by monitoring the number of cells expressing F4/80 while CD206 expression was used to discriminate M1 from M2 macrophages. The overwhelming majority of mouse mMDSC differentiated into phenotypically M1 macrophages when incubated with PGN or LPS. Stimulation of mMDSC with PAM3 resulted a similar fraction of the cells maturing but ≈40% of these cells were phenotypically M2 macrophages (Figure 3.29A). The experiment was repeated using all monocytes (not just mMDSC) cultured from the bone marrow. Again both TLR2 and TLR4 agonists generated M1 macrophages, with the exception of PAM3 which generated both M1 and M2 macrophages at an approximate ratio of 2:1 (Figure 3.29B). Further examining of M1:M2 ratios showed that the TLR4 agonists LPS and MPL were slightly stronger inducers of M1 macrophages than the TLR2 agonists PGN and FSL-1 (Figure 3.29C). These findings indicated that the activity of PAM3 was different from the other TLR agonists and showed that PAM3 was able to support the generation of M2 macrophages in rodents as well as primates. Nevertheless, unlike human mMDSC and HLA-DR$^+$ monocytes that responded to PAM3 by primarily differentiating into M2-like macrophages; PAM3 stimulated mouse mMDSC and monocytes were more likely to differentiate into M1 macrophages. While these conclusions depended upon our ability to classify macrophages based on CD206 expression, in our hands it was a reliable marker of M2 macrophages in both rodents and humans. These results discouraged use of mice to evaluate the *in vivo* activity of M2 macrophages generated by PAM3, since most of the macrophages produced by PAM3 in mice were M1.

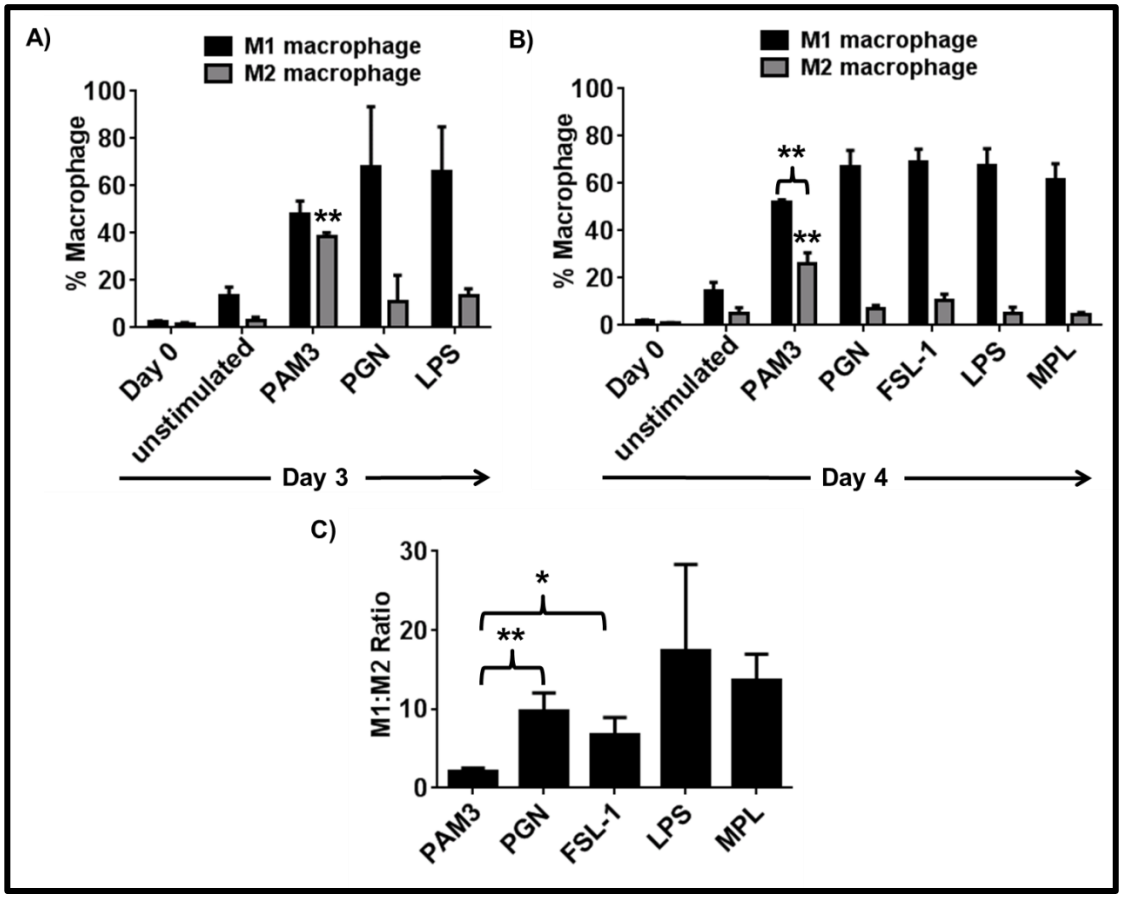


**Figure 3.29: Mouse mMDSC and monocytes do not primarily differentiate into M2 macrophages in response to PAM3.**

*A) Percentages of M1 and M2 macrophages derived from mMDSC (mean ± SD from 2 independently analyzed samples). B) Percentages of M1 and M2 macrophages derived from bone-marrow monocytes (mean ± SD from 4 independently analyzed samples). C) Ratio of M1:M2 macrophages derived from bone-marrow monocytes (mean ± SD of 4 independently analyzed samples). * p<0.05; ** p<0.01 PAM3 treated samples vs. untreated samples.*

### 3.1.22 PAM3 and M-CSF generate M2-like macrophages from HLA-DR$^+$ monocytes

The polarizing activity of PAM3 was compared to that of M-CSF, a cytokine known to drive human monocytes to differentiate into M2-like macrophages [163, 519]. HLA-DR$^+$ monocytes were stimulated with 1 μg/ml of PAM3 and 500 ng/ml of M-CSF for 5 days and their differentiation efficiency determined by staining with the macrophage marker 25F9. Expression of the M2-like macrophage associated markers CD163 and CD206 were used to identify the type of macrophage generated. In the absence of stimulation, <20% of the monocytes survived or differentiated into macrophages (Figure 3.30A-C). In contrast, treatment with either PAM3 or M-CSF resulted >80% of the cells acquiring 25F9 expression consistent with their becoming macrophages (Figure 3.30A-C). In the PAM3 treated group, ≈65% of the cells were also positive for CD206 and CD163 identifying these cells as phenotypically M2-like macrophages. The remaining 15% were positive only for 25F9 and were classified as M1-like macrophages

(Figure 3.30B-D). 72% of the cells generated in the presence of M-CSF were phenotypically M2-like whereas ≈7% were M1-like macrophages (Figure 3.30B-D). This difference in frequency of M1- vs M2-like macrophages in PAM3 and M-CSF treated samples is most easily understood by comparing their M2-to-M1-like macrophage ratio (Figure 3.30E). Results from this study support the conclusion that PAM3 preferentially induces MDSC to mature into M2-like macrophages and that M-CSF accomplished that goal even more effectively.

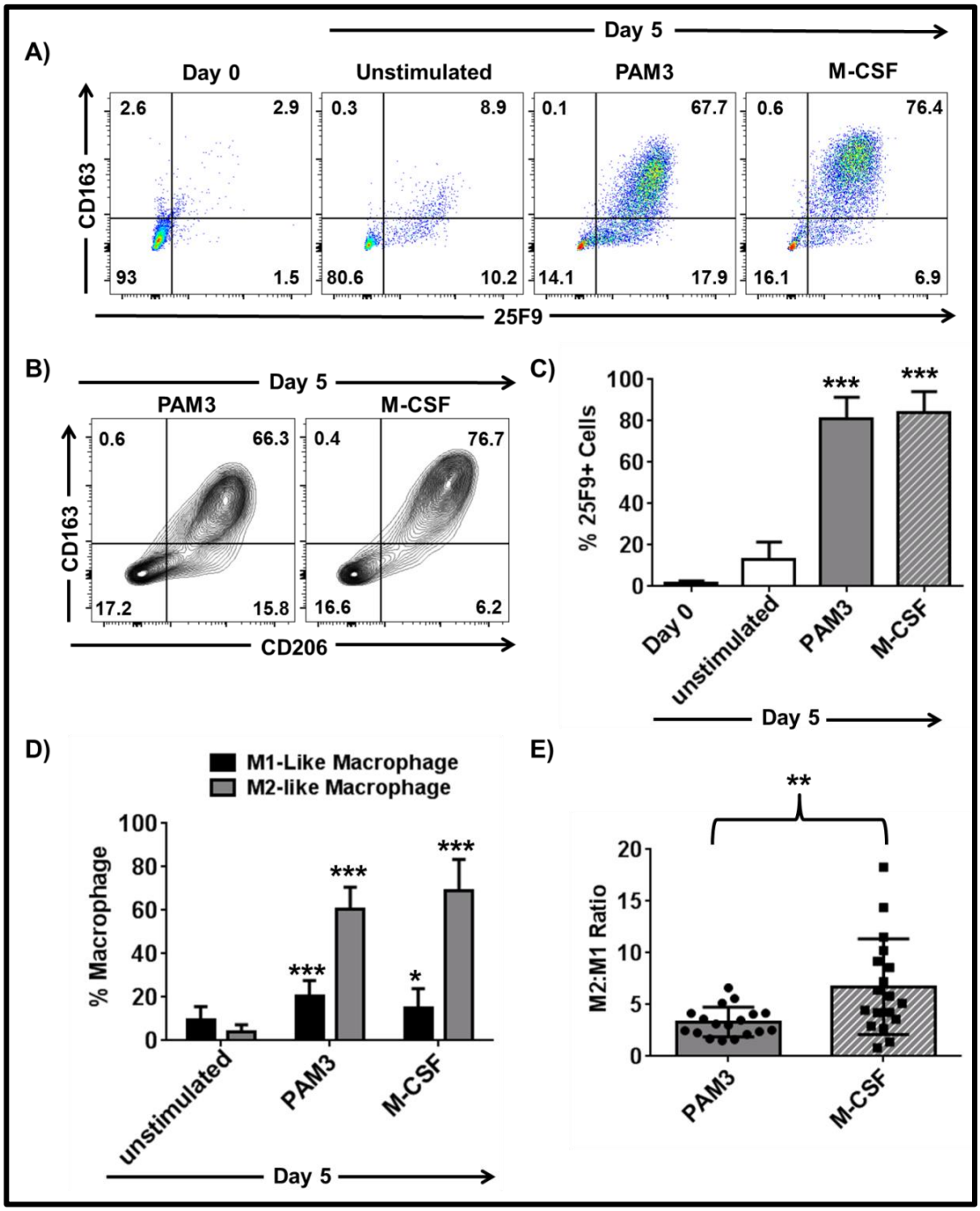


**Figure 3.30: M-CSF and PAM3 polarized HLA-DR$^+$ monocytes towards M2-like macrophage phenotype.**

*A) Representative dot plots depicting changes in CD163 and 25F9 expression upon differentiation. B) Representative dot plots showing co-expression pattern of M2-like macrophage markers CD163 and CD206. C) Percent of cells expressing the active macrophage marker 25F9 (mean ± SD of 18 independently analyzed donors). D) Percentages of M1- and M2-like macrophages (mean ± SD of 18 independently analyzed donors). E) Ratio of M2-to-M1-like macrophages (mean ± SD of 18 independently analyzed donors). * p<0.05; ** p<0.01; *** p<0.001 unstimulated vs. PAM3/M-CSF stimulated samples.*

### 3.1.23 PAM3 and M-CSF differ in their ability to induce HLA-DR$^+$ monocytes to differentiate into M2-like macrophage

After observing the profound ability of M-CSF to drive M2-like macrophage differentiation, we hypothesized that the effect of PAM3 might be mediated via the induction of M-CSF from monocytes which in turn would polarize cells towards the M2 phenotype in an autocrine or paracrine fashion. To test this hypothesis 25 μg/ml anti M-CSF neutralizing antibody was added to cultures for 5 days. As expected, the addition of anti-M-CSF antibody to M-CSF stimulated cultures almost completely blocked cell differentiation (Figure 3.31A). However, neutralization of M-CSF did not alter the frequency with which M2-like macrophages were generated in PAM3 stimulated cultures (Figure 3.31B).

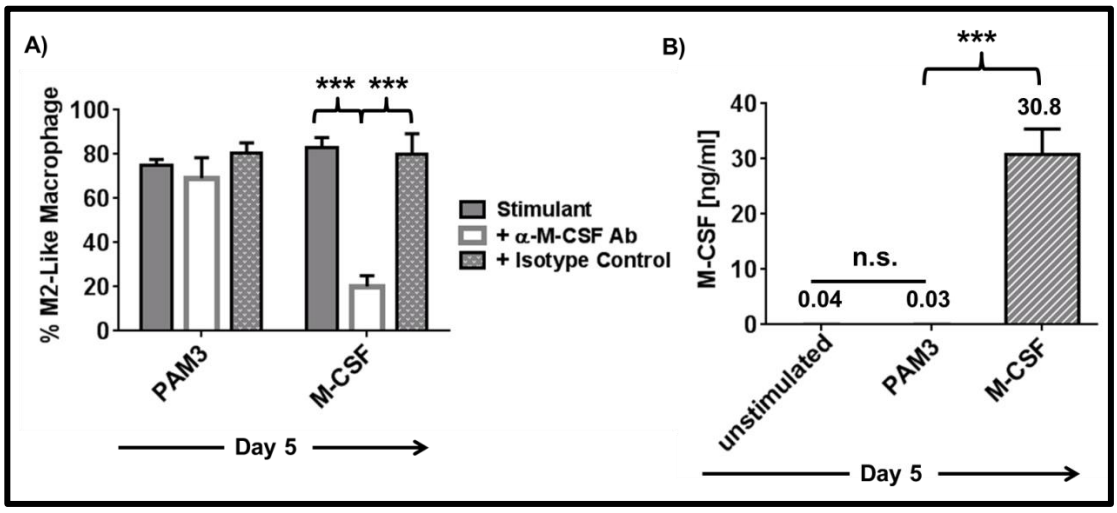


**Figure 3.31: PAM3-induced M2-like macrophage differentiation of HLA-DR$^+$ monocytes is independent of M-CSF.**

*A) Percent of M2-like macrophage present in cultures in the presence or absence of anti-M-CSF neutralizing antibody (mean ± SD of four independently analyzed donors). B) Quantification of secreted M-CSF levels (mean ± SD of four independently analyzed donors). *** p<0.001.*

### 3.1.24 Functional activity of PAM3 and M-CSF induced M2-like macrophages

Previous results established that both PAM3 and M-CSF treatment generated phenotypically M2-like macrophages from HLA-DR$^+$ monocytes. The function of these macrophages was evaluated by measuring their ability to suppress the proliferation of autologous naïve CD4$^+$ T

cells as described in Section 2.2.6.2. As expected, the addition of anti-CD3/CD28 beads to culture stimulated the T cells to proliferate as detected by the dilution in CFSE content (Figure 3.32A; Plots 1 and 2). When PAM3 or M-CSF was added to the pure T cell cultures (in the absence of monocytes), their rate of proliferation was unchanged suggesting that these agents had no direct effect on T cells (Figure 3.32A; Plots 3 and 4). Similarly, untreated monocytes did not alter proliferation of the T cells (Figure 3.32B; Plot 2). ). In contrast, PAM3 or M-CSF stimulated monocytes reduced T cell proliferation by >80% (Figure 3.32B; Plots 3 and 4). These results suggested that M2-like macrophages generated in the presence of PAM3 or M-CSF were functionally active.

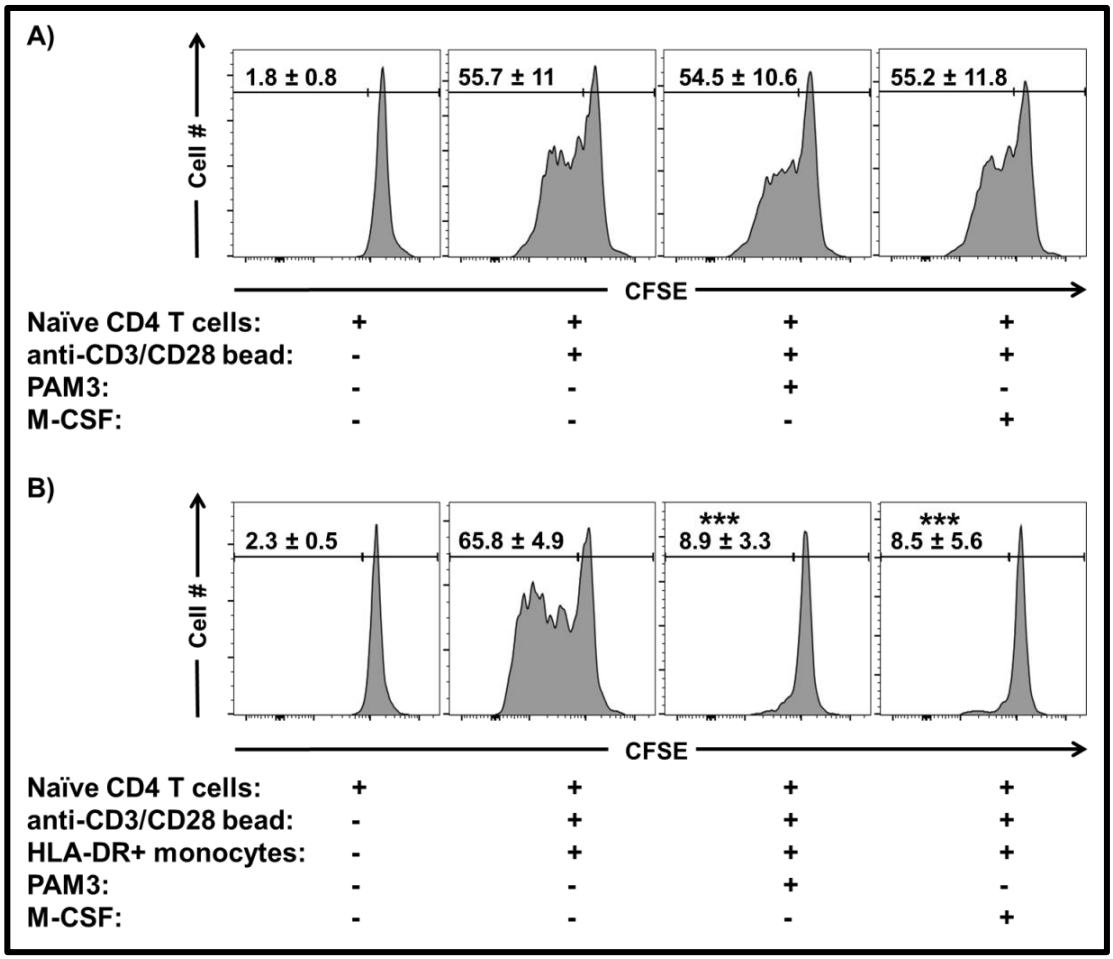


**Figure 3.32: Macrophages generated from HLA-DR$^+$ monocytes in the presence of PAM3 and M-CSF suppress proliferation of T cells.**

*A) Effect of PAM3 and M-CSF on proliferation of naïve CD4$^+$ T cell in the absence of HLA-DR$^+$ monocytes (mean ± SD of four independently analyzed donors). B) Effect of PAM3 and M-CSF on proliferation of naïve CD4$^+$ T cell in the presence of HLA-DR$^+$ monocytes (mean ± SD of four independently analyzed donors). *** p<0.001 stimulated monocyte containing cultures vs. unstimulated monocyte containing cultures.*

### 3.1.25 Morphology of PAM3 and M-CSF induced M2-like macrophages

To address possible differences in PAM3- vs. M-CSF-induced M2-like macrophages, cellular morphologies were investigated. HLA-DR$^+$ monocytes stimulated with PAM3 or M-CSF for 5 days were imaged under bright-field microscopy. Undifferentiated monocytes are typically round and ≈10 μm in diameter. By day 5 a majority of unstimulated macrophages were smaller in size and had high granularity, characteristics of dead/dying cells. PAM3 stimulated cells retained their circular shaped but were slightly enlarged. These cells tended to form layered clusters. In contrast, M-CSF stimulant cells underwent extensive changes and acquired a dendritic morphology, consistent with the phenotype of M2-like macrophages (Figure 3.33). This difference in cellular morphology suggested that PAM3 and M-CSF had independent and distinguishable effects on M2-like macrophages.

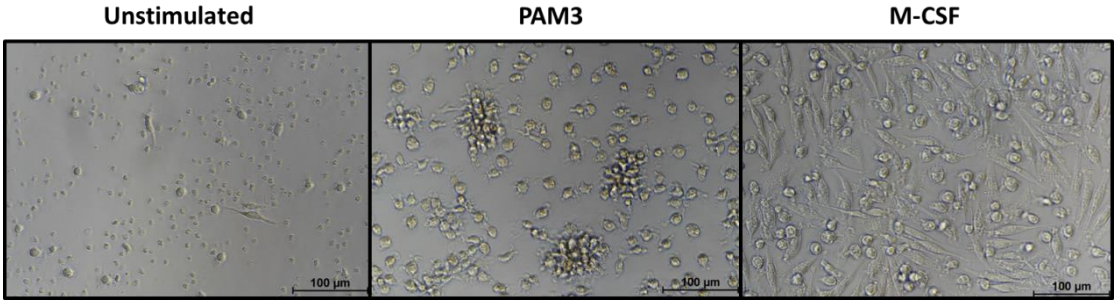


**Figure 3.33: Distinct morphology of unstimulated, PAM3 or M-CSF stimulated HLA-DR$^+$ monocytes at Day 5.**

### 3.1.26 PAM3 and M-CSF-induced M2-like macrophages originated from HLA-DR$^+$ monocytes differ in lineage and functional marker expression

Differences in the cellular morphology and the observation that PAM3-induced M2-like macrophage differentiation is not dependent on M-CSF suggested that macrophages generated by PAM3 might have characteristics distinct from those generated by M-CSF (Figure 3.31)(Figure 3.33). To further characterize these macrophages, their pattern of expression of selected surface/intracellular markers was analyzed. This included analysis of the i) percentage of cells up-regulating each marker and ii) change in the mean fluorescence intensity. Human monocytes can be discriminated based on their expression of the myeloid markers CD11b and CD14 [23]. On Day 0 all HLA-DR$^+$ monocytes were positive for both CD11b and CD14. Yet >60% of the cells further up-regulated these markers following PAM3- and M-CSF treatment consistent to express a pattern consistent with that of active macrophages ($p<.01$; Figure 3.34)[524]. CD11b and CD14 levels also increase following stimulation with PAM3 or M-CSF ($p<.001$; 6-8-fold; Figure 3.35). Expression of the co-stimulatory molecule CD40 and scavenger receptor CD68 were also analyzed to assess the functional activity of these macrophages. Although CD40 is primarily expressed by M1-like macrophages it is also present in tissue-resident macrophages [525]. Similar to 25F9, CD68 is a marker of active macrophages [523].

Thus, we expected to observe an increase in expression levels of both markers coincident with differentiation. Indeed, CD40 and CD68 were up-regulated by >60% of the cells and MFI values increased 10-15-fold ($p<.01$; Figure 3.34; Figure 3.35).

CD16 (FcγRIII) is differentially expressed by human monocyte populations [21]. Interestingly, stimulation of monocytes with M-CSF resulted in >80% of the macrophages acquiring 6-fold higher levels of CD16 expression (p. <.01) whereas in PAM3 stimulated samples this rate not significantly greater than background (Figure 3.34, Figure 3.35). These findings suggest that CD16 can be used to discriminate between macrophages generated by M-CSF vs. PAM3.

Additional markers were analyzed due to their close association with different aspects of M2-like macrophage function. CD273 (PD-L2) is a ligand for PD1 which is responsible for the suppression of T cell activation [526]. CD204 (SR-A) and CD209 (DC-SIGN) are expressed by tissue-resident macrophages and are associated with the capacity to endocytose particles [153]. The percent of macrophages with enhanced expression of these markers was similar following PAM3 and M-CSF stimulation (Figure 3.34). However macrophages generated in the presence of M-CSF expressed these markers at higher levels. While the same trend was detected for CD273 and CD209, only for CD204 did this difference achieve statistical significance (Figure 3.35).

In addition to these markers, changes in the expression of another PD-1 ligand CD274, scavenger receptor CD36, and co-stimulatory molecules CD80 and CD86 were analyzed. These markers were either not significantly or modestly ($p<0.05$) increased following PAM3 and M-CSF-induced macrophage polarization (Figure B2). Therefore, we concluded that they are not essential for M2-like macrophage characteristics.

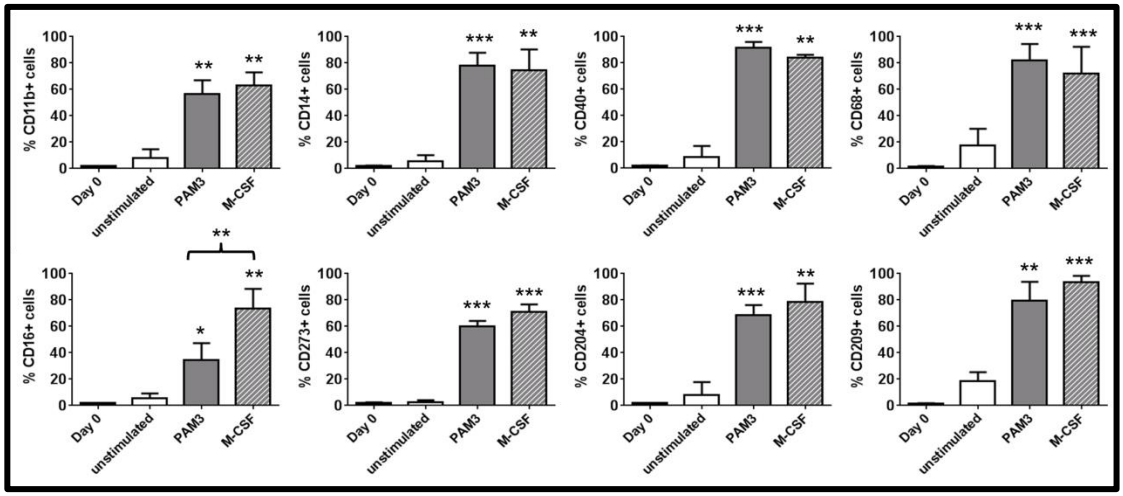


**Figure 3.34: CD16 is differentially up-regulated in PAM3 and M-CSF macrophages.**

*Percentage of cells up-regulate CD11b, CD14, CD40, CD68, CD16, CD273, CD204 and CD209 with PAM3 and M-CSF-induced macrophage differentiation (mean ± SD of four independently analyzed donors). ** p<0.01; *** p<0.001.*

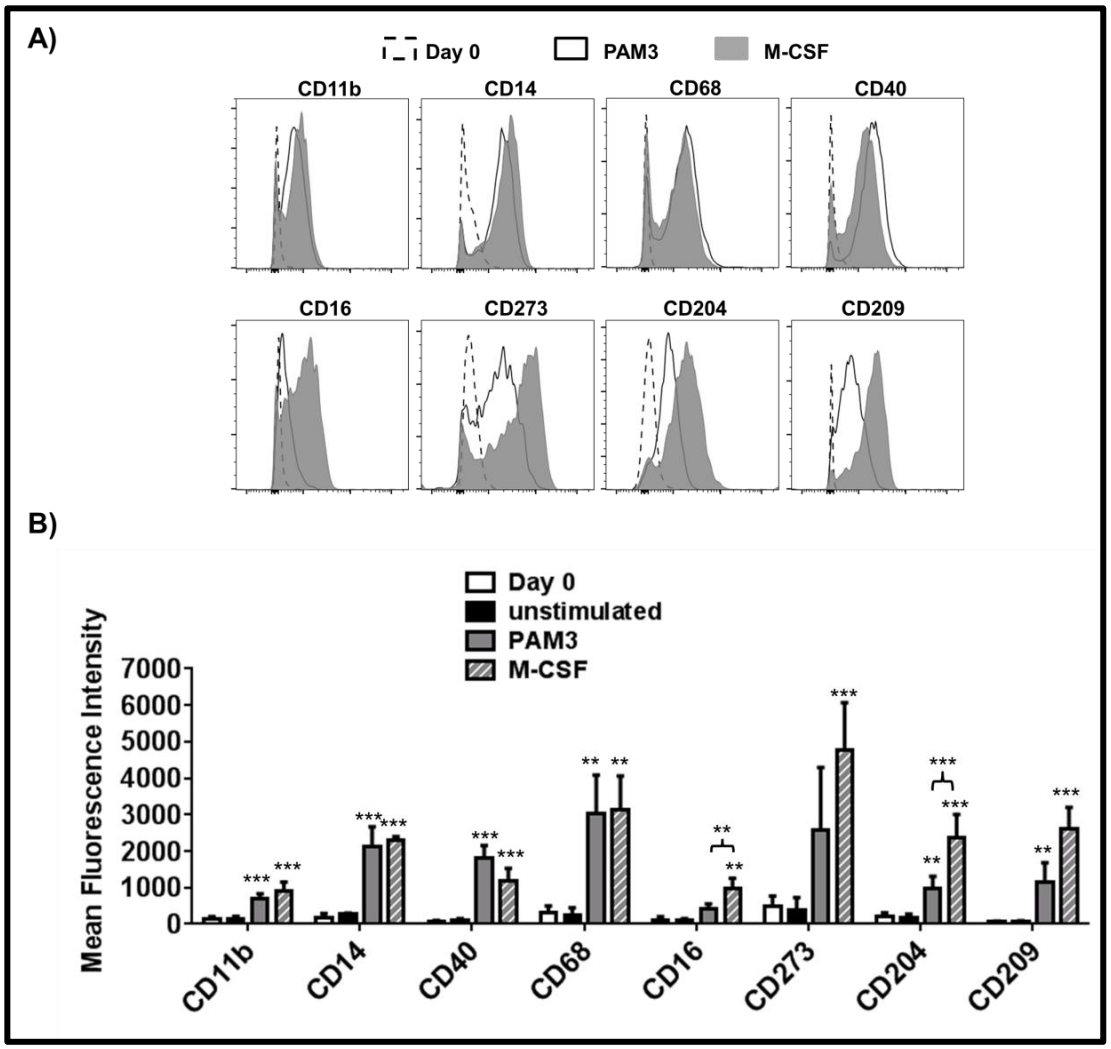


**Figure 3.35: PAM3 and M-CSF induced macrophages slightly differ in marker expression.**

*A) Representative histograms depicting change in the expression levels of CD11b, CD14, CD40, CD68, CD16, CD273, CD204 and CD209 following stimulation with PAM3 and M-CSF for 5 days. B) Mean fluorescence intensity of selected markers (mean ± SD of four independently analyzed donors). ** p<0.01; *** p<0.001 PAM3/M-CSF stimulated vs. unstimulated.*

### 3.1.27 PAM3 and M-CSF generate M2-like macrophages from HLA-DR$^+$ monocytes that differ in phagocytic activity

Scavenger and C-type lectin receptors mediate particle phagocytosis by macrophages [527, 528]. Higher levels of the scavenger receptor CD204 and the C-type lectin receptor CD209 expression in M-CSF-induced macrophages when compared to macrophages generated by

PAM3 suggested that the phagocytic ability of these macrophages might differ. To test this hypothesis, macrophage generated after 5 days in culture were incubated with labelled dextran for 45 minutes and their mean fluorescence intensity normalized by subtracting background values from untreated macrophages. Consistent with the morphological observation showing that PAM3 generated macrophages form clusters, background fluorescence of the PAM3-stimualated macrophages was slightly but non-significantly higher than that those treated with M-CSF (Figure 3.36A). The increase in MFI following exposure to dextran showed that M2-like macrophages from both cultures were phagocytic (Figure 3.36A). Yet the magnitude of their activity was quite different. The MFI of PAM3 cultured macrophages increased 9.7 ± 3.5 fold over the background whereas that of M-CSF derived macrophages rose 77.5 ±37.6 fold ($p<.05$; Figure 3.36B). The M-CSF-induced macrophages also contained 2.5 fold more dextran particles than those treated with PAM3 ($p<.05$; Figure 3.36C). Collectively, these results indicate that macrophages differentiated in the presence of M-CSF had greater phagocytic ability.

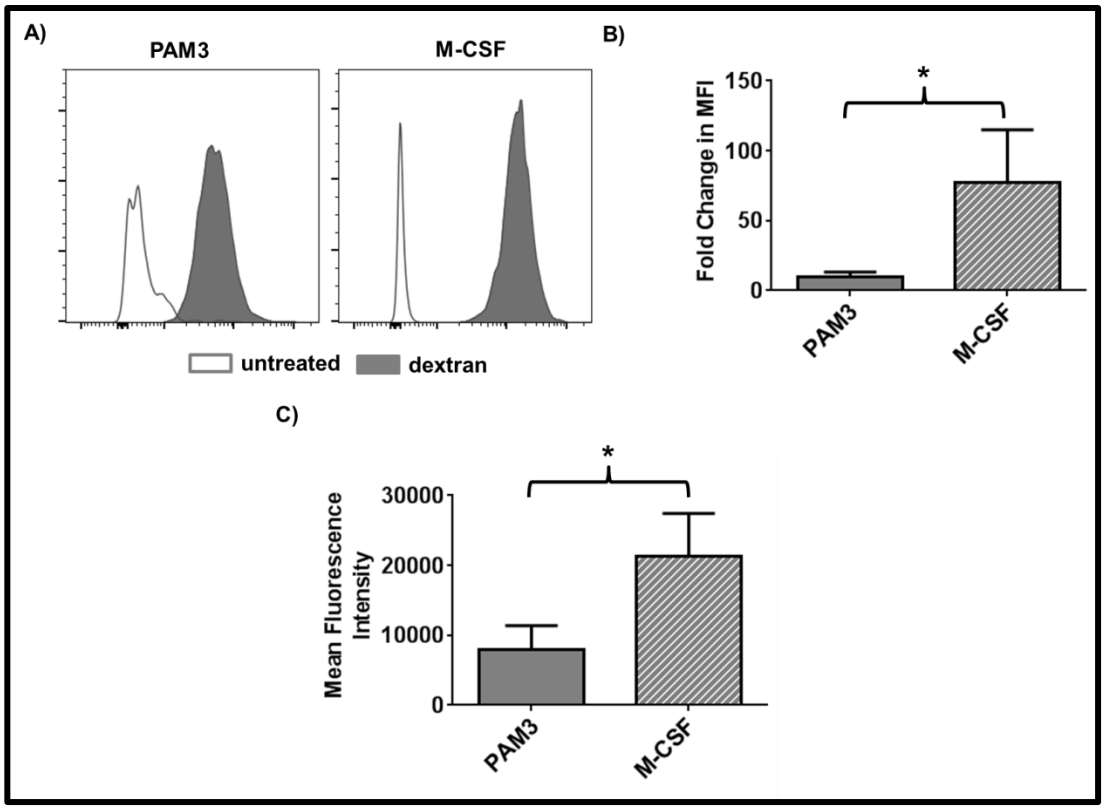


**Figure 3.36: PAM3 vs M-CSF-induced macrophages differ in their ability to phagocytose.**

*A) Representative histograms showing change in the MFI values following incubation with fluorescein-labelled dextran. B) Fold change in the MFI values of dextran treated vs. untreated macrophages C) Mean MFI value of dextran treated macrophages generated in the presence of PAM3- vs. M-CSF (mean ± SD of four independently analyzed donors). * $p<0.05$.*

### 3.1.28 Regulatory network underlying PAM3 and M-CSF-induced M2-like macrophage differentiation of HLA-DR$^+$ monocytes

Differences between PAM3 vs. M-CSF-induced M2-like macrophages led us to examine the regulatory networks involved in their generation. HLA-DR$^+$ monocytes were stimulated with PAM3 or M-CSF for 4 hours (N=6). To compensate for inter-donor variation in baseline gene expression, up-regulated genes were identified in each sample by comparison to baseline expression of untreated cells from the same donor. All genes up-regulated more than two-fold are shown in the Appendix Table 2. To identify relevant regulatory networks, IPA analysis was performed on all genes significantly up-regulated in a majority of donors. Those genes up-regulated by both PAM3 and M-CSF are expected to play a role in the general process of M2-like macrophage differentiation. Mapping those genes into networks identified two intercommunicating pathways: 1) NF-κB-related and 2) IL-10-linked. The NF-κB network along with the MAPK pathway was predicted to have two main effects: i) activation of PTGS2 (COX-2, an enzyme that catalyzes both pro- and anti-inflammatory lipid mediators) and ii) secretion of IL-1RA, a decoy receptor for pro-inflammatory cytokine IL-1β (Figure 3.37)[529, 530]. IL-10, on the other hand, was more directly linked to production of other cytokines and chemokines, such as IL-6, suggesting that this arm might be related to the function rather than the differentiation of M2-like macrophages (Figure 3.37).

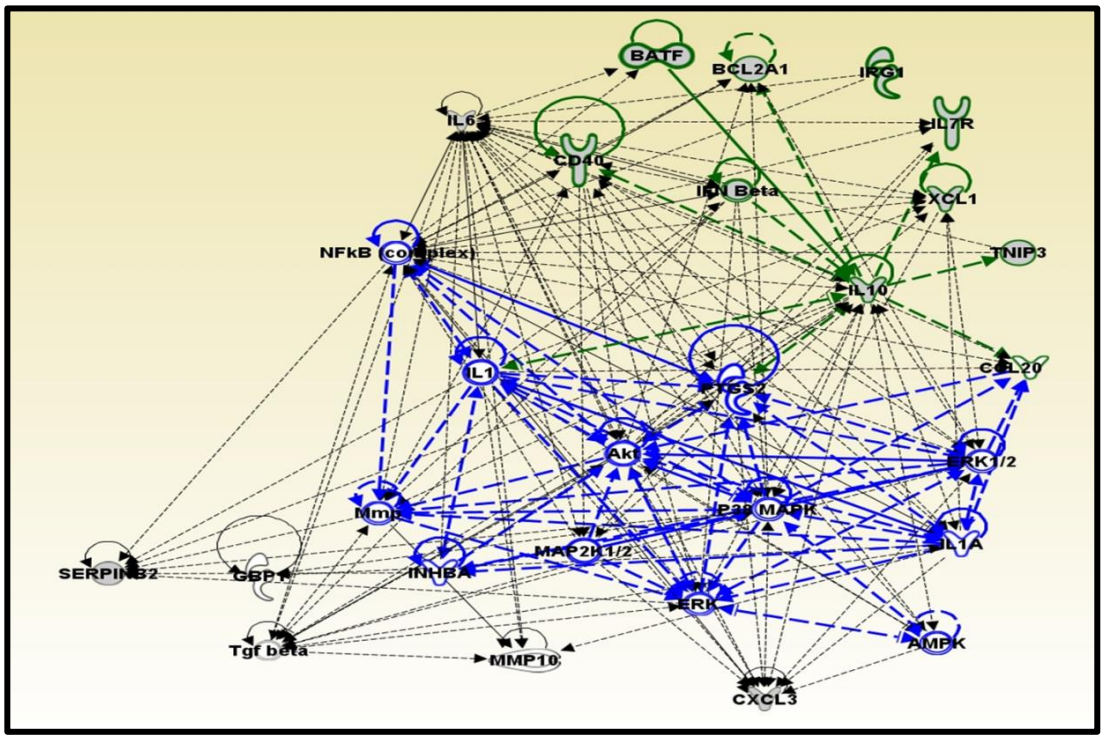


**Figure 3.37: Shared network of genes up-regulated during the course of PAM3- and M-CSF-induced macrophage differentiation.**

*Scheme depicting gene networks up-regulated in both PAM3 and M-CSF stimulated macrophages. Blue network represents NF-κB-related genes and green network is the genes linked to IL-10. (based on N=6).*

In addition to the shared networks, both PAM3 and M-CSF stimulation up-regulated unique sets of genes. Each would be expected to provide the basis for the distinct characteristics of thes resultant macrophages. Genes unique to PAM3 were linked to both the NF-κB complex and IL-6 (Figure 3.38) whereas genes specific to M-CSF were strongly associated with NF-κB but not IL-6. These findings confirm the central role of these pathways in M2-like macrophage biology and suggest that NF-κB is dominant while IL-6 might have a distinctive role in PAM3- but not M-CSF-driven polarization.

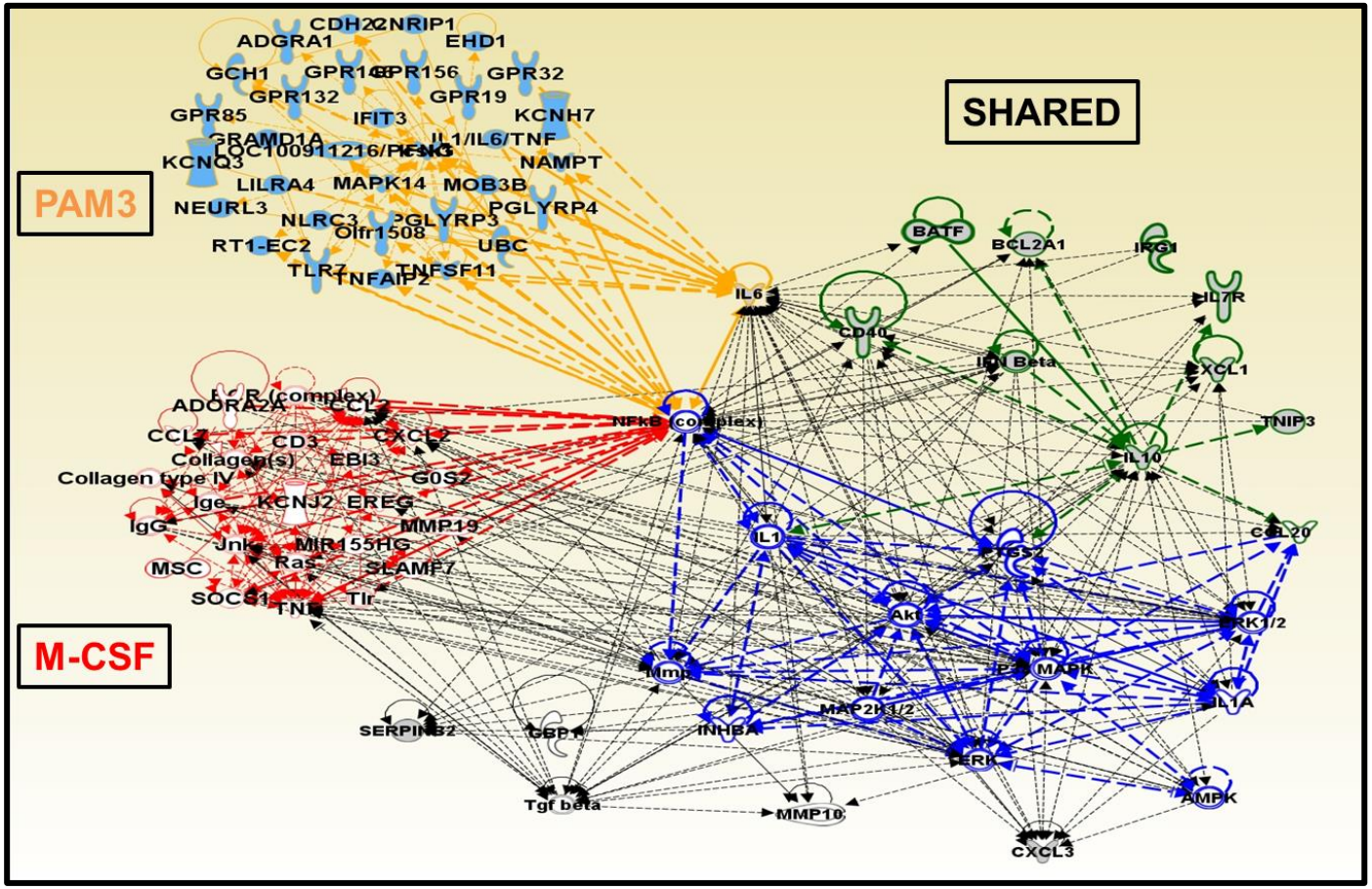


**Figure 3.38: Interaction of distinct set of genes up-regulated by PAM3 vs M-CSF with shared regulatory network.**

*Scheme demonstrating interaction of PAM3- (orange) or M-CSF- (red) specific networks with the shared networks (green and blue)(based on N=6).*

### 3.1.29 Validation of selected targets identified with microarray

IPA results indicated that PAM3- and M-CSF-induced M2-like macrophage differentiation utilized the same regulatory network. To test this hypothesis, candidate genes were targeted using specific inhibitors or neutralizing antibodies. NF-κB was predicted to be the major pathway driving M2-like macrophage polarization. Consistent with that expectation, adding 2.5 μM of Celastrol, an inhibitor NF-κB, completely blocked M-CSF-dependent M2-like macrophage polarization and reduced PAM3-induced differentiation by 80%, verifying the central role of NF-κB (Figure 3.39).

The IPA results further predicted that IL-6 was important for PAM3 but not M-CSF dependent M2-like macrophage polarization (38). We therefore added IL-6 neutralizing antibody to PAM3 and M-CSF cultures. Neutralization of IL-6 reduced the PAM3-driven macrophage polarization by 20%, whereas M-CSF-induced differentiation remained unaffected, verifying the IPA analysis (Figure 3.39). Consistent with these findings, PAM3 stimulated macrophages secreted higher amounts of IL-6 compared to the macrophages generated in the presence of M-CSF (Figure B3).

p38 MAPK was identified as a target by IPA and was previously shown to be a downstream modulator of the M-CSF signaling pathway. Therefore HLA-DR$^+$ monocytes were incubated with an inhibitor of p38 MAPK phosphorylation for 1 hour prior to the addition of the stimulants (Figure 3.38)[531, 532]. Blockade of p38 MAPK signaling reduced M-CSF dependent macrophage differentiation by 90%. In contrast, only ~30% of the PAM3-dependent macrophage polarization was affected, indicating that p38 MAPK has a differential role in PAM3- and M-CSF-induced maturation (Figure 3.39). Transcription of COX-2 is regulated by both NF-κB and p38 MAPK, leading us to examine the effect of the COX-2 specific inhibitor Celecoxib [533, 534]. COX-2 was active in PAM3- and M-CSF-induced polarization as Celecoxib decreased differentiation rates by ~70% (Figure 3.39). This confirmed that COX-2 is downstream of NF-κB, since inhibition of NF-κB signaling more efficiently prevented macrophage polarization. To test the specificity of COX-2-dependent macrophage polarization, COX-1 was also inhibited. Unlike inducible COX-2, COX-1 is constitutively expressed by macrophages [535]. Although inhibition of the COX-1 signaling pathway slightly impaired M2-like macrophage polarization the magnitude of this decrease did not achieve statistical significance (Figure 3.39). Similarly, neutralization of IL-10 or IFNβ, which were linked to the IL-6 pathway, had no significant effect on M2-like macrophage generation, suggesting they are not required for maturation (Figure 3.39).

Nicotinamide phosphoribosyltransferase (NAMPT) was one of the genes selectively upregulated during PAM3-induced M2-like macrophage differentiation. It was recently shown

that extracellular NAMPT acts as an M2 polarizing agent in patients with chronic lymphocytic leukemia [536]. We therefore investigated the role of NAMPT in PAM3-induced M2-like macrophage differentiation by adding its inhibitor FK866 during culture. A concentration of 10 nM was used as higher concentrations led to cell death. Blockade of NAMPT reduced PAM3-induced M2-like macrophage differentiation by 15% ($p<.05$) but did not affect M-CSF induced M2-like macrophage differentiation (Figure 3.39).

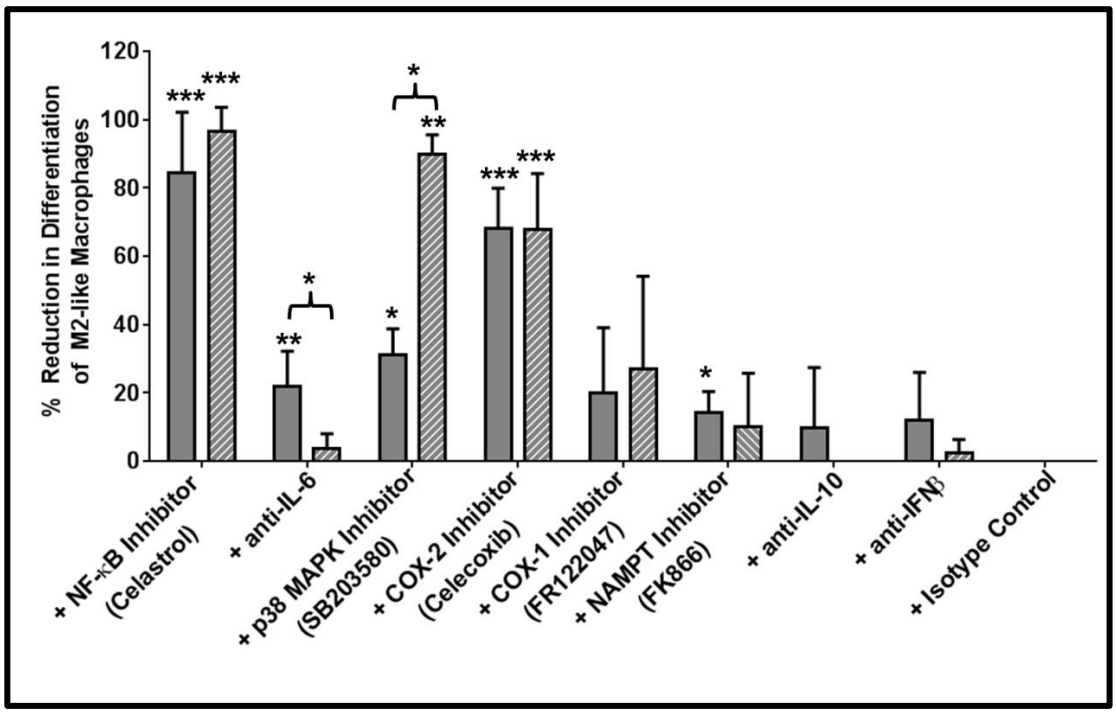


**Figure 3.39: NF-κB is the main regulator of PAM3- and M-CSF-induced M2-like macrophage differentiation.**

*Percent reduction in the frequency of M2-like macrophage derived from PAM3 or M-CSF stimulated HLA-DR$^+$ monocytes in the presence of indicated inhibitors or neutralizing antibodies (mean ± SD of 4-6 independently analyzed donors). * $p<0.05$; ** $p<0.01$; *** $p<0.001$ inhibitor containing samples vs. PAM3/M-CSF stimulated samples.*

**Efforts to Regulate Uptake of Extracellular Vesicles**

### 3.1.30 Mouse macrophage cell line uptakes EV in Scavenger Receptor Class A-dependent manner

Because EV are exposing phosphatidylserine on the surface, we hypothesized that their uptake might be at least partially dependent on Scavenger Receptor Class A. To test this hypothesis, a panel of mouse cell lines was first screened for expression of SR-A (MSR1, CD204). We found that the RAW264.7 macrophage-like cell line expressed high levels of this receptor when compared to other mouse cancer cell lines (Figure 3.40A). Dextran sulfate (DS) is a negatively charged sulfated sugar multimer that acts as an antagonist of class A scavenger receptors.

Chondroitin sulfate (CS) shares structural similarities with DS and serves as a control for nonspecific activity [537, 538]. Following treatment with DS and CS, cells were incubated with EV whose uptake was monitored by changes in mean fluorescence intensity (MFI). Within each cell type, the baseline was determined by background MFI of untreated samples (this value was subtracted from EV treated samples). Consistent with the expression pattern of SR-A, DS treatment significantly interfered with the EV uptake only by RAW264.7 cells (a decrease of 30-50%). Treatment with CS had no effect on the EV uptake in any of the cell lines (Figure 3.40B). As expected, no change in cell viability was following exposure to DS or CS observed supporting the conclusion that any effect on EV uptake rate was not due to reduced number of live cells (Figure B4).

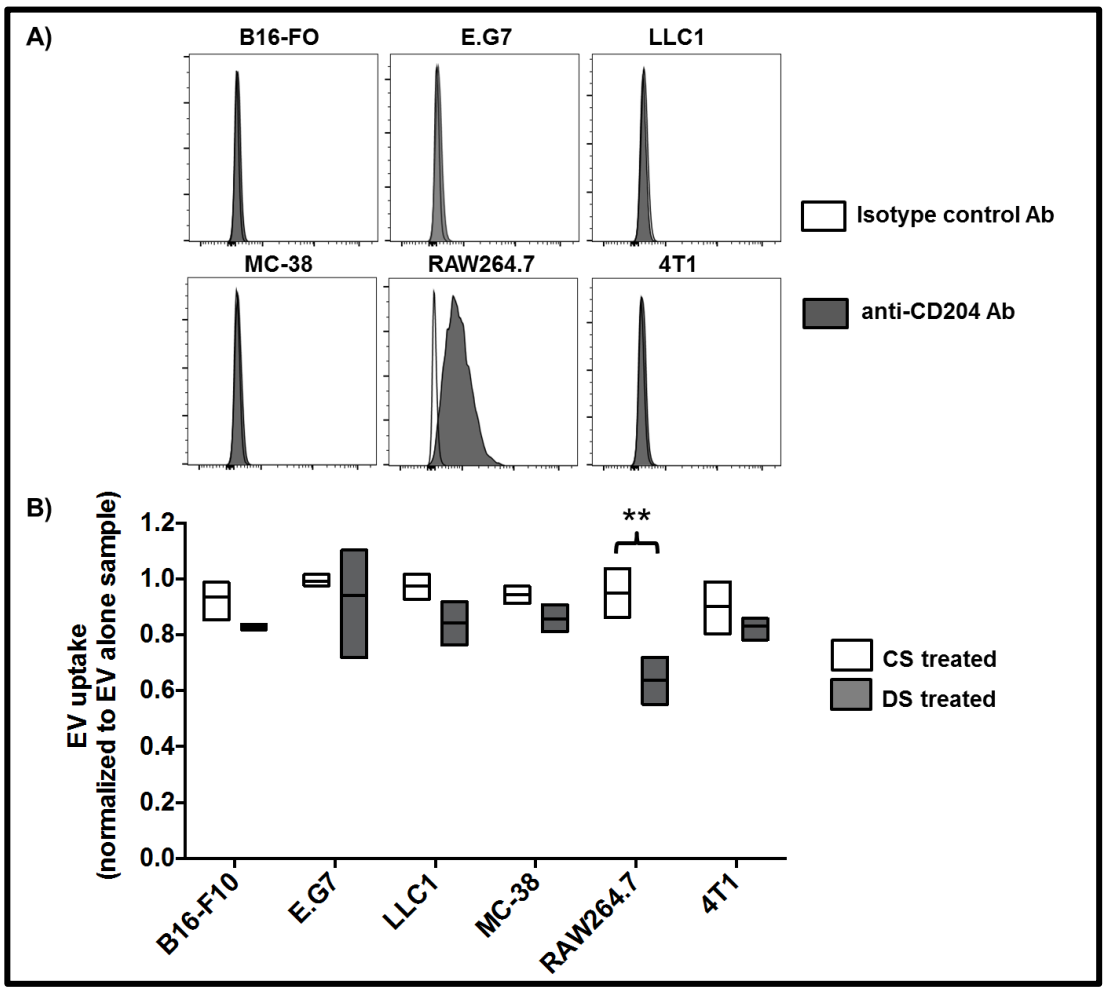


**Figure 3.40: Scavenger receptor class A blockade with DS interferes with EV uptake of murine macrophage cell line.**

*A) Representative histograms depicting SR-A (CD204) staining of B16-FO, E.G7, LLC1, MC-38, RAW264.7 and 4T1 cell lines. B) Change in total EV uptake (mean ± SD of three independent experiments performed in two technical replicates). Boxes represent range of values (min to max), and line in box denotes group mean ** $p<0.01$ as calculated with multiple t-test with Bonferroni correction.*

### 3.1.31 Primary mouse macrophages differentially uptake EV depending on the level of scavenger receptor expression

Although RAW264.7 is a useful screening tool, its behavior can differ substantially from that of primary macrophage. To assess whether freshly isolated macrophages behave in the manner predicted by RAW264.7, monocytes isolated from the bone marrow of C57BL/6 mice were stimulated with LPS or FSL-1 *in vitro*. ≈80% of the monocytes expressed F4/80 after 4 days of culture (Figure 3.41A). Despite this similarity, the resulting macrophage populations differed in their expression of SR-A. Macrophages generated in the presence of LPS expressed 2-fold more SR-A than FSL-1-induced macrophages (N=3, Figure 3.41B). A DS-dependent reduction in the uptake of EV by macrophages correlated with this difference in SR-A expression: DS reduced EV uptake by 41% in LPS polarized macrophages but by only 32% in FSL-1 macrophages ($p<.05$, Figure 3.41C). These findings provided indirect evidence that scavenger receptor class A contributes to the uptake of EV by primary murine macrophages.

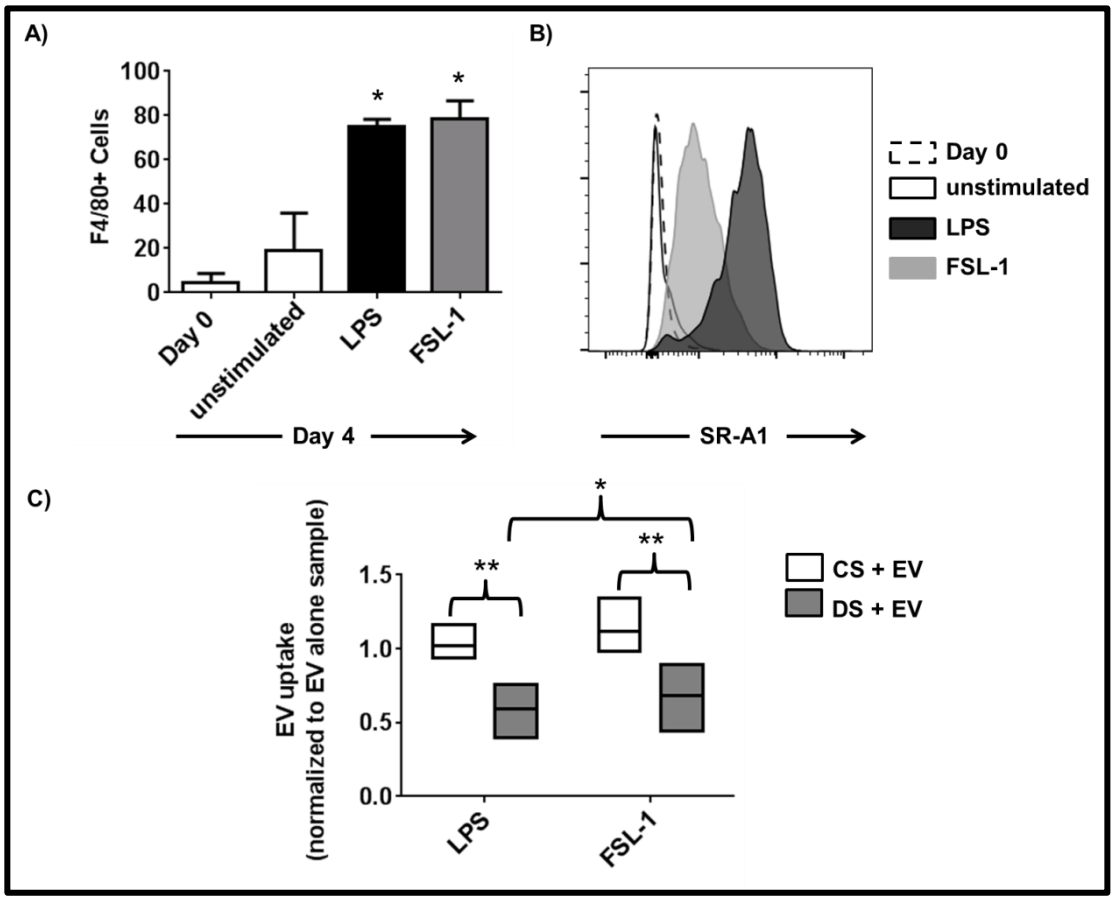


**Figure 3.41: Scavenger receptor class A blockade with DS interferes reduces EV uptake of primary murine macrophages.**

*A) Percent F4/80+ monocytes following 4 days of stimulation (mean ± SD of three experiments). B) Representative histogram depicting SR-A staining of unstimulated, LPS or FSL-1 stimulated monocytes. C) Change in total EV uptake (mean ± SD of five independent*

*experiments). Boxes represent range of values (min to max), and line in box denotes group mean.*

### 3.1.32 Human monocytes uptake EV in scavenger receptor-dependent manner

Human peripheral blood mononuclear cells (PBMCs) were used to investigate whether human monocytes participated in EV clearance. Initial studies identified 0.8 μg/ml of EV as optimal for detecting cellular uptake as it resulted in a 3-fold increase over the autofluorescence of monocytes after 2 hours of incubation (Figure 3.42A). The experiment was repeated after exposure to DS or CS using this optimal concentration (N=4). As above, the background level of fluorescence was subtracted from EV treated samples and normalized to the fluorescence of each donor's monocytes in the EV alone sample.

Monocytes showed the greatest interaction with EV, whereas NK, B and T cells showed less than a 5-fold change in EV signal. DS reduced the uptake of EV in monocytes by ≈40% and at the same time caused a significant increase in the EV signal of T cells As expected, pre-exposure to CS had no effect on the EV uptake by any cell type (Figure 3.42B). These results suggest that the uptake of EV by human myeloid cells is mediated at least partially through a scavenger receptor dependent mechanism and that blocking such receptors may provide a mechanism for directly EV to different cell populations.

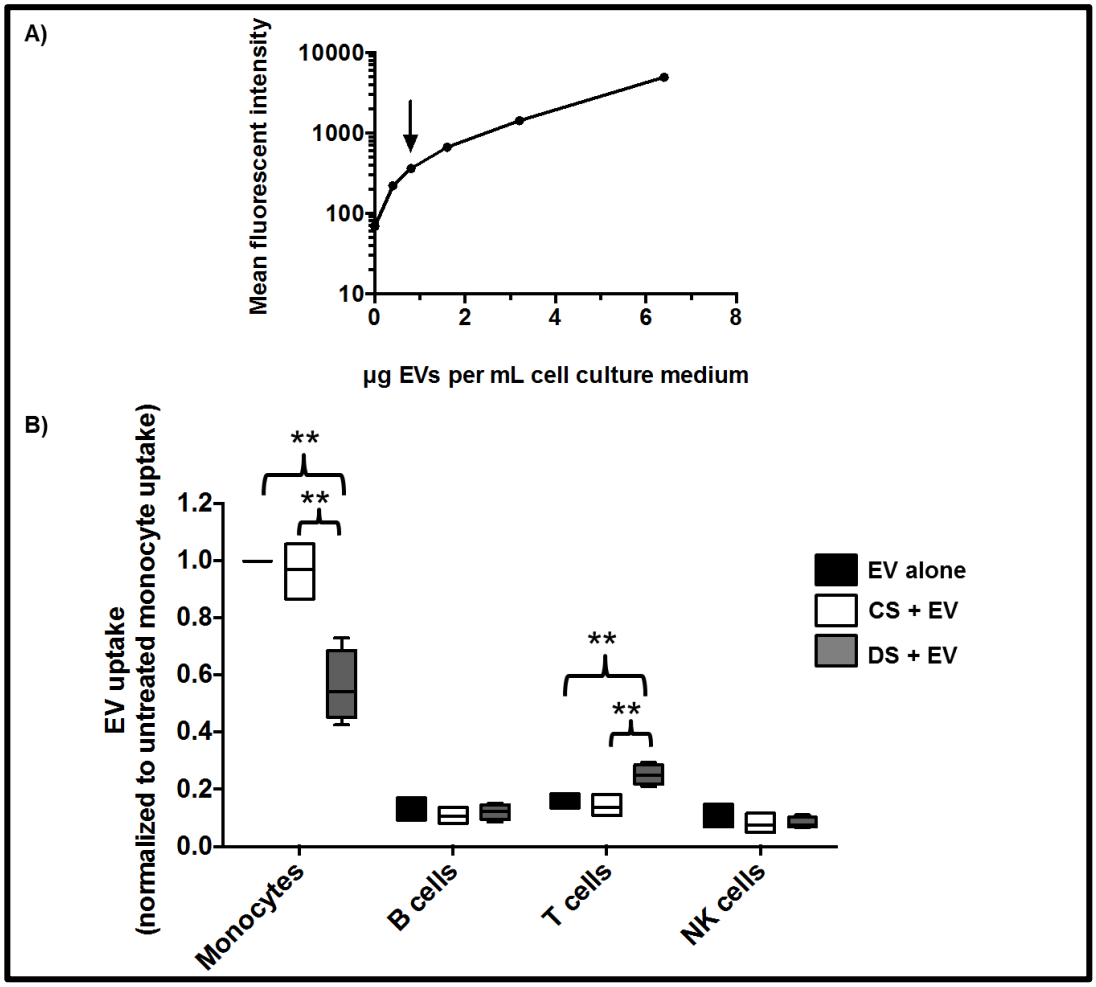


**Figure 3.42: Human monocytes take up EV in a scavenger receptor class A dependent manner.**

*A) Dose dependent increase in the uptake of EV by human monocytes B) Change in total EV uptake of different cell populations in PBMC (mean ± SD of four independently analyzed donors).*

### 3.1.33 Administration of scavenger-receptor inhibitor alters the biodistribution of EV

The above results established that scavenger receptors contribute EV uptake by monocytes and macrophages *in vitro*. One of the difficulties associated with EV-based therapy is the rapid clearance of EV by liver macrophages [439, 539]. We therefore considered whether blocking class A scavenger receptors might alter the biodistribution of EV. FVB mice were injected with DS (or CS) and then EV as described in Section 2.2.16. DS treatment reduced liver uptake of EV by ≈50%. This decrease was accompanied by a nearly 2-fold increase in plasma EV concentration ($p<0.05$) (Figure 3.43A-B-D). The biodistribution pattern was unchanged after CS administration in that EV were cleared by the liver within two hours of i.v. injection (Figure 3.43A-B-C). These finding support our hypothesis that blocking class A scavenger receptors can alter the biodistribution and prolong the circulating half-life of EV. This strategy should

increase the bioavailability of EV to other cell types which might improve their therapeutic utility.

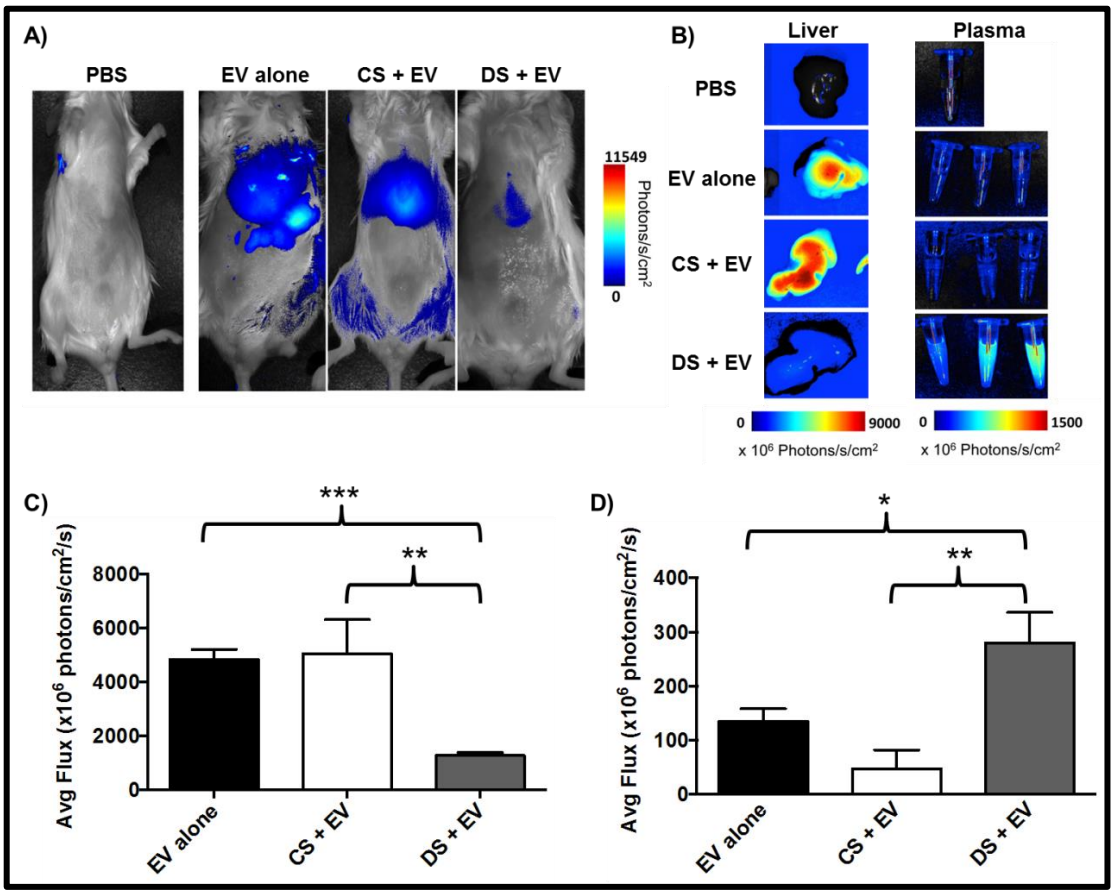


**Figure 3.43: Scavenger receptor blockade decreases the uptake of EV by the liver.**

*A) Representative images of live mice demonstrating localization of EV. B) Representative liver and plasma images showing intensity of EV signal C) Change in the liver uptake of stained EV as measured by photon flux (mean ± SD of three mice). D) Change in the plasma levels of stained EV as measured by photon flux (mean ± SD of three mice). * $p<0.05$; ** $p<0.01$; *** $p<0.001$.*

# Chapter 4

# Discussion

MDSC are immature myeloid cells that can differentiate into macrophages and dendritic cells under normal physiological conditions. In certain disease states they expand in numbers and migrate into tissues where they down-regulate T and NK cell responses [210]. The accumulation of MDSC at tumor sites facilitates immune evasion by tumor cells. For this reason MDSC are emerging as relevant targets for anti-cancer therapy [344]. Previous findings from our group indicated that TLR9 and TLR7/8 agonists can induce the differentiation of mMDSC into tumoricidal M1 macrophages, thereby aiding tumor elimination [360-362]. As human mMDSC lack TLR9, they could be stimulated to mature into M1-like macrophages by TLR7/8 agonists but not the TLR9 agonist CpG ODN [230]. The resultant macrophages were characterized by expression of the macrophage activation marker 25F9 but lacked of expression of the M2-associated markers CD200R, CD163 or CD206.

By comparison, a majority of the mMDSC cultured with the TLR2/1 dual agonist PAM3 showed enhanced expression of CD163, CD206 and CD200R consistent with phenotypic characterization as M2-like macrophages (Figure 3.1)[230, 540, 541]. The pro-inflammatory effect of R848 is consistent with previous reports indicating that TLR7/8 agonists could generate anti-viral and tumoricidal responses by activating human myeloid cells [542, 543]. However, there is little information concerning the immunosuppressive properties of PAM3 [544-546].

My thesis research detected several differences in the response of mMDSC to TLR agonists when compared to earlier findings from the Klinman lab. There are two possible explanations for this kind of variation: 1) markers used to detect M2-like macrophages, 2) differences in the culturing conditions. M2-like macrophages consist of a heterogenous population of cells that vary in surface marker expression [34]**.** Earlier phenotypic characterizations were primarily done based on expression of CD200R whereas my experiments relied preferentially on CD163. Thus, some difference in M1:M2-like macrophage ratio would be expected. Additionally, mMDSC were cultured in the media supplemented with 10% FCS in the previous study [230]. My work showed that high FCS levels increased the percentage of monocytes that spontaneously differentiated into macrophage leading me to reduce the FCS concentration to 2% (Figure B5). Despite these differences, we confirmed the general pattern of R848 and

PAM3-induced differentiation for human mMDSC (although greater heterogeneity among individual donor samples was observed when compared to earlier studies) (Figure 3.1).

Although R848 is a stronger inducer of Th1 responses, its use has been limited to intratumoral injection or topical administration because systemically administered R848 causes side effects including leukopenia [547-549]. For this reason and to dissect the role of different TLRs on macrophage differentiation, we separately tested the polarizing capacity of ligands specific for TLR7 and TLR8. Interestingly, the TLR7 agonist 3M-055 had no significant effect on the differentiation of mMDSC when used alone. In contrast, stimulation with the TLR8 agonist CL-075 generated a mixed population of macrophages the majority of which (~60%) were phenotypically M2-like (Figure 3.2). Although TLR7 and TLR8 belong to the same family of receptors that evolved to recognize ssRNA and support anti-viral immunity, several differences in their target cell selectivity have been described [550]. TLR8 ligands activate monocytes and monocyte-derived dendritic cells whereas TLR7-specific agonists act primarily on plasmacytoid dendritic cells [551]. Those findings are consistent with our observation that the TLR7 agonist 3M-055 was less effective at inducing mMDSC maturation but are somewhat different from previous findings indicating that both TLR7 and TLR8 agonists recapitulate the activity of R848 [230].

One possible explanation for these differences is variability between donors as expression of TLR7 reportedly differs between monocytes vs DC subsets from different individuals [552-554]. As some of our experiments were performed using a limited number of donor samples, this could have biased our findings (a concern that could be remedied by increasing the number of subjects evaluated). Still subtle differences in the TLR7 and TLR8 signaling pathways have been identified. Although both receptors activate the NF-κB, JNK and p38 MAPK pathways, different sets of DC-associated markers can be up-regulated [555]. Furthermore, TLR7 and TLR8 receptors induce different set of pro-inflammatory mediators with TLR7 triggering expression of IFN-inducible mediators, including IFNα, IP-10 and I-TAC while TLR8 induced the production of IL-6, IL-12, IL-8, IL-1 and TNFα [551]. This dichotomy is consistent with the results of mouse studies. The inability of murine TLR8 to respond to ssRNA suggested it might be inactive in mice [556]. Yet further investigation revealed that a combination of TLR8-specific agonists plus poly T ODNs led to NF- κB activation in mouse PBMC and cell lines transfected with mouse TLR8 gene. Those findings suggest that the receptor can be active [557]. Analysis of TLR8-deficient mice indicated that signaling via this receptor might have protective role against systemic inflammation. DC and monocytes from TLR8 KO mice manifest enhanced expression of TLR7, increased NF-κB activation and elevated levels of MHC Class II, consistent with the phenotype of activated APC. Furthermore, these mice had significantly higher levels of serum autoantibodies and developed glomerulonephritis consistent

with the symptoms of lupus-related diseases [558, 559]. These findings indicate that TLR8 might have a restraining role on TLR7 signaling and support our observation that TLR7 and TLR8 have slightly different roles in polarizing human mMDSC towards M1-like macrophages.

M1 and M2 macrophages express distinct cytokine profiles [39]. We hypothesized that R848 and PAM3 triggered the production of different cytokines and that that these might influence macrophage maturation. This possibility was evaluated using two approaches: i) neutralizing cytokines produced in TLR stimulated cultures and ii) incubating mMDSC with various cytokines and cytokine combinations. Initial results identified IL-6 as a possible regulator of macrophage polarization as this cytokine is expressed over the course of both R848- and PAM3-induced differentiation [230]. ELISA results confirmed that IL-6 was present in cultures stimulated by either TLR agonist (Figure 3.3). In this context, IL-6 has a complex role in the generation of both pro- and anti-inflammatory macrophages by controlling the phosphorylation of STAT1 and STAT3 [560]. We found that neutralization of IL-6 reduced the percentage of both M1- and M2-like macrophages by approximately 50% (Figure 3.4). Yet IL-6 alone could not fully recapitulate the activity of either TLR agonist as it induced the maturation of only ~40% of the mMDSC and generate a macrophage population of phenotype (Figure 3.5). Based on these findings, we concluded that IL-6 has a secondary role in mMDSC maturation and is not a main determinant of the macrophage subtypes.

Intracellular cytokine staining of mMDSC demonstrated that IL-12 and IL-10 were differentially expressed by R848 and PAM3 treated mMDSC [230]. Unexpectedly, soluble IL-10 but not IL-12 could be detected in R848 stimulated cultures by ELISA (Figure 3.3). One possible explanation to this discrepancy involves the antibodies used to detect intracellular vs. secreted cytokines. ELISA antibodies recognize IL-12p70, which is composed of p35 and p40 subunits. In contrast, intracellular cytokine staining antibodies might be directed against only the p40 subunit, which is shared by IL-23 as well. In this context, R848 was recently shown to induce secretion of IL-23 but that priming with IFNγ was needed to produce IL-12 [561]. IFNγ is an upstream modulator of IL-12 and induces expression of the p35 subunit of IL-12. It also primes monocytes to respond the TLR agonists by producing more p40 subunit [47]. Neutralization of IL-12 or IFNγ had only a limited effect on R848-induced M1-like macrophage differentiation and IL-12 alone was insufficient to drive macrophage polarization (Figure 3.8)(Figure 3.9)(Figure 3.14).

IPA analysis predicted that IL-12 does not have central role in generating M1-like macrophages, consistent with these other observations

Figure 3.15). These findings involving human MDSC differ from reports concerning mouse MDSC, which were shown to differentiate into macrophages in response to IL-12 in the tumor microenvironment [562, 563]. However, because the tumor microenvironment contains multiple cytokines and growth factors, this effect might not be due to IL-12 alone [564]. Indeed, our results confirm that combinations of cytokines are significantly more of effective than single cytokines in driving the maturation of mMDSC (Figure 3.10)(Figure 3.22).

A less likely explanation is that the intracellular staining was conducted within 12 hour of stimulation whereas the ELISA experiments were performed after 3 days such that early vs later patterns of cytokine production might have been detected. Consistent with such a possibility, IL-10 is up-regulated as part of a negative feedback loop that downregulates IL-12 production [55, 134]. Thus, as IL-10 levels increase over time they might cause a decrease in IL-12 production.

Secretion of IL-10 might also be a major driver of M2-like macrophage differentiation in R848 stimulated cultures (Figure 3.1). However neutralization of IL-10 interferes with R848-driven M1-like macrophage differentiation as well, suggesting that the effect of IL-10 is not limited to M2-like macrophages (Figure 3.4). Moreover, IL-10 supports M1-like macrophage polarization both alone and in combination with TNFα (Figure 3.5)(Figure 3.10). Although IL-10 is generally considered to be an anti-inflammatory factor, its effects seem to be context-dependent and cell-specific [135, 565]. For example, IL-10 augments the expression of IFNγ-related genes by activating STAT1 signaling in patients with systemic lupus erythematosus and healthy donors injected with LPS [566, 567]. Thus, as was the case for IL-6, differential activation of STAT1 vs STAT3 might determine the fate of the mMDSC. However, combination of IL-6 and IL-10 does not have a synergistic or additive effect (Figure 3.6). These findings can be linked to activation of the same downstream JAK/STAT pathway (dominantly STAT3) by IL-6 and IL-10 receptor signaling [568-570].

Several line of evidence suggests that TNFα plays a critical role in the differentiation of mMDSC into M1-like macrophages. Neutralization of TNFα almost completely blocked R848-dependent M1-like macrophage differentiation, whereas TNFα alone was almost as effective as R848 at inducing M1-like macrophage differentiation (Figure 3.8)(Figure 3.9). Moreover, combinations of TNFα with IL-6, IL-10 and/or IL-12 suggested that TNFα determines the phenotype, whereas the other cytokines have a supporting role in increasing the magnitude of mMDSC differentiation (Figure 3.10). Phenotypic evaluation of TNFα plus IL-6 vs R848 shows that the cytokine combination is more effective at inducing M1-like macrophage maturation

(Figure 3.11). Functional evaluation of the cytotoxic activity with tumor cell lysis assay using A549 human lung carcinoma cell line also indicated that the combination generates macrophages with greater tumoricidal ability (Figure 3.11)[571]. To further evaluate the specificity and magnitude of this effect, it is important to test this cytotoxic activity using other tumor and non-tumor cell lines. Indeed TNFα is both an inducer of M1 macrophage polarization and is a product of the resultant cells [39]. Unfortunately, the pleotropic effects of TNFα in driving the initiation and progression of inflammation-induced cancer and autoimmune disorders suggests that this cytokine is not safe to use in the tumor microenvironment [70, 73, 572]. Rather, it provides a tool to allow us to better understand the response of mMDSC under different physiological conditions and identify targetable pathways that regulate their differentiation.

The effect of R848 on mMDSC maturation was replicated by the combination of TNFα plus IL-6 and to a lesser extent by IFNγ (Figure 3.14). For this reason, gene expression signatures of R848, IFNγ, and IL-6 plus TNFα stimulated mMDSC were compared to determine whether a conserved pathway associated with M1-like macrophage differentiation by mMDSC could be identified. Despite some differences among the gene sets up-regulated by these agents, a shared network was found. This pathway included NF-κB, TNFα and IFNγ signaling linked to activation IRF7 and STAT1 (Figure 3.15). The roles of these molecules in the generation and function of M1 macrophages was previously defined [50]. IRF7 is activated in response to endosomal TLR signaling and controls the expression of type I IFN genes [573, 574] whereas NF-κB and STAT1 collectively are responsible for the translation of additional pro-inflammatory cytokines [575]. Although the importance of these pathways should be verified empirically, initial results indicate that mMDSC share the same M1-like macrophage polarization pathways as classical monocytes (Figure 4.1).

In contrast, IL-10 was only up-regulated in R848 treated samples, consistent with a role in R848-induced macrophage differentiation (Appendix Table 1)(Figure 3.15). Furthermore, increased expression of IDO and IL-1RA, which are closely associated with the function and polarization of M2 macrophages, was only detected in samples stimulated with R848 [576, 577] (Appendix Table 1)(Figure 3.15). These genes could be responsible for the generation of M2-like macrophages in R848 cultures (Figure 3.1). Yet, microarray analysis is limited in its ability to detect changes in the expression level of genes but not post-transcriptional modification. Therefore, it is important to extend initial findings from the microarrays using proteomics. Proteomic analysis of M1 macrophages identified a unique fingerprint [578, 579]. This approach might be applied to study differentiation of mMDSC and identify possible targets.

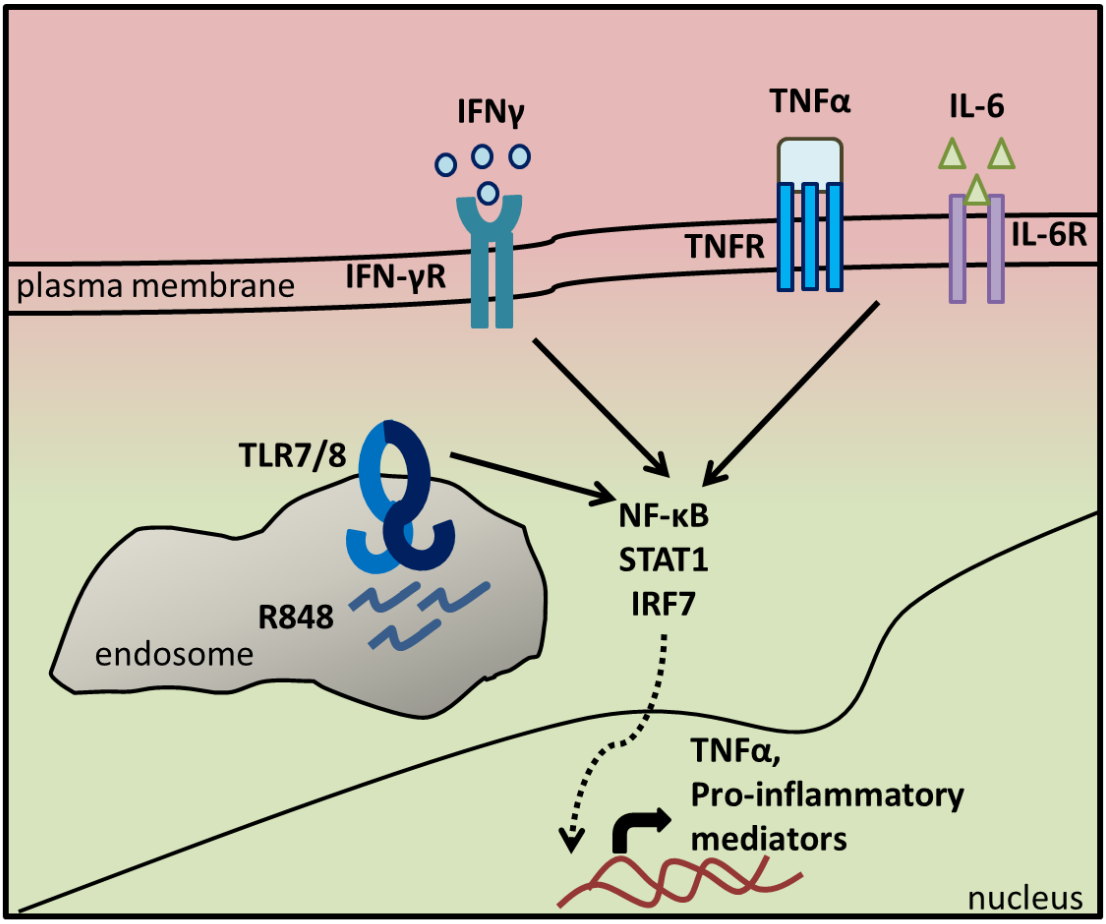


**Figure 4.1: Schematic representation of differentiation of mMDSC into M1-like macrophages.**

GM-CSF is commonly added to cultures of bone marrow cells or peripheral blood monocytes to increase the percentage of MDSC in mixed cultures and to maintain MDSC cell viability *in vitro* [210, 222, 237, 520]. Our findings confirmed that GM-CSF stimulation does not induce human mMDSC to differentiate into dendritic cells or activated macrophages, as neither CD11c nor 25F9 was up-regulated. Yet we detected a significant increase in the expression levels of CD11b and CD206 in GM-CSF treated human mMDSC (Figure 3.16). CD11b is part of the MAC-1 complex that can inhibit T cell activation [580, 581]. Notably, elevation of CD11b was associated with the suppressive activity of the PAM3-induced M2-like macrophage [230]. CD206 is a marker of M2-like macrophages and is expressed by tumor-infiltrating MDSCs possibly as a consequence of GM-CSF exposure [582]**.** These findings elucidate a significant difference in GM-CSF stimulated vs unstimulated human mMDSC in that the former appears to occupy an intermediate state between mMDSC and M2-like macrophages. Additional characterization of signaling pathways, function and surface markers would be required to precisely define the properties of this population. Considering the important role of GM-CSF in

MDSC physiology, we evaluated whether GM-CSF could prevent mMDSC from differentiating into macrophages. Initial results suggested that the response of mMDSC to TLR stimulation was not altered by the presence of GM-CSF, although these findings should be further verified (Figure 3.16).

Another factor that was shown to be crucial for MDSC generation and migration is $PGE_2$**,** which is constitutively present in the tumor microenvironment [235, 323, 325]. $PGE_2$ was also reported to drive tumor infiltrating myeloid cells into TAM [583]. For these reasons we hypothesized that $PGE_2$ might reduce R848-driven polarization of human mMDSC. Interestingly, $PGE_2$ triggered the maturation of ~20% of mMDSC into M1-like macrophages and augmented the polarizing capacity of R848 by skewing the phenotype of macrophages towards M1-like. Indeed, when co-administered with PAM3 $PGE_2$ primarily generated M1-like macrophages (Figure 3.17). In light of the suppressive activity associated with $PGE_2$ this was an unexpected finding. However, recent reports demonstrate that $PGE_2$ accelerates the maturation of DC but at the same time blocks their ability to attract T cells [584]. As mMDSC are immature myeloid cells, if a similar acceleration effect was induced it could be detected as increased M1-like macrophage polarization. Of note, the functionality of these cells was not evaluated in a tumor lysis assay. Another possibility is that addition of $PGE_2$ activated the PGE2-COX-2 positive feedback loop, which plays an important role in MDSC metabolism [325, 585]. COX-2 has pleotropic effects depending on the context in which it is activated. Although our results demonstrated that COX-2 is required for polarization of human monocytes towards M2-like macrophages it is also known that COX-2 is up-regulated in response to inflammatory stimuli [586, 587] (Figure 3.39). Moreover, the dual role of COX-2 is linked to its ability to catalyze both pro- anti-inflammatory lipid mediators [530]. Thus it is possible that activation of COX-2 could have an effect on TLR-induced macrophage differentiation. Analysis of lipid mediators in the cultures could provide insight to altered patterns of macrophage polarization.

Efforts to identify the cytokine milieu responsible for PAM3-induced M2-like macrophage differentiation initially focused on investigating the polarizing capacity of TGF-β, IL-8, IL-4 and IL-13. IL-4 and IL-13 are regulators of the "M2a" subset of the M2 macrophages. This pathway is well characterized *in vivo* using mouse models and *in vitro* using human and murine monocytes [81, 91, 97, 102, 523]. In addition, human MDSC express the IL-4Rα subunit which required for both IL-4R and IL-13R complexes [588]. Although the effect of IL-4 on human mMDSC, had not previously been investigated, exposure of mouse MDSC to IL-4 enhanced their suppressive activity by increasing ARG1 expression *in vitro* [290]. We therefore expected to observe M2-like macrophage differentiation when human mMDSC were stimulated with IL-4 and IL-13. Yet neither of these cytokines had any effect on the survival or differentiation of

human mMDSC. Furthermore, neutralization of IL-4 did not interfere with PAM3-induced macrophage polarization (Figure 3.18). These results suggested that M2-like macrophages generated in the presence of PAM3 should not be classified as "M2a". It should be noted that unlike other groups we did not prime the cells with GM-CSF or M-CSF [147, 589]. While a commonly used strategy, inclusion of those chemokines can polarize monocytes towards M2- and M1-like macrophages [162, 519, 590]. Indeed, analysis of the gene expression profiles of human macrophages generated by M-CSF vs. M-CSF plus IL-4 identified no significant differences, indicating that M-CSF alone is sufficient to polarize M2-like macrophages [163]. Thus, we conclude that activities attributed to IL-4 might reflect, at least in part, inclusion of M-CSF during culture. As discussed below our results confirm that M-CSF is sufficient to polarize human mMDSC and monocytes into M2-like macrophages (Figure 3.20)(Figure 3.30).

Similar to IL-10, TGF-β was found to polarize classically activated macrophages towards a deactivated state [136, 591]. TGF-β released by alternatively activated macrophages can contribute to the generation of Treg and to resolution of inflammation [592-594]. For these reasons, we checked for the effect of TGF-β on mMDSC differentiation. The addition of TGF-β alone failed support mMDSC polarization *in vitro* (Figure 3.18). Since we did not measure secreted levels of TGF-β following mMDSC differentiation, it is possible that TGF-β influences the activity but not polarization of macrophage. IL-8 is a chemokine produced by both epithelial cells and macrophages [595]. Although the effect of IL-8 as a pro-inflammatory mediator is controversial, it was shown that IL-8 was responsible for the generation of TAM in patients with oral squamous cell carcinoma [596]. In addition, microarray analysis revealed that IL-8 is significantly up-regulated during the course of PAM3- but not R848-induced macrophage differentiation from human mMDSC [230]. Similar to IL-4, IL-13 and TGF-β, IL-8 alone did not influence mMDSC differentiation (Figure 3.18). Collectively, these experiments demonstrate human mMDSC are unresponsive to a wide variety of cytokines with anti-inflammatory properties. Our studies did not eliminate the possibility that some combination of these cytokines may contribute to macrophage polarization. In this context, our findings are slightly different from what is reported about the maturation of murine monocytes although murine and human cells differ substantially. We conclude that the response of mMDSC to cytokines differs from that of classical monocytes.

Consistent with the hypothesis that mMDSC and monocytes have distinct patterns of cytokine response our results showed that IL-1β triggers mMDSC to differentiate primarily into M2-like macrophages (Figure 3.19). Studies with monocytes established that IL-1β both triggers the generation of pro-inflammatory macrophages and is secreted by these cells as part of their anti-microbial response [597-599]. On the other hand, IL-1β contributed to the accumulation and suppressive activity of MDSC in the tumor microenvironment [306, 330, 331]. Our results

indicated that besides mediating the accumulation of MDSC, IL-1β might contribute to the immunosuppressive microenvironment by driving M2 macrophage/TAM differentiation of mMDSC. However, the combination of IL-1β with IL-6 and IL-10 did not further augment the frequency of M2-like macrophages and failed to duplicate the number of M2-like macrophages generated by PAM3 in culture (Figure 3.19)(Table 3.1). These findings suggest that additional factor(s) might be required to the produce M2-like macrophages.

The activity of M-CSF on human mMDSC was tested because of the essential role of this growth factor on generation of tissue-resident macrophages with suppressive phenotype [162, 519, 589]. Importantly, M-CSF was not secreted during the course of PAM3-induced macrophage differentiation and neutralization of the cytokine had no impact this process. Yet, M-CSF at high doses was capable of inducing M2-like macrophage differentiation with the same (or higher) efficiency as PAM3, suggesting presence of an alternative route of macrophage generation (Figure 3.20). This mechanism was further investigated and discussed for HLA-DR$^+$ monocytes. However, at lower doses (5 ng/ml), M-CSF had a slightly different effect. 5 ng/ml M-CSF less efficiently induced polarization of mMDSC but its combination with IL-6 and IL-10 exceeded the effect of PAM3 (Figure 3.22). At this concentration M-CSF was required for the maintenance cell survival and also determined the phenotype of the macrophage polarization. As previously observed for TNFα, under these circumstances IL-6 and IL-10 had supporting roles increasing the magnitude of the macrophage differentiation. Importantly, in humans circulatory levels of biologically active M-CSF is determined as 10 ng/ml [600]. Thus our results indicated that under normal conditions mMDSC might actively be differentiating or at least become pre-determined to differentiate into M2-like macrophages due to constant M-CSF exposure.

The literature has not determined whether the mMDSC differentiation is a random process (such that any cell can become M1- or M2-like depending on the environment) vs individual mMDSC being pre-committed to respond to maturation signals in a predefined and restricted pattern. It is likely that mMDSC encounter opposing stimuli under physiologic conditions. To test the response of mMDSC to such conditions, the cells were incubated with a combination of IL-6, TNFα and M-CSF. The majority of mMDSC polarizing towards M1-like macrophages switched phenotype and became M2-like in cultures containing M-CSF (Figure 3.24). These findings demonstrate that most mMDSC maintain the capacity to differentiate into either M1- or M2-like macrophage. Still ~10% of the mMDSC exposed to M-CSF remained phenotypically M1-like. These cells might represent the portion of mMDSC pre-committed to become M1-like macrophages (or that had differentiated beyond the point where they were susceptible to other stimuli). This experiment also confirmed that mMDSC preferentially differentiate into M2-like

macrophages which some believe to be their default maturation pathway [163, 601]. If that is the case, TNFα plus IL-6 may not be strong enough convert the cells towards M1 fate.

M1- and M2-like macrophages represent two functionally distinct populations and are generated sequentially during the initiation and resolution of an inflammatory response. For this reason it has been suggested that macrophage phenotypes are dynamic and reversible [602]. This problem was tackled by several groups by counter-stimulating macrophages with opposing stimuli. Following polarization of human monocytes into M1-like macrophages with IFNγ and removal of the initial stimulus, cells were stimulated with IL-4, which resulted in an increase in the levels of M2 macrophage-associated mediators IL-1Rα and CCL18. Yet, these levels were 5-fold lower than the cultures of M2-like macrophages. Conversely, addition of IFNγ to M2 macrophages triggered significant levels of IL-12, IL-1β and TNFα production [603]. Another study took advantage of the dichotomy between the M-CSF and GM-CSF response of human macrophages. Although M1-like macrophages cultured with M-CSF for 6 days up-regulated CD163, showed enhanced phagocytosis and acquired the ability to suppress T cell proliferation, compared to M-CSF cultured macrophages the magnitude of the response was limited. Similarly, secreted TNFα levels were lower for M2-like macrophages re-polarized with GM-CSF than macrophages generated in the presence of GM-CSF [604]. Although that study concluded that macrophage phenotype was reversible, the weakness of the immune response could instead indicate that a small fraction of undifferentiated monocytes were present in the cultures that subsequently responded to the counter-stimulant. To eliminate this possibility, we sorted M1- or M2-like macrophages following TNFα or M-CSF treatment. Counter-stimulation of M-CSF-generated M2-like macrophages with TNFα for 5 days re-directed approximately 50% of the cells to become M1-like. Conversely, M-CSF re-polarized 65% of M1-like into M2-like macrophages (Figure 3.24). These findings indicate that neither M1- nor M2-like macrophages are terminally differentiated and that a single monocyte can differentiate in either direction depending on the factors to which it is exposed. However, 40-50% of the macrophages exposed to the counter-stimulus preserved their original phenotype suggesting either these cells had differentiated beyond a point where they could respond to a different stimulus or that a fraction of monocytes are irreversibly pre-committed to mature into a specific type of macrophage.

Findings involving mMDSC suggested that the TLR2/1 agonist PAM3 might have anti-inflammatory properties (Figure 3.1). This conclusion was confirmed by testing the activity of PAM3 on human monocyts. TLR2 contributes to the recognition of a wide spectrum of ligands including peptidoglycans, tri- or di-acetylated lipoproteins, lipoglycans and lipotheic acids, or endogenous ligands, such as extracellular cellular matrix component hyaluronan or tumor-released factors Hsp72 and versican [212, 605-607]. This heterogeneity in ligand recognition is

linked to the ability of TLR2 to form complexes with several other receptors including TLR1, TLR6, CD14, CD36, GD1a and Dectin-1 [606, 608-613]. TLR2/TLR1 and TLR2/TLR6 heterodimers are believed to be pre-formed in the absence of stimulant. Recognition of ligands alters their structure and initiates downstream signaling [614, 615]. Studies with mouse BMDM suggested that heterodimerization of TLR2 with TLR1 vs TLR6 serves to enhance the spectrum of pathogenic motifs recognized without altering the downstream signaling pathway [616]. Indeed, signaling through all TLRs (with the exception of TLR3) relies on the same downstream mediators including MyD88, NF-κB and MAPK [617].

Thus, we screened a panel of TLR agonists including PGN, (which does not discriminate between the heterodimers) and FSL-1, which specifically recognizes the TLR2/6 heterodimer. PAM3 was the only TLR agonist that induced a majority of HLA-DR$^{+}$ monocytes to differentiate into M2-like macrophages (Figure 3.26)(Figure 3.28). The difference between PAM3 vs FSL-1 suggests that this differentiation pattern is mediated specifically through TLR2/1 heterodimer signaling (Figure 3.27). Although TLR2 can be activated in response to microbial infection to protect the host, several reports suggest that PAM3 might also have an immunosuppressive function in humans [607]. In human DC, TLR2/1 or TLR2/6 signaling restrained the pro-inflammatory response initiated by TLR4 or TLR7/8 activation by reducing IL-12 and TNFα secretion [546]. Similarly, pre-exposure to PAM3 impaired the ability of human monocytes to respond to IFNγ efficiently due to disruption in the transcription machinery [544]. TLR2/1 signaling not only blocked the pro-inflammatory response but also influenced the phenotype of the macrophages generated.

It has been showed that stimulation of human monocytes with PAM3 results in generation of CD209+ macrophages with high phagocytic activity compared to classical macrophages. Although these cells were not characterized as M2-like macrophages, PAM3 was unique in its ability to generate this population of macrophages [618]. Comparison between the PAM3 responses of human monocytes with other TLR2/1 ligands (such as β-defensin 3) indicate several differences among the agonists [545]. Despite eliciting a similar pro-inflammatory cytokine profile (IL-6, IL-18 and IL-1β), PAM3 treated samples also secreted IL-10 and had lower levels of CD86 expression. These effects were associated with PAM3-dependent activation of SOCS1 and the alternative NF-κB complex [545, 546]. These findings are in line with our observation that PAM3 generated macrophages with immunosuppressive properties.

On the other hand, in mouse system PAM3-mediated response is strictly pro-inflammatory. It was shown to PAM3 alone or in combination of IFNγ triggers NF-κB and STAT1 activation to induce production of pro-inflammatory mediators (IL-6, TNFα and NO) from murine monocytes and DCs and combines with for augmented response [619-621]. These results are

consistent with our observation that mouse bone marrow monocytes and mMDSC primarily mature into pro-inflammatory type of macrophages in response to PAM3 (Figure 3.29). Notably, comparison of human vs mouse TLR2 revealed that the homology between extracellular parts is 64% and intracellular parts is 85%. It was established that this variation influences the ligand recognition pattern [622]. However, it is not clear whether there is a difference in the downstream mediators activated following ligand recognition. Still, when compared to the other TLR agonists, PAM3 treatment generated the highest rates of M2 macrophages, suggesting that evolutionarily TLR1/2 signaling triggers an anti-inflammatory response.

The polarizing capacity of PAM3 was investigated with respect to M-CSF because of the important role of this growth factor in generation of tissue resident macrophages. In comparison to PAM3, M-CSF response of donors was more consistent. Interestingly, samples from a limited number of individuals failed to differentiate into macrophages in the presence of PAM3 (Figure 3.30). This difference might be related to polymorphism of the TLR1 and TLR2. It has been shown that polymorphism of TLR2 (also TLR1) associates with higher risk of infection due to impaired ligand recognition [623, 624]. This might be a possible explanation to unresponsiveness of limited number of individuals. As a tendency, there were more M2- and less M1-like macrophages in the cultures of M-CSF, suggesting that M-CSF was more effective than PAM3 (Figure 3.30). This pattern is also observed with other cytokines (in mMDSC), indicating that TLR response is influenced by other factors such as expression levels, whereas cytokine response is more uniform.

As observed previously with mMDSC, PAM3-induced M2-like macrophage differentiation was not dependent on M-CSF as this cytokine was undetectable in PAM3 cultures and neutralization had no influence on the polarization rates (Figure 3.31). These observations suggested that PAM3 and M-CSF macrophages might differ in characteristics and/or functions. Morphological analysis of PAM3- vs M-CSF-induced M2-like macrophages supports the hypothesis that these macrophages had distinct properties (Figure 3.33**)**. Thus, PAM3- and M-CSF-induced macrophages were analyzed for markers related to origin, activation status and function. CD11b and CD14 are markers of myeloid cells, particularly monocytes [19]. Increased expression of these markers confirmed that cells generated in the presence of PAM3- and M-CSF- were macrophages (Figure 3.34)(Figure 3.35). CD11b is also important for the suppression of T cell proliferation mediated by PAM3-driven M2-like macrophages [230]. Similar levels of CD11b up-regulation might be the basis of the functional similarity between PAM3- and M-CSF-dependent macrophages in terms of their ability to suppress T cell proliferation (Figure 3.32).

CD16 expression defines subset of circulatory human monocytes. CD16 is expressed in non-classical and intermediate monocytes but not classical monocytes [21]. The fraction of macrophages that up-regulated CD16 was significantly higher in M-CSF than PAM3 treated samples (Figure 3.34). Human monocytes were sorted based on CD14 and HLA-DR$^{+}$ expression. Thus, the starting population contained both classical (CD14+CD16-) and intermediate (CD14+CD16+) monocytes. M-CSF could either have triggered CD16 up-regulation in classical monocytes or selectively stimulated intermediate monocytes to proliferate. However the mechanism responsible for differential CD16 up-regulation by PAM3 vs M-CSF and the functional significance of CD16 expression by macrophages have not been defined.

The B7 family of receptors regulates the interaction of APC with T cells and subsequent activation or inhibition of T cell responses [625]. CD80 (B7-1) and CD86 (B7-2) expressed by APC are co-stimulatory molecules of MHC-TCR (T cell receptor) signaling. These receptors either bind to CD28 with strong avidity to promote T cell activation or to CTL4 (cytotoxic T lymphocyte-associated antigen 4) with lower affinity to inhibit activated T cells [626]. Although CD80 and CD86 are present on both kinds of macrophages, their expression is lower in M2 macrophages vs M1 macrophages [590, 627]. Our results confirmed that M2 macrophages generated by either PAM3 or M-CSF only modestly increased CD80 and CD86 levels when compared to undifferentiated monocytes (Figure B2). In parallel, we checked for the expression pattern of CD273 (B7-H2, PD-L2) and CD274 (B7-H1, PD-L1). Programmed cell death 1 (PD1) is an immune checkpoint inhibitor that prevents activation of T cells and thus a target for cancer immunotherapy [628]. PD-1 is primarily expressed by T cells and interacts with CD273 and CD274 [629]. While CD274 is constitutively expressed by many different cell types including T cells, B cells, monocytes, DC and stem cells; expression of CD273 is inducible and largely limited to myeloid cells [526, 629, 630]. Our findings indicated that CD274 levels did not increase significantly (Figure B2). In contrast, CD273 levels rose significantly following PAM3- and M-CSF-induced polarization, suggesting that this molecule might play a more important role in suppressing T cell proliferation (Figure 3.35)(Figure 3.34). Consistent with our findings, studies using murine macrophages showed that up-regulation of CD273 in a STAT6-dependent manner following exposure to IL-4/IL-13 is required for contact-dependent inhibition of T cell activation [631, 632].

M-CSF regulates the differentiation of tissue resident macrophages whose primary role is to clear apoptotic/necrotic cells and phagocytose foreign/altered molecules through scavenger and C-type lectin receptors, particularly CD204, MARCO and CD209 [36, 153]. These markers are also expressed (but at lower levels) by alternatively activated macrophages generated by IL-

4/IL-13 or IL-10 (p< .001,

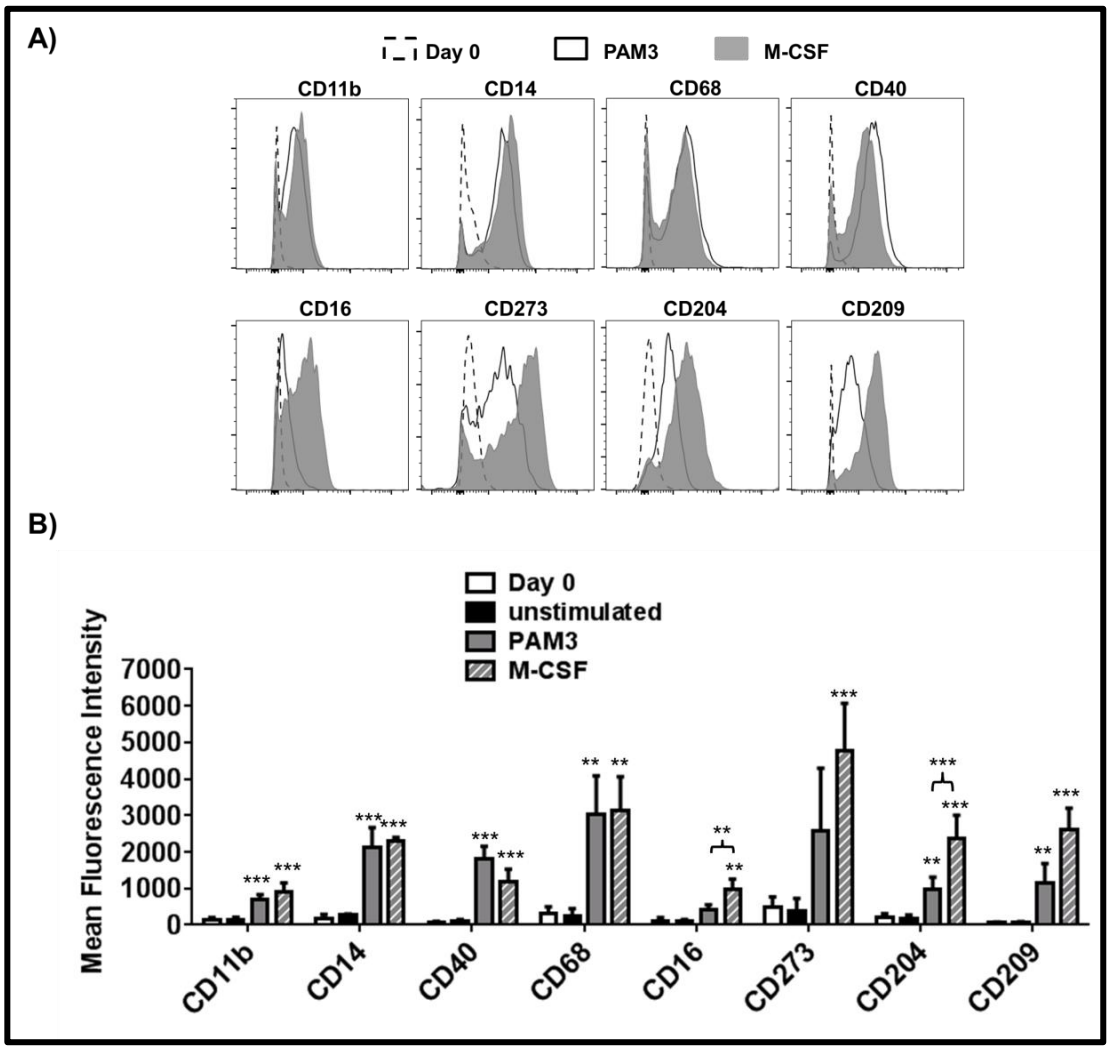


Figure 3.35) [523]. As expected, this difference in marker expression was reflected by phagocytic ability, which was lower in PAM3 generated macrophages (Figure 3.36). Such distinctions raise the possibility that PAM3 vs M-CSF macrophages are represent distinct subsets that serve distinct functions. For example, PAM3 macrophages might mimic those generated in response to commensal organisms, as such bacteria elicit a suppressive environment characterized by anti-inflammatory mediators, allowing them to evade immune elimination [633].

Differences in the morphology, surface marker expression and phagocytic ability of macrophages generated by PAM3 vs. M-CSF led us to examine the regulatory networks associated with M2-like macrophage differentiation. Pathways activated by both agents may be essential for the generation of M2-like macrophages (Figure 3.37). By comparison, genes up-regulated only by M-CSF were identified, including collagenases and metalloproteinases, consistent with the role of resident macrophages in tissue repair and remodeling (Figure 3.38) [153]. In contrast, most of the genes uniquely triggered by PAM3 were G-protein-coupled

receptors (GPCR). Signaling through GPCR regulates many aspects of macrophage biology including activation, survival and chemotaxis [634]. It has been shown expression of different classes of GPCR accompanies polarization towards M1 vs M2 macrophages; although the significance of such differences is not well established [163]. It was recently shown that the anti-inflammatory lipid mediator Resolvin D1 acts as a ligand to GPR32, one of the receptors up-regulated in response to PAM3. This receptor-ligand interaction was sufficient to polarize human monocytes towards an anti-inflammatory phenotype [635]. These findings suggest that although shared pathways are responsible for the differentiation of human monocytes to M2-like macrophages, differentially up-regulated genes following PAM3 and M-CSF stimulation might be linked to specialized functions of the resultant macrophages.

IPA predicted that the NF-κB complex plays a central role in M2-like macrophage polarization (Figure 3.37). Consistent with that interpretation, the addition of Celastrol, and NF-κB blocker, during PAM3 and M-CSF stimulation prevented polarization of human monocytes into M2-like macrophages (Figure 3.39). NF-κB transcription factors are master regulators of the inflammatory response [636]. The classical NF-κB complex (p65/p50) is responsible for transcription of pro-inflammatory genes and is activated as a consequence of TLR, IL-1R and TNFR signaling [637]. In contrast, developmental signals induce alternative NF-κB (p52/RelB) activation, which is required for the production of chemokines related to lymphoid organogenesis [636]. A third p105 pathway (p50/p50) related to classical pathway is required for generation of TAM. p50/p50 homodimer, which lacks transactivator domain, competes with p65/p50 heterodimer for binding of promoter regions of inflammatory mediators [171].

The essential role of NF-κB signaling in TAM was supported by the studies investigating upstream regulators. Activation of NF-κB is controlled by the activator kinase IκB complex, which is comprised of two catalytic subunits IKKα and IKKβ. IKKα and IKKβ phosphorylates and degrades the inhibitor molecules attached the NF-κB complex subunits. IKKβ is required for classical NF-κB activation, whereas IKKα promotes alternative NF-κB signaling [637]. Macrophage-specific deletion of IKKβ revealed its role in resolving inflammatory responses by negatively regulating Stat1 activation [638]. This is powerful approach to re-direct TAM into tumoricidal M1 macrophages [639]. Similarly, IKKα-deficient mice had significantly higher levels of IFNγ producing M1-like macrophages at the site of the tumor [640]. These studies indicated that both classical and alternative NF-κB signaling could potentially contribute to M2-like macrophage polarization. However, because celastrol binds to both IKKα and IKKβ subunits, it does not discriminate between the two arms of the NF-κB pathway [641, 642]. Thus, our findings do not explicitly demonstrate which NF-κB signal is responsible for polarization of M2-like macrophages. Absence of selective inhibitor targeting either one of the arms makes it

difficult to tackle this question. Yet analysis of the expression pattern of NF-κB subunits might provide insight to the mechanism.

COX-2 was predicted to be important for M2-like macrophage differentiation as well (Figure 3.37). COX-2 is an inducible enzyme that catalyzes arachidonic acid into prostaglandins. Although initially shown to be up-regulated mainly in response to proinflammatory agents, primarily to IL-1β and TNFα, in human monocytes, osteoblast and chondrocytes, it is appreciated that COX-2 has a more complex role in progression and resolution of the inflammatory response [534, 643-645]. Up-regulation of COX-2 in an inflammatory setting was described to be a consequence of signaling through NF-κB, AP1 and p38 MAPK pathways [533, 534]. However, COX-2 is also expressed by the tumor infiltrating macrophages and cancerous tissue [646, 647]. COX-2 expression in TAM is regulated by p50/p50 NF-κB complex [647, 648]. Furthermore, anti-inflammatory prostaglandins such as $PGE_2$ catalyzed by COX-2, favors production of Th2 cytokines such as IL-4 and IL-13, while inhibiting IL-2 and IFNγ from helper T cells [649]. All these studies established the role of COX-2 in generation of alternatively activated macrophages. We found that inhibition of COX-2 reduced the generation of M2-like macrophages by ~70% (Figure 3.39). As the magnitude of this effect is modest, we conclude that COX-2 is a downstream modulator of NF-κB signaling. This observation suggested that the same NF-κB – COX-2 axis responsible for generation of TAM can be activated in response to PAM3 or M-CSF. Unlike COX-2, COX-1 is constitutively active in most human cells [650]. Based on microarray results, COX-1 was suggested to be important for polarization of M2 macrophages [163]. Yet we could not verify this finding using a specific inhibitor against COX-1. Suppression of COX-1 had no effect on either PAM3- or M-CSF-induced M2-like macrophage polarization (Figure 3.39).

The difference in the PAM3 vs M-CSF macrophages was reflected by differential dependence on IL-6 vs p38 MAPK. IL-6 was required for only PAM3-dependetn macrophage polarization. Although p38 MAPK was required for both pathways, the relative importance was different (Figure 3.39). It is well established that p38 MAPK is activated both in response to TLR2/1 and CSF-1R signaling pathways [531, 651]. M2-like macrophage polarization can be related to p38 MAPK pathway in two ways: i) activation of AP-1 or ii) regulation of STAT phosphorylation can be more important for translation of the genes required for M-CSF-induced macrophage differentiation. Dependence of PAM3 on IL-6 could be explained by its ability to trigger SOCS1 to prevent Th1 polarization [652]. Because M-CS also up-regulates SOCS1, it may not require IL-6 (Figure 3.38)(Figure 4.2).

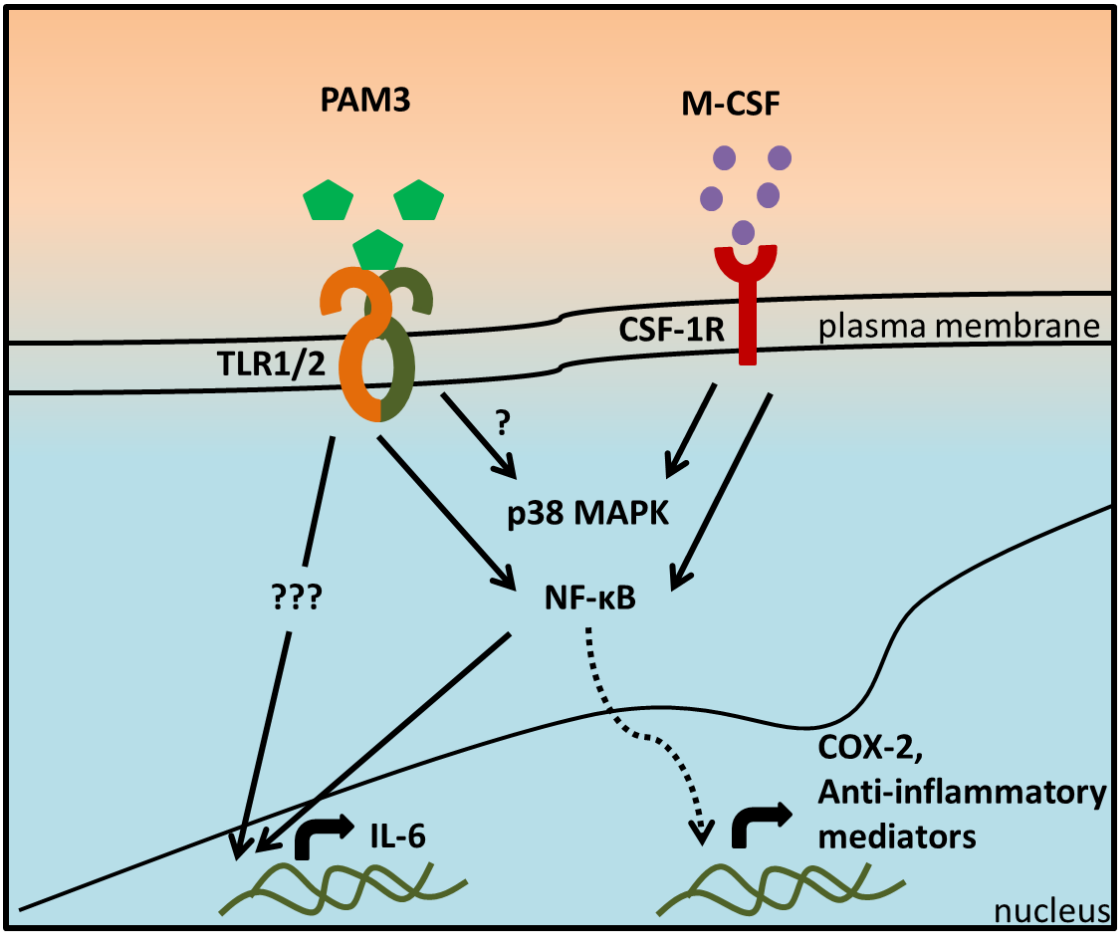


**Figure 4.2: Schematic representation of differentiation of mMDSC HLA-DR$^+$ monocytes into M2-like macrophages.**

Both IL-10 and IFNβ support the generation of M2 macrophages during the recuperative phase of an infection. These cells are required to suppress the ongoing inflammatory response [135, 653]. These cytokines were found to be part of the shared network triggered during PAM3- and M-CSF-induced macrophage differentiation (Figure 3.37). Yet neutralizing IL-10 or IFNβ did not alter the frequency of M2-like macrophages indicating that neither of the cytokines is essential for PAM3- or M-CSF-induced macrophage differentiation (Figure 3.39). The observed increase in IL-10 levels might be a consequence of NF-κB signaling, since the p50/p50 homodimer was shown to regulate secretion of this cytokine by TAM [654]. These findings do not exclude the possibility that IL-10 is important for the immunosuppressive function of the macrophages [565], a possibility that could be tested by monitoring the interaction of macrophages with T cells.

These findings identify the TLR2/1 agonist PAM3 as a novel inducer of M2-like macrophages. Studies using both mMDSC and HLA-DR$^+$ monocytes revealed that PAM3-dependent M2-like

macrophage polarization is independent of IL-4, IL-10 and M-CSF and does not require co-stimulation mediated by ligation of immunoglobulin complex to FcR. For these reasons, PAM3 macrophages do not fall into any category typical of M2 macrophages [132]. Whether PAM3-like macrophages are generated under physiologic conditions is not known. The TLR2/1 heterodimer recognizes a variety of endogenous and exogenous ligands. It is possible that recognition of endogenous ligands by TLR2/1 might induce TAM [212, 606]. For example, TLR ligands from commensal organisms are required for the maintenance of colonic homeostasis [655]. Thus, the TLR2/1 pathway could potentially be involved in generation of commensal bacteria driven M2 macrophages. This line of investigation is constrained by differences in the response of human vs mouse monocytes.

Despite such limitations, our studies suggest that PAM3 may be of use in the treatment of patients with autoimmune disease. Although PAM3 was slightly less effective than M-CSF in generating M2-like macrophage, the *in vivo* use of M-CSF is limited by its role in myelopoeiosis and maintenance tissue-resident macrophage [18, 600]. PAM3 as a lipoprotein can safely be administered and thus represents a therapeutic alternative to M-CSF. This possibility requires further investigation as discussed below.

The final part of my thesis sought to find a strategy that might overcome RES clearance of EV, which is the major problem limiting the therapeutic potential of EV as delivery vehicles [395, 433, 434]. Kupffer cells are tissue-resident macrophages that are maintained by M-CSF [656]. We and others detected high levels of CD204 (SR-A) expression by human and murine M2 macrophages, particularly those generated by M-CSF treatment (Figure 3.35)[39, 657-659]. As Class A scavenger receptors recognize anionic particles, we hypothesized that they might be responsible for the recognition of negatively charged EV [499]. To test this hypothesis, DS was used as a competitive inhibitor.

Pre-treatment of a macrophage cell line or primary macrophages with DS reduced the uptake of EVs by ~30% (Figure 3.40)(Figure 3.41). However several problems were associated with the use of DS to block SR-A. First, DS did not uniquely inhibit only Class A but also slightly altered endocytosis mediated by other receptors. Although though the magnitude of the effect of DS correlated with the CD204 levels, our findings do not exclude the possibility that MARCO is also differentially expressed in cell lines and discrete activation states of the macrophages (Figure 3.40)(Figure 3.41). Yet an antibody against MARCO that can be used reproducibly in FACS analysis is not commercially available. Thus, we couldn't analyze the pattern of MARCO expression. However existing reports suggest that MARCO is up-regulated by pro-inflammatory stimuli and that M-CSF treatment of macrophage decreases its expression *in vitro* [660]. To further evaluate the contribution of different members of scavenger receptor

class A, the RAW264.7 macrophage cell line or primary mouse macrophage were transfected with siRNAs. However that approach resulted in either 1) massive cell death or 2) failed to reduce protein levels by >20%. The other problem with DS is off-target effects. Indeed, dextran shows low affinity interaction with lectin and mannose receptors [661]. Although there are no reports of CD209 being expressed by mouse Kupffer cells, the receptor is present on human counterparts [662] and in human DC, CD209 is partially responsible for EV uptake [459]. Thus, blockade of CD209 in addition class A scavenger receptors might explain the effect of DS on macrophages. Moreover, DS was reported to cause cell detachment and trigger cell cycle arrest in cancer cells [663]. This non-specificity in activity could explain the modest decrease in EV uptake rates of cancer cell lines that lack scavenger receptor A, although decreased cell viability was not detected (Figure 3.40)(Figure B4).

Despite these side effects indirect evidence suggests that SR-A is important for the EV uptake as the level of receptor expression correlates with the magnitude of DS response. LPS treatment result in higher levels of SR-A expression by macrophages compared to FSL-1 treatment. Consistently the reduction in the EV uptake of LPS macrophages, after DS pre-treatment, was significantly higher than that of FSL-1 macrophages (Figure 3.41). Still, it is possible that other scavenger and C-type lectin receptors are differentially expressed in macrophages generated by LPS vs FSL-1 stimulation..

SR-A is expressed by human monocytes with levels increasing during differentiation into macrophages [664]. Human PBMC were used to evaluate the effect of DS in a mixed population and determine whether data from mouse studies applied to humans. Monocytes had higher levels of EV uptake than did T, B and NK cells and this was partially blocked (~35%) by DS pretreatment. This decrease was accompanied by a significant increase in EV uptake by T cells, suggesting that DS treatment can enhance the availability of EV for other cell types (Figure 3.42). The selective increase in EV uptake by T but not B or NK cells may reflect the widespread expression of the Tim family of receptors (Tim1, Tim3 and Tim4) by various subsets of naive and activated T cells [665]. Indeed, the role of Tim3 and Tim4 in EV uptake by immune cells was previously demonstrated [400, 460, 461, 666]. All of these receptors recognize the phosphatidylserine exposed on EV. Thus, it is probable that EV is recognized and internalized via these receptors by T cells.

These *in vitro* findings suggest an approach to alter the biodistribution of EV *in vivo*. As shown in Figure 3.43, administration of DS blocks the accumulation of EV in the liver while significantly increasing EV levels in the plasma EV. These observations indicate that preventing RES clearance enhances the half-life of circulating EV. This mechanism could particularly be important for targeting the tumor microenvironment. Enhanced permeability and a retention

(EPR) effect is a paradigm describing the differences between the vasculature of tumor vs healthy tissue. Blood vessels at the site of tumors have enhanced permeability to nutrients and oxygen. Furthermore, inefficient lymphatic drainage of tumors enables these molecules to be retained in the tumor microenvironment [667]. The combination of these effects results in nonselective accumulation of macromolecules in solid tumors and forms a basis for therapy [668]. By avoiding RES clearance and taking advantage of the EPR effect, on could enhance targeting of therapeutic EV to tumor cells. Consequently, our findings confirming the importance of monocyte/macrophages in the clearance of EV and identifying Scavenger Receptor Class A as a novel and targetable regulator of EV biodistribution has potential implications in humans.

# Chapter 5

# Future Perspectives

The mechanism underlying the differential response of mMDSC to TLR7- vs TLR8-specific agonists requires further investigation. Identifying and understanding the role of downstream mediators could provide insights into M1-like macrophage differentiation and lead to identification of targetable pathways. It is also important to investigate whether the responses detected in this word are conserved among all monocyte populations.

The functionality of macrophages generated from mMDSC in the presence of IFNγ should be confirmed. Microarray and IPA analyses predict TNFα and NF-κB play central roles in M1-like macrophage differentiation. These pathways should be validated using inhibitors or neutralizing antibodies. We expect that the neutralization of TNFα after IFNγ stimulation will clarify whether TNFα plays a central role in M1-like macrophage generation as predicted by IPA. IFNγ was shown to prime murine and human monocytes to respond LPS by differentiating into pro-inflammatory macrophages more effectively [47]. Combining R848 with IFNγ might therefore enhance the maturation of mMDSC into M1-like macrophages.

The combination of IL-6, IL-10 and low dose M-CSF generated phenotypically and functionally suppressive macrophages. Yet the signaling pathways mediating this process remain to be investigated. Microarray analysis could be useful in identifying critical regulatory networks. It is also possible that low dose M-CSF will synergize with other cytokines such as IL-4, IL-13, TGFβ and IL-1β as these cytokines/chemokines were inactive when used alone. Such combinations could identify additional routes of M2-like macrophage differentiation and provide a means to predict the behavior of MDSC under different conditions.

Our initial findings suggested differences in the outcome of TLR2/1 vs TLR2/6 heterodimer signaling. As both receptors rely on the MyD88-dependent signaling cascade, analysis of downstream mediators (particularly the differential up-regulation or phosphorylation of p38 MAPK, ERK, classical and alternative NF-κB, COX-1, COX-2 and STAT) could clarify the mechanism(s) of M2-like macrophage polarization [616]. Although TLR2 signaling primarily triggers STAT1 phosphorylation, limited evidence suggests that PAM3 might also induce activation of STAT3 which is required for polarization of a subset of M2 macrophages [139, 669, 670]. This mechanism should be evaluated further. In addition to p38 MAPK, CSF-1R signaling also activates ERK pathway [671]. The role of this pathway on PAM3- and M-CSF induced M2-like macrophage differentiation can be verified using specific inhibitors.

Inhibition of autologous T cell proliferation by macrophages generated by PAM3 and M-CSF confirmed the functionality of the M2-like macrophages. Yet interactions with specific T cell subsets were not investigated. Generation of M2 macrophages and Treg are supported reciprocally by the cross-talk between these populations [672, 673]. Therefore PAM3- and/or M-CSF-induced macrophages might support the differentiation of Treg from naïve $CD4^+$ T cells. Possible relationship between these cell types should be investigated by co-culture experiments. Moreover, the cytokines produced by PAM3- and M-CSF-induced macrophages were not analyzed in detailed. IPA analysis predicts that production of IL-1Ra should he high. This cytokine can block systemic inflammation and is therefore of interest [576]. Confirmation of IL-1Ra release accompanied by quantification of other cytokines/chemokines could provide clues concerning the physiological roles of these macrophages.

*In vitro* findings with PAM3 suggest that it may be useful for treating patients with inflammatory or autoimmune disease. M-CSF is not suitable for therapeutic use due to its role in myelopoeiosis and tissue-resident macrophage maintenance [18, 600]. Further characterization of PAM3 in terms of its interactions with different cell populations, capacity to reverse the phenotype of pro-inflammatory macrophages, and activity *in vivo* is essential to developed it as a therapeutic alternative for patients with inflammatory or autoimmune diseases. Although human monocytes express the highest levels of TLR2, the receptor is also expressed by DC and granulocytes [674, 675]. Initial findings indicate that NK, B and T cells isolated from human peripheral blood lack TLR2 [674, 676]. Yet recent studies report that TLR2 is expressed by human splenic B cells and activated T cells, where it triggers an inflammatory Th17 and memory T cell response [677-679]. In light of these findings, it is possible that the TLR2 has complex and pleotropic effects. It is important to investigate the nature of the PAM3 mediated immune response in different cell types and in mixed populations. Moreover, the activity of PAM3 might be altered within an inflammatory environment. To test that possibility, monocytes from patients autoimmune diseases include systemic lupus erythematosus (SLE), myositis and RA should be evaluated for their response to PAM3. SLE is a systemic autoimmune disease characterized high M1 and low M2 macrophage frequency [680]. It is therefore a suitable model to test PAM3-driven differentiation of monocytes/macrophages exposed to pro-inflammatory mediators. In this context, preliminary in vivo experiments found significant differences in the response to PAM3 by murine vs human monocytes. Thus we believe that primates are a more suitable model in which to examine the *in vivo* activity of PAM3. As there are no publications concerning the use of PAM3 in non-human primates, our first experiments will identify the effective dose, regimen and pharmacodynamics of PAM 3 in NHPs.

It would be important to confirm our finding concerning the use of DS to discriminate among class A members using specific inhibitors. Knockout animals could provide a useful tool to assess the contribution of each Class A member on EV uptake. Several *in vitro* studies support the conclusion that TIM4 and SR-BI recognize PS and influence EV uptake [400, 460, 463]. However the contribution of CD36 remains unclear. There is no specific inhibitor of CD36 but neutralizing antibodies can be used to evaluate the role of this receptor. Moreover, it is possible that targeting multiple receptors (SR-A, SR-B and TIM) with a combination of inhibitors may further increase circulatory EV in the circulation by mediating more efficient RES escape. Small molecule inhibitors and neutralizing peptides of scavenger receptors with higher specificity are being developed for human clinical usage [681-683]. Administration of EV together with these inhibitors could provide physiologically more relevant results. However, charge is not the only determinant of the EV biodistribution and glycosylation pattern also influences the uptake of EV by cancer cells [684, 685]. This mechanism can potentially be important for targeting of EV to tumor site. Furthermore, it was shown that tailoring EV increases their delivery to target tissue by ~2-fold [439, 442, 445]. Existing findings and our results indicate that combination of modified EV and RES blockade may further overcome the limitation of EV-based therapeutics.

# Bibliography


1. Janeway, C.A., Jr., *Approaching the asymptote? Evolution and revolution in immunology.* Cold Spring Harb Symp Quant Biol, 1989. **54 Pt 1**: p. 1-13.
2. Parkin, J. and B. Cohen, *An overview of the immune system.* Lancet, 2001. **357**(9270): p. 1777-89.
3. Medzhitov, R. and C.A. Janeway, Jr., *Decoding the patterns of self and nonself by the innate immune system.* Science, 2002. **296**(5566): p. 298-300.
4. Kawai, T. and S. Akira, *The role of pattern-recognition receptors in innate immunity: update on Toll-like receptors.* Nat Immunol, 2010. **11**(5): p. 373-84.
5. Wu, J. and Z.J. Chen, *Innate immune sensing and signaling of cytosolic nucleic acids.* Annu Rev Immunol, 2014. **32**: p. 461-88.
6. Rathinam, V.A., S.K. Vanaja, and K.A. Fitzgerald, *Regulation of inflammasome signaling.* Nat Immunol, 2012. **13**(4): p. 333-42.
7. Pandey, S., T. Kawai, and S. Akira, *Microbial sensing by Toll-like receptors and intracellular nucleic acid sensors.* Cold Spring Harb Perspect Biol, 2015. **7**(1): p. a016246.
8. Matzinger, P., *The danger model: a renewed sense of self.* Science, 2002. **296**(5566): p. 301-5.
9. Janeway, C.A., Jr. and R. Medzhitov, *Innate immune recognition.* Annu Rev Immunol, 2002. **20**: p. 197-216.
10. Serhan, C.N., et al., *Resolution of inflammation: state of the art, definitions and terms.* FASEB J, 2007. **21**(2): p. 325-32.
11. Boehm, T., *Design principles of adaptive immune systems.* Nat Rev Immunol, 2011. **11**(5): p. 307-17.
12. Iwasaki, A. and R. Medzhitov, *Control of adaptive immunity by the innate immune system.* Nat Immunol, 2015. **16**(4): p. 343-53.
13. Hume, D.A., *The mononuclear phagocyte system.* Curr Opin Immunol, 2006. **18**(1): p. 49-53.
14. Volkman, A. and J.L. Gowans, *The Origin of Macrophages from Bone Marrow in the Rat.* Br J Exp Pathol, 1965. **46**: p. 62-70.
15. Ginhoux, F. and S. Jung, *Monocytes and macrophages: developmental pathways and tissue homeostasis.* Nat Rev Immunol, 2014. **14**(6): p. 392-404.
16. Dai, X.M., et al., *Targeted disruption of the mouse colony-stimulating factor 1 receptor gene results in osteopetrosis, mononuclear phagocyte deficiency, increased primitive progenitor cell frequencies, and reproductive defects.* Blood, 2002. **99**(1): p. 111-20.
17. Cecchini, M.G., et al., *Role of colony stimulating factor-1 in the establishment and regulation of tissue macrophages during postnatal development of the mouse.* Development, 1994. **120**(6): p. 1357-72.

18. Hume, D.A., et al., *The effect of human recombinant macrophage colony-stimulating factor (CSF-1) on the murine mononuclear phagocyte system in vivo.* J Immunol, 1988. **141**(10): p. 3405-9.

19. Auffray, C., M.H. Sieweke, and F. Geissmann, *Blood monocytes: development, heterogeneity, and relationship with dendritic cells.* Annu Rev Immunol, 2009. **27**: p. 669-92.

20. Van Furth, R., M.C. Diesselhoff-den Dulk, and H. Mattie, *Quantitative study on the production and kinetics of mononuclear phagocytes during an acute inflammatory reaction.* J Exp Med, 1973. **138**(6): p. 1314-30.

21. Ziegler-Heitbrock, L., et al., *Nomenclature of monocytes and dendritic cells in blood.* Blood, 2010. **116**(16): p. e74-80.

22. Passlick, B., D. Flieger, and H.W. Ziegler-Heitbrock, *Identification and characterization of a novel monocyte subpopulation in human peripheral blood.* Blood, 1989. **74**(7): p. 2527-34.

23. Abeles, R.D., et al., *CD14, CD16 and HLA-DR reliably identifies human monocytes and their subsets in the context of pathologically reduced HLA-DR expression by CD14(hi) /CD16(neg) monocytes: Expansion of CD14(hi) /CD16(pos) and contraction of CD14(lo) /CD16(pos) monocytes in acute liver failure.* Cytometry A, 2012. **81**(10): p. 823-34.

24. Geissmann, F., S. Jung, and D.R. Littman, *Blood monocytes consist of two principal subsets with distinct migratory properties.* Immunity, 2003. **19**(1): p. 71-82.

25. Sunderkotter, C., et al., *Subpopulations of mouse blood monocytes differ in maturation stage and inflammatory response.* J Immunol, 2004. **172**(7): p. 4410-7.

26. Wong, K.L., et al., *Gene expression profiling reveals the defining features of the classical, intermediate, and nonclassical human monocyte subsets.* Blood, 2011. **118**(5): p. e16-31.

27. Kurihara, T., et al., *Defects in macrophage recruitment and host defense in mice lacking the CCR2 chemokine receptor.* J Exp Med, 1997. **186**(10): p. 1757-62.

28. Tsou, C.L., et al., *Critical roles for CCR2 and MCP-3 in monocyte mobilization from bone marrow and recruitment to inflammatory sites.* J Clin Invest, 2007. **117**(4): p. 902-9.

29. Jia, T., et al., *Additive roles for MCP-1 and MCP-3 in CCR2-mediated recruitment of inflammatory monocytes during Listeria monocytogenes infection.* J Immunol, 2008. **180**(10): p. 6846-53.

30. Landsman, L., et al., *CX3CR1 is required for monocyte homeostasis and atherogenesis by promoting cell survival.* Blood, 2009. **113**(4): p. 963-72.

31. Auffray, C., et al., *Monitoring of blood vessels and tissues by a population of monocytes with patrolling behavior.* Science, 2007. **317**(5838): p. 666-70.

32. Cros, J., et al., *Human CD14dim monocytes patrol and sense nucleic acids and viruses via TLR7 and TLR8 receptors.* Immunity, 2010. **33**(3): p. 375-86.

33. Medzhitov, R., *Inflammation 2010: new adventures of an old flame.* Cell, 2010. **140**(6): p. 771-6.

34. Gordon, S. and F.O. Martinez, *Alternative activation of macrophages: mechanism and functions.* Immunity, 2010. **32**(5): p. 593-604.

35. Wynn, T.A., A. Chawla, and J.W. Pollard, *Macrophage biology in development, homeostasis and disease.* Nature, 2013. **496**(7446): p. 445-55.

36. Murray, P.J. and T.A. Wynn, *Protective and pathogenic functions of macrophage subsets.* Nat Rev Immunol, 2011. **11**(11): p. 723-37.

37. Biswas, S.K. and A. Mantovani, *Macrophage plasticity and interaction with lymphocyte subsets: cancer as a paradigm.* Nat Immunol, 2010. **11**(10): p. 889-96.

38. Italiani, P. and D. Boraschi, *From Monocytes to M1/M2 Macrophages: Phenotypical vs. Functional Differentiation.* Front Immunol, 2014. **5**: p. 514.

39. Mantovani, A., et al., *The chemokine system in diverse forms of macrophage activation and polarization.* Trends Immunol, 2004. **25**(12): p. 677-86.

40. Kawai, T. and S. Akira, *Toll-like receptors and their crosstalk with other innate receptors in infection and immunity.* Immunity, 2011. **34**(5): p. 637-50.

41. Oppenheim, J.J. and D. Yang, *Alarmins: chemotactic activators of immune responses.* Curr Opin Immunol, 2005. **17**(4): p. 359-65.

42. Barton, G.M. and J.C. Kagan, *A cell biological view of Toll-like receptor function: regulation through compartmentalization.* Nat Rev Immunol, 2009. **9**(8): p. 535-42.

43. Kawasaki, T. and T. Kawai, *Toll-like receptor signaling pathways.* Front Immunol, 2014. **5**: p. 461.

44. Akira, S. and K. Takeda, *Toll-like receptor signalling.* Nat Rev Immunol, 2004. **4**(7): p. 499-511.

45. Trinchieri, G., *Interleukin-12: a cytokine at the interface of inflammation and immunity.* Adv Immunol, 1998. **70**: p. 83-243.

46. Kobayashi, M., et al., *Identification and purification of natural killer cell stimulatory factor (NKSF), a cytokine with multiple biologic effects on human lymphocytes.* J Exp Med, 1989. **170**(3): p. 827-45.

47. Ma, X., et al., *The interleukin 12 p40 gene promoter is primed by interferon gamma in monocytic cells.* J Exp Med, 1996. **183**(1): p. 147-57.

48. D'Andrea, A., et al., *Production of natural killer cell stimulatory factor (interleukin 12) by peripheral blood mononuclear cells.* J Exp Med, 1992. **176**(5): p. 1387-98.

49. Hayes, M.P., J. Wang, and M.A. Norcross, *Regulation of interleukin-12 expression in human monocytes: selective priming by interferon-gamma of lipopolysaccharide-inducible p35 and p40 genes.* Blood, 1995. **86**(2): p. 646-50.

50. Wang, N., H. Liang, and K. Zen, *Molecular mechanisms that influence the macrophage m1-m2 polarization balance.* Front Immunol, 2014. **5**: p. 614.

51. Krausgruber, T., et al., *IRF5 promotes inflammatory macrophage polarization and TH1-TH17 responses.* Nat Immunol, 2011. **12**(3): p. 231-8.

52. Ohmori, Y. and T.A. Hamilton, *Requirement for STAT1 in LPS-induced gene expression in macrophages.* J Leukoc Biol, 2001. **69**(4): p. 598-604.

53. MacMicking, J., Q.W. Xie, and C. Nathan, *Nitric oxide and macrophage function.* Annu Rev Immunol, 1997. **15**: p. 323-50.

54. Edwards, J.P., et al., *Biochemical and functional characterization of three activated macrophage populations.* J Leukoc Biol, 2006. **80**(6): p. 1298-307.

55. Verreck, F.A., et al., *Human IL-23-producing type 1 macrophages promote but IL-10-producing type 2 macrophages subvert immunity to (myco)bacteria.* Proc Natl Acad Sci U S A, 2004. **101**(13): p. 4560-5.

56. Nathan, C.F., *Secretory products of macrophages.* J Clin Invest, 1987. **79**(2): p. 319-26.

57. Trinchieri, G. and F. Gerosa, *Immunoregulation by interleukin-12.* J Leukoc Biol, 1996. **59**(4): p. 505-11.

58. O'Shea, J.J. and P.J. Murray, *Cytokine signaling modules in inflammatory responses.* Immunity, 2008. **28**(4): p. 477-87.

59. Strieter, R.M., et al., *CXC chemokines in angiogenesis.* Cytokine Growth Factor Rev, 2005. **16**(6): p. 593-609.

60. Sindrilaru, A., et al., *An unrestrained proinflammatory M1 macrophage population induced by iron impairs wound healing in humans and mice.* J Clin Invest, 2011. **121**(3): p. 985-97.

61. Grivennikov, S.I., F.R. Greten, and M. Karin, *Immunity, inflammation, and cancer.* Cell, 2010. **140**(6): p. 883-99.

62. de Martel, C., et al., *Global burden of cancers attributable to infections in 2008: a review and synthetic analysis.* Lancet Oncol, 2012. **13**(6): p. 607-15.

63. Coussens, L.M. and Z. Werb, *Inflammation and cancer.* Nature, 2002. **420**(6917): p. 860-7.

64. Sangiovanni, A., et al., *Increased survival of cirrhotic patients with a hepatocellular carcinoma detected during surveillance.* Gastroenterology, 2004. **126**(4): p. 1005-14.

65. Balkwill, F., K.A. Charles, and A. Mantovani, *Smoldering and polarized inflammation in the initiation and promotion of malignant disease.* Cancer Cell, 2005. **7**(3): p. 211-7.

66. Dedon, P.C. and S.R. Tannenbaum, *Reactive nitrogen species in the chemical biology of inflammation.* Arch Biochem Biophys, 2004. **423**(1): p. 12-22.

67. Barcellos-Hoff, M.H., D. Lyden, and T.C. Wang, *The evolution of the cancer niche during multistage carcinogenesis.* Nat Rev Cancer, 2013. **13**(7): p. 511-8.

68. Mussi, A., et al., *Serum TNF-alpha levels correlate with disease severity and are reduced by effective therapy in plaque-type psoriasis.* J Biol Regul Homeost Agents, 1997. **11**(3): p. 115-8.

69. Sharief, M.K. and R. Hentges, *Association between tumor necrosis factor-alpha and disease progression in patients with multiple sclerosis.* N Engl J Med, 1991. **325**(7): p. 467-72.

70. Reinecker, H.C., et al., *Enhanced secretion of tumour necrosis factor-alpha, IL-6, and IL-1 beta by isolated lamina propria mononuclear cells from patients with ulcerative colitis and Crohn's disease.* Clin Exp Immunol, 1993. **94**(1): p. 174-81.

71. Braun, J., et al., *Use of immunohistologic and in situ hybridization techniques in the examination of sacroiliac joint biopsy specimens from patients with ankylosing spondylitis.* Arthritis Rheum, 1995. **38**(4): p. 499-505.

72. Brennan, F.M., R.N. Maini, and M. Feldmann, *TNF alpha--a pivotal role in rheumatoid arthritis?* Br J Rheumatol, 1992. **31**(5): p. 293-8.

73. Koski, H., et al., *Tumor necrosis factor-alpha and receptors for it in labial salivary glands in Sjogren's syndrome.* Clin Exp Rheumatol, 2001. **19**(2): p. 131-7.

74. Segal, B.M., D.M. Klinman, and E.M. Shevach, *Microbial products induce autoimmune disease by an IL-12-dependent pathway.* J Immunol, 1997. **158**(11): p. 5087-90.

75. Martinez, F.O. and S. Gordon, *The evolution of our understanding of macrophages and translation of findings toward the clinic.* Expert Rev Clin Immunol, 2015. **11**(1): p. 5-13.

76. Tang, C., et al., *Interleukin-23: as a drug target for autoimmune inflammatory diseases.* Immunology, 2012. **135**(2): p. 112-24.

77. Kollias, G. and D. Kontoyiannis, *Role of TNF/TNFR in autoimmunity: specific TNF receptor blockade may be advantageous to anti-TNF treatments.* Cytokine Growth Factor Rev, 2002. **13**(4-5): p. 315-21.

78. Efimov, G.A., et al., *Cell-type-restricted anti-cytokine therapy: TNF inhibition from one pathogenic source.* Proc Natl Acad Sci U S A, 2016.

79. Ramos-Casals, M., et al., *Autoimmune diseases induced by TNF-targeted therapies: analysis of 233 cases.* Medicine (Baltimore), 2007. **86**(4): p. 242-51.

80. Mosser, D.M. and J.P. Edwards, *Exploring the full spectrum of macrophage activation.* Nat Rev Immunol, 2008. **8**(12): p. 958-69.

81. Voehringer, D., K. Shinkai, and R.M. Locksley, *Type 2 immunity reflects orchestrated recruitment of cells committed to IL-4 production.* Immunity, 2004. **20**(3): p. 267-77.

82. Jenkins, S.J., et al., *Local macrophage proliferation, rather than recruitment from the blood, is a signature of TH2 inflammation.* Science, 2011. **332**(6035): p. 1284-8.

83. Anthony, R.M., et al., *Memory T(H)2 cells induce alternatively activated macrophages to mediate protection against nematode parasites.* Nat Med, 2006. **12**(8): p. 955-60.

84. Siracusa, M.C., et al., *Dynamics of lung macrophage activation in response to helminth infection.* J Leukoc Biol, 2008. **84**(6): p. 1422-33.

85. Stein, M., et al., *Interleukin 4 potently enhances murine macrophage mannose receptor activity: a marker of alternative immunologic macrophage activation.* J Exp Med, 1992. **176**(1): p. 287-92.

86. Raes, G., et al., *Differential expression of FIZZ1 and Ym1 in alternatively versus classically activated macrophages.* J Leukoc Biol, 2002. **71**(4): p. 597-602.

87. Doyle, A.G., et al., *Interleukin-13 alters the activation state of murine macrophages in vitro: comparison with interleukin-4 and interferon-gamma.* Eur J Immunol, 1994. **24**(6): p. 1441-5.

88. Buechler, C., et al., *Regulation of scavenger receptor CD163 expression in human monocytes and macrophages by pro- and antiinflammatory stimuli.* J Leukoc Biol, 2000. **67**(1): p. 97-103.

89. Cornicelli, J.A., et al., *Interleukin-4 augments acetylated LDL-induced cholesterol esterification in macrophages.* J Lipid Res, 2000. **41**(3): p. 376-83.

90. Relloso, M., et al., *DC-SIGN (CD209) expression is IL-4 dependent and is negatively regulated by IFN, TGF-beta, and anti-inflammatory agents.* J Immunol, 2002. **168**(6): p. 2634-43.

91. Junttila, I.S., et al., *Tuning sensitivity to IL-4 and IL-13: differential expression of IL-4Ralpha, IL-13Ralpha1, and gammac regulates relative cytokine sensitivity.* J Exp Med, 2008. **205**(11): p. 2595-608.

92. Pauleau, A.L., et al., *Enhancer-mediated control of macrophage-specific arginase I expression.* J Immunol, 2004. **172**(12): p. 7565-73.

93. Liao, X., et al., *Kruppel-like factor 4 regulates macrophage polarization.* J Clin Invest, 2011. **121**(7): p. 2736-49.

94. Cao, H., et al., *Differential regulation of class II MHC determinants on macrophages by IFN-gamma and IL-4.* J Immunol, 1989. **143**(11): p. 3524-31.

95. D'Andrea, A., et al., *Stimulatory and inhibitory effects of interleukin (IL)-4 and IL-13 on the production of cytokines by human peripheral blood mononuclear cells: priming for IL-12 and tumor necrosis factor alpha production.* J Exp Med, 1995. **181**(2): p. 537-46.

96. Fenton, M.J., J.A. Buras, and R.P. Donnelly, *IL-4 reciprocally regulates IL-1 and IL-1 receptor antagonist expression in human monocytes.* J Immunol, 1992. **149**(4): p. 1283-8.

97. Cheung, D.L., et al., *Contrasting effects of interferon-gamma and interleukin-4 on the interleukin-6 activity of stimulated human monocytes.* Immunology, 1990. **71**(1): p. 70-5.

98. Standiford, T.J., et al., *Gene expression of macrophage inflammatory protein-1 alpha from human blood monocytes and alveolar macrophages is inhibited by interleukin-4.* Am J Respir Cell Mol Biol, 1993. **9**(2): p. 192-8.

99. Schebesch, C., et al., *Alternatively activated macrophages actively inhibit proliferation of peripheral blood lymphocytes and CD4+ T cells in vitro.* Immunology, 1997. **92**(4): p. 478-86.

100. Kodelja, V., et al., *Differences in angiogenic potential of classically vs alternatively activated macrophages.* Immunobiology, 1997. **197**(5): p. 478-93.

101. Munder, M., K. Eichmann, and M. Modolell, *Alternative metabolic states in murine macrophages reflected by the nitric oxide synthase/arginase balance: competitive regulation by CD4+ T cells correlates with Th1/Th2 phenotype.* J Immunol, 1998. **160**(11): p. 5347-54.

102. Becker, S. and E.G. Daniel, *Antagonistic and additive effects of IL-4 and interferon-gamma on human monocytes and macrophages: effects on Fc receptors, HLA-D antigens, and superoxide production.* Cell Immunol, 1990. **129**(2): p. 351-62.

103. Song, E., et al., *Influence of alternatively and classically activated macrophages on fibrogenic activities of human fibroblasts.* Cell Immunol, 2000. **204**(1): p. 19-28.

104. Reece, J.J., M.C. Siracusa, and A.L. Scott, *Innate immune responses to lung-stage helminth infection induce alternatively activated alveolar macrophages.* Infect Immun, 2006. **74**(9): p. 4970-81.

105. Wirth, J.J., F. Kierszenbaum, and A. Zlotnik, *Effects of IL-4 on macrophage functions: increased uptake and killing of a protozoan parasite (Trypanosoma cruzi).* Immunology, 1989. **66**(2): p. 296-301.

106. Barner, M., et al., *Differences between IL-4R alpha-deficient and IL-4-deficient mice reveal a role for IL-13 in the regulation of Th2 responses.* Curr Biol, 1998. **8**(11): p. 669-72.

107. Shirey, K.A., et al., *Francisella tularensis live vaccine strain induces macrophage alternative activation as a survival mechanism.* J Immunol, 2008. **181**(6): p. 4159-67.

108. Kahnert, A., et al., *Alternative activation deprives macrophages of a coordinated defense program to Mycobacterium tuberculosis.* Eur J Immunol, 2006. **36**(3): p. 631-47.

109. Holscher, C., et al., *Impairment of alternative macrophage activation delays cutaneous leishmaniasis in nonhealing BALB/c mice.* J Immunol, 2006. **176**(2): p. 1115-21.

110. Zhang, L., et al., *Oxidative stress and asthma: proteome analysis of chitinase-like proteins and FIZZ1 in lung tissue and bronchoalveolar lavage fluid.* J Proteome Res, 2009. **8**(4): p. 1631-8.

111. Moreira, A.P. and C.M. Hogaboam, *Macrophages in allergic asthma: fine-tuning their pro- and anti-inflammatory actions for disease resolution.* J Interferon Cytokine Res, 2011. **31**(6): p. 485-91.

112. Liravi, B., et al., *Dynamics of IL-4 and IL-13 expression in the airways of sheep following allergen challenge.* BMC Pulm Med, 2015. **15**: p. 101.

113. Woodruff, P.G., et al., *T-helper type 2-driven inflammation defines major subphenotypes of asthma.* Am J Respir Crit Care Med, 2009. **180**(5): p. 388-95.

114. Moreira, A.P., et al., *Serum amyloid P attenuates M2 macrophage activation and protects against fungal spore-induced allergic airway disease.* J Allergy Clin Immunol, 2010. **126**(4): p. 712-721 e7.

115. Mitchell, J., V. Dimov, and R.G. Townley, *IL-13 and the IL-13 receptor as therapeutic targets for asthma and allergic disease.* Curr Opin Investig Drugs, 2010. **11**(5): p. 527-34.

116. Wenzel, S., et al., *Effect of an interleukin-4 variant on late phase asthmatic response to allergen challenge in asthmatic patients: results of two phase 2a studies.* Lancet, 2007. **370**(9596): p. 1422-31.

117. Liew, F.Y., et al., *Negative regulation of toll-like receptor-mediated immune responses.* Nat Rev Immunol, 2005. **5**(6): p. 446-58.

118. Foster, S.L., D.C. Hargreaves, and R. Medzhitov, *Gene-specific control of inflammation by TLR-induced chromatin modifications.* Nature, 2007. **447**(7147): p. 972-8.

119. Porta, C., et al., *Tolerance and M2 (alternative) macrophage polarization are related processes orchestrated by p50 nuclear factor kappaB.* Proc Natl Acad Sci U S A, 2009. **106**(35): p. 14978-83.

120. Sutterwala, F.S., et al., *Reversal of proinflammatory responses by ligating the macrophage Fcgamma receptor type I.* J Exp Med, 1998. **188**(1): p. 217-22.

121. Sutterwala, F.S., et al., *Selective suppression of interleukin-12 induction after macrophage receptor ligation.* J Exp Med, 1997. **185**(11): p. 1977-85.

122. Marth, T. and B.L. Kelsall, *Regulation of interleukin-12 by complement receptor 3 signaling.* J Exp Med, 1997. **185**(11): p. 1987-95.

123. Wittmann, M., et al., *C5a suppresses the production of IL-12 by IFN-gamma-primed and lipopolysaccharide-challenged human monocytes.* J Immunol, 1999. **162**(11): p. 6763-9.

124. Grazia Cappiello, M., et al., *Suppression of Il-12 transcription in macrophages following Fc gamma receptor ligation.* J Immunol, 2001. **166**(7): p. 4498-506.

125. Anderson, C.F. and D.M. Mosser, *A novel phenotype for an activated macrophage: the type 2 activated macrophage.* J Leukoc Biol, 2002. **72**(1): p. 101-6.

126. Anderson, C.F. and D.M. Mosser, *Cutting edge: biasing immune responses by directing antigen to macrophage Fc gamma receptors.* J Immunol, 2002. **168**(8): p. 3697-701.

127. Gerber, J.S. and D.M. Mosser, *Reversing lipopolysaccharide toxicity by ligating the macrophage Fc gamma receptors.* J Immunol, 2001. **166**(11): p. 6861-8.

128. Sironi, M., et al., *Differential regulation of chemokine production by Fcgamma receptor engagement in human monocytes: association of CCL1 with a distinct form of M2 monocyte activation (M2b, Type 2).* J Leukoc Biol, 2006. **80**(2): p. 342-9.

129. Iellem, A., et al., *Unique chemotactic response profile and specific expression of chemokine receptors CCR4 and CCR8 by CD4(+)CD25(+) regulatory T cells.* J Exp Med, 2001. **194**(6): p. 847-53.

130. Oliveira, S.H., et al., *Increased responsiveness of murine eosinophils to MIP-1beta (CCL4) and TCA-3 (CCL1) is mediated by their specific receptors, CCR5 and CCR8.* J Leukoc Biol, 2002. **71**(6): p. 1019-25.

131. Miles, S.A., et al., *A role for IgG immune complexes during infection with the intracellular pathogen Leishmania.* J Exp Med, 2005. **201**(5): p. 747-54.

132. Mantovani, A., et al., *Macrophage polarization: tumor-associated macrophages as a paradigm for polarized M2 mononuclear phagocytes.* Trends Immunol, 2002. **23**(11): p. 549-55.

133. de Waal Malefyt, R., et al., *Interleukin 10(IL-10) inhibits cytokine synthesis by human monocytes: an autoregulatory role of IL-10 produced by monocytes.* J Exp Med, 1991. **174**(5): p. 1209-20.

134. D'Andrea, A., et al., *Interleukin 10 (IL-10) inhibits human lymphocyte interferon gamma-production by suppressing natural killer cell stimulatory factor/IL-12 synthesis in accessory cells.* J Exp Med, 1993. **178**(3): p. 1041-8.

135. Fiorentino, D.F., et al., *IL-10 inhibits cytokine production by activated macrophages.* J Immunol, 1991. **147**(11): p. 3815-22.

136. Bogdan, C., et al., *Contrasting mechanisms for suppression of macrophage cytokine release by transforming growth factor-beta and interleukin-10.* J Biol Chem, 1992. **267**(32): p. 23301-8.

137. Ehrchen, J., et al., *Glucocorticoids induce differentiation of a specifically activated, anti-inflammatory subtype of human monocytes.* Blood, 2007. **109**(3): p. 1265-74.

138. de Waal Malefyt, R., et al., *Interleukin 10 (IL-10) and viral IL-10 strongly reduce antigen-specific human T cell proliferation by diminishing the antigen-presenting capacity of monocytes via downregulation of class II major histocompatibility complex expression.* J Exp Med, 1991. **174**(4): p. 915-24.

139. Lang, R., et al., *Shaping gene expression in activated and resting primary macrophages by IL-10.* J Immunol, 2002. **169**(5): p. 2253-63.

140. Kane, M.M. and D.M. Mosser, *The role of IL-10 in promoting disease progression in leishmaniasis.* J Immunol, 2001. **166**(2): p. 1141-7.

141. Dai, W.J., G. Kohler, and F. Brombacher, *Both innate and acquired immunity to Listeria monocytogenes infection are increased in IL-10-deficient mice.* J Immunol, 1997. **158**(5): p. 2259-67.

142. Yang, X., et al., *IL-10 gene knockout mice show enhanced Th1-like protective immunity and absent granuloma formation following Chlamydia trachomatis lung infection.* J Immunol, 1999. **162**(2): p. 1010-7.

143. Murray, P.J. and R.A. Young, *Increased antimycobacterial immunity in interleukin-10-deficient mice.* Infect Immun, 1999. **67**(6): p. 3087-95.

144. Jacobs, M., et al., *Increased resistance to mycobacterial infection in the absence of interleukin-10.* Immunology, 2000. **100**(4): p. 494-501.

145. Maloy, K.J. and F. Powrie, *Intestinal homeostasis and its breakdown in inflammatory bowel disease.* Nature, 2011. **474**(7351): p. 298-306.

146. Martinez, F.O. and S. Gordon, *The M1 and M2 paradigm of macrophage activation: time for reassessment.* F1000Prime Rep, 2014. **6**: p. 13.

147. Murray, P.J., et al., *Macrophage activation and polarization: nomenclature and experimental guidelines.* Immunity, 2014. **41**(1): p. 14-20.

148. Gordon, S. and P.R. Taylor, *Monocyte and macrophage heterogeneity.* Nat Rev Immunol, 2005. **5**(12): p. 953-64.

149. Gordon, S., A. Pluddemann, and F. Martinez Estrada, *Macrophage heterogeneity in tissues: phenotypic diversity and functions.* Immunol Rev, 2014. **262**(1): p. 36-55.

150. Hashimoto, D., et al., *Tissue-resident macrophages self-maintain locally throughout adult life with minimal contribution from circulating monocytes.* Immunity, 2013. **38**(4): p. 792-804.

151. Davies, L.C., et al., *A quantifiable proliferative burst of tissue macrophages restores homeostatic macrophage populations after acute inflammation.* Eur J Immunol, 2011. **41**(8): p. 2155-64.

152. Morris, L., C.F. Graham, and S. Gordon, *Macrophages in haemopoietic and other tissues of the developing mouse detected by the monoclonal antibody F4/80.* Development, 1991. **112**(2): p. 517-26.

153. Davies, L.C., et al., *Tissue-resident macrophages.* Nat Immunol, 2013. **14**(10): p. 986-95.

154. Yona, S., et al., *Fate mapping reveals origins and dynamics of monocytes and tissue macrophages under homeostasis.* Immunity, 2013. **38**(1): p. 79-91.

155. Ginhoux, F., et al., *Fate mapping analysis reveals that adult microglia derive from primitive macrophages.* Science, 2010. **330**(6005): p. 841-5.

156. !!! INVALID CITATION !!!

157. Sherr, C.J., et al., *The c-fms proto-oncogene product is related to the receptor for the mononuclear phagocyte growth factor, CSF-1.* Cell, 1985. **41**(3): p. 665-76.

158. MacDonald, K.P., et al., *An antibody against the colony-stimulating factor 1 receptor depletes the resident subset of monocytes and tissue- and tumor-associated macrophages but does not inhibit inflammation.* Blood, 2010. **116**(19): p. 3955-63.

159. Wiktor-Jedrzejczak, W., et al., *Total absence of colony-stimulating factor 1 in the macrophage-deficient osteopetrotic (op/op) mouse.* Proc Natl Acad Sci U S A, 1990. **87**(12): p. 4828-32.

160. Gow, D.J., et al., *Characterisation of a novel Fc conjugate of macrophage colony-stimulating factor.* Mol Ther, 2014. **22**(9): p. 1580-92.

161. Pull, S.L., et al., *Activated macrophages are an adaptive element of the colonic epithelial progenitor niche necessary for regenerative responses to injury.* Proc Natl Acad Sci U S A, 2005. **102**(1): p. 99-104.

162. Fleetwood, A.J., et al., *Granulocyte-macrophage colony-stimulating factor (CSF) and macrophage CSF-dependent macrophage phenotypes display differences in cytokine profiles and transcription factor activities: implications for CSF blockade in inflammation.* J Immunol, 2007. **178**(8): p. 5245-52.

163. Martinez, F.O., et al., *Transcriptional profiling of the human monocyte-to-macrophage differentiation and polarization: new molecules and patterns of gene expression.* J Immunol, 2006. **177**(10): p. 7303-11.

164. Shand, F.H., et al., *Tracking of intertissue migration reveals the origins of tumor-infiltrating monocytes.* Proc Natl Acad Sci U S A, 2014. **111**(21): p. 7771-6.

165. Negus, R.P., et al., *The detection and localization of monocyte chemoattractant protein-1 (MCP-1) in human ovarian cancer.* J Clin Invest, 1995. **95**(5): p. 2391-6.

166. Barleon, B., et al., *Migration of human monocytes in response to vascular endothelial growth factor (VEGF) is mediated via the VEGF receptor flt-1.* Blood, 1996. **87**(8): p. 3336-43.

167. Lin, E.Y., et al., *The macrophage growth factor CSF-1 in mammary gland development and tumor progression.* J Mammary Gland Biol Neoplasia, 2002. **7**(2): p. 147-62.

168. Biswas, S.K., A. Sica, and C.E. Lewis, *Plasticity of macrophage function during tumor progression: regulation by distinct molecular mechanisms.* J Immunol, 2008. **180**(4): p. 2011-7.

169. Sica, A. and V. Bronte, *Altered macrophage differentiation and immune dysfunction in tumor development.* J Clin Invest, 2007. **117**(5): p. 1155-66.

170. Sica, A., et al., *Autocrine production of IL-10 mediates defective IL-12 production and NF-kappa B activation in tumor-associated macrophages.* J Immunol, 2000. **164**(2): p. 762-7.

171. Saccani, A., et al., *p50 nuclear factor-kappaB overexpression in tumor-associated macrophages inhibits M1 inflammatory responses and antitumor resistance.* Cancer Res, 2006. **66**(23): p. 11432-40.

172. Dinapoli, M.R., C.L. Calderon, and D.M. Lopez, *The altered tumoricidal capacity of macrophages isolated from tumor-bearing mice is related to reduce expression of the inducible nitric oxide synthase gene.* J Exp Med, 1996. **183**(4): p. 1323-9.

173. Hoves, S., et al., *Monocyte-derived human macrophages mediate anergy in allogeneic T cells and induce regulatory T cells.* J Immunol, 2006. **177**(4): p. 2691-8.

174. Liu, Y., et al., *Inhibition of STAT3 signaling blocks the anti-apoptotic activity of IL-6 in human liver cancer cells.* J Biol Chem, 2010. **285**(35): p. 27429-39.

175. Goswami, S., et al., *Macrophages promote the invasion of breast carcinoma cells via a colony-stimulating factor-1/epidermal growth factor paracrine loop.* Cancer Res, 2005. **65**(12): p. 5278-83.

176. Coniglio, S.J., et al., *Microglial stimulation of glioblastoma invasion involves epidermal growth factor receptor (EGFR) and colony stimulating factor 1 receptor (CSF-1R) signaling.* Mol Med, 2012. **18**: p. 519-27.

177. Murdoch, C., et al., *The role of myeloid cells in the promotion of tumour angiogenesis.* Nat Rev Cancer, 2008. **8**(8): p. 618-31.

178. Quail, D.F. and J.A. Joyce, *Microenvironmental regulation of tumor progression and metastasis.* Nat Med, 2013. **19**(11): p. 1423-37.

179. Nagakawa, Y., et al., *Histologic features of venous invasion, expression of vascular endothelial growth factor and matrix metalloproteinase-2 and matrix metalloproteinase-9, and the relation with liver metastasis in pancreatic cancer.* Pancreas, 2002. **24**(2): p. 169-78.

180. Sangaletti, S., et al., *Macrophage-derived SPARC bridges tumor cell-extracellular matrix interactions toward metastasis.* Cancer Res, 2008. **68**(21): p. 9050-9.

181. Qian, B.Z. and J.W. Pollard, *Macrophage diversity enhances tumor progression and metastasis.* Cell, 2010. **141**(1): p. 39-51.

182. Harris, J.A., et al., *CD163 versus CD68 in tumor associated macrophages of classical Hodgkin lymphoma.* Diagn Pathol, 2012. **7**: p. 12.

183. Ohri, C.M., et al., *The tissue microlocalisation and cellular expression of CD163, VEGF, HLA-DR, iNOS, and MRP 8/14 is correlated to clinical outcome in NSCLC.* PLoS One, 2011. **6**(7): p. e21874.

184. Hu, H., et al., *Tumor cell-microenvironment interaction models coupled with clinical validation reveal CCL2 and SNCG as two predictors of colorectal cancer hepatic metastasis.* Clin Cancer Res, 2009. **15**(17): p. 5485-93.

185. Niino, D., et al., *Ratio of M2 macrophage expression is closely associated with poor prognosis for Angioimmunoblastic T-cell lymphoma (AITL).* Pathol Int, 2010. **60**(4): p. 278-83.

186. Kryczek, I., et al., *B7-H4 expression identifies a novel suppressive macrophage population in human ovarian carcinoma.* J Exp Med, 2006. **203**(4): p. 871-81.

187. Espinosa, I., et al., *Myometrial invasion and lymph node metastasis in endometrioid carcinomas: tumor-associated macrophages, microvessel density, and HIF1A have a crucial role.* Am J Surg Pathol, 2010. **34**(11): p. 1708-14.

188. Forssell, J., et al., *High macrophage infiltration along the tumor front correlates with improved survival in colon cancer.* Clin Cancer Res, 2007. **13**(5): p. 1472-9.

189. Medrek, C., et al., *The presence of tumor associated macrophages in tumor stroma as a prognostic marker for breast cancer patients.* BMC Cancer, 2012. **12**: p. 306.

190. Shabo, I., et al., *Breast cancer expression of CD163, a macrophage scavenger receptor, is related to early distant recurrence and reduced patient survival.* Int J Cancer, 2008. **123**(4): p. 780-6.

191. Kurahara, H., et al., *Significance of M2-polarized tumor-associated macrophage in pancreatic cancer.* J Surg Res, 2011. **167**(2): p. e211-9.

192. Bronkhorst, I.H., et al., *Detection of M2-macrophages in uveal melanoma and relation with survival.* Invest Ophthalmol Vis Sci, 2011. **52**(2): p. 643-50.

193. Mantovani, A. and P. Allavena, *The interaction of anticancer therapies with tumor-associated macrophages.* J Exp Med, 2015. **212**(4): p. 435-45.

194. Laoui, D., et al., *Tumor-associated macrophages in breast cancer: distinct subsets, distinct functions.* Int J Dev Biol, 2011. **55**(7-9): p. 861-7.

195. Pyonteck, S.M., et al., *CSF-1R inhibition alters macrophage polarization and blocks glioma progression.* Nat Med, 2013. **19**(10): p. 1264-72.

196. DeNardo, D.G., et al., *Leukocyte complexity predicts breast cancer survival and functionally regulates response to chemotherapy.* Cancer Discov, 2011. **1**(1): p. 54-67.

197. Aharinejad, S., et al., *Colony-stimulating factor-1 blockade by antisense oligonucleotides and small interfering RNAs suppresses growth of human mammary tumor xenografts in mice.* Cancer Res, 2004. **64**(15): p. 5378-84.

198. Paulus, P., et al., *Colony-stimulating factor-1 antibody reverses chemoresistance in human MCF-7 breast cancer xenografts.* Cancer Research, 2006. **66**(8): p. 4349-4356.

199. Abraham, D., et al., *Stromal cell-derived CSF-1 blockade prolongs xenograft survival of CSF-1-negative neuroblastoma.* Int J Cancer, 2010. **126**(6): p. 1339-52.

200. West, R.B., et al., *A landscape effect in tenosynovial giant-cell tumor from activation of CSF1 expression by a translocation in a minority of tumor cells.* Proc Natl Acad Sci U S A, 2006. **103**(3): p. 690-5.

201. Ries, C.H., et al., *Targeting tumor-associated macrophages with anti-CSF-1R antibody reveals a strategy for cancer therapy.* Cancer Cell, 2014. **25**(6): p. 846-59.

202. Sandhu, S.K., et al., *A first-in-human, first-in-class, phase I study of carlumab (CNTO 888), a human monoclonal antibody against CC-chemokine ligand 2 in patients with solid tumors.* Cancer Chemother Pharmacol, 2013. **71**(4): p. 1041-50.

203. Pienta, K.J., et al., *Phase 2 study of carlumab (CNTO 888), a human monoclonal antibody against CC-chemokine ligand 2 (CCL2), in metastatic castration-resistant prostate cancer.* Invest New Drugs, 2013. **31**(3): p. 760-8.

204. Brana, I., et al., *Carlumab, an anti-C-C chemokine ligand 2 monoclonal antibody, in combination with four chemotherapy regimens for the treatment of patients with solid tumors: an open-label, multicenter phase 1b study.* Target Oncol, 2015. **10**(1): p. 111-23.

205. Bonapace, L., et al., *Cessation of CCL2 inhibition accelerates breast cancer metastasis by promoting angiogenesis.* Nature, 2014. **515**(7525): p. 130-3.

206. Colombo, N., et al., *Anti-tumor and immunomodulatory activity of intraperitoneal IFN-gamma in ovarian carcinoma patients with minimal residual tumor after chemotherapy.* Int J Cancer, 1992. **51**(1): p. 42-6.

207. Pujade-Lauraine, E., et al., *Intraperitoneal recombinant interferon gamma in ovarian cancer patients with residual disease at second-look laparotomy.* J Clin Oncol, 1996. **14**(2): p. 343-50.

208. Beatty, G.L., et al., *CD40 agonists alter tumor stroma and show efficacy against pancreatic carcinoma in mice and humans.* Science, 2011. **331**(6024): p. 1612-6.

209. Beatty, G.L., et al., *A phase I study of an agonist CD40 monoclonal antibody (CP-870,893) in combination with gemcitabine in patients with advanced pancreatic ductal adenocarcinoma.* Clin Cancer Res, 2013. **19**(22): p. 6286-95.

210. Gabrilovich, D.I. and S. Nagaraj, *Myeloid-derived suppressor cells as regulators of the immune system.* Nat Rev Immunol, 2009. **9**(3): p. 162-74.

211. Gabrilovich, D.I., et al., *The terminology issue for myeloid-derived suppressor cells.* Cancer Res, 2007. **67**(1): p. 425; author reply 426.

212. Chalmin, F., et al., *Membrane-associated Hsp72 from tumor-derived exosomes mediates STAT3-dependent immunosuppressive function of mouse and human myeloid-derived suppressor cells.* J Clin Invest, 2010. **120**(2): p. 457-71.

213. Kodumudi, K.N., et al., *A novel chemoimmunomodulating property of docetaxel: suppression of myeloid-derived suppressor cells in tumor bearers.* Clin Cancer Res, 2010. **16**(18): p. 4583-94.

214. Nefedova, Y., et al., *Regulation of dendritic cell differentiation and antitumor immune response in cancer by pharmacologic-selective inhibition of the janus-activated kinase 2/signal transducers and activators of transcription 3 pathway.* Cancer Res, 2005. **65**(20): p. 9525-35.

215. Eruslanov, E., et al., *Pivotal Advance: Tumor-mediated induction of myeloid-derived suppressor cells and M2-polarized macrophages by altering intracellular PGE(2) catabolism in myeloid cells.* J Leukoc Biol, 2010. **88**(5): p. 839-48.

216. Marigo, I., et al., *Tumor-induced tolerance and immune suppression depend on the C/EBPbeta transcription factor.* Immunity, 2010. **32**(6): p. 790-802.

217. Nefedova, Y., et al., *Activation of dendritic cells via inhibition of Jak2/STAT3 signaling.* J Immunol, 2005. **175**(7): p. 4338-46.

218. Corzo, C.A., et al., *HIF-1alpha regulates function and differentiation of myeloid-derived suppressor cells in the tumor microenvironment.* J Exp Med, 2010. **207**(11): p. 2439-53.

219. Ugel, S., et al., *Therapeutic targeting of myeloid-derived suppressor cells.* Curr Opin Pharmacol, 2009. **9**(4): p. 470-81.

220. Montero, A.J., et al., *Myeloid-derived suppressor cells in cancer patients: a clinical perspective.* J Immunother, 2012. **35**(2): p. 107-15.

221. Crook, K.R. and P. Liu, *Role of myeloid-derived suppressor cells in autoimmune disease.* World J Immunol, 2014. **4**(1): p. 26-33.

222. Bronte, V., et al., *Unopposed production of granulocyte-macrophage colony-stimulating factor by tumors inhibits CD8+ T cell responses by dysregulating antigen-presenting cell maturation.* J Immunol, 1999. **162**(10): p. 5728-37.

223. Movahedi, K., et al., *Identification of discrete tumor-induced myeloid-derived suppressor cell subpopulations with distinct T cell-suppressive activity.* Blood, 2008. **111**(8): p. 4233-44.

224. Youn, J.I., et al., *Subsets of myeloid-derived suppressor cells in tumor-bearing mice.* J Immunol, 2008. **181**(8): p. 5791-802.

225. Almand, B., et al., *Increased production of immature myeloid cells in cancer patients: a mechanism of immunosuppression in cancer.* J Immunol, 2001. **166**(1): p. 678-89.

226. Ochoa, A.C., et al., *Arginase, prostaglandins, and myeloid-derived suppressor cells in renal cell carcinoma.* Clin Cancer Res, 2007. **13**(2 Pt 2): p. 721s-726s.

227. Schmielau, J. and O.J. Finn, *Activated granulocytes and granulocyte-derived hydrogen peroxide are the underlying mechanism of suppression of t-cell function in advanced cancer patients.* Cancer Res, 2001. **61**(12): p. 4756-60.

228. Dumitru, C.A., et al., *Neutrophils and granulocytic myeloid-derived suppressor cells: immunophenotyping, cell biology and clinical relevance in human oncology.* Cancer Immunol Immunother, 2012. **61**(8): p. 1155-67.

229. Vuk-Pavlovic, S., et al., *Immunosuppressive CD14+HLA-DRlow/- monocytes in prostate cancer.* Prostate, 2010. **70**(4): p. 443-55.

230. Wang, J., et al., *Effect of TLR agonists on the differentiation and function of human monocytic myeloid-derived suppressor cells.* J Immunol, 2015. **194**(9): p. 4215-21.

231. Huang, A., et al., *Increased CD14(+)HLA-DR (-/low) myeloid-derived suppressor cells correlate with extrathoracic metastasis and poor response to chemotherapy in non-small cell lung cancer patients.* Cancer Immunol Immunother, 2013. **62**(9): p. 1439-51.

232. Brimnes, M.K., et al., *Increased level of both CD4+FOXP3+ regulatory T cells and CD14+HLA-DR(-)/low myeloid-derived suppressor cells and decreased level of dendritic cells in patients with multiple myeloma.* Scand J Immunol, 2010. **72**(6): p. 540-7.

233. Lin, Y., et al., *Immunosuppressive CD14+HLA-DR(low)/- monocytes in B-cell non-Hodgkin lymphoma.* Blood, 2011. **117**(3): p. 872-81.

234. Hoechst, B., et al., *A new population of myeloid-derived suppressor cells in hepatocellular carcinoma patients induces CD4(+)CD25(+)Foxp3(+) T cells.* Gastroenterology, 2008. **135**(1): p. 234-43.

235. Mao, Y., et al., *Inhibition of tumor-derived prostaglandin-e2 blocks the induction of myeloid-derived suppressor cells and recovers natural killer cell activity.* Clin Cancer Res, 2014. **20**(15): p. 4096-106.

236. Yang, L., et al., *Abrogation of TGF beta signaling in mammary carcinomas recruits Gr-1+CD11b+ myeloid cells that promote metastasis.* Cancer Cell, 2008. **13**(1): p. 23-35.

237. Pak, A.S., et al., *Mechanisms of immune suppression in patients with head and neck cancer: presence of CD34(+) cells which suppress immune functions within cancers that secrete granulocyte-macrophage colony-stimulating factor.* Clin Cancer Res, 1995. **1**(1): p. 95-103.

238. Lathers, D.M., et al., *Phase 1B study to improve immune responses in head and neck cancer patients using escalating doses of 25-hydroxyvitamin D3.* Cancer Immunol Immunother, 2004. **53**(5): p. 422-30.

239. Mirza, N., et al., *All-trans-retinoic acid improves differentiation of myeloid cells and immune response in cancer patients.* Cancer Res, 2006. **66**(18): p. 9299-307.

240. Fricke, I., et al., *Vascular endothelial growth factor-trap overcomes defects in dendritic cell differentiation but does not improve antigen-specific immune responses.* Clin Cancer Res, 2007. **13**(16): p. 4840-8.

241. Diaz-Montero, C.M., et al., *Increased circulating myeloid-derived suppressor cells correlate with clinical cancer stage, metastatic tumor burden, and doxorubicin-cyclophosphamide chemotherapy.* Cancer Immunol Immunother, 2009. **58**(1): p. 49-59.

242. Alizadeh, D., et al., *Doxorubicin eliminates myeloid-derived suppressor cells and enhances the efficacy of adoptive T-cell transfer in breast cancer.* Cancer Res, 2014. **74**(1): p. 104-18.

243. Brandau, S., et al., *Myeloid-derived suppressor cells in the peripheral blood of cancer patients contain a subset of immature neutrophils with impaired migratory properties.* J Leukoc Biol, 2011. **89**(2): p. 311-7.

244. Srivastava, M.K., et al., *Lung cancer patients' CD4(+) T cells are activated in vitro by MHC II cell-based vaccines despite the presence of myeloid-derived suppressor cells.* Cancer Immunol Immunother, 2008. **57**(10): p. 1493-504.

245. Rodriguez, P.C., et al., *Arginase I-producing myeloid-derived suppressor cells in renal cell carcinoma are a subpopulation of activated granulocytes.* Cancer Res, 2009. **69**(4): p. 1553-60.

246. Eruslanov, E., et al., *Circulating and tumor-infiltrating myeloid cell subsets in patients with bladder cancer.* Int J Cancer, 2012. **130**(5): p. 1109-19.

247. Gabitass, R.F., et al., *Elevated myeloid-derived suppressor cells in pancreatic, esophageal and gastric cancer are an independent prognostic factor and are associated with significant elevation of the Th2 cytokine interleukin-13.* Cancer Immunol Immunother, 2011. **60**(10): p. 1419-30.

248. Porembka, M.R., et al., *Pancreatic adenocarcinoma induces bone marrow mobilization of myeloid-derived suppressor cells which promote primary tumor growth.* Cancer Immunol Immunother, 2012. **61**(9): p. 1373-85.

249. Shen, P., et al., *Increased circulating Lin(-/low) CD33(+) HLA-DR(-) myeloid-derived suppressor cells in hepatocellular carcinoma patients.* Hepatol Res, 2014. **44**(6): p. 639-50.

250. OuYang, L.Y., et al., *Tumor-induced myeloid-derived suppressor cells promote tumor progression through oxidative metabolism in human colorectal cancer.* J Transl Med, 2015. **13**: p. 47.

251. Wang, L., et al., *Increased myeloid-derived suppressor cells in gastric cancer correlate with cancer stage and plasma S100A8/A9 proinflammatory proteins.* J Immunol, 2013. **190**(2): p. 794-804.

252. Angell, T.E., et al., *Circulating Myeloid-Derived Suppressor Cells Predict Differentiated Thyroid Cancer Diagnosis and Extent.* Thyroid, 2016.

253. Young, M.R., et al., *Human squamous cell carcinomas of the head and neck chemoattract immune suppressive CD34(+) progenitor cells.* Hum Immunol, 2001. **62**(4): p. 332-41.

254. Ko, J.S., et al., *Sunitinib mediates reversal of myeloid-derived suppressor cell accumulation in renal cell carcinoma patients.* Clin Cancer Res, 2009. **15**(6): p. 2148-57.

255. Yang, L., et al., *Expansion of myeloid immune suppressor Gr+CD11b+ cells in tumor-bearing host directly promotes tumor angiogenesis.* Cancer Cell, 2004. **6**(4): p. 409-21.

256. Bronte, V., et al., *Identification of a CD11b(+)/Gr-1(+)/CD31(+) myeloid progenitor capable of activating or suppressing CD8(+) T cells.* Blood, 2000. **96**(12): p. 3838-46.

257. Talmadge, J.E. and D.I. Gabrilovich, *History of myeloid-derived suppressor cells.* Nat Rev Cancer, 2013. **13**(10): p. 739-52.

258. Goni, O., P. Alcaide, and M. Fresno, *Immunosuppression during acute Trypanosoma cruzi infection: involvement of Ly6G (Gr1(+))CD11b(+ )immature myeloid suppressor cells.* Int Immunol, 2002. **14**(10): p. 1125-34.

259. Voisin, M.B., et al., *Both expansion of regulatory GR1+ CD11b+ myeloid cells and anergy of T lymphocytes participate in hyporesponsiveness of the lung-associated immune system during acute toxoplasmosis.* Infect Immun, 2004. **72**(9): p. 5487-92.

260. Van Ginderachter, J.A., et al., *Myeloid-derived suppressor cells in parasitic infections.* Eur J Immunol, 2010. **40**(11): p. 2976-85.

261. De Santo, C., et al., *Invariant NKT cells reduce the immunosuppressive activity of influenza A virus-induced myeloid-derived suppressor cells in mice and humans.* J Clin Invest, 2008. **118**(12): p. 4036-48.

262. Fortin, C., X. Huang, and Y. Yang, *NK cell response to vaccinia virus is regulated by myeloid-derived suppressor cells.* J Immunol, 2012. **189**(4): p. 1843-9.

263. Chen, S., et al., *Immunosuppressive functions of hepatic myeloid-derived suppressor cells of normal mice and in a murine model of chronic hepatitis B virus.* Clin Exp Immunol, 2011. **166**(1): p. 134-42.

264. Tacke, R.S., et al., *Myeloid suppressor cells induced by hepatitis C virus suppress T-cell responses through the production of reactive oxygen species.* Hepatology, 2012. **55**(2): p. 343-53.

265. Goh, C.C., et al., *Hepatitis C Virus-Induced Myeloid-Derived Suppressor Cells Suppress NK Cell IFN-gamma Production by Altering Cellular Metabolism via Arginase-1.* J Immunol, 2016. **196**(5): p. 2283-92.

266. Qin, A., et al., *Expansion of monocytic myeloid-derived suppressor cells dampens T cell function in HIV-1-seropositive individuals.* J Virol, 2013. **87**(3): p. 1477-90.

267. Vollbrecht, T., et al., *Chronic progressive HIV-1 infection is associated with elevated levels of myeloid-derived suppressor cells.* AIDS, 2012. **26**(12): p. F31-7.

268. Garg, A. and S.A. Spector, *HIV type 1 gp120-induced expansion of myeloid derived suppressor cells is dependent on interleukin 6 and suppresses immunity.* J Infect Dis, 2014. **209**(3): p. 441-51.

269. Sui, Y., et al., *Vaccine-induced myeloid cell population dampens protective immunity to SIV.* J Clin Invest, 2014. **124**(6): p. 2538-49.

270. Dietlin, T.A., et al., *Mycobacteria-induced Gr-1+ subsets from distinct myeloid lineages have opposite effects on T cell expansion.* J Leukoc Biol, 2007. **81**(5): p. 1205-12.

271. Dietlin, T.A., et al., *T cell expansion is regulated by activated Gr-1+ splenocytes.* Cell Immunol, 2005. **235**(1): p. 39-45.

272. Martino, A., et al., *Mycobacterium bovis bacillus Calmette-Guerin vaccination mobilizes innate myeloid-derived suppressor cells restraining in vivo T cell priming via IL-1R-dependent nitric oxide production.* J Immunol, 2010. **184**(4): p. 2038-47.

273. Delano, M.J., et al., *MyD88-dependent expansion of an immature GR-1(+)CD11b(+) population induces T cell suppression and Th2 polarization in sepsis.* J Exp Med, 2007. **204**(6): p. 1463-74.

274. Makarenkova, V.P., et al., *CD11b+/Gr-1+ myeloid suppressor cells cause T cell dysfunction after traumatic stress.* J Immunol, 2006. **176**(4): p. 2085-94.

275. Haile, L.A., et al., *Myeloid-derived suppressor cells in inflammatory bowel disease: a new immunoregulatory pathway.* Gastroenterology, 2008. **135**(3): p. 871-81, 881 e1-5.

276. Ioannou, M., et al., *Crucial role of granulocytic myeloid-derived suppressor cells in the regulation of central nervous system autoimmune disease.* J Immunol, 2012. **188**(3): p. 1136-46.

277. Fujii, W., et al., *Myeloid-derived suppressor cells play crucial roles in the regulation of mouse collagen-induced arthritis.* J Immunol, 2013. **191**(3): p. 1073-81.

278. Tu, Z., et al., *Myeloid suppressor cells induced by retinal pigment epithelial cells inhibit autoreactive T-cell responses that lead to experimental autoimmune uveitis.* Invest Ophthalmol Vis Sci, 2012. **53**(2): p. 959-66.

279. Guan, Q., et al., *The role and potential therapeutic application of myeloid-derived suppressor cells in TNBS-induced colitis.* J Leukoc Biol, 2013. **94**(4): p. 803-11.

280. Zhang, R., et al., *Dextran sulphate sodium increases splenic Gr1(+)CD11b(+) cells which accelerate recovery from colitis following intravenous transplantation.* Clin Exp Immunol, 2011. **164**(3): p. 417-27.

281. Dugast, A.S., et al., *Myeloid-derived suppressor cells accumulate in kidney allograft tolerance and specifically suppress effector T cell expansion.* J Immunol, 2008. **180**(12): p. 7898-906.

282. Luan, Y., et al., *Monocytic myeloid-derived suppressor cells accumulate in renal transplant patients and mediate CD4(+) Foxp3(+) Treg expansion.* Am J Transplant, 2013. **13**(12): p. 3123-31.

283. Highfill, S.L., et al., *Bone marrow myeloid-derived suppressor cells (MDSCs) inhibit graft-versus-host disease (GVHD) via an arginase-1-dependent mechanism that is up-regulated by interleukin-13.* Blood, 2010. **116**(25): p. 5738-47.

284. Bronte, V., et al., *Apoptotic death of CD8+ T lymphocytes after immunization: induction of a suppressive population of Mac-1+/Gr-1+ cells.* J Immunol, 1998. **161**(10): p. 5313-20.

285. Ostrand-Rosenberg, S., *Myeloid-derived suppressor cells: more mechanisms for inhibiting antitumor immunity.* Cancer Immunol Immunother, 2010. **59**(10): p. 1593-600.

286. Bronte, V. and P. Zanovello, *Regulation of immune responses by L-arginine metabolism.* Nat Rev Immunol, 2005. **5**(8): p. 641-54.

287. Rodriguez, P.C., D.G. Quiceno, and A.C. Ochoa, *L-arginine availability regulates T-lymphocyte cell-cycle progression.* Blood, 2007. **109**(4): p. 1568-73.

288. Rodriguez, P.C., et al., *Regulation of T cell receptor CD3zeta chain expression by L-arginine.* J Biol Chem, 2002. **277**(24): p. 21123-9.

289. Ezernitchi, A.V., et al., *TCR zeta down-regulation under chronic inflammation is mediated by myeloid suppressor cells differentially distributed between various lymphatic organs.* J Immunol, 2006. **177**(7): p. 4763-72.

290. Bronte, V., et al., *IL-4-induced arginase 1 suppresses alloreactive T cells in tumor-bearing mice.* J Immunol, 2003. **170**(1): p. 270-8.

291. Mazzoni, A., et al., *Myeloid suppressor lines inhibit T cell responses by an NO-dependent mechanism.* J Immunol, 2002. **168**(2): p. 689-95.

292. Raber, P.L., et al., *Subpopulations of myeloid-derived suppressor cells impair T cell responses through independent nitric oxide-related pathways.* Int J Cancer, 2014. **134**(12): p. 2853-64.

293. Rodriguez, P.C., et al., *Arginase I production in the tumor microenvironment by mature myeloid cells inhibits T-cell receptor expression and antigen-specific T-cell responses.* Cancer Res, 2004. **64**(16): p. 5839-49.

294. Cimen Bozkus, C., et al., *Expression of Cationic Amino Acid Transporter 2 Is Required for Myeloid-Derived Suppressor Cell-Mediated Control of T Cell Immunity.* J Immunol, 2015. **195**(11): p. 5237-50.

295. Gmunder, H., et al., *Macrophages regulate intracellular glutathione levels of lymphocytes. Evidence for an immunoregulatory role of cysteine.* Cell Immunol, 1990. **129**(1): p. 32-46.

296. Angelini, G., et al., *Antigen-presenting dendritic cells provide the reducing extracellular microenvironment required for T lymphocyte activation.* Proc Natl Acad Sci U S A, 2002. **99**(3): p. 1491-6.

297. Srivastava, M.K., et al., *Myeloid-derived suppressor cells inhibit T-cell activation by depleting cystine and cysteine.* Cancer Res, 2010. **70**(1): p. 68-77.

298. Corzo, C.A., et al., *Mechanism regulating reactive oxygen species in tumor-induced myeloid-derived suppressor cells.* J Immunol, 2009. **182**(9): p. 5693-701.

299. Kusmartsev, S. and D.I. Gabrilovich, *Inhibition of myeloid cell differentiation in cancer: the role of reactive oxygen species.* J Leukoc Biol, 2003. **74**(2): p. 186-96.

300. Kusmartsev, S., et al., *Antigen-specific inhibition of CD8+ T cell response by immature myeloid cells in cancer is mediated by reactive oxygen species.* J Immunol, 2004. **172**(2): p. 989-99.

301. Lu, T., et al., *Tumor-infiltrating myeloid cells induce tumor cell resistance to cytotoxic T cells in mice.* J Clin Invest, 2011. **121**(10): p. 4015-29.

302. Hanson, E.M., et al., *Myeloid-derived suppressor cells down-regulate L-selectin expression on CD4+ and CD8+ T cells.* J Immunol, 2009. **183**(2): p. 937-44.

303. Mao, Y., et al., *Melanoma-educated CD14+ cells acquire a myeloid-derived suppressor cell phenotype through COX-2-dependent mechanisms.* Cancer Res, 2013. **73**(13): p. 3877-87.

304. Parker, K.H., et al., *HMGB1 enhances immune suppression by facilitating the differentiation and suppressive activity of myeloid-derived suppressor cells.* Cancer Res, 2014. **74**(20): p. 5723-33.

305. Liu, C., et al., *Expansion of spleen myeloid suppressor cells represses NK cell cytotoxicity in tumor-bearing host.* Blood, 2007. **109**(10): p. 4336-42.

306. Elkabets, M., et al., *IL-1beta regulates a novel myeloid-derived suppressor cell subset that impairs NK cell development and function.* Eur J Immunol, 2010. **40**(12): p. 3347-57.

307. Li, H., et al., *Cancer-expanded myeloid-derived suppressor cells induce anergy of NK cells through membrane-bound TGF-beta 1.* J Immunol, 2009. **182**(1): p. 240-9.

308. Sinha, P., et al., *Cross-talk between myeloid-derived suppressor cells and macrophages subverts tumor immunity toward a type 2 response.* J Immunol, 2007. **179**(2): p. 977-83.

309. Pan, P.Y., et al., *Reversion of immune tolerance in advanced malignancy: modulation of myeloid-derived suppressor cell development by blockade of stem-cell factor function.* Blood, 2008. **111**(1): p. 219-28.

310. Huang, B., et al., *Gr-1+CD115+ immature myeloid suppressor cells mediate the development of tumor-induced T regulatory cells and T-cell anergy in tumor-bearing host.* Cancer Res, 2006. **66**(2): p. 1123-31.

311. Hoechst, B., et al., *Plasticity of human Th17 cells and iTregs is orchestrated by different subsets of myeloid cells.* Blood, 2011. **117**(24): p. 6532-41.

312. Pan, P.Y., et al., *Immune stimulatory receptor CD40 is required for T-cell suppression and T regulatory cell activation mediated by myeloid-derived suppressor cells in cancer.* Cancer Res, 2010. **70**(1): p. 99-108.

313. Serafini, P., et al., *Myeloid-derived suppressor cells promote cross-tolerance in B-cell lymphoma by expanding regulatory T cells.* Cancer Res, 2008. **68**(13): p. 5439-49.

314. Parker, K.H., D.W. Beury, and S. Ostrand-Rosenberg, *Myeloid-Derived Suppressor Cells: Critical Cells Driving Immune Suppression in the Tumor Microenvironment.* Adv Cancer Res, 2015. **128**: p. 95-139.

315. Lechner, M.G., et al., *Functional characterization of human Cd33+ and Cd11b+ myeloid-derived suppressor cell subsets induced from peripheral blood mononuclear cells co-cultured with a diverse set of human tumor cell lines.* J Transl Med, 2011. **9**: p. 90.

316. Serafini, P., et al., *High-dose granulocyte-macrophage colony-stimulating factor-producing vaccines impair the immune response through the recruitment of myeloid suppressor cells.* Cancer Res, 2004. **64**(17): p. 6337-43.

317. Morales, J.K., et al., *GM-CSF is one of the main breast tumor-derived soluble factors involved in the differentiation of CD11b-Gr1- bone marrow progenitor cells into myeloid-derived suppressor cells.* Breast Cancer Res Treat, 2010. **123**(1): p. 39-49.

318. Wright, M.A., et al., *Stimulation of immune suppressive CD34+ cells from normal bone marrow by Lewis lung carcinoma tumors.* Cancer Immunol Immunother, 1998. **46**(5): p. 253-60.

319. Gabrilovich, D.I., et al., *Mechanism of immune dysfunction in cancer mediated by immature Gr-1+ myeloid cells.* J Immunol, 2001. **166**(9): p. 5398-406.

320. Ko, J.S., et al., *Direct and differential suppression of myeloid-derived suppressor cell subsets by sunitinib is compartmentally constrained.* Cancer Res, 2010. **70**(9): p. 3526-36.

321. Melani, C., et al., *Myeloid cell expansion elicited by the progression of spontaneous mammary carcinomas in c-erbB-2 transgenic BALB/c mice suppresses immune reactivity.* Blood, 2003. **102**(6): p. 2138-45.

322. Lechner, M.G., D.J. Liebertz, and A.L. Epstein, *Characterization of cytokine-induced myeloid-derived suppressor cells from normal human peripheral blood mononuclear cells.* J Immunol, 2010. **185**(4): p. 2273-84.

323. Sinha, P., et al., *Prostaglandin E2 promotes tumor progression by inducing myeloid-derived suppressor cells.* Cancer Res, 2007. **67**(9): p. 4507-13.

324. Rodriguez, P.C., et al., *Arginase I in myeloid suppressor cells is induced by COX-2 in lung carcinoma.* J Exp Med, 2005. **202**(7): p. 931-9.

325. Obermajer, N., et al., *Positive feedback between PGE2 and COX2 redirects the differentiation of human dendritic cells toward stable myeloid-derived suppressor cells.* Blood, 2011. **118**(20): p. 5498-505.

326. Obermajer, N., et al., *PGE(2)-induced CXCL12 production and CXCR4 expression controls the accumulation of human MDSCs in ovarian cancer environment.* Cancer Res, 2011. **71**(24): p. 7463-70.

327. Salcedo, R. and J.J. Oppenheim, *Role of chemokines in angiogenesis: CXCL12/SDF-1 and CXCR4 interaction, a key regulator of endothelial cell responses.* Microcirculation, 2003. **10**(3-4): p. 359-70.

328. Gabrilovich, D., et al., *Vascular endothelial growth factor inhibits the development of dendritic cells and dramatically affects the differentiation of multiple hematopoietic lineages in vivo.* Blood, 1998. **92**(11): p. 4150-66.

329. Shojaei, F., et al., *Tumor refractoriness to anti-VEGF treatment is mediated by CD11b+Gr1+ myeloid cells.* Nat Biotechnol, 2007. **25**(8): p. 911-20.

330. Song, X., et al., *CD11b+/Gr-1+ immature myeloid cells mediate suppression of T cells in mice bearing tumors of IL-1beta-secreting cells.* J Immunol, 2005. **175**(12): p. 8200-8.

331. Bunt, S.K., et al., *Inflammation induces myeloid-derived suppressor cells that facilitate tumor progression.* J Immunol, 2006. **176**(1): p. 284-90.

332. Bunt, S.K., et al., *Reduced inflammation in the tumor microenvironment delays the accumulation of myeloid-derived suppressor cells and limits tumor progression.* Cancer Res, 2007. **67**(20): p. 10019-26.

333. Skabytska, Y., et al., *Cutaneous innate immune sensing of Toll-like receptor 2-6 ligands suppresses T cell immunity by inducing myeloid-derived suppressor cells.* Immunity, 2014. **41**(5): p. 762-75.

334. Ozao-Choy, J., et al., *The novel role of tyrosine kinase inhibitor in the reversal of immune suppression and modulation of tumor microenvironment for immune-based cancer therapies.* Cancer Res, 2009. **69**(6): p. 2514-22.

335. Sinha, P., et al., *Proinflammatory S100 proteins regulate the accumulation of myeloid-derived suppressor cells.* J Immunol, 2008. **181**(7): p. 4666-75.

336. Cheng, P., et al., *Inhibition of dendritic cell differentiation and accumulation of myeloid-derived suppressor cells in cancer is regulated by S100A9 protein.* J Exp Med, 2008. **205**(10): p. 2235-49.

337. Gebhardt, C., et al., *S100A8 and S100A9 in inflammation and cancer.* Biochem Pharmacol, 2006. **72**(11): p. 1622-31.

338. Ryzhov, S., et al., *Adenosinergic regulation of the expansion and immunosuppressive activity of CD11b+Gr1+ cells.* J Immunol, 2011. **187**(11): p. 6120-9.

339. Ohta, A., et al., *A2A adenosine receptor protects tumors from antitumor T cells.* Proc Natl Acad Sci U S A, 2006. **103**(35): p. 13132-7.

340. Iannone, R., et al., *Blockade of A2b adenosine receptor reduces tumor growth and immune suppression mediated by myeloid-derived suppressor cells in a mouse model of melanoma.* Neoplasia, 2013. **15**(12): p. 1400-9.

341. Sorrentino, C., et al., *Myeloid-derived suppressor cells contribute to A2B adenosine receptor-induced VEGF production and angiogenesis in a mouse melanoma model.* Oncotarget, 2015. **6**(29): p. 27478-89.

342. Cekic, C., et al., *Myeloid expression of adenosine A2A receptor suppresses T and NK cell responses in the solid tumor microenvironment.* Cancer Res, 2014. **74**(24): p. 7250-9.

343. Parker, K.H., L.A. Horn, and S. Ostrand-Rosenberg, *High-mobility group box protein 1 promotes the survival of myeloid-derived suppressor cells by inducing autophagy.* J Leukoc Biol, 2016.

344. Najjar, Y.G. and J.H. Finke, *Clinical perspectives on targeting of myeloid derived suppressor cells in the treatment of cancer.* Front Oncol, 2013. **3**: p. 49.

345. Vincent, J., et al., *5-Fluorouracil selectively kills tumor-associated myeloid-derived suppressor cells resulting in enhanced T cell-dependent antitumor immunity.* Cancer Res, 2010. **70**(8): p. 3052-61.

346. Kusmartsev, S., et al., *All-trans-retinoic acid eliminates immature myeloid cells from tumor-bearing mice and improves the effect of vaccination.* Cancer Res, 2003. **63**(15): p. 4441-9.

347. Nefedova, Y., et al., *Mechanism of all-trans retinoic acid effect on tumor-associated myeloid-derived suppressor cells.* Cancer Res, 2007. **67**(22): p. 11021-8.

348. Melani, C., et al., *Amino-biphosphonate-mediated MMP-9 inhibition breaks the tumor-bone marrow axis responsible for myeloid-derived suppressor cell expansion and macrophage infiltration in tumor stroma.* Cancer Res, 2007. **67**(23): p. 11438-46.

349. Fujita, M., et al., *COX-2 blockade suppresses gliomagenesis by inhibiting myeloid-derived suppressor cells.* Cancer Res, 2011. **71**(7): p. 2664-74.

350. Suzuki, E., et al., *Gemcitabine selectively eliminates splenic Gr-1+/CD11b+ myeloid suppressor cells in tumor-bearing animals and enhances antitumor immune activity.* Clin Cancer Res, 2005. **11**(18): p. 6713-21.

351. Le, H.K., et al., *Gemcitabine directly inhibits myeloid derived suppressor cells in BALB/c mice bearing 4T1 mammary carcinoma and augments expansion of T cells from tumor-bearing mice.* Int Immunopharmacol, 2009. **9**(7-8): p. 900-9.

352. Ko, H.J., et al., *A combination of chemoimmunotherapies can efficiently break self-tolerance and induce antitumor immunity in a tolerogenic murine tumor model*. Cancer Res, 2007. **67**(15): p. 7477-86.

353. De Santo, C., et al., *Nitroaspirin corrects immune dysfunction in tumor-bearing hosts and promotes tumor eradication by cancer vaccination.* Proc Natl Acad Sci U S A, 2005. **102**(11): p. 4185-90.

354. Serafini, P., et al., *Phosphodiesterase-5 inhibition augments endogenous antitumor immunity by reducing myeloid-derived suppressor cell function.* J Exp Med, 2006. **203**(12): p. 2691-702.

355. Meyer, C., et al., *Chronic inflammation promotes myeloid-derived suppressor cell activation blocking antitumor immunity in transgenic mouse melanoma model.* Proc Natl Acad Sci U S A, 2011. **108**(41): p. 17111-6.

356. Shojaei, F., et al., *Bv8 regulates myeloid-cell-dependent tumour angiogenesis.* Nature, 2007. **450**(7171): p. 825-31.

357. Bose, A., et al., *Sunitinib facilitates the activation and recruitment of therapeutic anti-tumor immunity in concert with specific vaccination.* Int J Cancer, 2011. **129**(9): p. 2158-70.

358. van Cruijsen, H., et al., *Sunitinib-induced myeloid lineage redistribution in renal cell cancer patients: CD1c+ dendritic cell frequency predicts progression-free survival.* Clin Cancer Res, 2008. **14**(18): p. 5884-92.

359. Nagaraj, S., et al., *Anti-inflammatory triterpenoid blocks immune suppressive function of MDSCs and improves immune response in cancer.* Clin Cancer Res, 2010. **16**(6): p. 1812-23.

360. Shirota, Y., H. Shirota, and D.M. Klinman, *Intratumoral injection of CpG oligonucleotides induces the differentiation and reduces the immunosuppressive activity of myeloid-derived suppressor cells.* J Immunol, 2012. **188**(4): p. 1592-9.

361. Zoglmeier, C., et al., *CpG blocks immunosuppression by myeloid-derived suppressor cells in tumor-bearing mice.* Clin Cancer Res, 2011. **17**(7): p. 1765-75.

362. Zhao, B.G., et al., *Combination therapy targeting toll like receptors 7, 8 and 9 eliminates large established tumors.* J Immunother Cancer, 2014. **2**: p. 12.

363. Forghani, P. and E.K. Waller, *Poly (I: C) modulates the immunosuppressive activity of myeloid-derived suppressor cells in a murine model of breast cancer.* Breast Cancer Res Treat, 2015. **153**(1): p. 21-30.

364. Shime, H., et al., *Myeloid-derived suppressor cells confer tumor-suppressive functions on natural killer cells via polyinosinic:polycytidylic acid treatment in mouse tumor models.* J Innate Immun, 2014. **6**(3): p. 293-305.

365. Arora, M., et al., *TLR4/MyD88-induced CD11b+Gr-1 int F4/80+ non-migratory myeloid cells suppress Th2 effector function in the lung.* Mucosal Immunol, 2010. **3**(6): p. 578-93.

366. Bunt, S.K., et al., *Inflammation enhances myeloid-derived suppressor cell cross-talk by signaling through Toll-like receptor 4.* J Leukoc Biol, 2009. **85**(6): p. 996-1004.

367. Liu, Y., et al., *Contribution of MyD88 to the tumor exosome-mediated induction of myeloid derived suppressor cells.* Am J Pathol, 2010. **176**(5): p. 2490-9.

368. Xiang, X., et al., *TLR2-mediated expansion of MDSCs is dependent on the source of tumor exosomes.* Am J Pathol, 2010. **177**(4): p. 1606-10.

369. Li, S., et al., *TLR2 limits development of hepatocellular carcinoma by reducing IL18-mediated immunosuppression.* Cancer Res, 2015. **75**(6): p. 986-95.

370. Dolcetti, L., et al., *Hierarchy of immunosuppressive strength among myeloid-derived suppressor cell subsets is determined by GM-CSF.* Eur J Immunol, 2010. **40**(1): p. 22-35.

371. Yanez-Mo, M., et al., *Biological properties of extracellular vesicles and their physiological functions.* J Extracell Vesicles, 2015. **4**: p. 27066.

372. Lee, Y., S. El Andaloussi, and M.J. Wood, *Exosomes and microvesicles: extracellular vesicles for genetic information transfer and gene therapy.* Hum Mol Genet, 2012. **21**(R1): p. R125-34.

373. Valadi, H., et al., *Exosome-mediated transfer of mRNAs and microRNAs is a novel mechanism of genetic exchange between cells.* Nat Cell Biol, 2007. **9**(6): p. 654-9.

374. Yuana, Y., A. Sturk, and R. Nieuwland, *Extracellular vesicles in physiological and pathological conditions.* Blood Rev, 2013. **27**(1): p. 31-9.

375. Raposo, G., et al., *B lymphocytes secrete antigen-presenting vesicles.* J Exp Med, 1996. **183**(3): p. 1161-72.

376. Robbins, P.D. and A.E. Morelli, *Regulation of immune responses by extracellular vesicles.* Nat Rev Immunol, 2014. **14**(3): p. 195-208.

377. Thery, C., M. Ostrowski, and E. Segura, *Membrane vesicles as conveyors of immune responses.* Nat Rev Immunol, 2009. **9**(8): p. 581-93.

378. Thery, C., et al., *Indirect activation of naive CD4+ T cells by dendritic cell-derived exosomes.* Nat Immunol, 2002. **3**(12): p. 1156-62.

379. Giri, P.K. and J.S. Schorey, *Exosomes derived from M. Bovis BCG infected macrophages activate antigen-specific CD4+ and CD8+ T cells in vitro and in vivo.* PLoS One, 2008. **3**(6): p. e2461.

380. Andre, F., et al., *Exosomes as potent cell-free peptide-based vaccine. I. Dendritic cell-derived exosomes transfer functional MHC class I/peptide complexes to dendritic cells.* J Immunol, 2004. **172**(4): p. 2126-36.

381. Coppieters, K., et al., *No significant CTL cross-priming by dendritic cell-derived exosomes during murine lymphocytic choriomeningitis virus infection.* J Immunol, 2009. **182**(4): p. 2213-20.

382. Danzer, K.M., et al., *Exosomal cell-to-cell transmission of alpha synuclein oligomers.* Mol Neurodegener, 2012. **7**: p. 42.

383. Simons, M. and G. Raposo, *Exosomes--vesicular carriers for intercellular communication.* Curr Opin Cell Biol, 2009. **21**(4): p. 575-81.

384. Andreola, G., et al., *Induction of lymphocyte apoptosis by tumor cell secretion of FasL-bearing microvesicles.* J Exp Med, 2002. **195**(10): p. 1303-16.

385. Clayton, A., et al., *Human tumor-derived exosomes selectively impair lymphocyte responses to interleukin-2.* Cancer Res, 2007. **67**(15): p. 7458-66.

386. Rak, J., *Extracellular vesicles - biomarkers and effectors of the cellular interactome in cancer.* Front Pharmacol, 2013. **4**: p. 21.

387. Ghidoni, R., L. Benussi, and G. Binetti, *Exosomes: The Trojan horses of neurodegeneration.* Medical Hypotheses, 2008. **70**(6): p. 1226-1227.

388. Amabile, N., et al., *Microparticles: key protagonists in cardiovascular disorders.* Semin Thromb Hemost, 2010. **36**(8): p. 907-16.

389. De Toro, J., et al., *Emerging roles of exosomes in normal and pathological conditions: new insights for diagnosis and therapeutic applications.* Front Immunol, 2015. **6**: p. 203.

390. S, E.L.A., et al., *Extracellular vesicles: biology and emerging therapeutic opportunities.* Nat Rev Drug Discov, 2013. **12**(5): p. 347-57.

391. van der Meel, R., et al., *Extracellular vesicles as drug delivery systems: lessons from the liposome field.* J Control Release, 2014. **195**: p. 72-85.

392. Lakhal, S. and M.J. Wood, *Exosome nanotechnology: an emerging paradigm shift in drug delivery: exploitation of exosome nanovesicles for systemic in vivo delivery of RNAi heralds new horizons for drug delivery across biological barriers.* Bioessays, 2011. **33**(10): p. 737-41.

393. Wahlgren, J., et al., *Plasma exosomes can deliver exogenous short interfering RNA to monocytes and lymphocytes.* Nucleic Acids Res, 2012. **40**(17): p. e130.

394. Maguire, C.A., et al., *Microvesicle-associated AAV vector as a novel gene delivery system.* Mol Ther, 2012. **20**(5): p. 960-71.

395. Sun, D., et al., *A novel nanoparticle drug delivery system: the anti-inflammatory activity of curcumin is enhanced when encapsulated in exosomes.* Mol Ther, 2010. **18**(9): p. 1606-14.

396. Tang, K., et al., *Delivery of chemotherapeutic drugs in tumour cell-derived microparticles.* Nat Commun, 2012. **3**: p. 1282.

397. Jang, S.C., et al., *Bioinspired exosome-mimetic nanovesicles for targeted delivery of chemotherapeutics to malignant tumors.* ACS Nano, 2013. **7**(9): p. 7698-710.

398. Mizrak, A., et al., *Genetically engineered microvesicles carrying suicide mRNA/protein inhibit schwannoma tumor growth.* Mol Ther, 2013. **21**(1): p. 101-8.

399. Erbs, P., et al., *In vivo cancer gene therapy by adenovirus-mediated transfer of a bifunctional yeast cytosine deaminase/uracil phosphoribosyltransferase fusion gene.* Cancer Res, 2000. **60**(14): p. 3813-22.

400. Feng, D., et al., *Cellular internalization of exosomes occurs through phagocytosis.* Traffic, 2010. **11**(5): p. 675-87.

401. Zech, D., et al., *Tumor-exosomes and leukocyte activation: an ambivalent crosstalk.* Cell Commun Signal, 2012. **10**(1): p. 37.

402. Wu, H., K. Hu, and X. Jiang, *From nose to brain: understanding transport capacity and transport rate of drugs.* Expert Opin Drug Deliv, 2008. **5**(10): p. 1159-68.

403. Zhuang, X., et al., *Treatment of brain inflammatory diseases by delivering exosome encapsulated anti-inflammatory drugs from the nasal region to the brain.* Mol Ther, 2011. **19**(10): p. 1769-79.

404. Zitvogel, L., et al., *Eradication of established murine tumors using a novel cell-free vaccine: dendritic cell-derived exosomes.* Nat Med, 1998. **4**(5): p. 594-600.

405. Lamparski, H.G., et al., *Production and characterization of clinical grade exosomes derived from dendritic cells.* J Immunol Methods, 2002. **270**(2): p. 211-26.

406. Hsu, D.H., et al., *Exosomes as a tumor vaccine: enhancing potency through direct loading of antigenic peptides.* J Immunother, 2003. **26**(5): p. 440-50.

407. Escudier, B., et al., *Vaccination of metastatic melanoma patients with autologous dendritic cell (DC) derived-exosomes: results of thefirst phase I clinical trial.* J Transl Med, 2005. **3**(1): p. 10.

408. Morse, M.A., et al., *A phase I study of dexosome immunotherapy in patients with advanced non-small cell lung cancer.* J Transl Med, 2005. **3**(1): p. 9.

409. Viaud, S., et al., *Updated technology to produce highly immunogenic dendritic cell-derived exosomes of clinical grade: a critical role of interferon-gamma.* J Immunother, 2011. **34**(1): p. 65-75.

410. Lener, T., et al., *Applying extracellular vesicles based therapeutics in clinical trials - an ISEV position paper.* J Extracell Vesicles, 2015. **4**: p. 30087.

411. Chaput, N., et al., *Exosomes as potent cell-free peptide-based vaccine. II. Exosomes in CpG adjuvants efficiently prime naive Tc1 lymphocytes leading to tumor rejection.* J Immunol, 2004. **172**(4): p. 2137-46.

412. Taieb, J., et al., *Chemoimmunotherapy of tumors: cyclophosphamide synergizes with exosome based vaccines.* J Immunol, 2006. **176**(5): p. 2722-9.

413. Gehrmann, U., et al., *Synergistic induction of adaptive antitumor immunity by codelivery of antigen with alpha-galactosylceramide on exosomes.* Cancer Res, 2013. **73**(13): p. 3865-76.

414. Le Blanc, K., et al., *Mesenchymal stem cells for treatment of steroid-resistant, severe, acute graft-versus-host disease: a phase II study.* Lancet, 2008. **371**(9624): p. 1579-86.

415. Baron, F. and R. Storb, *Mesenchymal stromal cells: a new tool against graft-versus-host disease?* Biol Blood Marrow Transplant, 2012. **18**(6): p. 822-40.

416. Kordelas, L., et al., *MSC-derived exosomes: a novel tool to treat therapy-refractory graft-versus-host disease.* Leukemia, 2014. **28**(4): p. 970-3.

417. Chen, T.S., et al., *Enabling a robust scalable manufacturing process for therapeutic exosomes through oncogenic immortalization of human ESC-derived MSCs.* J Transl Med, 2011. **9**: p. 47.

418. Witwer, K.W., et al., *Standardization of sample collection, isolation and analysis methods in extracellular vesicle research.* J Extracell Vesicles, 2013. **2**.

419. Li, J., et al., *Serum-free culture alters the quantity and protein composition of neuroblastoma-derived extracellular vesicles.* J Extracell Vesicles, 2015. **4**: p. 26883.

420. Eitan, E., et al., *Extracellular vesicle-depleted fetal bovine and human sera have reduced capacity to support cell growth.* J Extracell Vesicles, 2015. **4**: p. 26373.

421. Shelke, G.V., et al., *Importance of exosome depletion protocols to eliminate functional and RNA-containing extracellular vesicles from fetal bovine serum.* J Extracell Vesicles, 2014. **3**.

422. Thery, C., et al., *Isolation and characterization of exosomes from cell culture supernatants and biological fluids.* Curr Protoc Cell Biol, 2006. **Chapter 3**: p. Unit 3 22.

423. Yuana, Y., et al., *Handling and storage of human body fluids for analysis of extracellular vesicles.* J Extracell Vesicles, 2015. **4**: p. 29260.

424. Kalra, H., et al., *Comparative proteomics evaluation of plasma exosome isolation techniques and assessment of the stability of exosomes in normal human blood plasma.* Proteomics, 2013. **13**(22): p. 3354-64.

425. Gallart-Palau, X., et al., *Extracellular vesicles are rapidly purified from human plasma by PRotein Organic Solvent PRecipitation (PROSPR).* Sci Rep, 2015. **5**: p. 14664.

426. Nordin, J.Z., et al., *Ultrafiltration with size-exclusion liquid chromatography for high yield isolation of extracellular vesicles preserving intact biophysical and functional properties.* Nanomedicine, 2015. **11**(4): p. 879-83.

427. Lorincz, A.M., et al., *Effect of storage on physical and functional properties of extracellular vesicles derived from neutrophilic granulocytes.* J Extracell Vesicles, 2014. **3**: p. 25465.

428. Larson, M.C., et al., *Calcium-phosphate microprecipitates mimic microparticles when examined with flow cytometry.* Cytometry A, 2013. **83**(2): p. 242-50.

429. Lotvall, J., et al., *Minimal experimental requirements for definition of extracellular vesicles and their functions: a position statement from the International Society for Extracellular Vesicles.* J Extracell Vesicles, 2014. **3**: p. 26913.

430. Maas, S.L., et al., *Possibilities and limitations of current technologies for quantification of biological extracellular vesicles and synthetic mimics.* J Control Release, 2015. **200**: p. 87-96.

431. Dragovic, R.A., et al., *Sizing and phenotyping of cellular vesicles using Nanoparticle Tracking Analysis.* Nanomedicine, 2011. **7**(6): p. 780-8.

432. Peinado, H., et al., *Melanoma exosomes educate bone marrow progenitor cells toward a pro-metastatic phenotype through MET.* Nat Med, 2012. **18**(6): p. 883-91.

433. Takahashi, Y., et al., *Visualization and in vivo tracking of the exosomes of murine melanoma B16-BL6 cells in mice after intravenous injection.* J Biotechnol, 2013. **165**(2): p. 77-84.

434. Morelli, A.E., et al., *Endocytosis, intracellular sorting, and processing of exosomes by dendritic cells.* Blood, 2004. **104**(10): p. 3257-66.

435. Alemany, R., K. Suzuki, and D.T. Curiel, *Blood clearance rates of adenovirus type 5 in mice.* J Gen Virol, 2000. **81**(Pt 11): p. 2605-9.

436. Tao, N., et al., *Sequestration of adenoviral vector by Kupffer cells leads to a nonlinear dose response of transduction in liver.* Mol Ther, 2001. **3**(1): p. 28-35.

437. Liu, D.X., *Biological factors involved in blood clearance of liposomes by liver.* Advanced Drug Delivery Reviews, 1997. **24**(2-3): p. 201-213.

438. Rahman, Y.E., et al., *Differential uptake of liposomes varying in size and lipid composition by parenchymal and kupffer cells of mouse liver.* Life Sci, 1982. **31**(19): p. 2061-71.

439. Wiklander, O.P., et al., *Extracellular vesicle in vivo biodistribution is determined by cell source, route of administration and targeting.* J Extracell Vesicles, 2015. **4**: p. 26316.

440. Imai, T., et al., *Macrophage-dependent clearance of systemically administered B16BL6-derived exosomes from the blood circulation in mice.* J Extracell Vesicles, 2015. **4**: p. 26238.

441. Alvarez-Erviti, L., et al., *Delivery of siRNA to the mouse brain by systemic injection of targeted exosomes.* Nat Biotechnol, 2011. **29**(4): p. 341-5.

442. Cooper, J.M., et al., *Systemic exosomal siRNA delivery reduced alpha-synuclein aggregates in brains of transgenic mice.* Mov Disord, 2014. **29**(12): p. 1476-85.

443. Nazarenko, I., et al., *Cell surface tetraspanin Tspan8 contributes to molecular pathways of exosome-induced endothelial cell activation.* Cancer Res, 2010. **70**(4): p. 1668-78.

444. Rana, S. and M. Zoller, *Exosome target cell selection and the importance of exosomal tetraspanins: a hypothesis.* Biochem Soc Trans, 2011. **39**(2): p. 559-62.

445. Rana, S., K. Malinowska, and M. Zoller, *Exosomal tumor microRNA modulates premetastatic organ cells.* Neoplasia, 2013. **15**(3): p. 281-95.

446. Mulcahy, L.A., R.C. Pink, and D.R. Carter, *Routes and mechanisms of extracellular vesicle uptake.* J Extracell Vesicles, 2014. **3**.

447. Parolini, I., et al., *Microenvironmental pH is a key factor for exosome traffic in tumor cells.* J Biol Chem, 2009. **284**(49): p. 34211-22.

448. Tian, T., et al., *Visualizing of the cellular uptake and intracellular trafficking of exosomes by live-cell microscopy.* J Cell Biochem, 2010. **111**(2): p. 488-96.

449. Barres, C., et al., *Galectin-5 is bound onto the surface of rat reticulocyte exosomes and modulates vesicle uptake by macrophages.* Blood, 2010. **115**(3): p. 696-705.

450. Dasgupta, S.K., et al., *Lactadherin and clearance of platelet-derived microvesicles.* Blood, 2009. **113**(6): p. 1332-9.

451. Skokos, D., et al., *Mast cell-derived exosomes induce phenotypic and functional maturation of dendritic cells and elicit specific immune responses in vivo.* J Immunol, 2003. **170**(6): p. 3037-45.

452. Rieu, S., et al., *Exosomes released during reticulocyte maturation bind to fibronectin via integrin alpha4beta1.* Eur J Biochem, 2000. **267**(2): p. 583-90.

453. Hao, S., et al., *Mature dendritic cells pulsed with exosomes stimulate efficient cytotoxic T-lymphocyte responses and antitumour immunity.* Immunology, 2007. **120**(1): p. 90-102.

454. Xie, Y., et al., *Dendritic cells recruit T cell exosomes via exosomal LFA-1 leading to inhibition of CD8+ CTL responses through downregulation of peptide/MHC class I and Fas ligand-mediated cytotoxicity.* J Immunol, 2010. **185**(9): p. 5268-78.

455. Nanjundappa, R.H., et al., *GP120-specific exosome-targeted T cell-based vaccine capable of stimulating DC- and CD4(+) T-independent CTL responses.* Vaccine, 2011. **29**(19): p. 3538-47.

456. Nolte-'t Hoen, E.N., et al., *Activated T cells recruit exosomes secreted by dendritic cells via LFA-1.* Blood, 2009. **113**(9): p. 1977-81.

457. Segura, E., et al., *CD8+ dendritic cells use LFA-1 to capture MHC-peptide complexes from exosomes in vivo.* J Immunol, 2007. **179**(3): p. 1489-96.

458. Segura, E., et al., *ICAM-1 on exosomes from mature dendritic cells is critical for efficient naive T-cell priming.* Blood, 2005. **106**(1): p. 216-23.

459. Naslund, T.I., et al., *Exosomes from breast milk inhibit HIV-1 infection of dendritic cells and subsequent viral transfer to CD4+ T cells.* AIDS, 2014. **28**(2): p. 171-80.

460. Miyanishi, M., et al., *Identification of Tim4 as a phosphatidylserine receptor.* Nature, 2007. **450**(7168): p. 435-9.

461. Klibi, J., et al., *Blood diffusion and Th1-suppressive effects of galectin-9-containing exosomes released by Epstein-Barr virus-infected nasopharyngeal carcinoma cells.* Blood, 2009. **113**(9): p. 1957-66.

462. Saunderson, S.C., et al., *CD169 mediates the capture of exosomes in spleen and lymph node.* Blood, 2014. **123**(2): p. 208-16.

463. Plebanek, M.P., et al., *Nanoparticle Targeting and Cholesterol Flux Through Scavenger Receptor Type B-1 Inhibits Cellular Exosome Uptake.* Sci Rep, 2015. **5**: p. 15724.

464. Nishikawa, K., H. Arai, and K. Inoue, *Scavenger receptor-mediated uptake and metabolism of lipid vesicles containing acidic phospholipids by mouse peritoneal macrophages.* J Biol Chem, 1990. **265**(9): p. 5226-31.

465. Xu, Z., et al., *Clearance of adenovirus by Kupffer cells is mediated by scavenger receptors, natural antibodies, and complement.* J Virol, 2008. **82**(23): p. 11705-13.

466. Haisma, H.J., et al., *Polyinosinic acid enhances delivery of adenovirus vectors in vivo by preventing sequestration in liver macrophages.* J Gen Virol, 2008. **89**(Pt 5): p. 1097-105.

467. Willekens, F.L., et al., *Liver Kupffer cells rapidly remove red blood cell-derived vesicles from the circulation by scavenger receptors.* Blood, 2005. **105**(5): p. 2141-5.

468. Canton, J., D. Neculai, and S. Grinstein, *Scavenger receptors in homeostasis and immunity.* Nat Rev Immunol, 2013. **13**(9): p. 621-34.

469. Mukhopadhyay, S. and S. Gordon, *The role of scavenger receptors in pathogen recognition and innate immunity.* Immunobiology, 2004. **209**(1-2): p. 39-49.

470. Pluddemann, A., C. Neyen, and S. Gordon, *Macrophage scavenger receptors and host-derived ligands.* Methods, 2007. **43**(3): p. 207-17.

471. Prabhudas, M., et al., *Standardizing scavenger receptor nomenclature.* J Immunol, 2014. **192**(5): p. 1997-2006.

472. Kennedy, D.J. and S.R. Kashyap, *Pathogenic role of scavenger receptor CD36 in the metabolic syndrome and diabetes.* Metab Syndr Relat Disord, 2011. **9**(4): p. 239-45.

473. Kzhyshkowska, J., C. Neyen, and S. Gordon, *Role of macrophage scavenger receptors in atherosclerosis.* Immunobiology, 2012. **217**(5): p. 492-502.

474. Neyen, C., et al., *Macrophage scavenger receptor a promotes tumor progression in murine models of ovarian and pancreatic cancer.* J Immunol, 2013. **190**(7): p. 3798-805.

475. Wang, X.Y., et al., *Scavenger receptor-A negatively regulates antitumor immunity.* Cancer Res, 2007. **67**(10): p. 4996-5002.

476. Wilkinson, K. and J. El Khoury, *Microglial scavenger receptors and their roles in the pathogenesis of Alzheimer's disease.* Int J Alzheimers Dis, 2012. **2012**: p. 489456.

477. Armengol, C., et al., *Role of scavenger receptors in the pathophysiology of chronic liver diseases.* Crit Rev Immunol, 2013. **33**(1): p. 57-96.

478. Terpstra, V., et al., *Hepatic and extrahepatic scavenger receptors: function in relation to disease.* Arterioscler Thromb Vasc Biol, 2000. **20**(8): p. 1860-72.

479. Kodama, T., et al., *Type I macrophage scavenger receptor contains alpha-helical and collagen-like coiled coils.* Nature, 1990. **343**(6258): p. 531-5.

480. Freeman, M., et al., *An ancient, highly conserved family of cysteine-rich protein domains revealed by cloning type I and type II murine macrophage scavenger receptors.* Proc Natl Acad Sci U S A, 1990. **87**(22): p. 8810-4.

481. Gough, P.J., D.R. Greaves, and S. Gordon, *A naturally occurring isoform of the human macrophage scavenger receptor (SR-A) gene generated by alternative splicing blocks modified LDL uptake.* J Lipid Res, 1998. **39**(3): p. 531-43.

482. Kraal, G., et al., *The macrophage receptor MARCO.* Microbes Infect, 2000. **2**(3): p. 313-6.

483. Bickel, P.E. and M.W. Freeman, *Rabbit aortic smooth muscle cells express inducible macrophage scavenger receptor messenger RNA that is absent from endothelial cells.* J Clin Invest, 1992. **90**(4): p. 1450-7.

484. Zhou, Y.F., et al., *Human cytomegalovirus increases modified low density lipoprotein uptake and scavenger receptor mRNA expression in vascular smooth muscle cells.* J Clin Invest, 1996. **98**(9): p. 2129-38.

485. Pitas, R.E., *Expression of the acetyl low density lipoprotein receptor by rabbit fibroblasts and smooth muscle cells. Up-regulation by phorbol esters.* J Biol Chem, 1990. **265**(21): p. 12722-7.

486. Stein, O. and Y. Stein, *Bovine aortic endothelial cells display macrophage-like properties towards acetylated 125I-labelled low density lipoprotein.* Biochim Biophys Acta, 1980. **620**(3): p. 631-5.

487. Hughes, D.A., I.P. Fraser, and S. Gordon, *Murine macrophage scavenger receptor: in vivo expression and function as receptor for macrophage adhesion in lymphoid and non-lymphoid organs.* Eur J Immunol, 1995. **25**(2): p. 466-73.

488. Elomaa, O., et al., *Cloning of a novel bacteria-binding receptor structurally related to scavenger receptors and expressed in a subset of macrophages.* Cell, 1995. **80**(4): p. 603-9.

489. Han, H.J., T. Tokino, and Y. Nakamura, *CSR, a scavenger receptor-like protein with a protective role against cellular damage causedby UV irradiation and oxidative stress.* Hum Mol Genet, 1998. **7**(6): p. 1039-46.

490. Jiang, Y., et al., *Identification and characterization of murine SCARA5, a novel class A scavenger receptor that is expressed by populations of epithelial cells.* J Biol Chem, 2006. **281**(17): p. 11834-45.

491. Ohtani, K., et al., *The membrane-type collectin CL-P1 is a scavenger receptor on vascular endothelial cells.* J Biol Chem, 2001. **276**(47): p. 44222-8.

492. Doi, T., et al., *Charged collagen structure mediates the recognition of negatively charged macromolecules by macrophage scavenger receptors.* J Biol Chem, 1993. **268**(3): p. 2126-33.

493. Gu, X., et al., *The efficient cellular uptake of high density lipoprotein lipids via scavenger receptor class B type I requires not only receptor-mediated surface binding but also receptor-specific lipid transfer mediated by its extracellular domain.* J Biol Chem, 1998. **273**(41): p. 26338-48.

494. Platt, N., R.P. da Silva, and S. Gordon, *Class A scavenger receptors and the phagocytosis of apoptotic cells.* Biochem Soc Trans, 1998. **26**(4): p. 639-44.

495. Platt, N. and S. Gordon, *Scavenger receptors: diverse activities and promiscuous binding of polyanionic ligands.* Chem Biol, 1998. **5**(8): p. R193-203.

496. Van Berkel, T.J., Y.B. De Rijke, and J.K. Kruijt, *Different fate in vivo of oxidatively modified low density lipoprotein and acetylated low density lipoprotein in rats. Recognition by various scavenger receptors on Kupffer and endothelial liver cells.* J Biol Chem, 1991. **266**(4): p. 2282-9.

497. Dahl, M., et al., *Protection against inhaled oxidants through scavenging of oxidized lipids by macrophage receptors MARCO and SR-AI/II.* J Clin Invest, 2007. **117**(3): p. 757-64.

498. Platt, N., et al., *Role for the class A macrophage scavenger receptor in the phagocytosis of apoptotic thymocytes in vitro.* Proc Natl Acad Sci U S A, 1996. **93**(22): p. 12456-60.

499. Brown, M.S. and J.L. Goldstein, *Lipoprotein metabolism in the macrophage: implications for cholesterol deposition in atherosclerosis.* Annu Rev Biochem, 1983. **52**: p. 223-61.

500. Terpstra, V., N. Kondratenko, and D. Steinberg, *Macrophages lacking scavenger receptor A show a decrease in binding and uptake of acetylated low-density lipoprotein and of apoptotic thymocytes, but not of oxidatively damaged red blood cells.* Proc Natl Acad Sci U S A, 1997. **94**(15): p. 8127-31.

501. Platt, N., et al., *Apoptotic thymocyte clearance in scavenger receptor class A-deficient mice is apparently normal.* J Immunol, 2000. **164**(9): p. 4861-7.

502. Acton, S.L., et al., *Expression cloning of SR-BI, a CD36-related class B scavenger receptor.* J Biol Chem, 1994. **269**(33): p. 21003-9.

503. Webb, N.R., et al., *Alternative forms of the scavenger receptor BI (SR-BI).* J Lipid Res, 1997. **38**(7): p. 1490-5.

504. Navazo, M.D., et al., *Identification of a domain (155-183) on CD36 implicated in the phagocytosis of apoptotic neutrophils.* J Biol Chem, 1996. **271**(26): p. 15381-5.

505. Puente Navazo, M.D., et al., *Identification on human CD36 of a domain (155-183) implicated in binding oxidized low-density lipoproteins (Ox-LDL).* Arterioscler Thromb Vasc Biol, 1996. **16**(8): p. 1033-9.

506. Thorne, R.F., et al., *CD36 forms covalently associated dimers and multimers in platelets and transfected COS-7 cells.* Biochem Biophys Res Commun, 1997. **240**(3): p. 812-8.

507. Reaven, E., et al., *Dimerization of the scavenger receptor class B type I: formation, function, and localization in diverse cells and tissues.* J Lipid Res, 2004. **45**(3): p. 513-28.

508. Terpstra, V. and T.J. van Berkel, *Scavenger receptors on liver Kupffer cells mediate the in vivo uptake of oxidatively damaged red blood cells in mice.* Blood, 2000. **95**(6): p. 2157-63.

509. Greenberg, M.E., et al., *Oxidized phosphatidylserine-CD36 interactions play an essential role in macrophage-dependent phagocytosis of apoptotic cells.* J Exp Med, 2006. **203**(12): p. 2613-25.

510. Nieland, T.J., et al., *Negatively cooperative binding of high-density lipoprotein to the HDL receptor SR-BI.* Biochemistry, 2011. **50**(11): p. 1818-30.

511. Kawasaki, Y., et al., *Phosphatidylserine binding of class B scavenger receptor type I, a phagocytosis receptor of testicular sertoli cells.* J Biol Chem, 2002. **277**(30): p. 27559-66.

512. Rigotti, A., S.L. Acton, and M. Krieger, *The class B scavenger receptors SR-BI and CD36 are receptors for anionic phospholipids.* J Biol Chem, 1995. **270**(27): p. 16221-4.

513. Fukasawa, M., et al., *SRB1, a class B scavenger receptor, recognizes both negatively charged liposomes and apoptotic cells.* Exp Cell Res, 1996. **222**(1): p. 246-50.

514. McWhorter, F.Y., et al., *Modulation of macrophage phenotype by cell shape.* Proc Natl Acad Sci U S A, 2013. **110**(43): p. 17253-8.

515. Nathan, C.F., et al., *Identification of interferon-gamma as the lymphokine that activates human macrophage oxidative metabolism and antimicrobial activity.* J Exp Med, 1983. **158**(3): p. 670-89.

516. Gifford, G.E. and M.L. Lohmann-Matthes, *Gamma interferon priming of mouse and human macrophages for induction of tumor necrosis factor production by bacterial lipopolysaccharide.* J Natl Cancer Inst, 1987. **78**(1): p. 121-4.

517. Lehtonen, A., et al., *Gene expression profiling during differentiation of human monocytes to macrophages or dendritic cells.* J Leukoc Biol, 2007. **82**(3): p. 710-20.

518. Klaschik, S., D. Tross, and D.M. Klinman, *Inductive and suppressive networks regulate TLR9-dependent gene expression in vivo.* J Leukoc Biol, 2009. **85**(5): p. 788-95.

519. Lacey, D.C., et al., *Defining GM-CSF- and macrophage-CSF-dependent macrophage responses by in vitro models.* J Immunol, 2012. **188**(11): p. 5752-65.

520. Helft, J., et al., *GM-CSF Mouse Bone Marrow Cultures Comprise a Heterogeneous Population of CD11c(+)MHCII(+) Macrophages and Dendritic Cells.* Immunity, 2015. **42**(6): p. 1197-211.

521. Chapuis, F., et al., *Differentiation of human dendritic cells from monocytes in vitro.* Eur J Immunol, 1997. **27**(2): p. 431-41.

522. Kalinski, P., *Regulation of immune responses by prostaglandin E2.* J Immunol, 2012. **188**(1): p. 21-8.

523. Gordon, S., *Alternative activation of macrophages.* Nat Rev Immunol, 2003. **3**(1): p. 23-35.

524. Beyer, M., et al., *High-resolution transcriptome of human macrophages.* PLoS One, 2012. **7**(9): p. e45466.

525. Suttles, J. and R.D. Stout, *Macrophage CD40 signaling: a pivotal regulator of disease protection and pathogenesis.* Semin Immunol, 2009. **21**(5): p. 257-64.

526. Latchman, Y., et al., *PD-L2 is a second ligand for PD-1 and inhibits T cell activation.* Nat Immunol, 2001. **2**(3): p. 261-8.

527. Kerrigan, A.M. and G.D. Brown, *C-type lectins and phagocytosis.* Immunobiology, 2009. **214**(7): p. 562-75.

528. Peiser, L., S. Mukhopadhyay, and S. Gordon, *Scavenger receptors in innate immunity.* Curr Opin Immunol, 2002. **14**(1): p. 123-8.

529. Mantovani, A., et al., *Decoy receptors: a strategy to regulate inflammatory cytokines and chemokines.* Trends Immunol, 2001. **22**(6): p. 328-36.

530. Chen, C., *COX-2's new role in inflammation.* Nat Chem Biol, 2010. **6**(6): p. 401-2.

531. Curry, J.M., et al., *M-CSF signals through the MAPK/ERK pathway via Sp1 to induce VEGF production and induces angiogenesis in vivo.* PLoS One, 2008. **3**(10): p. e3405.

532. Nikolic, D., et al., *SR-A ligand and M-CSF dynamically regulate SR-A expression and function in primary macrophages via p38 MAPK activation.* BMC Immunol, 2011. **12**: p. 37.

533. Chen, C., Y.H. Chen, and W.W. Lin, *Involvement of p38 mitogen-activated protein kinase in lipopolysaccharide-induced iNOS and COX-2 expression in J774 macrophages.* Immunology, 1999. **97**(1): p. 124-9.

534. Yamamoto, K., et al., *Transcriptional roles of nuclear factor kappa B and nuclear factor-interleukin-6 in the tumor necrosis factor alpha-dependent induction of cyclooxygenase-2 in MC3T3-E1 cells.* J Biol Chem, 1995. **270**(52): p. 31315-20.

535. Crofford, L.J., *COX-1 and COX-2 tissue expression: implications and predictions.* J Rheumatol Suppl, 1997. **49**: p. 15-9.

536. Audrito, V., et al., *Extracellular nicotinamide phosphoribosyltransferase (NAMPT) promotes M2 macrophage polarization in chronic lymphocytic leukemia.* Blood, 2015. **125**(1): p. 111-23.

537. Thelen, T., et al., *The class A scavenger receptor, macrophage receptor with collagenous structure, is the major phagocytic receptor for Clostridium sordellii expressed by human decidual macrophages.* J Immunol, 2010. **185**(7): p. 4328-35.

538. Limmon, G.V., et al., *Scavenger receptor class-A is a novel cell surface receptor for double-stranded RNA.* FASEB J, 2008. **22**(1): p. 159-67.

539. Smyth, T., et al., *Biodistribution and delivery efficiency of unmodified tumor-derived exosomes.* J Control Release, 2015. **199**: p. 145-55.

540. Ambarus, C.A., et al., *Systematic validation of specific phenotypic markers for in vitro polarized human macrophages.* J Immunol Methods, 2012. **375**(1-2): p. 196-206.

541. Singh, M., et al., *Effective innate and adaptive antimelanoma immunity through localized TLR7/8 activation.* J Immunol, 2014. **193**(9): p. 4722-31.

542. Tomai, M.A., et al., *Immunomodulating and antiviral activities of the imidazoquinoline S-28463.* Antiviral Res, 1995. **28**(3): p. 253-64.

543. Sioud, M., et al., *Signaling through toll-like receptor 7/8 induces the differentiation of human bone marrow CD34+ progenitor cells along the myeloid lineage.* J Mol Biol, 2006. **364**(5): p. 945-54.

544. Benson, S.A. and J.D. Ernst, *TLR2-dependent inhibition of macrophage responses to IFN-gamma is mediated by distinct, gene-specific mechanisms.* PLoS One, 2009. **4**(7): p. e6329.

545. Funderburg, N.T., et al., *The Toll-like receptor 1/2 agonists Pam(3) CSK(4) and human beta-defensin-3 differentially induce interleukin-10 and nuclear factor-kappaB signalling patterns in human monocytes.* Immunology, 2011. **134**(2): p. 151-60.

546. Wenink, M.H., et al., *TLR2 promotes Th2/Th17 responses via TLR4 and TLR7/8 by abrogating the type I IFN amplification loop.* J Immunol, 2009. **183**(11): p. 6960-70.

547. Gunzer, M., et al., *Systemic administration of a TLR7 ligand leads to transient immune incompetence due to peripheral-blood leukocyte depletion.* Blood, 2005. **106**(7): p. 2424-32.

548. Woodmansee, C., J. Pillow, and R.B. Skinner, Jr., *The role of topical immune response modifiers in skin cancer.* Drugs, 2006. **66**(13): p. 1657-64.

549. Dockrell, D.H. and G.R. Kinghorn, *Imiquimod and resiquimod as novel immunomodulators.* J Antimicrob Chemother, 2001. **48**(6): p. 751-5.

550. Schon, M.P. and M. Schon, *TLR7 and TLR8 as targets in cancer therapy.* Oncogene, 2008. **27**(2): p. 190-9.

551. Gorden, K.B., et al., *Synthetic TLR agonists reveal functional differences between human TLR7 and TLR8.* J Immunol, 2005. **174**(3): p. 1259-68.

552. Krug, A., et al., *Toll-like receptor expression reveals CpG DNA as a unique microbial stimulus for plasmacytoid dendritic cells which synergizes with CD40 ligand to induce high amounts of IL-12.* Eur J Immunol, 2001. **31**(10): p. 3026-37.

553. Ito, T., et al., *Interferon-alpha and interleukin-12 are induced differentially by Toll-like receptor 7 ligands in human blood dendritic cell subsets.* J Exp Med, 2002. **195**(11): p. 1507-12.

554. Visintin, A., et al., *Secreted MD-2 is a large polymeric protein that efficiently confers lipopolysaccharide sensitivity to Toll-like receptor 4.* Proc Natl Acad Sci U S A, 2001. **98**(21): p. 12156-61.

555. Larange, A., et al., *TLR7 and TLR8 agonists trigger different signaling pathways for human dendritic cell maturation.* J Leukoc Biol, 2009. **85**(4): p. 673-83.

556. Jurk, M., et al., *Human TLR7 or TLR8 independently confer responsiveness to the antiviral compound R-848.* Nat Immunol, 2002. **3**(6): p. 499.

557. Gorden, K.K., et al., *Cutting edge: activation of murine TLR8 by a combination of imidazoquinoline immune response modifiers and polyT oligodeoxynucleotides.* J Immunol, 2006. **177**(10): p. 6584-7.

558. Demaria, O., et al., *TLR8 deficiency leads to autoimmunity in mice.* J Clin Invest, 2010. **120**(10): p. 3651-62.

559. Tran, N.L., C. Manzin-Lorenzi, and M.L. Santiago-Raber, *Toll-like receptor 8 deletion accelerates autoimmunity in a mouse model of lupus through a Toll-like receptor 7-dependent mechanism.* Immunology, 2015. **145**(1): p. 60-70.

560. Fuster, J.J. and K. Walsh, *The good, the bad, and the ugly of interleukin-6 signaling.* EMBO J, 2014. **33**(13): p. 1425-7.

561. Roses, R.E., et al., *Differential production of IL-23 and IL-12 by myeloid-derived dendritic cells in response to TLR agonists.* J Immunol, 2008. **181**(7): p. 5120-7.

562. Kerkar, S.P., et al., *IL-12 triggers a programmatic change in dysfunctional myeloid-derived cells within mouse tumors.* J Clin Invest, 2011. **121**(12): p. 4746-57.

563. Steding, C.E., et al., *The role of interleukin-12 on modulating myeloid-derived suppressor cells, increasing overall survival and reducing metastasis.* Immunology, 2011. **133**(2): p. 221-38.

564. Dranoff, G., *Cytokines in cancer pathogenesis and cancer therapy.* Nat Rev Cancer, 2004. **4**(1): p. 11-22.

565. Ouyang, W., et al., *Regulation and functions of the IL-10 family of cytokines in inflammation and disease.* Annu Rev Immunol, 2011. **29**: p. 71-109.

566. Sharif, M.N., et al., *IFN-alpha priming results in a gain of proinflammatory function by IL-10: implications for systemic lupus erythematosus pathogenesis.* J Immunol, 2004. **172**(10): p. 6476-81.

567. Lauw, F.N., et al., *Proinflammatory effects of IL-10 during human endotoxemia.* J Immunol, 2000. **165**(5): p. 2783-9.

568. Niemand, C., et al., *Activation of STAT3 by IL-6 and IL-10 in primary human macrophages is differentially modulated by suppressor of cytokine signaling 3.* J Immunol, 2003. **170**(6): p. 3263-72.

569. Riley, J.K., et al., *Interleukin-10 receptor signaling through the JAK-STAT pathway. Requirement for two distinct receptor-derived signals for anti-inflammatory action.* J Biol Chem, 1999. **274**(23): p. 16513-21.

570. Heinrich, P.C., et al., *Interleukin-6-type cytokine signalling through the gp130/Jak/STAT pathway.* Biochem J, 1998. **334 ( Pt 2)**: p. 297-314.

571. Cox, G.W., *Assay for macrophage-mediated anti-tumor cytotoxicity.* Curr Protoc Immunol, 2001. **Chapter 14**: p. Unit 14 7.

572. Landskron, G., et al., *Chronic inflammation and cytokines in the tumor microenvironment.* J Immunol Res, 2014. **2014**: p. 149185.

573. Taniguchi, T., et al., *IRF family of transcription factors as regulators of host defense.* Annu Rev Immunol, 2001. **19**: p. 623-55.

574. Sato, M., et al., *Distinct and essential roles of transcription factors IRF-3 and IRF-7 in response to viruses for IFN-alpha/beta gene induction.* Immunity, 2000. **13**(4): p. 539-48.

575. Tugal, D., X. Liao, and M.K. Jain, *Transcriptional control of macrophage polarization.* Arterioscler Thromb Vasc Biol, 2013. **33**(6): p. 1135-44.

576. Dinarello, C.A., *Blocking IL-1 in systemic inflammation.* J Exp Med, 2005. **201**(9): p. 1355-9.

577. Wang, X.F., et al., *The role of indoleamine 2,3-dioxygenase (IDO) in immune tolerance: focus on macrophage polarization of THP-1 cells.* Cell Immunol, 2014. **289**(1-2): p. 42-8.

578. Brown, J., et al., *Proteome bioprofiles distinguish between M1 priming and activation states in human macrophages.* J Leukoc Biol, 2010. **87**(4): p. 655-62.

579. Reales-Calderon, J.A., et al., *Proteomic characterization of human proinflammatory M1 and anti-inflammatory M2 macrophages and their response to Candida albicans.* Proteomics, 2014. **14**(12): p. 1503-18.

580. Varga, G., et al., *Active MAC-1 (CD11b/CD18) on DCs inhibits full T-cell activation.* Blood, 2007. **109**(2): p. 661-9.

581. Pillay, J., et al., *A subset of neutrophils in human systemic inflammation inhibits T cell responses through Mac-1.* J Clin Invest, 2012. **122**(1): p. 327-36.

582. Umemura, N., et al., *Tumor-infiltrating myeloid-derived suppressor cells are pleiotropic-inflamed monocytes/macrophages that bear M1- and M2-type characteristics.* J Leukoc Biol, 2008. **83**(5): p. 1136-44.

583. Eruslanov, E., et al., *Aberrant PGE(2) metabolism in bladder tumor microenvironment promotes immunosuppressive phenotype of tumor-infiltrating myeloid cells.* Int Immunopharmacol, 2011. **11**(7): p. 848-55.

584. Muthuswamy, R., et al., *PGE(2) transiently enhances DC expression of CCR7 but inhibits the ability of DCs to produce CCL19 and attract naive T cells.* Blood, 2010. **116**(9): p. 1454-9.

585. Serafini, P., *Editorial: PGE2-producing MDSC: a role in tumor progression?* J Leukoc Biol, 2010. **88**(5): p. 827-9.

586. Bachwich, P.R., et al., *Tumor necrosis factor stimulates interleukin-1 and prostaglandin E2 production in resting macrophages.* Biochem Biophys Res Commun, 1986. **136**(1): p. 94-101.

587. Lee, S.H., et al., *Selective expression of mitogen-inducible cyclooxygenase in macrophages stimulated with lipopolysaccharide.* J Biol Chem, 1992. **267**(36): p. 25934-8.

588. Mandruzzato, S., et al., *IL4Ralpha+ myeloid-derived suppressor cell expansion in cancer patients.* J Immunol, 2009. **182**(10): p. 6562-8.

589. Jaguin, M., et al., *Polarization profiles of human M-CSF-generated macrophages and comparison of M1-markers in classically activated macrophages from GM-CSF and M-CSF origin.* Cell Immunol, 2013. **281**(1): p. 51-61.

590. Rey-Giraud, F., M. Hafner, and C.H. Ries, *In vitro generation of monocyte-derived macrophages under serum-free conditions improves their tumor promoting functions.* PLoS One, 2012. **7**(8): p. e42656.

591. Gong, D., et al., *TGFbeta signaling plays a critical role in promoting alternative macrophage activation.* BMC Immunol, 2012. **13**: p. 31.

592. Huynh, M.L., V.A. Fadok, and P.M. Henson, *Phosphatidylserine-dependent ingestion of apoptotic cells promotes TGF-beta1 secretion and the resolution of inflammation.* J Clin Invest, 2002. **109**(1): p. 41-50.

593. Reed, S.G., *TGF-beta in infections and infectious diseases.* Microbes Infect, 1999. **1**(15): p. 1313-25.

594. Chen, W. and J.E. Konkel, *TGF-beta and 'adaptive' Foxp3(+) regulatory T cells.* J Mol Cell Biol, 2010. **2**(1): p. 30-6.

595. Eckmann, L., M.F. Kagnoff, and J. Fierer, *Epithelial cells secrete the chemokine interleukin-8 in response to bacterial entry.* Infect Immun, 1993. **61**(11): p. 4569-74.

596. Fujita, Y., et al., *Prognostic significance of interleukin-8 and CD163-positive cell-infiltration in tumor tissues in patients with oral squamous cell carcinoma.* PLoS One, 2014. **9**(12): p. e110378.

597. Schenk, M., et al., *Interleukin-1beta triggers the differentiation of macrophages with enhanced capacity to present mycobacterial antigen to T cells.* Immunology, 2014. **141**(2): p. 174-80.

598. Jayaraman, P., et al., *IL-1beta promotes antimicrobial immunity in macrophages by regulating TNFR signaling and caspase-3 activation.* J Immunol, 2013. **190**(8): p. 4196-204.

599. Lopez-Castejon, G. and D. Brough, *Understanding the mechanism of IL-1beta secretion.* Cytokine Growth Factor Rev, 2011. **22**(4): p. 189-95.

600. Hume, D.A. and K.P. MacDonald, *Therapeutic applications of macrophage colony-stimulating factor-1 (CSF-1) and antagonists of CSF-1 receptor (CSF-1R) signaling.* Blood, 2012. **119**(8): p. 1810-20.

601. Klimchenko, O., et al., *Monocytic cells derived from human embryonic stem cells and fetal liver share common differentiation pathways and homeostatic functions.* Blood, 2011. **117**(11): p. 3065-75.

602. Stout, R.D. and J. Suttles, *Functional plasticity of macrophages: reversible adaptation to changing microenvironments.* J Leukoc Biol, 2004. **76**(3): p. 509-13.

603. Gratchev, A., et al., *Mphi1 and Mphi2 can be re-polarized by Th2 or Th1 cytokines, respectively, and respond to exogenous danger signals.* Immunobiology, 2006. **211**(6-8): p. 473-86.

604. Xu, W., et al., *Reversible differentiation of pro- and anti-inflammatory macrophages.* Mol Immunol, 2013. **53**(3): p. 179-86.

605. Fraser, J.R., T.C. Laurent, and U.B. Laurent, *Hyaluronan: its nature, distribution, functions and turnover.* J Intern Med, 1997. **242**(1): p. 27-33.

606. Kim, S., et al., *Carcinoma-produced factors activate myeloid cells through TLR2 to stimulate metastasis.* Nature, 2009. **457**(7225): p. 102-6.

607. Oliveira-Nascimento, L., P. Massari, and L.M. Wetzler, *The Role of TLR2 in Infection and Immunity.* Front Immunol, 2012. **3**: p. 79.

608. Liang, S., et al., *Ganglioside GD1a is an essential coreceptor for Toll-like receptor 2 signaling in response to the B subunit of type IIb enterotoxin.* J Biol Chem, 2007. **282**(10): p. 7532-42.

609. Rahaman, S.O., et al., *A CD36-dependent signaling cascade is necessary for macrophage foam cell formation.* Cell Metab, 2006. **4**(3): p. 211-21.

610. Takeuchi, O., et al., *Cutting edge: role of Toll-like receptor 1 in mediating immune response to microbial lipoproteins.* J Immunol, 2002. **169**(1): p. 10-4.

611. Takeuchi, O., et al., *Discrimination of bacterial lipoproteins by Toll-like receptor 6.* Int Immunol, 2001. **13**(7): p. 933-40.

612. Ozinsky, A., et al., *The repertoire for pattern recognition of pathogens by the innate immune system is defined by cooperation between toll-like receptors.* Proc Natl Acad Sci U S A, 2000. **97**(25): p. 13766-71.

613. Ferwerda, G., et al., *Dectin-1 synergizes with TLR2 and TLR4 for cytokine production in human primary monocytes and macrophages.* Cell Microbiol, 2008. **10**(10): p. 2058-66.

614. Jin, M.S., et al., *Crystal structure of the TLR1-TLR2 heterodimer induced by binding of a tri-acylated lipopeptide.* Cell, 2007. **130**(6): p. 1071-82.

615. Kang, J.Y., et al., *Recognition of lipopeptide patterns by Toll-like receptor 2-Toll-like receptor 6 heterodimer.* Immunity, 2009. **31**(6): p. 873-84.

616. Farhat, K., et al., *Heterodimerization of TLR2 with TLR1 or TLR6 expands the ligand spectrum but does not lead to differential signaling.* J Leukoc Biol, 2008. **83**(3): p. 692-701.

617. O'Neill, L.A. and A.G. Bowie, *The family of five: TIR-domain-containing adaptors in Toll-like receptor signalling.* Nat Rev Immunol, 2007. **7**(5): p. 353-64.

618. Krutzik, S.R., et al., *TLR activation triggers the rapid differentiation of monocytes into macrophages and dendritic cells.* Nat Med, 2005. **11**(6): p. 653-60.

619. Gambhir, V., et al., *The TLR2 agonists lipoteichoic acid and Pam3CSK4 induce greater pro-inflammatory responses than inactivated Mycobacterium butyricum.* Cell Immunol, 2012. **280**(1): p. 101-7.

620. Tsolmongyn, B., et al., *A Toll-like receptor 2 ligand, Pam3CSK4, augments interferon-gamma-induced nitric oxide production via a physical association between MyD88 and interferon-gamma receptor in vascular endothelial cells.* Immunology, 2013. **140**(3): p. 352-61.

621. Schroder, K., M.J. Sweet, and D.A. Hume, *Signal integration between IFNgamma and TLR signalling pathways in macrophages.* Immunobiology, 2006. **211**(6-8): p. 511-24.

622. Grabiec, A., et al., *Human but not murine toll-like receptor 2 discriminates between tri-palmitoylated and tri-lauroylated peptides.* J Biol Chem, 2004. **279**(46): p. 48004-12.

623. Brown, R.A., et al., *R753Q single-nucleotide polymorphism impairs toll-like receptor 2 recognition of hepatitis C virus core and nonstructural 3 proteins.* Transplantation, 2010. **89**(7): p. 811-5.

624. Stappers, M.H., et al., *TLR1, TLR2, and TLR6 gene polymorphisms are associated with increased susceptibility to complicated skin and skin structure infections.* J Infect Dis, 2014. **210**(2): p. 311-8.

625. Greenwald, R.J., G.J. Freeman, and A.H. Sharpe, *The B7 family revisited.* Annu Rev Immunol, 2005. **23**: p. 515-48.

626. van der Merwe, P.A. and S.J. Davis, *Molecular interactions mediating T cell antigen recognition.* Annu Rev Immunol, 2003. **21**: p. 659-84.

627. Boehm, U., et al., *Cellular responses to interferon-gamma.* Annu Rev Immunol, 1997. **15**: p. 749-95.

628. Topalian, S.L., C.G. Drake, and D.M. Pardoll, *Targeting the PD-1/B7-H1(PD-L1) pathway to activate anti-tumor immunity.* Curr Opin Immunol, 2012. **24**(2): p. 207-12.

629. Okazaki, T. and T. Honjo, *The PD-1-PD-L pathway in immunological tolerance.* Trends Immunol, 2006. **27**(4): p. 195-201.

630. Chen, L., *Co-inhibitory molecules of the B7-CD28 family in the control of T-cell immunity.* Nat Rev Immunol, 2004. **4**(5): p. 336-47.

631. Huber, S., et al., *Alternatively activated macrophages inhibit T-cell proliferation by Stat6-dependent expression of PD-L2.* Blood, 2010. **116**(17): p. 3311-20.

632. Loke, P. and J.P. Allison, *PD-L1 and PD-L2 are differentially regulated by Th1 and Th2 cells.* Proc Natl Acad Sci U S A, 2003. **100**(9): p. 5336-41.

633. Kamada, N., et al., *Role of the gut microbiota in immunity and inflammatory disease.* Nat Rev Immunol, 2013. **13**(5): p. 321-35.

634. Lattin, J., et al., *G-protein-coupled receptor expression, function, and signaling in macrophages.* J Leukoc Biol, 2007. **82**(1): p. 16-32.

635. Schmid, M., et al., *Resolvin D1 Polarizes Primary Human Macrophages toward a Proresolution Phenotype through GPR32.* J Immunol, 2016. **196**(8): p. 3429-37.

636. Bonizzi, G. and M. Karin, *The two NF-kappaB activation pathways and their role in innate and adaptive immunity.* Trends Immunol, 2004. **25**(6): p. 280-8.

637. Vallabhapurapu, S. and M. Karin, *Regulation and function of NF-kappaB transcription factors in the immune system.* Annu Rev Immunol, 2009. **27**: p. 693-733.

638. Fong, C.H., et al., *An antiinflammatory role for IKKbeta through the inhibition of "classical" macrophage activation.* J Exp Med, 2008. **205**(6): p. 1269-76.

639. Hagemann, T., et al., *"Re-educating" tumor-associated macrophages by targeting NF-kappaB.* J Exp Med, 2008. **205**(6): p. 1261-8.

640. Goktuna, S.I., et al., *IKKalpha promotes intestinal tumorigenesis by limiting recruitment of M1-like polarized myeloid cells.* Cell Rep, 2014. **7**(6): p. 1914-25.

641. Lee, J.H., et al., *Inhibition of NF-kappa B activation through targeting I kappa B kinase by celastrol, a quinone methide triterpenoid.* Biochem Pharmacol, 2006. **72**(10): p. 1311-21.

642. Salminen, A., et al., *Celastrol: Molecular targets of Thunder God Vine.* Biochem Biophys Res Commun, 2010. **394**(3): p. 439-42.

643. Geng, Y., et al., *Regulation of cyclooxygenase-2 expression in normal human articular chondrocytes.* J Immunol, 1995. **155**(2): p. 796-801.

644. O'Banion, M.K., V.D. Winn, and D.A. Young, *cDNA cloning and functional activity of a glucocorticoid-regulated inflammatory cyclooxygenase.* Proc Natl Acad Sci U S A, 1992. **89**(11): p. 4888-92.

645. Arias-Negrete, S., K. Keller, and K. Chadee, *Proinflammatory cytokines regulate cyclooxygenase-2 mRNA expression in human macrophages.* Biochem Biophys Res Commun, 1995. **208**(2): p. 582-9.

646. Eruslanov, E., et al., *Altered expression of 15-hydroxyprostaglandin dehydrogenase in tumor-infiltrated CD11b myeloid cells: a mechanism for immune evasion in cancer.* J Immunol, 2009. **182**(12): p. 7548-57.

647. Klimp, A.H., et al., *Expression of cyclooxygenase-2 and inducible nitric oxide synthase in human ovarian tumors and tumor-associated macrophages.* Cancer Res, 2001. **61**(19): p. 7305-9.

648. Wadleigh, D.J., et al., *Transcriptional activation of the cyclooxygenase-2 gene in endotoxin-treated RAW 264.7 macrophages.* J Biol Chem, 2000. **275**(9): p. 6259-66.

649. Snijdewint, F.G., et al., *Prostaglandin E2 differentially modulates cytokine secretion profiles of human T helper lymphocytes.* J Immunol, 1993. **150**(12): p. 5321-9.

650. Simmons, D.L., R.M. Botting, and T. Hla, *Cyclooxygenase isozymes: the biology of prostaglandin synthesis and inhibition.* Pharmacol Rev, 2004. **56**(3): p. 387-437.

651. Vasselon, T., et al., *Toll-like receptor 2 (TLR2) mediates activation of stress-activated MAP kinase p38.* J Leukoc Biol, 2002. **71**(3): p. 503-10.

652. Diehl, S., et al., *Inhibition of Th1 differentiation by IL-6 is mediated by SOCS1.* Immunity, 2000. **13**(6): p. 805-15.

653. Shirey, K.A., et al., *Control of RSV-induced lung injury by alternatively activated macrophages is IL-4R alpha-, TLR4-, and IFN-beta-dependent.* Mucosal Immunol, 2010. **3**(3): p. 291-300.

654. Banerjee, A., et al., *Diverse Toll-like receptors utilize Tpl2 to activate extracellular signal-regulated kinase (ERK) in hemopoietic cells.* Proc Natl Acad Sci U S A, 2006. **103**(9): p. 3274-9.

655. Rakoff-Nahoum, S., et al., *Recognition of commensal microflora by toll-like receptors is required for intestinal homeostasis.* Cell, 2004. **118**(2): p. 229-41.

656. Yamamoto, T., et al., *Macrophage colony-stimulating factor is indispensable for repopulation and differentiation of Kupffer cells but not for splenic red pulp macrophages in osteopetrotic (op/op) mice after macrophage depletion.* Cell Tissue Res, 2008. **332**(2): p. 245-56.

657. Ohtaki, Y., et al., *Stromal macrophage expressing CD204 is associated with tumor aggressiveness in lung adenocarcinoma.* J Thorac Oncol, 2010. **5**(10): p. 1507-15.

658. Kawamura, K., et al., *Detection of M2 macrophages and colony-stimulating factor 1 expression in serous and mucinous ovarian epithelial tumors.* Pathol Int, 2009. **59**(5): p. 300-5.

659. Kaku, Y., et al., *Overexpression of CD163, CD204 and CD206 on alveolar macrophages in the lungs of patients with severe chronic obstructive pulmonary disease.* PLoS One, 2014. **9**(1): p. e87400.

660. Jozefowski, S., et al., *Disparate regulation and function of the class A scavenger receptors SR-AI/II and MARCO.* J Immunol, 2005. **175**(12): p. 8032-41.

661. Pustylnikov, S., et al., *Targeting the C-type lectins-mediated host-pathogen interactions with dextran.* J Pharm Pharm Sci, 2014. **17**(3): p. 371-92.

662. Lai, W.K., et al., *Expression of DC-SIGN and DC-SIGNR on human sinusoidal endothelium: a role for capturing hepatitis C virus particles.* Am J Pathol, 2006. **169**(1): p. 200-8.

663. Takagi, T., et al., *Dextran sulfate suppresses cell adhesion and cell cycle progression of melanoma cells.* Anticancer Res, 2005. **25**(2A): p. 895-902.

664. Sakamoto, H., et al., *Biomechanical strain induces class a scavenger receptor expression in human monocyte/macrophages and THP-1 cells: a potential mechanism of increased atherosclerosis in hypertension.* Circulation, 2001. **104**(1): p. 109-14.

665. Kuchroo, V.K., et al., *New roles for TIM family members in immune regulation.* Nat Rev Immunol, 2008. **8**(8): p. 577-80.

666. Freeman, G.J., et al., *TIM genes: a family of cell surface phosphatidylserine receptors that regulate innate and adaptive immunity.* Immunol Rev, 2010. **235**(1): p. 172-89.

667. Maeda, H., *The enhanced permeability and retention (EPR) effect in tumor vasculature: the key role of tumor-selective macromolecular drug targeting.* Adv Enzyme Regul, 2001. **41**: p. 189-207.

668. Maeda, H. and Y. Matsumura, *EPR effect based drug design and clinical outlook for enhanced cancer chemotherapy.* Adv Drug Deliv Rev, 2011. **63**(3): p. 129-30.

669. Rhee, S.H., et al., *Toll-like receptors 2 and 4 activate STAT1 serine phosphorylation by distinct mechanisms in macrophages.* J Biol Chem, 2003. **278**(25): p. 22506-12.

670. Park, D.W., et al., *Role of JAK2-STAT3 in TLR2-mediated tissue factor expression.* J Cell Biochem, 2013. **114**(6): p. 1315-21.

671. Gobert Gosse, S., et al., *M-CSF stimulated differentiation requires persistent MEK activity and MAPK phosphorylation independent of Grb2-Sos association and phosphatidylinositol 3-kinase activity.* Cell Signal, 2005. **17**(11): p. 1352-62.

672. Liu, G., et al., *Phenotypic and functional switch of macrophages induced by regulatory CD4+CD25+ T cells in mice.* Immunol Cell Biol, 2011. **89**(1): p. 130-42.

673. Tiemessen, M.M., et al., *CD4+CD25+Foxp3+ regulatory T cells induce alternative activation of human monocytes/macrophages.* Proc Natl Acad Sci U S A, 2007. **104**(49): p. 19446-51.

674. Flo, T.H., et al., *Differential expression of Toll-like receptor 2 in human cells.* J Leukoc Biol, 2001. **69**(3): p. 474-81.

675. Muzio, M., et al., *Differential expression and regulation of toll-like receptors (TLR) in human leukocytes: selective expression of TLR3 in dendritic cells.* J Immunol, 2000. **164**(11): p. 5998-6004.

676. Zarember, K.A. and P.J. Godowski, *Tissue expression of human Toll-like receptors and differential regulation of Toll-like receptor mRNAs in leukocytes in response to microbes, their products, and cytokines.* J Immunol, 2002. **168**(2): p. 554-61.

677. Komai-Koma, M., et al., *TLR2 is expressed on activated T cells as a costimulatory receptor.* Proc Natl Acad Sci U S A, 2004. **101**(9): p. 3029-34.

678. Nyirenda, M.H., et al., *TLR2 stimulation drives human naive and effector regulatory T cells into a Th17-like phenotype with reduced suppressive function.* J Immunol, 2011. **187**(5): p. 2278-90.

679. Ganley-Leal, L.M., X. Liu, and L.M. Wetzler, *Toll-like receptor 2-mediated human B cell differentiation.* Clin Immunol, 2006. **120**(3): p. 272-84.

680. Orme, J. and C. Mohan, *Macrophage subpopulations in systemic lupus erythematosus.* Discov Med, 2012. **13**(69): p. 151-8.

681. Neyen, C., et al., *Macrophage scavenger receptor A mediates adhesion to apolipoproteins A-I and E.* Biochemistry, 2009. **48**(50): p. 11858-71.

682. Marleau, S., et al., *EP 80317, a ligand of the CD36 scavenger receptor, protects apolipoprotein E-deficient mice from developing atherosclerotic lesions.* FASEB J, 2005. **19**(13): p. 1869-71.

683. Sulkowski, M.S., et al., *Safety and antiviral activity of the HCV entry inhibitor ITX5061 in treatment-naive HCV-infected adults: a randomized, double-blind, phase 1b study.* J Infect Dis, 2014. **209**(5): p. 658-67.

684. Christianson, H.C., et al., *Cancer cell exosomes depend on cell-surface heparan sulfate proteoglycans for their internalization and functional activity.* Proc Natl Acad Sci U S A, 2013. **110**(43): p. 17380-5.

685. Atai, N.A., et al., *Heparin blocks transfer of extracellular vesicles between donor and recipient cells.* J Neurooncol, 2013. **115**(3): p. 343-51.

# Appendices

## Appendix A - Gene Lists

**Appendix Table 1: Symbol of genes upregulated more 2-fold in R848, IL-6 plus TNFα or IFNγ stimulated HLA-DR$^+$ monocytes (alphabetically ordered).**

| **R848** | | | **IL-6 + TNFα** | | **IFNγ** | | |
|---|---|---|---|---|---|---|---|
| ADORA2A | GADD45B | LOC101930081 | ACSL1 | KCNG4 | ABCC9 | GBP2 | NLRC5 |
| BCL2A1 | GCH1 | MAFF | ADORA2A | NOTCH2 | ACSL1 | GBP4 | OASL |
| BIRC3 | GJB2 | MIR155HG | ARFRP1 | OOSP1 | ANKRD22 | GBP5 | PARP12 |
| C11orf96 | GRAMD1A | MMP1 | BCL3 | OR2T8 | APOL4 | GCH1 | PARP14 |
| CCL2 | HAPLN3 | MMP10 | BTLA | PLAUR | BATF | GCNT1 | PSMB9 |
| CCL20 | IDO1 | MMP19 | CCL2 | POU2F2 | BCL3 | GIMAP6 | RARRES3 |
| CD83 | IER3 | NFKBIA | CD40 | PTGER4 | C4orf32 | GLIPR2 | RGL1 |

| **R848** | | | **IL-6 + TNFα** | | **IFNγ** | | |
|---|---|---|---|---|---|---|---|
| CMPK2 | IL10 | PTGS2 | CD84 | Q8N649_HUMAN | C9orf72 | GPBAR1 | SCO2 |
| CSF2 | IL12B | SERPINB2 | CXCL1 | RALGAPA2 | CMPK2 | HERC5 | SERPING1 |
| CXCL1 | IL19 | SLC22A1 | CXCL8 | RGL1 | CXCL10 | HSD11B1 | SNX10 |
| CXCL2 | IL1A | SPINK1 | DCTN1 | RNF144B | CXCL9 | IL15 | SP110 |
| CXCL3 | IL36G | TNF | DPYSL2 | SCD5 | ETV7 | IRF7 | STAT1 |
| CXCL8 | IL6 | TNFAIP3 | EBI3 | SEMA6B | FAM26F | JAK2 | STAT2 |
| DNAAF1 | IL7R | TNFAIP6 | FBXW10 | TMPRSS7 | FCGR1A | KMO | TAGAP |
| DUSP2 | INHBA | TNFRSF4 | GRAMD1A | TNFAIP3 | FYB | LOC102724907 | |
| DUSP5 | IRG1 | TNFSF15 | HSD11B1 | TNFRSF4 | GADD45B | LRRK2 | |
| EBI3 | ISG20 | TNIP3 | IL7R | | GBP1 | MAGEB3 | |
| G0S2 | KCNJ2 | TRIM6 | ITSN2 | | GBP1P1 | MMP25 | |

**Appendix Table 2: Symbol of genes upregulated more than 2-fold in PAM3 and M-CSF stimulated HLA-DR$^+$ monocytes (alphabetically ordered).**

| PAM3 | | | | | M-CSF | | | | |
|---|---|---|---|---|---|---|---|---|---|
| ABCB4 | EFCAB1 | KANK1 | PDE4B | STAP1 | A1CF | DHRS4-AS1 | IL1RN | NT5C3 | SOCS1 |
| ADM | EHD1 | KBTBD8 | PDE4DIP | STAT4 | ABHD11 | DNHD1 | IL6 | NTS | SPAST |
| ADORA2A | EHF | KCNJ2 | PDSS1 | STX19 | ABLIM1 | DRAM1 | IL7R | NUMA1 | SRSF9 |
| ADPRHL1 | EIF1B | KCNQ3 | PEAR1 | SVIL | ACAT2 | DSP | INHBA | OPCML | ST20 |
| AK4 | EIF2S2 | KIAA0226L | PHKA2 | SYNJ1 | ACBD7 | DUSP1 | ITGB3BP | OPTN | SUPT4H1 |
| ALCAM | ELOVL6 | KIAA1211L | PHLDA2 | TBC1D9 | ACSL1 | EBI3 | ITIH2 | OR10C1 | SYTL4 |
| ALKBH8 | ELOVL7 | KIR2DS1 | PHLPP2 | TCHHL1 | ACSM3 | ECEL1 | ITPR3 | OR1J1 | TAAR9 |
| ALS2CL | ENTHD1 | KLF12 | PI4K2B | TMCO5A | ADAMTS13 | ECHDC2 | JPX | OR2T6 | TCL6 |
| ANKRD26P3 | EPB41L3 | KRT16P2 | PIK3AP1 | TMEM252 | ADAMTS9 | EHD1 | KANK1 | OR52N4 | TECPR2 |
| APCDD1L-AS1 | ETS2 | KRT79 | PIM1 | TMPRSS3 | ADORA2A | EMR3 | KCNJ2 | ORC4 | TGFB2 |
| ARL5B | F3 | KRT82 | PLAC8 | TNF | AFP | ENAH | KCNQ1OT1 | PAPOLG | THPO |

| PAM3 | | | | | M-CSF | | | | |
|---|---|---|---|---|---|---|---|---|---|
| ASPA | FAM120A | LAMA4 | PLAGL2 | TNFAIP2 | AGR2 | EXO1 | KDELC2 | PAR5 | TLL1 |
| ATP2B1 | FAM129A | LAMB3 | PLEKHF2 | TNFAIP3 | AK4 | EZH2 | KDR | PARP14 | TLR10 |
| B4GALT5 | FAM188A | LIMS3 | PNPLA8 | TNFSF9 | AMY1A | FAM43A | KERA | PBK | TLR2 |
| BAALC | FAM198A | LOC100128505 | PNRC1 | TNIK | ANKRD26P3 | FAM93B | KIF20A | PCLO | TMEM106C |
| BATF | FAM205B | LOC100129940 | POTEA | TNIP3 | ANKRD36 | FBLN1 | KLC3 | PCM1 | TMEM182 |
| BATF3 | FAM208B | LOC100506725 | POU6F2 | TRIM36 | ANO7 | FCRLB | KRT79 | PDSS1 | TMSB15A |
| BCL2A1 | FAM49A | LOC100507172 | PPP4R2 | TRIM77 | APOA2 | FGF14 | KRT85 | PHKA2 | TNFAIP3 |
| BIRC3 | FBXO15 | LOC100509195 | PRRC2B | TRIP10 | APOH | FGF7 | L2HGDH | PHLDA2 | TNFAIP6 |
| BPIFA2 | FLJ37505 | LOC440864 | PRUNE2 | TSPAN33 | ASTN2 | FGG | LAMP3 | PLAC8 | TNFRSF19 |
| BTBD9 | FLJ43879 | LOC440896 | PRY | TTC40 | ATP6V0D2 | FGL1 | LAPTM4B | PLAUR | TNFRSF9 |
| BTG3 | FMO1 | LOC646329 | PSMA6 | TTC40 | ATPAF1 | FLJ11292 | LEF1 | PLS3 | TNIP3 |

| PAM3 | | | | | M-CSF | | | | |
|---|---|---|---|---|---|---|---|---|---|
| C11orf96 | FNBP1 | LPPR4 | PSTPIP2 | TTN | ATPBD4 | FLJ34503 | LIN7C | PMEL | TP73-AS1 |
| C22orf23 | FREM3 | LRRC8C | PTGER3 | UPB1 | B4GALNT3 | FLJ37786 | LINC00115 | PODXL | TPM1 |
| C7orf60 | FSD1L | LRRN4 | PTGS2 | UPP1 | BATF | FLJ38109 | LINC00355 | PPFIBP2 | TPPP3 |
| C8orf12 | GABPB1 | LSS | PTPN2 | USF2 | BBS9 | FLJ42200 | LINC00485 | PPP1R3F | TPTEP1 |
| CAPN13 | GABRD | LUZP1 | PTPRQ | USP12 | BCL2A1 | FLJ46284 | LINC00575 | PRICKLE2-AS1 | TPX2 |
| CASP4 | GADD45B | MAP1A | PTX3 | UXS1 | BDH2 | FREM2 | LOC100129434 | PRSS1 | TRAF1 |
| CATSPERG | GBP1 | MAP3K4 | RAB33A | WNT5B | BIRC3 | FSD1L | LOC100130581 | PRSS2 | TRAF3IP2 |
| CCDC15 | GBP1P1 | MAP3K8 | RALGAPA1 | WTAP | BMPR1A | FST | LOC100505664 | PRSS23 | TRIM11 |
| CCL1 | GBP2 | MAPK6 | RASGRP1 | YRDC | BNIP3L | FSTL4 | LOC100506725 | PRSS3 | TRIM15 |
| CCL20 | GBP5 | MARCKS | RBM44 | ZAK | BPIFB1 | FUT3 | LOC100507654 | PSKH2 | TRIM25 |
| CCL23 | GCH1 | MCTP1 | RDX | ZBTB10 | C14orf119 | G0S2 | LOC157562 | PSTPIP2 | TTK |

| PAM3 | | | | | M-CSF | | | | |
|---|---|---|---|---|---|---|---|---|---|
| CCL5 | GGT6 | MECOM | REPS2 | ZBTB40 | C1orf177 | GAB1 | LOC254559 | PTGS2 | TTR |
| CD274 | GIT2 | MEP1A | RGS1 | ZC3H12C | C3P1 | GABPB1 | LOC280665 | PTPN14 | TTTY9A |
| CD40 | GJB2 | MFSD2A | RGS16 | ZFR2 | C4orf26 | GATA3 | LOC340515 | PTTG1 | TUSC3 |
| CD44 | GLS | MGLL | RHBDF2 | ZNF154 | C7orf60 | GBP1 | LOC440313 | PTTG3P | UACA |
| CDKL4 | GNG2 | MIR155HG | RHOH | ZNF28 | CAV1 | GBP2 | LOC440716 | PTX3 | UBE2C |
| CEACAM6 | GOLGA1 | MLL5 | RIF1 | ZNF544 | CCDC67 | GBX1 | LOC440716 | PURG | UGDH-AS1 |
| CEP135 | GOLGA6C | MMP7 | RIPK2 | ZNF583 | CCL2 | GCH1 | LOC91948 | PUS10 | UGT2B15 |
| CFB | GPR132 | MSC | RND1 | ZNF679 | CCL20 | GDAP1L1 | LRCH1 | RCN1 | USP12 |
| CFLAR | GRAMD1A | MSS51 | RNF148 | ZNF77 | CCNA2 | GDF15 | LRFN2 | RGPD1 | UXS1 |
| CHRDL1 | GUSBP1 | MST4 | RNF39 | ZNF774 | CCNB2 | GFRA1 | LUM | RGS16 | VHLL |
| CHRM1 | HAS1 | MTF1 | RRAGB | | CD24P4 | GIGYF2 | MALAT1 | RHCE | VLDLR |

| PAM3 | | | | M-CSF | | | | |
|---|---|---|---|---|---|---|---|---|
| CKB | HCAR3 | MYADML2 | RTN4RL1 | CD38 | GINS1 | MAMDC4 | RHOBTB3 | VPS13A |
| CLCNKB | HCFC1 | MYO1A | SAV1 | CD3D | GJB2 | MAPKAPK2 | RIN2 | VPS13B |
| CLIC4 | HIVEP2 | NACC2 | SCML1 | CD40 | GPC3 | MARCKS | RIPK2 | WNT5B |
| CNDP1 | HK1 | NAMPT | SCN1B | CD59 | GRAMD1A | MCAM | RND1 | WNT7A |
| CNPPD1 | HMCN1 | NCMAP | SEMA3C | CD69 | GREM1 | MCC | RNF144A | XIAP |
| CNTFR | HMGCS1 | NDP | SERPINA9 | CDC14C | GTSF1 | MCM4 | RNF170 | XPO6 |
| CPD | HS3ST3B1 | NELL1 | SERPINB13 | CDC42EP4 | GUCY1B2 | MDM4 | ROBO2 | YRDC |
| CRIM1 | HSFY1 | NFASC | SERPINB2 | CDCA3 | HAPLN3 | MGP | RSL1D1 | ZDHHC20 |
| CSF2 | IL12B | NFE2 | SGMS2 | CDK1 | HAS1 | MIPOL1 | S100PBP | ZFP42 |
| CXCL1 | IL15 | NFKBIZ | SGPP2 | CDO1 | HBE1 | MIR155HG | SARDH | ZFP64 |
| CXCL2 | IL18 | NPM2 | SH3BGRL2 | CELA3A | HCAR3 | MLLT4 | SARM1 | ZMAT1 |

| PAM3 | | | | M-CSF | | | | |
|---|---|---|---|---|---|---|---|---|
| CXCL3 | IL18R1 | NPSR1-AS1 | SLAMF1 | CENPF | HELLS | MORN1 | SEPP1 | ZNF205-AS1 |
| CYP7B1 | IL19 | NR4A3 | SLC22A1 | CENPK | HES1 | NAMPT | SERPINB2 | ZNF23 |
| DCAF16 | IL1A | NUP62CL | SLC36A4 | CFLAR | HIST1H1E | NCAPG | SERPINB9 | ZNF250 |
| DENND4A | IL23A | NUP98 | SLC39A8 | CHCHD7 | HJURP | NCKAP1 | SFRP1 | ZNF337 |
| DEXI | IL2RA | NXNL2 | SLC8A1 | CKS2 | HLA-DQA1 | NEFL | SLAMF7 | ZNF43 |
| DNAAF1 | IL2RB | OR14C36 | SMARCA2 | CLEC9A | HMGCS1 | NFIB | SLC16A11 | ZNF532 |
| DNAH6 | IL5RA | OR2F1 | SMPDL3A | CSRP2 | HUWE1 | NFKBIA | SLC19A3 | ZNF586 |
| DNAJC3 | IL6 | OR2M5 | SNAI1 | CTGF | ICAM1 | NFKBID | SLC24A4 | ZNF614 |
| DOCK6 | IL7R | OR4K1 | SNX10 | CTSL1 | IDO1 | NLRC4 | SLC2A10 | ZNF705D |
| DPY19L1P1 | INHBA | OSM | SOCS1 | CXCL1 | IFNAR2 | NLRP11 | SLC36A2 | ZNF774 |
| DRAM1 | IPCEF1 | OTOA | SOCS5 | CXCL3 | IGDCC4 | NOTCH3 | SLC39A8 | ZSCAN1 |

| PAM3 | | | | M-CSF | | | | |
|---|---|---|---|---|---|---|---|---|
| DUSP1 | IRAK2 | PANX1 | SPEG | CYSLTR2 | IGFBP7 | NPIPL3 | SLC7A2 | ZZEF1 |
| DUSP5 | IRF1 | PAX2 | SPHK1 | DACT2 | IGLC1 | NR3C1 | SLITRK3 | |
| DVL3 | IRG1 | PBX4 | SPTBN2 | DACT3 | IL19 | NR4A3 | SMOC2 | |
| EBI3 | ITGAD | PCNXL2 | ST20 | DFFB | IL1A | NRN1 | SNX29P2 | |

## Appendix B - Figures

**Figure B1: Confirmation of IL-10 and TNFα neutralization with ELISA**

*Data shown are the mean cytokine concentration (± SD) of four donors. * p<0.05.*

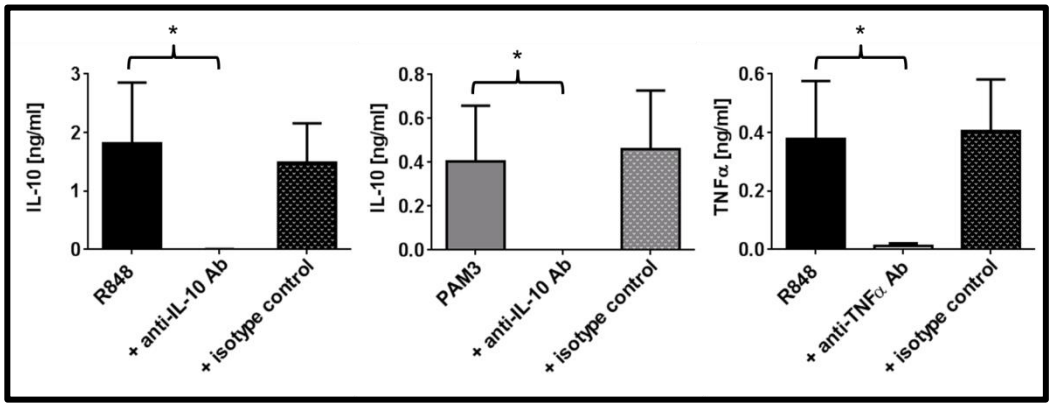


**Figure B2: Expression pattern of additional surface markers in PAM3 vs M-CSF stimulated HLA-DR$^+$ monocytes.**

*Mean fluorescence intensity of CD36, CD80, CD86 and CD274 following stimulation of HLA-DR$^+$ monocytes with PAM3 or M-CSF for 5 days (mean ± SD of four donors). * p<0.05 unstimulated monocytes vs. PAM3/M-CSF stimulated macrophages.*

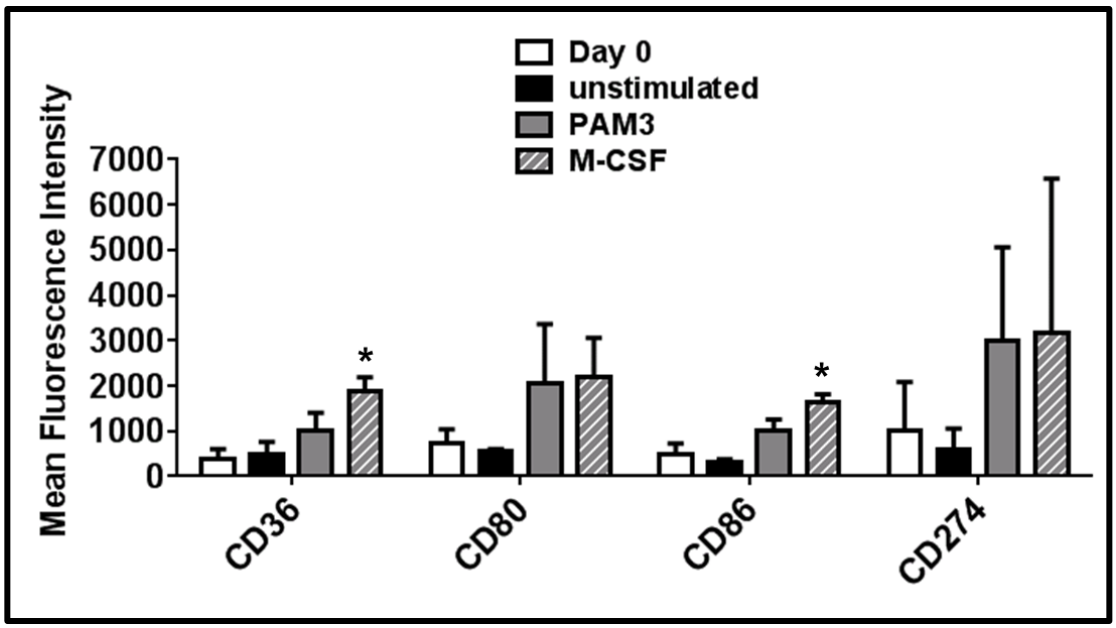

**Figure B3: Secreted IL-6 levels are higher in PAM3 treated cultures as compared to M-CSF treated cultures.**

*Data shown are the mean cytokine concentration (± SD) of six donors. * p<0.05; ** p<0.01 PAM3 or M-CSF cultures vs. untreated cultures.*

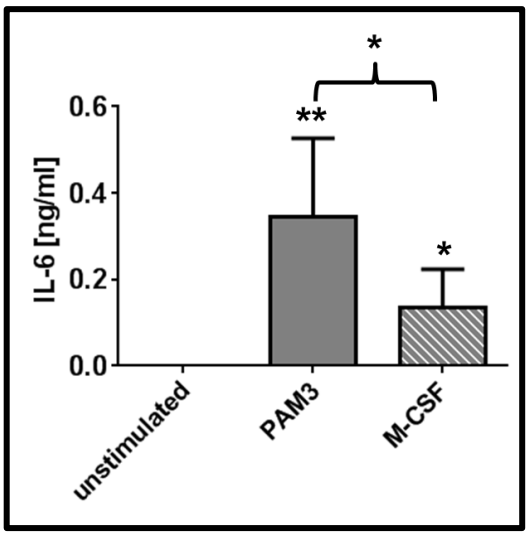


**Figure B4: DS and CS-treatment has no influence on the viability of cells.**

*A) Representative histograms demonstrating live/dead percentage of RAW264.7 cells. B) Percentage of viable cells following exposure to DS and CS.*

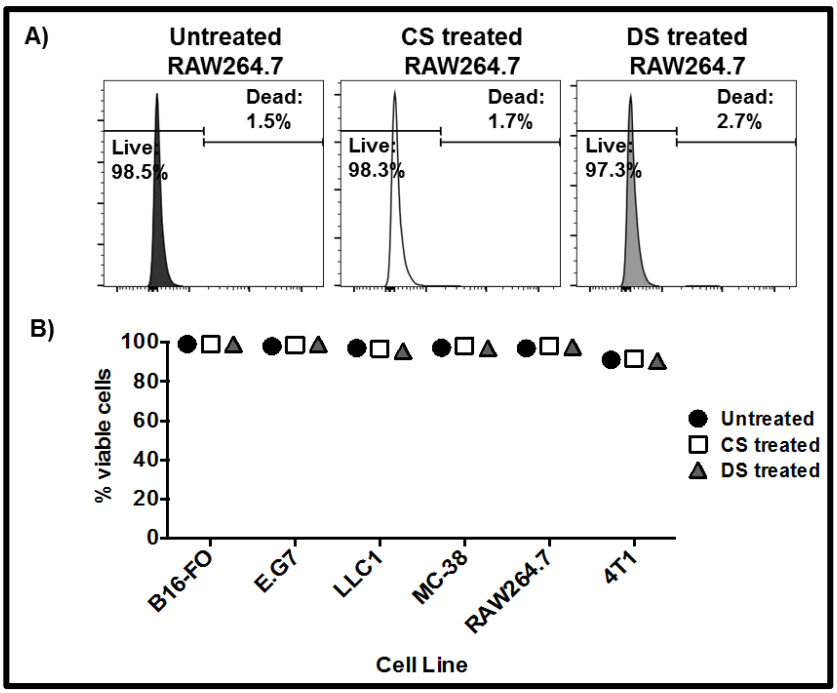

**Figure B5: FCS concentration determines the level of spontaneous macrophage differentiation from human monocytes.**

*A) Representative dot plots showing change in the CD206 and 25F9 levels of unstimulated HLA-DR$^+$ monocytes cultured in various FCS concentrations for 3 days. B) Percentage of spontaneously differentiated following culturing of HLA-DR$^+$ with media containing indicated FCS amounts (mean ± SD of two independently analyzed donors).*

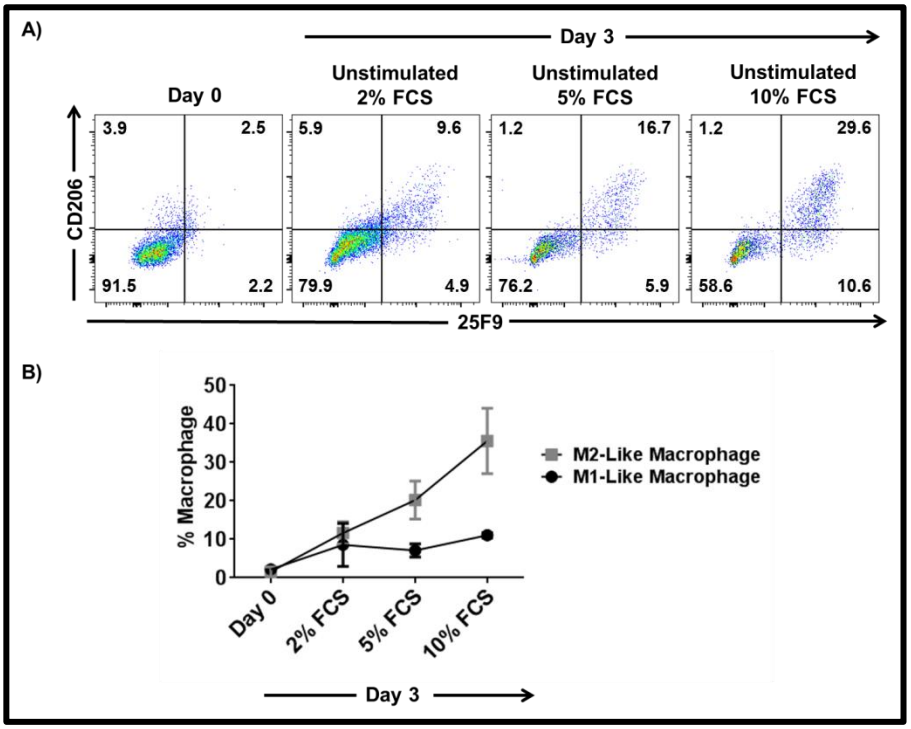

# Curriculum Vitae and Publications

Personal Information:


| | |
|---|---|
| Name: | Defne Bayık |
| Date of Birth: | 05.November.1989 |
| Citizenship: | Turkey |
| Languages: | Turkish (native) |
| | English (fluent) |
| Address: | 1050 Boyles Street, Bldg 567, Rm203 |
| | Frederick, MD, 21702, U.S.A. **OR** |
| | Bilkent University, Faculty of Science, SB Building |
| | Department of Molecular Biology and Genetics |
| | Cankaya, Ankara, Turkey 06800 |
| Contact Information: | defne.bayik@nih.gov **OR** |
| | dbayik@bilkent.edu.tr |


Education:

| | |
|---|---|
| 2010-present | Ph.D., (Molecular Biology and Genetics), Bilkent University, Ankara, Turkey |
| 2010 | B.S., (Molecular Biology and Genetics), Bilkent University, Ankara, Turkey |

Brief Chronology of Employment:

| | |
|---|---|
| 2014-present | Pre-doctoral Trainee, Cancer and Inflammation Program, Center for Cancer Research, National Cancer Institute, Frederick, MD |

| | |
|---|---|
| 2010-present | Graduate Research Assistant, Department of Molecular Biology and Genetics, Bilkent University, Ankara Turkey |
| 2010-2014 | Graduate Teaching Assistant, Department of Molecular Biology and Genetics, Bilkent University, Ankara Turkey |
| 2009 | Undergraduate Summer Research Fellow, Department of Obstetrics & Gynecology, New York Medical College, Valhalla, NY |
| 2008 | Undergraduate Summer Research Fellow, Department of Obstetrics & Gynecology Reproductive Sciences, Yale University School of Medicine, New Haven, CT |
| 2007 | Undergraduate Summer Research Fellow, Faculty of Medicine, Department of Physiology, Akdeniz University, Antalya, Turkey |

Professional Societies:

- Turkish American Scientist and Scholars Association, Washington DC, USA, 2015-present
- American Association of Immunologists Rockville, MD, USA, 2015-present
- Turkish Society of Immunology, Istanbul, Turkey, 2014-present

Honors, Awards:

- Travel Award for Outstanding Poster Presentation, Center for Cancer Research Office of the Director, National Institutes of Health, 2016
- NIH Graduate Student Research Award (NGSRA) for Poster Presentation, Office of Intramural Training and Education, National Institutes of Health, 2016
- The Scientific and Technological Research Council of Turkey Scholarship for Graduate Students, 2010-2015.
- Travel Award for Poster Presentation, Turkish Society of Immunology, 2014
- Travel and Accommodation Award for Poster Presentation, Oxford University, 2011
- Bilkent University, Department of Molecular Biology and Genetics, the Second Highest Ranking Graduate, 2010
- Bilkent University Full Scholarship, 2007-2010
- Bilkent University High Honors Student, 2006-2010

Other Activities:

- Reviewer for Peer J, 2015-present.
- Journal Club Leader of Extracellular Vesicles in Health and Disease, Office of Intramural Training and Education, National Institutes of Health, 2015
- Session Chair/Judging Committee of 19th Annual Spring Research Festival, National Interagency Confederation of Biological Research (NICBR), 2015

Workshops:

- Scientist Teaching Science, OITE, NIH, September 2015
- Scientific Writing and Publishing, OITE, NIH, June 2015
- Mentoring a Summer Intern and Leading a Journal Club, OITE, NIH, May 2015
- Grant Writing, OITE, NIH, February 2015

Teaching and Mentorship Experience:

- Instructor at Science Skills Boot Camp Faculty, Office of Intramural Training and Education, National Institutes of Health Spring 2016
- Undergraduate Microbiology Course Teaching Assistant, Department of Molecular biology and Genetics, Bilkent University, Spring 2013
- Undergraduate Molecular Biology of the Cell II Course Teaching Assistant, Department of Molecular biology and Genetics, Bilkent University, Spring 2011, Spring 2012
- Undergraduate Introduction to Bioinformatics Course Teaching Assistant, Department of Molecular biology and Genetics, Bilkent University, Fall 2010, Fall 2011
- Ece Yildiz, Junior Research Fellow, "Identification of potential mechanisms of extracellular vesicle internalization by macrophages" THORLAB., Bilkent University, Fall 2014.
- Ezgi Alkan, Summer Research Fellow, "Identification of differences in extracellular vesicle uptake potential of various cell types." THORLAB., Bilkent University, Summer 2014.
- Hakan Koksal, Junior Research Fellow, "Cloning and characterization of *Homo Sapiens* TLR9 gene isoforms." THORLAB., Bilkent University, 2013-2014.

Selected Abstracts and Presentations:

- **Bayik D.**, Tross D., Gursel I. and Klinman D.M. Modulating the differentiation of human monocytes into immunosuppressive macrophages via TLR2/1 signaling. 3rd International Molecular Immunology & Immunogenetics Congress (MIMIC III). Antalya, Turkey. 27-30 Apr. 2016 (Oral presentation).
- **Bayik D.**, Tross D. and Klinman D.M. TLR2/1 Signaling Generates Immunosuppressive Macrophage from Human Monocytes. 16th Annual CCR Fellows and Young Investigators Colloquium. Rockville, MD, U.S.A. 31 Mar.-1 Apr. 2016 (Poster presentation).
- **Bayik D.**, Tross D. and Klinman D.M TLR2/1 signaling drives the differentiation of human monocytes into M2-like macrophages. 12th Annual NIH Graduate Student Research Symposium. Bethesda, MD, U.S.A. 12 Jan. 2016 (Poster presentation).
- **Bayik D.** and Klinman D.M. Cytokine combinations selectively drive the differentiation of human monocytic myeloid derived suppressor cells into M1- or M2-like macrophages. IIG 2015 Workshop. Bethesda, MD, U.S.A. 9-10 Sep. 2015 (Oral presentation).
- Gucluler G., Kahraman T., **Bayik D.**, Gursel M. and Gursel I. Improved immunostimulatory activity of D-type CpG oligonucleotides encapsulated into exosomes in cancer treatment. 4th European Congress of Immunology. Vienna, Austria 06-09 Sep 2015.
- Kayali E.S., **Bayik D.**, Kahraman T., Gucluler G. and Gursel I. Targeting and sub-cellular localization of extracellular vesicles by phagocytic cells. 4th European Congress of Immunology. Vienna, Austria 06-09 Sep 2015.
- **Bayik D.**, Wang J., Gursel I. and Klinman D.M. Defined combinations of cytokines plus survival factors drive the differentiation of human monocytic myeloid derived suppressor cells into M1- or M2-like macrophages. Immunology 2015. New Orleans, LA, U.S.A. 8-12 May 2015 (Poster presentation).
- **Bayik D.** and Klinman D.M. Cytokine combinations selectively drive the differentiation of human monocytic myeloid derived suppressor cells into M1- or M2-like macrophages. 19th Annual Spring Research Festival. Frederick, MD, U.S.A. 4-7 May 2015 (Oral & poster presentation).
- **Bayik D.**, Kahraman T., Gucluler G., Klinman D.M. and Gursel I. Targeting and sub-cellular localization of cell-derived microparticles to macrophages. ISEV 2015 Annual Meeting. Bethesda, MD, U.S.A. 23-26 Apr. 2015 (Poster presentation).
- **Bayik D.** and Klinman D.M. Defined combinations of cytokines plus survival factors drive the differentiation of human monocytic myeloid derived suppressor cells into M1-

and M2-like macrophages. 15th Annual CCR Fellows and Young Investigators Colloquium. Rockville, MD, U.S.A. 23-24 Mar. 2015 (Poster presentation).

- **Bayik D.** and Klinman D.M. Regulating the Differentiation of Monocytic Myeloid Derived Suppressor Cells. Fellows and Young Investigators Seminar Series. 18. Feb. 2015 (Oral presentation).
- **Bayik D.**, Yildiz E. Kahraman T. and Gursel I. Scavenger-Receptor Mediated and Clathrin-Dependent Endocytosis Regulate Internalization of Extracellular Vesicles by Immune Cells. 2nd International Molecular Immunology & Immunogenetics Congress (MIMIC II). Antalya, Turkey. 27-30 Apr. 2014 (Poster presentation).
- Güçlüler G., Kahraman T., **Bayık D.**, Horuluoğlu B.H., Gürsel A. and Gürsel İ. CpG ODN Loaded Extracellular Nanovesicles: Enhanced Immunotherapeutic Activity. ILS Liposome Advanced Conference, London, United Kingdom. 13-17 Dec. 2013.
- Alpdündar E., Yıldız S., Bayyurt B., Özcan M., Güçlüler G., **Bayık D.,** Güngör B., Gürsel İ. and Gürsel M. Commensal bacteria-derived membrane vesicles suppress Th-1 dominated immune responses in vaccinated and tumor-bearing mice. 15th International Congress of Immunology. Milan, Italy. 22-27 Aug. 2013.
- Güçlüler G., Kahraman T., **Bayık D.,** Gürsel A., Gürsel M. and Gürsel İ. D Type CpG oligonucleotide loaded E.G7 exosomes act as strong vaccine adjuvant and anti-cancer agent. 15th International Congress of Immunology. Milan, Italy. 22-27 Aug. 2013.
- Bayyurt B., Güçlüler G., **Bayık D.,** Alpdündar E., Yıldız S., Horuluoğlu B.H., Özcan M., Gürsel M. and Gürsel İ. Extended anti-cancer immunity by liposomes coencapsulating nucleic acid TLR-ligands and antigen. 15th International Congress of Immunology. Milan, Italy. 22-27 Aug. 2013.
- Kahraman T., Güçlüler G., **Bayık D.,** Gürsel A., Gürsel M. and Gürsel İ. EXOLIGOS: a CpG oligonucleotide loaded exosome nanovesicles delivery platform suitable for effective immune modulation. 15th International Congress of Immunology. Milan, Italy. 22-27 Aug. 2013.
- Yıldız S., Alpdündar E., Bayyurt B., Özcan M., Güçlüler G., **Bayık D.,** Güngör B., Gürsel İ. and Gürsel M. Cyclic-di-GMP based immune stimulatory formulations as novel vaccine adjuvants and anti-cancer agents. 15th International Congress of Immunology. Milan, Italy. 22-27 Aug. 2013.
- Telkoparan P., Erkek S., Alotaibi H., Yaman E., **Bayık D.,** Tazebay U.H. Coiled-coil domain containing protein 124 is a novel centrosome and midbody protein that interacts with the Ras-guanine nucleotide exchange factor 1B and is involved in cytokinesis. 1st International Congress of the Molecular Biology Association of Turkey. İstanbul,Turkey, 23-24 Nov. 2012.

- **Bayık, D.,** Telkoparan, P., Erdoğan, M. and Tazebay U.H. A novel PIKK target coiled-coil-domain containing protein (Ccdc) is associated with double strand-breaks. EMBO Chromosome Structure, Damage & Repair Workshop. Cape Sounio, Greece. 25-28 Sept. 2011 (Poster presentation).

**BIBLIOGRAPHY**


- Watson D.C., **Bayik D.,** Srivatsan A., Bergamaschi C., Niu G., Bear J., Monninger M., Sun M., Kastraesana-Morales A., Jones J.C., Felber B.K., Chen X., Gursel I., Pavlakis G.N. Efficient production and enhanced tumor delivery of engineered extracellular vesicles. (Biomaterials, under revision, April 2016).
- **Bayik D.**, Gursel I., and Klinman D.M. Structure, Mechanism and Therapeutic Utility of Immunosuppressive Oligonucleotides. Pharmaco Res. 105:216-25. 2016.
- Wang J., Shirota Y., **Bayik D.**, Shirota H., Tross D., Gulley J.L., Wood L., Berzofsky J.A., and Klinman D.M. Effect of TLR Agonists on the Differentiation and Function of Human Monocytic Myeloid Derived Suppressor Cells. J Immunol. 194(9):4215-21. 2015.
- Telkoparan P., Erkek S., Yaman E., Alotaibi H., **Bayık D.,** and Tazebay U.H. Coiled-coil domain containing protein 124 is a novel centrosome and midbody protein that is involved in cytokinetic abscission, and it connects cell division to Rap2 signaling. PloS One. 9;8(7):e69289. 2013. (doi: 10.1371/journal.pone.0069289).

Pharmacological Research 105 (2016) 216–225

Contents lists available at ScienceDirect

Pharmacological Research

journal homepage: www.elsevier.com/locate/yphrs

Invited review

# Structure, mechanism and therapeutic utility of immunosuppressive oligonucleotides

Defne Bayik[a,b], Ihsan Gursel[b,**], Dennis M. Klinman[a,*]

[a] Cancer and Inflammation Program, Frederick National Laboratory for Cancer Research, Frederick, MD 21702, USA
[b] Bilkent University, Molecular Biology and Genetic Department, Therapeutic ODN Research Laboratory, Ankara, Turkey

ARTICLE INFO

*Article history:*
Received 13 November 2015
Accepted 13 November 2015
Available online 15 January 2016

*Keywords:*
CpG oligonucleotide
IRF8
IRF5
Dendritic cell
TLR9

ABSTRACT

Synthetic oligodeoxynucleotides that can down-regulate cellular elements of the immune system have been developed and are being widely studied in preclinical models. These agents vary in sequence, mechanism of action, and cellular target(s) but share the ability to suppress a plethora of inflammatory responses. This work reviews the types of immunosuppressive oligodeoxynucleotide (Sup ODN) and compares their therapeutic activity against diseases characterized by pathologic levels of immune stimulation ranging from autoimmunity to septic shock to cancer (see graphical abstract). The mechanism(s) underlying the efficacy of Sup ODN and the influence size, sequence and nucleotide backbone on function are considered.

Published by Elsevier Ltd.

**Contents**

1. Introduction ..... 217
   1.1. Historical overview ..... 217
2. Broadly acting Sup ODN ..... 217
   2.1. Mechanisms of action ..... 217
   2.2. Therapeutic activity ..... 218
      2.2.1. A151 for the treatment of autoimmune and infectious diseases ..... 218
      2.2.2. A151 for the treatment of toxic shock ..... 218
      2.2.3. A151 for the treatment of organ specific inflammation ..... 218
      2.2.4. A151 for the treatment of fungal infection ..... 219
      2.2.5. A151 for the treatment of atherosclerosis ..... 219
      2.2.6. A151 for the treatment of stroke ..... 219
      2.2.7. A151 for the prevention of inflammation-induced cancer ..... 219
3. TLR specific Sup ODN ..... 219
   3.1. Mechanism of action ..... 219
   3.2. *H154* sequence: 5′-CCTCAAGCTTGAGGGG-3′ ..... 219
   3.3. Inhibitory (INH) ODNs (*e.g.*, TCCTGGCGGGGAAGT) ..... 220
   3.4. 'G' ODN ..... 220
      3.4.1. Modified ODNs ..... 220
   3.5. Sup ODNs whose mechanisms of action has not been established ..... 220
   3.6. Therapeutic activity ..... 220
      3.6.1. Autoimmune disease ..... 220
      3.6.2. Organ-specific inflammation ..... 220
      3.6.3. Toxic shock ..... 222

* Corresponding author at: Bldg 567 Rm 205, Frederick National Laboratory for Cancer Research, Frederick, MD 21702, USA. Fax: +1 302 118 4281.
** Corresponding author at: Biotherapeutic ODN Research Laboratory, Faculty of Sciences, Bilkent University, Bilkent, Ankara 06800, Turkey. Fax: +90 312 266 50 97.
*E-mail addresses:* ihsangursel@bilkent.edu.tr (I. Gursel), klinmand@mail.nih.gov (D.M. Klinman).

http://dx.doi.org/10.1016/j.phrs.2015.11.010
1043-6618/Published by Elsevier Ltd.

4. General observations concerning Sup ODN activity ..... 222
4.1. Influence of structure and size on ODN function ..... 222
4.2. Effect of nucleotide backbone on ODN activity ..... 223
4.3. Influence of dose and site of administration of the activity of Sup ODN ..... 223
4.4. Comparative activity of different Sup ODN classes ..... 223
Conflict of interest ..... 223
Funding ..... 223
Acknowledgments ..... 223
References ..... 223

## 1. Introduction

Nucleic acids are the "blueprint of life" and thus essential components of all living organisms. DNA and RNA also have multiple and complex effects on the immune system [1–3]. The nucleic acids present in pathogenic microorganisms can trigger toll-like receptors on immune cells, stimulating them to mount a protective response [4–9]. Conversely, the telomeres that cap mammalian DNA contain repetitive TTAGGG motifs that inhibit immune reactions [1]. The release of inhibitory DNA as host cells die may serve to down-regulate pathologic inflammatory and autoimmune responses. This work reviews the use of synthetic oligonucleotides containing immunosuppressive motifs (Sup ODN) for the treatment of cancer, inflammation and autoimmune disorders.

### 1.1. Historical overview

The ability of DNA to inhibit immune reactions was first observed in studies of phosphorothioate modified ODN. ODNs (particularly those expressing poly-G motifs) suppressed IFN production by activated murine splenocytes. However neither the precise sequence nor mechanism of action underlying that suppressive activity was carefully investigated. Indeed, 30-mers of widely varying sequence were reported to mediate various degrees of immune suppression [10–12].

In 1998, Krieg et al. reported that DNA from certain adenovirus serotypes contained in "immunoinhibitory" motifs that could down-regulate TLR-induced immune activation [13]. Other suppressive motifs were subsequently described, some of which blocked other forms of immune activation as well [1,14–18]. Much of this activity was linked to the presence of extended G and C-rich sequence motifs [13,19]. In studies of mammalian DNA, Gursel et al. found that immune suppression was largely mediated by the repetitive TTAGGG motifs present in mammalian telomeres [1]. G-rich and microsatellite regions were later found to further contribute to the suppressive activity of mammalian DNA [20]. Of interest, the genomes of immunomodulatory commensal bacteria are now known to contain suppressive DNA motifs [16].

Oligodeoxynucleotides that mimic the immunosuppressive activity of mammalian DNA (referred to hereafter as "Sup ODN") were synthesized and tested by many groups. As described below, these vary in sequence and mechanism of action. Several groups sought to categorize these different types of Sup ODN. Trieu et al. proposed grouping them into four classes based on their sequence and probable mode of action [21] whereas Lenert categorized them based on their ability to form secondary structures (including G tetrads and palindromes) [22]. This review describes the sequence, mechanism of action and therapeutic potential of multiple classes of Sup ODN that are categorized based on the breadth of their inhibitory activity. Broadly acting Sup ODNs act on multiple cell types and suppress the immune activation elicited by many different stimulants. By comparison, TLR-specific Sup ODN primarily antagonize TLR9 and/or TLR7 induced responses and their activity is limited to cells expressing those receptors.

## 2. Broadly acting Sup ODN

### 2.1. Mechanisms of action

A151 is the archetypal example and best studied of the broadly acting Sup ODN. A151 is composed of four TTAGGG motifs designed to mimic the repetitive elements present at high frequency in mammalian telomeres. Telomeric DNA inhibits the activation and differentiation of macrophages, dendritic cells, B cells and multiple subsets of T cells [1,16,18,23–27].

A151 blocks the immune stimulation induced by bacterial DNA, an effect initially attributed to competition for binding between A151 and CpG ODN to TLR9. Subsequent research showed that the broad immunosuppressive activity of A151 was primarily attributable to its effect on STAT phosphorylation. STAT proteins are transcription factors that influence the maturation of many types of immune cell (reviewed in Ref. [28]). Evidence that A151 interfers with the phosphorylation of STAT1 and STAT4 was obtained in studies of TLR4-stimulated macrophages [23]. Inhibition of STAT3 phosphorylation was then observed in studies of naive CD4 T cell differentiation. A151 binds to STATs 1, 3 and 4 to inhibit downstream signaling, thereby inhibiting the production of IFNg and IL-12 which interferes with the generation of proinflammatory Th1 lymphocytes. This skews the cytokine milieu and supports the generation of Th2 responses *in vivo* [24].

The effect of A151 on STAT phosphorylation pre-dated the discovery of Th17 and regulatory T cells (Treg) whose influence on the development of autoimmune and inflammatory diseases is now appreciated. A151 supports the generation of Th17 cells by blocking the generation of SOCS3, a negative regulator of phospho-STAT3 [15]. A151 also promotes the generation of Tregs. This arises from a direct effect of A151 in blocking STAT1 phosphorylation which enables naive $CD4^+CD25^-$ T cells to differentiate into $CD4^+CD25^+FoxP3^+$ iTregs and an indirect effect whereby A151 interferes with the generation of LpDC that would otherwise reduce Treg generation [16,27]. Studies of human B cells indicates that A151 can suppress B cell activation, Ab production and the generation of plasma/memory cells [18]. This activity is attributed to the ability of A151 to suppress AICDA (activation induced cytidine deaminase) which is known to regulate class switch and somatic mutation in B cells [29] (Fig. 1).

An additional target of A151 was recently described. AIM2 and IFNg-inducible protein-16 (IFI16) are DNA-binding proteins that recognize cytosolic bacterial and viral dsDNA. Activation of these proteins recruits caspase-1 to mediate the cleave of pro-IL-1B and pro-IL-18 into their functional forms [30–32]. A151 directly binds to AIM2 which prevents the recruitment of ASC and the subsequent assembly of the inflammasome complex [26]. Thus, the ability of A151 to broadly suppress the differentiation and activation of

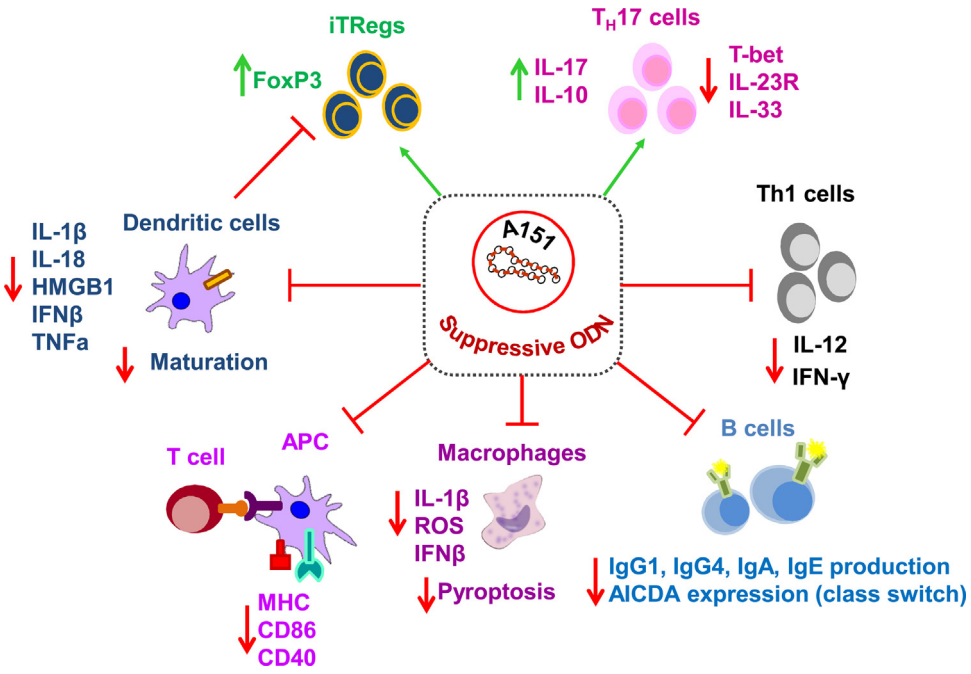


**Fig. 1.** Suppressive ODN A151 has diverse effects on cellular elements of the immune system.
Treatment with A151 supports the generation of Th17 and iTregulatory cells with immunosuppresive activity. It down-regulates activated Th1 cells resulting in a Th2 bias in subsequent responses. It inhibits the continued activation of dendritic cells, macrophages and other APCs resulting in decreased expression of activation markers and reduced production of proinflammatory cytokines. B cell maturation, class switching and Ig production are also suppressed.

multiple cell types derives from its ability to act on multiple signaling pathways (Fig. 1).

### 2.2. Therapeutic activity

#### 2.2.1. A151 for the treatment of autoimmune and infectious diseases

The first therapeutic uses of Sup ODN were for the prevention and/or treatment of autoimmune diseases. As these studies were performed over a decade ago and have already been reviewed [33], only a brief overview of salient findings is provided below.

1) Lupus. The effect of delivering A151 to lupus-prone NZB/W mice was examined in this spontaneous disease model both before and after immune complex mediated kidney damage had developed. Early treatment slowed the onset and reduced the magnitude of autoimmune-mediated renal inflammation leading to significantly prolonged survival [34]. Starting treatment after mice were already sick slowed but did not prevent disease progression.
2) Arthritis. Intra-articular delivery of A151 significantly reduced the incidence and severity of arthritis in an animal model of collagen-induced arthritis. This treatment also decreased serum titers of pathogenic IgG autoAb [14].
3) Autoimmune uveitis. Three different models of autoimmune uveitis were examined: acute, recurrent, and persistent. In each case, treatment with A151 significantly reduced the magnitude of ocular inflammation and subsequent tissue damage [3,35,36].
4) Atopic dermatitis. A recent report by Wang et al. broke new ground in the therapeutic use of Sup ODN by showing they can be delivered orally to treat skin disease. A151 was encapsulation in acid stable nanoparticles to protect them from degradation in the stomach. After oral delivery the nanoparticles reached the small intestine where they were selectively taken up by macrophages in the Peyers patches. Repeated delivery resulted in systemic changes in cytokine production (reducing levels of IL 4 and IL 33) and reduced the differentiation of allergen-activated Th2 cells thereby attenuating the development of chemically induced atopic dermatitis [17].

#### 2.2.2. A151 for the treatment of toxic shock

Toxic shock arises from the cytokine storm triggered by overwhelming bacterial sepsis. This effect can be replicated by the delivery of high dose LPS to normal mice. Treatment with A151 at the same time as LPS challenged significantly reduced cytokine storm and improved survival [23]. The longer therapy was delayed, the less effective it became.

#### 2.2.3. A151 for the treatment of organ specific inflammation

Studies of A151 document the ability of this class of ODN to ameliorate organ-specific inflammation. Pulmonary inflammation was evaluated in a murine model of silicosis. Similar to coal dust and asbestos, inhalation of silica particles causes progressive fibrosis, reduced blood oxygenation, and increased susceptibility to cancer [37]. Silicosis is elicited in mice by instilling silica particles into the lungs which causes an inflammatory infiltrate, increased production of pro-inflammatory cytokines and chemokines (including IL-6, IL-1, TNFa, IL-12 and keratinocyte chemoattractant (KC)), and alveolar hemorrhage (reviewed in Ref. [38]). Treating mice with A151 shortly before silica instillation significantly reduced cellular infiltration of the lungs and local production of pro-inflammatory cytokines [25]. Of clinical relevance, A151 prevented silica-induced weight loss and significantly improved survival. Thus, A151 both reduced local inflammation and ameliorated systemic symptoms. However treatment was ineffective if delayed until chronic silicosis had developed.

Inflammation of the GI tract has been shown to contribute to the development of autoimmune disease and cancer (reviewed in Ref. [39]). The effect of Sup ODN treatment in two different murine models of gut inflammation was examined. The first involved infection with the *Toxoplasma gondii* parasite and the second topical exposure to the chemical irritant dextran sulfate (DSS). In both

systems, repeated oral delivery of A151 down-regulated the production of pro-inflammatory cytokines (IFNg, TNFa, IL-6 and IL-22) and maintained the integrity of the gut epithelium [16]. This was linked to the ability of A151 to down-regulate LpDC activation, thereby maintaining IL-10 production and sustaining Treg activity [16]. Independent studies showed that A151 directly supported the generation of Tregs [27]. Together these findings indicate that A151 supports gut homeostasis by maintaining Treg function that would otherwise be dysregulated in inflammatory bowel disease (reviewed in Ref. [40]).

#### 2.2.4. A151 for the treatment of fungal infection

Although healthy individuals rarely suffer from major fungal infections, some fungal strains are pathogenic particularly in immunosuppressed hosts [41]. Recent evidence suggests Th17 immunity plays an important role in clearing fungal infections [35]. *In vitro* studies showed that A151 promoted the generation of Th17 cells by inhibiting SOCS3 which is a negative regulator of Th17 differentiation [15]. Using *Candida albicans* as a model pathogen, the ability of A151 to generate Th17 cells capable of protecting against fungi was examined in mice. Results showed that systemic treatment with A151 increased Th17 immunity and that this was associated with reduced weight loss and a lower infectious burden in *C. albicans* challenged animals when compared to untreated controls [15].

#### 2.2.5. A151 for the treatment of atherosclerosis

Atherosclerosis is characterized by the deposition of plaque (composed of macrophages, fat, cholesterol and calcium) in the arteries. Advanced atherosclerosis increases the risk of myocardial infarction, peripheral vascular disease and stroke. Inflammation is an important component of the atherosclerotic process. Activated T cells produce factors that stimulate macrophages to internalize lipoproteins and become artery-occluding foam cells. ApoeE KO mice are widely used to model this atherosclerotic process [42]. These animals rapidly develop extensive plaques associated with markers of atherosclerotic inflammation including MCP-1 and VCAM-1.

The effect of treating ApoE mice with A151 was evaluated. Serum levels of MCP-1 and VCAM fell by 30–50% ($p < .05$ for both factors) while the size of the atherosclerotic lesions was reduced by half [43]. Levels of the Th1 cytokines IFNg and TNFa were significantly reduced, an effect that correlated with reduced size of the atherosclerotic lesions. Mechanistically, Sup ODN treatment reduced the phosphorylation of STAT1 and STAT4 thereby reducing the T-bet expression needed to support Th1 cell differentiation. As a result, the frequency of IFNg production Th1 cells declined while the ratio of Th2:Th1 cells rose.

#### 2.2.6. A151 for the treatment of stroke

The ability of Sup ODN to prevent ischemic stroke was examined using stroke-prone hypertensive (SHR-SP) rats. Stroke is a major cause of chronic debilitation and the second most common cause of death worldwide. While strokes are caused by a reduction in blood supply to the brain, the resulting tissue damage triggers an inflammatory response that further increases lesion size [44–46].

Zhao et al. examined the effect of treatment with A151 on strokes generated by surgically occluding the middle cerebral artery of SHR-SP rats [47]. Results indicate that A151 had broad anti-inflammatory properties, associated with decreased production of caspase-1, IL-1ß, iNOS and NLRP3 by activated macrophages. Sup ODN treatment limited the magnitude of ischemia-induced brain damage in a time and dose dependent fashion. A151 was most effective when administered 1 day prior to infarct induction. The highest dose tested (3 mg) was more effective than 1 mg. Under optimal conditions, Sup ODN reduced the extent of brain damage by >25% [47]. These observations are relevant to patients scheduled to undergo cardiac or carotid surgery whose high risk of stroke may be reduced by treatment with Sup ODN prior to surgery.

#### 2.2.7. A151 for the prevention of inflammation-induced cancer

Chronic inflammation contributes to the development and progression of many types of cancer (reviewed in Ref. [48]). The possibility that Sup ODN might interfere with the inflammation that supports tumorigenesis was therefore explored. The first study in the field focused on a common murine model of skin cancer in which TPA was used to drive inflammation after transformation was initiated by DMBA. Mice treated with DMBA/TPA typically develop skin papillomas that transform into squamous cell carcinomas (SCC) over time [49].

Ikeuchi et al. examined the effect of administering A151 at the same time as TPA. Results showed that Sup ODN therapy reduced papilloma formation by 95% and that this effect was dose-dependent. Histological analyses revealed that A151 limited the development of edema, leukocyte infiltration and the production of various markers of inflammation (including CCL2, CXCL2, COX2 and ornithine decarboxylase) [50]. Discontinuing or delaying the initiation of Sup ODN therapy slowed but did not prevent papillomas from arising [50].

A large body of data suggests that pulmonary inflammation increases the risk of cigarette smoke induced lung cancer (reviewed in Ref. [51]). To evaluate whether A151 could alter susceptibility to lung cancer by reducing inflammation, a murine model was developed in which NNK (a highly carcinogenic component of cigarette smoke) was delivered to mice with silica-induced pulmonary inflammation. The combination of NKK plus silica increased the fraction of mice that developed lung tumors (incidence) and the number of tumors per mouse (multiplicity) [52]. Treating these mice with A151 starting at the time of silica administration reduced pulmonary inflammation as evidenced by a significant decrease in macrophage and neutrophil infiltration, lower levels of pro-inflammatory cytokines (including IL-1B and TNFa) and less fibrosis [52]. Treatment with A151 also reduced to background the incidence and multiplicity of lung tumors in NNK-treated silicotic mice. Additional studies showed that A151 improved the anti-proliferative effects of several chemotherapeutic drugs [53]. These results strongly suggest that Sup ODN may help prevent inflammation-driven cancers from developing.

## 3. TLR specific Sup ODN

### 3.1. Mechanism of action

A variety of Sup ODN function by selectively blocking the effects of TLR9 and/or TLR7 agonists. Various types of TLR-specific Sup ODN act on different stages of the TLR signaling cascade: some compete for uptake, others inhibit receptor binding and/or block downstream signaling. The following represents an overview of the effects of these types of Sup ODN.

### 3.2. H154 *sequence: 5′-CCTCAAGCTTGAGGGG-3′*

H154 is a specific inhibitor of the immune activation induced *via* TLR9. H154 interferes with downstream signaling rather than by inhibiting the binding or uptake of CpG DNA [8]. This results in a significant reduction in cytokine and Ab production by cells activated via TLR9 [8,54]. Reflecting its specificity for TLR9, H154 cannot downregulate immune responses triggered by other immune stimulants such as LPS or ConA [8]. Thus, while effective for treating inflammatory conditions triggered via TLR9 the therapeutic utility of H154 is more limited than that of A151 [55–57].

### 3.3. Inhibitory (INH) ODNs (e.g., TCCTGGCGGGGAAGT)

INH ODNs selectively interfere with TLR9-mediated immune activation by competing with CpG ODN for binding to the C-terminal region of TLR9 [58,59]. Most INH ODNs have sequences similar to CpG ODN with the critical difference that the receptor activation residues are absent [60–62]. The interaction of INH ODN with TLR9 fails to induce the conformational changes necessary for activation of the downstream signaling cascade *via* MyD88 with the result that NF-kB and AP1 activation never occurs [59,63–65]. Cells that express TLR9, including B cells, dendritic cells and murine monocytes, are all inhibited by INH ODN. INH ODNs are also reported to down-regulate TLR7-mediated immune activation to some extent, although that effect may not be sequence specific [66–68].

There is limited evidence that INH ODN might increase host susceptibility to bacterial infection. The gram negative bacterium *Salmonella typhimurium* replicates within macrophages and is a common cause of food-borne illnesses [69]. Independent of any effect on TLR9 signaling, INH ODN increase bacterial load in macrophages due to partial inhibition of TLR1/2 signaling, a side-effect that might alter the host-microbe response [70].

### 3.4. 'G' ODN

'G' ODN contain a string a five guanines with a representative sequence being CTCCTATTGGGGGTTTCCTAT. 'G' ODN bind to the C-terminal region of TLR9 thereby preventing CpG-receptor interaction [59]. As a result, this class of ODN dampens TLR9 mediated activation of APC and the production of pro-inflammatory cytokines including IFNa, TNFa and IL-12 [71].

#### 3.4.1. Modified ODNs

Modified ODNs are generated by reversing stimulatory CpG motifs to GpC or GpG. While their mechanism of action has not been clarified, their sequence similarity to CpG ODN strongly suggests that competition for uptake, binding and/or receptor activation underllies their activity. Sequences such as 5′-TGACTGTGAAGGTTAGAGATGA-3′ antagonize CpG-mediated immunity by limiting the activation of APC and production of pro-inflammatory cytokines [72]. In various *in vivo* models, GpG ODNs support Th2 rather than Th1 responses, an effect accompanied by decreased production in pro-inflammatory cytokines [73,74].

An atypical example of this class of ODN is GpC-1826. GpC-1826 utilizes the TLR7/TRIF signaling pathway to increase indoleamine 2,3-dioxygenase (IDO) expression thereby producing tolerogenic pDCs [75,76]. A modified version of this ODN supported the generation of Treg indirectly by promoting tolerogenic pDC [77]. GpC-1826 antagonizes immune response mediated by TLR7 agonists while its effect on responses elicited *via* TLR9 is unknown.

A different mechanism of action was described for GpC-1668 and GpG-1668. These mediate immune suppression by binding to high-mobility group box proteins (HMGBs) [78]. HGMBs are essential for the recognition of nucleic acids that trigger receptor mediated immune responses [78]. By competing with stimulatory nucleic acids for intracellular HMGB, these Sup ODN inhibit dsDNA, ssDNA and dsRNA-mediated immune activation.

### 3.5. Sup ODNs whose mechanisms of action has not been established

Several groups described novel ODNs with inhibitory activity but failed to examine the mechanism through which they blocked immune responses. Immunoregulatory DNA sequences (IRS) and microsatellite sequences are examples of such ODNs.

IRS 869 (TGCTCCTGGAGGGGTTGT) is a G-rich TLR9 antagonist that prevents TLR9-mediated endotoxic shock by blocking the release of pro-inflammatory cytokines [79]. Given the similarity in sequence between IRS 869 and INH ODNs, it is likely that this effect is mediated by competition for binding with CpG DNA to TLR9. IRS 661 blocks TLR7 signaling while IRS 954 down-regulates responses elicited by both TLR7 and TLR9 agonists [73]. While inhibition by IRS ODN was observed in multiple cell types of mouse and human origin, no information was provided on whether their activity involved competition at the uptake/receptor-binding level or modulation of downstream signaling.

Other groups evaluated 24-mer ODNs consisting of multiple TC, AAAG or CCT repeats and reported that several impaired IFN production by human PBMC [20,80]. Similar sequences are present in a subset of human microsatellite regions, leading the investigators to name them microsatellite (MS) ODN.

However no evidence that human microsatellites are immunosuppressive has been provided. MS08, a prototypic MS ODN, blocks the uptake of CpG ODNs and thus suppresses TLR9 mediated immune activation. However MS08 also down-regulates TLR independent immune responses although no underlying mechanism was identified [20]. Other MS ODNs vary in their ability to influence CpG-induced inflammation and discrepancies exist between the *in vitro vs in vivo* activity of this class of ODN, raising uncertainty over their potential therapeutic utility [20,80,81].

### 3.6. Therapeutic activity

#### 3.6.1. Autoimmune disease

1) In a murine model of reactive arthritis (an inflammatory condition triggered by bacterial infection), Zeuner et al. showed that injecting H154 into an affected joint significantly reduced both inflammation and swelling. Since arthritis can affect multiple joints, H154 ODN was also administered i.p. and found to reduce systemic inflammatory arthritis [56,57].
2) In the NZB × NZW F1 mouse model of lupus, GpG ODN treatment promoted Th2 biased immune responses that delayed the onset of proteinuria [74]. Treatment with IRS 661 and 954 reduced serum anti-nuclear Ab levels, the deposition of immune complexes in the kidneys and delayed disease progression [67,79,82–87]. In lupus prone MRL lpr/lpr mice, INH ODNs suppressed autoreactive B cell and DC responses leading to reduced autoantibody production [22,66]. In a murine model of lupus induced by chronic graft *versus* host disease, He et al. reported that MS ODNs and Sat05f reduced anti ssDNA antibody levels and delayed disease progression [88].
3) In the EAE model of multiple sclerosis, adding GpC ODN to a toleragenic DNA vaccine reduced disease severity by inducing autoreactive B and T cell responses to shift to a protective IgG1 isotype and Th2 type cytokine pattern [72,73]. In those studies, Sup ODN competed with CpG sequences in the vaccine to inhibit Th1 responses.
4) Experimental autoimmune neuritis provides a model of Guillain Barre Syndrome characterized by demyelination and inflammation of the peripheral nervous system. It is induced by injecting P2 peptide in complete Freund's adjuvant into the hind footpads of Lewis rats. When animals with EIN were treated with H154, markers of inflammation and disease severity were significantly reduced [89].

#### 3.6.2. Organ-specific inflammation

In a murine model of acute lung inflammation, MS19 significantly inhibited weight loss and hemorrhage, reduced intra-alveolar edema and lessened the accumulation of neutrophils in the lungs [81,88,90]. H154 inhibited the pulmonary inflammation induced by the delivery of immunostimulatory bacterial products

**Table 1**
Overview of suppressive oligonucleotides.

Name: A151

Sequence: TTAGGGTTAGGGTTAGGGTTAGGG

Mechanism of action
Binds to and prevents the phosphorylation of STATs 1, 3 and 4 [24]
Inhibits SOCS 3 [15,27]
Inhibits activation of the AIM2 inflammasome [26]

*In vitro* effects: suppresses the production of pro-inflammatory cytokines/chemokines. Down-regulates expression of co-stimulatory molecules
Acts on T cells, B cells, pDC and macrophages from multiple species [1,18,24]
Supports the generation of Th17 cells and Tregs [15,16,27]
Reduces the generation of alarmins [26]

*In vivo* activity reported in murine models of
Endotoxic shock [23]
Collagen induced arthritis [34]
SLE [14]
Pulmonary inflammation [16,25]
Uveitis/iritis [3,35,36]
Inflammation driven oncogenesis [50,52]
Allergy [18]
Atopic dermatitis [50]
Atheroscleosis [43]
Stroke [47]

Name: H154

Sequence: CCTCAAGCTTGAGGGG

Mechanism of action
Inhibits immune signalling viaTLR9 [8,54]

*In vitro* effects
Inhibits CpG induced production of pro-inflammatory cytokines/chemokines. Active on mouse spleen cells and macrophages, human PBMC and B cells [8,54,60,68,103]

*In vivo* activity reported in murine models of
Reactive arthritis [56,57]
Myocardial dysfunction [93]
Pulmonary inflammation [54]

–

Name: INH ODN

Representative sequence: TCCTGGCGGGGAAGT

Mechanism of action
Competes for binding to TLR9 and blocks the downstream signalling pathway [59,63–65]

*In vitro* effects
Inhibits CpG induced cytokine and NO production
Protects against apoptosis and cell-cycle entry [58,67,68,79,86,87,100,103]

*In vivo* activity reported in murine models of
SLE [66,104]

Name: Modified CpG ODN

Representative sequences
TGACTGTGAAGGTTAGAGATGA
TCCATGAGCTTCCTGATGCT

Mechanism of action
Inhibits TLR9-induced phosphorylation of I6B-. [72]
Induces IDO through non-canonical NF-kB signaling [77]
Binds to HMGB1 [77]

*In vitro* effects
Inhibits CpG induced cytokine production and B cell proliferation
Acts on mouse spleen cells, DC and macrophages [72,78]
Generates tolerogenic DC [77]

*In vivo* activity reported in murine models of
Experimental autoimmune encephalomyelitis [72,105]
SLE [104]
Endotoxic shock [78]

Name: S ODN

Representative sequence: GGGGGGGGGGGGGGGGGGGG
Mechanism of action

*In vitro* effects
Blocks Th1 cytokine production induced by various TLR agonists [10,106,107]
Blocks TLR induced NO production [11,12]
Active on monocytes and dendritic cells

Table 1 (*Continued*)

| |
|---|
| Name: A151 |
| No *in vivo* activity reported |
| Name: IRS ODN |
| Representative sequence: TGCTCCTGGAGGGGTTGT |
| Mechanism of action<br>Inhibits TLR9 and TLR7 mediated immune activation [73] |
| *In vitro* effects<br>Inhibits TLR9 mediated cytokine production<br>Acts on mouse spleen cells, human B cells and pDC [82] |
| *In vivo* activity reported in murine models of<br>SLE [79,82,85]<br>Skin inflammation [83]<br>Endotoxic shock [79] |
| Name: "G" ODN |
| Representative sequence: CTCCTATTGGGGGTTTCCTAT |
| Mechanism of action<br>Competes for binding to TLR9 [59] |
| *In vitro* effects<br>Blocks CpG induced production of pro-inflammatory cytokines<br>Acts on DC and macrophages [71] |
| *In vivo* activity reported in murine models of<br>SLE [108]<br>Endotoxic shock [71] |
| Name: Microsatellite ODN |
| Representative sequences<br>AAAGAAAGAAAGAAAGAAAGAAAG<br>CCTCCTCCTCCTCCTCCTCCTCCT |
| Mechanism of action<br>Inhibits TLR7 and TLR9 mediated immune activation<br>Competes for CpG uptake [20] |
| *In vitro* effects<br>Inhibits TLR mediated activation of human PBMC and macrophage<br>Blocks up-regulation of co-stimulatory signals [20,80] |
| *In vivo* activity reported in murine models of<br>GVHD [80,88,90]<br>Lung inflammation [81]<br>Endotoxic shock [80] |

(such as CpG DNA) into the lungs of mice was evaluated [91]. CpG instillation triggered a local response characterized by neutrophil accumulation and increased TNFa, IL-6, MIP-2, and KC production. Co-delivery of Sup ODN H154 significantly lessened the magnitude of these inflammatory changes [54].

In a murine model of myocardial dysfunction elicited by activation of TLR9, Boehm et al. found that ODN H154 significantly ameliorated cardiac inflammation, preserved cardiac function, and improved survival [92,93].

#### 3.6.3. Toxic shock

MS ODNs and Sat05f inhibited TLR7 and TLR9 mediated innate immune responses thereby protecting mice from D GalN/CpG ODN induced lethal shock [81].

'G' ODN protected mice from cytokine-mediated lethal shock induced by bacterial DNA [71]. GpG 1668 protected against LPS-induced toxin shock by reducing the production of pro-inflammatory cytokines. While this effect was attributed to HMGB targeting, it should be noted that GpG-1668 was unable to down-regulate LPS-induced immune responses *in vitro*.

## 4. General observations concerning Sup ODN activity

### 4.1. Influence of structure and size on ODN function

While distinct classes of Sup ODN differ in length, sequence and functional activity, most contain a string of poly-Gs [1,8,62,64,71,79]. Suppressive activity typically requires a minimum of 3 G's, with several studies suggesting that longer runs of poly-G increase potency further [58,60,62,79]. Conversely, reducing the number of G's typically reduces or ablates suppressive activity [1,26,94].

Poly-G sites enable the formation of higher order quadruplex structures *via* inter-chain Hoogsteen hydrogen bonding (reviewed in Ref. [95]). This binding is disrupted by insertion of a 7-deazaguanine (7-DG) nucleotide which prevents hydrogen bond formation but does not affect Watson–Crick pairing [96]. In studies of INH ODN, monomeric structures (generated by substituting 7-DG for one or more G's) remained functional, indicating that quadruplex formation was not required for their inhibitory activity [58,67,68,79,97]. In contrast, the ability to form G-tetrads was required for A151 to its maintain broad immunosuppressive activity since substituting a 7-DG for any G significantly reduced inhibitory function [1].

This difference in the role of quadruplex structures may distinguish between ODN that act in a TLR-specific *versus* broadly suppressive manner. Whereas single stranded ODN might effectively compete with single-stranded CpG ODN for binding to TLR9, quadruplex structures may be necessary to facilitate the interaction of A151 with molecular targets including STATs and inflammasome components. In this context, G-tetrads are known to make a critical contribution to the binding of ODN to STAT3, an important target of A151 [98].

Length also influences the activity of Sup ODN. A single TTAGGG 6-mer has no activity yet the same motif conjugated to a random 8-mer exhibits suppressive activity [1]. Similarly, a 5-mer poly-G is suppressive only when incorporated into a longer ODN [71]. Studies of various classes of Sup ODN indicate that sequences shorter than 11 nucleotides have little suppressive activity while those longer than 24 nucleotides gain little additional function [8,62,72,77,78,90]. This pattern was also observed in studies of TTAGGG multimers: suppressive activity increased as more motifs were added but only to a point, with ODN containing 5 repeats being no more active than those with 4 TTAGGG repeats [1,90].

### 4.2. Effect of nucleotide backbone on ODN activity

Native DNA is composed of nuclease-sensitive phosphodiester (PO) base pairs that are rapidly degraded *in vivo*. To improve therapeutic half life, the non-bridging oxygen can be replaced with sulfur to yield phosphorothioate (PS) modified ODN. PS are superior to PO ODN in terms of both nuclease resistance and cellular uptake (reviewed in Ref. [99]). The potency of PS *vs* PO was examined for several classes of Sup ODN. *In vitro* studies show that A151-PS and A151-PO are equally efficient in suppressing CpG induced responses whereas only A151-PS was much more effective in blocking dsDNA-induced inflammasome activation *in vivo* [1,26]. Other studies confirmed the superior potency of PS over PO versions of the same Sup ODN *in vivo* [71,78,79,100]. It should be noted that sequence-independent inhibition of immune responses has been reported for some PS ODNs [10,11,66,101].

### 4.3. Influence of dose and site of administration of the activity of Sup ODN

*In vitro* studies by many groups establish that Sup ODN can inhibit the production of pro-inflammatory cytokines and chemokines (including IL6, IL-12, IFNg, TNFa and MIP2a) [1,12,24,33]. These effects are summarized in Table 1. We draw the following general conclusions from analysis of multiple autoimmune and inflammatory disease models.

1) Sup ODN are most effective when administered immediately prior to or concomitant with the delivery of the inflammatory stimulus [3,102]. This is consistent with evidence that Sup ODN effectively block the activation of inflammatory immune cells but are relatively ineffective at down-regulating cells that have already been activated [8].
2) The effect of Sup ODN is dose and location dependent. In studies where A151 was delivered systemically, the effective dose in mice was typically 300 μg [3,34]. However much lower doses were sufficient when A151 was delivered locally. For the treatment of arthritis, as little as 10 ug injected into the knee was sufficient whereas 30–50 μg prevented pulmonary inflammation [25,54].

### 4.4. Comparative activity of different Sup ODN classes

Very few studies have compared the activity of different classes of Sup ODN. Those comparisons that were conducted generally used *in vitro* assays to examine a single immune parameter and cell type and thus are unlikely to reflect broad *in vivo* efficacy. For example, experiments indicate that INH ODN 2114 and H154 are equivalent in terms of stimulating cytokine production *in vitro* but that H154 is a less potent suppressor of B cell activation and proliferation [60,62,103]. Other studies focusing on B cell activation suggest that INH ODN 2114 is superior to 'G' ODN but inferior to IRS954 and IRS869 [103]. A151 and microsatellite ODN have similar capacities to block PBMC proliferation and pro-inflammatory cytokine production [20,80]. Another study revealed that INH ODN 2114 and A151 inhibited CpG-driven NF-kB up-regulation in macrophage to the same degree [21]. Lacking adequate *in vivo* comparisons, the extent and breadth of immune suppression mediated by A151 marks it as a superior candidate for clinical development.

## Conflict of interest

Dr. Dennis Klinman and members of his lab are co-inventors on a number of patents concerning Sup ODN and their use. All rights to these patents have been assigned to the Federal government.

## Funding

This research was supported by the Intramural Research Program of the National Cancer Institute of the National Institutes of Health.

## Acknowledgments

This manuscript was supported by the Intramural Research Program of the NIH, NCI. The content of this publication does not necessarily reflect the views or policies of the Department of Health and Human Services, nor does mention of trade names, commercial products, or organizations imply endorsement by the United States government. The funders had no role in study design, data collection and analysis, decision to publish, or preparation of the manuscript.

## References

[1] I. Gursel, M. Gursel, H. Yamada, K.J. Ishii, F. Takeshita, D.M. Klinman, Repetitive elements in mammalian telomeres suppress bacterial DNA-induced immune activation, J. Immunol. 171 (2003) 1393–1400.
[2] K.J. Ishii, S. Akira, Innate immune recognition of nucleic acids: beyond toll-like receptors, Int. J. Cancer 117 (2005) 517–523.
[3] F.C. Yagci, O. Aslan, M. Gursel, G. Tincer, Y. Ozdamar, K. Karatepe, et al., Mammalian telomeric DNA suppresses endotoxin-induced uveitis, J. Biol. Chem. 285 (2010) 28806–28811.
[4] S. Yamamoto, T. Yamamoto, S. Shimada, E. Kuramoto, O. Yano, T. Kataoka, et al., DNA from bacteria, but not vertebrates, induces interferons: activate NK cells and inhibits tumor growth, Microbiol. Immunol. 36 (1992) 983–997.
[5] D.M. Klinman, A. Yi, S.L. Beaucage, J. Conover, A.M. Krieg, CpG motifs present in bacterial DNA rapidly induce lymphocytes to secrete IL-6, IL-12 and IFNg, Proc. Natl. Acad. Sci. U. S. A. 93 (1996) 2879–2883.
[6] T. Sparwasser, E. Koch, R.M. Vabulas, K. Heeg, G.B. Lipford, J.W. Ellwart, et al., Bacterial DNA and immunostimulatory CpG oligonucleotides trigger maturation and activation of murine dendritic cells, Eur. J. Immunol. 28 (1998) 2045–2054.
[7] A.M. Krieg, The role of CpG motifs in innate immunity, Curr. Opin. Immunol. 12 (2000) 35–43.
[8] H. Yamada, I. Gursel, F. Takeshita, J. Conover, K.J. Ishii, M. Gursel, et al., Effect of suppressive DNA on CpG-induced immune activation, J. Immunol. 169 (2002) 5590–5594.
[9] D.M. Klinman, S. Klaschik, T. Sato, D. Tross, CpG oligonucleotides as adjuvants for vaccines targeting infectious diseases, Adv. Drug Deliv. Rev. 61 (2009) 248–255.
[10] D.S. Pisetsky, C.F. Reich, Inhibition of murine macrophage IL-12 production by natural and synthetic DNA, Clin. Immunol. 96 (2000) 198–204.
[11] F.G. Zhu, C.F. Reich, D.S. Pisetsky, Inhibition of murine macrophage nitric oxide production by synthetic oligonucleotides 9, J. Leukoc. Biol. 71 (2002) 686–694.

[12] F.G. Zhu, C.F. Reich, D.S. Pisetsky, Inhibition of murine dendritic cell activation by synthetic phosphorothioate oligodeoxynucleotides, J. Leukoc. Biol. 72 (2002) 1154–1163.
[13] A.M. Krieg, T. Wu, R. Weeratna, S.M. Efler, L. Love, L. Yang, et al., Sequence motifs in adenoviral DNA block immune activation by stimuatory CpG motifs, Proc. Natl. Acad. Sci. U. S. A. 95 (1998) 12631–12636.
[14] L. Dong, S. Ito, K. Ishii, D. Klinman, Suppressive Oligodeoxynucleotides Delay the Onset of Glomerulonephritis and Prolong the Survival of Lupus-prone NZB/W Mice, Arthritis Rheum. 52 (2004) 651–658.
[15] C. Bode, X.P. Yang, H. Kiu, D.M. Klinman, Suppressive oligodeoxynucleotides promote the development of Th17 cells, PLoS One 8 (2013) e67991.
[16] N. Bouladoux, J.A. Hall, J.R. Grainger, L.M. dos Santos, M.G. Kann, V. Nagarajan, et al., Regulatory role of suppressive motifs from commensal DNA, Mucosal Immunol. 5 (2012) 623–634.
[17] Y. Wang, Y. Yamamoto, S. Shigemori, T. Watanabe, K. Oshiro, X. Wang, et al., Inhibitory/suppressive oligodeoxynucleotide nanocapsules as simple oral delivery devices for preventing atopic dermatitis in mice, Mol. Ther. 23 (2015) 297–309.
[18] C. Sackesen, V. van d, M. Akdis, O. Soyer, J. Zumkehr, B. Ruckert, et al., Suppression of B-cell activation and IgE, IgA: IgG1 and IgG4 production by mammalian telomeric oligonucleotides, Allergy 68 (2013) 593–603.
[19] Q. Zhao, J. Temsamani, R.Z. Zhou, S. Agrawal, Pattern and kinetics of cytokine production following administration of phosphorothiate oligonucleotides in mice, Antisense Nucleic Acid Drug Dev. 7 (1997) 495–502.
[20] D. Hu, X. Su, R. Sun, G. Yang, H. Wang, J. Ren, et al., Human microsatellite DNA mimicking oligodeoxynucleotides down-regulate TLR9-dependent and -independent activation of human immune cells, Mol. Immunol. 46 (2009) 1387–1396.
[21] A. Trieu, T.L. Roberts, J.A. Dunn, M.J. Sweet, K.J. Stacey, DNA motifs suppressing TLR9 responses, Crit. Rev. Immunol. 26 (2006) 527–544.
[22] P. Lenert, Nucleic acid sensing receptors in systemic lupus erythematosus: development of novel DNA- and/or RNA-like analogues for treating lupus, Clin. Exp. Immunol. 161 (2010) 208–222.
[23] H. Shirota, I. Gursel, M. Gursel, D.M. Klinman, Suppressive oligodeoxynucleotides protect mice from lethal endotoxic shock, J. Immunol. 174 (2005) 4579–4583.
[24] H. Shirota, M. Gursel, D.M. Klinman, Suppressive oligodeoxynucleotides inhibit Th1 differentiation by blocking IFNg and IL-12 mediated signaling, J. Immunol. 173 (2004) 5002–5007.
[25] T. Sato, T. Shimosato, W.G. Alvord, D.M. Klinman, Suppressive oligodeoxynucleotides inhibit silica-induced pulmonary inflammation, J. Immunol. 180 (2008) 7648–7654.
[26] J.J. Kaminski, S.A. Schattgen, T.C. Tzeng, C. Bode, D.M. Klinman, K.A. Fitzgerald, Synthetic oligodeoxynucleotides containing suppressive TTAGGG motifs inhibit AIM2 inflammasome activation, J. Immunol. 191 (2013) 3876–3883.
[27] C. Bode, J. Wang, D.M. Klinman, Suppressive oligodeoxynucleotides promote the generation of regulatory T cells by inhibiting STAT1 phosphorylation, Int. Immunopharmacol. 23 (2014) 516–522.
[28] H.S. Li, S.S. Watowich, Innate immune regulation by STAT-mediated transcriptional mechanisms, Immunol. Rev. 261 (2014) 84–101.
[29] M. Muramatsu, K. Kinoshita, S. Fagarasan, S. Yamada, Y. Shinkai, T. Honjo, Class switch recombination and hypermutation require activation-induced cytidine deaminase (AID) a potential RNA editing enzyme, Cell 102 (2000) 553–563.
[30] V.A. Rathinam, Z. Jiang, S.N. Waggoner, S. Sharma, L.E. Cole, L. Waggoner, et al., The AIM2 inflammasome is essential for host defense against cytosolic bacteria and DNA viruses, Nat. Immunol. 11 (2010) 395–402.
[31] V. Hornung, A. Ablasser, M. Charrel-Dennis, F. Bauernfeind, G. Horvath, D.R. Caffrey, et al., AIM2 recognizes cytosolic dsDNA and forms a caspase-1-activating inflammasome with ASC, Nature 458 (2009) 514–518.
[32] L. Unterholzner, S.E. Keating, M. Baran, K.A. Horan, S.B. Jensen, S. Sharma, et al., IFI16 is an innate immune sensor for intracellular DNA, Nat. Immunol. 11 (2010) 997–1004.
[33] D.M. Klinman, D. Tross, S. Klaschik, H. Shirota, T. Sato, Therapeutic applications and mechanisms underlying the activity of immunosuppressive oligonucleotides, Ann. N. Y. Acad. Sci. 1175 (2009) 80–88.
[34] L. Dong, S. Ito, K.J. Ishii, D.M. Klinman, Suppressive oligonucleotides protect against collagen-induced arthritis in mice, Arthritis Rheum. 50 (2004) 1686–1689.
[35] N. Hernandez-Santos, S.L. Gaffen, Th17 cells in immunity to *Candida albicans*, Cell Host Microbe 11 (2012) 425–435.
[36] C. Fujimoto, D.M. Klinman, G. Shi, H. Yin, B.P. Vistica, J.D. Lovaas, et al., A suppressive oligodeoxynucleotide inhibits ocular inflammation, Clin. Exp. Immunol. 156 (2009) 528–534.
[37] J.M. Mazurek, P.L. Schleiff, J.M. Wood, S.A. Hendricks, A. Weston, Notes from the field: update: silicosis mortality—United States, 1999–2013, MMWR Morb. Mortal Wkly. Rep. 64 (2015) 653–654.
[38] H. Kawasaki, A mechanistic review of silica-induced inhalation toxicity, Inhal. Toxicol. 27 (2015) 363–377.
[39] A.L. Franks, J.E. Slansky, Multiple associations between a broad spectrum of autoimmune diseases: chronic inflammatory diseases and cancer, Anticancer Res. 32 (2012) 1119–1136.
[40] M.J. Barnes, F. Powrie, Regulatory T cells reinforce intestinal homeostasis, Immunity 31 (2009) 401–411.
[41] P.B. De, T.J. Walsh, J.P. Donnelly, D.A. Stevens, J.E. Edwards, T. Calandra, et al., Revised definitions of invasive fungal disease from the European organization for research and treatment of cancer/invasive fungal infections cooperative group and the National Institute of Allergy and Infectious Diseases Mycoses study group (eortc/msg) consensus group, Clin. Infect. Dis. 46 (2008) 1813–1821.
[42] J. Jawien, The role of an experimental model of atherosclerosis: apoE-knockout mice in developing new drugs against atherogenesis, Curr. Pharm. Biotechnol. 13 (2012) 2435–2439.
[43] X. Cheng, Y. Chen, J.J. Xie, R. Yao, X. Yu, M.Y. Liao, et al., Suppressive oligodeoxynucleotides inhibit atherosclerosis in ApoE(−/−) mice through modulation of Th1/Th2 balance, J. Mol. Cell. Cardiol. 45 (2008) 168–175.
[44] C. Iadecola, J. Anrather, The immunology of stroke: from mechanisms to translation, Nat. Med. 17 (2011) 796–808.
[45] N. Zhang, X. Zhang, X. Liu, H. Wang, J. Xue, J. Yu, et al., Chrysophanol inhibits NALP3 inflammasome activation and ameliorates cerebral ischemia/reperfusion in mice, Mediators Inflamm. (2014), 370530.
[46] N. Deroide, X. Li, D. Lerouet, V.E. Van, L. Baker, J. Harrison, et al., MFGE8 inhibits inflammasome-induced IL-1beta production and limits postischemic cerebral injury, J. Clin. Invest. 123 (2013) 1176–1181.
[47] J. Zhao, Y. Mou, J.D. Bernstock, D. Klimanis, S. Wang, M. Spatz, et al., Synthetic oligodeoxynucleotides containing multiple telemeric TTAGGG motifs suppress inflammasome activity in macrophages subjected to oxygen and glucose deprivation and reduce ischemic brain injury in stroke-prone spontaneously hypertensive rats, PLoS One 10 (2015) e0140772.
[48] L.M. Coussens, Z. Werb, Inflammation and cancer, Nature 420 (2002) 860–867.
[49] E.L. Abel, J.M. Angel, K. Kiguchi, J. DiGiovanni, Multi-stage chemical carcinogenesis in mouse skin: fundamentals and applications, Nat. Protoc. 4 (2009) 1350–1362.
[50] H. Ikeuchi, T. Kinjo, D.M. Klinman, Effect of suppressive oligodeoxynucleotides on the development of inflammation-induced papillomas, Cancer Prev. Res. (Phila.) 4 (2011) 752–757.
[51] T. Brown, Silica exposure, smoking: silicosis and lung cancer–complex interactions, Occup. Med. (Lond.) 59 (2009) 89–95.
[52] C. Bode, T. Kinjo, W.G. Alvord, D.M. Klinman, Suppressive oligodeoxynucleotides reduce lung cancer susceptibility in mice with silicosis, Carcinogenesis 35 (2014) 1078–1083.
[53] R. Takahashi, T. Sato, D.M. Klinman, T. Shimosato, T. Kaneko, Y. Ishigatsubo, Suppressive oligodeoxynucleotides synergistically enhance antiproliferative effects of anticancer drugs in A549 human lung cancer cells, Int. J. Oncol. 42 (2013) 429–436.
[54] H. Yamada, K.J. Ishii, D.M. Klinman, Suppressive oligodeoxynucleotides inhibit CpG-induced inflammation of the mouse lung, Crit. Care Med. 32 (2004) 2045–2049.
[55] P. Utaisincharoen, W. Kespichayawattana, N. Anuntagool, P. Chaisuriya, S. Pichyangkul, A.M. Krieg, et al., CpG ODN enhances uptake of bacteria by mouse macrophages, Clin. Exp. Immunol. 132 (2003) 70–75.
[56] R.A. Zeuner, K.J. Ishii, M.J. Lizak, I. Gursel, H. Yamada, D.M. Klinman, et al., Reduction of GpG-induced arthritis by suppressive oligodeoxynucleotides, Arthritis Rheum. 46 (2002) 2219–2224.
[57] R.A. Zeuner, D. Verthelyi, M. Gursel, K.J. Ishii, D.M. Klinman, Influence of stimulatory and suppressive DNA motifs on host susceptibility to inflammatory arthritis, Arthritis Rheum. 48 (2003) 1701–1707.
[58] L.L. Stunz, P. Lenert, D. Peckham, A.K. Yi, S. Haxhinasto, M. Chang, et al., Inhibitory oligonucleotides specifically block effects of stimulatory CpG oligonucleotides in B cells, Eur. J. Immunol. 32 (2002) 1212–1222.
[59] A.M. Avalos, H.L. Ploegh, Competition by inhibitory oligonucleotides prevents binding of CpG to C-terminal TLR9, Eur. J. Immunol. 41 (2011) 2820–2827.
[60] P. Lenert, W. Rasmussen, R.F. Ashman, Z.K. Ballas, Structural characterization of the inhibitory DNA motif for the type A (D)-CpG-induced cytokine secretion and NK-cell lytic activity in mouse spleen cells, DNA Cell Biol. 22 (2003) 621–631.
[61] P. Lenert, A.J. Goeken, R.F. Ashman, Extended sequence preferences for oligodeoxyribonucleotide activity, Immunology 117 (2006) 474–481.
[62] R.F. Ashman, J.A. Goeken, J. Drahos, P. Lenert, Sequence requirements for oligodeoxyribonucleotide inhibitory activity, Int. Immunol. 17 (2005) 411–420.
[63] E. Latz, A. Verma, A. Visintin, M. Gong, C.M. Sirois, D.C. Klein, et al., Ligand-induced conformational changes allosterically activate toll-like receptor 9, Nat. Immunol. 8 (2007) 772–779.
[64] P. Lenert, L. Stunz, A.K. Yi, A.M. Krieg, R.F. Ashman, CpG stimulation of primary mouse B cells is blocked by inhibitory oligodeoxyribonucleotides at a site proximal to NF-kappaB activation, Antisense Nucleic Acid Drug Dev. 11 (2001) 247–256.
[65] P. Lenert, A.K. Yi, A.M. Krieg, L.L. Stunz, R.F. Ashman, Inhibitory oligonucleotides block the induction of AP-1 transcription factor by stimulatory CpG oligonucleotides in B cells, Antisense Nucleic Acid Drug Dev. 13 (2003) 143–150.
[66] P. Lenert, K. Yasuda, L. Busconi, P. Nelson, C. Fleenor, R.S. Ratnabalasuriar, et al., DNA-like class R inhibitory oligonucleotides (INH-ODNs) preferentially block autoantigen-induced B-cell and dendritic cell activation in vitro and autoantibody production in lupus-prone MRL-Fas(lpr/lpr) mice in vivo, Arthritis Res. Ther. 11 (2009) R79.

[67] F. Rommler, M. Jurk, E. Uhlmann, M. Hammel, A. Waldhuber, L. Pfeiffer, et al., Guanine modification of inhibitory oligonucleotides potentiates their suppressive function, J. Immunol. 191 (2013) 3240–3253.
[68] F. Rommler, M. Hammel, A. Waldhuber, T. Muller, M. Jurk, E. Uhlmann, et al., Guanine-modified inhibitory oligonucleotides efficiently impair, PLoS One 10 (2015) e0116703.
[69] P.I. Fields, R.V. Swanson, C.G. Haidaris, F. Heffron, Mutants of *Salmonella typhimurium* that cannot survive within the macrophage are avirulent, Proc. Natl. Acad. Sci. U. S. A. 83 (1986) 5189–5193.
[70] A. Trieu, N. Bokil, J.A. Dunn, T.L. Roberts, D. Xu, F.Y. Liew, et al., TLR9-independent effects of inhibitory oligonucleotides on macrophage responses to *S. typhimurium*, Immunol. Cell Biol. 87 (2009) 218–225.
[71] M. Peter, K. Bode, G.B. Lipford, F. Eberle, K. Heeg, A.H. Dalpke, Characterization of suppressive oligodeoxynucleotides that inhibit toll-like receptor-9-mediated activation of innate immunity, Immunology 123 (2008) 118–128.
[72] P.P. Ho, P. Fontoura, P.J. Ruiz, L. Steinman, H. Garren, An immunomodulatory GpG oligonucleotide for the treatment of autoimmunity via the innate and adaptive immune systems, J. Immunol. 171 (2003) 4920–4926.
[73] P.P. Ho, P. Fontoura, M. Platten, R.A. Sobel, J.J. DeVoss, L.Y. Lee, et al., A suppressive oligodeoxynucleotide enhances the efficacy of myelin cocktail/IL-4-tolerizing DNA vaccination and treats autoimmune disease, J. Immunol. 175 (2005) 6226–6234.
[74] K.L. Graham, L.Y. Lee, J.P. Higgins, L. Steinman, P.J. Utz, P.P. Ho, Treatment with a toll-like receptor inhibitory GpG oligonucleotide delays and attenuates lupus nephritis in NZB/W mice, Autoimmunity 43 (2010) 140–155.
[75] M. Heikenwalder, M. Polymenidou, T. Junt, C. Sigurdson, H. Wagner, S. Akira, et al., Lymphoid follicle destruction and immunosuppression after repeated CpG oligodeoxynucleotide administration, Nat. Med. 10 (2004) 187–192.
[76] F. Fallarino, P. Puccetti, Toll-like receptor 9-mediated induction of the immunosuppressive pathway of tryptophan catabolism, Eur. J. Immunol. 36 (2006) 8–11.
[77] C. Volpi, F. Fallarino, R. Bianchi, C. Orabona, L.A. De, C. Vacca, et al., A GpC-rich oligonucleotide acts on plasmacytoid dendritic cells to promote immune suppression, J. Immunol. 189 (2012) 2283–2289.
[78] H. Yanai, A. Matsuda, J. An, R. Koshiba, J. Nishio, H. Negishi, et al., Conditional ablation of HMGB1 in mice reveals its protective function against endotoxemia and bacterial infection, Proc. Natl. Acad. Sci. U. S. A. 110 (2013) 20699–20704.
[79] O. Duramad, K.L. Fearon, B. Chang, J.H. Chan, J. Gregorio, R.L. Coffman, et al., Inhibitors of TLR-9 act on multiple cell subsets in mouse and man in vitro and prevent death in vivo from systemic inflammation, J. Immunol. 174 (2005) 5193–5200.
[80] R. Sun, L. Sun, M. Bao, Y. Zhang, L. Wang, X. Wu, et al., A human microsatellite DNA-mimicking oligodeoxynucleotide with CCT repeats negatively regulates TLR7/9-mediated innate immune responses via selected TLR pathways, Clin. Immunol. 134 (2010) 262–276.
[81] M. Fang, M. Wan, S. Guo, R. Sun, M. Yang, T. Zhao, et al., An oligodeoxynucleotide capable of lessening acute lung inflammatory injury in mice infected by influenza virus, Biochem. Biophys. Res. Commun. 415 (2011) 342–347.
[82] F.J. Barrat, T. Meeker, J. Gregorio, J.H. Chan, S. Uematsu, S. Akira, et al., Nucleic acids of mammalian origin can act as endogenous ligands for toll-like receptors and may promote systemic lupus erythematosus, J. Exp. Med. 202 (2005) 1131–1139.
[83] C. Guiducci, C. Tripodo, M. Gong, S. Sangaletti, M.P. Colombo, R.L. Coffman, et al., Autoimmune skin inflammation is dependent on plasmacytoid dendritic cell activation by nucleic acids via TLR7 and TLR9, J. Exp. Med. 207 (2010) 2931–2942.
[84] F.J. Barrat, T. Meeker, J.H. Chan, C. Guiducci, R.L. Coffman, Treatment of lupus-prone mice with a dual inhibitor of TLR7 and TLR9 leads to reduction of autoantibody production and amelioration of disease symptoms, Eur. J. Immunol. 37 (2007) 3582–3586.
[85] R.D. Pawar, A. Ramanjaneyulu, O.P. Kulkarni, M. Lech, S. Segerer, H.J. Anders, Inhibition of toll-like receptor-7 (TLR-7) or TLR-7 plus TLR-9 attenuates glomerulonephritis and lung injury in experimental lupus, J. Am. Soc. Nephrol. 18 (2007) 1721–1731.
[86] P. Lenert, Inhibitory oligodeoxynucleotides—therapeutic promise for systemic autoimmune diseases? Clin. Exp. Immunol. 140 (2005) 1–10.
[87] P.S. Patole, D. Zecher, R.D. Pawar, H.J. Grone, D. Schlondorff, H.J. Anders, G-Rich DNA suppresses systemic lupus, J. Am. Soc. Nephrol. 16 (2005) 3273–3280.
[88] C. He, L. Zhou, R. Sun, T. Zhao, Y. Zhang, Y. Fu, et al., Effects of oligodeoxynucleotide with CCT repeats on chronic graft versus host disease induced experimental lupus nephritis in mice, Clin. Immunol. 140 (2011) 300–306.
[89] Y.Z. Wang, Q.H. Liang, H. Ramkalawan, W. Zhang, W.B. Zhou, B. Xiao, et al., Inactivation of TLR9 by a suppressive oligodeoxynucleotides can ameliorate the clinical signs of EAN, Immunol. Invest. 41 (2012) 171–182.
[90] Y.S. Zhang, X.L. Wu, Y. Wang, R. Sun, Y.L. Yu, L.Y. Wang, Structure-activity relationship of a guanine-free oligodeoxynucleotide as immunopotent inhibitor, Int. Immunopharmacol. 13 (2012) 446–453.
[91] D.A. Schwartz, T.J. Quinn, P.S. Thorne, S. Sayeed, Y. Ae, A.M. Krieg, CpG motifs in bacterial DNA cause inflammation in the lower respiratory tract, J. Clin. Invest. 100 (1997) 68–73.
[92] P. Markowski, O. Boehm, L. Goelz, A.L. Haesner, H. Ehrentraut, K. Bauerfeld, et al., Pre-conditioning with synthetic CpG-oligonucleotides attenuates myocardial ischemia/reperfusion injury via IL-10 up-regulation, Basic Res. Cardiol. 108 (2013) 376.
[93] O. Boehm, P. Markowski, G.M. van der, V. Gielen, A. Kokalova, C. Brill, et al., In vivo TLR9 inhibition attenuates CpG-induced myocardial dysfunction, Mediators Inflamm. 2013 (2013) 217297.
[94] Y. Ito, S. Shigemori, T. Sato, T. Shimazu, K. Hatano, H. Otani, et al., Class I/II hybrid inhibitory oligodeoxynucleotide exerts Th1 and Th2 double immunosuppression, FEBS Open Bio 3 (2013) 41–45.
[95] H. Han, L.H. Hurley, G-Quadruplex DNA: a potential target for anti-cancer drug design, Trends Pharmacol. Sci. 21 (2000) 136–142.
[96] A.I. Murchie, D.M. Lilley, Retinoblastoma susceptibility genes contain 5′ sequences with a high propensity to form guanine-tetrad structures, Nucleic Acids Res. 20 (1992) 49–53.
[97] R.F. Ashman, J.A. Goeken, P.S. Lenert, Aggregation and secondary loop structure of oligonucleotides do not determine their ability to inhibit TLR9, Int. Immunopharmacol. 11 (2011) 1032–1037.
[98] N. Jing, Y. Li, X. Xu, W. Sha, P. Li, L. Feng, et al., Targeting Stat3 with G-quartet oligodeoxynucleotides in human cancer cells, DNA Cell Biol. 22 (2003) 685–696.
[99] C.A. Stein, Y.C. Cheng, Antisense oligonucleotides as therapeutic agents—is the bullet really magical? Science 261 (1993) 1004–1012.
[100] K.J. Stacey, G.R. Young, F. Clark, D.P. Sester, T.L. Roberts, S. Naik, et al., The molecular basis for the lack of immunostimulatory activity of vertebrate DNA, J. Immunol. 170 (2003) 3614–3620.
[101] M. Jurk, A. Kritzler, B. Schulte, S. Tluk, C. Schetter, A.M. Krieg, et al., Modulating responsiveness of human TLR7 and 8 to small molecule ligands with T-rich phosphorothiate oligodeoxynucleotides, Eur. J. Immunol. 36 (2006) 1815–1826.
[102] D.M. Klinman, I. Gursel, S. Klaschik, L. Dong, D. Currie, H. Shirota, Therapeutic potential of oligonucleotides expressing immunosuppressive TTAGGG motifs, Ann. N. Y. Acad. Sci. 1058 (2005) 87–95.
[103] R.F. Ashman, J.A. Goeken, E. Latz, P. Lenert, Optimal oligonucleotide sequences for TLR9 inhibitory activity in human cells: lack of correlation with TLR9 binding, Int. Immunol. 23 (2011) 203–214.
[104] K.L. Graham, L.Y. Lee, J.P. Higgins, L. Steinman, P.J. Utz, P.P. Ho, Treatment with a toll-like receptor inhibitory GpG oligonucleotide delays and attenuates lupus nephritis in NZB/W mice, Autoimmunity 43 (2010) 140–155.
[105] P.P. Ho, P. Fontoura, M. Platten, R.A. Sobel, J.J. DeVoss, L.Y. Lee, et al., A suppressive oligodeoxynucleotide enhances the efficacy of myelin cocktail/IL-4-tolerizing DNA vaccination and treats autoimmune disease, J. Immunol. 175 (2005) 6226–6234.
[106] M.K. Wloch, S. Pasquini, H.C. Ertl, D.S. Pisetsky, The influence of DNA sequence on the immunostimulatory properties of plasmid DNA vectors, Hum. Gene Ther. 9 (1998) 1439–1447.
[107] M.D. Halpern, D.S. Pisetsky, In vitro inhibition of murine IFN gamma production by phosphorothioate deoxyguanosine oligomers, Immunopharmacology 29 (1995) 47–52.
[108] P.S. Patole, H.J. Grone, S. Segerer, R. Ciubar, E. Belemezova, A. Henger, et al., Viral double-stranded RNA aggravates lupus nephritis through toll-like receptor 3 on glomerular mesangial cells and antigen-presenting cells, J. Am. Soc. Nephrol. 16 (2005) 1326–1338.

The Journal of Immunology

# Effect of TLR Agonists on the Differentiation and Function of Human Monocytic Myeloid-Derived Suppressor Cells

Jing Wang, Yuko Shirota, Defne Bayik, Hidekazu Shirota, Debra Tross, James L. Gulley, Lauren V. Wood, Jay A. Berzofsky and Dennis M. Klinman

*J Immunol* 2015; 194:4215-4221; Prepublished online 30 March 2015;
doi: 10.4049/jimmunol.1402004
http://www.jimmunol.org/content/194/9/4215



*The Journal of Immunology* is published twice each month by
The American Association of Immunologists, Inc.,
9650 Rockville Pike, Bethesda, MD 20814-3994.

Print ISSN: 0022-1767 Online ISSN: 1550-6606.

# Effect of TLR Agonists on the Differentiation and Function of Human Monocytic Myeloid-Derived Suppressor Cells

**Jing Wang,*[,1,2] Yuko Shirota,*[,1,3] Defne Bayik,* Hidekazu Shirota,*[,4] Debra Tross,* James L. Gulley,[†] Lauren V. Wood,[‡] Jay A. Berzofsky,[‡] and Dennis M. Klinman***

**Tumors persist by occupying immunosuppressive microenvironments that inhibit the activity of tumoricidal T and NK cells. Monocytic myeloid-derived suppressor cells (mMDSC) are an important component of this immunosuppressive milieu. We find that the suppressive activity of mMDSC isolated from cancer patients can be reversed by treatment with TLR7/8 agonists, which induce human mMDSC to differentiate into tumoricidal M1-like macrophages. In contrast, agonists targeting TLR1/2 cause mMDSC to mature into immunosuppressive M2-like macrophages. These two populations of macrophage are phenotypically and functionally discrete and differ in gene expression profile. The ability of TLR7/8 agonists to reverse mMDSC-mediated immune suppression suggests that they might be useful adjuncts for tumor immunotherapy.** ***The Journal of Immunology*****, 2015, 194: 4215–4221.**

Cancers survive by creating an immunosuppressive microenvironment that inhibits the activity of cytotoxic T and NK cells (1, 2). Myeloid-derived suppressor cells (MDSC) constitute most of these tumor-infiltrating leukocytes and are key contributors to the immunosuppressive milieu that protects tumors from elimination. MDSC arise in the bone marrow from myeloid progenitors (3, 4) and expand in patients with cancer. Although both granulocytic and monocytic MDSC (mMDSC) inhibit T and NK cell responses, mMDSC are more suppressive on a per cell basis (5–7) and promote the generation and expansion of regulatory T cells that further interfere with antitumor immunity (8). In clinical trials, agents that block the activity of mMDSC reduce Treg frequency and improve the efficacy of cancer immunotherapy (9–11). These observations support efforts to identify strategies that can be used in the clinic to inhibit mMDSC-mediated immune suppression.

Murine mMDSC express TLR9 and respond to stimulation by the TLR9 agonist CpG oligodeoxynucleotide (ODN) by differentiating into tumoricidal macrophages (12). In vivo administration of CpG ODN prevents the growth of murine tumors, an outcome linked to increased activity by tumoricidal T cells (12). These findings led us to examine whether the maturation and function of human mMDSC might also be altered by TLR agonists. Consistent with the finding that human mMDSC express TLRs 2, 7, and 8 (but not 9), stimulation with the TLR1/2 agonist $Pam_3CSK_4$ (PAM3) induced them to differentiate into immunosuppressive M2-like macrophages that expressed high levels of CD11b. In contrast, stimulation via TLR7/8 caused these mMDSC to differentiate into tumoricidal M1-like macrophages with low CD11b expression. Microarray analysis identified genes that were upregulated during the process of mMDSC differentiation and additional genes uniquely associated with the generation of M1-like macrophages. Because TLR7/8 agonists induce mMDSC from patients with cancer to lose their immunosuppressive capability and differentiate into tumoricidal M1-like macrophages, we propose their use as adjuncts during tumor immunotherapy.

## Materials and Methods

### *Reagents*

R848 and PAM3 were purchased from InvivoGen (San Diego, CA). The Live/Dead cell stain kit was purchased from Invitrogen (Eugene, OR). 3M-052 and CL-075 were gifts of Dr. John Vasilakos (3M Drug Delivery Systems, St. Paul, MN). Immunostimulatory CpG ODN was synthesized at the Core Facility of the Center for Biologics Evaluation and Research of the Food and Drug Administration (Bethesda, MD). All Abs used to purify and stain human MDSC were obtained from BD Biosciences (Franklin Lakes, NJ) except for anti-CD200 glycoprotein receptor (CD200R), which was obtained from R&D Systems (Minneapolis, MN).

### *Cell preparation*

Leukapheresis, buffy coats, and PBMC were obtained from patients and healthy volunteers who gave written informed consent to participate in an Institutional Review Board–approved study for the collection of blood samples for in vitro research use (National Institutes of Health, Bethesda, MD). In some cases, PBMC were frozen and stored at −80° until use. These samples were thawed, washed, and resuspended in RPMI 1640 containing 10% FBS. Fresh or previously frozen PBMC were isolated over a Ficoll-Hypaque gradient, stained with fluorochrome-conjugated Abs against CD33, CD3, CD19, CD57, HLA-DR, CD11b, and/or CD14 and then FACS sorted to isolate mMDSC as defined by the following characteristics: $CD33^+$, $Lin^-$ ($CD3/19/57^-$), $HLA\text{-}DR^-$, $CD11b^+$, and $CD14^{hi}$. Syngeneic $CD4^+$ T cells were isolated from PBMC by negative selection using the naive $CD4^+$ T cell isolation kit II from Miltenyi Biotec (Auburn, CA) as recommended by the manufacturer.

### *T cell proliferation assay*

$CD4^+$ T cells were purified using MACS, labeled with 1 μM CFSE, and stimulated with anti-CD3/28–coated beads at a bead/cell ratio of 1:1. FACS-purified mMDSC plus R848 (3 μg/ml), PAM3 (1 μg/ml), and/or

*Cancer and Inflammation Program, Frederick National Laboratory for Cancer Research, National Cancer Institute, Frederick, MD 21702; [†]Genitourinary Malignancies Branch, National Cancer Institute, Bethesda, MD 20892; and [‡]Vaccine Branch, Center for Cancer Research, National Cancer Institute, Bethesda, MD 20892

[1]J.W. and Y.S. contributed equally to this work.

[2]Current address: Hebei Provincial Cancer Institute, Shijiazhuang, Hebei, China.

[3]Current address: Departments of Hematology and Rheumatology, Tohoku University Hospital, Sendai, Japan.

[4]Current address: Department of Clinical Oncology, Tohoku University Hospital, Sendai, Japan.

Received for publication August 11, 2014. Accepted for publication March 1, 2015.

The microarray data presented in this article have been submitted to the National Center for Biotechnology Information Gene Expression Omnibus under accession number GSE57032.

Address correspondence and reprint requests to Dr. Dennis M. Klinman, Frederick National Laboratory for Cancer Research, Building 567, Room 205, Frederick, MD 21702. E-mail address: klinmand@mail.nih.gov

The online version of this article contains supplemental material.

Abbreviations used in this article: aRNA, amplified RNA; CD200R, CD200 glycoprotein receptor; MDSC, myeloid-derived suppressor cell; MFI, mean fluorescence intensity; mMDSC, monocytic MDSC; ODN, oligodeoxynucleotide; PAM3, $Pam_3CSK_4$.

www.jimmunol.org/cgi/doi/10.4049/jimmunol.1402004

anti-CD11b were added for 3 d. Cell division as determined by CFSE content was determined using an LSR II (BD Biosciences).

### *Surface marker expression by mMDSC*

FACS-purified mMDSC were cultured with 1 μg PAM3 or 3 μg R848 for 3 d and stained with fluorescence-conjugated Abs against 25F9, CD200R, CD206, CD80, CD86, and/or CD11b for 30 min on ice. Cells were washed, resuspended in PBS/0.1% BSA plus sodium azide, and analyzed using the LSR II.

### *Detection of intracytoplasmic and secreted cytokines*

FACS-purified mMDSC were cultured for 72 h with PAM3 or R848 as described above. PMA (50 ng/ml), ionomycin (500 ng/ml), and brefeldin A (10 μg/ml) (Sigma-Aldrich, St. Louis, MO) were added during the final 5 h of culture. Cells were then treated with permeabilization solution (BD Pharmingen, Franklin Lakes, NJ) and stained with Abs specific for IL-6, IL-12, and/or IL-10. The frequency of internally stained mMDSC was determined by LSR II.

### *Cytotoxicity function assay*

MDSC were FACS sorted from PBMC of healthy donors and cultured for 3 d with R848 or PAM3 as described above. A549 tumor cells were then mixed with the MDSC for 6 h at a 1:40 ratio. The cells were then stained with Fl-conjugated anti-EGFR Ab and fluorescent-reactive dye for 30 min on ice. Cells were washed, resuspended in PBS/0.1% BSA plus sodium azide, and lysed tumor cells were identified using an LSR II.

### *Microarray analysis of gene expression*

Total RNA was extracted from FACS-purified mMDSC using the RNeasy mini kit (Qiagen) as previously described (13). The RNA was reverse transcribed into cDNA and transcribed in vitro using T7 RNA polymerase into antisense amplified RNA (aRNA) using the Amino Allyl MessageAmp II aRNA kit (Ambion/Life Technologies, Grand Island, NY). aRNA from mMDSC samples was labeled with Cy5 monoreactive dye (Amersham Biosciences, Piscataway, NJ). A reference human sample (Stratagene) was processed in parallel and labeled with Cy3. For the coupling reaction, 10 μl aRNA (2–4 μg) in 0.1 M bicarbonate buffer (pH 8.7) was added to Cy3 or Cy5 in DMSO for 2 h in a final volume of 20 μl. Unreacted Cy dye was quenched with 18 μl 4 M hydroxylamine and labeled aRNA isolated using an RNeasy MinElute kit (Qiagen).

Human ODN microarrays were produced by Microarrays (Huntsville, AL). Cy3-labeled reference and Cy5-labeled sample aRNAs (15 μl each) were combined, denaturated by heating for 2 min at 98°C, and mixed with 18 μl hybridization solution at 42°C (Ambion, Austin, TX). Microarrays were overlaid with this solution and hybridized for 18 h at 42°C using an actively mixing MAUI hybridization system (BioMicro Systems, Salt Lake City, UT). The arrays were washed after hybridization, dried, and scanned using an Axon scanner equipped with GenePix software 5.1 (Axon Instruments, Foster City, CA). Data were uploaded to the mAdb (a collaboration of the Center for Information Technology/Bioinformatics and Molecular Analysis Section and National Cancer Institute/Center for Cancer Research at the National Institutes of Health; http://nciarray.nci.nih.gov/) and formatted.

Raw microarray data from four independent donors were processed as previously described (13). The gene expression profile of treated cells was compared with baseline values of untreated cells from the same donor. Genes that were upregulated by >5-fold in all donors were identified.

### *Accession codes*

Microarray data were deposited in the National Center for Biotechnology Information Gene Expression Omnibus (http://www.ncbi.nlm.nih.gov/geo/) and are accessible through accession number GSE57032.

### *Statistical analysis*

A two-sided unpaired Student *t* test was used to analyze cellular responses. A *p* value <0.05 was considered to be statistically significant.

## Results

### *Human mMDSC suppress T cell proliferation*

Normal healthy volunteers were leukapheresed and mMDSC isolated by FACS sorting based on their expression of CD14, CD11b, and CD33 coupled with the absence of HLA-DR and the lineage markers CD3, CD19, and CD57 (Fig. 1A). mMDSC constituted 0.4 ± 0.3% of PBMC in normal donors.

To examine the functional activity of these purified mMDSC, their interaction with $CD4^+$ T cells was examined. Syngeneic $CD4^+$ T cells were labeled with CFSE and stimulated to proliferate with anti-CD3/anti-CD28–coated beads. Adding mMDSC to these activated T cells resulted in a dose-dependent inhibition of proliferation ($p < 0.05$, Fig. 1B, 1C) (12, 14).

### *Effect of TLR agonists on the phenotype of human mMDSC*

Previous studies showed that stimulating murine mMDSC with a TLR9 agonist prevented tumor growth (12). This led us to examine the effect of treating human mMDSC with various TLR agonists targeting TLRs 1, 2, 3, 4, 7, 8, and 9. Cell yields after 3 d showed the greatest increase in cultures containing the TLR1/2 agonist PAM3 or the TLR7/8 agonist R848. Eighty to 90% of the viable cells in these cultures upregulated expression of 25F9, a surface marker identifying mature macrophages ($p < 0.01$, Fig. 2A, 2B). In the absence of stimulation, <20% of human mMDSC survived and <10% of those typically upregulated 25F9 expression (Fig. 2A, 2B). Subsequent experiments focused on clarifying the effects of PAM3 and R848 on human mMDSC.

Macrophages are categorized into classically activated M1-like or alternatively activated M2-like subsets (15). Although both M1- and M2-like macrophages express 25F9, those of the M2 subset can also express the CD200R and the mannose receptor CD206 (16, 17). When human mMDSC were cultured with PAM3, >70% of the resulting $25F9^+$ macrophages expressed the two M2-

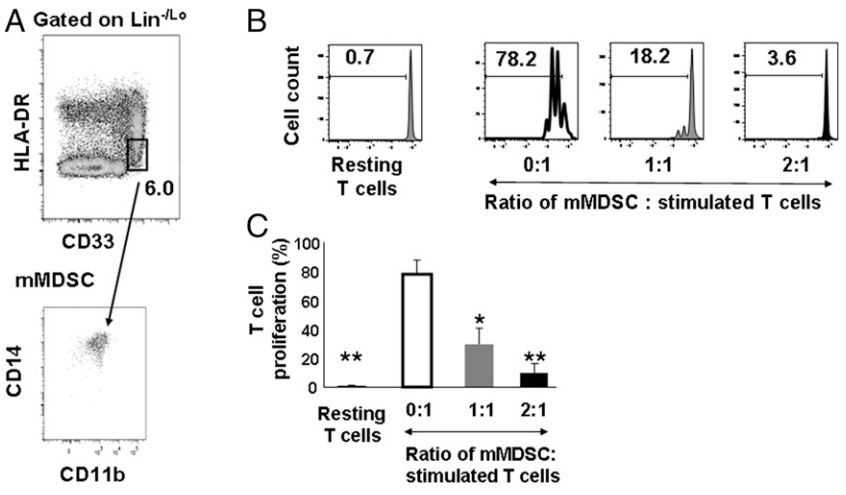


**FIGURE 1.** mMDSC from normal volunteers suppress T cell proliferation. (**A**) mMDSC were identified based on their pattern of surface marker expression: $Lin^-$, $HLA\text{-}DR^-$, $CD33^+$, $CD14^{hi}$, and $CD11b^+$. (**B** and **C**) mMDSC were FACS purified whereas syngeneic $CD4^+$ T cells were purified from the same donor sample by MACS. T cells ($10^5$) were labeled with CFSE, stimulated with anti-CD3/28–coated beads, and cultured with 1–2 × $10^5$ mMDSC. T cell proliferation was examined on day 3. (B) Representative example and (C) combined results (mean ± SD) of nine independently studied donors are shown. *$p < 0.05$, **$p < 0.01$ versus anti-CD3/28–treated T cells alone.

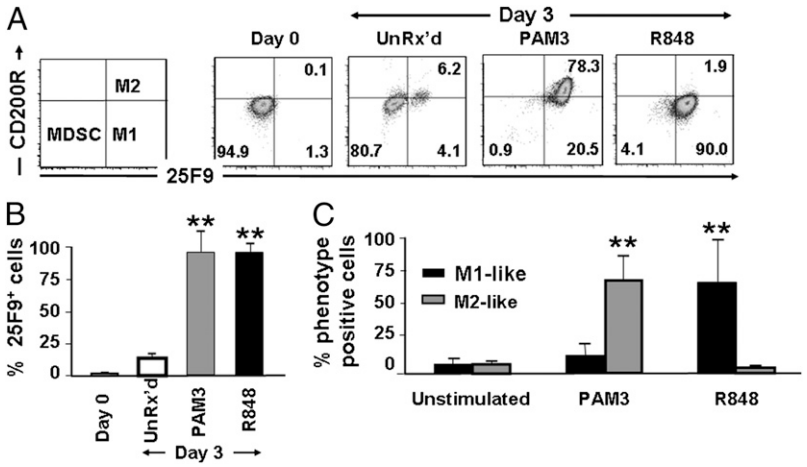


**FIGURE 2.** R848 and PAM3 induce mMDSC to differentiate into macrophages. mMDSC were purified from normal donors as described in Fig. 1 and stimulated in vitro with PAM3 (1 μg/ml) or R848 (3 μg/ml). 25F9 and CD200R expression was examined on day 3. (**A**) Representative example showing changes in surface marker expression over time. (**B**) Change in the percentage of $25F9^+$ cells (mean ± SD) of nine independently studied donors. (**C**) The percentage of cultured cells bearing an M1-like ($25F9^+/CD200R^-$) versus M2-like ($25F9^+/CD200R^+$) phenotype was determined by independently analyzing 12 donors/group (mean ± SD). $^{**}p < 0.01$ versus unstimulated cultures.

associated surface markers, CD200R and CD206 (Fig. 2A, 2C, Supplemental Fig. 1). In contrast, >70% of the cells cultured with R848 upregulated 25F9 but failed to express these M2-associated surface markers and thus were phenotypically M1-like. The same effect was observed when mMDSC were cultured with the selective TLR7 agonist 3M-055 or the TLR8 selective agonist CL-075 (Supplemental Fig. 2). In the absence of stimulation, only a small fraction (generally <10%) of mMDSC survived or expressed 25F9. Those displayed a balanced M1/M2 phenotypic ratio (Fig. 2A, 2C, Supplemental Fig. 2).

*Cytokine production by mMDSC cultured with TLR agonists*

Previous studies established that M1 macrophages protect the host from infection and support tumor destruction in vivo (18–23). Classical M1-like macrophages are characterized by their ability to present Ag, support the development of type I polarized immune responses, and produce proinflammatory cytokines (including IL-12). In contrast, M2-like macrophages have been shown to produce immunosuppressive factors (such as IL-10), to support Th2 immunity, and to support tumor growth (24, 25). The cytokine profile of macrophages generated when human mMDSC were triggered via their TLRs was therefore analyzed. After 3 d in culture with PAM3, ≈90% of the cells produced IL-10 but not IL-12 (consistent with an M2 profile) whereas the cells generated in the presence of R848 produced IL-12 but not IL-10 (consistent with an M1 profile; Fig. 3, Supplemental Fig. 3). Nearly all of the cells cultured in the presence of either PAM3 or R848 produced IL-6.

*Functional activity of mMDSC cultured with TLR agonists*

Two assays were used to assess the function of cells generated after human mMDSC were stimulated with PAM3 or R848. In the first, their ability to kill A549 tumor targets was evaluated. mMDSC incubated with PAM3 did not acquire the ability to lyse tumor targets, consistent with their M2-like character (Fig. 4). In contrast, mMDSC cultured with R848, 3M-052, or CL-075 gained the ability to lyse A549 tumor cells ($p < 0.01$, Fig. 4, Supplemental Fig. 3A).

The second assay examined their ability to inhibit T cell proliferation. Syngeneic $CD4^+$ T cells and mMDSC were copurified from leukapheresis samples. The T cells were stimulated to proliferate by the addition of anti-CD3/28–coated beads. This proliferation was inhibited by freshly isolated mMDSC (Fig. 5). The same outcome was observed when mMDSC cultured for 3 d with PAM3 were added: the M2-like macrophages generated in vitro suppressed T cell proliferation. In contrast, mMDSC cultured with R848, 3M-052, or CL-075 lost their ability to inhibit T cell proliferation and thus behaved similar to M1-like macrophages (Fig. 5, Supplemental Fig. 3B). This outcome could not be attributed to any direct effect of PAM3 or R848 on T cells, as anti-CD3/CD28–stimulated T cells proliferated normally in cultures supplemented with these TLR agonists but lacking mMDSC.

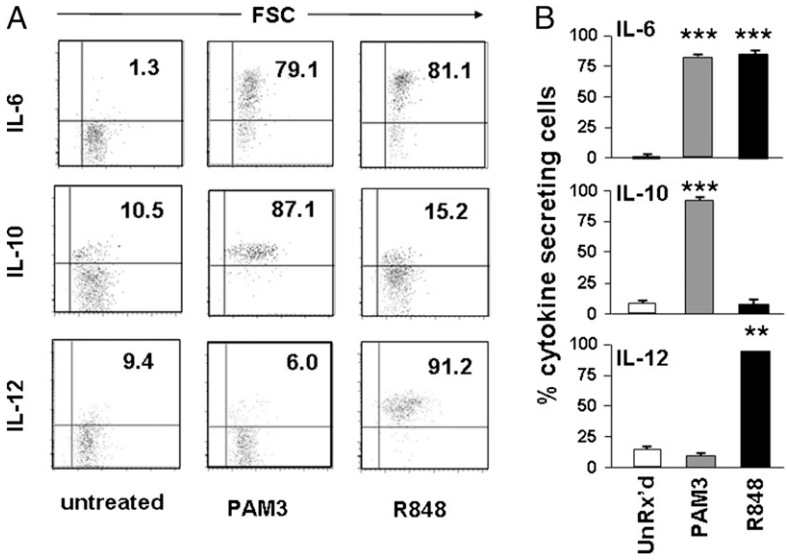


**FIGURE 3.** Effect of TLR stimulation on cytokine production by mMDSC. mMDSC were purified as described in Fig. 1 and stimulated with PAM3 or R848 as described in Fig. 2. The cells were cultured for 1–3 d with brefeldin A being added during the final 5 h. The cells were then permeabilized and stained with Abs specific for IL-6, IL-10, or IL-12. The frequency of mMDSC containing intracytoplasmic cytokine was determined by LSR II. (**A**) Representative example of cytokine production by cells stimulated with R848 or PAM3. (**B**) Mean ± SD of samples from four independently analyzed donors per group. $^{**}p < 0.01$, $^{***}p < 0.001$ versus unstimulated cells.

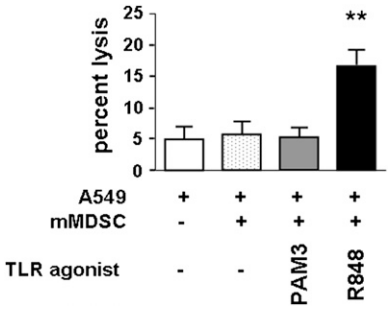


**FIGURE 4.** Effect of TLR stimulation on tumoridal activity. mMDSC were purified as described in Fig. 1 and stimulated with TLR ligands for 3 d as described in Fig. 2. Labeled A549 tumor cells were added to these cultures at an E:T ratio of 40:1, and their viability was determined after 6 h. Data represent the means ± SD of samples from four independently analyzed donors per group. $^{**}p < 0.01$ versus control mMDSC.

*Expression of CD11b is associated with differences in the suppressive activity of mMDSC cultured with R848 versus PAM3*

The above findings establish that both PAM3 and R848 could induce mMDSC to mature into 25F9$^+$ macrophages but that the phenotype and functional activity of mMDSC incubated with PAM3 differed from those exposed to R848. Insight into the mechanism underlying these differences was provided by studies of CD11b. CD11b is a $\beta_2$ integrin expressed by macrophages that plays a critical role in the formation of cell–cell contacts required to suppress T cell activity. Virtually all of the M2-like macrophages generated after 3 d of culture with PAM3 expressed high levels of CD11b$^+$ (Fig. 6A; mean fluorescence intensity [MFI], 4180 ± 636). This contrasted with the M1-like macrophages generated by R848 whose expression of CD11b was markedly lower (Fig. 6A; MFI, 1465 ± 193, $p < 0.02$). The relevance of these findings was clarified by adding neutralizing anti-CD11b Ab to cultures of TCR-stimulated T cells plus syngeneic mMDSC. In the absence of neutralizing Ab, the mMDSC efficiently inhibited T cell proliferation (Fig. 6B, 6C). In the presence of anti-CD11b, this suppressive activity was significantly reduced.

*Effect of TLR agonists on mMDSC from cancer patients*

mMDSC contribute to the suppressive milieu that protects human tumors from immune-mediated elimination. To examine the response of mMDSC from cancer patients to TLR stimulation, peripheral blood was collected from 22 individuals with colon, prostate, pancreatic, or liver cancer (Supplemental Table I). The frequency of mMDSC in these samples ranged from 0.5–9.2%, significantly exceeding the frequency found in normal volunteers

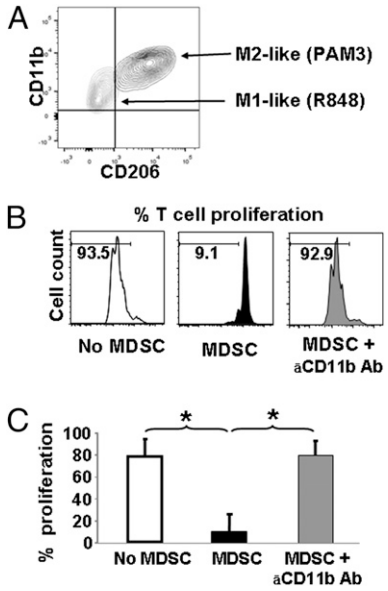


**FIGURE 6.** Effect of R848 and PAM3 on CD11b expression. mMDSC were FACS purified from PBMC and cultured for 3 d in the presence of R848 or PAM3 as described in Fig. 1. (**A**) Representative example of the level of CD11b expression by M1-like macrophages generated by R848 and by M2-like macrophages generated by PAM3. Similar results were observed in three independent experiments and the MFI of each treatment is described in *Results*. (**B** and **C**) mMDSC and CD4$^+$ T cells were purified as described Fig. 1. CFSE-labeled CD4 T cells ($10^5$) were stimulated with anti-CD3/28–coated beads and cultured with $10^5$ syngeneic mMDSC for 3 d in the presence of 10 μg/ml neutralizing anti-CD11b Ab. A representative example of the effect of anti-CD11b on the inhibition of T cell proliferation mediated by the mMDSC is shown in (B). The mean ± SD of this effect in four independently studied donors per group is shown in (C). $^*p < 0.05$ compared with stimulated T cells mixed with mMDSC.

($p < 0.02$). The behavior of mMDSC from cancer patients cultured with TLR agonists was indistinguishable from that of normal controls. PAM3 induced these mMDSC to differentiate into 25F9$^+$, CD200R$^+$ M2-like macrophages that secreted IL-10 and inhibited the proliferation of TCR-stimulated syngeneic T cells (Fig. 7). R848 treatment primarily generated 25F9$^+$, CD200R$^-$ M1-like macrophages that secreted IL-12 and could not suppress T cell proliferation (Fig. 7). mMDSC from patients with different tumor types responded similarly to TLR agonist treatment.

*Changes in gene expression induced by TLR ligation*

Microarrays were used to examine changes in gene expression that accompanied the differentiation of human mMDSC into either M1-

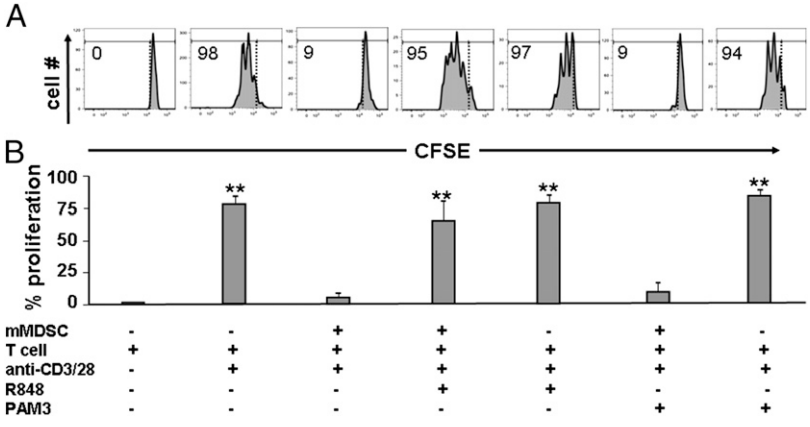


**FIGURE 5.** Effect of TLR stimulation on the ability of mMDSC to inhibit T cell proliferation. mMDSC and CD4$^+$ T cells were purified as described in Fig. 1. mMDSC ($2 \times 10^5$) were cultured with $10^5$ syngeneic CSFE-labeled CD4$^+$ T cells in the presence of anti-CD3/28–coated beads, 3 μg/ml R848, or 1 μg/ml PAM3. T cell proliferation was examined on day 3. (**A**) Representative example of the effect of R848 and PAM3 on the ability of mMDSC to inhibit T cell proliferation. (**B**) The percentage of T cells proliferating (mean ± SD) was determined independently in four to eight donors per treatment group. $^{**}p < 0.01$ versus mMDSC-suppressed cultures.

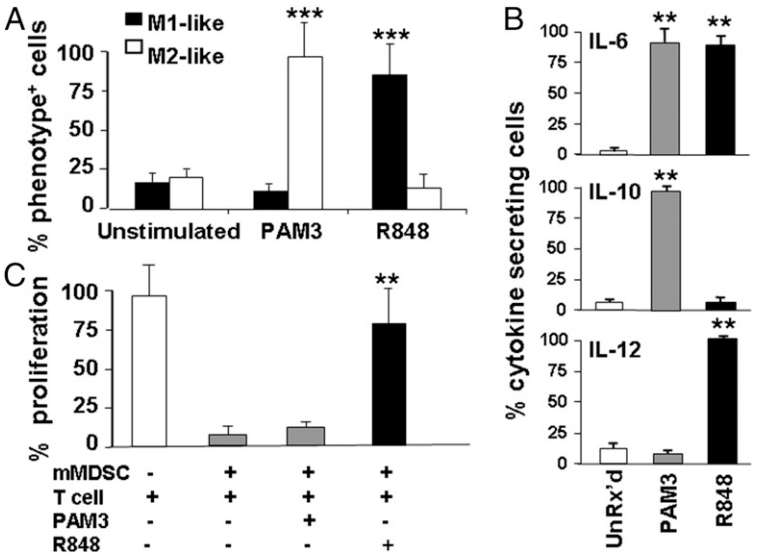


**FIGURE 7.** Effect of TLR stimulation on mMDSC isolated from cancer patients. mMDSC and $CD4^+$ T cells were purified from patient PBMC as described in Fig. 1. The types of cancer studied included: liver ($n$ = 8), pancreatic ($n$ = 5), prostate ($n$ = 4), and GI ($n$ = 5). A description of patient characteristics is provided in Supplemental Table I. The purified cells were cultured in the presence of R848 or PAM3 as described in Fig. 2. (**A**) Cells were stained for surface expression of 25F9 and CD200R on day 3. The percentage of cells (mean ± SD) expressing an M1-like ($25F9^+/CD200R^-$) versus M2-like ($25F9^+/CD200R^+$) phenotype was determined independently in 22 patients. (**B**) The accumulation of intracytoplasmic cytokine was examined in 14 patients as described in Fig. 3. (**C**) mMDSC and syngeneic CSFE-labeled $CD4^+$ T cells were treated as described in Fig. 5. The proliferation of T cells (mean ± SD) was determined independently in samples from four patients. $^{**}p < 0.01$, $^{***}p < 0.001$ versus unstimulated cultures.

or M2-like macrophages. Preliminary experiments revealed extensive variation in baseline mRNA levels among individual volunteers. To compensate for this variability, microarray profiles from TLR-stimulated samples were compared with unstimulated controls from the same donor. A gene was considered to be significantly upregulated when its level of expression rose >5-fold (exceeding the mean ± 3 SD of all upregulated genes) in all donors at any time during the period from 0.5 through 3.5 h poststimulation.

Results showed that >50% of the genes stimulated by R848 were never upregulated by PAM3 whereas >90% of the genes upregulated by PAM3 were also upregulated by R848 (Table I). Because PAM3 treatment generates M2-like macrophages, we hypothesized that the genes upregulated by both TLR agonists were associated with the differentiation of mMDSC into M2-like macrophages. Conversely, as R848 treatment generated M1-like macrophages, we hypothesized that genes uniquely upregulated by R848 influenced the differentiation of M1-like macrophages.

To examine this process of differentiation, mMDSC were incubated with PAM3 for 2 d, washed, and then cultured with R848 for a final day (Table II). Whereas most of the macrophages present after 2 d in culture with PAM3 expressed the M2-associated marker CD200R, exposure to R848 solely on day 3 yielded cultures in which most cells expressed an M1-like phenotype ($25F9^+/CD200R^-$) (Table II). Indeed, the frequency of macrophages with this M1-like phenotype in cultures treated for 2 d with PAM3 and 1 final day with R848 was statistically indistinguishable from that of mMDSC treated for all 3 d with R848. In contrast, treatment with R848 for 2 d induced nearly half of the mMDSC to differentiate into M1-like macrophages, and the frequency of these $25F9^+/CD200R^-$ macrophages was not changed by the addition of PAM3 on day 3 (Table II). These findings are consistent with the interpretation that genes induced by both PAM3 and R848 drive the differentiation of mMDSC into M2-like macrophages whereas the genes uniquely activated by R848 divert this differentiation toward the M1 lineage.

## Discussion

MDSC facilitate the growth and survival of cancer cells by inhibiting the activity of tumoricidal NK and T cells and by secreting factors that support tumor proliferation (3, 4, 7). The importance of mMDSC is underscored by clinical findings showing that their frequency in the peripheral blood of cancer patients correlates with tumor progression and metastatic potential (26–30). Treatments that reduce mMDSC activity have been shown to improve tumor-specific immunity (9, 31–34). Current results demonstrate that agonists targeting TLR7 and TLR8 represent an effective and previously unrecognized means of reducing the immunosuppressive activity of human mMDSC.

Rodent mMDSC express TLR9. When treated in vitro with the TLR9 agonist CpG ODN, murine mMDSC differentiate into tumoricidal M1 macrophages (12). When large established murine

Table I. Genes upregulated by PAM3 and/or R848

| Only PAM3 | Only R848 | Both PAM3 and R848 |
|---|---|---|
| IL8 | BCL2 | ARL5B |
| KBTD8 | BCL2A1 | BAG3 |
| NSMAF | CA2 | C13orf15 |
| OLR1 | CCL2 | CCL20 |
| | CFLAR | CD44 |
| | EDN1 | CD83 |
| | EREG | CXCL1 |
| | FFAR2 | CXCL2 |
| | FLJ37505 | CXCL3 |
| | GEM | DNAJA4 |
| | KCNMA1 | ELOVL6 |
| | LOC338758 | ETNK1 |
| | LOC646329 | F3 |
| | LRRC50 | IL1A |
| | MAP3K8 | IL6 |
| | NFKBIZ | IRG1 |
| | NPR1 | KRT16P2 |
| | OR6K3 | LOC399884 |
| | PLAUR | LY6K |
| | PLLP | MIR155HG |
| | PMAIP1 | PHLDA1 |
| | PNRC1 | PURG |
| | PPP1R15A | RRAD |
| | PTGS2 | SERPINB2 |
| | RECQL4 | ST20 |
| | REPS2 | TNF |
| | RGS1 | ZC3H12C |
| | RGS20 | ZNF784 |
| | RRP7A | |
| | RRP7B | |
| | TNFAIP3 | |
| | TNFAIP6 | |
| | TRIB3 | |
| | ZNF544 | |

mMDSC from four donors were purified and stimulated with PAM3 or R848 for 0, 30, 75, and 225 min. Results show those genes that were reproducibly upregulated (>5-fold increase versus unstimulated cells) in all donors during this period.

Table II. Kinetics of TLR agonist–induced macrophage differentiation

| Day 1 | Day 2 | Day 3 | % M1 | % M2 |
|---|---|---|---|---|
| — | — | — | 5 ± 2 | 6 ± 4 |
| R848 | R848 | R848 | 83 ± 7 | 3 ± 1 |
| PAM3 | PAM3 | PAM3 | 3 ± 1 | 89 ± 5 |
| PAM3 | PAM3 | R848 | 74 ± 11 | 18 ± 4 |
| R848 | R848 | PAM3 | 42 ± 5 | 24 ± 4 |
| R848 | R848 | — | 45 ± 6 | 8 ± 2 |
| PAM3 | PAM3 | — | 7 ± 3 | 27 ± 1 |

mMDSC were purified from normal donors as described in Fig. 1 and stimulated in vitro with PAM3 (1 μg/ml) or R848 (3 μg/ml) for 2 d. The cells were then washed and restimulated with the same or different TLR agonist for a final day. Data show the mean percentage ± SD of cells bearing an M1-like ($25F9^+/CD200R^-$) versus M2-like ($25F9^+/CD200R^+$) phenotype in independent studies of three donors. Results of treating cells for only 2 d are also shown.

tumors were injected with CpG ODN in vivo, infiltrating mMDSC again differentiated into macrophages, an outcome associated with tumor elimination (12). Unfortunately human mMDSC do not express TLR9 or respond to CpG ODN, limiting the clinical applicability of the murine findings. We therefore sought to determine whether other TLR agonists might reduce the immunosuppressive activity of human mMDSC (28). Consistent with the observation that human mMDSC express TLRs 2, 7 and 8, the TLR1/2 agonist PAM3 and the TLR7/8 agonist R848 induced human mMDSC to differentiate into IL-6–secreting $25F9^+$ macrophages (Figs. 2, 3). This is consistent with an earlier finding that R848 caused human PBMC and $CD34^+$ bone marrow cells to differentiate along the myeloid lineage and produce Th1 cytokines (35–37).

Although the signaling pathways triggered by TLRs 2, 7, and 8 are alike in proceeding via MyD88, NF-κB, and MAPK (38, 39), the behavior and phenotype of the macrophages generated by their ligation differed. mMDSC treated with PAM3 matured into "alternatively activated" M2-like macrophages similar to those found in the Th2-polarized environment that characterizes large tumors (40, 41). M2-like macrophages are characterized phenotypically by their expression of CD200R, CD163, and/or CD206 and functionally by their production of factors that support tumor growth and suppress tumor-specific immunity (including glucocorticoids, IL-4, IL-13, and IL-10) (17, 18, 42). As seen in Figs. 2–5 and Supplemental Fig. 1, the $25F9^+$ macrophages generated when mMDSC were cultured with PAM3 expressed CD200R and/or CD206, produced IL-10 (but not IL-12), and inhibited the proliferation of TCR-activated T cells. In contrast, the macrophages generated from mMDSC cultured with R848 were M1-like in phenotype and function: they expressed 25F9 but not CD200R or CD206, secreted the proinflammatory cytokine IL-12 but not IL-10, and lost their ability to suppress T cell proliferation while gaining the ability to lyse tumor cells (Figs. 2–5, Supplemental Figs. 1–3).

Microarray analysis of mRNA isolated from TLR-stimulated mMDSC identified genes associated with 1) the general process of differentiation into macrophages and 2) the generation of M1- versus M2-like macrophages. We found that a common set of genes activated by both PAM3 and R848 supported the generation of M2-like macrophages from mMDSC (Table I). A distinct set of genes was upregulated by R848 but not PAM3 and was associated with the further differentiation of mMDSC into M1-like macrophages. The possibility of M2 macrophages being the "default" pathway is consistent with results obtained from mMDSC cultured sequentially with these TLR agonists. mMDSC treated with PAM3 for 2 d differentiated into M2-like macrophages. Adding R848 for the final day of culture diverted differentiation to yield predominantly M1-like macrophages (Table II). No such diversion was observed when mMDSC were incubated first with R848 and then with PAM3. We are in the process of defining the contribution of specific genes and regulatory pathways to the differentiation of mMDSC into M1- or M2-like macrophages.

CD11b is a $\beta_2$ integrin that forms heterodimers with CD18 to generate Mac-1. Mac-1 mediates much of the ICAM binding activity characteristic of mature macrophages (43). Recent reports suggest that the ability of macrophages to recognize T cells and suppress their proliferation is dependent on the expression of CD11b (43, 44). Indeed, Pillay et al. (44) speculated that CD11b is central to the suppression of T cell function mediated by myeloid cells. We found that R848 did not increase the expression of CD11b by $25F9^+/CD200R^-$ M1-like macrophages, consistent with their loss of immunosuppressive activity (Fig. 6B). Similiary, the addition of neutralizing anti-CD11b Ab abrogated the ability of mMDSC to suppress T cell proliferation (Fig. 6C).

R848 was developed as a topical immune response modifier. When administered systemically, undesirable side effects were observed (including a profound depletion of circulating leukocytes) (45–48). We therefore examined the activity of novel TLR7/8 agonists designed for in vivo use and found to be safe when administered to mice (49, 50). 3M-055 and CL-075 are selective TLR7 and TLR8 agonists, respectively (48, 51). Phenotypic and functional studies showed that each of these agonists duplicated the ability of R848 to induce human mMDSC to mature into M1-like macrophages and thus might be of clinical utility (Supplemental Figs. 2, 3) (52).

mMDSC isolated from patients with liver, pancreatic, prostate, and GI cancers (Supplemental Table I) responded to stimulation by TLR1/2 and TLR7/8 agonists in a manner indistinguishable from that of normal volunteers (Fig. 7). Of particular relevance, patient cells treated with TLR7/8 agonists (including 3M-055 and CL-075) lost their immunosuppressive activity. This parallels the effect of CpG ODN on murine mMDSC, an activity associated with the elimination of large tumors in mice (12, 53, 54). Current findings thus support clinical testing of TLR7/8 agonists as adjuncts to tumor immunotherapy. Conversely, PAM3 may be useful in generating M2-like macrophages that could be useful in the treatment of autoimmune diseases (55, 56).

## Acknowledgments

We thank Kathleen Noer and Roberta Matthai for performing the flow cytometry. We also thank Dr. John Vasilakos of 3M Drug Delivery Systems for providing the 3M-052 and CL-075 used in the supplemental studies.

## Disclosures

The authors have no financial conflicts of interest.

## References

1. Zitvogel, L., A. Tesniere, and G. Kroemer. 2006. Cancer despite immunosurveillance: immunoselection and immunosubversion. *Nat. Rev. Immunol.* 6: 715–727.
2. Muller, A. J., and P. A. Scherle. 2006. Targeting the mechanisms of tumoral immune tolerance with small-molecule inhibitors. *Nat. Rev. Cancer* 6: 613–625.
3. Ostrand-Rosenberg, S., and P. Sinha. 2009. Myeloid-derived suppressor cells: linking inflammation and cancer. *J. Immunol.* 182: 4499–4506.
4. Gabrilovich, D. I., and S. Nagaraj. 2009. Myeloid-derived suppressor cells as regulators of the immune system. *Nat. Rev. Immunol.* 9: 162–174.
5. Bronte, V., and P. Zanovello. 2005. Regulation of immune responses by L-arginine metabolism. *Nat. Rev. Immunol.* 5: 641–654.
6. Rodríguez, P. C., and A. C. Ochoa. 2008. Arginine regulation by myeloid derived suppressor cells and tolerance in cancer: mechanisms and therapeutic perspectives. *Immunol. Rev.* 222: 180–191.
7. Dolcetti, L., E. Peranzoni, S. Ugel, I. Marigo, A. Fernandez Gomez, C. Mesa, M. Geilich, G. Winkels, E. Traggiai, A. Casati, et al. 2010. Hierarchy of immunosuppressive strength among myeloid-derived suppressor cell subsets is determined by GM-CSF. *Eur. J. Immunol.* 40: 22–35.

8. Yin, B., G. Ma, C. Y. Yen, Z. Zhou, G. X. Wang, C. M. Divino, S. Casares, S. H. Chen, W. C. Yang, and P. Y. Pan. 2010. Myeloid-derived suppressor cells prevent type 1 diabetes in murine models. *J. Immunol.* 185: 5828–5834.
9. Ko, J. S., A. H. Zea, B. I. Rini, J. L. Ireland, P. Elson, P. Cohen, A. Golshayan, P. A. Rayman, L. Wood, J. Garcia, et al. 2009. Sunitinib mediates reversal of myeloid-derived suppressor cell accumulation in renal cell carcinoma patients. *Clin. Cancer Res.* 15: 2148–2157.
10. Mirza, N., M. Fishman, I. Fricke, M. Dunn, A. M. Neuger, T. J. Frost, R. M. Lush, S. Antonia, and D. I. Gabrilovich. 2006. All-*trans*-retinoic acid improves differentiation of myeloid cells and immune response in cancer patients. *Cancer Res.* 66: 9299–9307.
11. Nagaraj, S., J. I. Youn, H. Weber, C. Iclozan, L. Lu, M. J. Cotter, C. Meyer, C. R. Becerra, M. Fishman, S. Antonia, et al. 2010. Anti-inflammatory triterpenoid blocks immune suppressive function of MDSCs and improves immune response in cancer. *Clin. Cancer Res.* 16: 1812–1823.
12. Shirota, Y., H. Shirota, and D. M. Klinman. 2012. Intratumoral injection of CpG oligonucleotides induces the differentiation and reduces the immunosuppressive activity of myeloid-derived suppressor cells. *J. Immunol.* 188: 1592–1599.
13. Klaschik, S., D. Tross, and D. M. Klinman. 2009. Inductive and suppressive networks regulate TLR9-dependent gene expression in vivo. *J. Leukoc. Biol.* 85: 788–795.
14. Mao, Y., I. Poschke, E. Wennerberg, Y. Pico de Coaña, S. Egyhazi Brage, I. Schultz, J. Hansson, G. Masucci, A. Lundqvist, and R. Kiessling. 2013. Melanoma-educated $CD14^+$ cells acquire a myeloid-derived suppressor cell phenotype through COX-2-dependent mechanisms. *Cancer Res.* 73: 3877–3887.
15. Locati, M., A. Mantovani, and A. Sica. 2013. Macrophage activation and polarization as an adaptive component of innate immunity. *Adv. Immunol.* 120: 163–184.
16. Koning, N., M. van Eijk, W. Pouwels, M. S. Brouwer, D. Voehringer, I. Huitinga, R. M. Hoek, G. Raes, and J. Hamann. 2010. Expression of the inhibitory CD200 receptor is associated with alternative macrophage activation. *J. Innate Immun.* 2: 195–200.
17. Lolmede, K., L. Campana, M. Vezzoli, L. Bosurgi, R. Tonlorenzi, E. Clementi, M. E. Bianchi, G. Cossu, A. A. Manfredi, S. Brunelli, and P. Rovere-Querini. 2009. Inflammatory and alternatively activated human macrophages attract vessel-associated stem cells, relying on separate HMGB1- and MMP-9-dependent pathways. *J. Leukoc. Biol.* 85: 779–787.
18. Mantovani, A., A. Sica, S. Sozzani, P. Allavena, A. Vecchi, and M. Locati. 2004. The chemokine system in diverse forms of macrophage activation and polarization. *Trends Immunol.* 25: 677–686.
19. Noy, R., and J. W. Pollard. 2014. Tumor-associated macrophages: from mechanisms to therapy. *Immunity* 41: 49–61.
20. Sica, A., P. Larghi, A. Mancino, L. Rubino, C. Porta, M. G. Totaro, M. Rimoldi, S. K. Biswas, P. Allavena, and A. Mantovani. 2008. Macrophage polarization in tumour progression. *Semin. Cancer Biol.* 18: 349–355.
21. Griffith, T. S., S. R. Wiley, M. Z. Kubin, L. M. Sedger, C. R. Maliszewski, and N. A. Fanger. 1999. Monocyte-mediated tumoricidal activity via the tumor necrosis factor-related cytokine, TRAIL. *J. Exp. Med.* 189: 1343–1354.
22. Biswas, S. K., and A. Mantovani. 2010. Macrophage plasticity and interaction with lymphocyte subsets: cancer as a paradigm. *Nat. Immunol.* 11: 889–896.
23. Klimp, A. H., E. G. de Vries, G. L. Scherphof, and T. Daemen. 2002. A potential role of macrophage activation in the treatment of cancer. *Crit. Rev. Oncol. Hematol.* 44: 143–161.
24. Murdoch, C., M. Muthana, S. B. Coffelt, and C. E. Lewis. 2008. The role of myeloid cells in the promotion of tumour angiogenesis. *Nat. Rev. Cancer* 8: 618–631.
25. Sica, A., P. Allavena, and A. Mantovani. 2008. Cancer related inflammation: the macrophage connection. *Cancer Lett.* 267: 204–215.
26. Zea, A. H., P. C. Rodriguez, M. B. Atkins, C. Hernandez, S. Signoretti, J. Zabaleta, D. McDermott, D. Quiceno, A. Youmans, A. O'Neill, et al. 2005. Arginase-producing myeloid suppressor cells in renal cell carcinoma patients: a mechanism of tumor evasion. *Cancer Res.* 65: 3044–3048.
27. Hoechst, B., L. A. Ormandy, M. Ballmaier, F. Lehner, C. Krüger, M. P. Manns, T. F. Greten, and F. Korangy. 2008. A new population of myeloid-derived suppressor cells in hepatocellular carcinoma patients induces $CD4^+CD25^+Foxp3^+$ T cells. *Gastroenterology* 135: 234–243.
28. Gallina, G., L. Dolcetti, P. Serafini, C. De Santo, I. Marigo, M. P. Colombo, G. Basso, F. Brombacher, I. Borrello, P. Zanovello, et al. 2006. Tumors induce a subset of inflammatory monocytes with immunosuppressive activity on $CD8^+$ T cells. *J. Clin. Invest.* 116: 2777–2790.
29. Vuk-Pavlović, S., P. A. Bulur, Y. Lin, R. Qin, C. L. Szumlanski, X. Zhao, and A. B. Dietz. 2010. Immunosuppressive $CD14^+HLA^-DR^{low/-}$ monocytes in prostate cancer. *Prostate* 70: 443–455.
30. Montero, A. J., C. M. Diaz-Montero, C. E. Kyriakopoulos, V. Bronte, and S. Mandruzzato. 2012. Myeloid-derived suppressor cells in cancer patients: a clinical perspective. *J. Immunother.* 35: 107–115.
31. Serafini, P., K. Meckel, M. Kelso, K. Noonan, J. Califano, W. Koch, L. Dolcetti, V. Bronte, and I. Borrello. 2006. Phosphodiesterase-5 inhibition augments endogenous antitumor immunity by reducing myeloid-derived suppressor cell function. *J. Exp. Med.* 203: 2691–2702.
32. Nefedova, Y., M. Fishman, S. Sherman, X. Wang, A. A. Beg, and D. I. Gabrilovich. 2007. Mechanism of all-*trans* retinoic acid effect on tumor-associated myeloid-derived suppressor cells. *Cancer Res.* 67: 11021–11028.
33. Vincent, J., G. Mignot, F. Chalmin, S. Ladoire, M. Bruchard, A. Chevriaux, F. Martin, L. Apetoh, C. Rébé, and F. Ghiringhelli. 2010. 5-Fluorouracil selectively kills tumor-associated myeloid-derived suppressor cells resulting in enhanced T cell-dependent antitumor immunity. *Cancer Res.* 70: 3052–3061.
34. Le, H. K., L. Graham, E. Cha, J. K. Morales, M. H. Manjili, and H. D. Bear. 2009. Gemcitabine directly inhibits myeloid derived suppressor cells in BALB/c mice bearing 4T1 mammary carcinoma and augments expansion of T cells from tumor-bearing mice. *Int. Immunopharmacol.* 9: 900–909.
35. Sioud, M., Y. Fløisand, L. Forfang, and F. Lund-Johansen. 2006. Signaling through Toll-like receptor 7/8 induces the differentiation of human bone marrow $CD34^+$ progenitor cells along the myeloid lineage. *J. Mol. Biol.* 364: 945–954.
36. Tomai, M. A., S. J. Gibson, L. M. Imbertson, R. L. Miller, P. E. Myhre, M. J. Reiter, T. L. Wagner, C. B. Tamulinas, J. M. Beaurline, J. F. Gerster, et al. 1995. Immunomodulating and antiviral activities of the imidazoquinoline S-28463. *Antiviral Res.* 28: 253–264.
37. Wagner, T. L., V. L. Horton, G. L. Carlson, P. E. Myhre, S. J. Gibson, L. M. Imbertson, and M. A. Tomai. 1997. Induction of cytokines in cynomolgus monkeys by the immune response modifiers, imiquimod, S-27609 and S-28463. *Cytokine* 9: 837–845.
38. Kawai, T., and S. Akira. 2010. The role of pattern-recognition receptors in innate immunity: update on Toll-like receptors. *Nat. Immunol.* 11: 373–384.
39. Qian, C., and X. Cao. 2013. Regulation of Toll-like receptor signaling pathways in innate immune responses. *Ann. N. Y. Acad. Sci.* 1283: 67–74.
40. Sica, A., and A. Mantovani. 2012. Macrophage plasticity and polarization: in vivo veritas. *J. Clin. Invest.* 122: 787–795.
41. Mantovani, A., G. Germano, F. Marchesi, M. Locatelli, and S. K. Biswas. 2011. Cancer-promoting tumor-associated macrophages: new vistas and open questions. *Eur. J. Immunol.* 41: 2522–2525.
42. Ambarus, C. A., S. Krausz, M. van Eijk, J. Hamann, T. R. Radstake, K. A. Reedquist, P. P. Tak, and D. L. Baeten. 2012. Systematic validation of specific phenotypic markers for in vitro polarized human macrophages. *J. Immunol. Methods* 375: 196–206.
43. Varga, G., S. Balkow, M. K. Wild, A. Stadtbaeumer, M. Krummen, T. Rothoeft, T. Higuchi, S. Beissert, K. Wethmar, K. Scharffetter-Kochanek, et al. 2007. Active MAC-1 (CD11b/CD18) on DCs inhibits full T-cell activation. *Blood* 109: 661–669.
44. Pillay, J., V. M. Kamp, E. van Hoffen, T. Visser, T. Tak, J. W. Lammers, L. H. Ulfman, L. P. Leenen, P. Pickkers, and L. Koenderman. 2012. A subset of neutrophils in human systemic inflammation inhibits T cell responses through Mac-1. *J. Clin. Invest.* 122: 327–336.
45. Dockrell, D. H., and G. R. Kinghorn. 2001. Imiquimod and resiquimod as novel immunomodulators. *J. Antimicrob. Chemother.* 48: 751–755.
46. Jurk, M., F. Heil, J. Vollmer, C. Schetter, A. M. Krieg, H. Wagner, G. Lipford, and S. Bauer. 2002. Human TLR7 or TLR8 independently confer responsiveness to the antiviral compound R-848. *Nat. Immunol.* 3: 499.
47. Lee, J., T. H. Chuang, V. Redecke, L. She, P. M. Pitha, D. A. Carson, E. Raz, and H. B. Cottam. 2003. Molecular basis for the immunostimulatory activity of guanine nucleoside analogs: activation of Toll-like receptor 7. *Proc. Natl. Acad. Sci. USA* 100: 6646–6651.
48. Gunzer, M., H. Riemann, Y. Basoglu, A. Hillmer, C. Weishaupt, S. Balkow, B. Benninghoff, B. Ernst, M. Steinert, T. Scholzen, et al. 2005. Systemic administration of a TLR7 ligand leads to transient immune incompetence due to peripheral-blood leukocyte depletion. *Blood* 106: 2424–2432.
49. Butchi, N. B., S. Pourciau, M. Du, T. W. Morgan, and K. E. Peterson. 2008. Analysis of the neuroinflammatory response to TLR7 stimulation in the brain: comparison of multiple TLR7 and/or TLR8 agonists. *J. Immunol.* 180: 7604–7612.
50. Gorden, K. B., K. S. Gorski, S. J. Gibson, R. M. Kedl, W. C. Kieper, X. Qiu, M. A. Tomai, S. S. Alkan, and J. P. Vasilakos. 2005. Synthetic TLR agonists reveal functional differences between human TLR7 and TLR8. *J. Immunol.* 174: 1259–1268.
51. Du, J., Z. Wu, S. Ren, Y. Wei, M. Gao, G. J. Randolph, and C. Qu. 2010. TLR8 agonists stimulate newly recruited monocyte-derived cells into potent APCs that enhance HBsAg immunogenicity. *Vaccine* 28: 6273–6281.
52. Le Mercier, I., D. Poujol, A. Sanlaville, V. Sisirak, M. Gobert, I. Durand, B. Dubois, I. Treilleux, J. Marvel, J. Vlach, et al. 2013. Tumor promotion by intratumoral plasmacytoid dendritic cells is reversed by TLR7 ligand treatment. *Cancer Res.* 73: 4629–4640.
53. Balsari, A., M. Tortoreto, D. Besusso, G. Petrangolini, L. Sfondrini, R. Maggi, S. Ménard, and G. Pratesi. 2004. Combination of a CpG-oligodeoxynucleotide and a topoisomerase I inhibitor in the therapy of human tumour xenografts. *Eur. J. Cancer* 40: 1275–1281.
54. Wang, X. S., Z. Sheng, Y. B. Ruan, Y. Guang, and M. L. Yang. 2005. CpG oligodeoxynucleotides inhibit tumor growth and reverse the immunosuppression caused by the therapy with 5-fluorouracil in murine hepatoma. *World J. Gastroenterol.* 11: 1220–1224.
55. Jiang, Z., J. X. Jiang, and G. X. Zhang. 2014. Macrophages: a double-edged sword in experimental autoimmune encephalomyelitis. *Immunol. Lett.* 160: 17–22.
56. Parsa, R., P. Andresen, A. Gillett, S. Mia, X. M. Zhang, S. Mayans, D. Holmberg, and R. A. Harris. 2012. Adoptive transfer of immunomodulatory M2 macrophages prevents type 1 diabetes in NOD mice. *Diabetes* 61: 2881–2892.

**Supplemental Figure 1**

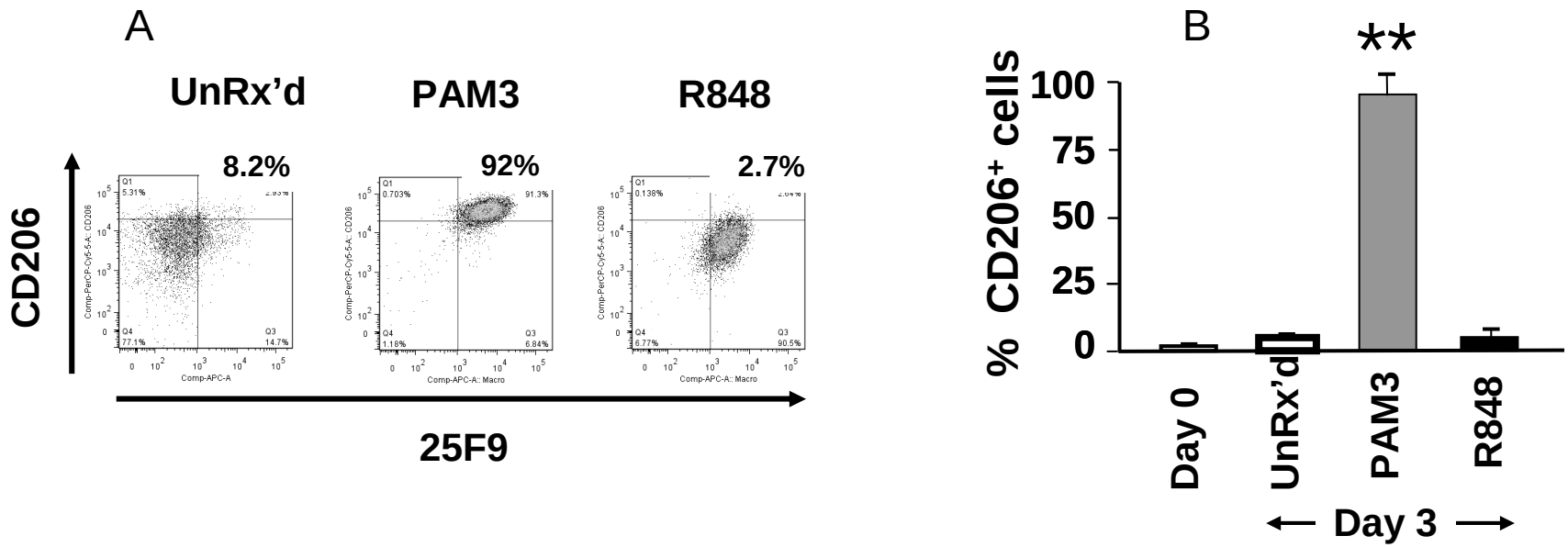


R848 and PAM3 induce mMDSC to differentiate into macrophages.

mMDSC were purified from normal donors as described in Fig 1 and stimulated *in vitro* with PAM3 (1 ug/ml) or R848 (3 ug/ml). 25F9 and CD206 expression were examined on day 3. A) Representative example showing changes in surface marker expression over time. B) Change in the percentage of 25F9+ cells (mean + SD) of 4 independently studied donors.

**, $p < .01$; vs unstimulated cultures

**Supplemental Figure 2**

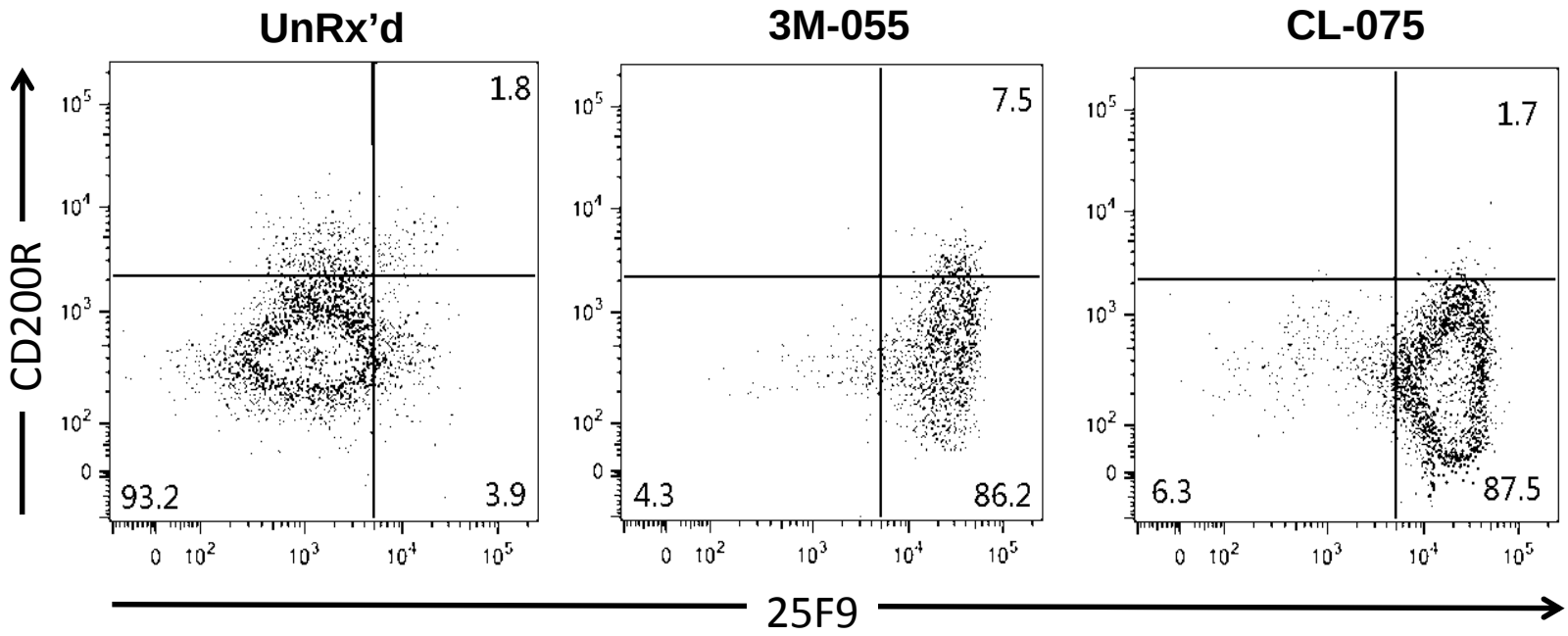


3M-055 and CL-075 induce mMDSC to differentiate into phenotypically M1-like macrophages.

mMDSC were purified from normal donors as described in Fig 1 and stimulated *in vitro* with optimal concentrations (determined by preliminary dose-ranging studies) of 3M-055 (100 ng/ml) or CL-075 (200 ng/ml). 25F9 and CD200R expression was examined on day 3. Data are representative of results from 4 independently studied donors.

## Supplemental Figure 3

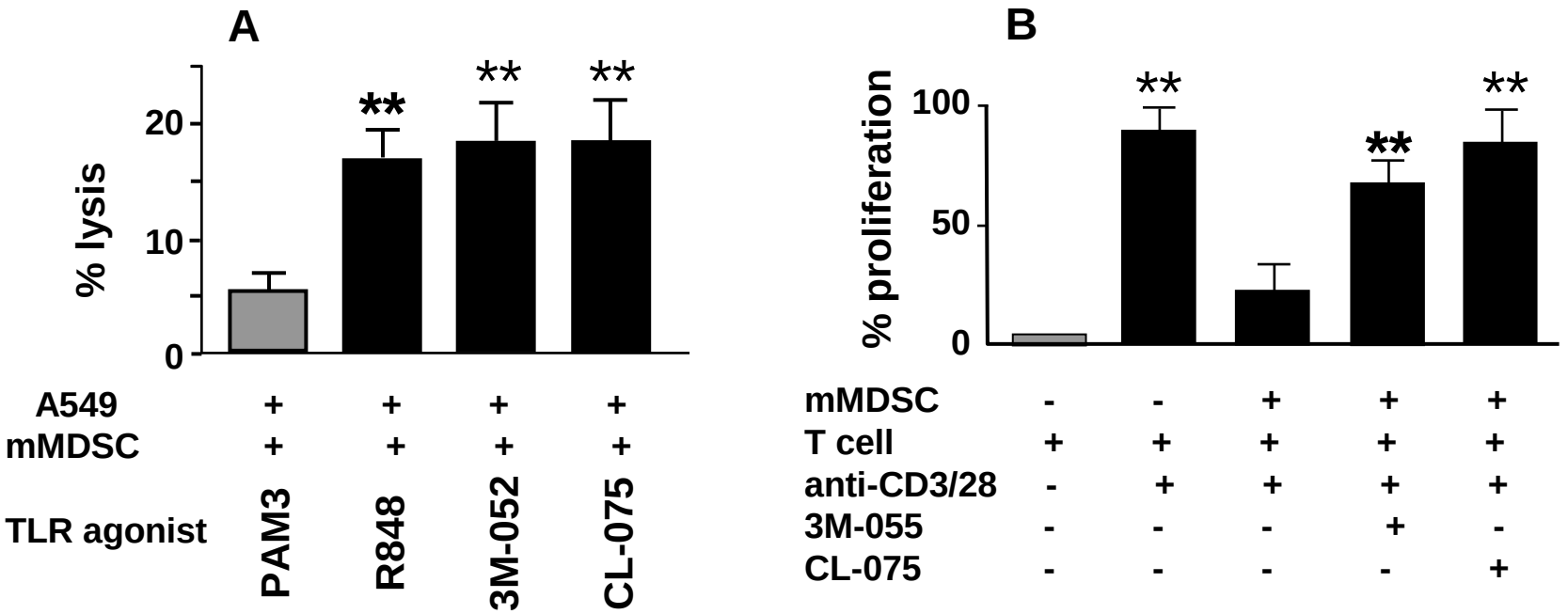


Effect of 3M055 and CL075 on mMDSC from cancer patients.

mMDSC and CD4+ T cells were purified from cancer patient samples as described in Fig 6. A) Purified mMDSC were cultured with 3 ug/ml R848, 100 ng/ml of 3M055 or 200 ng/ml of CL075 for 3 days as described in Fig 4. Labeled A549 tumor cells were added at a 1:40 ratio for the final 6 hr and the percent targeted for lysis determined. B) 2 x 105 mMDSC were cultured with 1 x $10^5$ syngeneic CSFE-labeled CD4 T cells in the presence of anti-CD3/28 coated beads, 100 ng/ml of 3M055 or 200 ng/ml of CL075. T cell proliferation was examined on day 3. The percent of T cells proliferating (mean + SD) was determined independently in samples from 4 patients/treatment group. Data represent the mean + SD of samples from 4 independently analyzed donors/group.

**, $p < .01$ vs control group.

Supplemental Table I: Characteristics of cancer patients

| Tumor type | # of patients per gender M | F | Age range | Stage | Failed therapies |
|---|---|---|---|---|---|
| GI | 4 | 1 | 49 – 71 | Stage III- IV | Chemo, surgery |
| prostate | 4 | - | 63 - 72 | Gleason 7-8 | Hormone, surgery |
| pancreatic | 2 | 3 | 50 – 67 | Stage III - IV | Chemo |
| hepatocellular | 6 | 2 | 53 – 68 | Stage III - IV | Chemo |

OPEN ACCESS Freely available online

PLOS ONE

# Coiled-Coil Domain Containing Protein 124 Is a Novel Centrosome and Midbody Protein That Interacts with the Ras-Guanine Nucleotide Exchange Factor 1B and Is Involved in Cytokinesis

**Pelin Telkoparan[1], Serap Erkek[1¤], Elif Yaman[1], Hani Alotaibi[1], Defne Bayık[1], Uygar H. Tazebay[1,2]***

**1** Department of Molecular Biology and Genetics, Faculty of Science, Bilkent University, Ankara, Turkey, **2** Department of Molecular Biology and Genetics, Gebze Institute of Technology, Kocaeli, Turkey

## Abstract

Cytokinetic abscission is the cellular process leading to physical separation of two postmitotic sister cells by severing the intercellular bridge. The most noticeable structural component of the intercellular bridge is a transient organelle termed as midbody, localized at a central region marking the site of abscission. Despite its major role in completion of cytokinesis, our understanding of spatiotemporal regulation of midbody assembly is limited. Here, we report the first characterization of coiled-coil domain-containing protein-124 (Ccdc124), a eukaryotic protein conserved from fungi-to-man, which we identified as a novel centrosomal and midbody protein. Knockdown of Ccdc124 in human HeLa cells leads to accumulation of enlarged and multinucleated cells; however, centrosome maturation was not affected. We found that Ccdc124 interacts with the Ras-guanine nucleotide exchange factor 1B (RasGEF1B), establishing a functional link between cytokinesis and activation of localized Rap2 signaling at the midbody. Our data indicate that Ccdc124 is a novel factor operating both for proper progression of late cytokinetic stages in eukaryotes, and for establishment of Rap2 signaling dependent cellular functions proximal to the abscission site.

**Citation:** Telkoparan P, Erkek S, Yaman E, Alotaibi H, Bayık D, et al. (2013) Coiled-Coil Domain Containing Protein 124 Is a Novel Centrosome and Midbody Protein That Interacts with the Ras-Guanine Nucleotide Exchange Factor 1B and Is Involved in Cytokinesis. PLoS ONE 8(7): e69289. doi:10.1371/journal.pone.0069289

**Editor:** Claude Prigent, Institut de Génétique et Développement de Rennes, France

**Received** February 1, 2013; **Accepted** June 6, 2013; **Published** July 19, 2013



**Funding:** The Turkish Scientific and Technological Research Council (TUBITAK) has supported the study with grants 109T049 and 109T925. The European Science Foundation-Functional Genomics Programme provided a mobility grant to P.T. The funders had no role in study design, data collection and analysis, decision to publish, or preparation of the manuscript.

**Competing Interests:** The authors have declared that no competing interests exist.

* E-mail: tazebay@gyte.edu.tr

¤ Current address: Friedrich Miescher Institute for Biomedical Research, Basel, Switzerland

## Introduction

Centrosomes are microtubule-organizing centers (MTOCs) that play a key role in determining the geometry of microtubule arrays in animal cells. They control and influence cell shape, polarity, motility, spindle formation, as well as chromosome segregation and cell division [1]. Each centrosome comprises a pair of centrioles that are surrounded by an amorphous and dynamic proteinaceous matrix referred to as the pericentriolar material (PCM), which is considered to be the site where microtubule nucleation initiates [2]. Associated with the multifunctional role of this primary MTOC in the cell, the total amount of PCM organized around centrioles (corresponding to centrosome size) and the composition of PCM vary considerably throughout the cell cycle [2–4].

Microtubule-nucleating capacities of centrosomes are increased by recruitment of key PCM proteins such as γ-tubulin and gamma-tubulin complex proteins (GCP) forming the γ-tubulin ring complexes (γ-tuRC), which orchestrate cell division-related MTOC activities leading to the formation of spindle asters and correct positioning of the two spindle poles. These cellular activities are required for genetically stable cells as it facilitates proper segregation of the duplicated chromosomes, ultimately resulting in diploid daughter cells [4–7].

Recently, a number of efforts aimed to establish both the precise composition of PCM at different stages of cell cycle, and the nature of dynamic networks of molecular interactions that lead to spatiotemporal regulation of PCM assembly. Jakobsen *et al.* [8] have obtained an extensive coverage of human centrosome proteome by using a mass spectrometry-based proteomics approach combined with an antibody based subcellular screen of candidate proteins [8]. In this study, the authors identified 126 known and 40 novel candidate centrosome proteins, of which 22 were validated as novel centrosome components, and 5 turned out to associate preferentially either with mother or daughter centrioles. These analyses also indicated that the majority (60%) of centrosomal proteins contain coiled-coil domain (CCD) type oligomerization motifs [8], [9], as their predominant structural features, which seem to be important for proper centrosome assembly.

Previous studies have indicated the presence of microtubule nucleation-related proteins that are shared between the centrosome and the midbody, which is the central region of the intercellular bridge that is rich in anti-parallel microtubule bundles

emanating from the central spindle [10]. These include for instance γ-tubulin, as the midbody is also a secondary MTOC associated with the contractile ring forming at the site of cleavage furrow ingression [1], [11]. Again, another protein with a CCD motif, Cep55, is centrosomal in interphase cells, but dissociates from the centrosome during entry into mitosis [12–14]. Precisely at cytokinetic abscission Cep55 is localized to the midbody where it plays an essential role in recruitment of the endosomal sorting complex required for transport (ESCRT) components such as Alix and tumor susceptibility gene 101 (tsg101, an ESCRT-I member), as well as endobrevin (v-SNARE) [15–17]. This is then followed by the recruitment of ESCRT-III components via interactions with Alix and Tsg101, resulting in the translocation of CHMP4B to the midbody [18]. According to current models, polymerization of CHMP4B subunits forms series of cortical rings extending away from the midbody, either as continuous helical contractile filaments [18], [19] or to give rise to a second immediately distal CHMP4B pool [20]. This then deforms the intercellular bridge membrane neck into a narrow constriction, and subsequently induces the abscission event.

Recent studies have also identified a number of factors other than Cep55 that similarly localize to centrosomes early in mitosis but then move to the midbody at cytokinesis where they execute essential functions in fission of the daughter cells [10], [16]. Among those proteins, Polo-like-kinase-1 (Plk1) plays critical roles in centrosome maturation and microtubule organization [7], [21], [22]. At the midzone Plk1 also phosphorylates Cep55 on Ser-436, thereby modulating its interaction with Mklp1, a kinesin-like component of centralspindlin. This provides a temporal control of abscission, by inhibiting functions of Cep55 in the midbody at stages earlier than late-anaphase [23].

During our earlier studies on specificities of Ras-guanine nucleotide exchange factor-1 (RasGEF1) family members [24], we obtained preliminary evidences regarding possible interactions between RasGEF1B and a previously uncharacterized protein known as the coiled-coil domain-containing protein 124 (Ccdc124). Here, we report the first characterization of this conserved human protein, Ccdc124, and show that it is a novel component of the centrosome during interphase and at the G2/M transition. During cell division, Ccdc124 relocates to the midbody at telophase and acts as an essential molecular component in cytokinesis. Ccdc124 interacts with RasGEF1B at the midbody where this GEF could activate the small G protein Rap2 [24] at pre-abscission stages. Our data propose a mechanistic link between cytokinesis and Rap signaling that is mainly linked to the formation of cell-cell junctions, regulation of cell-extracellular matrix adhesion, and establishment of cell polarity [25], i.e., molecular processes that must follow cell division while tissues are formed.

## Results

### Molecular Characterization of Ccdc124

The coiled-coil domain (CCD) is a motif that is found in most centrosome proteins [8]. Intrigued by its strict conservation in all eukaryotic genomes from fungi-to-man, we hypothesized that *CCDC124*, a human gene of unknown function encoding a putative CCD containing novel protein, could in fact be involved in centrosome biology. We carried-out a comparative sequence analysis on *CCDC124* which encodes a cDNA that is transcribed from chromosome 19p13.11, consisting of five exons, of which exon 1 is non-coding. BLAST analysis indicated that the protein encoded from this genetic locus shares, for instance, 70% identity/89.1% similarity with its orthologue NP_956859 in the vertebrate model *Danio rerio* (zebrafish), or 50.4% identity/72.6% similarity with Y73E7A.1 in the invertebrate *Caenorhabditis elegans*. *CCDC124* has also orthologues in lower eukaryotes such as the filamentous fungus *Aspergillus nidulans* (AN0879.2; 35.1% identity/58.2% similarity), or the fission yeast *Schizosaccharomyces pombe* (SPBC29A10.12; 33% identity/57.8% similarity), while it is not found in the budding yeast *Saccharomyces cerevisiae*.

Northern blot analysis have revealed that *CCDC124* is ubiquitously expressed in all tested human tissues, and relatively high levels of expression were detected in the brain, placenta, liver, spleen, and prostate (Fig. 1A). In these analyses, a transcript of ~1061 nucleotides was detectable in tested organs, in agreement with the predicted size of *CCDC124* mRNA in the NCBI databases (http://genome.ucsc.edu), except in the placenta where we observed a second shorter mRNA species indicative of a transcript variant (Fig. 1A). *CCDC124* cDNA would encode a protein of 223 amino acids with two putative coiled-coil domains between residues 18–82 in the N-terminal half of the protein as detected by the ELM (http://elm.eu.org) and COILS (www.ch.embnet.org/software/COILS_form.html) bioinformatics analysis platforms (Fig. S1). No significant homology to other proteins or domains were found.

We generated a rabbit polyclonal antibody recognizing the peptide corresponding to the N-terminal 24 amino acids of Ccdc124 and characterized its specificity towards Ccdc124 in immunoblots including peptide competition assays (Fig. 1B). We identified Ccdc124 as a ~32 kDa protein in immunoblots using different protein lysates obtained from Ccdc124 expression vector (CMV-Ccdc124) transfected or untransfected human HEK-293 cells (Figs. 1B–C). Furthermore, when the Ccdc124 ORF was tagged with an N-terminal flag-epitope in plasmid vectors, the antibody also detected the flag-Ccdc124 at the expected size (~35 kDa; Fig. 1C). When these bands were gel extracted and subjected to peptide analyses by mass-spectrometry, the band of ~35 kDa were identified as the full-size flag-Ccdc124, suggesting that without the flag epitope *CCDC124* would encode a protein of ~32 kDa (Pelin Telkoparan, Lars A.T. Meijer, and Uygar H. Tazebay, unpublished results). Surprisingly, anti-flag antibodies failed to detect a similar robust band of ~35 kDa when the epitope was inserted at the C-terminus, but instead they revealed a band of ~32 kDa in lysates of cells transfected with vectors expressing Ccdc124-flag (Fig. 1C). This indicated possible proteolytic cleavage of the protein at its N-terminus when flag-epitope is inserted to the C-terminus of Ccdc124. We have not further characterized the proteolytic cleavage of this protein at the molecular level, and we used the more stable N-terminus flag-tagged Ccdc124 expressing vector (flag-Ccdc124) in the rest of our studies.

### Ccdc124 is a Novel Centrosome Protein Relocated to Midbody at Telophase

In order to obtain insight into the biological function of Ccdc124, we assessed the subcellular localization of endogenous Ccdc124 by using generated or commercial anti-Ccdc124 antibodies in cellular immunofluorescence assays. When asynchronously growing HeLa cells were subjected to a preliminary immunofluorescence analysis by using an anti-mid-Ccdc124 antibody recognizing the central part of the protein (between residues 100–150), subcellular dot-like structures reminiscent of centrosomal staining patterns were detected (results not shown, but please see Fig. 2, below). We then synchronized the cells at G2/M stage of the cell cycle by the MT polymerization inhibitor nocodazole following double-thymidine treatments (Fig. S2, see *Methods s1*), and followed cell cycle stage-dependent subcellular

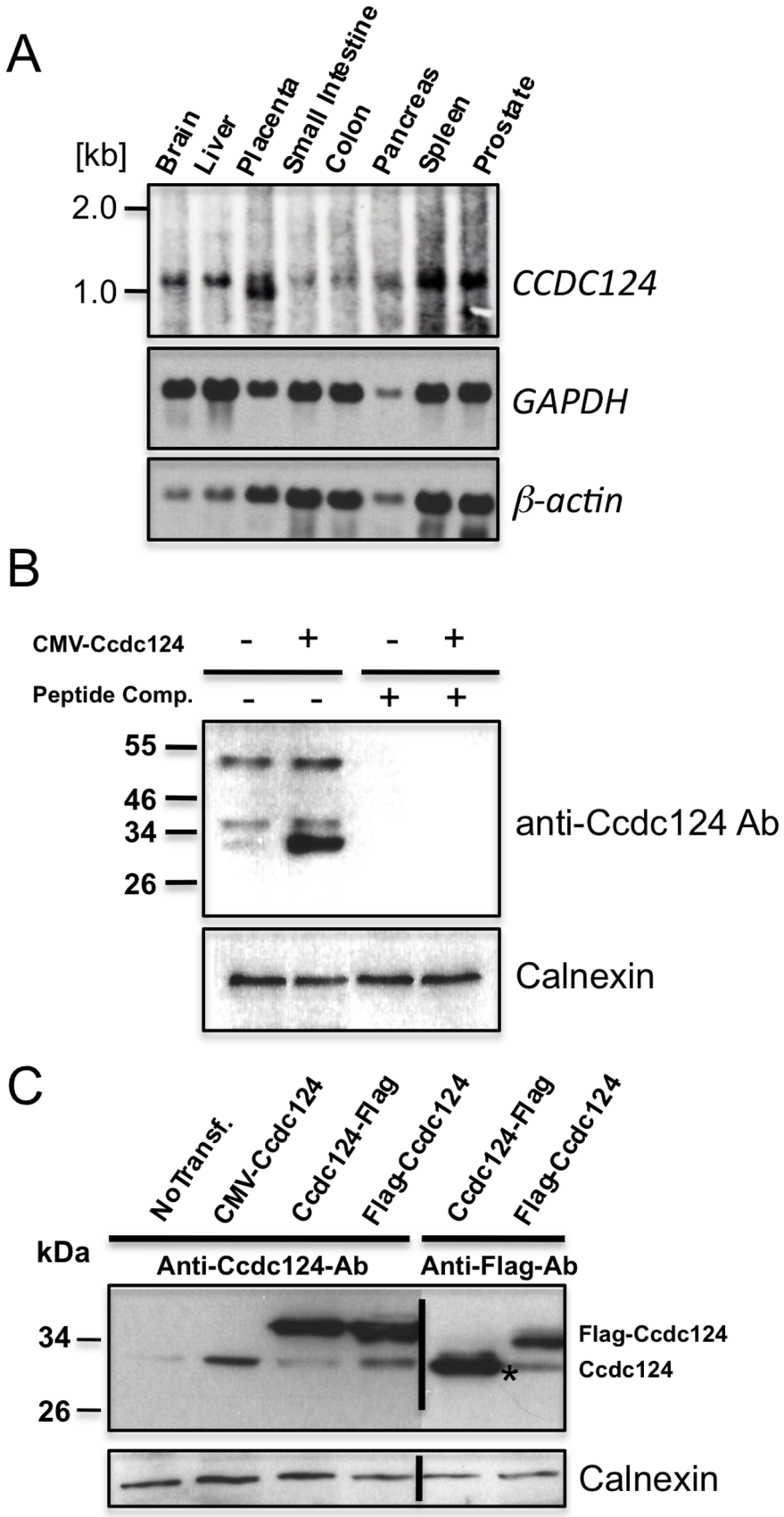


**Figure 1. *CCDC124* mRNA is ubiquitously expressed in human tissues, and it encodes a 32 kDa protein.** (A) Hybridization of part of the coding region of *CCDC124* to an adult human multiple tissues Northern blot containing 2 μg of polyA-mRNA each lane. A single transcript of ~1061

nucleotides was detectable in all human tissues analyzed, except the placenta with a second smaller transcript variant. The same blot was rehybridized with probes corresponding to two differentially expressed genes, β-actin and GAPDH, to monitor blotting quality. (**B**) Specific detection of ectopically expressed Ccdc124 by anti-Ccdc124 antibodies. HEK-293 cells, either non-transfected, or transfected with CMV-promoter controlled Ccdc124 were lysed, protein lysates were separated by SDS-PAGE, and immunoblot was performed either with anti-Ccdc124 antibodies alone, or same antibodies pre-incubated with 100 ng of competing peptide epitope corresponding to N-terminus 24mer peptide of Ccdc124. (**C**) Expression of Flag-tagged Ccdc124 protein was specifically detected by the anti-Ccdc124 or with anti-Flag antibodies, as indicated. Asterisk (*) indicates C-terminus flag-tag insertion dependent N-terminus cleaved form of Ccdc124. The expression of calnexin was confirmed in all cell lysates as an equal loading control.

doi:10.1371/journal.pone.0069289.g001

localization of endogenous Ccdc124 by immunofluorescence assays using Ccdc124 N-terminal epitope (residues 1 to 24), mid-region, or C-terminal epitope (residues 173 to 223)-specific antibodies. Independent of the Ccdc124 antibody used, these studies further indicated centrosome colocalization of Ccdc124 with γ-tubulin at interphase, prophase, metaphase, and anaphase stages, albeit it was relatively diffused to the pericentrosomal region at anaphase (Fig. 2A). Similar results were obtained when subcellular localization of an N-terminus flag-tagged version of Ccdc124 was monitored by immunofluorescence stainings using anti-flag antibodies on cells transfected with the corresponding vector construct (Fig. 2B). Moreover, endogenous centrosome immunostainings with anti-Ccdc124 Abs were very significantly reduced in response to Ccdc124 depletion by esiRNAs targeting its expression (see below, Fig. 4B), further supporting the notion that Ccdc124 is a novel centrosome protein. Centrosome localization of endogenous Ccdc124 was also observed in Retinal Pigment Epithelial cells (RPE1) containing another centrosomal marker, GFP-Centrin [26] (results not shown). Interestingly, at telophase and in cytokinesis Ccdc124 dissociates from centrosomes and relocalizes to the midzone, subsequently accumulating at the midbody at cytokinesis as assessed by its colocalization with the midzone-specific γ-tubulin (Fig. 2A–B, and Fig. 3A, C), or by its positioning at the midbody marked by the empty mid-space in α-tubulin stainings (Fig. 3B). Immunofluorescence studies with peptide competition assays further indicated that the Ccdc124 signal detected at the midbody was specific, as anti-N-ter-Ccdc124 antibodies pre-treated with the epitope peptide failed to recognize Ccdc124 at the midbody (Fig. 3C).

## Knock-down of CCDC124 by siRNAs Leads to Defects in Cytokinesis

A number of midbody localized proteins were previously shown to be involved in cytokinetic abscission [13], [16], [27]. In order to test a possible role of Ccdc124 during the separation of dividing sister cells, we initially knocked-down *CCDC124* in HeLa cells by separately transfecting them either with esiRNAs or with shRNA vectors specifically targeting this gene. We first monitored knock-down efficiencies by immunoblots that we carried-out using lysates obtained from Ccdc124-specific esiRNA or shRNA vector transfected cells as compared to scrambled esiRNA/shRNA vector transfected controls. We observed approximately 75–80% decrease in Ccdc124 levels in cells that received gene specific esiRNAs as compared to scrambled transfected controls (Fig. 4A). Again, depending on shRNA target sequence, close to 30–65% decrease were detected in Ccdc124 levels in cells separately transfected with three different sequences of shRNAs (Sh1, Sh2, and Sh3), as compared to scrambled controls. In these assays, Ccdc-Sh1 was identified as the vector containing the most potent Ccdc124-targeting shRNA sequence (Fig. 4A) We then analyzed cellular morphologies, centrosome localizations, and midbody functions of asynchronous growing cells that received either Ccdc124 specific esiRNAs, or shRNA vectors targeting the same gene. In Ccdc124-depleted cells interphase centrosomes still formed, as assessed by immunostainings that mark γ-tubulin complexes (Fig. 4B). This indicated that the absence of Ccdc124 does not impair centrosome formation. However, in Ccdc124-depleted cells cytokinesis was remarkably blocked as assessed by the significantly increased percentage of bi- and multinucleated cells (Fig. 4C–D) from 2.5±0.3% in scrambled control esiRNA transfected cases to 14.6±1.5% in Ccdc124-specific esiRNA received asynchronous cultures (Fig. 4C). The percentage of multinucleated cells in Ccdc124-depleted cultures were decreased significantly and nearly restored to normal levels (4.5±0.8%) when Ccdc124 was reintroduced in a strong expression vector (Fig. 4A, C). This indicated that the cytokinesis defect observed with the esiRNA against Ccdc124 was specific. Further supporting this observation, the ratio of multinucleated cells also raised from 3.1±0.2% in scrambled shRNA vector received cells to 11.6±2.7% in cells transfected with Ccdc-Sh1 (Fig. 4B), indicating that defects in cytokinesis was specific to endogenous Ccdc124 depletion in HeLa cells rather than an off-target effect of RNAi.

## Identification and Characterization of Interaction Partners of Ccdc124

In order to identify possible interaction partners of Ccdc124, a human liver cDNA library was screened in a yeast two-hybrid assay system as described in *Materials and Methods*. Colonies with interacting partners were selected, and the corresponding prey fragments were sequenced at their 5′ and 3′ junctions. All 15 positive colonies contained overlapping cDNA sequences belonging to only one gene, RasGEF1B, suggesting that this guanine nucleotide exchange factor (GEF) is a strong candidate as an interaction partner of Ccdc124. RasGEF1B was first identified in zebrafish as a protein expressed in neural cells during late embryogenesis and early larval stages [28]. Furthermore, by using *in vitro* assay systems [24] we previously characterized RasGEF1B as an exchange factor exclusively activating the small G protein Rap2. RasGEF1B was also identified in murine macrophages as a toll-like receptor inducible protein with a subcellular localization in early endosomal vesicles [29].

Following the yeast two-hybrid assays, we were able to confirm the interaction between Ccdc124 and RasGEF1B, first by *in vitro* GST pull-down methods (Fig. 5A), and then by analyzing their association in mammalian HEK-293 cells transfected with flag-Ccdc124 and GFP-RasGEF1B containing expression vectors (Fig. 5B). Coimmunoprecipitation of GFP-RasGEF1B and flag-Ccdc124 in transfected cells could indicate a functional interaction between these two proteins. In parallel to functional studies to establish cellular roles of Ccdc124 and RasGEF1B, we sought to determine whether the subcellular localizations of these two proteins were comparable throughout the cell cycle. In fact, in a previous study, RasGEF1B was shown to localize in endosomal vesicles when fluorescent protein-fused versions (YFP-RasGEF1B or mRFP-RasGEF1B) were ectopically expressed in asynchronous CHO cells [29]. However, the subcellular localization of RasGEF1B was not previously addressed in cell cycle-synchronized cells. Identification of an endosomal vesicle factor such as

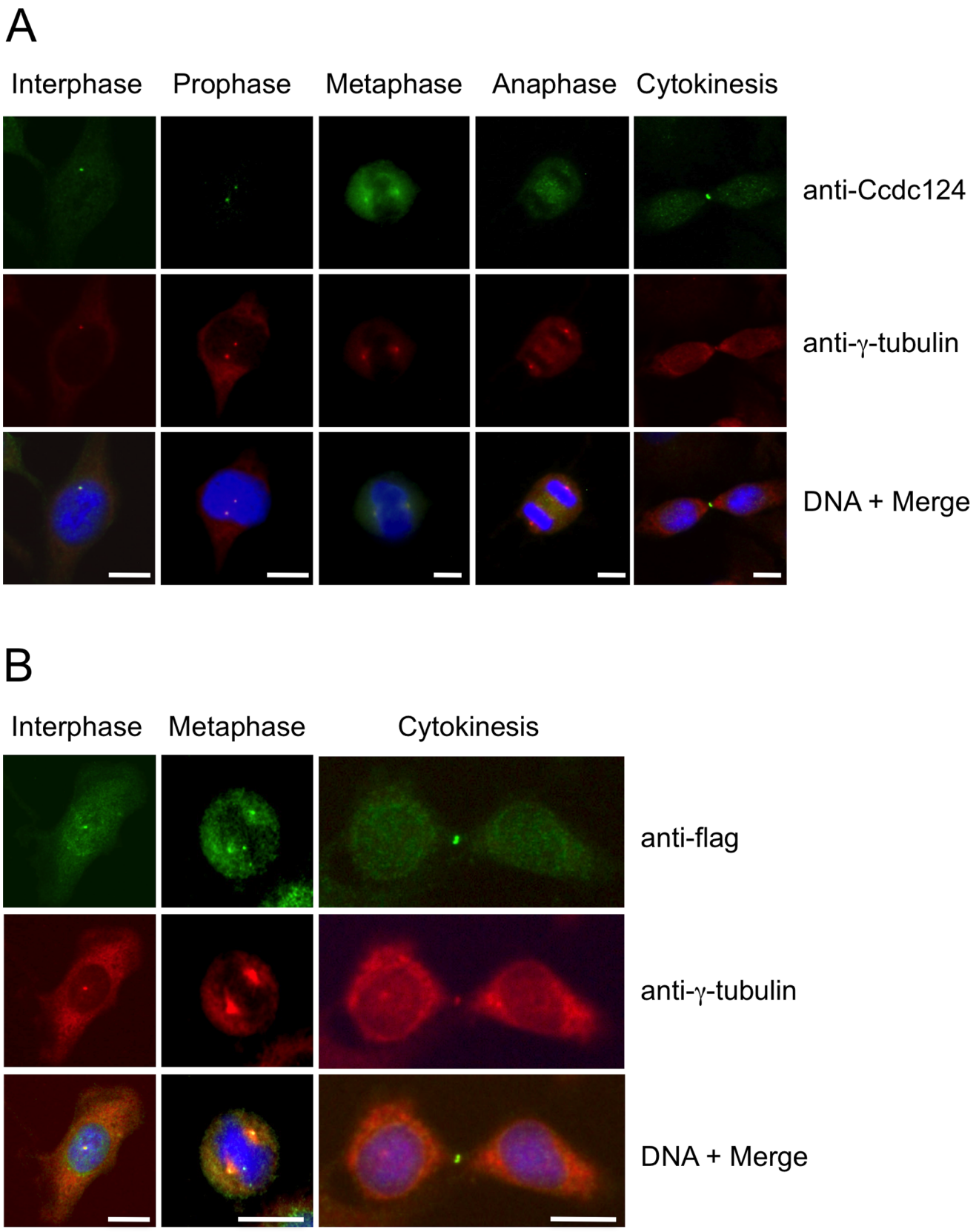


**Figure 2. Ccdc124 is present at the centrosome and it concentrates at the midbody in late stages of cytokinesis.** (A) HeLa cells were arrested at G2/M phase by sequential double thymidine and nocodazole treatments, then the drug was washed-off, cells were analyzed by immunofluorescence at time points with intervals of 15 minutes, and they were classified according to phases of mitosis, and cytokinesis. Samples of cells were then costained with anti-Ccdc124 and anti-γ-tubulin antibodies, and in interphase and prophase, Ccdc124 was observed as puncta in cells,

and it is located in the MTOC area. In metaphase and anaphase cells, Ccdc124 appeared at the spindle poles. Ccdc124 was present at the midzone and at the spindle poles in late anaphase, and concentrated in the midbody during cytokinesis. (**B**) HeLa cells were transfected with the N-ter flag-Ccdc124 vector construct as in Figure 1. 48 hours later samples of cells were subjected to immunofluorescence costainings using anti-flag and anti-γ-tubulin Abs together. Representative micrographs of cells at different stages of cell cycle are given. Bars represent 10 μm.
doi:10.1371/journal.pone.0069289.g002

RasGEF1B as an interaction partner of centrosomal and/or midbody localized Ccdc124 is particularly interesting, as critical roles of endosomes in physical separation of cells during cytokinetic abscission are well established in recent studies (for a review, see [30]). Subsequently, we generated a rabbit polyclonal antibody recognizing the C-terminal 19 amino acids epitope of the Zebrafish orthologue of RasGEF1B, and by immunoblotting analysis we first established that it also recognizes the human RasGEF1B protein (Fig. S3). Then, by using this antibody, we observed that even though in HeLa cells at interphase and prophase it displays characteristics of previously suggested cytoplasmic/early endosome localization [29], in metaphase cells RasGEF1B was located at a pericentrosomal/centrosomal position, as assessed by its co-localization with γ-tubulin, a subcellular localization similar to that Ccdc124 at metaphase cells (Fig. 6A, compare with Fig. 2).

Again similar to Ccdc124, at telophase and during cytokinesis RasGEF1B was detected at the midzone and in the midbody, and the RasGEF1B immunostaining at the midzone/midbody was sensitive to shRNAs (Fig. S4) targeting the expression of this GEF (Fig. 6B–C), indicating that the immunofluorescence signal was specific to the midbody localized RasGEF1B. Furthermore, during late stages of cytokinesis GFP-tagged RasGEF1B localized to the midbody as described for the endogenous protein (Fig. 6D). Noticeably, in these cell assays GFP-RasGEF1B clearly colocalized with Ccdc124 at the midbody puncta, suggesting that in late-cytokinesis the midbody forms a site of interaction for the two proteins. These results imply a possible role of Ccdc124 in linking cytokinesis to previously uncharacterized RasGEF1B dependent signaling at the midbody. As a note, we observed that bacteria purified Ccdc124 does not functionally interfere with the guanine nucleotide exchange activity of RasGEF1B in *in vitro* reconstituted assay systems (see below, Elif Yaman, Alfred Wittinghofer, and Uygar H. Tazebay, unpublished results), suggesting that Ccdc124 could affect spatial regulation of RasGEF1B, rather than modulating its GEF activity.

## RasGEF1B Stimulates Guanine Nucleotide Exchange of Rap2 in Mammalian Cells in Culture

Activation cycle of small G proteins is regulated by guanine nucleotide exchange factors (GEFs), which induce dissociation of bound GDP and its replacement by the more abundant GTP, and the resulting conformational change allows the binding of effector proteins and thereby stimulation of downstream signaling. Previous functional studies by Yaman *et al.* [24] indicated that under *in vitro* conditions RasGEF1B specifically activates Rap2 by stimulating guanine nucleotide exchange only of this small G protein, whereas it does not activate even its close family member, Rap1, or other members of Ras family. We decided to take these *in vitro* studies to one level up, and confirm the stimulatory effect of RasGEF1B on Rap2 GDP/GTP nucleotide exchange by knocking-down this GEF in HEK-293 cells, followed by assessing GTP-bound active Rap2 (Rap2·GTP) status in these cells. For this, we used a Rap-activity assay method based on immunoprecipitation of active Rap proteins by the Rap-binding domain of RalGDS (RBD-RalGDS), as previously described [31]. When RasGEF1B is knocked-down to nearly 55% in HEK-293 cells by specific down-regulatory shRNA-containing vectors (Fig. S4), significantly less Rap2·GTP were present in cells, even though total Rap2 amounts were not affected (Fig. 7). This indicated a functional link between RasGEF1B and Rap2 GTP-binding protein activation in this cell system. These results were consistent with our previous *in vitro* studies that established Rap2 as the sole RasGEF1B activated Ras-family GTP-binding protein [24].

## Active Rap2 GTP-binding Protein is Relocated to the Midbody at Cytokinesis

We then decided to assess if RasGEF1B substrate G protein Rap2 was also located in centrosomes and midbody during different stages of cell cycle. Our data indicated that at the midbody the position of Rap2 overlapped both with RasGEF1B and with Ccdc124 in binary comparisons (Fig. 8A, B). Depletion of endogenous Rap2 in HeLa cells by transfecting them with Rap2-specific shRNA vectors have led to the loss of endogenous Rap2 at the midbody (Fig. 8C, D). However, depletion of Rap2 did not result in a significant increase in percentages of multinucleated cells above scrambled controls (Fig. 8C, D). This result could suggest that although Rap2 is located at the midbody, its molecular function(s) at this organelle is(are) not essential for proper completion of cytokinesis. Subsequent immunofluorescence assays using anti-Rap2 antibodies on dividing HeLa cells indicated that Rap2 migrates to the midzone during anaphase/telophase (Fig. 9A, B), which is in contrast to its homologue Rap1 that is non-responsive to RasGEF1B [24] (Fig. S5). We also observed that in synchronously dividing cells 90 mins after they were released from nocodasole, at initial stages of cytokinesis Rap2 associates with microtubules originating at the midzone, and it migrates to the very center of intercellular bridge (boundaries marked with α-tubulin, Fig. 9B), relocating itself to midbody during cytokinetic abscission (Fig. 9A, B).

We then inquired whether Rap2 located at the midbody was functionally active during cytokinetic abscission, by transfecting HeLa cells with a GFP-labeled recombinant version of the Rap Binding Domain (RBD) of RalGDS referred as GFP-RBD(RalGDS). This GFP-labeled effector protein interacts with Rap2 specifically in the GTP-bound active state of the G protein, and thus serves as a subcellular Rap2 activity reporter [32]. When the signal coming from the GFP-RBD(RalGDS) that interacts with Rap2·GTP was followed at the subcellular level, at the interphase both endogenous Rap2 and GFP-RBD(RalGDS) were detected to localize diffusely at the cytoplasm with only a partial overlap (Fig. 10A, interphase). However, during cytokinetic abscission, GFP-RBD(RalGDS) very clearly colocalized with Rap2 at the midbody, indicating that Rap2 protein identified at the spindle midzone/midbody is in its GTP-bound active form (Fig. 10A, cytokinesis), and that it may potentially act on its specific effectors at this location. Midbody localization of GFP-labeled RBD(RalGDS) strictly depended on the presence of an active Rap2, as in cells co-transfected with dominant negative version of Rap2 (Rap2-S17N) the reporter protein GFP-RBD(RalGDS) did not relocate with the same efficiency to the midbody during cytokinesis as compared to cells transfected with wild-type Rap2 (Fig. 10B). The endogenous activation of local Rap2 signaling at midbody did not require pretreatment of cells with secondary messengers such as cAMP, diacylglycerol (DAG), or calcium that were previously shown to stimulate Rap signaling through

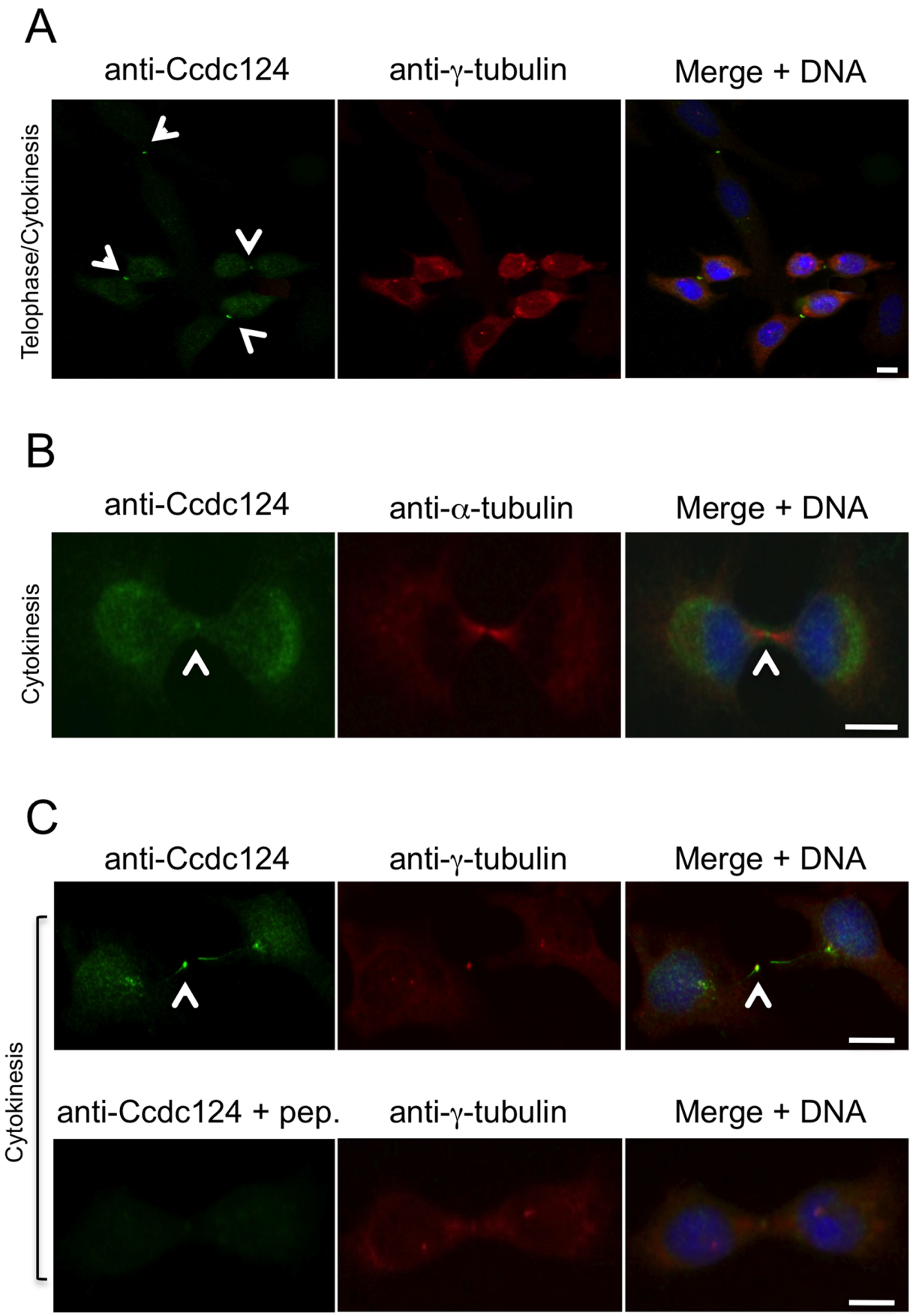
A
anti-Ccdc124
anti-γ-tubulin
Merge + DNA
Telophase/Cytokinesis
B
anti-Ccdc124
anti-α-tubulin
Merge + DNA
Cytokinesis
C
anti-Ccdc124
anti-γ-tubulin
Merge + DNA
anti-Ccdc124 + pep.
anti-γ-tubulin
Merge + DNA
Cytokinesis

**Figure 3. Ccdc124 accumulates at the midbody.** HeLa cells were synchronized as described in the legend of Fig. 2, and samples of cells were then stained with anti-Ccdc124 Ab together either with anti-γ-tubulin or with anti-α-tubulin Abs to monitor subcellular positions of centrosomes and the midbody. (**A–B**) At telophase and cytokinesis Ccdc124 is observed as puncta typically associated with the midbody positioned at the middle of intercellular bridge separating daughter cells, as detected in costainings with anti-γ-tubulin and anti-α-tubulin Abs, respectively. (**C**) Peptide competition assays were done by pre-incubating anti-N-ter-Ccdc124 antibody with the corresponding epitope peptide in 200-fold molar excess amounts. Signals generated by Ccdc124 localized at the midbody (shown with arrowhead) were lost in immunofluorescence assays where peptide pre-treated antibodies were used. Bars represent 10 μm.
doi:10.1371/journal.pone.0069289.g003

activation of various GEFs [33], [34]. This indicate that the recruitement of RasGEF1B to the midbody could be sufficient for regulation of Rap2 activity, as well as for translocation of Rap2 effectors to this subcellular location.

## Conclusion and Discussion

Previous biochemical studies and mass-spectrometry analyses on purified centrosomes have shown that proteins with CCD (coiled-coil domain) motifs are abundant in PCM [8], [35]. Close to 150 different proteins were identified in the PCM at different cellular stages, about 60% of which contain predicted CCD type oligomerization motifs [8]. In this work, by using molecular and cell biology methods we identified Ccdc124 as a novel component of the centrosome, as in cells at interphase and in mitotic cells up to the late-anaphase/telophase stage it clearly colocalized with two different centrosome markers, such as γ-tubulin and centrin (Fig. 2, and unpublished data). Despite multiple high throughput proteomics analyses targeting centrosome composition in the past, Ccdc124 was not in the list of PCM proteins prior to this study, indicating that combined genetic, cell biology and biochemical approaches are still necessary to identify all the components of PCM which has a remarkably dynamic composition [1], [36]. Conservation of Ccdc124 in lower eukaryotic species without centrosomes, such as *A. nidulans*, or *S. pombe* was not surprising, as also some major centrosome proteins (for instance, γ-tubulin) were common between this organelle and fungal spindle pole bodies [37]. The absence of an orthologue of Ccdc protein in *S. cerevisiae*, however, might indicate that Ccdc124 is not essential for fungi with budding-type of cell division.

Our data revealed that at late-anaphase/telophase stages of cell cycle Ccdc124 changes its subcellular localization: it dissociates from centrosomes, and first relocalizes to the midzone at late-anaphase, and then it accumulates at the midbody puncta at telophase and during cytokinetic abscission (Fig. 2–4). Currently, we do not know what triggers the displacement of Ccdc124 from

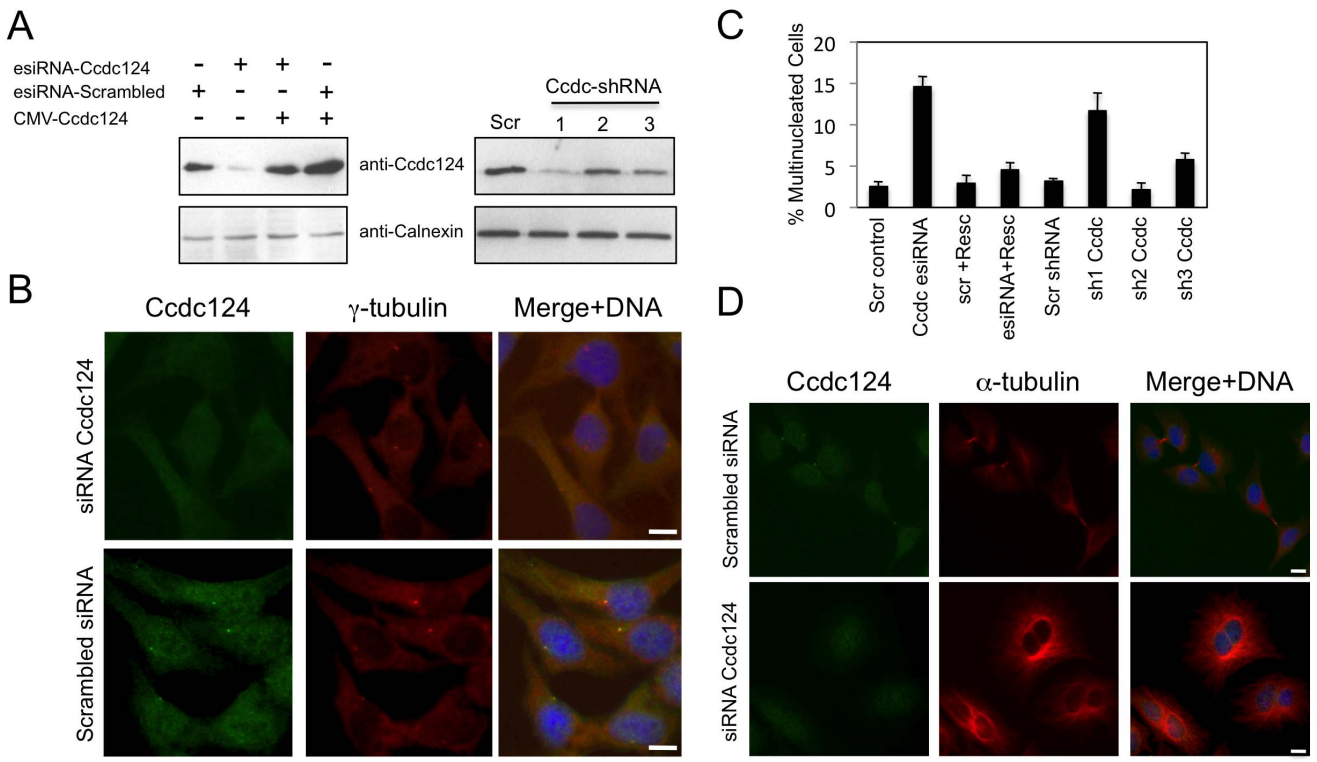


**Figure 4. Depletion of Ccdc124 in HeLa cells by RNAi leads to cytokinesis failure.** (A) HeLa cells were transfected with either esiRNAs or shRNA vectors (Sh1, Sh2, Sh3) targeting Ccdc124, cell lysates were collected at 48 hrs post-transfection, and immunoblotted with antisera to Ccdc124. Where indicated, Ccdc124 expression vector (CMV-Ccdc124) was cotransfected with gene-specific esiRNAs in order to rescue the cellular effect of Ccdc124 depletion. Scrambled control transfections were indicated (Scr). Calnexin expression was monitored as loading control. (**B**) Immunostainings of endogenous Ccdc124 in cells transfected with Ccdc124-specific esiRNA, or with scrambled control esiRNA were carried out with anti-Ccdc124 Ab. Costainings with γ-tubulin antisera have indicated subcellular positions of MTOCs (**C**) Cells described and analyzed in (A) were scored for bi- and multinucleation (n = 5± SD). (**D**) Representative micrographs of Ccdc124 depleted multinuclear or control esiRNA treated normal dividing cells described in (C). Bars represent 10 μm.
doi:10.1371/journal.pone.0069289.g004

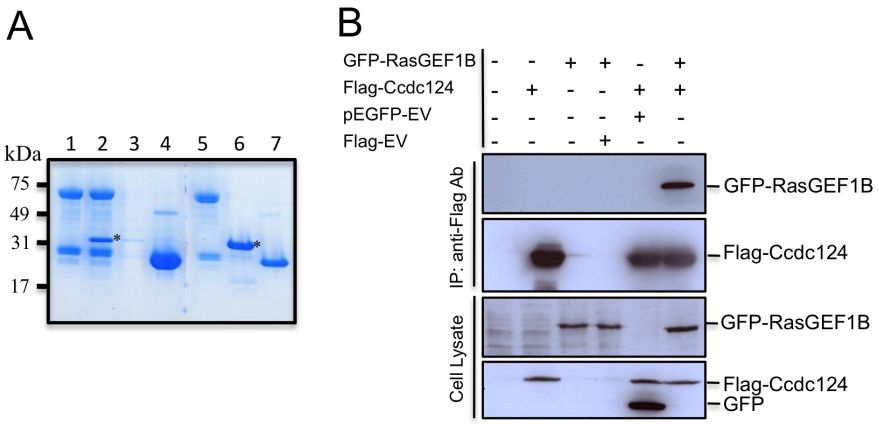


**Figure 5. RasGEF1B is an interaction partner of Ccdc124.** (A) *In vitro* GST pull-down assay indicating a possible interaction between RasGEF1B and Ccdc124. GST-RasGEF1B protein were immobilized on GSH-beads, followed by incubation with empty PBS buffer control (lane 1), or with bacteria purified His-tagged Ccdc124 (lane 2). As controls, GSH-beads w/o RasGEF1B protein incubated with His-Ccdc124 to monitor the amount of His-Ccdc124 proteins binding to GSH-beads in the absence of a putative interaction partner (lane 3), or GSH-beads immobilized with GST protein and incubated with His-Ccdc124 to monitor interaction capacity of Ccdc124 with GST (lane 4). Lanes 5, 6, 7 are stainings of 100 ng bacteria purified GST-RasGEF1B, His-Ccdc124, and GST proteins, respectively, run in the same gel to monitor their corresponding sizes. Bands corresponding to His-Ccdc124 were marked with asterisks (*). (**B**) HEK-293 cells were either transfected with Flag-Ccdc124 or GFP-RasGEF1B expression vectors alone or with indicated control plasmids, or alternatively they were co-transfected with Flag-Ccdc124 and GFP-RasGEF1B together, followed by immunoprecipitations (IP) on cell lysates using protein-G beads with anti-Flag antibodies. Subsequently, immunoblots were done on IP or cell lysate samples using anti-GFP (monitoring GFP-RasGEF1B) or anti-Flag-HRP (to assess Flag-Ccdc124) antibodies.
doi:10.1371/journal.pone.0069289.g005

the centrosome, or its association to the midzone/midbody. In fact, Cep55, a relatively well studied coiled-coil containing centrosome protein that relocates to the midbody and controls cytokinetic abscission, was shown to be a substrate of Plk1 [13]. Phosphorylation of Cep55 by Plk1 on its Ser436 residue is required for its interaction with centralspindlin and ESCRT complex proteins, leading to the recruitment of CHMP4B to the midbody [13], [16]. This is then followed by the assembly of this ESCRT-III component into a series of ring-like structures organizing the abscission site, mainly by bringing the two membranes of the intercellular bridge into close proximity for the scission [20], [38]. Even though in the current study we have not addressed post-translational modifications of Ccdc124, there are several reasons why we anticipate that its functions/stability could be regulated by phosphorylation dependent mechanisms. First, Ccdc124 is identified as a phosphoprotein in our preliminary phosphopeptide analysis by mass-spectrometry methods, and Ser141 residue of Ccdc124 (which is a consensus Plk1 phosphorylation site) was detected as a phosphorylated residue (Pelin Telkoparan, Lars A.T. Meijer, and Uygar H. Tazebay, unpublished results). Second, when we mutated predicted Ser, Thr, or Tyr phosphorylation sites to Ala residues in Ccdc124 by *in vitro* mutagenesis, the Ser121 residue conforming to a Casein Kinase-II phosphorylation consensus site turned out to be essential for the stability of Ccdc124 protein, even though phospho-mimicking mutations S121D, and S121E were normal in terms of protein stability (Fig. S6A, B), indicative of possible phosphorylation dependent regulatory mechanisms operating on Ccdc124.

We found that Ccdc124 depleted cells can still form MTOC, but they undergo cytokinesis failure inducing aneuploidy and generating genomic instability in cultured human cells (Fig. 4). According to current models of cytokinetic abscission, resolution of the membrane connection between two prospective daughter cells requires a concerted action of ESCRT proteins together with the targeting of three main types of recycling endosomes to midbody for an appropriate regulation of cytokinetic abscission (see below) [39], [40]. In an early work, Gromley *et al*, proposed a role for secretory vesicle fusion in the final stages of cytokinetic abscission, as they have shown that the coiled-coil protein centriolin relocates to midbody where, preceding abscission, it interacts with components of vesicle-targeting exocyst complexes and membrane-fusion inducing SNARE components [11]. However, subsequent studies indicated that even though the secretary pathway could contribute to formation of the intracellular bridge membrane, it is rather recycling endosome-dependent mechanisms that make major contributions to spatiotemporal regulation of cytokinetic abscission [40]. Furthermore, other than two Ral family G proteins RalA and RalB, endosome enriched complexes such as Rab35/OCRL and FYVE-CENT/TTC19 that were found on different types of endosomes, were previously shown to enable the completion of the final stages of abscission [41–43]. Our data suggested possible links between Ccdc124 and recycling endosomes. First, we identified an endosome localized nucleotide exchange factor RasGEF1B [29] as an interaction partner of the coiled-coil protein Ccdc124 (Fig. 5–6). Second, RasGEF1B activated small G protein Rap2 that we detected at the midzone/midbody, was previously reported to colocalize with Rab11-positive endosomes in *Xenopus* early embryos [44]. Importantly, Rab11-positive recycling endosomes containing the effector protein FIP3 (Rap11 Family of Interacting Protein 3) were previously shown to control the reorganization of the cortical actomyosin network during cytokinetic abscission, as they accumulate at the intercellular space between dividing cells and regulate local actin depolymerization by recruiting p50RhoGAP, and thus contributing to further thinning of the bridge [45].

In this study, we primarily focused on the biological significance of the interaction between Ccdc124 and RasGEF1B, rather than studying mechanistic aspects of it. Yet, our studies on the effect of bacteria purified Ccdc124 on the rate of nucleotide exchange by RasGEF1B on Rap2A in *in vitro* reconstituted assay systems suggested that Ccdc124 does not functionally interfere with RasGEF1B activity (Elif Yaman, Alfred Wittinghofer, Uygar H. Tazebay, unpublished observations). We could hypothesize that rather than modulating its GEF activity, Ccdc124 could recruit

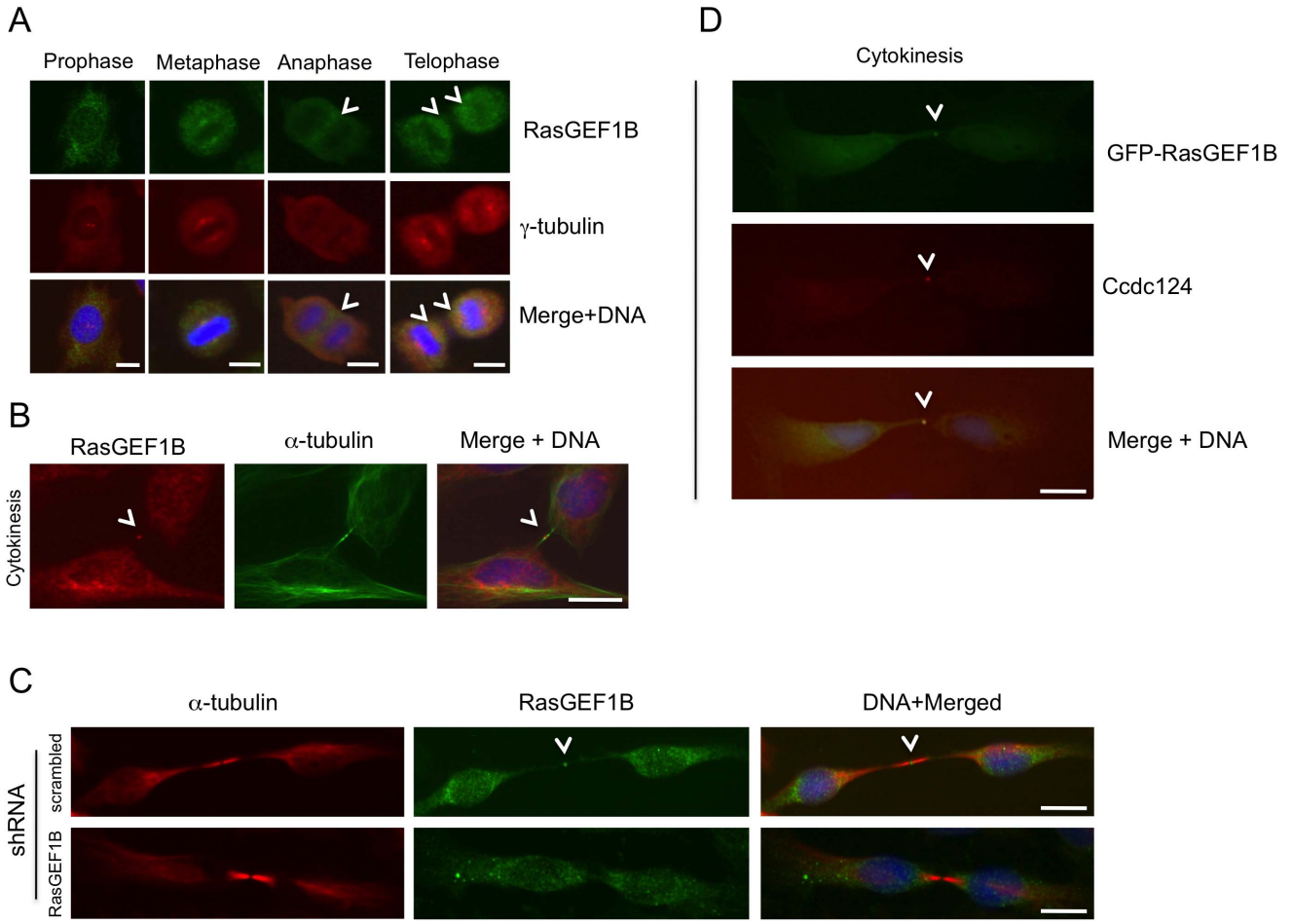


**Figure 6. RasGEF1B and Ccdc124 colocalize at the midbody.** (A–B) Subcellular localizations of RasGEF1B proteins in synchronously dividing HeLa cells were detected with specific anti-RasGEF1B antibodies. Cell divisions were synchronized as described in the legend of Figure 2, above. Representative immunofluorescence microscopy images of HeLa cells costained with anti-RasGEF1B, and either anti-γ-tubulin (A) or α-tubulin (B) antibodies illustrating the position of MTOCs and the midbody at cytokinesis. Arrowheads show RasGEF1B detected at the midzone and the midbody. (C) Immunofluorescence signals observed at midbody were significantly decreased when endogenous RasGEF1B were depleted by transfections with specific shRNA vectors (Sh-C or Sh-D, Fig. S4) and representative micrographs were shown. (D) HeLa cells transiently transfected with GFP-RasGEF1B were fixed and stained using anti-Ccdc124 Abs. Arrowheads indicate midbody positions of GFP-RasGEF1B, Ccdc124, and their colocalizations at the midbody. Bars represent 10 μm.
doi:10.1371/journal.pone.0069289.g006

RasGEF1B to midzone/midbody where the exchange factor activate its substrate G protein(s). A similar spatiotemporal regulation of Rap1 signaling localized at the plasma membrane by recruitement and translocation of its cAMP responsive GEF, Epac1, through activation of Ezrin-Radixin-Moesin (ERM) complex proteins was previously described [46].

We have shown that both the activator RasGEF1B and its partner G protein Rap2 have identical spatiotemporal subcellular distributions (Fig. 8). This indicated that RasGEF1B could potentially activate GDP/GTP exchange of Rap2 at midbody during late-telophase stage of cell cycle and at cytokinesis. Importantly, we observed the RasGEF1B substrate Rap2, but not its close homologue Rap1, accumulated in vesicular structures proximal to the midzone and at the midbody (Fig. 9A, see panels metaphase to cytokinesis, and Fig. S5). Detection of active Rap2 (Rap2·GTP) binding reporter protein GFP-RBD(RalGDS) in midbody further proved local activation of Rap2 at midbody puncta during cytokinesis (Fig. 10). This midbody localization of GFP-RBD(RalGDS), was only observed in cells having Rap2-WT, but not its dominant negative form, Rap2-S17N, indicating that midbody localization of Rap2 effectors requires activation of this small G protein (Fig. 10B). Neither cellular depletion of endogenous Rap2 by specific shRNA transfections, nor over-expression of the dominant negative form of Rap2 (S17N) has led to cytokinesis defects, as assessed by normal levels of bi- and multinucleated cells in corresponding cellular assays (Fig. 8, 10). Therefore, in our opinion rather than playing a direct role in cytokinesis, localization of Rap2 at the midbody might serve to modulate and/or functionalize local membrane environment for molecular events following cytokinetic abscission, such as establishment of cell-cell junctions, cell-extracellular matrix adhesions, or polarizations of cells after division of daughter cells fully accomplished. When we consider results obtained in this study altogether, we propose Ccdc124 as a novel factor that links cytokinesis to Rap signaling dependent junction/adhesion or cellular polarization promoting molecular mechanisms, thus bonding different cellular events that must closely follow each other in tissues of live organisms.

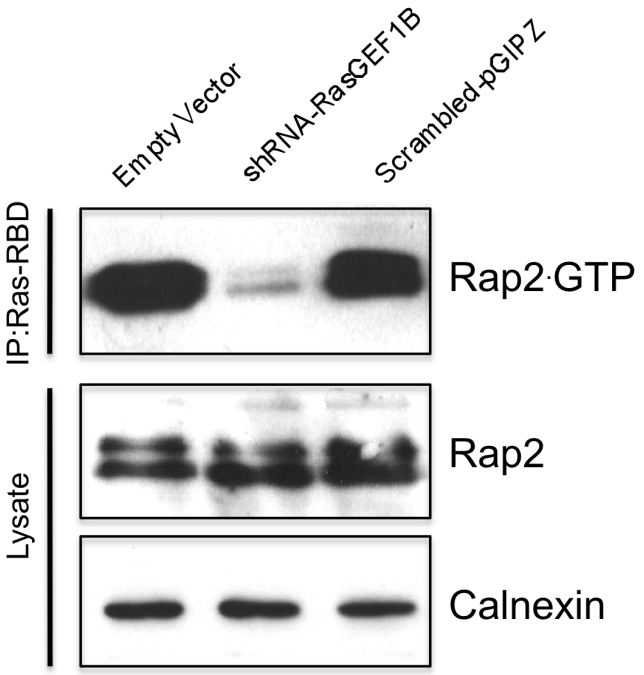


**Figure 7. The guanine nucleotide exchange factor RasGEF1B controls cellular Rap2·GTP status.** HEK-293 cells were transfected either with RasGEF1B specific shRNA expressing vector (Sh-D, Figure S4), scrambled shRNA expressing vector, or empty vector (negative control), 48 hrs later cells were lysed as described at Materials and Methods, they were cleared by centrifugation, and active Rap was precipitated with a glutathione *S*-transferase fusion protein of the Ras-binding domain of RalGDS precoupled to glutathione-Sepharose beads. Rap2 activation assay were carried-out by using anti-Rap2 monoclonal Abs. Results confirmed that shRNA mediated down-regulation of RasGEF1B expression effectively block generation of Rap2·GTP, although total cellular Rap2 was not affected. Calnexin expression was monitored as loading control.
doi:10.1371/journal.pone.0069289.g007

## Methods

### Ethics Statement

All cell lines of human origin used in this study were obtained legally either from commercial sources, or they were previously published. Material transfer agreements were duly signed between appropriate offices/persons-in-charge at donating and receiving institutions.

### Cell Culture and Reagents

Hek-293 and HeLa cells were maintained in DMEM and Retinal Pigment Epithelial-1 (RPE1) cells were grown in DMEM/F12 (1:1) supplemented with 10% FBS and kept at 37°C in a humidified 5% CO2 atmosphere. Cell lines used in this work were either from commercial sources, or described in previous publications. RPE1 cells [26] were obtained from Nurhan Özlü (Koç University, Istanbul), and RPE1 lines stably expressing GFP-Centrin [26], and GFP-Plk1 [47] were gifts from Greenfield Sluder (U. Mass. Medical School, MA), and Prasad Jallepalli (Memorial Sloan-Kettering, NY), respectively. 50 nM of Mission® esiRNA from Sigma-Aldrich (cat. EHU004061) was used for silencing Ccdc124 in HeLa cells by using Oligofectamine (Invitrogen) as transfection reagent. We have also targeted Ccdc124 expression by using the following three shRNA vector constructs prepared in pTRIPZ plasmids (Open Biosystems-Thermo) closely following the procedures described by Paddison *et al.* [48]. Ccdc124 specific shRNA sequences inserted in pTRIPZ vectors were as follows: shRNA #1: 5′-TGCTGTTGACAGTGAGCGACTCGACCAGCTGGAACGTAA|GTAGTGAAGCCACAGATGTACTTACGTTCCAGCTGGTCGAGGTGCCTACTGCCTCGGA-3′; shRNA #2: 5′-TGCTGTTGACAGTGAGCGACGAGACCATCAGCTCAGGGA|GTAGTGAAGCCACAGATGTACTCCCTGAGCTGATGGTCTCGGTGCCTACTGCCTCGGA-3; shRNA #3: 5′-TGCTGTTGACAGTGAGCGACCCAAGAAGTTCCAGGGTGA|GTAGTGAAGCCACAGATGTACTCACCCTGGAACTTCTTGGGCTGCCTACTGCCTCGGA-3. pTRIPZ vector containing scrambled shRNA control were purchased (Open Biosystems-Thermo, cat. no. RHS4750). In experiments to rescue cellular effects of Ccdc124 knock-downs by specific esiRNAs, 40 ng of pCDN3.1-CMV-Ccdc124 plasmids were cotransfected with the above indicated amounts of esiRNAs. In order to knock-down RasGEF1B expression, a set of five plasmids containing shRNA sequences specific for human RasGEF1B gene in pLKO1 vectors, and the corresponding scrambled shRNA control plasmid were purchased (Open Biosystems-Thermo) with the catalog number RHS4533 (TRC Lentiviral shRNAs) and following sequences: 1) Oligo ID: TRCN0000072963, 5′-CCGGGCTGACAGATAGACTCAGATTCTCGAGAATCTGAGTCTATCTGTCAGCTTTTTG-3′, renamed as sh-A; 2) Oligo ID: TRCN0000072964, 5′-CCGGCGGAAACATTTCCCTATGATTCTCGAGAATCATAGGGAAATGTTTCCGTTTTTG-3′, renamed as sh-B; 3) Oligo ID: TRCN0000072965, 5′-CCGGCGGTTATTTATGCATCCGTATCTCGAGATACGGATGCATAAATAACCGTTTTTG-3′, renamed as sh-C; 4) Oligo ID: TRCN0000072966, %'-CCGGGCTCTCTACTTGGCTTCTTATCTCGAGATAAGAAGCCAAGTAGAGAGCTTTTTG-3′, renamed as sh-D; 5) Oligo ID: TRCN0000072967, 5′-CCGGGAAGCACTCATCCAGCACTTACTCGAGTAAGTGCTGGATGAGTGCTTCTTTTTG-3′, renamed as sh-E. Similarly, for decreasing Rap2 expression, a set of three plasmids containing shRNA sequences specific for human Rap2 gene in pGIPZ vectors, together with the corresponding scrambled shRNA control vector were purchased (Open Biosystems-Thermo) with the catalog number RHS4531 (TRC Lentiviral shRNAs) and following sequences: 1) Oligo ID: V2LHS_34663, 5′-TGCTGTTGACAGTGAGCGCACTCAGAACAGGTTATGTAAATAGTGAAGCCACAGATGTATTTACATAACCTGTTCTGAGTTTGCCTACTGCCTCGGA-3′, renamed as sh-1; 2) Oligo ID: V2LHS_34666, 5′-TGCTGTTGACAGTGAGCGAAGAGATATAGTTCACAGTTAATAGTGAAGCCACAGATGTATTAACTGTGAACTATATCTCTGTGCCTACTGCCTCGGA-3′, renamed as sh-2; 3) Oligo ID: V2LHS_34662, 5′-TGCTGTTGACAGTGAGCGCTGACCTTGTGTCACTATTTATTAGTGAAGCCACAGATGTAATAAATAGTGACACAAGGTCAATGCCTACTGCCTCGGA-3′, renamed as sh-3. When indicated, cells were synchronized by a first thymidine block (2,5 mM) for 16 hours, released for 8 hours, and then blocked a second time with thymidine for 16 hours, followed by 200 nM nocodasole treatment/12 hours. Mitotic arrested cells were collected by "mitotic shake-off", and either they were analyzed directly (0 min.), or recultured for 15, 30, 45, 60, 120, 150, and 180 mins. At the beginning of the experiments cell cycle status of samples were established by FACS analysis as described in Fabbro *et al.* [13] and at each time point cells were processed for immunofluorescence.

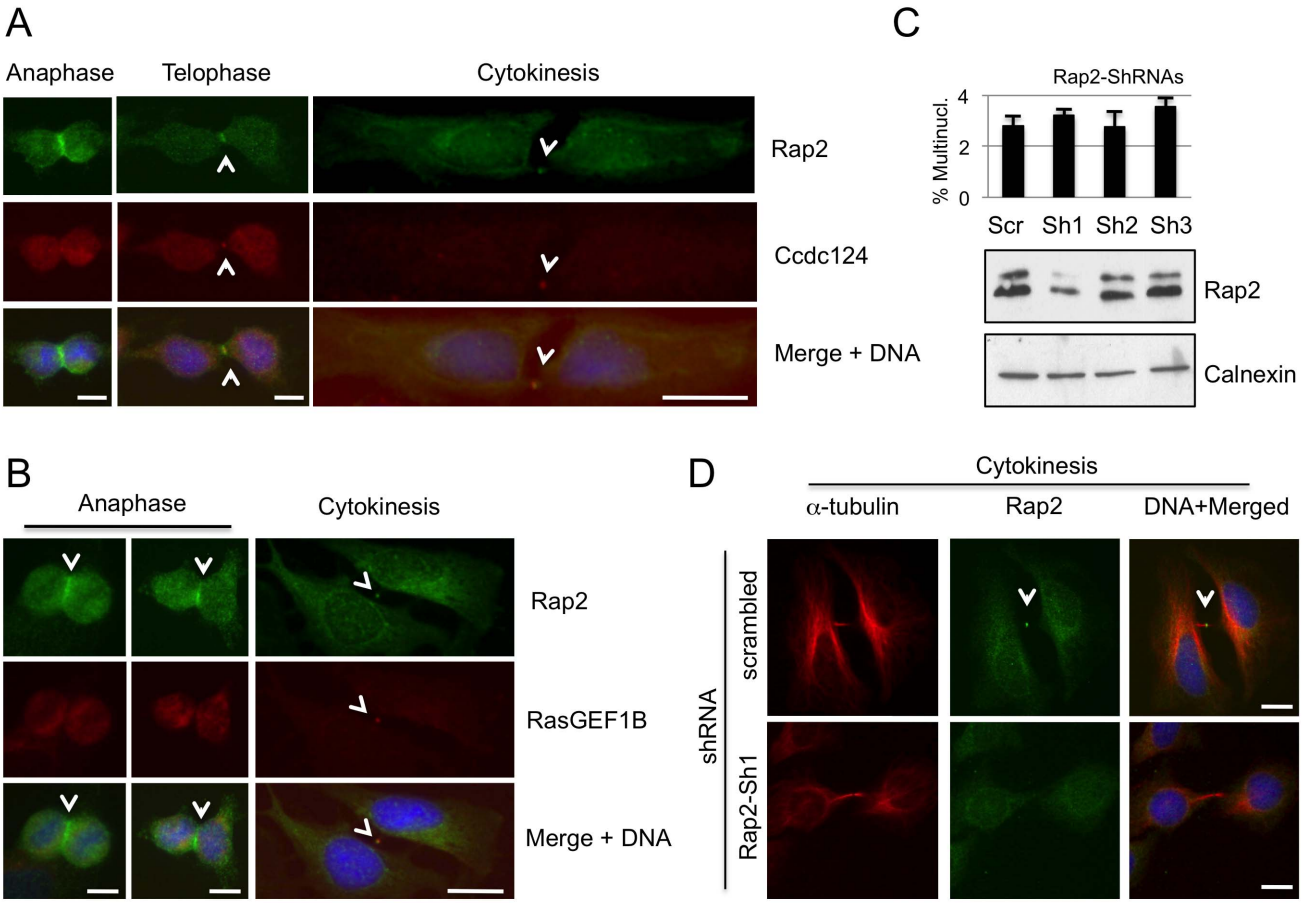


**Figure 8. Rap2 colocalize with Ccdc124 and RasGEF1B at the subcellular level.** Subcellular localizations of endogenous Rap2 and Ccdc124 or RasGEF1B proteins were studied in HeLa cells by immunofluorescence methods. (**A**) At anaphase, Rap2 was clearly localized at the midzone, while Ccdc124 concentration at the same localization was less pronounced. However, at telophase, both proteins were concentrated at the puncta characterizing the midbody, Rap2 rather surrounding Ccdc124. During cytokinetic abscission, a clear colocalization of both Rap2 and Ccdc124 were observed at the midbody. (**B**) Similar to panel (A), Rap2 translocation to the midzone has started during anaphase. Two representative images of anaphase cells were shown in the corresponding panel. Both Rap2 and RasGEF1B proteins colocalized at the midbody during cytokinetic abscission. Arrowheads either indicate subcellular localization of Rap2 at anaphase and telophase, or they indicate the colocalization of Rap2 with RasGEF1B/Ccdc124 at the midbody during cytokinesis. (**C**) HeLa cells were transfected with shRNA vectors (Sh1, Sh2, Sh3) targeting Rap2, then cell lysates were collected at 48 hrs post-transfection, and immunoblotted with anti-Rap2 Ab. Scrambled control transfection was indicated (Scr). Calnexin expression was monitored as loading control. In parallel experiments, similarly treated cells were immunostained with anti-Rap2 and anti-α-tubulin antibodies, followed by scorings for multinucleation ($n = 5 \pm$ SD), as reported on the graph above the immunoblot. (**D**) Representative micrographs of midbody stage cells depleted in endogenous Rap2 (C). Bars represent 10 μm.
doi:10.1371/journal.pone.0069289.g008

## Vector Constructions

pCDNA3.1 was used to generate CMV-promoter controlled Ccdc124 expression vector construct by using EcoRI/BamHI restriction sites and 5′-AAGCTTGAATTCATGCCCAAGAAGTTCCAGGGTGAG-3′ (forward) and 5′-GGTACCGGGATCCTCTTGGGGGCATTGAAGGGCAC-3′ (reverse) primers. Cloning of RasGEF1B into pEGFP-C1 (Clontech) was done by using 5′- GTCGACGAATTCTTAAACTCTGCCTAAGAGGCTCGACC-3′ (forward), and 5′-GTCGACGAATTCTTAAACTCTGCCTAAGAGGCTCGACC-3′ (reverse) primers and XhoI/EcoRI sites. Flag-tagged Ccdc124 expressing vectors were constructed by sub-cloning the gene in p3X-Flag-CMV10 or p3X-Flag-CMV14 vectors (Sigma) by using 5′-CTTGAATTCATGCCCAAGAAGTTCCAGGGTGAG-3′ (forward)/5′-GACCGGGATCCTCTTGGGGGCATTGAAGGGCAC-3′ (reverse) and 5′-CTTGAATTCATGCCCAAGAAGTTCCAGGGTGAG-3′ (forward)/5′-GGATCCTCTAGAGTCCTTGGGGGCATTGAAG-3′ (reverse) primers together with EcoRI/BamHI, and EcoRI/XbaI restriction enzyme sites, respectively. HA-epitope linked versions of Rap2 in Rap2-WT-HA, Rap2-G12V-HA, and Rap2-S17N-HA vectors were kind gifts of Daniel Pak (University of California, Berkeley). GFP-RBD(RalGDS) expression vector was a gift from Johannes L. Bos (University Medical Center Utrecht, the Netherlands).

## Rap Activity Assays

Rap activity assays were carried-out as described previously by van Triest and Bos [31]. Briefly, HEK-293 cells grown in 6-cm plates were lysed in buffer containing 1% NP-40, 150 mM NaCl, 50 mM Tris-HCl (pH 7.4), 10% glycerol, 2 mM $MgCl_2$, and protease and phosphatase inhibitors. Lysates were cleared by centrifugation, and active Rap was precipitated with a glutathione S-transferase fusion protein of the Rap-binding domain of RalGDS precoupled to glutathione-Sepharose beads.

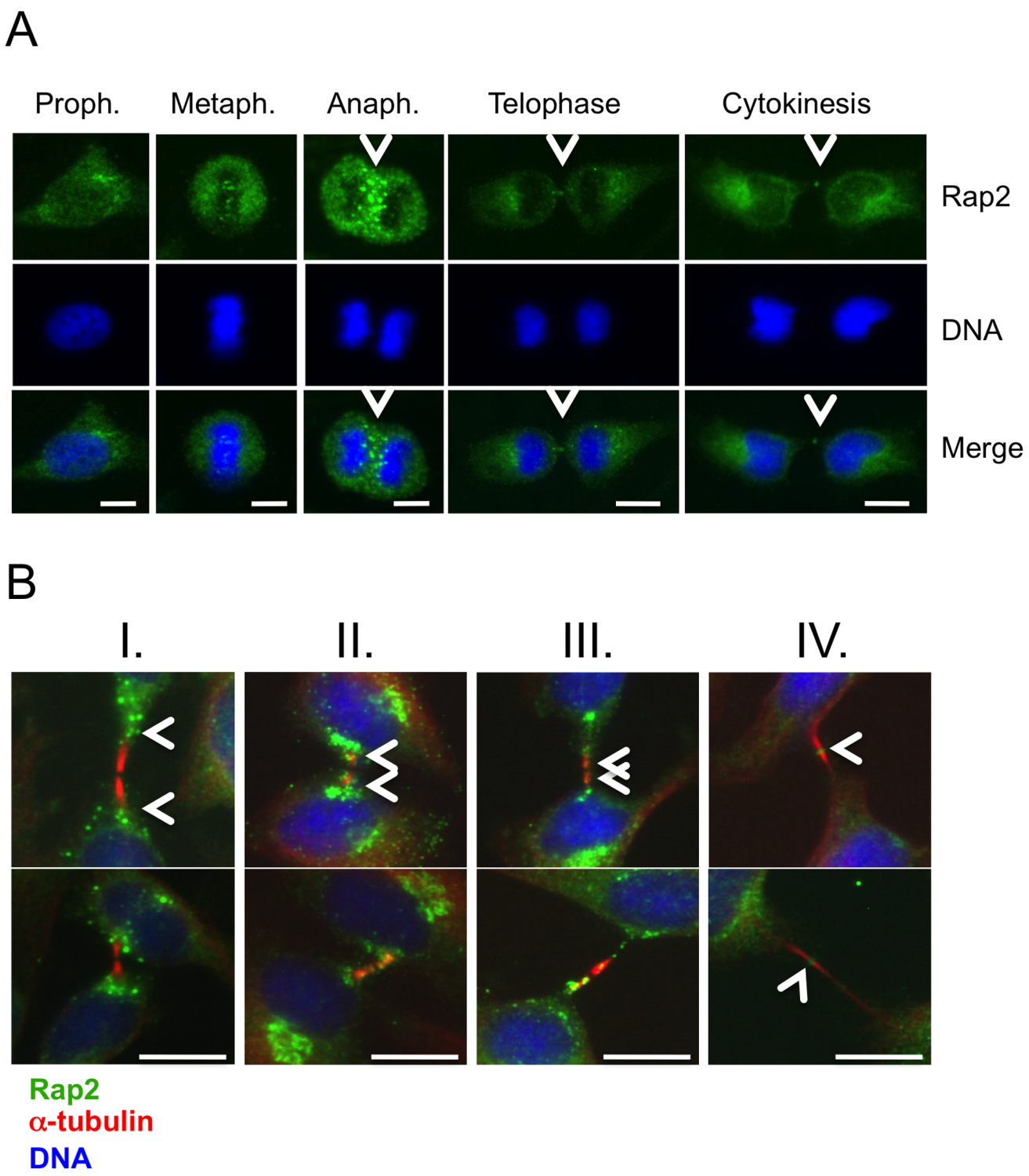


**Figure 9. Active endogenous Rap2 relocates to midzone at anaphase, and to midbody during cytokinetic abscission.** (A) HeLa cells were arrested at G2/M phase by sequential double thymidine and nocodazole treatments as described in the legend of Figure 2, and they were classified according to phases of mitosis, and cytokinesis. Samples of cells were then stained with anti-Rap2 antibody, and with DAPI to visualize DNA. At anaphase Rap2 was detected at the midzone with staining characteristics reminiscent of endosomes, and at telophase/cytokinesis Rap2 was observed as puncta at the middle of the intercellular bridge, a position typically occupied by midbody associated factors. (**B**) Following synchronization of cells as above, 80 mins. after nocodazole was washed-off samples were taken with four consecutive intervals of 10 minutes (I, II, III, and IV), the last one (IV) corresponding to ~120 minutes after the drug was removed, and dynamic positioning of Rap2 at the intercellular bridge in respect to α-tubulin was monitored. A time-dependent relocalization of Rap2 from peripheral flanking regions to the midbody was detected. Intercellular bridge localizations of Rap2 were concluded with observations from a sample of ~50 cells in which over 75% showed similar positioning patterns. Two sets of representative micrographs were displayed. Bars represent 10 μm.
doi:10.1371/journal.pone.0069289.g009

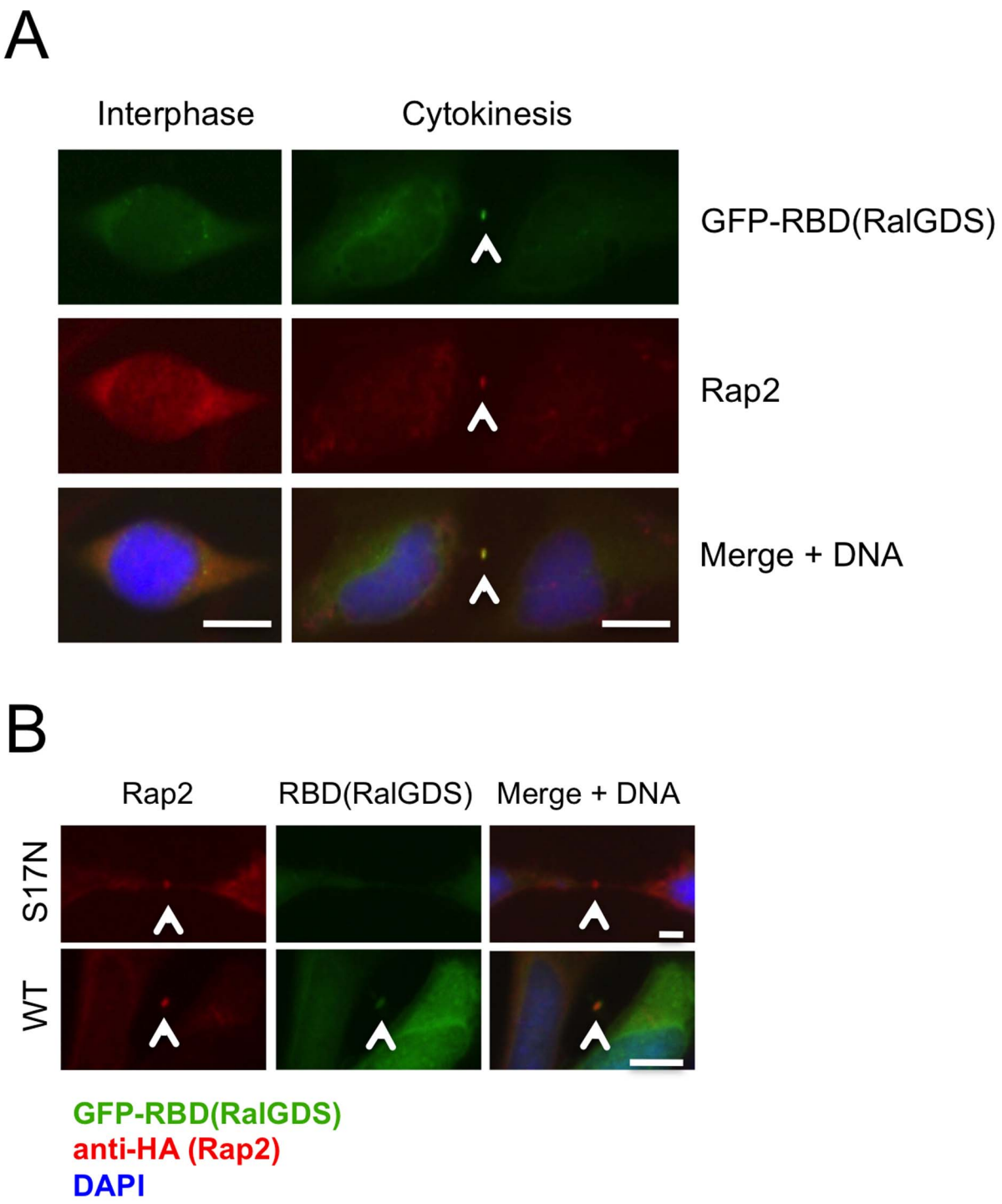


**Figure 10. Rap2 effector proteins translocate to the midbody depending on the signal transduction activity of Rap2.** (A) HeLa cells were transfected with the vector containing GFP-labeled Rap Binding Domain of RalGDS [GFP-RBD(RalGDS)] which interacts only with the GTP-bound active form of Rap2, and cells were monitored at interphase and at cytokinetic abscission following immunostainings involving anti-Rap2 monoclonal Abs and Alexa568-red labeled anti-mouse secondary Abs. Colocalization of GFP-RBD(RalGDS) with Rap2 indicated that at the midbody Rap2 is in its active (Rap2·GTP) form. (**B**) HeLa cells were cotransfected with GFP-RBD(RalGDS) either together with HA-Rap2-WT, or with HA-Rap2-S17N (inactive dominant negative form) and their localizations were monitored with anti-HA-epitope Abs. Positioning of GFP-RBD(RalGDS) were assessed by monitoring GFP-signal observed at the midbody. Localization of the GFP-RBD(RalGDS) depended on the presence of active Rap2 in cells. As in (A), at least 50 cells were monitored in each experiment, and representative pictures display Rap2 and GFP-RBD(RalGDS) localizations observed at least ~90% of cells cotransfected with indicated vectors. Bars represent 10 μm.
doi:10.1371/journal.pone.0069289.g010

## Immunoprecipitation, Immunoblotting and GST-Pull Down Assays

Cells lysed in 50 µl lysis buffer consisting of 50 mM Tris 8.0 Base, 250 mM NaCl, proteinase inhibitor cocktail (Roche), and 1% NP40. Protein concentrations were determined by using Bradford assay. 40 µg of whole cell extracts were denatured in gel loading buffer [50 mM Tris-HCl pH 6.8, 1% SDS, 0.02% bromophenol blue, 10% Glycerol and 5% 2-mercaptoethanol] at 95°C for 5 min, resolved by SDS-PAGE using a 12% gel, and electrotransferred onto PVDF membranes (Millipore). For RasGEF1B/Ccdc124 coimmunoprecipitation experiments, HEK-293 cells were transfected with flag-Ccdc124 and YFP-RasGEF1B vectors. 48 hours later, cells were lysed in NP-40 lysis buffer, flag-tagged agarose beads (A2220, Sigma-Aldrich) were used to precipitate proteins for two hours, followed by a centrifugation for 30 sec. at 8800 rpm, then beads were washed three times with NP-40 lysis buffer. 50 µl sample buffers were added to lysates and incubated at 95°C for 5 min, fractionated by SDS-PAGE for immunoblot analysis and transferred onto PVDF membranes (Millipore). Anti-GFP (G1544, Sigma-Aldrich) and anti-Flag-HRP M2 (A8592, Sigma-Aldrich) were used in Western blot analysis. Blotted proteins were visualized using the ECL detection system (Amersham). For GST pull-down assays, 100 µl 50% slurry (~50 µl packed) GSH beads were washed 3 times with wash buffer (50 mM Tris HCl pH 7.5, 100 mM NaCl, 3 mM β-Mercaptoethanol). First two vials were immobilized with 200 µg purified GST-RasGEF1B protein, second vial was immobilized with 200 µg GST protein, whereas the fourth vial was incubated with buffer only and rotated at 4°C for 1 hour. The first and the third vials incubated with wash buffer only, second and fourth vials incubated with 500 µg bacteria purified His-Ccdc124 protein and incubated at 4°C for 1 hour by rotating. Beads were washed 10 times with wash buffer, and samples were eluted with 40 µl 4xSDS loading buffer, boiled for 5 min and loaded on an SDS gel. For the control of protein sizes samples from a 10 µg/µl stock of each protein were loaded to the same gel. The gel then stained with commassie blue and destained with water.

## Generation of Polyclonal Antibodies

3 mg of N-terminus 24mer peptide MPKKFQGENTK-SAAARARRAEAK-[C]-amide of human Ccdc124, and [C]-NNMEKDR-W-KSLRSSLLNRT peptide corresponding to partly conserved C-terminus of the zebra fish homologue of RasGEF1B (*Danio rerio* RasGEF domain family member 1Ba, NCBI accession number: NM_199829) were coupled to KLH through their inserted cysteine residues via MBS, and Both peptides were used in rabbit immunizations at the Cambridge Research Biochemicals (Cambridge, United Kingdoms). 10 mg of each peptide affinity column purified (Glycine and TEA eluates) antibodies and pre-immune control sera were then received for use in molecular biology research.

## Immunofluorescence

HeLa cells on cover slips were fixed by ice cold 100% Methanol for 10 min at −20°C, washed three times with PBS-T; blocked in 2% BSA for 1 hour and incubated 1 hour with primary antibodies, washed again three times with PBS-T and incubated for 1 hour with suitable secondary antibodies. Sources of antibodies: Plk1 a gift from Nurhan Özlü, Koç University, Istanbul; monoclonal (ab17057), or polyclonal (ab109777) Abs were purchased from Abcam; anti-RasGEF1B-C-ter epitope Ab and anti-Ccdc124-N-ter epitope Ab were custom produced by Cambridge Research Biochemicals-UK (see above), Ccdc124 middle-epitope specific (A-301-835A) or C-ter epitope specific (A-301-834A) Abs were from BETHYL Laboratories; anti-γ-tubulin were either from Abcam (ab11316), or from BioLegend (rabbit polyclonal cat.620902); anti-α-tubulin were from Santa Cruz (SC-5286); rabbit anti-flag-Ab was from Sigma (F-7425); rabbit anti-Rap2 polyclonal was purchased from Genetex (GTX108831); mouse anti-Rap2 monoclonal was from BD Biosciences (610215), DNA dye (DAPI) was from Invitrogene (P36931); and Alexa Fluor 488, or 568 labeled anti-rabbit, and anti-mouse secondary antibodies were purchased from Invitrogene.

## Fluorescent Microscopy and Imaging

Fluorescent images were done by Zeiss Imager-A1 microscope with a Zeiss Acroplan 40X objective. Images were captured on the Zeiss Axia Cam MRc 5-CCD camera for fixed samples. Microscope control and image processing were done through Axiovision version 4.6 software program (Universal Imaging).

## Northern Blot Analysis

Northern blotting was performed on commercially obtained "FirstChoice Northern Human Blot-1 and Blot-2 Membranes" (Ambion) which contained 2 µg poly(A)-RNA from indicated human organs on each lane. Donor information is available at the suppliers (Ambion) documents; human derived materials have been prepared in the mentioned company from tissues obtained with consent from a fully informed donor, or a member of the donor's family, as certified by the company. DNA probes used in hybridizations were as follows: ApaI-XbaI DNA fragment (381 bp) of *CCDC124* cut-out from Flag-Ccdc124 plasmid vector, GAPDH fragment (408 bp) obtained after PCR amplification of a HeLa cell cDNA library by using forward primer 5′-GGCTGA-GAACGGGAAGCTTGTCAT-3′ and reverse primer 5′-CAGCCTTCTCCATGGTGGTGAAGA-3′ as amplification primers, and β-actin fragment (539 bp) obtained after PCR amplification of the same cDNA library by using forward 5′-GATGACCCAGATCATGTTTG-3′ and reverse 5′- CATG-GAGGAGCCGCCAGACAGC-3′ primers in PCR amplifications in the following conditions: 5 min initial denaturation at 95°C, 35 cycles of 30 sec denaturation at 95°C, 30 sec primer annealing at 60°C and 30 sec extension at 72°C, and a 5 min final extension at 72°C. Then, DNA templates corresponding to expected band sizes were isolated from agarose gels, labeled by North-2-South Biotin random prime labeling kit (Pierce). Nucleic acids hybridization and detection were done by North-2-South Chemiluminescent hybridization and detection kit (Pierce). Resulting blots were exposed to autoradiography films (Kodak).

## Identification of CCDC124-interacting Proteins by using the Yeast Two-hybrid (Y2H) Screening Method

Bait cloning and Y2H screening were performed by Hybrigenics, S.A., Paris, France (http://www.hybrigenics.com). Human CCDC124 cDNA (encoding 223 a.a protein) was PCR-amplified and cloned in a LexA C-terminal fusion vector. The bait construct was checked by sequencing the entire insert, and was subsequently transformed in the L40ΔGAL4 yeast strain [49]. Then, a human liver cDNA library containing ten million independent fragments were transformed into the Y187 yeast strain, which was used for mating. The screen was performed in conditions ensuring a minimum of 50 million interactions tested, in order to cover five times the primary complexity of the yeast-transformed cDNA library. After selection on medium lacking leucine, tryptophane, and histidine, 15 positive clones were picked, and the corresponding prey fragments were sequenced at their 5′ and 3′ junctions.

Sequences were contigued as described previously, and then they were compared to the latest release of the GenBank database using BLASTN [50]. A Predicted Biological Score (PBS) was attributed to assess the reliability of each interaction, as described previously [51].

## Supporting Information

**Figure S1 Ccdc124 contains two main coiled-coil domains at its N-terminal part.** Schematic representation of the coiled-coil prediction of Ccdc124 is presented. The graph was obtained by the COILS (www.ch.embnet.org/software/COILS_form.html) bioinformatics analysis platform.
(TIFF)

**Figure S2 Double-thymidine and nocodazole treatments synchronized HeLa cells at G2/M phase of cell cycle.** HeLa cells were treated with thymidine and MT polymerization inhibitor drug nocodazole as indicated in *Methods*. $1\times10^6$ unsynchronized **(A)** or synchronized **(B)** cells were collected as samples, and resuspended in 0.3 ml of PBS buffer. Cells were fixed by addition of 0.7 ml cold ethanol (70%), left on ice for 1 hr, and then washed and resuspended in 0.25 ml of PBS in which it is treated with 0.5 mg/ml RNAse-A for 1 hr at 37°C. Cellular DNA is then stained with 10 μg/ml propidium iodide (PI) solution, and cytometric analysis was performed by FACS at 488 nm. Percentages of cells in each sample at various stages of the cell cycle are indicated below each panel **(A–B)**.
(TIFF)

**Figure S3 Polyclonal Anti-RasGEF1B antibody raised against zebrafish homologue of RasGEF1B cross-reacts strongly with human RasGEF1B.** HEK-293 cells were transfected with mCherry-labeled human RasGEF1B or YFP-labeled human RasGEF1B expression vectors (mCherry-RasGEF1B and YFP-RasGEF1B, respectively), after 48 hours cells were lysed, proteins were separated by SDS-PAGE, and immunoblot was performed with anti-RasGEF1B antibody alone (1 μg at 1:1000 dilution), and then the membrane was stripped and sequentially reprobed first with the same antibody pre-incubated with 100 ng of competing 20mer peptide epitope [C]-NNMEKDR-W-KSLRSSLLNRT corresponding to C-terminus of ZF-RasGEF1B, and then with anti-GFP antibody recognizing YFP as its epitope in YFP-RasGEF1B. Calnexin expression was monitored as loading control.
(TIFF)

**Figure S4 Screening of RasGEF1B specific shRNA plasmids to monitor their down-regulatory capacities.** HEK-293 cells were transfected with RasGEF1B shRNA plasmids described in Materials and MethodsS1. 48 hours after transfections, cells were lysed and proteins were separated by SDS-PAGE. Immunoblot was performed with custom made anti-RasGEF1B antibody. Image-J software program were used to obtain densitometric readings of band intensities corrected by calnexin values, and these were indicated below each band. RasGEF1B specific shRNA expressing vector renamed as sh-D (see *Materials and Methods S1*) was selected to carry-out experiments described in Results. Calnexin expression was monitored as loading control.
(TIFF)

**Figure S5 Endogenous Rap1 does not relocate to the midzone/midbody during cytokinetic abscission.** HeLa cells were arrested at G2/M phase by sequential double thymidine and nocodazole treatments as described in the legend of Figure 2, and they were classified according to phases of mitosis, and cytokinesis. Samples of cells were then costained with anti-Rap1 and anti-α-tubulin antibodies, which were used to monitor intercellular bridge and the space containing midbody complexes. DAPI staining was used to visualize DNA. Bars represent 10 μm.
(TIFF)

**Figure S6 Mutating the consensus CK2 phosphorylation site Ser122 to Ala leads to compromised stability of Ccdc124. (A–B)** HEK-293 cells were transfected either with HA-tagged wild-type Ccdc124 expression vector, or with similar vectors carrying indicated mutations on Figures, and stabilities of mutants proteins were monitored by immunoblots using anti-Ccdc124 antibodies recognizing the N-terminus of the protein. Only one CK2 phosphorylation consensus site (Ser122) turned out to be essential for the stability of Ccdc124 protein as S122A mutants were cleaved at their C-terminus, whereas phospho-mimicking mutations S121D, and S121E were normal in terms of Ccdc124 stability (B). Calnexin expressions were monitored as loading control.
(TIFF)

**Methods S1.**
(DOCX)

## Acknowledgements

The authors would like to thank Mehmet Öztürk for a critical reading of the manuscript. We would like to thank Holger Rehmann and Johannes L. Bos for hosting P.T. in their laboratories for a short stay to learn analysis of Rap signaling, and for providing us GFP-RBD(RalGDS) vector. We are grateful to Greenfield Sluder for GFP-Centrin containing RPE1 cells, to Prasad Jallepalli for providing RPE1 cells with GFP-Plk1(WT), to Daniel Pak for Rap2-WT-HA, Rap2-G12V-HA, and Rap2-S17N-HA expression vectors, and to Nurhan Özlü for anti-Plk1 Abs.

## Author Contributions

Conceived and designed the experiments: PT SE DB UHT. Performed the experiments: PT SE EY HA DB. Analyzed the data: PT EY DB UHT. Contributed reagents/materials/analysis tools: UHT. Wrote the paper: UHT.

## References

1. Lüders J, Stearns T (2007) Microtubule-Organizing centres: A re-evaluation. Nat Rev Mol Cell Biol 8: 161–7.
2. Conduit PT, Brunk K, Dobbelaere J, Dix CI, Lucas EP, et al. (2010) Centrioles regulate centrosome size by controlling the rate of Cnn incorporation into the PCM. Curr Biol 20: 2178–86.
3. Debec A, Sullivan W, Bettencourt-Dias M (2010) Centrioles: active players or passengers during mitosis? Cell Mol Life Sci 67: 2173–94.
4. Nigg EA, Stearns T (2011) The centrosome cycle: Centriole biogenesis, duplication and inherent asymmetries. Nat Cell Biol 13: 1154–60.
5. Haren L, Stearns T, Lüders J (2009) Plk1-dependent recruitment of gamma-tubulin complexes to mitotic centrosomes involves multiple PCM components. PLoS ONE 4: e5976.
6. Schatten H, Sun QY (2010) The role of centrosomes in fertilization, cell division and establishment of asymmetry during embryo development. Semin Cell Dev Biol 21: 174–84.
7. Lee K, Rhee K (2011) PLK1 phosphorylation of pericentrin initiates centrosome maturation at the onset of mitosis. J Cell Biol 195: 1093–101.
8. Jakobsen L, Vanselow K, Skogs M, Toyoda Y, Lundberg E, et al. (2011) Novel asymmetrically localizing components of human centrosomes identified by complementary proteomics methods. EMBO J 30: 1520–35.
9. Cohen C, Parry DA (1990) Alpha-helical coiled coils and bundles: how to design an alpha-helical protein. Proteins 7: 1–15.
10. Fededa JP, Gerlich DW (2012) Molecular control of animal cell cytokinesis. Nat Cell Biol 14: 440–7.

11. Gromley A, Yeaman C, Rosa J, Redick S, Chen CT, et al. (2005) Centriolin anchoring of exocyst and SNARE complexes at the midbody is required for secretory-vesicle-mediated abscission. Cell 123: 75–87.
12. Skop AR, Liu H, Yates J, Meyer BJ, Heald R (2004) Dissection of the mammalian midbody proteome reveals conserved cytokinesis mechanisms. Science 305: 61–6.
13. Fabbro M, Zhou BB, Takahashi M, Sarcevic B, Lal P, et al. (2005) Cdk1/Erk2- and Plk1-dependent phosphorylation of a centrosome protein, Cep55, is required for its recruitment to midbody and cytokinesis. Dev Cell 9: 477–88.
14. van der Horst A, Simmons J, Khanna KK (2009) Cep55 stabilization is required for normal execution of cytokinesis. Cell Cycle 8: 3742–9.
15. Lee HH, Elia N, Ghirlando R, Lippincott-Schwartz J, Hurley JH (2008) Midbody targeting of the ESCRT machinery by a noncanonical coiled coil in CEP55. Science 322: 576–80.
16. Hu CK, Coughlin M, Mitchison TJ (2012) Midbody assembly and its regulation during cytokinesis. Mol Biol Cell 23: 1024–34.
17. Carlton JG, Martin-Serrano J (2007) Parallels between cytokinesis and retroviral budding: a role for the ESCRT machinery. Science 316: 1908–12.
18. Guizetti J, Schermelleh L, Mantler J, Maar S, Poser I, et al. (2011) Cortical constriction during abscission involves helices of ESCRT-III-dependent filaments. Science 331: 1616–20.
19. Hanson PI, Roth R, Lin Y, Heuser JE (2008) Plasma membrane deformation by circular arrays of ESCRT-III protein filaments. J Cell Biol 180: 389–402.
20. Elia N, Sougrat R, Spurlin TA, Hurley JH, Lippincott-Schwartz J (2011) Dynamics of endosomal sorting complex required for transport (ESCRT) machinery during cytokinesis and its role in abscission. Proc. Natl Acad Sci USA 108: 4846–51.
21. Lane HA, Nigg EA (1996) Antibody microinjection reveals an essential role for human polo-like kinase 1 (Plk1) in the functional maturation of mitotic centrosomes. J Cell Biol 135: 1701–13.
22. Tong C, Fan HY, Lian L, Li SW, Chen DY, et al. (2002) Polo-like kinase-1 is a pivotal regulator of microtubule assembly during mouse oocyte meiotic maturation, fertilization, and early embryonic mitosis. Biol Reprod 67: 546–54.
23. Bastos RN, Barr FA (2010) Plk1 negatively regulates Cep55 recruitment to the midbody to ensure orderly abscission. J Cell Biol 191: 751–60.
24. Yaman E, Gasper R, Koerner C, Wittinghofer A, Tazebay UH (2009) RasGEF1A and RasGEF1B are guanine nucleotide exchange factors that discriminate between Rap GTP-binding proteins and mediate Rap2-specific nucleotide exchange. FEBS J 276: 4607–16.
25. Gloerich M, Bos JL (2011) Regulating Rap small G-proteins in time and space. Trends Cell Biol 21: 615–23.
26. Uetake Y, Loncarek J, Nordberg JJ, English CN, La Terra S, et al. (2007) Cell cycle progression and de novo centriole assembly after centrosomal removal in untransformed human cells. J Cell Biol 176: 173–82.
27. Gromley A, Jurczyk A, Sillibourne J, Halilovic E, Mogensen M, et al. (2003) A novel human protein of the maternal centriole is required for the final stages of cytokinesis and entry into S phase. J Cell Biol 161: 535–45.
28. Epting D, Vorwerk S, Hageman A, Meyer D (2007) Expression of rasgef1b in zebrafish. Gene Expr Patterns 7: 389–95.
29. Andrade WA, Silva AM, Alves VS, Salgado AP, Melo MB, et al. (2010) Early endosome localization and activity of RasGEF1b, a toll-like receptor-inducible Ras guanine-nucleotide exchange factor. Genes Immun 11: 447–57.
30. Schiel JA, Prekeris R (2013) Membrane dynamics during cytokinesis. Curr. Opin. in Cell. Biol 25: 92–8.
31. van Triest M, Bos JL (2004) Pull-down assays for guanoside 5′-triphosphate-bound Ras-like guanosine 5′-triphosphatases. Methods Mol Biol 250: 97–102.
32. Bivona TG, Wiener HH, Ahearn IM, Silletti J, Chiu VK, et al. (2004) Rap1 up-regulation and activation on plasma membrane regulates T cell adhesion. J Cell Biol 164: 461–70.
33. de Rooij J, Zwartkruis FJ, Verheijen MH, Cool RH, Nijman SM, et al. (1998) Epac is a Rap1 guanine-nucleotide-exchange factor directly activated by cyclic AMP. Nature 396: 474–7.
34. Ghandour H, Cullere X, Alvarez A, Luscinskas FW, Mayadas TN (2007) Essential role for Rap1 GTPase and its guanine exchange factor CalDAG-GEFI in LFA-1 but not VLA-4 integrin mediated human T-cell adhesion. Blood 110: 3682–90.
35. Stearns T, Winey M (1997) The Cell Center at 100. Cell 91: 303–9.
36. Piel M, Nordberg J, Euteneuer U, Bornens M (2001) Centrosome-dependent exit of cytokinesis in animal cells. Science 291: 1550–3.
37. Oakley BR, Oakley CE, Yoon Y, Jung MK (1990) Gamma-tubulin is a component of the spindle pole body that is essential for microtubule function in *Aspergillus nidulans*. Cell 61: 1289–301.
38. Morita E, Sandrin V, Chung HY, Morham SG, Gygi SP, et al. (2007) Human ESCRT and ALIX proteins interact with proteins of the midbody and function in cytokinesis. EMBO J 26: 4215–27.
39. Steigemann P, Gerlich DW (2009) Cytokinetic abscission: cellular dynamics at the midbody. Trends Cell Biol 19: 606–16.
40. Schiel JA, Childs C, Prekeris R (2013) Endocytic transport and cytokinesis: from regulation of the cytoskeleton to midbody inheritence Trends Cell Biol (*in press*, http://dx.doi.org/10.1016/j.tcb.2013.02.003).
41. Cascone I, Selimoglu R, Ozdemir C, Del Nery E, Yeaman C, et al. (2008) Distinct roles of RalA and RalB in the progression of cytokinesis are supported by distinct RalGEFs. EMBO J 27: 2375–87.
42. Dambournet D, Machicoane M, Chesneau L, Sachse M, Rocancourt M, et al. (2011) Rab35 GTPase and OCRL phosphatase remodel lipids and F-actin for successful cytokinesis. Nat Cell Biol 13: 981–8.
43. Sagona AP, Nezis IP, Pedersen NM, Liestol K, Poulton J, et al. (2010) PtdIns(3)P controls cytokinesis through KIF13A-mediated recruitment of FYVE-CENT to the midbody. Nat Cell Biol 12: 362–71.
44. Choi SC, Kim GH, Lee SJ, Park E, Yeo CY, et al. (2008) Regulation of activin/nodal signaling by Rap2-directed receptor trafficking. Dev Cell 15: 49–61.
45. Schiel JA, Simon GC, Zaharris C, Weisz J, Castle D, et al. (2012) FIP3-endosome-dependent formation of the secondary ingression mediates ESCRT-III recruitment during cytokinesis. Nat Cell Biol 14: 1068–78.
46. Gloerich M, Ponsioen B, Vliem MJ, Zhang Z, Zhao J, et al. (2010) Spatial regulation of cyclic AMP-Epac1 signaling in cell adhesion by ERM proteins. Mol Cell Biol 30: 5421–31.
47. Burkard ME, Randall CL, Larochelle S, Zhang C, Shokat KM, et al. (2007) Chemical genetics reveals the requirement for Polo-like kinase 1 activity in positioning RhoA and triggering cytokinesis in human cells. Proc. Natl Acad Sci USA 104: 4383–8.
48. Paddison PJ, Cleary M, Silva JM, Chang K, Sheth N, et al. (2004) Cloning of short hairpin RNAs for gene knock-down in mammalian cells. Nat Methods 1: 163–167.
49. Fromont-Racine M, Rain JC, Legrain P (1997) Toward a functional analysis of the yeast genome through exhaustive two-hybrid screens. Nat Genet 16: 277–82.
50. Altschul SF, Madden TL, Schäffer AA, Zhang J, Zhang Z, et al. (1997) Gapped BLAST and PSI-BLAST: a new generation of protein database search programs. Nucleic Acids Res 25: 3389–402.
51. Formstecher E, Aresta S, Collura V, Hamburger A, Meil A, et al. (2005) Protein interaction mapping: a Drosophila case study. Genome Res 15: 376–84.

# Permissions to the Copy Righted Material

## NATURE PUBLISHING GROUP LICENSE TERMS AND CONDITIONS

May 10, 2016

---

This is a License Agreement between Defne Bayik ("You") and Nature Publishing Group ("Nature Publishing Group") provided by Copyright Clearance Center ("CCC"). The license consists of your order details, the terms and conditions provided by Nature Publishing Group, and the payment terms and conditions.

**All payments must be made in full to CCC. For payment instructions, please see information listed at the bottom of this form.**

| | |
|---|---|
| License Number | 3865330691186 |
| License date | May 10, 2016 |
| Licensed content publisher | Nature Publishing Group |
| Licensed content publication | Nature Reviews Immunology |
| Licensed content title | Toll-like receptor signalling |
| Licensed content author | Shizuo AkiraandKiyoshi Takeda |
| Licensed content date | Jul 1, 2004 |
| Volume number | 4 |
| Issue number | 7 |
| Type of Use | reuse in a dissertation / thesis |
| Requestor type | academic/educational |
| Format | print and electronic |
| Portion | figures/tables/illustrations |
| Number of figures/tables/illustrations | 1 |
| High-res required | no |
| Figures | Table1.1 |
| Author of this NPG article | no |
| Your reference number | None |
| Title of your thesis / dissertation | REGULATION OF HUMAN MONOCYTE DIFFERENTIATION INTO M1- AND M2-LIKE MACROPHAGES |
| Expected completion date | May 2016 |
| Estimated size (number of pages) | 250 |
| Total | 0.00 USD |

## NATURE PUBLISHING GROUP LICENSE TERMS AND CONDITIONS

May 10, 2016

---

This is a License Agreement between Defne Bayik ("You") and Nature Publishing Group ("Nature Publishing Group") provided by Copyright Clearance Center ("CCC"). The license consists of your order details, the terms and conditions provided by Nature Publishing Group, and the payment terms and conditions.

**All payments must be made in full to CCC. For payment instructions, please see information listed at the bottom of this form.**

| | |
|---|---|
| License Number | 3865330234290 |
| License date | May 10, 2016 |
| Licensed content publisher | Nature Publishing Group |
| Licensed content publication | Nature Reviews Immunology |
| Licensed content title | Myeloid-derived suppressor cells as regulators of the immune system |
| Licensed content author | Dmitry I. Gabrilovich and Srinivas Nagaraj |
| Licensed content date | Mar 1, 2009 |
| Volume number | 9 |
| Issue number | 3 |
| Type of Use | reuse in a dissertation / thesis |
| Requestor type | academic/educational |
| Format | print and electronic |
| Portion | figures/tables/illustrations |
| Number of figures/tables/illustrations | 1 |
| High-res required | no |
| Figures | Figure1.1 |
| Author of this NPG article | no |
| Your reference number | None |
| Title of your thesis / dissertation | REGULATION OF HUMAN MONOCYTE DIFFERENTIATION INTO M1- AND M2-LIKE MACROPHAGES |
| Expected completion date | May 2016 |
| Estimated size (number of pages) | 250 |
| Total | 0.00 USD |